

British Geological Survey

**Exploration methods and new targets
for epithermal gold mineralisation in
the Devonian rocks of northern Britain**



dti

**Minerals Programme
Department of Trade and Industry**



**Minerals Programme Publication No. 2
British Geological Survey Research Report RR/00/8**

BRITISH GEOLOGICAL SURVEY

BGS RESEARCH REPORT RR/00/08

is equivalent to

DTI MINERALS PROGRAMME PUBLICATION NO. 2

Exploration methods and new targets for epithermal gold mineralisation in the Devonian rocks of Northern Britain

A G Gunn and K E Rollin

(with contributions by M H Shaw, A M Denniss and J S Coats)

Bibliographical reference

Gunn, A G and Rollin, K E.

2000. Exploration methods and
new targets for epithermal gold
mineralisation in the Devonian
rocks of northern Britain.

BGS Research Report,
RR/00/08. DTI Minerals
Programme Publication
No. 2.

© NERC 2000. All
rights reserved.

Keyworth, Nottingham British Geological Survey 2000

BRITISH GEOLOGICAL SURVEY

The full range of Survey publications is available from the BGS Sales Desk at the Survey headquarters, Keyworth, Nottingham. The more popular maps and books may be purchased from BGS-approved stockists and agents and over the counter at the Bookshop, Gallery 37, Natural History Museum (Earth Galleries), Cromwell Road, London. Sales desks are also located at the BGS London Information Office, and at Murchison House, Edinburgh. The London Information Office maintains a reference collection of BGS publications including maps for consultation. Some BGS books and reports may also be obtained from the Stationery Office Publications Centre or from the Stationery Office bookshops and agents.

The Survey publishes an annual catalogue of maps, which lists published material and contains index maps for several of the BGS series.

The British Geological Survey carries out the geological survey of Great Britain and Northern Ireland (the latter as an agency service for the government of Northern Ireland), and of the surrounding continental shelf, as well as its basic research projects. It also undertakes programmes of British technical aid in geology in developing countries as arranged by the Department for International Development and other agencies.

The British Geological Survey is a component body of the Natural Environment Research Council.

*All communications regarding the content of this publication should be addressed to the Programme Manager, Onshore Minerals and Energy Resources, British Geological Survey, Keyworth, Nottingham NG12 5GG
☎ 0115-936 3493 Fax 0115 936 3520
E-mail minerals@bgs.ac.uk*

Authors

A G Gunn, BA, MSc
K E Rollin, BSc
BGS, Keyworth

This publication was prepared for the
Department of Trade and Industry

Maps and diagrams in this report use
topography based on Ordnance Survey
mapping. Ordnance Survey Licence
GD272191/2000.

Cover photograph

Lower Devonian rhyodacite lava flow at
Craig Rossie, Ochil Hills, Scotland. BGS
Photo D2182. © NERC 1977

Keyworth, Nottingham NG12 5GG

☎ 0115-936 3100 Fax 0115-936 3200

Murchison House, West Mains Road, Edinburgh EH9 3LA

☎ 0131-667 1000 Fax 0131-668 2683

London Information Office at the Natural History Museum (Earth Galleries), Exhibition Road, South Kensington, London SW7 2DE

☎ 020-7589 4090 Fax 020-7584 8270
☎ 020-7938 9056/57

St Just, 30 Pennsylvania Road, Exeter EX4 6BX

☎ 01392-278312 Fax 01392-437505

Geological Survey of Northern Ireland, 20 College Gardens,
Belfast BT9 6BS

☎ 01232-666595 Fax 01232-662835

Maclean Building, Crowmarsh Gifford, Wallingford,
Oxfordshire OX10 8BB

☎ 01491-838800 Fax 01491-692345

Parent Body

Natural Environment Research Council
Polaris House, North Star Avenue, Swindon, Wiltshire SN2 1EU

☎ 01793-411500 Fax 01793-411501

CONTENTS

| | |
|--|-----------|
| SUMMARY | 1 |
| 1. INTRODUCTION | 2 |
| 1.1. Objectives and methodology | 3 |
| 2. DEVONIAN VOLCANIC ROCKS OF NORTHERN BRITAIN | 4 |
| 2.1. Geology and tectonic setting | 4 |
| 2.1.1. <i>Precambrian to Lower Palaeozoic</i> | 4 |
| 2.1.2. <i>Lower Palaeozoic</i> | 4 |
| 2.1.3. <i>Lower Devonian volcanism</i> | 5 |
| 2.2. Epithermal mineralisation | 6 |
| 3. DEPOSIT MODELS FOR EPITHERMAL GOLD MINERALISATION | 7 |
| 3.1. Introduction | 7 |
| 3.2. Features of epithermal precious metal deposits | 8 |
| 3.2.1. <i>Low-sulphidation deposits</i> | 10 |
| 3.2.2. <i>High-sulphidation deposits</i> | 12 |
| 3.2.3. <i>Hot-spring gold deposits</i> | 13 |
| 3.2.4. <i>Associated mineral deposits</i> | 14 |
| 3.2.5. <i>Mining aspects</i> | 14 |
| 4. EXPLORATION GUIDES AND METHODS | 16 |
| 4.1. Structure and terrain characteristics | 16 |
| 4.2. Mineralisation and alteration patterns | 18 |
| 4.3. Geophysical signatures | 20 |
| 4.4. Geochemical signatures | 21 |
| 4.5. Multi-dataset integration and analysis | 23 |
| 5. MULTI-DATASET INTEGRATION AND PROSPECTIVITY ANALYSIS | 24 |
| 5.1. Introduction | 24 |
| 5.2. Details of the XMAP system | 25 |
| 5.2.1. <i>Logic model</i> | 25 |
| 5.2.2. <i>Pixel size</i> | 26 |
| 5.2.3. <i>Prospectivity parameters</i> | 27 |
| 5.3. Prospectivity map and grid | 28 |
| 6. OCHIL HILLS | 31 |
| 6.1. Geology | 31 |
| 6.1.1. <i>Volcanic rocks</i> | 31 |
| 6.1.2. <i>Intrusions</i> | 32 |
| 6.1.3. <i>Superficial deposits</i> | 33 |
| 6.1.4. <i>Structure</i> | 34 |
| 6.2. Mineralisation | 34 |
| 6.3. Geochemistry | 36 |
| 6.3.1. <i>Introduction</i> | 36 |
| 6.3.2. <i>Results</i> | 36 |
| 6.3.3. <i>Discussion</i> | 42 |
| 6.4. Investigations in the Borland Glen area | 43 |
| 6.4.1. <i>Introduction</i> | 43 |
| 6.4.2. <i>Geology of Borland Glen</i> | 43 |
| 6.4.3. <i>Overburden sampling</i> | 43 |
| 6.4.4. <i>Geophysical surveys</i> | 44 |
| 6.4.5. <i>Boreholes</i> | 44 |
| 6.4.6. <i>Alteration</i> | 47 |
| 6.4.7. <i>Discussion</i> | 48 |
| 6.5. Geophysics | 49 |
| 6.5.1. <i>Magnetic and gravity features</i> | 49 |
| 6.5.2. <i>Lineament analysis</i> | 50 |
| 6.6. Data integration and prospectivity analysis | 50 |

| | |
|--|------------|
| 7. LORN PLATEAU | 52 |
| 7.1. Geology | 52 |
| 7.1.1. <i>Introduction</i> | 52 |
| 7.1.2. <i>Devonian sedimentary rocks</i> | 53 |
| 7.1.3. <i>Volcanic rocks</i> | 54 |
| 7.1.4. <i>Intrusive rocks</i> | 56 |
| 7.1.5. <i>Structure</i> | 57 |
| 7.2. Mineralisation | 58 |
| 7.3. Geochemistry | 59 |
| 7.3.1. <i>Introduction</i> | 59 |
| 7.3.2. <i>Results</i> | 60 |
| 7.3.3. <i>Discussion</i> | 64 |
| 7.4. Geophysics | 65 |
| 7.4.1. <i>Magnetic features</i> | 65 |
| 7.4.2. <i>Gravity features</i> | 66 |
| 7.4.3. <i>Lineament analysis</i> | 66 |
| 7.4.4. <i>Discussion</i> | 67 |
| 7.5. Data integration and prospectivity analysis | 67 |
| 8. CHEVIOT HILLS | 69 |
| 8.1. Geology | 69 |
| 8.1.1. <i>Introduction</i> | 69 |
| 8.1.2. <i>Sedimentary and volcanic rocks</i> | 70 |
| 8.1.3. <i>Intrusions</i> | 71 |
| 8.1.4. <i>Structure</i> | 73 |
| 8.2. Mineralisation | 73 |
| 8.3. Geochemistry | 75 |
| 8.3.1. <i>Introduction</i> | 75 |
| 8.3.2. <i>Results</i> | 76 |
| 8.3.3. <i>Discussion</i> | 81 |
| 8.4. Geophysics | 82 |
| 8.4.1. <i>Bouguer gravity data</i> | 82 |
| 8.4.2. <i>Aeromagnetic data</i> | 83 |
| 8.4.3. <i>3-D gravity-magnetic model</i> | 83 |
| 8.4.4. <i>Geophysical lineaments</i> | 84 |
| 8.4.5. <i>Discussion</i> | 84 |
| 8.5. Investigations in the Kingsseat Burn area | 85 |
| 8.5.1. <i>Previous work</i> | 85 |
| 8.5.2. <i>PIMA analysis and magnetic susceptibility data</i> | 87 |
| 8.5.3. <i>Discussion</i> | 88 |
| 8.6. Data integration and prospectivity analysis | 89 |
| 9. DISCUSSION AND CONCLUSIONS | 91 |
| 9.1. Ochil Hills | 91 |
| 9.2. Lorn Plateau | 92 |
| 9.3. Cheviot Hills | 92 |
| 9.4. Exploration methods | 93 |
| 9.5. Computer-based data analysis | 93 |
| 10. RECOMMENDATIONS | 94 |
| 11. REFERENCES | 95 |
| 12. APPENDIX 1 | 107 |
| TABLES | |
| 3.1 Key features of epithermal gold deposits | 11 |
| 3.2 The size and grade of selected low-sulphidation epithermal gold deposits | 15 |
| 3.3 The size and grade of selected high-sulphidation epithermal gold deposits | 15 |
| 5.1 Summary of the main stages of knowledge-based prospectivity analysis | 25 |

| | | |
|-----|--|----|
| 5.2 | Hypothetical example of a table of index parameters | 27 |
| 5.3 | Exploration criteria and source datasets used in prospectivity analysis for epithermal gold mineralisation in this study | 29 |
| 6.1 | Summary statistics for G-BASE stream-sediment samples, Ochil and Sidlaw Hills (all values in ppm) | 37 |
| 6.2 | Summary statistics for MRP panned-concentrate samples, Ochil Hills (all values in ppm) | 38 |
| 6.3 | Specifications of boreholes in Borland Glen | 45 |
| 6.4 | Summary statistics for geochemical samples from boreholes in Borland Glen (344 samples; all values in ppm, except Au in ppb) | 46 |
| 6.5 | Index parameters used for prospectivity analysis, Ochil Hills | 51 |
| 6.6 | Main targets for epithermal gold, Ochil Hills | 52 |
| 7.1 | Generalised stratigraphy of the Lorn succession in the Oban–Kilmore region (after Kynaston and Hill, 1908) | 54 |
| 7.2 | Summary statistics for G-BASE stream-sediment samples, Lorn Plateau (all values in ppm) | 60 |
| 7.3 | Summary statistics for MRP stream-sediment samples, Lorn Plateau (all values in ppm) | 61 |
| 7.4 | Summary statistics for MRP panned-concentrate samples, Lorn Plateau (all values in ppm) | 61 |
| 7.5 | Main geochemical anomalies over the Lorn Plateau lavas | 65 |
| 7.6 | Index parameters used for prospectivity analysis, Lorn Plateau | 68 |
| 7.7 | Main targets for epithermal gold, Lorn Plateau | 69 |
| 8.1 | Documented metalliferous mineral occurrences in the Cheviot Hills | 74 |
| 8.2 | Summary statistics for G-BASE stream-sediment samples, Cheviot Hills (all values in ppm) | 76 |
| 8.3 | Summary statistics for MRP stream-sediment samples, Cheviot Hills (all values in ppm) | 77 |
| 8.4 | Summary statistics for MRP panned-concentrate samples, Cheviot Hills (all values in ppm) | 77 |
| 8.5 | Summary statistics for lithochemical samples, Kingsseat Burn area (all values in ppm, except Au ppb) | 87 |
| 8.6 | Index parameters used for prospectivity analysis, Cheviot Hills | 90 |
| 8.7 | Main targets for epithermal gold, Cheviot Hills | 90 |
| 9.1 | Key exploration criteria for Lower Devonian volcanic terrains in northern Britain | 92 |

FIGURES

| | |
|------|---|
| 1.1 | Devonian lavas and strata in northern Britain showing the locations of known epithermal gold mineralisation |
| 3.1 | Schematic cross-section showing the environments of formation for porphyry Cu-Mo-Au and high- and low-sulphidation epithermal precious metal deposits (modified from Hedenquist and Lowenstern, 1994) |
| 3.2 | Schematic cross-section showing the architecture of a typical low sulphidation epithermal vein deposit |
| 3.3 | Simplified alteration zoning in high- and low sulphidation epithermal precious metal deposits |
| 3.4 | Schematic cross-section showing the architecture of a typical high sulphidation epithermal deposit (after Silberman and Berger, 1985) |
| 5.1 | Event occurrences derived from digital geological and geophysical data |
| 5.2 | Prospectivity weight cosine function (f) for any pixel (n) is determined by the exponent (a) and the halo distance (x). |
| 6.1 | Solid geology of the Ochil Hills and surrounding area |
| 6.2 | Legend for the solid geology map Figure 6.1 |
| 6.3 | Ochils: selected elements of the geology based on the 1:50 000 map series |
| 6.4 | Ochils: occurrences of alluvial gold, copper and lead minerals |
| 6.5 | Ochils: location of G-BASE stream sediment samples |
| 6.6 | Ochils: location of MRP panned concentrate samples |
| 6.7 | Ochils: antimony (Sb) in G-BASE stream sediment data |
| 6.8 | Ochils: antimony (Sb) in MRP panned concentrate data |
| 6.9 | Ochils: arsenic (As) in G-BASE stream sediment data |
| 6.10 | Ochils: barium (Ba) in G-BASE stream sediment data |
| 6.11 | Ochils: bismuth (Bi) in G-BASE stream sediment data |
| 6.12 | Ochils: bismuth (Bi) in MRP panned concentrate data |
| 6.13 | Ochils: boron (B) in G-BASE stream sediment data |
| 6.14 | Ochils: copper (Cu) in G-BASE stream sediment data |

- 6.15** Ochils: copper (Cu) in MRP panned concentrate data
- 6.16** Ochils: gold (Au) in MRP panned concentrate data
- 6.17** Ochils: lead (Pb) in G-BASE stream sediment data
- 6.18** Ochils: lead (Pb) in MRP panned concentrate data
- 6.19** Ochils: manganese (Mn) in G-BASE stream sediment data
- 6.20** Ochils: molybdenum (Mo) in MRP panned concentrate data
- 6.21** Ochils: silver (Ag) in G-BASE stream sediment data
- 6.22** Ochils: silver (Ag) in MRP panned concentrate data
- 6.23** Ochils: zinc (Zn) in G-BASE stream sediment data
- 6.24** Ochils: zinc (Zn) in MRP panned concentrate data
- 6.25** Ochils: detailed geology of Borland Glen showing gold (Au) in panned concentrate data
- 6.26** Ochils: distribution of alluvial gold in Borland Glen, geophysical anomalies and elevated mercury (Hg) values in overburden
- 6.27** Ochils: geochemical log for borehole 2, Borland Glen
- 6.28** Ochils: geochemical log for borehole 5, Borland Glen
- 6.29** Ochils: summary of PIMA analysis for borehole 2, Borland Glen
- 6.30** Ochils: summary of PIMA analysis for borehole 5, Borland Glen
- 6.31** Ochils: Bouguer gravity anomaly, contour interval 0.5 mGal
- 6.32** Ochils: Residual gravity anomaly, contour interval 0.5 mGal
- 6.33** Ochils: Total magnetic field anomaly, contour interval 25 nT
- 6.34** Ochils: Residual magnetic anomaly, contour interval 25 nT
- 6.35** Ochils: gravity lineaments
- 6.36** Ochils: magnetic lineaments
- 6.37** Ochils: lineaments from Ordnance Survey digital topography. Area of digital topography shown by dashed red line
- 6.38** Ochils: Landsat TM lineaments
- 6.39** Ochils: selected geology layers for prospectivity analysis
- 6.40** Ochils: selected geochemistry layers for prospectivity analysis
- 6.41** Ochils: selected geophysical layers for prospectivity analysis
- 6.42** Ochils: all selected data layers for prospectivity analysis
- 6.43** Ochils: binary weights-of-evidence (BWE) prospectivity map for epithermal gold mineralisation

- 7.1** Solid geology of the Lorn Plateau region
- 7.2** Legend for the solid geology map Figure 7.1
- 7.3** Geology of the Lorn Plateau region based on the 1:50,000 map series. Inset shows the orientations of mapped dykes in the area.
- 7.4** Cartoon cross-section through the SW Grampian Highlands showing the location of the Lorn Plateau lavas
- 7.5** Lorn: location of G-BASE stream sediment samples
- 7.6** Lorn: location of MRP drainage geochemical samples
- 7.7** Lorn: antimony (Sb) in G-BASE stream sediment data
- 7.8** Lorn: antimony (Sb) in MRP panned concentrate data
- 7.9** Lorn: arsenic (As) in G-BASE stream sediment data
- 7.10** Lorn: bismuth (Bi) in G-BASE stream sediment data
- 7.11** Lorn: copper (Cu) in G-BASE stream sediment data
- 7.12** Lorn: copper (Cu) in MRP panned concentrate data
- 7.13** Lorn: lead (Pb) in G-BASE stream sediment data
- 7.14** Lorn: lead (Pb) in MRP panned concentrate data
- 7.15** Lorn: molybdenum (Mo) in G-BASE stream sediment data
- 7.16** Lorn: tin (Sn) in MRP stream sediment data
- 7.17** Lorn: zinc (Zn) in G-BASE stream sediment data
- 7.18** Lorn: total magnetic field anomaly (contour interval 25 nT)
- 7.19** Lorn: residual magnetic field anomaly (contour interval 25 nT)
- 7.20** Lorn: Bouguer gravity anomaly (contour interval 1 mGal)
- 7.21** Lorn: residual gravity anomaly (contour interval 0.5 mGal)
- 7.22** Lorn: gravity lineaments
- 7.23** Lorn: magnetic lineaments
- 7.24** Lorn: Landsat TM lineaments
- 7.25** Lineament azimuths over the Lorn Plateau region
- 7.26** Lorn: selected geological data layers
- 7.27** Lorn: selected geochemical data layers

- 7.28** Lorn: selected geophysical data layers
- 7.29** Lorn: all selected prospective data layers
- 7.30** Lorn: binary weights-of-evidence (BWE) prospectivity map for epithermal gold mineralisation

- 8.1** Solid geology of the Cheviot Hills area. Boxed region is the Kingsseat Burn area.
- 8.2** Cheviot: legend for the solid geology map Figure 8.1
- 8.3** Cheviot: location of gold, copper and lead occurrences
- 8.4** Cheviot: location of G-BASE stream-sediment samples
- 8.5** Cheviot: location of MRP stream-sediment and panned concentrate samples
- 8.6** Cheviot: antimony (Sb) in G-BASE stream sediment data
- 8.7** Cheviot: antimony (Sb) in MRP panned concentrate data
- 8.8** Cheviot: arsenic (As) in G-BASE stream sediment data
- 8.9** Cheviot: arsenic (As) in MRP stream sediment data
- 8.10** Cheviot: barium (Ba) in MRP panned concentrate data
- 8.11** Cheviot: beryllium (Be) in G-BASE stream sediment data
- 8.12** Cheviot: bismuth (Bi) in G-BASE stream sediment data
- 8.13** Cheviot: bismuth (Bi) in MRP panned concentrate data
- 8.14** Cheviot: cobalt (Co) in G-BASE stream sediment data
- 8.15** Cheviot: copper (Cu) in G-BASE stream sediment data
- 8.16** Cheviot: copper (Cu) in MRP panned concentrate data
- 8.17** Cheviot: lead (Pb) in G-BASE stream sediment data
- 8.18** Cheviot: lead (Pb) in MRP stream sediment data
- 8.19** Cheviot: manganese (Mn) in G-BASE stream sediment data
- 8.20** Cheviot: molybdenum (Mo) in MRP stream sediment data
- 8.21** Cheviot: molybdenum (Mo) in MRP panned concentrate data
- 8.22** Cheviot: tin (Sn) in G-BASE stream sediment data
- 8.23** Cheviot: tin (Sn) in MRP panned concentrate data
- 8.24** Cheviot: zinc (Zn) in G-BASE stream sediment data
- 8.25** Cheviot: Bouguer gravity anomaly map. Line A-B is the location of the 2D modelled profile in Figure 8.32.
- 8.26** Cheviot: residual gravity anomaly based on a continued (+5 km) regional field. Contour interval 0.5 mGal
- 8.27** Cheviot: regional gravity anomaly based on subsampled data away from the granites. Contour interval 1.0 mGal
- 8.28** Cheviot: residual gravity anomaly over the granite based on subsampled regional field. Contour interval 0.5 mGal
- 8.29** Cheviot: total field magnetic anomaly at 305m above ground level. Contour interval 20 nT
- 8.30** Cheviot: polar total field magnetic anomaly at 800m above ground level. Contour interval 20 nT
- 8.31** Cheviot: modelled depth (km) to top of the granite. Contour interval 0.5 km
- 8.32** Cheviot: part of a 2-D north-west – south-east section through the granite and lava field
- 8.33** Cheviot: gravity lineaments
- 8.34** Cheviot: magnetic lineaments
- 8.35** Cheviot: Landsat TM lineaments
- 8.36** Cheviot: azimuthal frequency plots for faults and lineaments
- 8.37** Kingsseat Burn: arsenic (As) in MRP stream sediment data
- 8.38** Kingsseat Burn: copper (Cu) in MRP stream sediment data
- 8.39** Kingsseat Burn: arsenic (As) in MRP panned concentrate data
- 8.40** Kingsseat Burn: copper (Cu) in MRP panned concentrate data
- 8.41** Kingsseat Burn: antimony (Sb) in MRP panned concentrate data
- 8.42** Kingsseat Burn: molybdenum (Mo) in MRP panned concentrate data
- 8.43** Kingsseat Burn: lead (Pb) in MRP panned concentrate data
- 8.44** Kingsseat Burn: distribution of anomalous values of Au, As, Sb and Cu in rock samples
- 8.45** Kingsseat Burn: abundance of selected elements in rock samples
- 8.46** Kingsseat Burn: summary of alteration minerals in rock samples identified by The Spectral Geologist
- 8.47** Kingsseat Burn: distribution of magnetic susceptibility in rock samples
- 8.48** Cheviot: selected geological data for prospectivity analysis
- 8.49** Cheviot: selected geochemical data for prospectivity analysis
- 8.50** Cheviot: selected geophysical data for prospectivity analysis
- 8.51** Cheviot: all selected data for prospectivity analysis
- 8.52** Cheviot: binary weights-of-evidence (BWE) prospectivity map for epithermal gold mineralisation

SUMMARY

Epithermal deposits are important sources of gold with major resources occurring worldwide in volcanic rocks ranging in age from Proterozoic to Quaternary. Epithermal mineralisation forms at shallow levels in the crust from circulating low-temperature fluids in either geothermal or volcanic hydrothermal systems. Descriptive and genetic models for the principal deposit types are well established and provide a sound basis for exploration. The aim of this study was to establish best practice guidelines for detection of this type of deposit in the Devonian volcanic rocks of northern Britain and apply them to determine prospective areas.

During the Lower Devonian, calc-alkaline volcanic rocks were erupted over extensive areas of northern Britain in a continental-margin setting between 425 and 395 Ma ago. Today these rocks are preserved in several areas, the largest of which are in the Ochil Hills of the Scottish Midland Valley, the Lorn Plateau of the south-west Scottish Highlands and the Cheviot Hills in north-eastern England. Epithermal mineralisation is known at several localities in these terrains and evidence from various sources indicates potential for further significant occurrences. Important examples include the oldest known hot-spring occurrence in the world at Rhynie in north-east Scotland and the diatreme-hosted deposit at Lagalochan in south-west Scotland.

The BGS has developed a knowledge-based prospectivity mapping system which maximises the value of multi-disciplinary digital datasets for mineral exploration. The user identifies key exploration parameters on the basis of established deposit models and empirical observations in the target area. These parameters are combined, each with its own weight, style and zone of influence in relation to the occurrence pixel. Boolean and fuzzy logic data models are used to integrate the quantified spatial relationships into a single prospectivity map showing the distribution of relative favourability for the occurrence of a mineral deposit. The combination of advanced technology for data integration and modelling with soundly-based predictive deposit models is a powerful and versatile tool for the identification and ranking of prospective targets and for the estimation of mineral potential. This method has been used to produce prospectivity maps showing the distribution of potential for the occurrence of epithermal gold mineralisation in the three major Lower Devonian volcanic terrains in northern Britain. The main features taken into account in the analysis include tectonic setting, geological structure, geochemistry, geophysics, stratigraphy, lithology, mineralisation and buried intrusions.

In the Ochil Hills prospectivity analysis has identified significant potential to the north and west of Borland Glen, where alluvial gold is widespread and associated intense hydrothermal alteration has been recorded. Other targets in the Ochil Hills include areas around Culteuchar Hill and on the north Fife coast. Favourability for epithermal mineralisation is also demonstrated in several parts of the Lorn Plateau. In particular, high prospectivity is indicated close to a major fault at Bragleenbeg, where coincident geochemical and geophysical anomalies suggest the presence of mineralisation related to a buried intrusion emplaced in or beneath the lavas. In the Cheviot Hills two prospective areas have been identified. In the Kingsseat Burn area favourability is indicated by coincident geophysical and multi-element geochemical anomalies close to a major structure. The altered volcanic and intrusive rocks contain advanced argillic and sericitic alteration and low-tenor enrichment of gold. The second area is around the Breamish Fault, where geochemical anomalies occur in a favourable structural setting.

Further investigations for epithermal gold deposits are recommended in the target areas highlighted by these studies. The investigations should include detailed geological mapping, alteration studies and drainage and overburden geochemical surveys. Ground geophysical surveys may provide useful information on the extent and form of hydrothermal alteration, especially where transported overburden cover is prevalent.

The same methodology may be used to identify prospective targets for epithermal gold mineralisation elsewhere in Britain. Other potentially favourable areas include the Lower Devonian rocks of east Sutherland, the Pentland Hills and the area around the Southern Upland Fault near Maybole. Volcanic rocks of Devonian and Carboniferous age in south-west England are also prospective. The generic nature of this technology allows it to be applied to other styles of mineralisation where deposit models are well established. In this way expensive field exploration programmes for a wide range of mineral deposit types in various terrains can be focused more effectively leading to cost reductions for industry.

1. INTRODUCTION

Predicting the quantity and quality of undiscovered mineral resources is fraught with uncertainties and difficulties. Nevertheless these forecasts are of great importance not only to mining companies but also to planners and policy-makers. With the increased availability of multiple geoscience datasets in digital form, improved metallogenic models and the capabilities of modern GIS systems, the ability to produce prospectivity maps showing the distribution of favourability for the occurrence of mineral deposits has become a reality.

The BGS has developed a GIS-based prospectivity mapping system based on the integration of relevant key features of multiple spatial datasets held in its corporate databases. The prototype system was established in 1997 under a Technology Access project funded by the Department of Trade and Industry (DTI) (Gunn et al., 1997). Initial testing comprised mapping the potential for the occurrence of mesothermal lode deposits in the Scottish Highlands. However, the generic nature of the system allows it to be readily applied to prospectivity mapping for other styles of mineralisation. Accordingly it has been used as the principal tool in this study of epithermal gold deposits, both for the display of multivariate data and for the production of prospectivity maps.

Epithermal deposits are an important class of gold deposit which form near the surface of the earth, most commonly in volcanic terrains. They are major sources of gold, producing several million ounces per annum from mines in more than 25 countries. Most production is derived from the circum-Pacific region, particularly USA, Mexico, Peru, Chile, Japan, Papua New Guinea, the Philippines and Indonesia. However there are also many epithermal deposits in Europe, with important examples in Spain, Greece, Italy, Bulgaria and Hungary. The largest gold deposit in Europe, located at Chelopech in Bulgaria, is of epithermal type. It contains more than 5.5 millions ounces of gold in a total resource of 52.1 Mt grading 3.3 g/t Au and 1.4% Cu (Andrew, 1997).

Epithermal deposits possess various characteristics which make them attractive exploration targets. They occur in a range of settings where they form either large, bulk-tonnage low-grade resources or smaller higher-grade vein deposits. In bulk-tonnage deposits a major part of the ore may be oxidised allowing it to be mined by cheap open-pit methods and the gold to be extracted by simple, low-cost metallurgical processing. Small, high-grade vein deposits are more attractive to SMEs: they require less capital investment and can be developed with minimal environmental impact. The fact that epithermal deposits commonly cluster in districts with dimensions of the order of ten to a few tens of kilometres also contributes to their economic attractiveness. For example, in the Yanacocha district of northern Peru there is a cluster of 4 heap leach gold mines and at least 5 undeveloped deposits with a proven and probable reserve at the end of 1998 of 702 Mt grading about 0.9 g/t Au, equivalent to more than 20 million contained ounces of gold. Yanacocha is South America's largest gold producer, with an annual production exceeding 1.3 million ounces at a cash cost of about US\$95 per ounce.

In the UK, epithermal mineralisation is known to occur widely in Lower Devonian volcanic sequences and associated high-level intrusions in northern Britain. These occurrences are shown in Figure 1.1 and described in Section 2 of this report.

1.1. Objectives and methodology

The objectives of this study are:

1. to develop a predictive model for the occurrence of economic deposits of epithermal gold mineralisation in the Devonian volcanic rocks of northern Britain;
2. to identify new prospective targets;
3. to define the most effective exploration methods for mineralisation of this type;
4. to transfer the new concepts and methodologies to the minerals industry.

The study areas comprise the main Lower Devonian volcanic terrains in northern Britain: the Cheviot Hills in north-east England, the Lorn Plateau in the south-west Highlands of Scotland, and the Ochil Hills in the Midland Valley of Scotland. Various surveys carried out by the BGS, most funded by the DTI Mineral Reconnaissance Programme (MRP), in and around the Cheviot Hills targetted principally base-metal mineralisation in Carboniferous sediments and contiguous Lower Devonian strata (Haslam, 1975; Leake and Haslam, 1978; Bateson et al., 1983). However, in one area of the Devonian outcrop highly altered volcanic rocks with potential for the occurrence of epithermal gold mineralisation were identified (Cameron et al., 1988). In the Lorn Plateau, Lower Devonian rocks outcrop over an area exceeding 300 km². Little systematic exploration for gold has been carried out in this area, but geological and geochemical features of these rocks, together with the occurrence of the Lagalochan Cu-Mo-Au deposit immediately to the south, indicate that they are prospective for the occurrence of epithermal gold mineralisation. The potential of the Ochil Hills has been demonstrated by regional surveys conducted by the MRP which led to the discovery of epithermal mineralisation in one area (Coats et al., 1991). Elsewhere in the Ochils, extensive areas remain largely unexplored, but the favourable geology and drainage geochemical data suggest that additional investigations are warranted.

The work was undertaken in a number of discrete phases. First, an extensive review of deposit models and case history studies in the scientific literature was undertaken. On this basis key exploration criteria for epithermal gold deposits were defined at various scales. In the next stage information relevant to these criteria for the UK was acquired from digital spatial datasets. This involved extraction of archived geological, geophysical, geochemical, remotely-sensed and mineral occurrence data from BGS databases, together with the capture of new pertinent geoscience data. Following data acquisition, further data manipulation was carried out to maximise the utility of the information for identifying areas prospective for epithermal gold mineralisation. For geochemical data this involved processes such as simple filtering above selected thresholds and calculation of various multi-element indices. For geophysical field data, gradients and partial derivatives were calculated where they offered potentially significant new information concerning key exploration criteria. Given the importance of geological structure in localising hydrothermal mineralisation, new event or occurrence datasets were also generated from various intersecting lineaments selected according to their type and orientation.

The next stage of the analysis involved preparation of multi-dataset maps for each area at various scales to examine and analyse the spatial relationships among the variables and in particular their distributions relative to occurrences of known epithermal mineralisation in bedrock. The final step was the calculation of

prospectivity for each area and the integration of quantified spatial relationships into a single prospectivity map.

2. DEVONIAN VOLCANIC ROCKS OF NORTHERN BRITAIN

2.1. Geology and tectonic setting

Much of northern Britain is underlain by metamorphic and igneous rocks which are the eroded remains of the Caledonian mountain belt which developed in late Precambrian and early Palaeozoic times.

The Caledonian orogenic belt contains the deformed remains of Cambrian to Silurian volcano-sedimentary sequences deposited and accreted at opposing continental margins during the evolution and destruction of the Iapetus Ocean. Final closure of the ocean had occurred by the early Devonian, at which time the orogen formed a sinuous deformation zone extending from what is now northern Scandinavia to the southern Appalachians of North America. More recent formation of the Atlantic Ocean has fragmented the original geological continuity but close similarity of geological evolution can still be demonstrated between Britain, Ireland and maritime Canada. Britain provides a virtually complete cross-section through the orogen from the Laurentian continental margin sliver preserved in the extreme north-west of Scotland to the volcanic arc and back arc sequences formed at the Avalonian margin and now seen in the English Lake District and Wales. Between the two continental margin assemblages the overall structure of the orogen can be conveniently reviewed in terrain terms: the principal terrain-bounding faults are shown in Figure 1.1.

2.1.1. Precambrian to Lower Palaeozoic

To the north-west of the Moine Thrust Zone the Hebridean Terrain consists of Archaean and early Proterozoic gneissose basement unconformably overlain by undeformed late Proterozoic (Torridonian) and Cambro-Ordovician shallow-water sedimentary assemblages. The Northern Highlands Terrain has been carried north-west by the Moine Thrust Zone onto the continental basement and extends south-east as far as the Great Glen Fault. It consists mainly of early Proterozoic clastic shelf sequences of the Moine Supergroup and shows complex, polyphase deformation and metamorphism ranging from a possible Grenville event to Caledonian folding at about 450 Ma. Between the Great Glen and Highland Boundary faults the Central Highlands or Grampian Terrain contains a late Precambrian to possible Cambrian shelf sediment to turbidite assemblage. Most of this is assigned to the Dalradian Supergroup which accumulated during the progressive rifting and deepening of extensional basins. Basic extrusive rocks in the upper part of the Dalradian sequence indicate limited generation of oceanic crust: the first, late Precambrian attempt at continental rifting and sea-floor spreading which finally led to the Cambro-Ordovician growth of the Iapetus Ocean. The Dalradian Supergroup was subjected to polyphase metamorphism and deformation culminating at about 450–500 Ma.

2.1.2. Lower Palaeozoic

To the south of the Highland Boundary Fault, terrains consist mainly of Lower Palaeozoic volcano-sedimentary sequences with a simpler deformation history and a metamorphic grade rarely exceeding the greenschist facies. The Caledonian geology of the Midland Valley Terrain, between the Highland Boundary and Southern Upland faults, is largely obscured by Upper Palaeozoic strata. A complex metamorphic basement seems likely, onto which early Ordovician ophiolites (e.g. Ballantrae and Highland Border) were obducted in the mid-Ordovician. A continental-margin magmatic arc then developed through the mid to upper Ordovician with proximal, forearc sedimentary fans overlying the obducted ophiolites. Subsequent Silurian sedimentation indicates a progressive shallowing from deep-water turbidites to terrestrial red beds of the Old Red Sandstone facies. To the south of the Southern Upland Fault the Southern Uplands Terrain consists of a thrust complex containing Ordovician to Silurian turbidite strata overlying a basal mudstone and chert assemblage. An origin by sequential accretion above a north-west-directed subduction zone during

closure of the Iapetus Ocean seems likely. To the south of the Iapetus Suture the Lakesman-Leinster Terrain records events at the southern (Avalonia) margin of the Iapetus Ocean during its destruction by southward-directed subduction. In the English Lake District early Ordovician continental-margin clastic strata, mid-Ordovician calc-alkaline volcanic rocks and a post-collision, mainly Silurian foreland basin sequence are preserved. Deformation was largely end-Caledonian (late Silurian to early Devonian) and has been linked to the continued southwards propagation of the Southern Uplands thrust belt across the Iapetus Suture.

Extensive calc-alkaline and lesser alkaline magmatism accompanied collision in the late Silurian to mid-Devonian (425–395 Ma) with late and post-tectonic granitoid intrusions emplaced through the belt southwards from the Moine Thrust. Voluminous complexes are intruded in the eastern sector of the Grampian Highlands of Scotland, the Caledonides of northern and southern Ireland and beneath the Lake District and the North Pennines of England. Smaller intrusions were emplaced in the Moine of northern Scotland, the Dalradian of the south-west Highlands and the western Southern Uplands. There was also extensive andesitic volcanism in the Grampian and Midland Valley terrains and in the Cheviot Hills of northern England during Lower Devonian times. The youngest plutons have been suggested to be the product of melting after subduction had ceased following continent-continent collision and crustal recovery. At this time major sinistral movements also took place along terrain boundaries with associated north-east–south-west faults in the culmination of a regime of sinistral transpressive strain.

2.1.3. Lower Devonian volcanism

The Lower Devonian volcanic rocks in Britain are dominated by sub-aerial andesitic lavas and subordinate pyroclastic rocks, with minor developments of more basic and acidic compositions. They are calc-alkaline in character but become generally increasingly alkaline towards the north-west. They outcrop in three major tracts: the Ochil Hills of the Midland Valley; the Lorn Plateau of Argyllshire, south-west Scotland; and the Cheviot Hills on the England-Scotland border. On account of their size, the incidence of known mineralisation and their perceived potential, these areas were selected as the principal targets for prospectivity analysis in this study.

Elsewhere in northern Britain smaller developments of Devonian volcanic rocks occur in Lochaber at Glen Coe and Ben Nevis, in Shetland and Northern Ireland. To the north of the Highland Boundary Fault volcanic rocks form minor components of Lower Old Red Sandstone sequences at Rhynie in Aberdeenshire, in the Cabrach, Banffshire, at Gollachy Burn near the Moray Firth coast and in Kintyre, Argyll. Small outliers of Lower Devonian rocks including lavas are found in the Highland Boundary Fault zone in the Forest of Alyth and Monzie areas where they unconformably overlie Dalradian and Highland Border Complex rocks. Lower Devonian sequences including lavas and tuffs also occur in the southern part of the Midland Valley. The most important localities are around the Pentland Hills where up to 1800 m of volcanic rocks ranging from basaltic to rhyolitic in composition are intercalated with about 600 m of conglomerates and sandstones. In the south-west of the Midland Valley Lower Devonian sequences with significant volcanic components occur near Maybole and parallel to the Southern Upland Fault near Dalmellington. Several Lower Devonian outcrops occur in the eastern part of the Southern Uplands, although volcanic rocks generally form only a minor part of the sequence. The most extensive development of volcanic rocks occurs near St Abbs and Eyemouth where about 1000 m of lavas and tuffs of basic and intermediate compositions are preserved. Lower Old Red Sandstone sedimentary rocks were also deposited in several fault-bounded basins in the northern Highlands, including Caithness, Easter Ross and Invernesshire and in the Brora outlier in eastern Sutherland. No volcanic rocks are recorded in these areas.

Thirlwall (1988) provided a critical review of geochronological studies of Caledonian magmatism in northern Britain. This included evaluation of radiometric age dates on the Lower Devonian volcanic rocks and associated post-tectonic intrusions. He concluded that volcanism in the south-west Highlands (Lorn) took

place around 420 Ma and overlapped with plutonic activity which continued until ca. 408 Ma. In the Midland Valley all Caledonian igneous activity took place between 415–411 Ma. Although the data are somewhat sparse he concluded that magmatism in the Midland Valley and the Highlands was coeval and hence genetically related. Magmatism in the northern part of the Southern Uplands is essentially contemporaneous with that in the Midland Valley. On this basis, in conjunction with an examination of the spatial variations in geochemical data, Thirlwall demonstrated that the Lower Devonian lavas were generated in the mantle above a descending lithospheric plate. This is consistent with the geochronological evidence which indicates that the magmatism occurred prior to closure of the Iapetus Ocean during the interval 410–396 Ma. In the southern part of the Southern Uplands the Fleet, Criffell and Cheviot plutons, and the Cheviot lavas, are much younger, 392–397 Ma, which corresponds to a late Lower Devonian stratigraphic age and post-dates closure of the Iapetus Ocean. Their origin cannot therefore be related directly to subduction processes.

2.2. Epithermal mineralisation

Epithermal gold mineralisation has been identified at a number of localities in Scotland, mainly in the last 10–15 years. The majority of these occurrences are related to outcropping Lower Devonian rocks or postulated to be associated with magmatic activity of that age. Commercial exploration has been carried out at most of these localities but no economic mineralisation has been discovered to date. These localities are shown in Figure 1.1.

In the Ochil Hills reconnaissance drainage surveys by the BGS led to the identification of extensive hydrothermal alteration and low-tenor gold mineralisation in the Borland Glen area. (Coats et al., 1991). An origin related to a low-sulphidation epithermal system developed in the Lower Devonian andesitic volcanic rocks was proposed. Subsequent exploration by commercial companies failed to identify economic mineralisation in this area (Crummy, 1993), but the MRP surveys indicated potential for the occurrence of epithermal gold deposits elsewhere in the central Ochils. Details of the mineralisation in the Borland Glen and the work carried out are given in section 6 of this report.

Epithermal gold mineralisation also occurs in a Lower Devonian hot spring system at Rhynie in the north-east Grampian Highlands of Scotland in an outlier of Old Red Sandstone overlying Dalradian Southern Highland Group rocks (Rice and Trewin, 1988; Rice et al., 1995). The Devonian rocks are locally intensely altered to quartz, K-feldspar, calcite, hematite, pyrite and illitic and chloritic clays. Silicified areas show evidence of repeated veining and brecciation. Chert sinters and the altered rocks contain high levels of Au, As and Sb and are locally enriched in W, Mo and Hg. Overall the alteration and mineralisation characteristics at Rhynie may be compared with low-sulphidation epithermal systems developed in the south-western USA and the south-west Pacific. Commercial exploration has failed to identify economic mineralisation at Rhynie, but potential exists for underlying more extensive, high-grade vein and stockwork ores.

Another area where there is good evidence for epithermal gold mineralisation is eastern Sutherland, which is well known for its historical alluvial gold production near Helmsdale. In this area mineralised pyritic quartz-cemented breccias, containing up to 12 ppm Au, were discovered in the headwaters of the River Brora, about 25 km north of Lairg (Crummy 1993; Crummy et al., 1997). Fluid inclusion studies yield trapping temperatures of 170–140°C for the hydrothermal fluid indicating an epithermal setting. Further supporting evidence is provided by the quartz textures in the auriferous rocks, which range from cherty and chalcedonic to vuggy open-space filling. A Lower Devonian outlier occurs within 2 km of the in-situ mineralisation, which is hosted by basement migmatites of Precambrian age. This, together with the presence of several other small Lower Devonian outliers in the district, indicates that the present level of erosion is not far below the Lower Devonian palaeosurface. It is therefore suggested that the eroded remains of a Lower Devonian

hydrothermal system are preserved in the area and that potential exists for the occurrence of further epithermal mineralisation, including feeder veins in the basement.

Several porphyry-type gold occurrences in the Scottish Highlands are associated with alteration of high-sulphidation epithermal type. The most important example occurs in the Lagalochoan sub-volcanic complex of the Kilmelford calc-alkaline centre emplaced in Argyll Group rocks in the south-west Highlands (Harris et al., 1988; Zhou, 1988). This complex is thought to reflect a vented diatreme-type structure with mineralisation comprising early Cu-Mo-Au in veinlets and disseminations within a central core of breccias and diorite to granodiorite intrusions. This was followed by shear-related Pb-Zn-Ag-Au-As-Sb mineralisation and, finally, by a suite of Pb-Zn-Ag carbonate veins. Sericite-quartz-pyrite and carbonate alteration are widespread, with K-silicate alteration locally present.

Sub-volcanic porphyry-style gold mineralisation also occurs at Fore Burn, near Straiton, in the northern section of the western Southern Uplands. During the 1970s commercial exploration in this area focused on copper, but, following the discovery of gold and silver by BGS (Allen et al., 1982), subsequent exploration activity targetted precious metals. The mineralisation is associated with an eroded volcanic centre of probable Lower Devonian age, immediately north of the Southern Upland Fault. The igneous complex comprises a central core of quartz diorite with an associated series of subaerial lavas, volcanic breccias, agglomerates and tuffs of intermediate to acid composition. The Au-Ag mineralisation occurs in quartz veins and stockworks in faults at the margins of the complex (Charley et al., 1989).

Further evidence of intrusion-related gold mineralisation with a possible epithermal overprint was identified by regional geochemical surveys conducted by the BGS over south-east Scotland (British Geological Survey, 1993; Shand, 1989). Follow-up investigations by the BGS confirmed the existence of elevated Au, As, Ag and Hg in stream sediments over a broad area around the Priestlaw intrusion and other late-Caledonian intrusions in the Duns area (Shaw et al., 1995). Detailed prospecting identified high concentrations of Au and As in overburden and bedrock samples at several localities. Gold values up to 5 ppm are found in fracture-controlled veins and breccias in altered greywackes and minor intrusions. Further studies are required to clarify the metallogensis of this occurrence and to identify additional targets for follow-up.

3. DEPOSIT MODELS FOR EPITHERMAL GOLD MINERALISATION

3.1. Introduction

A mineral deposit model can be defined as ‘systematically arranged information describing the essential attributes (properties) of a class of mineral deposits’ (Cox and Singer, 1986). Deposit models can be divided into two end members: empirical or descriptive models based on observational data; and genetic or conceptual models, based on theoretical concepts. Deposit models include geological, tectonic and structural features, geochemical, geophysical and mineralogical characteristics, ore controls, deposit morphology, grade and tonnage profiles and environmental characteristics.

Deposit models synthesise large amounts of geological data and provide an effective means of classification and communication within the scientific and technological sectors at large. Deposit models are also valuable exploration tools, for the identification of new targets and for providing a general guide to the size and grade of a potential target type. Deposit signatures or ‘fingerprints’ can be established and used as a basis for the identification of exploration targets. As such they can influence the exploration strategy of companies and assist in the selection of appropriate exploration and evaluation techniques.

The utility of deposit models in exploration is enhanced if essential features, which show the closest spatial association with mineralisation, can be recognised and separated from non-essential accessory features. The area-selection criteria can be scale-dependent. For example, large-scale features are useful to identify geological environments favourable for mineralisation, whereas smaller-scale features indicate controls on the location of individual deposits. However, at all scales deposit models have their drawbacks and their non-critical use can lead to erroneous judgements. They may emphasise local, parochial features, or may be based on inadequate observations or understanding. The best models should stress the important and essential characteristics and be based upon the study of many deposits. They must be continually re-evaluated and refined to accommodate new knowledge and understanding of the processes responsible for their genesis.

Economic gold mineralisation occurs in a range of deposit types hosted by a wide variety of lithologies in many different tectonic settings. Various classification schemes have been proposed to handle the large amounts of information relating to gold deposits available from exploration and mining, much of which has been generated in the last 20 years (Boyle, 1979; Cox and Singer, 1986; Nesbitt, 1988; Robert et al., 1997). These schemes are based on many different parameters, geological, tectonic, geochemical, genetic and economic, which has led to great diversity of nomenclature, often contrasting, unclear or ambiguous. Nevertheless a number of major groups of deposit types can be defined with reasonable confidence:

- i. Placer deposits
- ii. Mesothermal lode deposits
- iii. Intrusion-related deposits (including porphyry-style, breccia-hosted and skarn)
- iv. Sediment-hosted Carlin-type deposits
- v. Volcanogenic massive sulphide deposits
- vi. Banded iron formation or Homestake-type gold deposits
- vii. Epithermal deposits.

Epithermal deposits form near the surface of the earth, generally at depths of less than 1 km, most commonly in volcanic terrains. Metals are dissolved from the volcanic rocks by circulating fluids and are deposited as a result of complex chemical reactions at temperatures in the range 100–300°C. They occur in a variety of geological structures and environments in response to the changing conditions as the pressurised metalliferous fluids ascend through the crust and react with the rocks. Cooling, fluid mixing and boiling are among the processes responsible for deposition of the ore minerals.

Active geothermal systems in modern volcanic belts are analogues for ancient epithermal systems and their study contributes to an improved understanding of the generation of mineral deposits within them and thus provides valuable guidance for exploration (Hedenquist and Lowenstern, 1994). The active precipitation of gold from hot springs and the reported concentrations of gold in other magmatic fluids in active volcanic settings provides insight into the processes responsible for the generation of epithermal precious metal deposits (e.g. Krupp and Seward, 1987).

3.2. Features of epithermal precious metal deposits

Most epithermal deposits occur in volcano-plutonic arcs in subduction-related tectonic settings, mainly at continental margins and in island arcs. This is clearly evident from the concentration of major deposits in the circum-Pacific region, extending from New Zealand, through the south-west Pacific and Japan, and continuing into North and South America. They are normally found on the back-arc side, but may occur in

grabens produced as pull-apart structures associated with strike-slip movement. They do not occur in submarine back-arc basin settings, but may be found in continental volcanic fields.

The gold deposits are hosted mainly by subaerial lavas and pyroclastic rocks and their sub-volcanic intrusive equivalents. Contemporaneous intercalated epiclastic and sedimentary strata and underlying basement units may also be mineralised. The volcanic rocks cover a broad spectrum of compositions, ranging from intermediate to acid. They belong mainly to the calc-alkaline series, but shoshonitic and alkaline varieties host important deposits in both intraoceanic and continental settings.

Favoured structural settings for the development of epithermal gold mineralisation are provided wherever permeability is enhanced. In volcanic terrains such sites are commonly found in andesitic vent complexes, silicic calderas, resurgent domes and maar-diatreme complexes. Major regional faults are also widely recognised as important controls on the location of epithermal deposits, both as favoured sites for magma emplacement and for subsequent hydrothermal fluid flow. Subsidiary faults, dilational jogs, hydrothermal and phreatomagmatic breccia zones, lithological contacts and a range of minor structural features may also control the distribution of hydrothermal activity and thus the location of mineralisation.

Until recently the majority of known epithermal deposits were restricted to Tertiary and Quaternary volcanic belts. In older terrains primary geological features of epithermal style mineralisation are commonly obscured by later deformation and metamorphism. However, a more critical factor in exploration for these deposits in older terrains is their preservation from erosion. Although rates of erosion in tectonically active volcanic settings are generally high, where early tilting of the host successions took place or where rapid burial occurred, epithermal mineralisation may be preserved in older rocks. For example, the Jacinto deposit in the Camagüey district in Cuba is hosted by rocks of Cretaceous age (Simon et al., 1999), with preservation related to rapid burial beneath a sedimentary basin shortly after the mineralising event.

In the last decade important epithermal deposits have been identified in older rocks where appropriate geological conditions of high-level magmatism and associated hydrothermal activity have been recognised. Deposits hosted by Proterozoic rocks occur at Enåsen in Sweden (Hallberg, 1994), at Brewer in South Carolina, USA (Zwaschka and Scheetz, 1995), and at Hope Brook, Newfoundland, Canada (Dubé et al., 1995). Examples of epithermal deposits hosted by Palaeozoic rocks are found in northern Queensland and south-eastern Australia (Morrison and Beams, 1995; Thompson et al., 1986; White et al., 1995), in the Appalachians (Kiff and Spence, 1988) and in the southern Urals in Russia (Lehmann et al., 1999). Important Mesozoic deposits occur at Pueblo Viejo in the Dominican Republic (Russell and Kessler, 1991), at Cerro Vanguardia in Patagonia, Argentina (Schalumak et al., 1997) and in the Toodoggone River district in British Columbia (Diakow et al., 1991, Thiersch et al., 1997). High-sulphidation epithermal gold mineralisation has also recently been reported for the first time in Cretaceous rocks on the Chinese mainland (So et al., 1998).

Two principal classes of epithermal deposits have been established on the basis of the nature and distribution of associated hydrothermal alteration, the deposit morphology and the textures of the ore and gangue minerals. These classes are known as:

- i. low-sulphidation or adularia-sericite deposits.
- ii. high-sulphidation or alunite-kaolinite deposits.

This division reflects fundamental differences in fluid chemistry which are related to the environments in which the deposits form. High-sulphidation deposits are derived from oxidised, acidic, sulphur-rich fluids generated in the volcanic-hydrothermal environment. In contrast, low-sulphidation deposits are produced by

reduced, near neutral, sulphur-poor fluids comparable to those found in modern geothermal settings (Figure 3.1).

The nature and distribution of alteration in these systems can provide important information on the parent hydrothermal system, the distribution of palaeotemperatures and the location of mineralised targets. Where low temperatures are indicated this suggests preservation of all or most of the epithermal system and hence potential exists for the discovery of underlying mineralisation. Where higher palaeotemperatures are suggested by the alteration assemblage, high-level epithermal mineralisation may have been removed by erosion.

An overview of the main characteristics of epithermal gold deposits is provided by Hedenquist et al. (1996). Table 3.1 summarises the key features of the two main classes of epithermal precious metal deposits and highlights their differences.

3.2.1. Low-sulphidation deposits

A schematic cross-section showing the architecture of a typical low-sulphidation epithermal vein deposit is illustrated in Figure 3.2.

The alteration in low-sulphidation systems is produced by the interaction of hypogene magmatic fluids with deeply convecting meteoric fluids which produces a near-neutral fluid in the epithermal environment. Although the alteration zoning may vary between deposits and may have a limited areal extent or be overprinted by later contrasting assemblages, it can nevertheless often provide useful general exploration guidance (Figure 3.3). In these deposits the alteration typically comprises a central ore-bearing zone of silicification, locally accompanied by adularia and rarely chlorite. This passes laterally into assemblages dominated by sericite or illite and, in lower temperature zones, argillic assemblages may be developed with mixed-layer smectite-illite or smectite. Outwards from these zones propylitic alteration, characterised by chlorite, albite, epidote, carbonate and pyrite, typically occurs over a wide area.

In some cases a steam-heated alteration assemblage may overprint the upper sections of low-sulphidation systems in the vadose zone above the palaeo-watertable. Oxidation of hydrogen sulphide in this setting produces moderately acid fluids resulting in the deposition of various low-temperature minerals, such as kaolinite, alunite and cristobalite, which are more usually associated with the high-sulphidation environment. These normally occur above the low-sulphidation ore zone, but may overprint it if the fluids percolate down sufficiently. Discrimination between hypogene and supergene advanced argillic assemblages, especially alunite, is often not easy, but it is an important distinction to make when exploring for hypogene ores. Sillitoe (1993a) has discussed this problem in some detail.

Epithermal deposits are highly varied in morphology because of the low-pressure conditions under which they form and their dependence on fluid pathways determined by local geology and structure. Structural control is especially common in low-sulphidation systems, with ore zones commonly focused on hydrothermal conduits (faults, fractures, breccia zones, etc) at deeper levels which may broaden upwards towards the palaeosurface. Veins and stockworks are the most common styles of mineralisation, while disseminated and replacement ores are less important in this setting. The vein systems may extend laterally over large areas giving rise to a cluster of several deposits within a district. For example, the Cerro Vanguardia district in Patagonia, Argentina extends over an area of 350 km² and hosts precious-metal veins with a total strike length of more than 140 km (Schalumak et al., 1997). The Osilo low-sulphidation vein field in northern Sardinia which is currently being explored extends over an area of at least 300 km². The deposit at Round Mountain, Nevada, USA, is an example of a major low-sulphidation deposit in which the bulk of the ore is essentially stratabound, occurring as disseminations within a body of poorly welded tuffs.

Table 3.1 Key features of epithermal gold deposits

| | Low sulphidation | High sulphidation |
|---------------------------------|---|---|
| Tectonic setting | Volcano-plutonic continental margin and oceanic arcs and back-arcs. Continental volcanic fields. | Volcano-plutonic continental margin and oceanic arcs and back-arcs. |
| Geological / structural setting | Regional fault systems, grabens, silicic calderas, andesitic stratovolcanoes, flow-dome complexes, maar-diatremes. | Regional fault systems, grabens, silicic calderas, andesitic stratovolcanoes, flow-dome complexes, maar-diatremes. May overlie mineralised porphyry systems. |
| Country rocks | Andesite – rhyodacite – rhyolite and associated epiclastic rocks. Some associated with alkaline or sub-alkaline (shoshonitic) volcanics. | Andesite – dacite – rhyodacite and associated epiclastics. Subvolcanic intrusions. |
| Age of host rock | Any age. Tertiary to Quaternary most common. Important Mesozoic and Palaeozoic examples. | Any age. Tertiary to Quaternary most common. Important Mesozoic and Palaeozoic examples. |
| Age of mineralisation | Commonly 0.5–1.0 Ma younger than host rocks | Similar to age of host rocks. |
| Deposit form | Veins and stockwork ores dominant. Feeder veins may pass upwards into broad ore zones. Extensive vein fields may occur. | Fine-grained massive replacement and disseminated ores in pods, lenses and irregular masses. |
| Ore controls | Zones of increased permeability such as faults, fractures, permeable lithologies, breccias (intrusive, tectonic or hydrothermal), radial and ring faults at caldera margins, minor structures associated with craters, flow-domes, maar-diatreme complexes. | Zones of increased permeability such as faults, fractures, permeable lithologies, breccias (intrusive, tectonic or hydrothermal), radial and ring faults at caldera margins, minor structures associated with craters, flow-domes, maar-diatreme complexes. |
| Alteration zoning | Commonly restricted and inconspicuous: (proximal) silicification, sericitic, argillic, propylitic (distal). | Extensive and conspicuous: (proximal) silicification, advanced argillic, argillic, propylitic (distal). |
| Ore textures | Open-space filling quartz textures: banding (colloform to crustiform), comb, bladed, cockade and carbonate-replacement textures, drusy cavities. | Massive silica replacements and residual, slaggy or vuggy silica. |
| Ore minerals | Pyrite, electrum, gold, silver, argentite. Subordinate sphalerite, galena, chalcopyrite, tetrahedrite. | Pyrite, enargite-luzonite, chalcocite, bornite, covellite, gold, electrum. Subordinate chalcopyrite, galena, sphalerite, tetrahedrite, tennantite, marcasite, arsenopyrite, silver sulphosalts, tellurides. |
| Gangue minerals | Quartz, chalcedony, amethyst, carbonate (commonly manganoan), adularia, sericite, barite, fluorite. | Quartz, barite, gypsum, anhydrite. |
| Alteration minerals | Sericite, illite, adularia, chlorite, smectite. | Alunite, kaolinite, dickite, pyrophyllite, jarosite, smectite. |
| Metals present | Au, Ag. Local or minor Zn, Pb, Cu, Mo, Sb, As, Te, Se, Hg, Ba, F, Mn. | Cu, Au, As. Local or minor Ag, Pb, Bi, Sb, Mo, Sn, Zn, Te, Hg, W, B. |
| Metal zoning | Upper: As, Sb, Hg, B, Tl, Au, Ag. Lower: Cu, Pb, Zn, Bi, Te, Se, Co. | Upper: As, Sb, Hg, B, Tl, Au, Ag. Lower: Cu, Pb, Zn, Bi, Te, Se, Co. |

Low-sulphidation systems commonly have distinctive quartz textures. Spatial variations in the distribution of the textural assemblages can help to identify the level of exposure relative to the palaeosurface (Figure 3.2). Where the uppermost parts of the palaeosystems are preserved, sinter terraces and hydrothermal eruption breccias may be evident, although these are not commonly highly enriched in gold. At deeper levels in the systems the quartz textures are characterised by multiple generations of open-space filling textures and chalcedony. These include comb, bladed and cockade textures. Drusy cavities, vugs and banding, either crustiform or fine colloform, are also common. Silica pseudomorphs after calcite (carbonate replacement texture) are also widespread. In the idealised model quartz textures are dominated by massive chalcedonic silica in the upper parts of the system, passing downwards into a zone characterised mainly by crustiform and colloform banded quartz. Beneath this, below the boiling level, the quartz is mainly crystalline in form and is associated with crystalline adularia, sulphides and carbonate. This vertical variation in quartz-vein textural assemblages can therefore assist in locating zones that host gold mineralisation (Morrison et al., 1990).

The ore-mineral assemblage in low-sulphidation systems is dominated by base-metal sulphides, mainly pyrite, with minor or trace quantities of native gold, electrum, arsenopyrite, tetrahedrite, tellurides, pyrrargyrite and locally selenides. The overall sulphide content is generally low, about 5%, but may be as high as 20%. The principal gangue minerals are quartz, chalcedony, adularia, illite, calcite, manganoan carbonate and smectite, locally with chlorite, barite and fluorite.

Low-sulphidation systems may exhibit a gross vertical geochemical zonation. Volatile elements, As, Sb, and, locally, Hg and Tl are enriched in the uppermost levels. The main Au and Ag enrichment occurs beneath this and typically passes downwards into a zone relatively enriched in Cu, Pb and Zn. Local enrichments in Te, Se, Mo, Ba, F and Mn may also be present.

Most low-sulphidation deposits occur in calc-alkaline volcanic rocks which vary in composition from andesite to dacite and rhyolite. Some important examples also occur in alkaline to sub-alkaline (shoshonitic) rhyolitic rocks. These include the bulk tonnage deposit at Ladolam on Lihir Island, Papua New Guinea (Table 3.2) and the Cripple Creek deposit in Colorado, USA (Kelley et al., 1998).

3.2.2. *High-sulphidation deposits*

A schematic cross-section showing the architecture of a typical high-sulphidation epithermal deposit is illustrated in Figure 3.4.

In contrast to the low-sulphidation systems, the hydrothermal alteration in high-sulphidation systems is commonly more extensive and visually distinctive and therefore potentially a more useful guide to the location of mineralisation. The alteration is related to the ascent of magmatic volatiles with little modification to high levels in the crust where they are absorbed by meteoric water to form an acidic fluid that leaches wallrock around the fluid conduits. The ore is commonly hosted by a highly acid-leached siliceous residue from this process, termed vuggy silica, which is fringed by a zone of advanced argillic alteration characterised by alunite, kaolinite, dickite, pyrophyllite and diaspore. This typically passes outwards into argillic assemblages, dominated by mixed layer illite-smectite, and an outermost propylitic zone. The generalised distribution of alteration in these systems is shown in Figure 3.3.

The mineralisation style and textures typical of high-sulphidation systems differ from those in low-sulphidation systems. Disseminated and replacement ores are most common, with veins and stockworks normally comprising only minor components. The quartz in high-sulphidation deposits is normally fine grained. It occurs as massive replacements and in a characteristic slaggy form (vuggy silica) which is the residual product of acid leaching. Drusy cavities, banded veins and hydrothermal breccias may also occur as subordinate ore types. The ore mineralogy is dominated by pyrite and enargite-luzonite. Chalcocite, covellite,

bornite, gold, electrum, tetrahedrite-tennantite, tellurides and base metal sulphides are also common. Quartz is the predominant gangue mineral, although barite, alunite, kaolinite, pyrophyllite, diaspore and illite are commonly present. Native sulphur commonly infills vuggy cavities and other open spaces. Carbonate minerals and adularia are absent, while smectite and chalcedony are rare. The total abundance of sulphide, mainly pyrite, may vary widely up to about 90%. In some deposits massive enargite-pyrite ores are important sources not only of gold, but also of silver and copper e.g. El Indio, Chile (Siddeley and Araneda, 1986). More commonly the Au is contained within quartz-alunite assemblages with low sulphide contents e.g. Pierina (Volkert et al., 1998) and Yanacocha, both in Peru (Sillitoe, 1995).

The host rocks of high-sulphidation deposits are lavas and pyroclastics of andesitic, dacitic and rhyodacitic compositions. The dominant metals present in high-sulphidation deposits are Au, Cu and As. These are locally accompanied by high levels of Ag, B, Bi, Hg, Mo, Pb, Sb, Sn, Te, W and Zn.

The occurrence of economic mineralisation of both high and low-sulphidation types in a single district has not been documented in many areas. Normally one alteration type is dominant and carries the most important mineralisation. Also, where both are present, each is localised by a different set of structures. For example, in the Eocene Mount Skukum deposit in the Yukon, Canada, early barren high-sulphidation alteration follows closely after magmatism (less than 0.6 Ma), while the later gold-bearing low-sulphidation veins were emplaced approximately 1.6 Ma later (Love et al., 1998). Another example of hydrothermal activity in the epithermal environment continuing beyond the cessation of volcanic activity is described in the Baia Mare area of north-western Romania (Lang et al., 1994). In general, where high-quality geochronological data are available it is common for mineralisation in high-sulphidation systems to follow magmatism more closely (commonly by less than 0.5–1 Ma) than in the low-sulphidation environment. This is consistent with the direct link between magmatic fluids and mineralisation in the high-sulphidation environment in contrast with the processes involving deeply convecting meteoric fluids in the low-sulphidation geothermal setting.

3.2.3. Hot-spring gold deposits

Hot-spring gold deposits are a sub-class of epithermal mineralisation. They occur in the uppermost parts of hydrothermal systems, extending from the surface to a depth of up to a few hundred (<300) metres. They are associated with hot-spring deposits (siliceous sinter, fumarolic precipitates, geyserite) and hydrothermal eruption breccias (Nelson and Giles, 1985). The ores occur as very fine-grained disseminated sulphides, principally pyrite and marcasite, with minor gold, electrum, stibnite, cinnabar and realgar, in ponded sub-aerial precipitates. They form extensive tabular or lenticular siliceous replacements in their upper sections associated with the development of silica caps at the palaeo-watertable. They commonly exhibit multi-stage small-scale chalcedonic, locally opaline, quartz veining and silica-cemented eruption breccias. Beneath the zone of extensive lateral silicification, mineralisation is associated with stockwork veining and hydrothermal brecciation. Hot-spring deposits are characterised by enrichments in Au, Ag, Hg, Sb and As in the upper parts of the systems, decreasing with depth. Levels of Ag and Ba increase with depth, while base-metal contents are low. They are locally enriched in W, B and NH₄.

Hot-spring gold deposits are mined at relatively few locations. The major McLaughlin deposit, located in the Knoxville mercury mining district of California, has a long history of mining mercury but not gold (Table 3.2: Sherlock et al., 1995). This deposit is localised by a fault zone separating ophiolitic footwall rocks and overlying Jurassic mudstones. Associated igneous activity is related to late Tertiary volcanic and sub-volcanic bodies associated with the hydrothermal activity which led to alteration, veining and mineralisation in the fault zone. Prior to mining, the deposit was overlain by a silica sinter enriched in Hg. Gold enrichment occurs principally in multiple generations of opal, chalcedony and quartz veins in the altered rocks in the fault zone and in silicified eruption breccias. The trace-metal assemblage in the McLaughlin deposit is typical

of low-sulphidation deposits, being enriched in Au, Ag, Sb, As, Hg and Tl. The Round Mountain deposit in Nevada, USA, is another important example included in the hot-spring sub-class (Tingley and Berger, 1985).

Hot-spring deposits are highly variable in the nature and distribution of their ore, gangue and alteration-mineral assemblages. This may be attributed to local structural, lithological and hydrological features of the near-surface environment in which these deposits were formed. Alteration and geochemical zoning may therefore be expected to vary markedly between individual deposits.

3.2.4. Associated mineral deposits

In the majority of cases epithermal mineralisation is not directly observed to overlie deeper subvolcanic mineralisation. However in some districts, particularly where there is high relief, a close spatial relationship can be demonstrated between epithermal and porphyry Cu-Au-Mo mineralisation. The best-documented example is in the Mankayan district of northern Luzon in the Philippines, where several porphyry Cu-Au deposits and epithermal gold and base-metal deposits of both low and high-sulphidation type occur within an area of 25 km² (Hedenquist et al., 1998). In this area integrated geological, geochemical and isotopic studies show that the porphyry and high-sulphidation deposits at Far Southeast – Lepanto were derived from a single evolving hydrothermal system. The vertical interval occupied by ore is more than 1.5 km and the lateral extent at least 4 km in this system. Both porphyry and epithermal mineralisation were deposited from a dominantly magmatic fluid over a time interval of less than 100 000 years.

A more common situation occurs in areas of rapid erosion and gravitational collapse of volcanoes where epithermal mineralisation may overprint, or be telescoped over, intrusion-related mineralisation. This scenario has been documented at the Porgera and Ladolam deposits in Papua New Guinea (Sillitoe, 1995; White et al., 1995).

3.2.5. Mining aspects

Both high and low-sulphidation deposits represent attractive exploration targets in volcanic terrains. Low-grade, large-tonnage disseminated ores and high-grade veins are the two most important deposit morphologies which support mining. The former are mined exclusively by low-cost mining methods (open pit), commonly in combination with heap-leach extraction of the gold. For example, the disseminated low-sulphidation deposit at Round Mountain in south-west Nevada is economically viable on account of its scale and the amenability of the ore to heap leaching (Sander and Einaudi, 1990; Sillitoe, 1995). Similarly, the high-sulphidation deposits at Pierina and in the Yanacocha district, both in northern Peru, enjoy low production costs for the same reasons of scale and ease of mining and processing (Volkert et al., 1998; Sillitoe, 1995). In contrast, high-grade, so-called bonanza veins, often steeply inclined, can be exploited economically by underground mining. For example, the Hishikari deposits in southern Kyushu, Japan have exceptionally high grades and large proven gold reserves (Shikazono et al., 1993; Izawa et al., 1990). Dependent upon grade and weathering history, the uppermost sections of high-grade veins may be amenable to low-cost open-pit mining e.g. Chelopech, Bulgaria (Andrew, 1997). In Britain bonanza vein targets mined underground are likely to be environmentally more acceptable than large low-grade resources exploited by open-cast methods.

Tables 3.2 and 3.3 show reserves and grades for a number of epithermal precious-metal deposits of low and high-sulphidation types for which published data are available. The figures quoted do not adhere to a single reporting standard and should therefore be regarded only as a guide. Nevertheless it is clear that epithermal deposits vary markedly in size and grade, and several giant deposits, containing more than 100 tonnes of gold (ca. 3.3 million ounces), are included. Many deposits, particularly those of high-sulphidation style in the central Andes, are also important sources of silver. Some high-sulphidation deposits, notably El Indio, Lepanto and Chelopech, also contain significant copper resources.

Table 3.2 The size and grade of selected low-sulphidation epithermal gold deposits

| Deposit | Location | Reserve (Mt) | Gold grade (g/t) | Silver grade (g/t) | Contained gold (millions oz) |
|----------------|-------------------------|------------------------------|------------------------------|---------------------------|-------------------------------------|
| Hishikari | Japan | 3.2 | 63 | | 6.48 |
| Round Mountain | Nevada | 317 | 0.86 | | 8.76 |
| Pajingo | Queensland | 1.4 | 12 | 40 | 0.54 |
| Shasta | British Columbia | 1.6 | 2.84 | 132.2 | 0.15 |
| Kelian | Indonesia | 95 | 1.85 | | 5.65 |
| Sleeper | Nevada | 50 | 1.58 | 13.0 | 2.54 |
| Ladolam | Lihir, Papua New Guinea | 4.7 oxide; 168.2 sulphide | 1.96 oxide; 3.48 sulphide | | 0.30; 18.82 |
| Gosowong | Indonesia | 1.0 | 29 | 45 | 0.93 |
| Pongkor | Indonesia | 5.98 | 16.4 | 171.2 | 3.15 |
| Kori Kollo | Bolivia | 55 | 2.3 | 15.1 | 4.48 |
| El Peñon | Chile | 4.7 | 6 | 96 | 0.89 |
| McLaughlin | California | 24.3 | 4.49 | | 2.93 |

Table 3.3 The size and grade of selected high-sulphidation epithermal gold deposits

| Deposit | Location | Reserve (Mt) | Gold grade (g/t) | Grade – silver (g/t); copper, (%) | Contained gold (millions oz) |
|---------------------------|--------------------|--------------------------|-------------------------|--|-------------------------------------|
| Paradise Peak | Nevada | 20 | 3.9 | 125.9 | 2.51 |
| Summitville | Colorado | 9.25 | 1.6 | | 0.48 |
| Pueblo Viejo | Dominican Republic | > 50 oxide; 100 sulphide | 4 3 | 20 23 | 6.43 9.65 |
| Yanacocha | Peru | 702 | 0.9 | | 20.6 |
| Pierina | Peru | 67.7 | 2.98 | 22 | 6.49 |
| El Indio | Chile | 23.2 | 6.6 | 50 Ag + 4% Cu | 4.92 |
| Rodalquilar | Spain | 4 | 4.5 | | 0.58 |
| Lepanto | Philippines | 33 | 3.5 | 11 Ag + 4%Cu | 3.72 |
| Chelopech | Bulgaria | 52 | 3.3 | 1.4% Cu | 5.52 |
| Julcani | Peru | 6 | 1 | 400 | 0.21 |
| Ladera-Farallon, La Coipa | Maricunga, Chile | 52.1 | 1.58 | 60.4 | 2.9 |
| Lobo | Maricunga, Chile | 90 | 1.5 | | 4.75 |

4. EXPLORATION GUIDES AND METHODS

Descriptive and genetic mineral-deposit models provide a framework for the interpretation of geological and exploration data. They can assist in the identification of new targets and also provide guidance on the selection of the most appropriate methods to be used in exploration. At the regional scale, deposit models can be used to identify favourable districts on the basis of geological setting, major structures and the presence of known mineralisation of the type sought. At the local scale, models can be used to guide prospect evaluation by helping to predict the location of mineralised zones at depth or along strike.

Epithermal systems are complex and highly varied in size and shape at both local and prospect scales and consequently the application of models to exploration for epithermal deposits may not be straightforward. The fundamental control on the location of mineralisation in these environments is the palaeohydrology of the parent system. This is determined by numerous factors including: multiple generations of complex structures; variations in host-rock properties such as permeability and chemical reactivity; overprinting of one event by another due to changes in water table and boiling levels; and shifts in the position of active vents. Nevertheless models remain powerful predictive tools, especially when used in conjunction with detailed mapping to determine the controls on palaeofluid flow and hence on the distribution of ores.

Processes responsible for the genesis of epithermal deposits have been studied in modern volcanic environments and are relatively well understood. These deposits are the products of large-scale hydrothermal systems operating at high water/rock ratios and can form under a variety of physical and chemical conditions given a suitable heat supply and sources of metals and sulphur. If the magmatic heat source is emplaced at shallow levels in the crust then magmatic volatiles rise to the surface with little modification. Here mixing with meteoric waters produces a low pH fluid which has the potential to produce ore, gangue and alteration minerals characteristic of high-sulphidation systems. In contrast, low-sulphidation systems are related to deeper magmatic bodies degassing into an overlying groundwater system.

4.1. Structure and terrain characteristics

Epithermal deposits generally occur at convergent plate boundaries, commonly in volcano-plutonic continental margin settings, as reviewed in Section 3 and summarised in Table 3.1. They are generally hosted by calc-alkaline sub-aerial volcanic sequences of intermediate to acid composition. In several deposits the host rocks are sub-alkaline or shoshonitic in character (i.e. high total alkalies, high K/Na and enriched in LILE). Shoshonitic rocks are commonly formed during the late stages of arc evolution at sites distant from the trench (Müller and Groves, 1993).

In northern Britain, Devonian volcanic rocks were deposited in a continental-margin setting related to the closure of the Iapetus Ocean at about 425 Ma. They are mainly calc-alkaline but become generally increasingly alkaline towards the north-west, such that the lavas of the Lorn Plateau are shoshonitic in character.

Given an appropriate tectonic setting, a critical aspect in the assessment of regional favourability is the presence of underlying igneous intrusions which provided heat for the circulation of fluids and also may have acted as a source of various components of the hydrothermal system. Sub-volcanic intrusions emplaced at a high level in the crust above large deep magma chambers provide an appropriate mechanism for the transfer of heat and for the generation of fluid circulation. The locations of these intrusions on a regional scale are controlled by major faults, both normal and strike-slip, that extend into basement. The mineralisation is localised by secondary structures subsidiary to these structural zones. In this study the role of structure in controlling the location of epithermal mineralisation has been addressed by examination of mapped faults and

of lineaments picked from remotely-sensed Landsat TM images, and from images of regional magnetic and gravity fields.

Within favourable districts, epithermal mineralisation is localised by high-level intrusions and secondary structures and is preferentially developed within appropriate fluid conduits. The geometrical configuration of epithermal deposits is determined principally by the permeability of the host rocks which controls the plumbing of the hydrothermal system that brought fluids from deep sources into the shallow epithermal environment. Enhanced permeability may be related to geological structures, to lithological variations or brecciation by hydrothermal fluids. Particularly favoured structures are second-order faults, fault intersections and fault bends and zones of rapid change of local strike. The fluid flow is focused along structures, and ore deposition occurs in zones of dilation and extension where physical and chemical conditions are appropriate. Disseminated mineralisation is produced where pervasive flow is permitted by relatively permeable lithologies such as poorly consolidated pyroclastic or volcanoclastic rocks. Pervasive acid leaching in the high-sulphidation environment is probably an important stage of ground preparation for the development of mineralisation in these systems in some areas. For example, there is strong lithological control on the location of alteration and mineralisation in the major Pierina deposit in northern Peru. Here gold is concentrated in a permeable pumice tuff unit associated with the development of residual vuggy silica and alunite (Volkert et al., 1998).

Lithological contacts and regional unconformities may also be favoured sites for the development of epithermal mineralisation, especially if the contact juxtaposes rocks of significantly different physical or chemical properties. Various types of breccias, especially of hydrothermal origin, also provide effective fluid conduits which may host mineralisation.

In the caldera environment there are many potential sites for epithermal mineralisation that may develop during evolution of the caldera system over prolonged periods. Particularly favoured locations occur in proximity to the ring fractures and associated structures created during caldera collapse and the later stages of the caldera cycle. Resurgent intrusions, especially where flow domes are produced, are particularly prospective.

The tectonically active arc settings in which epithermal deposits form are subject to rapid uplift and erosion. Given the shallow depths of their emplacement, typically in the upper 1 km of the crust, preservation from erosion is an important factor in their exploration and discovery. This explains why epithermal deposits are most common in relatively young rocks, mostly of Tertiary or Quaternary age. However the recognition of important epithermal mineralisation in Palaeozoic and older rocks testifies to the efficacy of rapid subsidence and burial as a means of preserving mineralisation of this type. Where sinters or poorly consolidated and reworked volcanoclastic rocks are preserved in a potentially favourable terrain this indicates that burial was rapid and that underlying mineralisation may have been preserved. The preservation of silica sinter and plant remains in the Lower Devonian basin at Rhynie in Aberdeenshire, north-east Scotland (Rice and Trewin, 1988), provides good evidence for the nearly complete preservation of an epithermal system capped by a hot spring and indicates potential for underlying precious-metal mineralisation. In the Brora district of east Sutherland the present erosion level is close to the Lower Devonian palaeosurface and so high-level epithermal mineralisation may be preserved (Crummy, 1997).

Silicic alteration in epithermal systems may help to preserve associated mineralisation as it is usually erosionally resistant and is therefore less likely to be removed than associated argillic alteration. This feature is most significant where vuggy silica alteration is extensive, either in stratiform or structurally controlled zones.

The effects of supergene processes on the distribution of gold in surficial materials should be taken into account when designing any exploration programme for epithermal gold. The long-held view that gold is inert in the weathering environment and is dispersed only by mechanical processes has been challenged in recent decades and there is now good evidence from a variety of sources which supports supergene chemical mobility of gold (Nichol et al., 1994). This mobility is ascribed principally to the transport and precipitation of gold in chloride, thiosulphate and organic complexes (Lawrance, 1995). Such processes have been shown to be particularly important in tropical terrains where deep, commonly lateritic, regoliths are developed and significant lateral and vertical dispersion of gold from its primary source have been documented (Freyssinet et al., 1989; Freyssinet and Itard, 1997). Studies by Butt and co-workers in Western Australia over a long period (Butt and Zeegers, 1992; Butt et al., 1997) have permitted the development of effective exploration practices for these terrains. Of particular importance are the effects of changes in geomorphology and climate on gold mobilisation mechanisms and their consequent impacts on the exploration process. Where there has been a change to increased aridity in areas of low relief, as in Western Australia, then the combined effects of prolonged erosion and subsequent deposition of transported materials can produce a complex, thick and highly variable regolith. In many other areas of the world, including the UK, relicts of Mesozoic and younger tropical weathering have survived to the present day. The influence of these earlier periods of deep weathering on the distribution of gold in the surficial environment and consequently on the effectiveness of target recognition should not be overlooked.

Glaciation has affected large parts of the northern hemisphere, including Britain, during the Pleistocene, most recently in the last 10 000 to 20 000 years. The impacts of glacial processes on the underlying land surface and hence on exploration procedures are diverse and may be highly significant. Extensive erosion, reworking and deposition remote from the original source may be involved. Subsequent glaciofluvial and alluvial processes may also lead to further disturbance of element distribution patterns and hence hinder identification of a mineralised source in bedrock. Elsewhere depositional processes may lead to masking of bedrock mineralisation by exotic deposits. In the last few decades techniques for identification of mineral deposits by sampling and analysis of glacial sediments have been developed, particularly in Canada and Scandinavia. This methodology has been underpinned by improved understanding of ice-flow dynamics and mechanisms of glacial erosion, transport and deposition, and by the production of high-quality maps of the glacial deposits. In the UK integrated geochemical and geophysical methods have been developed for precious metal exploration in prospective terrains characterised by thinner overburden cover, including glacial deposits. Panning and geochemical analysis of basal overburden samples have been successfully used to identify drilling targets (e.g. Coats et al., 1991; Gunn et al., 1991; Shaw et al., 1995).

In northern Britain the Ochil Hills have been the main exploration target for epithermal mineralisation (Section 6). Alluvial gold has been discovered over a wide area, and is especially abundant in the western part of the central Ochils, but no discrete bedrock source of ore-grade material has been identified. Crummy (1993) has suggested that this may be explained by gold remobilisation under tropical weathering conditions of an extensive area without discrete gold concentrations, followed by glacial, fluvioglacial and fluvial reworking. However, the existence of economic epithermal mineralisation in bedrock in the Ochil Hills cannot be ruled out and potential remains in several areas.

4.2. Mineralisation and alteration patterns

Information on the nature of the epithermal system, the depth of erosion and fluid pathways can be derived by studying a range of features including the nature and zoning of hydrothermal alteration, the deposit form and various geochemical and mineralogical parameters. This information helps to identify the controls on ore distribution and hence provides valuable guidance for further exploration.

The geometry of the ore-controlling structures and host-rock permeability are the dominant controls on the morphology of alteration and mineralisation in epithermal systems. Although they are highly varied in shape and size, low-sulphidation ores are typically localised in structures, and consequently veins, sheeted vein systems and stockworks are the most common deposit forms (Figure 3.2). In high-sulphidation systems stockworks, breccias, disseminated and replacement ores are most common (Figure 3.4).

The alteration halo around an epithermal deposit commonly provides a larger exploration target than the mineralisation itself and is therefore a valuable exploration guide. The alteration-mineral assemblages provide important information on the chemistry of the fluid from which they were produced and hence facilitates identification of the style of the deposit. Characteristic alteration zoning patterns may occur around high- and low-sulphidation style mineralisation (Figure 3.3) which, in conjunction with a range of other parameters, can be used as a guide to indicate the level in the palaeosystem of the present land surface and to provide vectors to mineralisation. Where low-temperature alteration minerals are identified preservation of much of the epithermal system is indicated and underlying precious-metal mineralisation may be present. In both high- and low-sulphidation environments the transition from smectite through mixed layer illite-smectite to illite is indicative of increasing temperatures and hence may help to determine the erosion level of the system. Similarly the identification of dickite and pyrophyllite in advanced argillic assemblages indicates a relatively high temperature, hypogene origin.

In the high-sulphidation environment the zoning of alteration minerals is commonly more conspicuous than in low-sulphidation systems and is therefore potentially more useful as an exploration tool. Vuggy silica alteration passing laterally into advanced argillic assemblages dominated by kaolinite and alunite is characteristic of deposits of this type. Furthermore Hedenquist and Arribas (1999) have pointed out that the silicic and advanced argillic alteration zones in high-sulphidation deposits commonly taper downwards. The roots of these systems may be represented by narrow quartz-pyrite veins and be associated with sericitic alteration, sometimes accompanied by pyrophyllite.

The Portable Infrared Mineral Analyser (PIMA) is a valuable tool for in-situ determination of a wide range of alteration minerals which are often difficult to identify in the field on account of their very fine grain size and non-diagnostic colours. The PIMA is a compact portable spectrometer which measures spectral reflectance in the short-wave infra-red, between 1300 and 2500 nm. This wavelength range includes diagnostic absorption features of many rock-forming and alteration minerals, including phyllosilicates, hydroxylated silicates, sulphates and carbonates. Spectra can be obtained rapidly, in the field or laboratory, from small samples of rocks and soils with minimal prior preparation. Data processing is normally carried out by an experienced spectral geologist, but computer software packages providing automated mineral identification are becoming widely used as their reliability improves.

There are two basic approaches to using the PIMA in studies of mineral deposits. First, it can be employed for direct mapping of alteration systems whereby the distribution of diagnostic minerals identified by the PIMA can be interpreted in terms of established deposit models to provide vectors to mineralisation. Second, systematic PIMA analysis on an individual deposit or in a particular orefield or mine-camp may permit recognition of empirical relationships between the mineral assemblage identified, or particular features of the PIMA spectra, and geochemical patterns. These empirical relationships can then be used in a predictive manner to guide local exploration. Thus, when used in conjunction with other methods, the PIMA can help improve exploration effectiveness and thereby reduce costs. A good example of the utility of the PIMA is provided by a recent study led by the BGS of the volcanogenic massive sulphide deposit at Parys Mountain, Anglesey (Colman and Cooper, 1998). The PIMA has been used in the present investigation to determine its potential for use in the Devonian volcanic terrains of northern Britain. Spectral analysis has been conducted on archived drillcore and rock specimens from the Ochil and Cheviot Hills (Sections 6.4 and 8.5).

A range of simple, readily observed textural and mineralogical features can also provide useful information on the nature of the epithermal system, its degree of preservation and other parameters which may help to locate ore. Discrimination between high and low-sulphidation settings may be made from the nature of the ore and gangue-mineral textures. Open-space filling textures are dominant in the low-sulphidation environment while vuggy residual silica is characteristic of high-sulphidation deposits. In low-sulphidation systems further insight may be gained from study of the assemblages of quartz textures present which may vary systematically with depth as discussed in Section 3 and illustrated in Figure 3.2. Carbonate-replacement texture and the presence of adularia have been widely used as indicators of boiling in low-sulphidation systems.

Other potentially useful diagnostic features include remnants of silica sinters, characterised by laminated banding, which are indicative of the tops of low-sulphidation systems. Also, the presence of opaline silica indicates low temperature deposition from low pH fluids at shallow depth, normally in the high-sulphidation environment.

4.3. Geophysical signatures

Geophysical techniques have an important role to play in exploration for epithermal mineral deposits principally through study of the physical properties of the hydrothermal alteration products rather than the ores themselves (Allis, 1990). The application of each method is based on the response to altered country rocks which may be silicified, clay-altered or contain disseminated sulphide mineralisation of hydrothermal origin (White and Hedenquist, 1990). The value of each technique will vary according to the stage of the exploration programme, the erosion level of the system, and specific geological and structural features of the target area which may have influenced fluid flow and mineral deposition. Several case histories and the anticipated responses from various geophysical methods to epithermal mineralisation have been discussed by Irvine and Smith (1990).

On the regional scale, the use of aeromagnetic surveys for the identification of extensive alteration zones and to assist geological mapping in volcanic terrains is well established. In general, fresh or propylitically altered andesitic rocks are more magnetic than the same lithologies that have undergone argillic or advanced argillic alteration. Consequently the alteration systems are evident as circular or ovoid magnetic lows without significant magnetic relief. Aeromagnetic surveys are useful for mapping geological structures and for the identification of buried high-level intrusions which may localise epithermal mineralisation. Airborne radiometric data provide geological information and may help to identify adularia and sericite in alteration zones around epithermal deposits. Regional gravity surveys provide information on buried intrusions, on basement topography and, in some instances, on alteration. For example, Criss et al. (1985) reported positive Bouguer gravity anomalies over epithermal deposits in Idaho which they attributed to infilling of pore spaces by hydrothermal minerals. However, in the high-sulphidation environment it is more likely that negative gravity anomalies related to acid leaching may be produced, at least on a local scale.

Ground IP, resistivity and electromagnetic methods are particularly useful at the prospect scale for the delineation of alteration, silicified structures and silica caps. In particular, conductivity and resistivity contrasts may be detected in or around silicified zones or veins which are typically enveloped by clay alteration with low resistivity and high conductivity. The extent and thickness of highly resistive silica caps can also be evaluated by these techniques. The widespread occurrence of disseminated sulphides in epithermal systems may preclude good target definition by electrical methods alone.

A notable example of the successful application of geophysical techniques to exploration for epithermal mineralisation is provided by the discovery of the Hishikari deposit in Kyushu, Japan. The results of a

helicopter-borne EM and magnetic survey flown in 1978 over an area including known mineralisation suggested that a low resistivity signature, related to clay alteration, might be used as a guide to promising targets (Johnson and Fujita, 1985). Drilling of one such anomaly yielded high-grade intersections of gold and silver mineralisation and ultimately led to the identification of the multi-million ounce Hishikari low-sulphidation vein deposit (see Table 3.2).

4.4. Geochemical signatures

Epithermal deposits may be enriched in a wide range of metallic and volatile trace elements as summarised in Table 2.1. In general, the volatile elements As, Sb, Tl and Hg are concentrated in the uppermost zones of epithermal systems. In low-sulphidation vein deposits the main level of Au and Ag enrichment normally underlies these zones and in turn passes downwards into a base-metal interval enriched in Cu, Pb and Zn, possibly accompanied by elevated Bi, Te, Se and Co (Figure 3.2). Silica sinters deposited at the palaeosurface may be enriched in As, Sb, Tl and Hg locally with elevated Au and Ag. Zones of steam-heated advanced argillic alteration may be enriched in Hg, but are not usually anomalous in Au or Ag. An understanding of the vertical geochemical zonation in epithermal systems can therefore help to interpret rock geochemical data, to determine the erosion level and thus to provide vectors to mineralisation. It should be emphasised, however, that these relationships are of a general nature and should be refined for local use in the light of empirical observations in individual deposits or districts. In this way, relationships useful to exploration can be established and applied. For example, So et al. (1998) identified vertical and horizontal metal-zoning patterns in the Zijinshan high-sulphidation deposit in Fujian Province, China. The pattern in this deposit is characterised by Au-Ag-As in silicic shallower and central parts, through a Cu zone, to Cu±Pb-Zn-Mo in the deeper and outer parts of the system.

Drainage geochemical sampling has been used successfully in exploration for epithermal gold mineralisation in a variety of geomorphic terrains and at various stages of the exploration process. However, in contrast to large porphyry systems which commonly have extensive geochemical and alteration signatures developed around them, epithermal deposits are commonly much smaller exploration targets. Furthermore, on account of their relatively simple mineralogy and low contents of base metals, they may not be associated with conspicuous multi-element anomalies. As a result potentially significant epithermal occurrences may be indicated by a single-site anomaly for only one or two elements in regional drainage survey data. Normalisation of reported element concentrations with respect to background geology can help to identify anomalies related to lithological variations and thereby increase the probability of identifying subtle anomalies related to other causes, such as the presence of metallic mineralisation. Given these constraints it is particularly important to maintain quality control at all stages of a drainage geochemical survey. This includes collection and sub-sampling of the most appropriate material, as well as all subsequent stages of sample preparation and analysis. The representativeness of the samples and the reliability of the collection procedures should also be monitored. Comprehensive guidance on recommended procedures for drainage geochemical surveys is available in a recent UNESCO publication (Darnley et al., 1995).

The utility of drainage geochemical techniques in exploration for epithermal deposits and the predicted generation of anomalies for particular trace elements are also dependent on the erosion level of the palaeosystem. Where erosion has been limited and the system is well preserved the volatile elements, As, Sb, Tl and Hg, will be prevalent and may form extensive low-tenor anomalies which are useful for reconnaissance purposes but do not pinpoint targets closely. Where erosion has been more important Au, Ag and the base metals may be present at higher values and may be more readily related to bedrock mineralisation at the local scale.

Drainage geochemistry is particularly useful in areas of tropical rain forest where geological and remote-sensing studies are less informative. For example, the Gosowong low-sulphidation epithermal deposit on Halmahera island in eastern Indonesia was discovered by regional geochemical surveys carried out over favourable geological terrain identified on the basis of established genetic models (Carlile et al., 1998). Following bulk-leach extractable gold (BLEG) and conventional stream-sediment reconnaissance sampling, mineralised float and outcrop were discovered by detailed drainage surveys, ridge-and-spur soil sampling and mapping.

Modern analytical techniques are capable of providing sensitive determinations of a wide range of elements in various sample media down to very low concentrations. For example, analytical detection limits for Au in the range 1–2 ppb are widely available at low cost, and sub-ppb levels can also be readily determined. However, when dealing with these very low concentrations the importance of analysing representative samples and avoiding contamination acquires fundamental importance. The BLEG technique developed in Australia in the 1980s offers one solution to the sampling problem (Radford, 1996). In this method between 2 and 5 kg of sample is leached in a cold cyanide solution over an extended period. Gold is then determined in the leachate and the Au content of the bulk sample calculated, normally to detection limits of 0.05 to 0.1 ppb. This method has been fairly widely used in exploration for epithermal and porphyry systems, mainly in tropical terrains, and provides increased confidence in anomaly detection. However the collection and transport of very large samples may preclude the use of this technique in some circumstances. The effects of contamination are minimised by the use rigorous quality control procedures including the use of duplicate and standard samples.

Partial or selective extraction techniques applied to solid sample media from the surficial environment offer another potentially useful approach in gold exploration. These methods involve the selective dissolution of certain minerals or the release of ions at specific sites in order to obtain better responses to mineralisation than conventional ‘total’ or strong acid leaches, especially where buried beneath exotic overburden. The underlying premise is that oxidation of sulphide mineralisation releases elements to groundwater and that these elements migrate towards the surface in aqueous or gaseous forms and are fixed there on suitable substrates. Certain oxide phases and clay minerals provide such substrates and are capable of scavenging trace elements to high concentrations relative to the bulk soil matrix, and thus often produce superior peak-to-background responses to mineralisation. A wide range of analytical attacks have been evaluated, including deionised water, sodium acetate, hydroxylamine hydrochloride, sodium pyrophosphate and enzyme leach analysis (Seneshen, 1997). The merits of each should be evaluated according to the objectives of particular programmes, and orientation studies are generally recommended.

Enzyme leach (EL) analysis, a selective extraction for the dissolution of amorphous Mn oxides, has attracted considerable interest and discussion in recent years. It has been shown to offer good anomaly contrasts over deeply buried mineralisation which may otherwise exhibit no surface geochemical expression (Clark, 1997; Bajc, 1998). The genetic and morphological characteristics of EL anomalies have been described in detail by Clark (1997). Critical to data interpretation is the differentiation of discrete halo (oxidation-type) and apical anomaly forms which are, by definition, antipathetic. Oxidation halos, typically incorporating halogens (Cl, Br, I) and elements with a propensity for the formation of volatile halides (e.g. As, Sb, Mo, W, Re, Se, Te, V, U, Th), are believed to be the product of anodic migration within electrochemical cells developed above any reducing sub-surface body (e.g. a sulphide deposit). Apical anomalies are related to vertical diffusion from a highly concentrated source and, in contrast to oxidation anomalies, generally display some compositional affinity to the orebody. Consequently the EL method may be particularly useful in exploration for epithermal mineralisation in areas covered by younger deposits. However, the mechanisms responsible for the generation of anomalies detected by EL analysis are not well understood and it is therefore recommended that data interpretation should be carried out by appropriate experienced personnel. The utility of the EL

method in exploration for epithermal mineralisation has been documented in the desert environment of Nevada by Smee (1997) and in the glaciated terrain of the Andes in Ecuador by Williams (1999) and Williams and Gunn (1999). However the general robustness of the technique and the repeatability of the results are not well substantiated and it has not been tested in northern Britain.

Several other techniques for the selective extraction of mobile and weakly bonded elements have been developed in various countries (Goldberg et al., 1997; Alekseev, 1996). These include the mobile metal ion (MMI) leach from Australia (Mann et al., 1999) and various geoelectrochemical methods, such as CHIM, MDE, MPF and TMGM, which originated mainly in Russia (Roy and Putikov, 1997). The efficacy of these methods in exploration for epithermal deposits has not been well documented and they have not been tested in northern Britain.

Surface water and ground-water geochemistry were widely used in the 1970s as a tool in exploration for uranium. More recently, with the advent of inductively-coupled plasma mass spectrometry (ICP-MS) technology, it has become possible to determine at least 60 elements simultaneously, including many commodity metals, pathfinders and alteration indicators, to detection limits in the low ppb or ppt range of concentrations. Hydrochemical techniques have not been widely used in routine gold exploration, although they offer advantages in simplicity, reduced collection and preparation times and cost over techniques using solid media. Their effectiveness in detecting epithermal mineralisation in the low-sulphidation epithermal vein field at Osilo, northern Sardinia, was demonstrated by Cidu et al. (1996). Gold contents up to 3 ppb were detected against a regional background of less than 0.4 ppb. Anomalies of a similar magnitude were reported by Grimes et al. (1993) in groundwaters of the Getchell Trend in Nevada, which hosts important disseminated gold deposits.

4.5. Multi-dataset integration and analysis

The multi-disciplinary approach to mineral exploration, using a combination of techniques and expertise from geology, geochemistry and geophysics, is not new. Traditionally various datasets are integrated by time-consuming, manual methods in an essentially qualitative manner. Not only is this an inefficient use of human resources but it is also commonly subjective and inconsistent.

With the advent of modern GIS systems, numerous digital exploration datasets can be accessed, visualised and integrated rapidly and consistently. When underpinned by soundly-based genetic or descriptive mineral-deposit models these systems can be used to evaluate the mineral potential of an area. This approach optimises the use of human resources and of the increasingly abundant digital geoscience datasets. It can be applied consistently and objectively and thus leads to more effective exploration. Some of the earliest examples of the application of this approach were provided by Bonham-Carter (1994). A major study of this type led by the BGS was undertaken in western Europe to develop exploration models for mainly mesothermal lode gold deposits (Plant et al., 1998).

Bonham-Carter (1997) discussed developments in the use of GIS in mineral exploration in the decade 1987–1997 and reviewed the rationale underlying mineral-potential mapping. He provided an example involving analysis of the prospectivity of the Snow Lake area of Manitoba for the occurrence of VMS deposits. Generally similar methodologies have been applied by various workers to other deposit types and commodities: for example, sediment-hosted gold deposits in north-central Nevada (Turner, 1997), lead-zinc massive sulphide deposits in the Bathurst camp, New Brunswick (Chinn and Ascough, 1997) and Archaean lode gold deposits in the Yilgarn block of Western Australia (Knox-Robinson and Groves, 1997). In Britain Gunn et al. (1997) carried out knowledge-based prospectivity mapping for mesothermal lode gold deposits in the Dalradian terrain of the Scottish Highlands.

The availability in BGS databases of digital geological, geochemical, geophysical and remotely-sensed data for northern Britain allows this approach to be used to evaluate the potential for epithermal precious metal mineralisation in the Lower Devonian volcanic terrains.

5. MULTI-DATASET INTEGRATION AND PROSPECTIVITY ANALYSIS

5.1. Introduction

Genetic or empirical mineral deposit models are syntheses of large amounts of data and provide an essentially qualitative basis for exploration and resource assessment. Such models can be used to identify the key exploration criteria for a particular type of deposit and thus form the basis for analysis of the mineral potential of a region. However, with increased availability of digital geoscience datasets of all types there is a need for systems which use this information to maximum advantage by providing structured integration and modelling of the datasets in a quantitative manner.

In its simplest form, mineral-potential mapping or prospectivity analysis involves appraisal of the region for the presence or absence of the identified criteria. However, this assessment is subjective as it depends on the emphasis given to particular criteria and on the availability of appropriate data relevant to each criterion. In some areas crucial geological or geochemical data might be absent or incomplete. Elsewhere there may be several phases of data acquisition of varying quality and relevance, possibly collected for other deposit types, and the explorationist has to decide which of the data are suitable to include in the prospectivity appraisal. In many cases the abundance of data of different types makes the use of traditional exploration methods of visual inspection and transparent overlays impractical.

GIS systems allow the manipulation and analysis of individual layers of spatial data and also provide the capability for analysing, modelling and displaying the relationships between the layers. Modern prospectivity appraisal is carried out on a GIS platform, using digital data and specific computer applications devised for a *data-driven* analysis of the data relationships or a *knowledge-based* analysis using exploration expertise. Data-driven analysis aims to relate all specified data to known occurrences of the particular deposit type within the region and, by association, highlight those data relationships which closely mimic the patterns at the known occurrences. Knowledge-based systems may be applied to regions with no known occurrences. Such systems use expertise from the explorationist to determine the relative significance of the exploration data and then search for patterns which reflect the total effect of such significance. In practice exploration criteria are identified for the deposit type sought and relevant data are then acquired for use in the analysis. The user assigns weights to these features, which are then combined in the GIS environment to produce a prospectivity map (Table 5.1).

Various *classes* of multivariate geoscience data may be available in digital form for use in prospectivity analysis. These include geological maps, geochemical analyses and geophysical, remotely-sensed and mineralogical data. These classes may include several *types* of data: points, grids, vectors, sets. In addition particular relationships between data *layers* can give rise to *event* occurrences which may be included in a prospectivity model. Examples of event occurrences might include the intersection of a fault plane with a particular geological unit or the intersection of known or inferred geological structures with geophysical lineaments of a particular orientation (Figure 5.1).

Table 5.1 Summary of the main stages of knowledge-based prospectivity analysis

| | |
|---|--|
| 1 | Selection of mineral deposit type and project area |
| 2 | Review of published mineral deposit models and determination of exploration criteria |
| 3 | Acquisition of digital spatial datasets |
| 4 | Data processing and extraction of features relevant to the selected mineral-deposit model |
| 5 | Preparation of maps displaying derived features, e.g. lineation intersections, geophysical gradients |
| 6 | Assignment of weights to, and combination of, key features and derived evidence |
| 7 | Combination of weighted criteria to produce prospectivity map |

BGS has developed a knowledge-based prospectivity system, known as XMAP, to integrate exploration-related multivariate data. The system uses simple Boolean, Binary-weights-of-evidence (BWE) and Fuzzy Logic (FL) models to assess prospectivity scores across a region. FL analysis allows for data layers to have a 'range of uncertainty' across which the significance of the data will vary from zero to unity. Outside this range the data will be either significant or not significant. Each individual data parameter is treated as a layer of evidence in the subsequent analysis. Each data layer has associated parameters which determine the significance of the data elements and the style of influence they exert.

XMAP is a knowledge-based system, in that the user provides the parameters for the relative weight of influence, zone of influence and style of influence for a particular input data layer and the system responds with an analysis in the form of a pixel-based prospectivity grid. The definition of weights for each data layer relies on knowledge of the importance of such data in controlling the location of the targetted deposit type. This knowledge is derived from published mineral deposit models, from empirical observations of known occurrences in the study area and from the experience of the user. The degree of confidence and value attached to the prospectivity maps depends on the availability, quality and relevance of data together with the reliability of the exploration model.

5.2. Details of the XMAP system

5.2.1. Logic model

XMAP uses various logic models for GIS prospectivity analysis:

i) Boolean Logic (BL) model

In the simplest form, this displays a set of information which has a binary code representing present (1) or absent (0). More commonly the model is used to produce binary-weights-of-evidence maps to incorporate the effects of numerous populations. For example, if 5 populations were plotted together, each with a weight of 1.0 then the maximum prospectivity score would be 5 and the minimum 0. By normalising the score to the sum of the weights a binary-weights-of-evidence map in the range 0.0–1.0 can be generated.

The operation of the Boolean model in XMAP is as follows:

$$x_{ij} = 0$$

Then for each active option:

$$x_{ij} = x_{ij} + wa_{ij}$$

$$\text{Then: } x_{ij} = x_{ij} / ws$$

where wa is the apparent weight of the pixel (ij) for each active option, ws is the sum of the weights for all active options and x_{ij} is the prospectivity for pixel ij .

This method has been used to produce the prospectivity maps shown in this report.

ii) Fuzzy Logic (FL) model

In the Fuzzy Logic model, the definition of the anomalous population or set boundaries is less clear (i.e. fuzzy). In stream-sediment geochemical data for example, a value of 100 ppm arsenic might be regarded as highly anomalous (1.00), whereas a value less than 10 ppm would normally be part of the background population and assigned a weighting of 0.0. In the Fuzzy Logic model data values in the range 10–100 ppm might be weighted by a simple linear function to produce a weighting between 0.0 and 1.0.

In the Fuzzy Logic model XMAP uses the Fuzzy Algebraic Sum which is additive for all positive weights (Bonham-Carter, 1994). The operation of the model is as follows:

$$x_{ij} = -1.0$$

Then, for each active option:

$$x_{ij} = x_{ij} * (1.00 - wa_{ij})$$

$$\text{Then: } x_{ij} = x_{ij} + 1.00$$

where wa is the apparent weight of the pixel (ij) for each active option and x_{ij} is the Fuzzy Logic prospectivity for pixel ij .

Note that use of the Fuzzy Logic model will not mean that all data layers are assigned ‘fuzzy’ values. For example the intersection of two vectors provides a ‘real’ event and is given a weight defined by the index parameters selected for that option. Fuzziness in XMAP is applied to those data-posting options which have minimum and maximum limits defined during plotting. These limits determine the ‘fuzziness’ such that values above the maximum have a weight factor of 1.0, values below the minimum have a weight factor of 0.0 and values in between have factors in the range 0.0–1.0. Geochemical data are the data class most commonly assigned fuzzy weightings in prospectivity analysis.

In the present study many trial prospectivity maps were prepared using the Fuzzy Logic Model. However the results were generally less satisfactory than those produced using binary-weights-of-evidence and they are not therefore shown in this report.

5.2.2. Pixel size

The resolution of the prospectivity model is determined by the pixel size for analysis and is independent of the plot area or any of the plot option parameters. However if the plot options include gridded data the user should consider the effects of the pixel size in relation to the plotted grid size. The size of the pixel used depends on the specifications of the available datasets. In the UK typical pixel sizes used for regional prospectivity analyses are normally in the range 0.25–1 km.

The contribution of any vector to prospectivity is based on the [x,y] pairs which define the line. These [x,y] pairs form the occurrence pixels so that ‘simple’ vectors defined by a few widely spaced points will not give the same prospectivity as a vector defined by closely-spaced points.

5.2.3. Prospectivity parameters

The prospectivity analysis is based on a table of index parameters which is completed by the user. For each active data layer the zone of influence (buffer), the style of influence (exponent, distance) and the weight of influence are entered into the table. A hypothetical example is shown in Table 5.2. By default the table of index parameters is set to a negative (-0.1) weight. Since zones with zero or negative weights are not cumulative in either of the logic models this would generate a prospectivity grid of zero.

Table 5.2 Hypothetical example of a table of index parameters

| parameter code | zone of influence | exponent | peak distance | weight | parameter description |
|----------------|-------------------|----------|---------------|--------|---|
| 1 | 0 | 2.0 | 0 | 0.1 | andesitic lavas from 1:250K map |
| 2 | 2 | 2.5 | 0 | 0.2 | diorites from 1:50K maps |
| 3 | 0 | 2.5 | 0 | 0.1 | porphyry from 1:50K maps |
| 15 | 4 | 2.5 | 0 | 0.1 | occurrences of copper and lead minerals |
| 17 | 4 | 2.5 | 0 | 0.4 | alluvial gold occurrences |
| 41 | 4 | 1.5 | 0 | 0.2 | stream-sediment data, As > 20 ppm |
| 43 | 3 | 2.5 | 0 | 0.1 | panned-concentrate data, Bi > 10 ppm |
| 61 | 0 | 2.0 | 0 | 0.3 | residual gravity anomalies < -2 Mgal |
| 67 | 3 | 2.5 | 0 | 0.2 | intersections of inferred faults and gravity lineaments |

For Fuzzy algebraic logic, the defined index weights are always less than 1.00, whereas for Boolean models individual index weights can be greater than unity. The sum of weights, essential for normalisation of the prospectivity map, is defined by the sum of weights for all plotted data layers. Each data layer is treated therefore as a level of evidence. Consequently if files contain non-unique data, (i.e. duplicate data points, or overlapping polygons) then these will be scored twice in the prospectivity analysis although the sum of weights will not reflect this. This results in final prospectivity scores at or above 1.00 for some BWE models. To overcome this, XMAP checks the sum of weights against the final prospectivity scores. If the non-normalised prospectivity grid contains elements greater than the sum of weights, then the maximum prospectivity score is used to normalise the BWE map before plotting.

Zone of influence

The zone of influence or buffer-zone allows the user to specify the extent of the prospectivity contribution for an individual data layer around the occurrence pixel. For example, the user may wish to emphasise the significance of the intersection of two vectors or of known occurrences of gold in bedrock. For a buffer zone value of zero, only the occurrence pixel which contains the data element (vector intersection or gold occurrence) would contribute to the prospectivity model. For a zone value of 1 the 8 pixels immediately adjacent to the occurrence pixel are also included in the proximity window and scored into the prospectivity model. A buffer zone of 3 will mean that each data element affects a window of 7x7 pixels centred on the occurrence pixel into the analysis. The maximum zone of influence allowed in XMAP is 20 pixel widths.

However, it should be noted that the style of influence will also affect the actual width of the buffer zone in which there is a prospectivity contribution.

Style of influence

The style of influence is the mathematical function which determines the variation in influence away from the occurrence pixel within the buffer zone. The influence may be constant, decrease or increase away from the occurrence pixel according to a simple cosine distance law. The user defines the nature of this relationship by the exponent and distance parameters in the table of index parameters. The style of influence assumes the value f in the relationship:

$$f = \cos [|(n-x)|^a]$$

where n is the distance from the occurrence pixel in pixel widths, x is the peak distance (see below), a is the distance exponent and $f = 0$.

Suitable values of the distance exponent are in the range between 0.0 and 3.0. This function is illustrated in Figure 5.2 for various values of the distance exponent, a , in this range. For example, where the zone of influence is specified as 10 pixels and a distance exponent of 2.0 is selected, the relative weight at a pixel distance of 10 would be zero. At a distance of 6 pixels the relative weight would be 0.8 and beyond this it would be zero. Similarly, for a zone of influence of 20 and a distance exponent of 1.5, the relative weight at 14 pixels from the occurrence pixel will be about 0.6 of the maximum weight.

Peak distance

For certain datasets the influence of the data layer might not be a maximum at the occurrence point. For example 'halo' effects might be important at specified distances from data occurrences. XMAP allows a simple shifting of the zone of maximum weight away from the occurrence pixel by use of the peak distance (x) parameter. A peak distance of 0 (pixels) will mean maximum relative weights occur at the occurrence pixel. A peak distance of 5 will mean maximum weights occur at a radius of 5 pixels from the occurrence and decrease at greater or lesser distances.

Weight of influence

The weight of influence (w) is defined in the table of index parameters by any real value. It is the maximum value of the function describing the effect within the zone of influence. Negative weights will not be scored into the prospectivity grid. For Boolean and Binary-weights-of-evidence prospectivity maps any positive values can be used. For Fuzzy Logic maps then all weights should be less than or equal to 1.00. The weight for any data layer can only be scored in the occurrence pixel (assuming a distance parameter of zero). The apparent weight within the zone of influence is given by the product of the weight and the distance function as described above.

5.3. Prospectivity map and grid

The key criteria used in this study of the Lower Devonian volcanic rocks of northern Britain are summarised in Table 5.3. The datasets from which these criteria are extracted and the source databases are also listed.

The results of the prospectivity analysis are displayed either to the screen or to the specified driver for plotting. The prospectivity analysis grid as generated can be saved to a USGS standard grid file for use in other applications.

Table 5.3 Exploration criteria and source datasets used in prospectivity analysis for epithermal gold mineralisation in this study

| <i>Feature</i> | <i>Prospectivity criteria</i> | <i>Data class</i> | <i>Datasets</i> | <i>Source</i> | <i>Data used</i> |
|--|--|---------------------|---|--|------------------|
| Geological setting | sub-aerial volcanic rocks of intermediate to acid composition. Devonian age | geology | chronostratigraphy, lithostratigraphy | digital geological map, 1:250 000 | ✓ |
| Regional structure | proximity to major fault zones or terrain boundaries | geology | Faults | digital geological map, 1:250 000 | ✓ |
| Regional structure | proximity to faults, terrain boundaries, unconformities | geophysics | aeromagnetic lineations derived from analysis of images of data | UK Aeromagnetic database | ✓ |
| Regional structure | proximity to faults, terrain boundaries, unconformities | geophysics | gravity lineations derived from analysis of images of data | UK Gravity database | ✓ |
| Known metalliferous mineralisation | occurrence of minerals containing Au, Ag, Cu, As, Sb, Pb, Zn, Bi, Mo, Hg, Tl, W, B, Ba, F, Sn, Te, Se in bedrock | mineral occurrences | mineral occurrence data | UK Mineral Occurrence Database and published | ✓ |
| Indicator of proximity to mineralisation | observations of gold grains in pan concentrates | mineral occurrences | regional geochemistry (G-BASE) and reconnaissance exploration surveys (MRP) | UK Mineral Occurrence Database | ✓ |
| Indicator of proximity to mineralisation | geochemical anomalies for Au, Ag, As, Cu, Sb, Pb, Zn, Bi, Hg, Mo, Ba in stream sediments and pan concentrates | geochemistry | regional geochemistry (G-BASE) and reconnaissance exploration surveys (MRP) | UK Geochemistry database | ✓ |
| Hydrothermal alteration | low or negative TMI due to destruction of magnetic minerals | geophysics | residual magnetic anomalies | UK Aeromagnetic database | ✓ |
| Indications of buried basic to intermediate intrusions | TMI anomalies | geophysics | residual magnetic anomalies derived from a regional polar field at 2 km above observation level | UK Aeromagnetic database | ✓ |
| Indications of faults, intrusion contacts | Bouguer anomalies | geophysics | horizontal gradient magnitude of Bouguer gravity derived from analysis of regional field | UK Gravity database | ✓ |
| Indications of buried intrusions | Bouguer anomalies; residual gravity anomalies | geophysics | Bouguer gravity contours | UK Gravity database | ✓ |

Table 5.3 continued Exploration criteria and source datasets used in prospectivity analysis for epithermal gold mineralisation in this study

| <i>Feature</i> | <i>Prospectivity criteria</i> | <i>Data class</i> | <i>Datasets</i> | <i>Source</i> | <i>Data used</i> |
|----------------------------------|---|-------------------|--|--|------------------|
| Structure and volcanic features | surface features related to topography, lithology, structure, volcanism, erosion | remote sensing | Landsat lineations derived from analysis of images of data | Landsat TM images | ✓ |
| Preservation from erosion | near surface geological features – silica sinters, eruption breccias, fluvial/lacustrine sediments, poorly welded ignimbrites | geology | local geology | digital geological maps, borehole logs, written accounts | ✓ |
| Ore controls | zones of increased permeability such as faults, fractures, breccias, permeable lithologies | geology | local geology – structure and lithology | digital geological maps, borehole logs, written accounts | ✓ |
| Alteration and alteration zoning | presence of silicification, advanced argillic, argillic, sericitic and propylitic alteration assemblages | mineralogy | PIMA, XRD and petrographic studies. Field observations | digital geological maps, borehole logs, written accounts | |
| Alteration and gangue minerals | LS – sericite, illite, adularia, chlorite, smectite, quartz, carbonate, chalcedony, amethyst, fluorite HS – alunite, kaolinite, dickite, pyrophyllite, jarosite, smectite, quartz, baryte, gypsum. | mineralogy | PIMA, XRD and petrographic studies. Field observations | digital geological maps, borehole logs, written accounts | |
| Ore textures | quartz textures: LS – open-space filling / banded HS – massive / vuggy silica | mineralogy | field and petrographic observations | digital geological maps, borehole logs, written accounts | |

6. OCHIL HILLS

6.1. Geology

The Lower Devonian volcanic rocks of the Ochil Hills form an east-north-east-trending tract of high ground in the Midland Valley of Scotland, extending over a distance of about 80 km from Bridge of Allan in the west to the coast north of St. Andrews in the east (Figures 6.1, 6.2). Smaller developments of similar lavas in the Midland Valley also occur in the Sidlaw Hills to the north of the Tay estuary, around Montrose and along the Highland Boundary Fault. These outcrops are shown in Figures 6.1/6.2 which are extracted from the BGS 1:250 000 digital geological map of the UK.

The Devonian strata of the Ochil and Sidlaw Hills extend over several 1:50 000 geological map sheets, 39, 40, 48 and 49. In terms of mineral potential sheet 39 (Stirling) is the most important of these. The geology of this sheet is described in detail in the Geological Survey Memoir (Francis et al., 1970). Accounts of the geology of other parts of the district are given by Geikie (1900 and 1902). Additional geological details from the 1:50 000 scale geological maps for the region are shown in Figure 6.3.

During the Devonian the Midland Valley of Scotland formed part of an intracontinental basin receiving clastic debris from the Highlands to the north and the Southern Uplands to the south. The sediments were deposited in proximal alluvial fans and distal flood-plains with braided, intermittent streams. Volcanic activity commenced in the Downtonian and increased in intensity and extent to a maximum in the Lower Devonian, ending in the late Lower Devonian. Thick successions of dominantly andesitic and basaltic lavas, with scarcer rhyolitic variants, were deposited, while contemporaneous erosion resulted in their incorporation into sediments, especially in the southern part of the area. Radiometric ages of Midland Valley volcanic rocks and associated intrusions fall within the range 415–411 Ma (Thirlwall, 1988).

6.1.1. Volcanic rocks

Lower Devonian rocks in the north-eastern part of the Midland Valley are assigned to the Arbutnott Group of Gedinian to lower Siegenian age. This group includes a thick sequence of lavas and volcanoclastic rocks of the Ochil Volcanic Formation which extends from the western Ochils in Perthshire north-eastwards to Fife and the Sidlaw Hills. Towards the north-east the Ochil Volcanic Formation thins out and passes into fluvial and lacustrine sediments of the Dundee Formation which contain Lower Devonian fossils.

Andesitic and basaltic lavas are predominant. They generally dip towards the north-west at about 15°, although locally this changes to a west or west-south-westerly direction. Together with intercalated beds of epiclastic origin, they attain a maximum thickness in the western Ochils exceeding 2500 m. Several varieties of andesite, notably pyroxene-andesite and hornblende-andesite, occur together with feldspar-phyric olivine basalt and subordinate flows of aphyric basalt, trachyandesite and rhyodacite. The andesitic lavas are commonly autobrecciated and are locally traversed by a network of interconnected fissures and voids which were filled with fine-grained sediment after consolidation of the flow. Individual flows are impersistent along strike and appear to be lenticular in form. Their consistent dips and the lack of volcanic vents indicate that most eruptions emanated from fissures. Deposition appears to have been sub-aerial, but rapid accumulation of the volcanic pile prevented widespread oxidation and reddening.

Field discrimination between the andesites and basalts is difficult. Most contain phenocrysts of plagioclase and one or more ferromagnesian minerals and they vary in colour from grey to purple. They are commonly streaked or mottled with red hematite. Vesicles filled with calcite, zeolites and agates are widespread. Most of the lavas show some degree of alteration: replacement by carbonate and chlorite is most common, while albitisation is locally important. There is also evidence for potassic metasomatism occurring at a late stage in the volcanic history of the western Ochil Hills (French et al., 1977).

Subordinate flows of trachyandesite are developed locally in the western Ochils. These rocks are fine grained, paler in colour than the andesites and basalts, and have a distinctive flow-banding. Minor rhyodacite flows occur in the area to the south and east of Auchterarder at high stratigraphic levels close to the northern edge of the volcanic outcrop. The main development, around Craig Rossie [2985 7121]¹, comprises a feldspar-phyric fine-grained, flow-banded rock.

Volcaniclastic rocks (coarse tuffs, lapilli tuffs and agglomerates) are confined to the western Ochils. Lateral variations in thickness are marked, but they are generally most abundant and coarse grained along the southern margin of the Ochil Hills close to the Ochils Fault, suggesting that this area was either proximal to the detrital source or that sediment influx was triggered by periodic tectonic activity.

Outside the main area of volcanism, sedimentary deposition continued for a long period. Along the Highland Border coarse conglomerates with components of metamorphic and igneous origin form the Johnshaven Formation, which is about 1800 m thick. Closer to the Ochil Hills, extensive and thick sequences of sandstone were deposited as the Dundee Formation, up to 1500 m thick. Several lenticular masses of olivine-basalt and andesitic lava occur within the Johnshaven and Dundee formations.

6.1.2. Intrusions

Several small stock-like intrusions cut the lower part of the Ochil Volcanic Formation in the western Ochils. At Tillicoultry [292 798] four dioritic stocks occur within a thermal aureole extending over an area of 6 km by 1 km. These bodies are truncated to the south by the Ochil Fault but geophysical evidence suggests that they extend, at depth, beneath Carboniferous rocks on the south side of the fault (Francis et al., 1970). Another stock and three associated small bosses occur in the area north of Glendevon village surrounded by a thermal aureole extending over 4 km by 1.5 km. Two small stocks also outcrop at Newhill, south-west of Glenfarg, in the central Ochils.

The diorites comprise mainly plagioclase with minor quartz and varying amounts of ferromagnesian minerals. They vary from almost granodioritic in composition, to types with abundant amphibole or two pyroxenes, to more basic varieties with olivine. They are generally weakly altered with plagioclase partly sericitised and locally replaced by albite or rimmed by orthoclase. Chlorite, biotite and carbonate are local minor constituents. The country rocks around the diorites are variably and irregularly thermally metamorphosed. The weakest alteration comprises clouding and sericitisation of plagioclase and replacement by carbonate and chlorite. In the hornfelses the original feldspars have albite overgrowths and the rocks are xenoblastic or granoblastic in texture. They also contain abundant poikiloblastic quartz and common biotite. Pink aplitic rocks occur as patchy segregations and veins, up to about 2 m wide, which cut both the diorites and the aureole rocks.

¹ square brackets are used throughout this report to identify locations according to the British National Grid

Some stocks have sharp, steep, outward-dipping intrusive margins while others have gradational hybridised, xenolithic contacts. Locally a ghost stratigraphy is evident with scarp features in the diorite conformable with the regional dip of the lavas. This suggests that the diorites were emplaced partly by simple intrusion and assimilation, associated with radial fracturing of the surrounding rocks, and partly by the metasomatic replacement of country rock. The wide development of thermal alteration in volcanic rocks elsewhere indicates the presence of additional concealed intrusions at shallow levels. For example, thermal alteration has been mapped for at least 5 km to the east of the exposed diorites at Tillicoultry in an elongate zone to the north of the Ochil Fault. Similarly, in the area to the north of Glendevon the effects of thermal metamorphism are evident over an area of about 4 km by 1.5 km, although the mapped diorite outcrop extends only about 1 km by about 250 m.

Minor intrusions emplaced mainly as dykes occur throughout the Ochils but are particularly concentrated around the diorite stocks in the west. They vary from basic to intermediate and acid compositions. In the Tillicoultry area they form a swarm of mainly microdiorites: these rocks have a fine-grained grey, green, purple or pink matrix containing microphenocrysts of altered plagioclase and variable amounts of altered hornblende or pyroxene. The majority of the dykes in this area have ragged, unchilled and locally gradational contacts with the diorites suggesting near simultaneous intrusion. The dykes sometimes display a crude radial relationship relative to the diorite bodies and also a marked concentration parallel to the main fault trends. It is therefore probable that the structural grain was already established before the intrusions were emplaced and may explain the fact that these trends can seldom be traced in the overlying sediments.

Lower Devonian minor intrusions of more acid composition, termed quartz and quartz-albite porphyries, occur fairly widely. Some are highly irregular in form, while others are dyke or sill-like. The largest of these occur in the western part of the central Ochils (at Mellock Hill, Thornton Hill and between Westrigg Burn and Borland Glen) and in the eastern Ochils at Forret Hill and Lucklaw Hill.

Various minor intrusions of quartz dolerite are also widespread within the Ochils. Five irregular discontinuous pod-like bodies occur along the Ochil Fault between Alva and Dollar. Elsewhere quartz dolerite occurs mainly as east-west-trending dykes, some of which may be traced over several kilometres. By analogy with other areas these bodies are thought to be of Permo-Carboniferous age.

6.1.3. Superficial deposits

The Ochil Hills are blanketed by an incomplete cover of glacial and fluvio-glacial deposits laid down on a deeply weathered pre-glacial regolith. Although the Ochil Hills have undergone more than one episode of glaciation, the existing drift deposits relate to the last glacial events of Late Devensian age (ca. 15 000–13 000 years ago). The presence of erratics of Highland origin on the high ground indicates that during the Late Devensian an ice-sheet originating in the Highlands extended over the Ochil Hills. The distribution of local erratics, notably those of the distinctive rhyodacite of Craig Rossie, indicates an ice-movement towards the south-east in the ground north of Glen Devon (Francis et al., 1970). Over high ground on the interfluvial boulder clay deposits are generally thin, less than 5 m. On lower ground, particularly in the main valleys, thicker boulder clay, between 10 and 20 m, is widespread.

Valleys in the Ochil Hills are characterised by fills of sandy head and stratified fluvio-glacial deposits, which give rise to sloping terraces, commonly with distinct uphill margins against the steeper valley sides. Present stream courses commonly cut deeply through these deposits into bedrock, locally revealing the composite nature of the

mapped till deposits and intercalated stratified silt and gravel. In such cases it is probable that deposits of till left behind by the melting ice sheet were later modified in form and composition by the down-hill movement of soliflucted material. These processes were probably most active during the renewal of arctic conditions in the period of the Loch Lomond Stadial, between 11 000 and 10 000 years ago, when glaciers were mainly confined to the Highlands of Scotland.

6.1.4. Structure

The Midland Valley is a graben which developed in Devonian times. It is about 80 km wide, bounded to the north by the Highland Boundary Fault and to the south by the Southern Upland Fault. The Devonian rocks are folded along north-east-trending axes which are tightest close to these marginal faults. Elsewhere the folds are more open structures of considerable amplitude. The Lower Old Red Sandstone sediments to the north of the Ochils lie within the major Strathmore Syncline which trends in a north-easterly direction and reaches the coast south of Stonehaven. The fold is asymmetrical with a steep north-western limb and a gently-dipping south-eastern limb. The rocks of the Ochil Hills lie to the south-east of the Strathmore Syncline on the flank of a broad complementary anticline which is the south-western continuation of the Sidlaw Anticline. Here the rocks dip more or less consistently towards the north-west at about 15°.

A number of faults affect the Ochil Volcanic Formation, most commonly along its southern margin (Figure 6.3). They are oriented in two main directions, north-west and north-east. These structures are considered to be of Lower Devonian age because of their close association with dykes of that age. A third, less common, trend is roughly east-west. By analogy with structures elsewhere in the Midland Valley, these faults are thought to be of Permo-Carboniferous age.

The major Ochil Fault, which trends approximately east-west, has had a long and complex history. It is a normal fault with its maximum downthrow occurring near Alva and decreasing towards the east and west. The minimum throw on the fault is estimated to be 2000 m and it may well be considerably greater. Limited field evidence indicates a southerly hade, but this is at variance with geophysical evidence which suggests a northerly hade (Davison, 1924). An alternative explanation for the geophysical evidence is that there is a second subsurface structure dipping towards the north, parallel to and north of the Ochil Fault. Recent comparatively shallow seismic activity appears to have been centred to the north of the fault (Davison, 1924) and along the fault (Dollar, 1951).

6.2. Mineralisation

Polymetallic vein mineralisation is widespread in the western Ochils where it was mined on a small scale at several localities intermittently between the seventeenth and nineteenth centuries. The mineralised lodes occur close to the southern fault-bounded margin of the Ochil Hills, within 3 km of the Ochils Fault (Figure 6.4). Francis et al. (1970) and Dickie and Forster (1974) provide the most recent and comprehensive descriptions of the main workings and occurrences.

All the known mineralisation is localised along fault planes and fracture zones, which in some cases are also the sites of minor intrusions. The three main trends of faulting have all been mineralised to some extent but are characterised by different associations of minerals (Francis et al., 1970). The most widespread mineral occurrences are narrow, steeply dipping baryte veins trending between north-west and north-north-west. They have a dominantly baryte-copper association, with iron and lead in small quantities and calcite and quartz as less

common gangue minerals. Most of the iron occurs as pyrite. Copper occurs as chalcopyrite, chalcocite and tetrahedrite, with some native copper, chrysocolla and malachite.

The north-east–south-west trend has a dominantly calcite-iron association with the iron occurring as an oxide. Silver with minor cobalt, copper and lead occur, while baryte and quartz are less common gangue minerals. East–west-trending mineralised veins are the least common. They are characterised by a dominantly calcite-iron association but in this case the iron occurs mostly as pyrite. Silver and copper also occur, with subordinate lead, arsenic and cobalt; quartz and minor baryte are gangue minerals. The Ochil Fault also follows this trend but no mineralisation is recorded at the few localities where it is exposed.

The most important mine workings were in the Silver Glen about 1 km north-east of Alva. Native silver was discovered here in 1711 and shortly after mining commenced a large body of ore containing 85.7% pure metal was discovered. This rich ore was soon exhausted to be replaced by lead and copper. The mine was reopened in 1759 when a large mass of cobalt ore, mainly erythrite, was discovered. The silver and cobalt occur in a steeply inclined fault breccia trending north-east. The breccia contains calcite, quartz, pyrite, chalcopyrite, arsenopyrite, argentite, galena, erythrite, ferruginous gouge and hydrocarbon coatings.

Silver was also produced from the mines at Airthrey [2815 6972], Carnaughton Glen [2878 6975] and Tillicoultry Burn [2912 6978]. At the latter site copper was the principal product from a north-east-trending fault breccia mineralised with calcite, pyrite, argentite and ferruginous gouge. The mineralisation occurs within lavas and volcanoclastic rocks about 300 m from the margin of the Wester Kirk Craig Diorite. Porphyrite dykes which cut and displace faults are widespread in the Tillicoultry Burn area.

Production of copper is recorded from several other localities in the district: from a steep north-east-trending vein at Airthrey Hill [2795 6978]; from a steep vein oriented at about 100° in Allan Water, near Bridge of Allan [2787 6983]; and from a north-north-west-trending mineralised fault at the Jerah mine [2832 6995]. In the Blairlogie area, about 5 km west of Alva, numerous veins carrying baryte and copper ores occur along north-west-trending faults. Many of these have been trialled, but no significant production reported (Wilson and Flett, 1921).

The occurrence of gold in the Ochil Hills is not widely documented. Collins (1976) refers to gold at Alva, but the original source is not quoted. Gold was recorded at the Airthrey Hill mine in a memorandum written by Robert Seton in the reign of James V of Scotland (quoted in Cochran-Patrick, 1878). The same source also notes the presence of cinnabar on the Perthshire side of the Water of Alqwharry, which is probably Old Wharry Burn [2850 7020], west of Glen Devon.

The distributions of alluvial and bedrock occurrences of copper, lead and gold minerals in the district are shown in Figure 6.4. Occurrences of metallic minerals and alteration indicators noted during the regional geochemical survey of the Ochil Hills in the late 1970s reflect the incidence of known mineralisation and provide evidence for the existence of additional mineralisation in bedrock. In particular, observations of alluvial gold grains in panned concentrates from the western and central Ochils and from the north Fife coast indicated potential for the occurrence of gold-bearing mineralisation in those districts (Coats et al., 1991). Follow-up investigations by BGS under the Mineral Reconnaissance Programme (MRP) in the late 1980s led to the discovery of epithermal gold mineralisation in Borland Glen in the western part of the central Ochil Hills. An extensive zone of hydrothermal alteration was identified, associated with low-tenor Au enrichment (up to 500 ppb) in bedrock. Detailed follow-up surveys were subsequently conducted by a commercial company, but few details are available (Crummy, 1993). The work carried out by BGS in the Borland Glen area is described in Section 6.4.

On the basis of field evidence and by analogy with similar mineralisation elsewhere in central Scotland, it is suggested that the north-east and east–west-trending faults (i.e. the calcite-iron associations) in the Ochil Hills were mineralised during the Permo-Carboniferous and that the north-westerly trend (dominated by baryte) was mineralised in Tertiary times (Francis et al., 1970). This interpretation is consistent with K-Ar ages on illite-rich concentrates from the mineralised rocks of the Alva area which are late Carboniferous to early Permian (260–300 Ma) (Ineson and Mitchell, 1974). Sulphur isotope compositions for baryte from three localities in the Alva area have an average of +9.2‰ (Jassim et al., 1983), which is close to the average for other baryte veins in the Midland Valley. These values rule out genesis during an early Carboniferous metallogenic epoch as suggested by Russell (1972) and indicate a genetic link to faulting and dyke intrusion during the Stephanian. The source of the metals in the deposits around Alva is thought to be the Lower Devonian volcanic host-rocks (Hall et al., 1982; Parnell and Swainbank, 1984).

6.3. Geochemistry

6.3.1. Introduction

Drainage geochemical surveys were conducted by BGS over the Ochil Hills in two phases of the MRP: a regional survey which targetted base-metals was carried out in 1978; this was followed by more detailed investigations for gold between 1987 and 1989. The regional MRP stream sediment data (Figure 6.5) were subsequently incorporated into the G-BASE database and described in the regional geochemical atlas covering southern Scotland (British Geological Survey, 1993). All samples were analysed by direct-reading DC arc emission spectrometry (DCOES). In addition, As and Sb were determined in about 50% of the samples by atomic absorption spectrophotometry (AAS).

During the MRP surveys, panned-concentrate samples were also collected and analysed (Figure 6.6). In the first programme 829 concentrates were analysed for As, Ba, Ca, Ce, Cu, Fe, Mn, Ni, Pb, Sb, Sn, Ti and Zn. During this survey 29 occurrences of visible gold in panned concentrates were recorded. In the follow-up survey for gold in 1987–89 attention focused on the central Ochils and a larger suite of elements was determined, including Au, Ag, Bi and Mo in samples collected at that time. Gold was determined by AAS following aqua regia leaching while the other elements were analysed by XRF.

For the purposes of this study regional stream sediment data were evaluated over an area covering the outcrop of Lower Devonian volcanic rocks in the Ochil and Sidlaw Hills and immediately adjacent strata (1209 samples). Univariate summary statistics for the stream-sediment and panned concentrate datasets are shown in Tables 6.1 and 6.2.

The locations of sites at which visible gold, copper and lead minerals were observed in the concentrates in the field are shown in Figure 6.4. In addition, sites where analytical values for Au in panned concentrates exceed 100 ppb are also shown.

6.3.2. Results

Antimony (Sb): the Lower Devonian lavas are characterised by low Sb values in stream sediments (Figure 6.7), with minor enhancement above background (0.5 ppm) at sporadic sites in the western Ochils e.g. near Glenfarg [313 710] and the upper part of the Water of May catchment [303 710]. In the eastern Ochils elevated values occur to the west of Cupar [335 715] and along the Tay coastal strip. The anomalies in the western Ochils are associated with enrichment in a suite of elements including Zn, Pb, Ba, Bi and As; most of them can be attributed to recorded sulphide mineralisation, either in bedrock or in panned concentrates. However associated high values

of Co, Mn and Fe indicate that some anomalies may be caused by coprecipitation on secondary Fe-Mn hydroxides. In the eastern Ochils the highest Sb value over the volcanics (5 ppm) occurs in the Dunbog area [328 719]. The nearby anomaly west of Cupar correlates with elevated Pb, Ba and Bi and may be associated with sulphide mineralisation.

Table 6.1 Summary statistics for G-BASE stream-sediment samples, Ochil and Sidlaw Hills
(all values in ppm)

| Element | no. samples | mean | minimum | maximum | median | 75% | 90% | 95% |
|---------|-------------|---------|---------|---------|--------|-------|---------|---------|
| Ag | 1209 | 0.1 | 0.1 | 6.7 | 0.1 | 0.1 | 0.1 | 0.3 |
| As | 629 | 11.8 | 2 | 160 | 10 | 10 | 20 | 25 |
| B | 1208 | 31.1 | 2 | 229 | 28 | 38 | 51 | 62 |
| Ba | 1209 | 755.1 | 128 | 7034 | 655 | 794 | 1008 | 1234 |
| Be | 1149 | 1.9 | 0.1 | 13.3 | 1.7 | 2.4 | 3.3 | 3.8 |
| Bi | 1209 | 1.1 | 0.2 | 40 | 0.2 | 0.2 | 5 | 6 |
| Co | 1209 | 19 | 2 | 82 | 17 | 23 | 28 | 34 |
| Cu | 1209 | 31.4 | 6 | 299 | 28 | 35 | 48 | 58 |
| Fe | 1209 | 48754 | 6854 | 166807 | 45601 | 54343 | 65324 | 73927 |
| K | 1209 | 20037.2 | 5396 | 56696 | 19424 | 22662 | 26065 | 28887 |
| Li | 1209 | 34.5 | 6.6 | 147 | 34.4 | 39.7 | 44.6 | 48.9 |
| Mn | 1208 | 1532.1 | 173 | 24700 | 1091 | 1726 | 2940 | 3950 |
| Mo | 1209 | 0.1 | 0.1 | 0.1 | 0.1 | 0.1 | 0.1 | 0.1 |
| Ni | 1209 | 49.8 | 5 | 211 | 45 | 62 | 79 | 90 |
| Pb | 1209 | 49.5 | 4 | 756 | 37 | 56 | 88 | 118 |
| Rb | 1208 | 63.1 | 22 | 197 | 55 | 76 | 97 | 111 |
| Sb | 629 | 0.5 | 0.1 | 5 | 0.5 | 0.5 | 0.5 | 0.5 |
| Sn | 1209 | 3.1 | 0.1 | 427 | 0.1 | 1 | 8 | 14 |
| Sr | 1209 | 283.3 | 73 | 760 | 277 | 346 | 400 | 440 |
| Ti | 1209 | 7786 | 419.6 | 22601.2 | 7373.9 | 8393 | 10011.6 | 11390.5 |
| V | 1209 | 94.1 | 12 | 305 | 89 | 107 | 129 | 147 |
| Zn | 1207 | 195.8 | 8 | 1443 | 151 | 224 | 350 | 507 |

Table 6.2 Summary statistics for MRP panned-concentrate samples, Ochil Hills
(all values in ppm)

| Element | no. samples | mean | minimum | maximum | median | 75% | 90% | 95% |
|---------|-------------|----------|---------|---------|--------|--------|--------|--------|
| Ag | 202 | 3.4 | 0.05 | 42 | 3 | 5 | 6 | 7 |
| As | 1003 | 16.7 | 0.5 | 65 | 16 | 21 | 26 | 31 |
| Au | 209 | 2.9 | 0.001 | 140 | 0.03 | 0.86 | 7.53 | 10 |
| Ba | 1116 | 5701.8 | 22 | 446500 | 376 | 596 | 1974 | 9760 |
| Bi | 196 | 0.7 | 0.2 | 59 | 0.2 | 0.2 | 1 | 2 |
| Co | 83 | 20.2 | 10 | 208 | 18 | 20 | 22 | 27 |
| Cr | 201 | 419.3 | 76 | 1143 | 385 | 516 | 691 | 803 |
| Cu | 1116 | 84.1 | 0.5 | 7737 | 16 | 23 | 49 | 132 |
| Fe | 1116 | 114634.7 | 2950 | 311540 | 106180 | 145265 | 185445 | 212980 |
| Mn | 1116 | 2914.6 | 50 | 15470 | 2110 | 3950 | 6335 | 7898 |
| Mo | 83 | 12.6 | 0.1 | 32 | 13 | 16 | 18 | 19 |
| Ni | 1116 | 34.7 | 1 | 161 | 32 | 41 | 54 | 64 |
| Pb | 1115 | 281.1 | 1 | 24684 | 38 | 64 | 197 | 393 |
| Sb | 1114 | 4.5 | 0.2 | 558 | 1 | 5 | 9 | 11 |
| Sn | 1060 | 22.3 | 0.5 | 1106 | 6 | 13 | 46 | 101 |
| Ti | 1116 | 18154.7 | 860 | 137000 | 13635 | 22160 | 35125 | 43600 |
| Zn | 1116 | 152.1 | 4 | 4258 | 98 | 141 | 222 | 342 |

High Sb values in panned concentrates are widespread with 25% of samples containing more than 5 ppm Sb (Figure 6.8). Elevated values in the eastern Ochils are accompanied by enrichments in Sn and Pb and are probably due to metallic contamination. For example, the maximum reported value (558 ppm Sb), from a site near Dunbog, about 8 km north-west of Cupar, is accompanied by 1.1% Pb and 312 ppm Sn. In the western Ochils many high Sb values (>50 ppm) are accompanied by elevated Ba, Pb, Zn and Cu, and are related to polymetallic vein mineralisation. An exceptional site occurs at the south-eastern end of Glen Eagles [295420 705520] where high Sb (532 ppm) is accompanied by anomalous Bi, Mo and Ag in a stream draining interbedded lavas and tuffs cut by a major porphyrite dyke.

Arsenic (As): the median As content of stream sediments from the Devonian volcanic rocks is 10 ppm (Figure 6.9). Higher values occur over the Kinfauns area [315 722], to the north-east of Perth, although the levels in this area may be enhanced by hydromorphic upgrading. Another zone of elevated values (15–30 ppm) occurs to the south of the Ochil Fault, between the Crook of Devon [304 700] and Kinross [311 705]. A small cluster of elevated values occurs on the northern margin of the volcanics at Newburgh [323 718]. These anomalies are not accompanied by high As values in heavy mineral concentrates. However, the Kinross anomaly is associated with Bi values up to 10 ppm and the Newburgh anomaly with elevated Pb and Cu. Gold grains were also observed in concentrates at Dunbog and Flisk, a few kilometres east of Newburgh.

The As content of panned concentrates is fairly uniform across the Ochil Hills, with an interquartile range of 11 to 21 ppm and a maximum value of 65 ppm. In general values are higher over the westernmost part of the Ochils, particularly on the northern flank of the main watershed. Elsewhere, medium-tenor enrichment is associated with the margins of the volcanics, particularly in the vicinity of the Duncricvie diorite intrusion [312 709].

Overall, the relatively low As contents of stream-sediment and panned-concentrate samples suggest absence of arsenopyrite and other minerals carrying significant amounts of As.

Barium (Ba): the Ba contents of stream sediments from the volcanic rocks vary widely (Figure 6.10). In the Sidlaws and eastern Ochils values are generally low. For example, the lavas of the Kinfauns Forest [316 722] contain less than 600 ppm. In contrast Ba levels over the western Ochils are much higher, with values near Bridge of Allan [282 700] commonly exceeding 2000 ppm. The high Ba values in the stream sediments and associated high levels in panned concentrates are consistent with visual observations of baryte in heavy-mineral concentrates and reflect baryte vein mineralisation (e.g. Silver Glen, Alva). The high Ba values in concentrates from this area are accompanied by elevated Pb, Zn, Cu and Sb, together with local low tenor As enrichment.

Beryllium (Be): there is little variation in the Be contents of stream sediments over the lavas, with most values in the range 2–5 ppm. Sporadic local enrichment occurs around the Tillicoultry diorite and adjacent catchments to the north-west.

Bismuth (Bi): the abundance of Bi in stream sediments varies markedly between the western and eastern Ochils (Figure 6.11). In the eastern Ochils most Bi values fall below the analytical detection limit, whereas in the west many sites have values in the upper 10% of the regional dataset (i.e. >5 ppm). The highest Bi value (40 ppm), accompanied by elevated Ag (6.7 ppm), occurs near Tillicoultry at [294 698] and probably reflects the polymetallic mineralisation developed around the high-level intrusions in the area.

Several other Bi stream-sediment anomalies over the lavas are associated with high Ba values, and may be related to local hydrothermal centres within the lavas (Cameron and Stephenson, 1985). There is also a cluster of elevated Bi values in the area of alluvial gold enrichment in the Glen Devon catchment.

Data for Bi in panned concentrates are available only for the phase of detailed follow-up for gold in the central Ochils (196 sites) (Figure 6.12). Values above the 95th percentile (2 ppm) occur mainly in the area between Glen Eagles and Mellock Hill in the western part of the central Ochils. The highest value (59 ppm) is associated with elevated Sb, Mo and Ag, as noted above.

Boron (B): sporadic high values of B in stream sediments occur in three areas: along the northern margin of the western Ochils; west of Glenfarg; and near Tillicoultry (Figure 6.13). Boron data are not available for the panned concentrates.

Copper (Cu): in the western Ochils elevated values (>110 ppm) in stream sediment occur in the Finglen-Danny Burn catchment area to the west of Glen Devon [287 703] and along the southern margin of the Ochil Hills close to Tillicoultry [290 696] (Figure 6.14). Over the eastern Ochils high values occur sporadically, notably to the north-east of Cupar [339 717] and in the Dunbog area [330 717]. Elevated Cu is commonly associated with enrichment in Zn, and locally with Pb and Ba, reflecting the occurrence of polymetallic vein mineralisation. For example, the highest Cu value (299 ppm) is accompanied by 556 ppm Zn [324 717].

Copper values in panned concentrates exceeding 200 ppm are fairly widespread in the Ochils (Figure 6.15), although most high values (>2000 ppm) are restricted to the western sector where vein mineralisation is widespread.

Gold (Au): in the 1978 reconnaissance survey visible gold was recorded at 29 out of 818 sites. These sites were resampled in 1987 and gold was observed at 40% of them. The sites where gold was not identified in the later samples were normally in drift-covered areas where sporadic occurrences of single gold grains might be expected. These observations highlighted the central Ochils and the north Fife areas as of particular interest. On this basis, together with an evaluation of the regional stream-sediment geochemical data, Coats et al. (1991) identified several target areas for follow-up. Panned concentrates from 209 sites were analysed for Au during this phase (Figure 6.16). The median Au content of these samples is 0.03 ppm, with 25% of them containing more than 0.86 ppm Au (Table 6.2). Stream-sediment samples were not collected during this phase of investigations.

In north Fife, sampling was carried out along a coastal strip on the south side of the Tay estuary and three smaller areas inland. In this region the topography is subdued and bedrock is blanketed by thick glacial and fluvioglacial deposits. The highest values were reported in the coastal belt, up to a maximum of 3.8 ppm at Flisk Point [33118 72250]. The source of these anomalies is unknown but coastal superficial deposits are one possibility. Weak to moderate anomalies (up to about 500 ppb Au) were reported from other areas in north Fife, but no bedrock sources were identified and no follow-up surveys carried out.

In the central Ochils, panned concentrates were collected from an area between the south side of Glen Devon and Bridge of Earn [313 718], about 20 km in length by 10 km wide. In this region the relief ranges from undulating to hilly (approaching 500 m in places), and the streams are well developed with abundant active sediment. Till covering the lower hill slopes and filling the main valleys has been reworked by fluvio-glacial action. Drift cover on the higher ground is generally thin, 1–2 m. Alluvial gold was observed widely throughout the area, with local upgrading from fluvioglacial terrace deposits by the present drainage. The area of greatest Au enrichment was found to the north of Glendevon village [299 704] extending along Borland Glen northwards into the Coul Burn catchment, beyond Green Law [2994 7075]. In this area analytical values for Au exceed 1 ppm in 14 out of 24 concentrates collected. Most gold grains observed were in the range 0.05–1.0 mm in size, but particles up to 10 mm were locally recovered. Cinnabar grains were also observed in association with high gold values at some localities. Limited analytical data for Hg yielded a maximum value of 22 ppm. The highest Au value (140 ppm) was reported from the Hodyclach Burn, to the north of Green Law, in the upper part of the Coul Burn catchment. Follow-up surveys carried out in the Borland Glen and Coul Burn catchments are described in Section 6.4 of this report. Other prominent high tenor anomalies and occurrences of visible gold were reported from Westrig Burn [2957 7075], Lee Burn [3035 7055], and the Kelty Burn catchment to the south of Culteuchar Hill [3089 7141] (Coats et al., 1991). No follow-up investigations were carried out at these localities.

The abundance of gold in panned concentrates correlates with few other elements. The distribution patterns of Fe, Mn and Ti are similar to that of gold because of the hydrodynamic equivalence of gold and grains of heavy minerals such as magnetite and ilmenite. Silver shows a weak positive correlation with Au, but base-metals and chalcophile pathfinder elements (As, Sb and Bi) are not generally correlated with Au abundance.

Lead (Pb): the highest Pb values in stream sediments are found mainly in the southern part of the western Ochils between Glen Devon and Tillicoultry where mineralisation is well known (Figure 6.17). Several single-site anomalies occur close to the contact between the lavas and sediments to the north. The highest value, 756 ppm, is

from the Balquhandy Burn area [303 712] and is associated with elevated Mo (5 ppm) and Sn (17 ppm). Minor Pb enrichment is also present at several sites in the eastern Ochils, up to a maximum value of 581 ppm [327 718]. However, there is no general association between Pb and other base metals or the chalcophile pathfinder elements here.

The data distribution for Pb in concentrates (Figure 6.18) is highly skewed, with nine values exceeding 2%. These sites are located in the western Ochils, to the south and west of Glen Devon, but are not associated with observations of visible gold. They are, however, accompanied by marked enrichments in Ba, Cu and Zn and are clearly related to the presence of vein mineralisation. Elsewhere sporadic single-site anomalies between 0.5 and 1% Pb occur over a wide area in the central and eastern Ochils, locally accompanied by low-tenor enrichment in As, Ba, Cu, Sb and Sn. These anomalies may, in some instances, be related to metallic contamination.

Manganese (Mn): in the eastern Ochils Mn values seldom exceed 2000 ppm in stream sediments (Figure 6.19). In contrast, levels are much higher in the west with values exceeding 8000 ppm in the Glen Devon area [300 705] and in the extreme west of the volcanic outcrop near Bridge of Alan. This regional contrast may relate to variations in erosion level between west and east, but some of the highest values may relate to mineralisation along south-east trending structures. At some localities the association of high Mn with enrichments in Fe, Co and Zn suggests the importance of secondary enrichment processes.

Molybdenum (Mo): no Mo values exceeding the analytical detection limit are reported in the stream-sediment dataset. Data for Mo in concentrates are available only for 83 sites, the majority of them located in the western part of the central Ochils in the area west of Glenfarg where alluvial Au occurrences are widespread. Molybdenum concentrations are low, with a median value of 13 ppm. Values exceeding the 90th percentile (18 ppm) occur in the Borland Glen, Westrig Burn, Kelty Burn and Lee Burn areas (Figure 6.20).

Silver (Ag): the majority of Ag values in stream sediments are very low with the concentrations at only 22 sites exceeding 1 ppm (Figure 6.21). In the western Ochils detectable Ag values, up to 2 ppm, occur fairly widely and include sites to the north of Glen Alva [285 703] and in the Glen Devon area. The highest value (6.7 ppm) occurs on the north side of the Tillicoultry diorite and, as mentioned above, is accompanied by elevated Bi and low-tenor enrichment in zinc (236 ppm). Low-tenor anomalies also occur in the eastern Ochils to the west of Cupar. Other elevated values are found at the northern end of the volcanic outcrop, to the north of Dundee.

Silver was determined in panned concentrates from 202 sites (Figure 6.22). The median value is 3 ppm, with 9 values exceeding 7 ppm (95th percentile). Most high values occur in the western central Ochils, specifically in and around Glen Devon and in the Cloan area, south-east of Auchterarder. Sporadic single site anomalies are found to the north and north-west of Cupar in the eastern Ochils.

Tin (Sn): there are sporadic low-tenor Sn anomalies in stream sediments and panned concentrates, mainly in the eastern Ochils, most of which can be attributed to contamination. Sporadic high values occur in the western Ochils, mostly between Kinross and Glen Devon, but are not related to known mineralisation.

Zinc (Zn): values in stream sediments from the western Ochils are generally within the upper quartile of the regional dataset (>224 ppm) (Figure 6.23). Some high values are associated with elevated Mn, Fe and Co, and can be attributed to secondary enrichment, while a small number associated with high Sn may be due to contamination. However, stream-sediment anomalies for Zn with attendant high Bi, Pb, Ba, Cu, As and Sb are probably due to vein or intrusion-related mineralisation. The distribution of Zn in panned concentrates (Figure

6.24) correlates closely with that of Pb. The highest values (>3000 ppm) are restricted to the western Ochils, to the south and west of Glen Devon, and relate to vein mineralisation. Low-tenor anomalies in the range 200–500 ppm are more widespread in the western part of the central Ochils, but occur only rarely in the east, around and to the north-west of Cupar.

6.3.3. Discussion

Drainage geochemical data provide useful information for mineral exploration in the Lower Devonian volcanic rocks of the Ochil and Sidlaw Hills. However, for gold exploration and prospectivity mapping the limited data availability for certain potential pathfinder elements and the lack of uniform survey cover over the region are problematic. In particular, if Au and pathfinder element data are included in the prospectivity analysis, then those areas where such data are lacking will be under-rated by comparison with others where such data are available. However, given that the areas targetted for gold follow-up surveys in the Ochil Hills were based on a regional assessment and were not arbitrarily selected, it is reasonable to expect that some, if not all, of the most prospective areas were identified at that stage. However it is likely that some targets will have been missed or under-rated as a result of their exclusion at the reconnaissance stage.

The main sources of drainage geochemical anomalies in the Ochil Hills are polymetallic mineral veins which occur widely, especially in the western part of the area. These occurrences are characterised by coincident enrichments in Ba, Pb, Zn and Cu which can generally be related to known occurrences in bedrock or to observations of baryte, galena and other metallic minerals in panned concentrates.

The chalcophile pathfinder elements for gold, As, Sb and Bi, are generally enriched in the western part of the Ochils. Antimony enrichment is locally associated with elevated Sn and Pb and in these cases may be due to anthropogenic contamination. However, where Sb accompanies Ba, Pb, Zn and Cu it is probably derived from polymetallic mineralised veins. Arsenic, Sb and Bi are also locally enriched, together with Ag and Mo, in proximity to mineralisation related to the exposed diorite bodies in the Alva area. Similar anomalies spatially related to exposed high-level intrusions or alteration haloes indicate the possibility for further mineral occurrences. At higher levels in the volcanic sequence epithermal mineralisation developed in association with these intrusions might be expected to be reflected in anomalies for these elements.

The geochemical anomalies in the Borland Glen area provide the strongest evidence for epithermal mineralisation in the region, but several other prospective targets in the central Ochils are also highlighted by the drainage geochemical data and warrant further investigation. The geology and geochemical data for the area west and south of Glen Devon indicate a deeper level of erosion in that sector and hence reduced favourability for the occurrence of epithermal gold.

The geochemical data for the eastern Ochils indicate lower prospectivity for epithermal gold mineralisation. This may be a function of erosion level, but the thick cover of superficial deposits in the area reduces the usefulness of drainage geochemical exploration and hinders follow-up surveys aimed at identifying mineralisation in bedrock. Accordingly geochemical anomalies in the eastern section of the Ochils should be assigned a lower priority than those farther west.

6.4. Investigations in the Borland Glen area

6.4.1. Introduction

Attention was first drawn to the Borland Glen area of the western Ochils by elevated Au values detected in the 1978 MRP reconnaissance survey in a stream east of White Creich Hill (Figure 6.25). Follow-up in 1987–89 identified higher Au values in the Creich Burn, which drains Borland Glen. The Au concentrations in 14 out of 24 panned concentrates exceeded 1000 ppb. Further evidence of mineralisation in this area was derived from Upper Cloan, to the north of Borland Glen, where numerous gold grains were observed during panning and high analytical values for Au were identified in the Hodyclach and Coul Burn catchments on the north side of Green Law.

In Borland Glen a general upstream increase in gold was observed, although between-site variations are marked due to the entrainment and resultant concentration of gold at certain sites. Abundant fine- to medium-grained gold particles were observed at many sites, mainly in the size range 0.05–1.0 mm. Panning of washed but unsieved terrace material near Heart Plantation [29930 70650] revealed gold particles up to 10 mm in size, commonly associated with abundant cinnabar grains. In Creich Burn rounded grains of cinnabar up to 1.5 mm in size are present in both stream sediment and overburden.

The MRP investigations conducted in the Borland Glen area are described in detail by Coats et al. (1991). Mineralogical and petrographic studies of rocks and drillcore are reported in Fortey (1990).

6.4.2. Geology of Borland Glen

The geology of Borland Glen comprises a series of Lower Devonian andesitic lavas and pyroclastics intruded by a diorite body and porphyry dykes (Figure 6.25). Minor hydrothermal alteration is visible locally at surface. The dominant rock types in the catchment are interbedded basic andesite lavas and agglomerates which dip towards the north-west at about 15°. They are best exposed in the lower part of Borland Glen, south of White Creich Hill [299 706]. Flows of distinctive pale-coloured, banded trachyandesite are a minor component of the sequence.

A large stock of diorite penetrates the volcanic rocks between Black Creich and White Creich Hill (Figure 6.25), and extends to the west side of Borland Glen. The diorite, mainly coarse-grained and grey or pink in colour, contains pink aplitic veinlets. An elongate metamorphic aureole, over one kilometre wide, extends in a north-east direction around the diorite outcrops. Within the aureole some lavas have been converted to grey hornfels, and locally they contain patches of dioritic material, as on White Creich Hill. In the outer parts of the aureole the altered rocks are in places rotted and weathered an ochreous colour. Lava scarps within the thermal aureole on White Creich Hill can be observed to continue into the outcrop of a small boss of diorite on the south side of the hill. This is consistent with the hypothesis of Francis et al. (1970) that the diorite formed by in-situ metasomatism of the lavas.

Minor intrusions within the Borland Glen area include dykes of hornblende andesite, basalt, acid porphyrite and quartz-albite-porphyry. A large intrusion of pink or buff quartz-albite porphyry extends for at least 3 km in a roughly east–west direction between the Westrig Burn [295 707] and Borland Glen.

6.4.3. Overburden sampling

Following the discovery of alluvial gold in the upper Borland Glen during drainage sampling, follow-up investigations were carried out to locate bedrock sources of gold. These comprised basal overburden geochemical

sampling and geophysical surveys over an area covering the northern part of Borland Glen extending northwards into the catchment of the Coul Burn (Figure 6.26).

The overburden sampling indicated a zone of sulphide mineralisation extending northwards to the watershed near Green Law. The zone of mineralisation has elevated Au, Hg, As, Sb, Cu, Pb and Zn values and is believed to be the source of the gold and cinnabar grains found in the Borland Glen drainage. A large Hg anomaly in the overburden adjacent to the track between Borland Glen and Coul Burn extends over the watershed into the catchment of the Coul Burn, where there are similar Au and Hg anomalies in the drainage. However, there are no anomalous Au values in the basal till extending that far north. Mercury in overburden samples forms a discontinuous halo around and overlapping the zone of high Au values (Figure 6.26).

The overburden sampling data also identified evidence of baryte mineralisation with minor base metals, concentrated at the margins of the major east–west quartz-porphyry dyke.

6.4.4. Geophysical surveys

Initial geophysical investigations using IP, VLF-EM and magnetic techniques were carried out over an area of about 1 km² in the Borland Glen area to map out the mineralisation identified in the geochemical surveys (Figure 6.26). Technical details of the survey methods and a detailed discussion of results are given by Coats et al. (1991).

In the northern part of Borland Glen the IP survey identified a zone of high chargeability (>40 msec, n=4) approximately 300 m in maximum dimension (Figure 6.26). This was interpreted as due to disseminated sulphide mineralisation within altered lavas. The source geometry was inferred to be a plug-like cylinder, or an ovoid, with its long axis trending north–south. The VLF electric-field data showed high resistivity values over the principal zone of alteration.

Ground magnetic survey data showed that the inferred northerly extension of the main diorite body is characterised by a magnetic anomaly in excess of 500 nT. The data also indicate a smaller, lower-amplitude anomaly (250nT) on the eastern flank of the main chargeability anomaly. This may be related to varying degrees of alteration or another body of diorite at shallow depth.

In order to identify any northward continuation of the IP anomaly from Borland Glen and other similar mineralised zones, the geophysical surveys were extended over an area to the north and west of Green Law in the catchment area of Coul Burn (Figure 6.26). However no coherent IP anomalies were found and it was concluded that, within the depth investigated by the survey, the sulphidic material detected to the south is absent. The minor chargeability anomalies may reflect local occurrences of pyrite or pyrrhotite associated with mineralogical changes within the lavas. West of the Hodyclach Burn, the magnetic data show some continuity across several profiles and this might be related to an extensive area of alteration within the andesite and basalt.

6.4.5. Boreholes

Seven boreholes were drilled in Borland Glen to investigate the sources of the chargeability anomalies and the high gold values in drainage and overburden samples. The locations of the holes are tabulated in Table 6.3 and shown in Figures 6.25 and 6.26.

Table 6.3 Specifications of boreholes in Borland Glen

| Borehole No. | Easting | Northing | Collar height (m) | Depth (m) | Inclination | Azimuth |
|--------------|---------|----------|-------------------|-----------|-------------|---------|
| 1 | 299170 | 706930 | 397 | 101.86 | 90° | |
| 2 | 299250 | 706950 | 414 | 95.31 | 70° | 256° |
| 3 | 299280 | 706850 | 383 | 82.32 | 70° | 256° |
| 4 | 299240 | 706740 | 356 | 57.50 | 90° | |
| 5 | 299400 | 707450 | 475 | 51.46 | 70° | 256° |
| 6 | 299710 | 707260 | 424 | 50.35 | 90° | |
| 7 | 299289 | 706645 | 345 | 88.91 | 90° | |

Boreholes 1, 2, 3 and 4 were drilled to intersect the main IP anomaly and associated gold enrichment in the overburden. Borehole 5 was drilled to locate the source of high gold values in overburden near the watershed between Borland and Cloan Glens, remote from the main IP anomaly. Borehole 6 was drilled to investigate a smaller IP anomaly to the east of the main anomaly, while borehole 7 targeted the southern extension of the chargeability anomaly and the metamorphic aureole of the diorite.

Boreholes 1, 2, 3 and 7 were logged using downhole probes for gamma activity, chargeability and resistivity. In general chargeability and resistivity peaks were correlated and reflect the degree of alteration, particularly silicification and associated disseminated pyrite. With the exception of boreholes 5 and 6, the geophysical logs indicate a zone of strong hydrothermal alteration of greater intensity than that evident at surface. The gamma-ray logging indicated a close correlation between count-rate and the degree of K-feldspar alteration.

A total of 344 samples of sliced half-core were collected from the boreholes after detailed logging. Gold was determined by lead fire assay with an ICP finish, while a range of trace elements was determined by XRF (Table 6.4).

The median Au content of the drillcore samples is 6 ppb, which is comparable with typical background concentrations in intermediate extrusive rocks. The upper 4% of the samples constitute a separate anomalous population with Au contents in the range 100–505 ppb. These samples were all derived from boreholes 1, 2 and 5.

In borehole 1, anomalous Au values (maximum 163 ppb) occur at a number of levels in a sequence of variably hydrothermally altered andesitic lavas with subordinate thin agglomerates. The gold abundance is not correlated with that of other metallic trace elements, although disseminated pyrite, up to about 15% by volume, is widespread together with sporadic traces of galena, sphalerite, chalcopyrite and molybdenite. Quartz-sericite alteration is common, with local chloritic patches and zones of K-feldspar alteration. Tourmaline was tentatively identified in minute patches in this borehole.

Table 6.4 Summary statistics for geochemical samples from boreholes in Borland Glen
(344 samples; all values in ppm, except Au in ppb)

| Element | Minimum | Maximum | Median | Mean | 75% | 90% | 95% |
|---------|---------|---------|--------|-------|-------|-------|-------|
| Ag | 0.05 | 5 | 2 | 2 | 2 | 3 | 3 |
| As | 3 | 301 | 24 | 29 | 33 | 43 | 53 |
| Au | 1 | 505 | 6 | 21 | 20 | 51 | 82 |
| Ba | 48 | 3237 | 585 | 658 | 813 | 1065 | 1199 |
| Bi | 0.05 | 9 | 1 | 2 | 2 | 3 | 4 |
| Ca | 400 | 163500 | 15350 | 16413 | 22525 | 31040 | 35070 |
| Ce | 28 | 104 | 54 | 55 | 61 | 70 | 76 |
| Co | 4 | 181 | 21 | 21 | 26 | 31 | 35 |
| Cr | 23 | 493 | 141 | 162 | 216 | 274 | 322 |
| Cu | 2 | 2393 | 28 | 79 | 63 | 127 | 252 |
| Fe | 12300 | 111800 | 37550 | 38882 | 48525 | 54970 | 57825 |
| La | 14 | 55 | 29 | 30 | 33 | 38 | 43 |
| Mn | 70 | 3600 | 940 | 967 | 1210 | 1580 | 1717 |
| Mo | 0.5 | 22 | 3 | 4 | 4 | 7 | 9 |
| Nb | 5 | 19 | 9 | 9 | 10 | 12 | 13 |
| Ni | 1 | 117 | 31 | 38 | 55 | 80 | 91 |
| Pb | 1 | 840 | 21 | 42 | 45 | 89 | 129 |
| Rb | 5 | 122 | 48 | 52 | 69 | 81 | 92 |
| Sb | 0.2 | 55 | 2 | 4 | 4 | 8 | 16 |
| Sr | 37 | 2909 | 339 | 434 | 553 | 717 | 908 |
| Ti | 1630 | 9800 | 4610 | 4459 | 5338 | 6530 | 7034 |
| U | 0.5 | 6 | 1 | 2 | 2 | 3 | 4 |
| V | 20 | 210 | 119 | 107 | 139 | 156 | 171 |
| W | 0.5 | 57 | 1 | 1 | 1 | 2 | 2 |
| Y | 6 | 35 | 15 | 15 | 17 | 20 | 22 |
| Zn | 11 | 650 | 90 | 103 | 124 | 161 | 187 |
| Zr | 102 | 367 | 184 | 194 | 211 | 251 | 265 |

In borehole 2, an interval of Au enrichment (130–295 ppb Au) occurs between 78.75 m and the base of the hole at 95.31 m in mainly andesitic agglomerates (Figure 6.27). Alteration in this borehole is dominantly sericitic, but argillic assemblages are locally important. Narrow zones of silicified hydrothermal breccias carry abundant disseminated and veinlet pyrite with traces of chalcopyrite and bornite, but with no attendant enrichment in Au. Minor tourmaline is also widespread in this borehole.

Borehole 5 yielded two anomalous samples, with 505 ppb and 143 ppb Au at 25.14–26.22 m and 46.91–48.21 m respectively (Figure 6.28). The upper interval is weakly enriched in As, Cu, Pb and Sb and is probably a minor fault zone. The lower interval contains high W (57 ppm) in addition to Au. Alteration and mineralisation in this borehole are generally weak, consistent with its location away from the main IP anomaly.

In borehole 7 low-tenor Au enrichment occurs in an upper agglomerate unit which also contains minor W. Most of the sequence of andesitic pyroclastic rocks and lavas in this borehole is strongly altered to quartz-sericite±chlorite±feldspar assemblages, locally overprinted by argillic alteration. Disseminated pyrite is widespread, while minor chalcopyrite and molybdenite occur locally in veinlets.

6.4.6. Alteration

All boreholes drilled in Borland Glen, with the exception of boreholes 5 and 6, intersected andesitic lavas and pyroclastic rocks that have been strongly hydrothermally altered. The main alteration is sericitic and consists of quartz-sericite-pyrite±carbonate-dominant assemblages. In local zones of hydrothermal brecciation the alteration is more intense and comprises strong silicification with the development of abundant pyrite, up to 35%. The agglomerates and breccia zones appear to have acted as preferred fluid conduits due to their high permeability relative to the lavas and, as a result, are more strongly altered and mineralised.

Hydrothermal alteration in Borland Glen was studied in this project by spectral analysis of drillcore from boreholes 1, 2, 5 and 7 using a Portable Infrared Mineral Analyser (PIMA) (Section 4.2). PIMA spectra were measured at intervals varying from a few metres to less than a metre, dependent on geochemical, mineralogical or lithological features of the core. Automated spectral analysis was carried out using The Spectral Geologist™ (TSG™) version 1.1 software package.

Summary logs for boreholes 2 and 5 are shown in Figures 6.29 and 6.30. The left-hand ‘Index’ column refers to the spectral file name which includes borehole number and depth. For example, BOR2_045 indicates a spectrum measured from borehole 2 at a depth of 4.5 m; BOR2_490 is from the same borehole at a depth of 49.0 m. The second column headed ‘Pet Code’ is a lithological code for which an explanation is given in Appendix 1. The third column shows stacked spectra, each represented as a colour bar, effectively providing an overview of the main downhole spectral variations in the wavelength range 1300 to 2500 nm. ‘TSA mineral1’ and ‘TSA mineral2’ are minerals identified by TSG using the Spectral Assistant™, a module of TSG used to automatically assess the likely mineral contributors to a spectrum, while ‘TSA Error’ gives an indication of the error associated with those identifications. In general the longer the error bar the less reliable the mineral identification. In such cases close examination of the spectra and comparison with reference-library spectra will be required to validate the mineral identification. Where a mineral identification is critical then corroboration by another method such as X-Ray Diffraction may be necessary.

The results show that kaolinite-dominant assemblages overprint earlier sericitic alteration (illite + muscovite) in the upper part of borehole 2 (Figure 6.29). The basal part of this borehole, below about 75 m, associated with Au enrichment is characterised by illite-muscovite- or chlorite-dominant alteration and lacks the kaolinite overprinting. The identification of dickite by TSG may not be reliable.

PIMA spectra for borehole 5 are illustrated in Figure 6.30. In the upper part of the borehole the spectra are dominated by either kaolinite and chlorite or illite and chlorite, representing respectively late clay and early sericitic alteration. In the lower section of the borehole, below about 30 m, the spectra are dominated by chlorite with local argillic alteration characterised by illite. Also shown in Figure 6.30 are magnetic susceptibility data

measured on the same drillcore specimens using a kappameter. The data, in 10^{-3} SI units, are shown both graphically and as numerical values in the two right hand columns headed 'Kappa'. Most values lie in the range $0.1-0.5 \times 10^{-3}$ SI, although in the upper, clay-altered interval they are generally less than 0.25. High values, up to 1.85, occur around 17–18 m in andesite lava that is relatively enriched in primary Fe-oxides. There are no particular spectral or magnetic features which characterise the gold-enriched intervals in this borehole.

PIMA analysis of drillcore from borehole 1 shows widespread propylitic alteration commonly overprinted by quartz-sericite-pyrite assemblages but without significant Au enrichment. Pink K-feldspar alteration occurs fairly widely in this borehole, as patches of new mineral growth, preferential clast replacements or marginal to quartz veinlets. K-feldspar also occurs sporadically in some of the other borehole sections. In general it appears to have developed at an early stage in the alteration history, possibly before the sericitic assemblages. Its occurrence correlates with an enhanced gamma count-rate in the downhole surveys carried out for the MRP.

Borehole 7 shows a generally similar pattern of alteration to boreholes 2 and 5. An upper kaolinite (\pm gypsum) zone, extending to a depth of about 42 m, overlies chlorite- and quartz-sericite-altered rocks, with local development of pink K-feldspar. The transition from the upper kaolinite zone is marked by a conspicuous downward increase in magnetic susceptibility from values less than 0.5×10^{-3} SI above to much higher values (up to 30×10^{-3} SI) below.

In addition to the pervasive alteration with associated abundant disseminated pyrite, thin fracture veinlets of quartz and/or calcite are common. Sphalerite, galena and molybdenite were recorded locally, mostly in or close to these veinlets. Vuggy veins of sparry calcite and quartz also carry minor amounts of baryte. Fibrous gypsum was recorded on a joint surface in one borehole, but PIMA analysis has indicated that gypsum is actually more widespread, mainly in association with the kaolinite-dominated clay alteration (Figure 6.29).

6.4.7. Discussion

The investigations carried out in Borland Glen have identified an area of epithermal alteration and mineralisation in a Lower Devonian sequence of subaerial andesitic lavas and pyroclastic rocks cut by high-level intrusions. Detailed paragenetic studies of the ore and alteration assemblages have not been carried out, so the history of the hydrothermal system is not fully established. However a model involving hydrothermal activity related to the high-level intrusions in an evolving calc-alkaline volcanic complex is suggested. Meteoric waters were focused along faults and permeable pyroclastic and breccia units, leading to the formation of the observed alteration and mineralisation.

Low-tenor Au enrichment has been identified in several boreholes associated with dominantly sericitic alteration and, in another borehole, along a minor fault zone. The controls on the gold distribution are unclear. Both surface and borehole evidence indicate the presence of a zone of intense hydrothermal alteration including early development of K-feldspar and quartz-sericite-pyrite-carbonate overprinted locally by kaolinite \pm gypsum. The predominance of sericitic alteration and the local illite-dominated argillic alteration indicate derivation from a low-sulphidation fluid. This is consistent with the occurrence of minor quantities of base-metal sulphides. The nature of the alteration and its association with base-metal sulphide mineralisation suggests that the present erosion level exposes a relatively deep level in the system, possibly more than 1 km below the palaeosurface. On the basis of models for low-sulphidation epithermal systems (section 3.2) any upper precious-metal-rich vein and stockwork ores would have been removed by erosion. Potential remains, however, for the discovery of underlying high-grade feeder veins and intrusion-related porphyry-style mineralisation.

The alteration style and zoning in Borland Glen may be compared with that described for gold-rich porphyry copper deposits by Sillitoe (1993b). In this setting early high-temperature K-silicate alteration is produced at deep levels. This passes outwards and upwards into intermediate argillic alteration comprising sericite, illite, smectite, chlorite and calcite. Sericitic alteration, comprising quartz-sericite-pyrite, typically occurs later in the development of the system in response to falling temperatures and ingress of cooler meteoric fluids.

The kaolinite-dominant alteration in the upper sections of some of the boreholes is probably the product of a late process, such as supergene oxidation, unrelated to gold mineralisation.

6.5. Geophysics

6.5.1. Magnetic and gravity features

The Bouguer gravity data for the northern part of the Midland Valley of Scotland are based on measurements made at a station density of about 1 km⁻². The Bouguer gravity anomaly map (Figure 6.31) shows minimum values of about -8 mGal a few kilometres offshore Methil. This reflects the effects of relatively low-density Namurian and Westphalian strata which extend to depths of about 2 km. Maximum Bouguer gravity anomalies occur around Kinghorn and the Burntisland volcanic centre, just south of Kirkcaldy, and can be related to a basement high. The gravity anomaly contours run approximately north-westwards from the north-east of the exposed Carboniferous volcanic rocks with a maximum horizontal gradient close to Dysart.

Secondary gravity lows occur over the Tillicoultry basin south of the Ochil Fault (OCF) and in the Firth of Tay between the North Tay Fault (NTF) and the South Tay Fault (STF). These anomalies are related in part to strata of the Stratheden and Inverclyde Groups (Upper Devonian-Carboniferous) which have low measured densities e.g. Knox Pulpit Formation, 2.41 Mgm⁻³; Kinneswood and Ballagan Formations, 2.47 Mgm⁻³ (Breerton et al., 1988).

Over the volcanic rocks of the Ochil Hills, minor positive residual gravity anomalies (Figure 6.32), derived from a regional field by upward continuation of the observed field by 2 km, occur in three areas: (i) associated with the Tillicoultry diorite; (ii) in the Borland Glen - Mellock Hill region and (iii) near the Glenfarg (Duncricvie) diorite. North of Cupar a residual gravity low is associated with minor outcrops of quartz-porphyry and some agglomeratic rocks.

Regional magnetic data have been collected along east-west flight lines approximately 2 km apart. Strong magnetic anomalies occur along the Highland Boundary Fault associated with the Comrie diorite intrusion [278 725] and near Blairgowrie (Figure 6.33). The latter anomaly is interpreted as due to magnetic basement beneath the Dalradian rocks of the Southern Highlands. The minor dioritic intrusions in the Ochil Hills volcanic terrain have susceptibilities of about 0.025 SI, while the andesitic lavas have susceptibilities up to about 0.02 SI. The diorites, especially at Tillicoultry, produce some localised anomalies in the residual magnetic anomaly map (Figure 6.34). At Glenfarg the diorites are partially surrounded by a thick basaltic lava flow which locally has a relatively high volume susceptibility (0.06 SI). This basalt is responsible for most of the features in this area of the magnetic anomaly map.

The aeromagnetic anomalies over the Carboniferous strata largely reflect the distribution of Dinantian volcanic rocks and associated quartz dolerite intrusions. The exposed parts of the quartz dolerite Midland Valley sill (susceptibility about 0.03 SI) produce localised high frequency anomalies indicative of shallow sources.

Occasionally similar anomalies are associated with minor intrusive teschenite or nepheline basanite bodies. Both of these sources could occur within the Devonian volcanic terrain.

6.5.2. Lineament analysis

Lineaments have been picked from colour and shaded relief images of the regional gravity and magnetic data (British Geological Survey, 1997 and 1998) and their derivatives (predominantly magnitude of the horizontal gradient) based on a grid of mesh size 0.5 km. These lineaments reflect alignment of anomalies, changes in the signature (frequency and amplitude) of the field and significant gradients in the data. In general, the lineaments reflect real variations in the density and magnetisation of the upper part of the crust and are therefore related to the geological structure. Landsat Thematic Mapper (TM) imagery has been interpreted to produce a lineament map for Northern Britain, with the aim of mapping any surface expressions of the structures. The data processing consisted of geometric correction to the British National Grid (BNG), edge-enhancement, contrast stretching and the writing of colour and black-and-white negatives. The black-and-white negatives consist of TM band 5 (1.55–1.65 micrometre) from the short-wave infrared region and were used to produce 1:250 000 scale photographic prints registered to BNG which were used for the lineament interpretation.

Gravity lineaments show significant populations at about 060° and 090° (Figure 6.35), while magnetic lineaments cluster at about 045° and 090° (Figure 6.36). Lineaments derived from analysis of a digital terrain model for the western and central Ochils cluster in three main groups: between 000° and 005°; 045°; and 130° (Figure 6.37). Landsat TM lineaments for the whole region have groupings at about 045°, 090°, 110° and 140° (Figure 6.38). The fault pattern based on 1:50 000 mapping over the northern part of the lava field only shows strong preferred orientations at about 020°, 090° and 130° (Figure 6.3).

The distribution of alluvial gold occurrences shows a general correlation with minor positive Bouguer gravity anomalies although no Au has been recorded close to the gravity anomaly associated with the Glenfarg diorite. Small local positive magnetic anomalies are associated with the Borland Glen gold occurrences but not all magnetic features have associated alluvial gold. There is a weak association with magnetic lineaments trending between north-west and west-north-west, and possibly with gravity lineaments trending north to north-east. The main zone of alluvial gold appears to be bounded by a pair of north-west lineaments which also link to mapped inflexions on the outcrop pattern of the lavas and are therefore considered to be fault structures (Figures 6.35 and 6.36). The inferred fault-controlled block with most of the alluvial gold occurrences includes the main outcrops of acid lavas on the northern margin of the volcanic terrain.

6.6. Data integration and prospectivity analysis

Key exploration parameters for analysis of the prospectivity for epithermal gold mineralisation in the Ochil and Sidlaw Hills were defined on the basis of published deposit models, on empirical observations of known mineralisation in the district and the availability of suitable multivariate digital data. Each parameter was assigned a zone of influence (number of cells), a style of influence (exponent) and a weighting (Table 6.5).

Fourteen parameters were considered in the analysis which used a pixel size of 250 m square. These include: bedrock geology; enrichment in a suite of trace elements in drainage geochemical data; presence of positive residual gravity and magnetic anomalies that may be related to high-level intrusions; and known mineral occurrences, including the distribution of gold in pan concentrates. Intersections of gravity or magnetic lineaments trending north-west (windowed between 290° and 340°) with any topographic or Landsat lineament

were also used to generate an event dataset used in the analysis. The distributions of these parameters in the area are shown in the multi-dataset maps (Figures 6.39, 6.40, 6.41 and 6.42).

Several geochemical parameters were used in this analysis. This has the effect of highlighting areas where sample density is greatest and where multiple-site multi-element anomalies were identified. Even though individual parameters are given a low weight the cumulative effect is to generate high prospectivity where follow-up MRP sampling was carried out. This effect has been reduced by using the 95th, rather than the 90th, percentile values as the anomaly thresholds for the MRP datasets. Selective or arbitrary exclusion of data points is considered inappropriate due to the effect on the data distributions and the risk of excluding critical anomalous values. For the only element (As) from the regional G-BASE data used in the analysis an anomaly threshold was set at the 90th percentile value.

Table 6.5 Index parameters used for prospectivity analysis, Ochil Hills

| zone of influence | exponent | weight | parameter |
|-------------------|----------|--------|--|
| 0 | 2.0 | 0.1 | andesitic lavas from 1:250K map |
| 2 | 2.5 | 0.2 | diorites from 1:50K maps |
| 0 | 2.5 | 0.1 | porphyry from 1:50K maps |
| 4 | 2.5 | 0.1 | occurrences of copper and lead minerals |
| 4 | 2.5 | 0.4 | alluvial gold occurrences |
| 4 | 2.5 | 0.2 | G-BASE stream-sediment data, As > 20 ppm |
| 4 | 2.5 | 0.1 | MRP panned-concentrate data, As > 31 ppm |
| 4 | 2.5 | 0.1 | MRP panned-concentrate data, Bi > 2 ppm |
| 4 | 2.5 | 0.1 | MRP panned-concentrate data, Sb > 11 ppm |
| 4 | 2.5 | 0.2 | MRP panned-concentrate data, Mo > 19 ppm |
| 4 | 2.5 | 0.1 | MRP panned-concentrate data, Ag > 7 ppm |
| 0 | 2.5 | 0.2 | residual gravity anomalies > 2 Mgal |
| 0 | 2.5 | 0.2 | magnetic residual > 50 nT |
| 4 | 2.5 | 0.1 | intersections of north-west gravity or magnetic lineaments with any topographic or Landsat lineament |

The prospectivity analysis was carried out using the Boolean logic data model normalised to produce a binary-weights-of-evidence map for the district (Figure 6.43). The main epithermal gold targets identified and their key features are summarised in Table 6.6.

This analysis has confirmed that the greatest potential exists along, and to the north of, Glen Devon in the western part of the central Ochils. The highest prospectivity occurs over an area of about 12 km², centred on Borland Glen, extending from there to the north and westwards towards Glen Eagles. This potential is derived from the occurrence of alluvial gold at many localities, coincident with geochemical anomalies for various

elements associated with epithermal gold. The favourable geological and structural setting derived from geophysical and geological evidence also make important contributions to the prospectivity. The Culteuchar Hill target area, about 12 km north-east of Borland Glen, is identified by the coincidence of several of the same parameters but lacks outcropping diorite and a positive gravity anomaly. The small target area on the Firth of Tay coast, about 10 km to the north of Cupar, is defined mainly on the basis of the occurrence of alluvial gold. However, associated corroborative evidence to support the presence of a bedrock source is lacking. The Tillicoultry area is favoured on geological and structural grounds, but its potential for epithermal gold mineralisation is relatively poor on account of the erosion level and the lack of favourable geochemical indicators, including the occurrence of alluvial gold.

Table 6.6 Main targets for epithermal gold, Ochil Hills

| Area | Centre | Approx size (km ²) | Geology | Drainage geochemical anomalies | Positive gravity anomaly | Positive magnetic anomaly | Faults & inter-sections |
|-----------------------------|------------|--------------------------------|--|--|--------------------------|---------------------------|-------------------------|
| Borland Glen and Glen Devon | 299 706 | 12 | andesite; diorites and minor porphyry intrusions | Au, Ag, Mo, As, Sb, Bi and alluvial gold occurrences | ✓ | ✓ | ✓ |
| Culteuchar Hill | 309 714 | 3 | andesite | Ag, Sb and alluvial gold occurrences | | ✓ | ✓ |
| Tay Firth coast | 335 724 | 3 | andesite | Ag, Sb and alluvial gold occurrences | | | ✓ |
| Tillicoultry | 293 698 | 2 | andesite, diorites, porphyry, minor intrusions | As and occurrences of Cu minerals | ✓ | ✓ | ✓ |

7. LORN PLATEAU

7.1. Geology

7.1.1. Introduction

Devonian rocks assigned to the Lower Old Red Sandstone megafacies were deposited in the Argyll Basin in the south-western part of the Highlands. The succession comprises mainly andesitic lavas of the Lorn Plateau which overlie Lower Devonian sedimentary rocks. Smaller areas of volcanic rocks of similar age are preserved at Glen Coe and Ben Nevis farther to the north-east. These comprise remnants of formerly much more extensive sequences of lavas, ignimbrites and sediments and are associated with ring structures, probably calderas.

The Lorn Plateau lavas form the largest area of Devonian volcanic rocks in the orthotectonic Caledonian belt of Scotland (Figures 7.1 and 7.2). They occupy an area of approximately 300 km² extending for about 25 km from the Pass of Brander in the north-east to the shores of Loch Melfort in the south-west. They form comparatively low ground, up to a maximum elevation of about 500 m, and give rise to a distinctive succession of scarped and terraced hills. The eruption of the basic and intermediate lavas overlapped with a minor suite of rhyolites, dacites

and ignimbrites, which are mainly exposed to the south of Loch Etive, in the north-eastern part of the Lorn Plateau, where they form flows no greater than 2 m thick.

K-Ar dating of the volcanic suite by Evans et al. (1971) gave an age of 394 ± 9 Ma. This was later revised by more extensive sampling which yielded K-Ar and Rb-Sr isochrons corresponding to 409 ± 13 and 401 ± 5 Ma respectively (Brown, 1975). Further revisions were made by Clayburn et al. (1983), at 400 ± 5 Ma using Rb/Sr whole rock analysis. This age is similar to the intrusion age for the probably genetically related Etive granites. However, more recent Ar-Ar studies by Thirlwall (1988) indicate an eruption age between 415 and 424 Ma, which is comparable with that of the lavas at Glencoe with which the Lorn Plateau lavas have been correlated. Thirlwall suggested that alteration associated with emplacement of the post-tectonic intrusions had reset the Rb/Sr isotope systematics of the volcanic rocks.

The dating by Thirlwall indicates that the Lorn Plateau lavas have a similar age to the Midland Valley volcanism. However, palaeomagnetic data indicates a single magnetic polarity for the whole Lorn sequence (Latham and Briden, 1974), in contrast to the several reversals evident in the Midland Valley (Sallomy and Piper, 1973). The Midland Valley polarity reversals indicate that volcanism in the area took place over a longer time span than the Lorn Plateau lavas. Indeed, the oldest horizons in the Midland Valley group have the opposite polarity to the Lorn sequence, suggesting that the onset of volcanism in the two areas was not synchronous.

The Dalradian metasedimentary strata underlying the Lorn Plateau are assigned mainly to the Easdale, Crinan and Tayvallich sub-groups of the Argyll Group. They comprise greenschist-facies pelites and psammites, with grits and limestones becoming important towards the top of the succession. Basic magmatism is an important component of the Tayvallich sub-group, represented by extensive developments of volcanic (Tayvallich Lavas) and subvolcanic rocks. On the eastern side of the Devonian outcrop, in the Loch Awe Syncline, the Tayvallich Lavas are overlain by psammites and slates of the Loch Avich Grit and the basaltic Loch Avich Lavas, which are assigned to the Southern Highland Group.

7.1.2. Devonian sedimentary rocks

The volcanic sequence of the Lorn Plateau rests on Lower Devonian sediments that contain fish fauna (Kynaston and Hill, 1908). A coarse conglomerate unit, approximately 30 m thick, of Upper Silurian to Lower Devonian age is overlain by Lower Devonian reddish and purple sandstones and shales. The generalised stratigraphy of the Lorn succession is summarised in Table 7.1.

The Lower Devonian volcano-sedimentary sequence rests unconformably on metamorphic rocks of the Dalradian Argyll Group. The Nant hydro-electric tunnel provides a near continuous sequence from the Devonian volcanic rocks at the south-eastern shore of Loch Nant [200 723] into the underlying Dalradian as far as Loch Awe [202 720] (Harris and Berridge, 1969).

The thick and distinctively coarse basal conglomerate of the Lower Old Red Sandstone is well exposed along the coastline around Oban and on the nearby island of Kerrera. It comprises boulders of olivine basalt and hornblende and biotite andesite, which locally exceed 1 m in diameter. Andesites derived from an earlier phase of volcanism are also present in the matrix. The variety and size of clasts present, apparently of restricted origin, suggest a mountainous and possibly glaciated source area, in which sediment input may have been triggered by tectonic activity.

Sedimentary breccias occur at a number of localities in the Oban–Kerrera area. They comprise generally angular clasts of quartzite and limestone, frequently within a matrix of smaller slaty fragments, and are interpreted as scree deposits laid down on the unconformable land surface of Dalradian rocks. The overlying basinward sequence comprises laterally discontinuous units of finer sediments (dominantly sandstone, with subordinate mudstone lenses). It is considered to be of local origin, deposited in shallow-water conditions in a small fault-bound basin. These closely resemble sediments of Lower Devonian age in the Midland Valley of Scotland, although deposition was not synchronous.

7.1.3. Volcanic rocks

Basic to intermediate lavas

The volcanic succession reaches a maximum thickness of approximately 800 m, although it gradually thins eastwards (Groome and Hall, 1974). It comprises a sequence of mainly basaltic and andesitic lavas, which are commonly porphyritic and vesicular, with subordinate rhyolitic ignimbrites and lavas. The lavas have a dominantly fresh and unaltered appearance and display little variation in texture on a gross scale. The succession of lavas dips gently and young towards the east-south-east. Individual basalt flows range in thickness from 5 m to 30 m, but restricted exposure allows them to be traced for only limited distances.

Table 7.1 Generalised stratigraphy of the Lorn succession in the Oban–Kilmore region (after Kynaston and Hill, 1908)

| <u>Lithology</u> | <u>Thickness</u> (metres) |
|---|------------------------------|
| Porphyritic hypersthene andesites, with some basic andesite flows | 90 – 120 |
| Basic andesites and basalt lavas, with occasional basic tuffs and agglomerates | 150 – 180 |
| Zone of red mudstones and sandstones with a thin concretionary limestone, locally developed, and underlain in places by tuffs and agglomerates | 10 – 12 |
| Basic andesite and basalt lavas and occasional basic tuffs and agglomerates | 120 |
| Zone of sandstone and red mudstones, and grey shales with plant remains (<i>Pachythea</i> sp., etc.) | 15 – 30 |
| Basic andesite lava flow | |
| Red and grey sandstones and shales with fossils, <i>Cephalaspis Lornesis</i> , <i>Mesacanthus mitchelli</i> , <i>Thelodus</i> sp., <i>Pterygotus anglicus</i> , <i>Kampecaris forfarenensis</i> , ostracods and plant remains | 15 – 30 |
| Coarse conglomerates with occasional sandstones and at least one lava flow. Clasts well rounded, up to 1 m diameter, consisting of quartzite, andesite, granite, porphyrite, epidiorite and various schists | 30 – 60 |

The main lava suite falls within the SiO₂ range 52 – 64 % (Fitton et al., 1982) and are essentially sub-alkaline (shoshonitic) in chemistry. It shows an AFM trend similar to those of other orogenic lava series (e.g. the Cascade Province). Overall the Lorn lavas are relatively richer in Sr, Ba, K, P and the LREE than the equivalent lavas in

the Midland Valley. Locally they are also enriched in Mg, Ni and Cr. Based on this geochemistry and associated isotope data, derivation from a mantle source with crustal contamination has been proposed (Groome and Hall, 1974; Thirlwall, 1981, 1982). Pyroclastic rocks are less common than in modern andesitic provinces, and are mainly represented by laharic deposits. However, the uniform appearance of the basalts and andesites belies their mineralogical variability, with over 30 different recognised phenocryst assemblages.

Fine-grained basalts, without conspicuous feldspar phenocrysts and with numerous small red pseudomorphs after olivine, are widespread (Lee and Bailey, 1925). They vary in texture from compact (generally dark grey in fresh section) towards the base of flows, passing upwards into slaggy, cavernous and sometimes flow-brecciated variants, which are somewhat purplish in colour. The cavernous portions of the lavas are frequently infilled with pale, sandy sediment which shows small-scale laminar bedding. Geikie (1897) and Kynaston and Hill (1908) suggested that these inclusions of sediment might indicate a sub-aqueous environment for extrusion of the lavas. However, the absence of meso-scale sub-aqueous features such as pillowing suggests that deposition took place in shallow water.

Basic andesites are well developed at a number of localities (Groome and Hall, 1974), including Cruach Airdenny [199 727], where they are generally fine grained and vesicular. The basic variants grade into the typical hypersthene andesites, which occupy a major part of the total outcrop of volcanic rocks, mainly in the centre of the volcanic plateau. They comprise plagioclase feldspar (andesine to oligoclase), which occurs as laths up to 0.3 mm in length, together with pseudomorphs after olivine, which frequently reach 1 mm in length. Common minor accessory constituents include apatite, and calcite and hematite (or other iron oxides) as secondary mineral phases.

Acid lavas

More evolved volcanic rocks occupy a small proportion (<2%) of the total volcanic outcrop (Figure 7.3). Typical exposures occur in Glen Nant [201 728] and Airds Park [198 732]. They comprise pale coloured, compact, cherty and flow-banded lithologies, possibly rhyolites or dacites, but without quartz phenocrysts. Other minor extrusive variants, including hornblende and mica andesites, are commonly associated with the acid lavas.

Ignimbrites, tuffs and agglomerates

These rocks form generally thin bodies outcropping over limited areas (Figure 7.3). They are poorly documented in the literature and generally not well defined on published maps. The most extensive areas of tuff, each occupying about 1.5 km², occur at Loch a Mhinn [187 713] and around Sior Lochs [197 723]. Discontinuous outcrops also occur in a north-east trending belt which stretches from Loch na Criathraich [196 720], through the Allt Coire Odhar area to the south-west of Loch Nant [197 723], to just east of Glen Nant [203 727].

The tuffs, mainly of andesitic composition, are generally poorly welded and have been divided into crystal and lithic variants (Kynaston and Hill, 1908). Two of these tuff horizons have been correlated with ignimbrites in Glencoe. Subordinate welded tuffs show strongly flattened pumice. A more acid type of tuff is exposed in the western portion of Benderloch, at Airds Point [198 732] and on Cruach Airdeny [199 727], south-south-west of Taynult. It has a compact flinty texture, and varies in colour from reddish-purple to pale yellow or grey. The matrix is mostly volcanic and is composed of minute sanidine, plagioclase, biotite and pseudomorphed amphibole. The lapilli are mainly andesitic, mostly of basic or pyroxene-bearing types. Locally, more acid fragments of felsite are common. Only rarely are fragments of schist or quartzite, derived from the underlying metasedimentary sequence, incorporated.

Agglomerates are rare, with the exception of the coastal section to the north-west of Gallanach Beg [183 728]. At this locality, a coarse dominantly basaltic agglomerate comprising unrounded blocks of basalt up to 2 m in size, within a matrix of water-rounded pebbles and cobbles, is exposed. Agglomeratic conglomerates also occur in an apparently higher horizon approximately 1 km to the south-east, immediately east of Gallanach Beg.

All volcanic rocks show some development of low-temperature secondary minerals in thin section, in particular chlorite, sericite, chalcedony and calcite. The alteration is more pervasive in the more permeable parts of the volcanic pile, particularly the pyroclastic rocks, although intense hydrothermal alteration of hypogene origin is uncommon. Such alteration in the north-east of the Lorn Plateau lavas is possibly due to the emplacement of the Etive (Ben Cruachan) Granite.

7.1.4. Intrusive rocks

Caledonian granites

Post-tectonic calc-alkaline intrusions are represented in the south-west Highlands by tonalite-granodiorite-granite complexes assigned to the Argyll Suite (Stephens and Halliday, 1984). In the Lorn district these include the Etive Complex and the Kilmelford Suite.

The Etive Complex is a post-tectonic composite pluton of elliptical shape, located at the north-eastern margin of the Lorn Plateau. It comprises three distinct phases: the earliest comprises several bosses and sheets of basic to intermediate material; the second, Cruachan phase, comprises monzodiorite to monzogranite; and the third, Starav phase, comprises a fine- to medium-grained monzogranite (Batchelor, 1987). The Cruachan body has been dated at 401 ± 6 Ma (Rb-Sr) and the Starav intrusion at 396 ± 12 Ma (Rb-Sr) (Clayburn et al., 1983). The complex is emplaced in Dalradian metasedimentary rocks within which a 2 km wide thermal aureole is developed. A shallow depth of emplacement, between 3 and 6 km, is inferred from the mineralogy developed in this aureole. The complex is characterised by a low initial $^{87}\text{Sr}/^{86}\text{Sr}$ ratio (around 0.705–0.706) which indicates a magmatic source with little input from Dalradian material.

In the Kilmelford district, located about 30 km south of Oban, small bodies of diorite, granodiorite, porphyrite and volcanic breccia outcrop over an area of 50 km² within the upper part of the Easdale Sub-group of the Argyll Group. Various exploration programmes have been carried out in this area, targeting mainly porphyry Cu-Au mineralisation (see below).

Minor intrusions

A major suite of late Caledonian dykes, termed the Etive dyke swarm, and is intruded widely into the Lorn Plateau lavas and the early plutonic phases of the Etive Complex (Figure 7.3). They comprise mostly north-east-trending porphyrites, composed of plagioclase phenocrysts (oligoclase to andesine), hornblende and rare biotite. Other subordinate members of the same suite include quartz-porphyries, lamprophyres and diorites, although these are only rarely found in the outcrop of the volcanic rocks.

The Etive dyke swarm has been divided into three classes: 1) those which cut all the pre-Starav plutonic phases, 2) those truncated by the Cruachan Granite and 3) rare microdiorites which, farther east, cut the margin of the Starav Granite (Speight and Mitchell, 1979). Analyses by Groome and Hall (1974) indicate that the porphyrites do not span the same compositional range as the lavas, and their silica content is restricted to between 63 and 70%. Furthermore, no connection is observed between any individual lava flow and these dykes.

Another suite of minor intrusions cutting the Lorn Plateau lavas comprises quartz-dolerites of Permo-Carboniferous age (Speight and Mitchell, 1979). These bodies are commonly oriented east–west. Tertiary intrusions related to the Mull centre are also widespread in the Lorn Plateau. They comprise mainly dolerite and basalt dykes trending north-west–south-east and are particularly abundant in the south-western part of the volcanic outcrop. Minor Tertiary volcanic vents and fissures also occur sporadically in the same area.

Several suites of appinite intrusions have been documented in the western Highlands. These include the complexes at Garabal Hill–Glen Fyne [390 717], Arrochar [388 708] and Rubha Mor (Ardsheal) [197 755], which have been dated in the range 422–427 Ma, similar to the age of the Lorn Plateau lavas.

7.1.5. Structure

The Dalradian strata of the south-west Highlands are disposed in large recumbent folds (Figure 7.4). The lower limbs of many of these folds are partly excised by low-angle extensional faults, termed ‘slides’. These folds diverge on either side of the early, upward-facing, Loch Awe Syncline (LAS). This structure appears to be dislocated between Loch Avich and Loch Awe with an inferred dextral offset of the axial trace by about 2.5 km. South-east of the LAS the Ardrishaig Anticline (ADA) is interpreted as the core of the large south-east-facing Tay Nappe (TN) which covers most of the south and south-east Highlands. Much of the Tay Nappe is flat lying and exposed at a level such that most of the strata form part of the lower inverted limb. Farther south-west in Knapdale, in the core of the Tay Nappe, the strata are not regionally inverted and the fold axial planes dip to the north-west. Near the Highland Boundary, the Tay Nappe lags downwards to form a synformal anticline, the Aberfoyle Anticline, which is downward-facing.

North-west of the LAS the large north-west upward-facing Islay Anticline exposes quartzites, marbles and schists of the Appin Group on Islay with an envelope of Argyll Group quartzites (Islay Quartzite). The western limb of the Islay Anticline is cut by the Loch Skerrols Thrust and underlain by the deformed Bowmore Sandstone, considered to be part of the Dalradian sequence (Fitches and Maltman, 1984).

Various features of the regional geophysical data for the south-west Highlands are consistent with this generalised structural model. The Tayvallich Subgroup of the Argyll Group consists in the type locality of dark oolitic limestones and phyllites overlain by up to 2000 m of submarine spilitic basalts. Further north–east the Tayvallich and Loch Avich Volcanic formations are part of the Southern Highland Group and consist predominantly of a contemporaneous basalt–dolerite–gabbro intrusive sill complex. The sill complex forms most of the meta–igneous amphibolites present in the Loch Awe region. These are relatively poorly magnetic (<0.003 SI) and do not produce significant aeromagnetic anomalies. In contrast, the spilitic parts of the formation are significantly magnetic and south-west of Tayvallich are associated with prominent aeromagnetic anomalies of over 400 nT.

The Devonian lavas of the Lorn Plateau unconformably overlie the Dalradian sequence, occupying a position approximately between the Islay Anticline and the Loch Awe syncline (Figure 7.4). They comprise a volcanic pile up to 800 m thick which dips gently towards the east-south-east. Vent agglomerates, tuffs and acid lavas are of relatively minor importance. The lavas may have been sourced from large vents or fissures now invaded by the late Caledonian granites of Etive, Glencoe and Nevis.

Various faults and lineaments identified in geophysical and remotely-sensed images cut the Devonian succession of the Lorn Plateau. These are discussed in Section 7.4.

7.2. Mineralisation

There are few reported occurrences of metalliferous mineralisation in the Devonian volcanic rocks of the Lorn Plateau). Gold grains have been recorded in pan concentrates collected during drainage geochemical surveys conducted by BGS at two localities (Figure 7.1). In the vicinity of Strontoiller [190720 728890], gold grains were reported from the River Lonan at a site associated with low-tenor enrichment in Cu, Sb and Sn. The second occurrence is at Allt Mor [195730 711410], just south of the southern edge of the outcrop of the Lorn Plateau lavas.

The identification by the MRP of extensive hydrothermal alteration in the Lower Devonian Kilmelford intrusive suite (Ellis et al., 1977) (Figure 7.1), immediately south of the Lorn Plateau, stimulated several commercial exploration programmes in the 1970s and early 1980s which targetted porphyry-style base- and precious-metal mineralisation. This resulted in the discovery of significant gold mineralisation in the Lagalochan sub-volcanic complex at the eastern end of the Kilmelford centre (Kay, 1985; Zhou, 1987a, 1987b, and 1988; Harris et al., 1988).

The Lagalochan felsic porphyry-breccia complex is thought to represent the basal sections of a vented diatreme-type structure that was emplaced by hydrovolcanic activity probably around 430 Ma. The intrusive activity at Lagalochan was accompanied by base- and precious-metal mineralisation and multiple phases of hydrothermal alteration. The first major stage of mineralisation comprised Cu-Mo-Au in veinlets and disseminations within a central core of breccias and diorite to granodiorite intrusions of calc-alkaline type in the North Hill section of the prospect. A zoned, shear-related Pb-Zn-Ag-Au-As-Sb assemblage is developed around this central core with the best ore intersections found in the south-eastern part of the prospect, known as the south-east Quadrant. The final phase of mineralisation is represented by a suite of Pb-Zn-Ag carbonate veins. Gold is concentrated mainly in the early-stage core with Cu-Mo, but there is sporadic enrichment in the south-east Quadrant associated with elevated As levels. Hydrothermal alteration is widespread, its intensity reflecting the degree of fracturing in the rocks. Sericite-quartz-pyrite and carbonate alteration affects almost all rocks, while K-silicate alteration assemblages, mainly the development of secondary biotite and orthoclase, are locally present. Late-stage propylitic and phyllic alteration are locally weakly developed. Visible gold was not observed in outcrop or drill core but was discovered, by electron microprobe analysis, as irregular inclusions and veinlets in pyrite and, more rarely, in chalcopyrite. Associated sulphides include galena, sphalerite and tennantite.

The site of intrusion of the Lagalochan complex was controlled by the intersection of two important faults: the east-north-east-trending Gleann Domhain fault and a large-scale north-north-east-trending fault with a movement history spanning intrusion. The latter fault cuts through the centre of the mineralised zone and has down-faulted the eastern block. This accounts for the presence of a high-level freibergite-bearing shear zone in the south-east Quadrant and indicates potential for additional North Hill-type mineralisation at depth. The east-north-east-trending Gleann Domhain fault is a deep, regional Caledonian structure and was probably fundamental in controlling the location of the complex. A series of mineralised north-east-trending faults are locally intruded by post-mineralisation, red-brown porphyry dykes.

The currently explored portions of the Lagalochan complex are interpreted as the basal sections of a vented phreatomagmatic event that was complexly intruded by stocks, dykes, sheets and breccia bodies. The evidence from isotope and fluid inclusion studies (Kay, 1985) indicates that the Cu-Au-(Mo) mineralisation intersected by drilling in the North Hill area was deposited by magmatic, hypersaline, boiling fluids at temperatures in excess of 400°C, which had equilibrated with magma. The peripheral Pb-Zn-Ag-Au-As-Sb suite and the later carbonate-

hosted Pb-Zn-Ag veining probably represent later; lower-temperature events derived from lower-salinity fluids, including a probable meteoric component, in a higher-level epithermal setting.

The mineralisation at Lagalochan has many features characteristic of a sub-volcanic porphyry system, including the element-zoning patterns, alteration assemblages and style of mineralisation. It is proposed that a resurgent, highly active Caledonian sub-volcanic complex was operative at Lagalochan, possibly centred on the Cu-Au-(Mo) hydrothermal system at North Hill. Calculations based on the isotope data of Kay (1985) indicate that about 1000 m of the porphyry system has been removed by erosion, limiting the potential for the discovery of bonanza-type epithermal precious-metal mineralisation. However, potential exists for the occurrence of epithermal gold mineralisation overlying similar intrusive centres beneath the Lorn Plateau lavas to the north.

Investigations carried out by BGS in the 1970s identified small-scale porphyry-copper mineralisation in the Beinn nan Chaorach intrusion [181 710] of the Kilmelford suite (Ellis et al., 1977). This composite body comprises a non-porphyrific, largely unmineralised, granodiorite and a younger suite of mineralised porphyritic dacite and intrusive breccias. The dacite porphyry is extensively altered to sericite and kaolinite, with secondary biotite locally developed. Sulphide mineralisation, comprising pyrite with subordinate chalcopyrite and minor molybdenite, locally reaches 5% by volume. Minor disseminated arsenopyrite occurs in the sericitised lithologies and in Pb-Zn-bearing veins located marginal to the main area of mineralisation. Limited diamond drilling identified Au concentrations up to 0.4 ppm in a small suite of samples.

In 1984 BP Minerals undertook further exploration at Beinn nan Chaorach. Anomalous base- and precious-metal values identified in stream sediments were followed up by soil sampling. Local coincident concentrations of up to 555 ppb Au and 13 ppm Ag were identified in this survey. Harris (in Patrick and Polya, 1993) reported up to 6.5 ppm Au in sphalerite- and galena-bearing veins peripheral to the main mineralised area at Beinn na Chaorach.

MRP investigations in the Etive Complex identified minor molybdenite, chalcopyrite and scheelite mineralisation, mainly in quartz veinlets, in the Starav intrusion (Haslam and Cameron, 1985). The host rock is a weakly altered monzogranite, but there is no evidence for extensive alteration such as might be produced by a major porphyry or epithermal system. A drainage geochemical survey conducted in the same programme did not provide evidence for metallic mineralisation elsewhere in the Etive Complex.

Copper mineralisation has also been documented in the late Caledonian appinite complex at Ardsheal, about 30 km north-north-east of Oban (Rice and Davies, 1979). High Cu grades, up to 5.8%, have been reported in chalcopyrite- and pyrite-bearing float boulders from the appinite breccia pipes, while similar mineralisation in bedrock comprises low grade copper as veins and disseminations in a propylitically altered host. Stockwork mineralisation comprising veinlets of quartz, pyrite, molybdenite, chalcopyrite and minor tetrahedrite and scheelite has been reported in the Ballachulish intrusion, a few km east of Ardsheal (Haslam and Kimbell, 1981; Haslam, 1986).

7.3. Geochemistry

7.3.1. Introduction

The Lorn Plateau has been covered by various drainage geochemical surveys conducted by both public-sector and commercial organisations. Most of these targeted base metals, and samples were analysed for a limited range of elements. The most extensive coverage is provided by the BGS regional geochemical survey (G-BASE) over the Argyll map sheet (British Geological Survey, 1990). Detailed follow-up surveys were carried out by BGS

under the MRP over the Kilmelford–Lagalochan area (Ellis et al., 1977) and parts of the Lorn lavas (J.S. Coats, pers. comm.).

For the current project, data were extracted from the BGS UK Geochemical Database for the area bounded by National Grid Eastings 175000 and 210000, and Northings 700000 and 745000 (a total of 1575 km²). For G-BASE a total of 1102 stream-sediment and panned-concentrate samples were collected from this area, but only the stream-sediment samples were analysed (Figure 7.5). With the exception of U, As and Sb, all elements were determined by direct-reading emission spectrometry (OES). Arsenic and Sb analyses were carried out on samples from 50% of the sites using solvent-extraction atomic absorption spectrophotometry (AAS), and for U by the delayed neutron method. Summary statistics for selected elements are presented in Table 7.2.

MRP investigations for base metals in the late 1970s involved local detailed surveys over the Lorn lavas and adjacent areas considered favourable for metalliferous mineralisation. Coverage of the Lorn Plateau lavas is therefore patchy and incomplete (Figure 7.6). The stream-sediment samples were analysed for Ba, Fe, Mn, Mo and Sn by OES and Ag, Cu, Ni, Pb and Zn by AAS (Table 7.3). Data for 12 elements determined by XRF in panned-concentrate samples are summarised in Table 7.4. Gold analyses were not carried out on these samples. Summary statistics for selected elements are presented in Tables 7.3 and 7.4.

7.3.2. Results

Antimony (Sb): G-BASE data indicate very low background levels of Sb, with 99.5 % of values falling below the analytical detection limit of 0.5 ppm (Figure 7.7). Slight enhancement, up to 3 ppm, occurs in the Kilmelford–Lagalochan area, where samples are also enriched in Pb, Zn, As, Bi and Mo. In general, however, the low sensitivity of the analytical method used restricts the value of the data over the Lorn lavas.

Table 7.2 Summary statistics for G-BASE stream-sediment samples, Lorn Plateau
(all values in ppm)

| Element | no. samples | mean | minimum | maximum | 50% | 75% | 90% | 95% |
|---------|-------------|---------|---------|---------|-------|-------|-------|-------|
| As | 661 | 10 | 2 | 160 | 5 | 10 | 20 | 30 |
| Bi | 1095 | 1.3 | 0.2 | 60 | 0.2 | 1 | 4 | 6 |
| Cu | 1101 | 29 | 1 | 599 | 25 | 36 | 49 | 62 |
| Fe | 1012 | 63101.8 | 10771 | 99804 | 63436 | 76724 | 86376 | 91412 |
| Mn | 1095 | 5625.4 | 68 | 76000 | 3079 | 5800 | 11500 | 19400 |
| Mo | 1095 | 0.4 | 0.1 | 15 | 0.1 | 0.1 | 0.1 | 2 |
| Pb | 1092 | 41.7 | 1 | 1197 | 30 | 46 | 71 | 96 |
| Sb | 1101 | 0.2 | 0.2 | 3 | 0.2 | 0.2 | 0.2 | 0.2 |
| Zn | 1100 | 230.4 | 18 | 1635 | 185 | 284 | 423 | 573 |

Table 7.3 Summary statistics for MRP stream-sediment samples, Lorn Plateau
(all values in ppm)

| Element | no. samples | mean | minimum | maximum | 50% | 75% | 90% | 95% |
|---------|-------------|---------|---------|---------|-------|-------|-------|-------|
| Ag | 560 | 0.9 | 0.1 | 2 | 1 | 1 | 1 | 1 |
| Ba | 562 | 866.5 | 195 | 6270 | 697 | 980 | 1400 | 1870 |
| Cu | 560 | 33.4 | 5 | 790 | 25 | 40 | 55 | 65 |
| Fe | 562 | 67335.1 | 17400 | 132000 | 65900 | 77700 | 86700 | 92800 |
| Mn | 562 | 9552 | 690 | 138000 | 5200 | 9950 | 19500 | 30100 |
| Mo | 562 | 0.4 | 0.1 | 5 | 0.1 | 1 | 1 | 2 |
| Pb | 560 | 39.8 | 10 | 550 | 30 | 40 | 60 | 70 |
| Sn | 562 | 1.4 | 0.5 | 48 | 0.5 | 0.5 | 3 | 6 |
| Zn | 560 | 328 | 30 | 15600 | 200 | 310 | 480 | 600 |

Table 7.4 Summary statistics for MRP panned-concentrate samples, Lorn Plateau
(all values in ppm)

| Element | no. samples | mean | minimum | maximum | 50% | 75% | 90% | 95% |
|---------|-------------|---------|---------|---------|-------|--------|--------|--------|
| Ca | 564 | 26161.3 | 3190 | 88110 | 22450 | 38710 | 49940 | 55510 |
| Ti | 564 | 13805.8 | 3340 | 79300 | 11590 | 15830 | 22110 | 28560 |
| Mn | 564 | 1469.5 | 300 | 8000 | 1320 | 1810 | 2360 | 2800 |
| Fe | 564 | 95547.9 | 12470 | 285190 | 90490 | 110240 | 134940 | 155170 |
| Ni | 564 | 86.4 | 4 | 526 | 72 | 100 | 135 | 173 |
| Cu | 563 | 51.4 | 2 | 5080 | 26 | 38 | 57 | 89 |
| Zn | 564 | 175.7 | 6 | 3957 | 148 | 189 | 254 | 299 |
| Sn | 563 | 7.5 | 0.5 | 1658 | 1 | 3 | 6 | 8 |
| Sb | 557 | 1.8 | 0.2 | 75 | 0.2 | 2 | 5 | 7 |
| Ba | 564 | 5490.1 | 27 | 181300 | 583 | 1260 | 11100 | 28100 |
| Ce | 530 | 39.1 | 0.5 | 130 | 37 | 49 | 64 | 77 |
| Pb | 562 | 47.1 | 1 | 2493 | 16 | 23 | 54 | 163 |

For the MRP surveys, Sb data are available only for the panned concentrates and not for the stream sediment samples (Figure 7.8). Low-tenor enrichment, within the range 5–10 ppm Sb, occurs sporadically although there is no general correlation between Sb and other chalcophile elements. Locally, however, Sb anomalies are accompanied by enrichment in other elements. For example, the highest Sb value of 75 ppm, derived from the north-eastern end of Loch Feochan [186 723], is accompanied by enrichment in Pb (1011 ppm). The second-highest Sb value (24 ppm), from the Loch Nell area [190 728], is accompanied by elevated Cu (407 ppm), Sn

(325 ppm) and Ba (1732 ppm). The third-highest Sb value (23 ppm), also located in the central-western part of the volcanic outcrop [190 724], has attendant enrichment in Sn (93 ppm).

Arsenic (As): low As values are present in G-BASE data over the Etive Complex and the Lorn lavas (Figure 7.9). Markedly higher levels occur over the Dalradian Argyll Group metasedimentary rocks to the south-east. The highest As contents occur on the north-east flank of the Lorn Plateau, between Loch Etive and Loch Creran. Here a zone of elevated As follows the fault-bounded western margin of the Etive Granite, largely in an area underlain by metasediments of the Islay Subgroup.

The late Caledonian Kilmelford Complex [184 710] is identified by many high As values in the G-BASE data. The highest values are confined to the area of subvolcanic intrusives and their immediate country rocks and do not extend northwards into the volcanics. However, there is low-tenor enrichment (>20 ppm) in the southern half of the Lorn lavas, with sporadic elevated values around Loch Scammadale [187 721] and along the eastern edge of the volcanics around Carn Dearg [199 722].

No data for As are available from the MRP surveys carried out in this district.

Barium (Ba): G-BASE stream sediment data indicate uniform Ba levels over the Lorn lavas. Field observations of baryte in pans indicated the presence of minor baryte mineralisation in association with the acid lavas, particularly where they are cut by north-east trending faults.

These baryte occurrences, followed up by detailed MRP surveys, are associated with an east-north-east-trending linear zone of elevated Ba in both panned concentrates and stream sediments, centred around Beinn Ghlas-Loch Nell [196 726]. Visual observation of abundant detrital baryte in panned concentrates corroborates the geochemical results. A smaller zone, with anomalous Ba values in stream sediments only, is located south-west of Loch Scammadale [184 716].

Bismuth (Bi): Bi values over the Lorn lavas in the G-BASE data are generally below detection limit, although minor enrichments occur in the tract around Loch Nell and Beinn Ghlas, and sporadically north-eastwards from there (Figure 7.10). The highest Bi value (60 ppm) occurs adjacent to the margin of the Etive Complex. Arsenic (45 ppm) and Mn (35400 ppm) are enriched at the same locality. A similar As-Bi-Mn association is present in several other samples from the same area. Bismuth and As enrichment is also locally accompanied by elevated Mo: for example at two sites in the upper part of the Gleann Dubh catchment, [201 742]. Sporadic Bi enrichment also occurs along the southern margin of the volcanics and in proximity to the Kilmelford intrusive suite.

Copper (Cu):— In the G-BASE dataset, moderate- to low-tenor Cu values (25–50 ppm) occur over most of the Lorn lavas (Figure 7.11). Copper levels are generally higher in the south-western part of the lavas compared to the north-east. An east-south-east-trending zone of elevated values transects the area, centred on Loch Scammadale and Bragleenbeg [189 720]. To the south of the volcanic outcrop anomalous Cu values, locally exceeding 100 ppm, occur over the Kilmelford–Lagalochan area. A wide range of Cu values occurs over the large, composite Etive pluton, with isolated medium-tenor Cu over the outer, earlier tonalitic components of the intrusion, and low values over the more evolved central core.

Copper values in the MRP stream sediment data over the Lorn lavas are similar to those in the G-BASE dataset, with a zone of elevated Cu occurring in an east-south-east-trending zone around Loch Scammadale [189 720]. MRP panned concentrate data show enrichment in Cu around Beinn Ghlas and Loch Nell, associated with high

Ba values (Figure 7.12). Elevated Cu values are also present in both stream sediments and panned concentrates along the fault which transects the Lagalochan Complex and about 7 km to the north-north-east along the same fault at Bragleenbeg.

Lead (Pb): A multiple-site high-tenor Pb anomaly is present in the G-BASE data in the Kilmelford–Lagalochan area, with a number of values exceeding 300 ppm (Figure 7.13). Concentrations over the Lorn lavas are generally low, although there is sporadic medium-tenor enrichment in the north-east of the outcrop and a single high value (316 ppm) about 3.5 km to the north of Bragleenbeg [190 723]. Slight enrichment also occurs marginal to the Etive Complex, along the line of the Glen Creran slide and the Glen Salach Fault, in the north-east of the map area.

Lead concentrations in the MRP stream-sediment data are slightly enhanced over the central part of the volcanic outcrop, particularly around Beinn Ghlas [195 726].

Sporadic medium-tenor Pb enrichment (>1000 ppm) in MRP panned concentrates is associated with enhancement in a suite of elements indicative of possible sulphide mineralisation, including Cu, Sb, Zn, Ba and Sn (Figure 7.14). In the Bragleenbeg area, around [190 719], several sites close to the mapped north-north-east-trending fault extending from Lagalochan are enriched in these elements. A second area of Pb enrichment occurs along the south-eastern shoreline of Loch Feochan [186 723], where locally elevated Pb levels are associated with high Sb values. A third area of Pb enrichment occurs around the acid volcanics to the north-east of Beinn Ghlas. Field observations from this area indicate the presence of galena, locally with baryte or pyrite, in heavy-mineral concentrates.

There is generally a poor correlation between the Pb contents of panned concentrates and stream sediments. Many of the sites where galena was observed during panning and where high analytical Pb values were reported in concentrates do not contain high Pb values in stream sediments. It is clear therefore that Pb levels in stream sediment samples do not provide a good indication of the presence of base-metal mineralisation in the Lorn lavas.

Molybdenum (Mo): Mo values in G-BASE data reach a maximum of 15 ppm over the Kilmelford intrusive suite (Figure 7.15). High values also occur widely over the Etive Complex. Over most of the Lorn lavas Mo values are below the detection limit of 0.1 ppm. Sporadic minor enrichment up to 4 ppm Mo occurs in the vicinity of Loch Scammadale and Beinn Ghlas. In the MRP stream sediment data several clusters of weakly anomalous Mo values occur in the central and southern parts of the volcanic outcrop.

Silver (Ag): data are available only for MRP stream sediments. Most reported values are close to or below the analytical detection limit, with a maximum of only 2 ppm Ag. There is therefore no evidence in these data of significant Ag enrichment in the area.

Tin (Sn): in the G-BASE dataset elevated Sn is associated with the more evolved Starav intrusion of the Etive Complex. The regional data also indicate locally enhanced levels within the tract of ground to the north of Glen Lonan [194 727], running roughly parallel to Loch Etive to the north.

High Sn values are present in MRP stream sediments over sporadic zones of the lava outcrop (Figure 7.16). The most conspicuous anomaly occurs between Loch Scammadale [185 722] and Loch Feochan [186 724] where several sites have high Sn levels in sediments and sporadic high values in concentrates. In the Strontoiller area [190 728], north-east of Loch Nell, high Sn values are present in both panned concentrates (105–325 ppm) and

stream sediments (17–48 ppm) from the MRP surveys. The elevated Sn values in this area are accompanied by local enrichment in Cu and Sb. A gold grain was also observed during panning in this area. Elevated Sn values also occur in the Beinn Ghlas area and around Bragleenbeg.

Zinc (Zn): levels are generally high over the volcanic rocks of the Lorn Plateau (Figure 7.17). The G-BASE data show a slight enhancement in the south-east of the outcrop, which is consistent with partitioning of Zn into lavas of intermediate composition, possibly the hypersthene andesites. The clustering of low- and medium- tenor Zn values in the central and northern parts of the Lorn Plateau may reflect variations in lithology, with the samples from more evolved volcanics having lower Zn levels than those of intermediate to basic composition.

Very high Zn values (15600 and 12000 ppm) occur in the MRP stream-sediment data at two sites in the vicinity of Loch Avich House [193 715], close to the south-eastern margin of the volcanic outcrop. The corresponding panned concentrates from the same sites have no Zn enrichment, indicating that this element occurs in a fine-grained phase, possibly co-precipitated on amorphous Mn oxides.

7.3.3. Discussion

The distributions of major and trace elements in drainage geochemical samples from archived records provide important information on the geology and mineral potential of the Lorn Plateau. Various elements, Ca, Mg, Fe, Cr, Ni, Co and Zn, reflect mainly primary lithological variations within the Lorn volcanic sequence. The least evolved lavas, in the south-west of the outcrop, are characterised by relative enrichments in Cr, Ni, Co, Fe, Mg and Zn, together with relatively low levels of Ca. Towards the central and northern parts of the outcrop these patterns are reversed.

The distribution patterns of other elements in the drainage geochemical datasets provide information on the possible location of metalliferous mineralisation. By virtue of its near-uniform cover of the entire area, the G-BASE stream-sediment data are most useful. The utility of the MRP datasets for prospectivity mapping is limited by their restricted areal coverage.

The known mineralisation associated with the Caledonian intrusive suite at Kilmelford, including porphyry-epithermal Cu-Mo-Au mineralisation at Lagalochan, is identified by anomalous values of Cu, Mo, As, Pb, Bi, Sb and Zn in stream sediments. Restricted panned concentrate cover in the Kilmelford area indicates anomalous levels of Sb, Pb and Zn. Several areas characterised by enrichment in various elements indicating the possible presence of base-metal and/or gold epithermal mineralisation have been identified over the Lorn Plateau lavas (Table 7.5).

Table 7.5 Main geochemical anomalies over the Lorn Plateau lavas

| Area | Centre | Anomalous elements in stream sediments | Anomalous elements in panned concentrates |
|-------------------------|---------|--|---|
| Kilmelford – Lagalochan | 187 712 | As, Bi, Cu, Mo, Pb, Sb, Zn | Pb, Sb, Zn |
| Bragleenbeg Fault | 191 720 | Bi, Cu, Sn | Cu, Pb, Sb, Sn |
| Scammadale – Feochan | 187 722 | As, Ba, Cu, Mo, Zn | Ba, Pb, Sb |
| Beinn Ghlas | 195 726 | Bi, Mo, Sn | Ba, Cu, Pb, Sb, Sn |
| Gleann Salach | 196 738 | Bi, Pb, Zn | no data |
| Loch Nell | 190 729 | Bi, Cu, Sn | Ba, Cu, Sb, Sn |

7.4. Geophysics

The Lorn Plateau Lavas occupy a significant position in the geophysical map of Scotland. They lie across the Cruachan Lineament, which is one of the main ‘lineaments’ thought to have affected the tectonic and structural development of the Highlands from Vendian time and possibly developed on an earlier Proterozoic structure. It approximately defines the south-western limit of the Grampian Group and late major granites and the north-eastern limit of abundant Tertiary dykes.

7.4.1. Magnetic features

A strong north-west-trending magnetic fabric crosses the Lorn Plateau lavas and continues across the main outcrop of Dalradian Tayvallich Subgroup between Loch Awe and Tayvallich (Figure 7.18). This is associated with numerous Tertiary dykes and is evident in the residual magnetic anomaly map (Figure 7.19). However, local positive magnetic features near the Kilmelford granite-porphry complex and at the Furnace porphyry intrusion [ca. 203 700] are probably caused by intrusive rocks. The magnetic Avich lavas south-west of Tayvallich have a localised strong magnetic anomaly. Susceptibility sampling of parts of the subgroup close to Loch Awe identified no significant magnetisation although the TMI data suggest zones of magnetic material between Loch Avich and the southern part of Loch Awe.

Significant minor magnetic anomalies are evident in the TMI data (Figure 7.18). The most extensive anomaly occurs over the eastern side of the Kilmelford granodiorite extending towards the Lagalochan Complex. A similar anomaly occurs 7–8 km to the north-north-east around Bragleenbeg, just north of Loch Scammadale adjacent to a mapped fault which extends from Lagalochan. A series of small positive anomalies extending across the lavas west of Loch Scammadale are probably related to Tertiary dykes. Significant magnetic anomalies are also associated with the marginal dioritic phases of the Etive Granite.

Another important magnetic anomaly occurs over the main outcrop of Tayvallich Subgroup on the south east side of Loch Awe [203 718]. In this region a semi-annular positive anomaly of up to 150 nT has a matched negative on the north side and is close to mapped basalt dykes in the core of the Loch Awe syncline. This anomaly might reflect magnetic lavas within the Tayvallich Subgroup but this has not been tested on the ground. An alternative explanation involves a buried diorite mass, possibly part of the Kilmelford suite, displaced about 15 km by sinistral movement on the Ericht–Laidon Fault (ELF). This suggests that epithermal or porphyry-style mineralisation similar to that at Lagalochan–Kilmelford might be present at depth on the east side of Loch Awe.

7.4.2. Gravity features

Assessment of the role and significance of the Cruachan Lineament is complicated by the positional uncertainty of the underlying structure. In the south-west Grampians, Hall (1986) places the Cruachan Lineament through Loch Lomond and the south of Lismore, trending 130°, approximately along the zero Bouguer gravity anomaly contour for a reduction density of 2.70 Mgm⁻³. Graham (1986) defines a zone about 10 km wide, trending 120°, centred on the Pass of Brander. Fettes et al. (1986) mark the lineament through the centre of Lismore trending about 120°.

To the south-west of the Cruachan Lineament the Bouguer gravity field (Figure 7.20) is generally positive reflecting either the bulk effects of Tertiary dyke intrusion (Hipkin and Hussain, 1983) or a thicker Dalradian sequence with mafic sills and basic volcanic rocks developed on a thinned crust (Hall 1985). The Cruachan Lineament may mark a change in basement type (Graham 1986) although there is no clear evidence for this from the magnetic data (Figure 7.18).

The Cruachan Lineament extends south-eastwards as far as the Highland Boundary (Hall 1986) and may even continue across the Midland Valley (Hipkin and Hussain, 1983). The most prominent geophysical expression of the lineament is a broad gravity gradient trending 130°, passing through Oban. Truncation of a strong north-east-trending lineament in the gravity data through the Tayvallich lavas just east of Loch Awe might be related to the underlying structure. The inferred north-west-trending Vendian rifting associated with the Tayvallich Volcanic Formation has a similar orientation to pre-Torridon Group structures in the northern Highlands. Subsequently the Cruachan Lineament appears to have influenced post-tectonic intrusion, Devonian volcanic activity and Tertiary intrusion.

A ridge in the gravity field over the Tayvallich Subgroup on the south side of the ELF can be traced to the north-east and is conspicuous on the residual gravity anomaly map (Figure 7.21). It is therefore suggested that the gravity and magnetic anomalies in this area might have a common source and be related to petrological variations in the Tayvallich Subgroup.

On the main outcrop of lavas a small trough in the Bouguer gravity anomaly map (Figure 7.20), extending south-west from Bragleenbeg, suggests a residual gravity low. The residual gravity map shows this to be in a similar position to a residual positive magnetic anomaly (Figures 7.21 and 7.19). These anomalies are in a similar structural position to the Lagalochan Complex and might represent an intermediate intrusion into or beneath the lava field, possibly with associated metallic mineralisation.

7.4.3. Lineament analysis

Lineaments have been picked from colour and shaded relief images of the regional geophysical gravity and magnetic data (British Geological Survey, 1997 and 1998) and their derivatives, based on a grid of mesh size 0.5 km (Figures 7.22 and 7.23). These lineaments reflect alignment of anomalies, changes in the signature (frequency and amplitude) of the field and significant gradients in the data. In general, the lineaments reflect real variations in the density and magnetisation of the upper part of the crust and are therefore related to the geological structure.

Landsat Thematic Mapper (TM) imagery has been interpreted to produce a lineament map for northern Britain, with the aim of mapping any surface expressions of the structures. The data processing consisted of geometric correction to the British National Grid (BNG), edge-enhancement, contrast stretching and the writing of colour and black and white negatives. The black-and-white negatives consist of TM band 5 (1.55–1.65 μm) from the short-wave infrared wavelength region and were used to produce 1:250 000 scale photographic prints registered

to BNG which were used for the lineament interpretation. Landsat TM lineaments for the Lorn Plateau are shown in Figure 7.24.

The gravity and magnetic lineament azimuth diagrams show similar features to the azimuthal diagram for the fault vectors from the 1:250 000 digital geological map (Figure 7.25). Significant populations of gravity vectors cluster at 050° and 135°. For magnetic data lineaments the clusters are at about 035° and 145°, similar to the observed bimodal clusters for dykes digitised from the 1:50,000 Series geological maps (Figure 7.3). The Landsat TM data have a preferred north-east orientation, typical of the regional Caledonian strike, but also show a cluster at 110° which is poorly represented in the geophysical data. Structures trending north-west, east-south-east and north-north-east are thought to be significant in the late-Caledonian extension which permitted the development of the voluminous granites. These features and their intersections with known and inferred faults are regarded as possible conduits for circulating fluids and hence as potentially favourable sites for the deposition of hydrothermal mineralisation.

7.4.4. Discussion

The Kilmelford–Lagalochoan intrusive suite, located immediately south of the Lorn Plateau lavas, is associated with a small residual gravity low and a local positive magnetic anomaly. Emplacement of the Lagalochoan Complex and associated mineralisation may have been controlled by the intersection of a regional north-east-trending fault and a north-north-east-trending fault.

Conspicuous north-east- and north-west-trending gravity lineaments which cross the Lorn Plateau lavas may also indicate the presence of structures which permitted the emplacement of intrusions and hydrothermal fluids. Examination of these gravity lineaments in conjunction with outcrop patterns and discontinuous mapped faults have led to the identification of a set of faults which cross the lavas. These faults include the north-north-east extension of the Bragleenbeg Fault which is inferred to extend from Lagalochoan as far as the sub-centre at Gleann Salach [around 197 738]. Other inferred faults extend north-westwards from Loch Awe to Oban and from Loch Avich to Loch Feochan.

On this basis the combination of residual gravity low, residual magnetic high and the inferred north-north-east-trending Bragleenbeg Fault provides the best geophysical target for epithermal gold mineralisation in the Lorn Plateau lavas.

7.5. Data integration and prospectivity analysis

Key exploration parameters for epithermal gold mineralisation in the Lorn Plateau lavas were defined on the basis of published deposit models, on empirical observations of mineralisation in the district and the availability of suitable multivariate digital data. Twenty parameters used in the analysis were each assigned a zone of influence (number of cells), a style of influence (exponent) and a weighting (Table 7.6).

Particular emphasis was given to features associated with the known mineralisation at Lagalochoan. These include enrichment in a suite of elements in drainage geochemical data; presence of negative residual gravity and positive observed TMI anomalies related to the host intrusions; site of intrusion controlled by intersection of two major faults, the east-north-east-trending Gleann Domhain Fault and the Bragleenbeg Fault, extending from Lagalochoan towards the north-north-east as far as Bragleenbeg, and possibly beyond. The distribution of these parameters in the area is shown in the multi-dataset maps (Figure 7.26, 7.27, 7.28 and 7.29)

Table 7.6 Index parameters used for prospectivity analysis, Lorn Plateau

| zone of influence | exponent | weight | parameter |
|-------------------|----------|--------|---|
| 0 | 2.0 | 0.1 | diorites from 1:250K map |
| 0 | 2.0 | 0.1 | andesitic lavas from 1:250K map |
| 1 | 2.0 | 0.1 | acid lavas from 1:50K maps |
| 1 | 2.0 | 0.3 | tuffs from 1:50K maps |
| 0 | 2.0 | 0.1 | north-west-trending dykes from 1:50K maps |
| 1 | 2.0 | 0.1 | large faults from 1:250K map |
| 1 | 2.0 | 0.2 | inferred faults across lavas |
| 4 | 2.5 | 0.4 | alluvial gold occurrences |
| 4 | 2.5 | 0.2 | G-BASE stream-sediment data, As > 20 ppm |
| 4 | 2.5 | 0.1 | G-BASE stream-sediment data, Bi > 4 ppm |
| 4 | 2.5 | 0.1 | G-BASE stream-sediment data, Cu > 49 ppm |
| 4 | 2.5 | 0.1 | G-BASE stream-sediment data, Pb > 71 ppm |
| 4 | 2.5 | 0.1 | G-BASE stream-sediment data, Zn > 422 ppm |
| 4 | 2.5 | 0.1 | MRP panned-concentrate data, Cu > 89 ppm |
| 4 | 2.5 | 0.1 | MRP panned-concentrate data, Pb > 163 ppm |
| 4 | 2.5 | 0.1 | MRP panned-concentrate data, Zn > 299 ppm |
| 4 | 2.5 | 0.2 | MRP panned-concentrate data, Sb > 7 ppm |
| 0 | 2.0 | 0.4 | residual gravity anomalies < -2 Mgal |
| 0 | 2.0 | 0.2 | observed TMI anomalies > 75 nT |
| 4 | 2.5 | 0.2 | intersections of inferred faults and gravity lineaments |

Several geochemical parameters are used in this analysis. This has the effect of highlighting areas where sample density is greatest and where multiple-site multi-element anomalies were identified. Even though individual parameters are given a low weight the cumulative effect is to generate high prospectivity where follow-up MRP sampling was carried out. This effect has been reduced by using the 95th, rather than the 90th, percentile values as the anomaly thresholds for the MRP datasets. Selective or arbitrary exclusion of data points is considered inappropriate due to the effect on the data distributions and the risk of excluding critical anomalous values. For the regional G-BASE data anomaly thresholds were set at the 90th percentile values.

The prospectivity analysis was carried out in X-MAP with a pixel size of 250 m square using the Boolean logic data model normalised to produce a binary-weights-of-evidence map (Figure 7.30). The main epithermal gold targets identified and their key features are summarised in Table 7.7.

Table 7.7 Main targets for epithermal gold, Lorn Plateau

| Area | Centre | Approx. size (km ²) | Geology | Geochemical anomalies | Negative gravity anomaly | Positive magnetic anomaly | Faults or intersections |
|-----------------------|---------|---------------------------------|--------------------------|----------------------------|--------------------------|---------------------------|-------------------------|
| Kilmelford–Lagalochan | 187 712 | 20 | sub-volcanic intrusion | As, Bi, Cu, Mo, Pb, Sb, Zn | ✓ | ✓ | ✓ |
| Bragleenbeg Fault | 191 720 | 5 | andesite | Bi, Cu, Sb, Sn | ✓ | ✓ | ✓ |
| Scammadale – Feochan | 187 722 | 7 | andesite | As, Ba, Cu, Mo, Pb, Sb, Zn | | | ✓ |
| Beinn Ghlas | 195 726 | 8 | rhyolite, tuff, andesite | Bi, Cu, Mo, Pb, Sb, Sn, Zn | | | ✓ |
| Gleann Salach | 196 738 | 4 | tuff, andesite | Bi, Pb, Zn | | | ✓ |
| Loch Nell | 190 729 | 3 | andesite | Bi, Cu, Sb, Sn | | | |

8. CHEVIOT HILLS

8.1. Geology

8.1.1. Introduction

The Lower Devonian succession of the Cheviot Hills occupies a roughly circular upland area approximately 30 km in diameter straddling the border between Scotland and England. The main geological units are the Cheviot Granite, volcanic rocks of Devonian age and country rocks of Silurian greywacke and Lower Carboniferous sandstone (Figures 8.1 and 8.2). There are few recent accounts of the geology of the area, and there has been no extensive resurvey of the Scottish part since it was mapped by Geikie in 1883. However, the English side was resurveyed in the 1920s (Carruthers et al., 1932). The geological descriptions given here are based partly on the aforementioned mapping, supplemented by the observations of Robson (1976, 1977).

Most of the study area is underlain by extrusive and intrusive volcanic rocks of Lower Devonian age - the Cheviot Volcanic Group, which lies unconformably on Silurian shales and greywackes (Figure 8.1). The volcanics are unconformably overlain by Upper Devonian sandstones followed by a succession of Carboniferous sediments comprising conglomerates, sandstones, mudstones, cementstones, dolomitic limestones and basaltic lavas. Probably the most up to date description of the volcanic rocks is provided by Allen in Cameron et al. (

Rb-Sr whole-rock and mineral ages for the Cheviot Granite average 395.9 ± 2.9 Ma (Thirlwall, 1988), and are similar to the K-Ar age of 385 Ma published by Mitchell (1972). Other major granitoid plutons in the southern part of the Southern Uplands, the Criffel and Fleet complexes, yield comparable Rb-Sr dates of 397 ± 2 Ma and 392 ± 2 Ma respectively. Rb-Sr dating of the lavas gave an Rb-Sr date on biotite of 395 ± 3.8 Ma (Thirlwall, 1988) which supports a comagmatic origin for the granitic and volcanic rocks.

The Lower Devonian igneous suite also includes numerous porphyrite intrusions, a volcanic vent filled with agglomerate at Fundhope Rig [3867 6178], and tuffs near Score Head [3878 6187] and Hexmoor Sike [3868 6172].

8.1.2. Sedimentary and volcanic rocks

Silurian

The oldest rocks, exposed in the west and south-west of the area, are a folded and cleaved sequence of Wenlockian greywackes, comprising mudstones, siltstones and sandstones. These rocks suffered deformation and low-grade metamorphism during late Caledonian (end Silurian) tectonism.

Cheviot Volcanic Group

The earliest Devonian rocks are those of the Cheviot Volcanic Group, which unconformably overlie the Silurian succession. The Group occupies an area of approximately 500 km², with minor intercalations of pyroclastic and sedimentary rocks, and additionally two main vent breccias and several other small bodies of volcanic breccia.

The lavas are presumed to be of Lower Devonian age, as the Middle Devonian is not present in this part of the British Isles. They are dominantly sub-aerial and locally contain minor intercalations of grey and red sandstone, marl and greenish mudstone. Most of the lavas have been mapped as andesite, although analyses by Leake and Haslam (1978) indicate that some are trachyandesites. The total thickness of the volcanic pile is uncertain, although Robson (1976) estimates that 2000 m of lavas may have been erupted and that at least 500 m remain.

The lower part of the volcanic succession comprises a series of agglomerates, tuffs and ashes, probably erupted from a number of separate centres. These rocks are best exposed on the south-western side of the Cheviot massif, where they directly overlie Silurian rocks and are estimated to be less than 60 m thick (Taylor et al., 1971). Carruthers et al. (1932) describe the basal agglomerate as a 'silicified breccia, the fragments of which are usually of a fine-grained purple mica-felsite'. Thin rhyolitic lavas are locally developed. They are reddish in colour and are composed of biotite and alkali-feldspar phenocrysts in a quartz-feldspar groundmass (Carruthers et al., 1932).

The major part of the volcanic suite comprises variably altered, grey, purple, reddish-brown to black, andesite and basaltic andesite, with minor amounts of pyroclastics. The lavas carry phenocrysts of andesine-labradorite feldspar and, invariably, altered orthopyroxene and clinopyroxene. They are commonly amygdaloidal, with small irregularly shaped vesicles, infilled with chalcedony or quartz and chlorite. Xenoliths of microdiorite and microtonalite are present in some rocks. Locally, flows of dark grey or black 'glassy andesite' are cut by red veinlets of jasper and chalcedony. These lavas are unusually fresh and contain phenocrysts of hypersthene, augite and labradorite. Oligoclase trachytes are recorded in the upper part of the Alwin basin [393 607] (Carruthers et al., 1932). They are fine grained and consist of rare feldspar phenocrysts set in a matrix of oligoclase feldspar and altered pyroxene.

Whole rock geochemical data presented by Cameron et al. (1988) and Thirlwall (1981) indicate that the lavas have a restricted compositional range and in the Kingsseat area are dacitic in composition rather than andesitic. Thirlwall (1981) demonstrated that the Cheviot Volcanics are geochemically distinct from the Lower Devonian lavas erupted elsewhere in Scotland. It is probable that the Cheviot lavas were erupted after subduction had ceased, and Cameron et al. (1988) consider the lavas might represent a transitional phase between subduction-related and within-plate types. The lavas show various geochemical features typical of continental-margin calc-alkaline volcanic rocks, including a low Ti contents, but other geochemical parameters indicate their possible transitional nature (Gill, 1981).

The Cheviot Volcanic Group is unconformably overlain along most of its western margin by conglomerates, sandstones, siltstones and marls of Upper Old Red Sandstone (Devonian) age. These are predominantly red in colour and contain cornstone bands. However, at Oxnam, near Jedburgh, red sandstones, shales and

conglomerates unconformably overlies near-vertical Wenlockian strata, and may have been deposited contemporaneously with the volcanism.

Carboniferous

In the north-west of the area the Upper Old Red Sandstone sequence is succeeded by basaltic lavas of the Birrenswark Volcanic Group (Kelso Traps) which form the base to the Carboniferous in this area. The lavas are overlain by the Cementstone Group of Dinantian age, in which locally developed lavas of Puy-type represent the waning phases of the Lower Carboniferous volcanic episode. Small exposures of olivine-basalts (the Cottonshope Lavas) also lie near the base of the Cementstone Group in the south-west of the area.

In the east and south of the area, the Lower Palaeozoic rocks are unconformably overlain by the Cementstone Group. This comprises a locally developed basal conglomerate, overlain by a cyclic sequence of mudstones, shales, cementstones, dolomitic limestones and sandstones. The basal conglomerate is exposed in Roddam Dene [4020 6205], at Ramshope [3732 6060] and Windy Gyle [3850 6155]. At the first two localities pebbles are mainly andesitic, while at the third granite pebbles and boulders are predominant.

8.1.3. Intrusions

Cheviot Granite

The Cheviot Granite is laccolithic in form and outcrops over an area of approximately 57 km² in the centre of the Cheviot massif. It intrudes the volcanic rocks and yields a Devonian Rb-Sr age of 395.9 ± 2.9 Ma (Thirlwall, 1988). The boundary between the granite and surrounding rocks is difficult to trace on account of its irregular nature and the widespread cover of peat and drift.

The granite has been subdivided into three varieties (Jhingran, 1942): a fine-grained marginal phase, termed either pyroxene granodiorite (Haslam, 1975) or quartz diorite (Lee, 1982); and a more acid phase split into the 'Standrop' and granophyric varieties (Jhingran, 1942). The Standrop variety is a light grey granodioritic rock containing diopside, whilst the granophyric type is pink and contains little or no pyroxene.

The marginal phase is dark grey and dioritic in appearance, and is frequently porphyritic in texture. It comprises quartz, usually interstitial, orthoclase, plagioclase, biotite, pyroxene and iron oxides with occasional hornblende and chlorite. Generally, orthoclase is subordinate to plagioclase. Usually the potash feldspar forms rims around plagioclase but intergrowth of orthoclase with albite and quartz frequently occur. Plagioclase, ranging from andesine to albite, almost always forms well-defined crystals and occasionally phenocrysts. Pyroxene is a characteristic constituent of this variety of granite (Haslam, 1986), being present in varying quantities. It is associated with large amounts of iron oxides which occur as fine dust and as large rounded grains.

Carruthers et al. (1932) suggested that the basic component of the intrusion was the product of contamination from the overlying lava roof. However, on the basis of geochemical data Jhingran (1942) concluded that this hypothesis was not tenable and that the most likely source was the underlying greywackes and shales. A third possibility, which is regarded as the most likely, is that the basic variant of the granite is an early magmatic differentiate, similar to that in other late Caledonian granites in Britain.

The Standrop variety, in contrast to the marginal type, is leucocratic, with conspicuous large crystals of feldspar, and a relatively small proportion of ferromagnesian minerals, mainly pyroxene with minor amphibole and biotite. It is rich in quartz and orthoclase is the dominant feldspar. The replacement relation of quartz to feldspar is pronounced, with large crystals of quartz often enclosing numerous fragments of orthoclase.

The granophyric variety is pink in colour and medium- to coarse-grained. It is granitic in composition, containing quartz, potash feldspar (often perthitic), biotite and minor iron oxide. Ferromagnesian constituents are almost absent and there are no reaction products after pyroxene. Coarse, micrographic intergrowth of quartz and perthitic feldspar is common usually occurring interstitially, creating a strong tendency towards a spherulitic texture. Occasionally the feldspar is strongly sericitised. Accessory minerals rarely occur in large quantities except where tourmaline is present. The tourmaline is invariably associated with veining and brecciation of the granite.

The contact metamorphic aureole around the granite is about 1 km wide, except where the boundary is faulted. Where unfaulted the contact is locally complex, with ramifying veins of fine-grained granite running into the andesitic host rocks. Rafts of metamorphosed lava, presumed to be part of the original roof, occur well within the granite boundary. These, together with the wide aureole, suggest that the present erosion level is near the laccolith roof and that the granite/lava contact is gently dipping (Robson, 1976). From geophysical data, Lee (1982) estimates that the granite has a diameter of 35 km at 9 km depth (see Section 8.4.3 for discussion).

The Cock Law Complex

Near the base of the volcanic succession in the western part of the Kingsseat Burn area (Figure 8.1), the pyroclastic rocks are overlain by some 15 m of porphyritic acid volcanics, described as mica felsites by Carruthers et al. (1932) and as rhyolites by Robson (1976). These rocks consist of a groundmass of quartz and feldspar, with prominent phenocrysts of biotite and, less commonly, alkali feldspar. A second group of rhyolitic rocks (Robson, 1976), which outcrop in the area between Cocklawfoot and the border, were reinterpreted during the MRP survey (Cameron et al., 1988) on the basis of field and petrographic evidence as part of a high level intrusive complex, termed the Cock Law Complex. Two main rock types are present, biotite porphyry and pyroxene-biotite porphyry, but minor varieties identified include pyroxene porphyry, biotite-quartz porphyry and granodiorite porphyry. The overall form of the complex is difficult to determine from the limited mapping carried out, but the available evidence suggests that it is laccolithic. On the basis of field and petrographic studies it was concluded that the Cock Law Complex predates intrusion of the Cheviot Granite.

Minor intrusions

Most minor intrusions in the area are associated with either the Devonian or Carboniferous volcanicity. Dykes of Devonian age intrude both the Cheviot Volcanic Group and the granite. The dykes, which trend north-north-west and north-north-east, appear to be concentrated in the southern part of the area (Robson, 1976) but it is uncertain how much this distribution is deceptive, affected by the location of the detailed geological mapping. Four varieties of dyke were distinguished on the English side of the border by Carruthers et al. (1932), namely mica porphyrites, quartz porphyries, felsites and pyroxene porphyries. Their relationship to the granite is uncertain; only a few can be traced into it, suggesting that at least some may be earlier, but aplite veins cutting granite and lavas are in turn cut by dykes (Taylor et al., 1971; Mitchell, 1972).

A laccolith of mica porphyrite occurs at Biddlestone, close to the southern margin of the Cheviot volcanics. Minor intrusions of basalt and dolerite, some marking vents, are associated with the Lower Carboniferous volcanism, while a dyke of fresh quartz dolerite outcropping at Windy Rigg is associated with the late Hercynian Whin Sill event (Robson, 1976). The Acklington Dyke of Tertiary age, composed of non-porphyritic tholeiitic basalt, crosses the southern part of the area in a roughly east-south-easterly direction. Volcanic breccias, probably indicating the sites of vents, have been noted at several localities, such as Fundhope Rig [3867 6178].

8.1.4. Structure

The structural history of the Cheviot igneous massif has been described by Robson (1977). The lavas generally dip towards the east or south-east, suggesting that the whole block has been tilted in this direction. The Lower Palaeozoic basement displays typical Caledonide structures, with major folds and faults striking north-east. Hercynian easterly compression generated north-north-east and north-north-west trending folds in sedimentary rocks adjacent to the massif as well as tear-faults, both in the sediments and in the block. These tear-faults, which include the major line of the Thieves–Gyle–Harthope fracture, all trend between 050° and 075°. In the central part of the area, the trend and disposition of the rocks on either side of the Gyle–Harthope fault zone suggests a dextral displacement.

Conjugate sinistral movement may have taken place along the Breamish Fault. The direction of faulting is probably controlled in part by the Lower Palaeozoic basement, which may also account for the weakly developed, sinistral, north-west trending conjugate set. Robson (1977) postulates that the anomalous trend of the College, Yetholm and Yeavinger Faults is accounted for by rotation of the stress pattern in the northern part of the block adjacent to the less resistant and thick sedimentary succession of the Tweed floodplain. Further faulting, in response to north-south compression, occurred in the Tertiary, probably causing sinistral movement along the Gyle–Harthope fracture. The relative displacement of the Cheviot Granite suggests that this movement was less than the dextral Hercynian displacement. Final movements involved tilting and normal faulting along pre-existing fractures at the boundaries of the volcanic rocks. On the southern side the Harthope, Ridlees and Ryle Faults downthrow to the south, while at the northern margin the Gyle, Pressen, Flodden and Yeavinger Faults downthrow to the north.

8.2. Mineralisation

There are few accounts of metal working in the Cheviot Hills and historic excavations appear to have comprised only trials. Most occurrences consist of quartz and calcite veins situated in faults and crush zones. Locally they contain minor amounts of copper ore, galena or hematite (Carruthers et al., 1932). The locations of known occurrences of mineralisation are shown in Figure 8.3 and their main features summarised in Table 8.1 (after Cameron et al., 1988).

Accounts of mineral occurrences in the area are given by Clough (1888). A vein at Craggy Glen (Raven's Crag) on the south side of Allerhope Burn [3920 6100] comprises ribs 2.5–10 cm thick, containing galena, pyrite and baryte. The host rock appears to have been a calcite-cemented porphyrite (andesite) breccia. In a stream 400 m south-south-west of Langlee [3963 6320] there is a strong vein trending slightly east of north with calcite and quartz breccias, containing strings of malachite varying in thickness between 3 and 13 mm. In the stream 1 mile east-north-east of Ridleeshope [3820 6070] (probably the Pudding Burn or its tributary), a calcite vein containing specks of chalcopyrite approximately 2 mm in size was reported by Clough (1888).

Further evidence of the existence of metalliferous mineralisation was provided by MRP surveys. Leake and Haslam (1978) identified three principal zones of mineralisation within the Cheviot Volcanic Group:

- i. An area with elevated values of Cu, Pb, Zn and Ba lies to the west of the Cheviot Granite and trends approximately south-east from Kingsseat Burn to Allerhope Burn. An anomalous panned concentrate sample from Kingsseat Burn [3869 6182], led to the discovery of a small mineralised structure containing malachite and baryte. South-east of the zone, samples from two western tributaries of the Usway Burn, [3885 6160] and [3884 6158], contain elevated levels of Cu, Ba and Zn and, at one site, Pb.

Table 8.1 Documented metalliferous mineral occurrences in the Cheviot Hills

| | <u>Locality</u> | <u>National Grid Coordinates</u> | <u>Mineralisation and Reference</u> |
|----|------------------|--------------------------------------|--|
| 1 | Heathery Hill | 3870 6060 | Calcite with galena (Miller, 1887) |
| 2 | Allerhope | 3930 6103 3934 6106 | North-west-trending calcite veins in andesite, with galena, pyrite and baryte (Clough, 1888) |
| 3 | Harden Edge | 3792 6068 | Vein with chalcopyrite (Clough, 1888) |
| 4 | Langlee | 3963 6230 | Veins with calcite, quartz and analcite (Clough, 1888) |
| 5 | Long Hill | 3860 6070 | Baryte strings (Clough, 1888) |
| 6 | Pudding Burn | 3840 6070 | Calcite vein with chalcopyrite (Clough, 1888) |
| 7 | Ridleeshope | 3820 6070 | Baryte strings (Clough, 1888) |
| 8 | Yeaming Hall | 3810 6120 | Calcite vein with galena (Clough, 1888) |
| 9 | Harden Edge | 3795 6072 | Cu-U occurrence (Haslam, 1975) |
| 10 | Biddlestone Burn | 3950 6100 | Mineralised zone; baryte and sphalerite in concentrate (Leake and Haslam, 1978) |
| 11 | Kingsseat Burn | 3869 6182 | Mineralised structure with malachite, hematite and baryte (Leake and Haslam, 1978) |
| 12 | R. Breamish | 3930 6155 | Mineralised zone; baryte, chalcopyrite, malachite and pyromorphite recorded in concentrates (Leake and Haslam, 1978) |
| 13 | Usway Burn | 3885 6160 | Baryte and secondary lead minerals in concentrate; pebbles of vein calcite (Leake and Haslam, 1978) |
| 14 | Cottonshope | 3790 6045 3803 6058 | Two east–west Pb veins (Geological Survey of England and Wales, sheet 8) |
| 15 | Middleton | 3990 6240 | Manganese oxide in crush (Geological Survey of Great Britain, Northumberland (New Series) XXI NW) |

- ii. The second mineralised area is associated with a north-west-trending linear crush zone, which runs for approximately 6 km in the headwater tributary area of the River Breamish, centred on [3920 6160]. This zone straddles the southern contact of the Cheviot Granite with the Cheviot Volcanic Group. In panned concentrates baryte, chalcopyrite, malachite, pyromorphite and goethite pseudomorphs after pyrite have been identified. Elevated Cu, Pb and Zn levels in panned concentrates occur in streams on the south-western side of the crush belt draining the volcanics. Mineralisation is inferred to occur in a cross-fractures of north-easterly trend.
- iii. A third, ill-defined area of elevated Zn values extends over approximately 10 km² from the southern margin of the Cheviot Granite to the Biddlestone Burn [3950 6100]. Some of the sites sampled also contain elevated Cu, Ba and Pb. Exposure in this area exposure is poor and the sources of the geochemical anomalies are unknown.

There are two historic reports of the occurrence of gold in the area. Firstly, Clough (1888) notes that a north-trending quartz vein at the head of Lambden Burn (Goldsleugh) [392 623] was purported to contain gold. Secondly, it is said in the area that gold has been panned from the stream above Cocklawfoot [385 618]. Neither observation has been corroborated by modern studies. During MRP surveys native gold was observed at two localities in the River Breamish catchment, at High Bleakhope [3910 6173] and at Shank [3964 6135] (Cameron et al., 1988). Both sites occur close to the south-east-trending Breamish Fault which crosses the volcanic sequence close to the south-western margin of the Cheviot Granite. The site at Shank is close to an area of Zn, Pb and Bi anomalies in panned concentrates which may be derived from mineralisation. Low-tenor enrichment in gold (maximum 43 ppb Au) was also documented by analysis of rock samples in the MRP surveys carried out in the Kingsseat Burn area (Cameron et al., 1988).

Minor quartz veins, quartz-filled tension gashes and quartz-cemented breccias with associated veins up to 30 cm thick are widespread in the lavas around Kingsseat Burn and Windy Gyle to the south-west of the Cheviot Granite. Larger quartz vein systems have been reported in the same area (Cameron et al., 1988). Elsewhere some quartz veins, locally with calcite, occur in vertical fractures within the Cheviot Volcanic Group and silicification may extend for up to 20 m into the lavas, e.g. at Raker Crag [385 609]. These siliceous zones pre-date Hercynian fractures but cut Devonian mica porphyrite dykes (Robson, 1976).

Tourmalinisation is also a relatively late-stage event, affecting dykes and crush zones which cut the Cheviot Granite (Carruthers et al., 1932). The granite contains tourmaline as an accessory mineral and the western part of it has been subjected to late hydrothermal alteration, with the crystallisation of ‘pneumatolitic micas’ and tourmaline.

Pervasive alteration has affected most of the Cheviot Volcanic Group. Robson (1976) records that most andesites are altered and that rhyolitic rocks, outcropping near the border, are so altered that they crumble readily. A petrographic study of samples from the Kingsseat area enabled seven alteration assemblages to be identified resulting from sericitisation, kaolinisation, silicification, tourmalinisation, hematitisation and carbonate alteration (Cameron et al., 1988). Except for hematitisation, all the alteration episodes are related to the Lower Devonian igneous activity. In this study PIMA analysis has been carried out on rock samples from the Kingsseat area to elucidate the alteration mineralogy (Section 8.5.2).

8.3. Geochemistry

8.3.1. Introduction

The Cheviot Volcanic Group and surrounding area have been covered by drainage geochemical surveys conducted by the BGS. These include the regional (G-BASE) survey (British Geological Survey, 1993), which covered all the area except the military ranges around Otterburn. Several projects, mostly carried out by the MRP, covered smaller parts of the area underlain by volcanic rocks together with adjacent Carboniferous strata (Haslam, 1975; Leake and Haslam, 1978; Bateson et al., 1983, Cameron et al., 1988). The MRP surveys were aimed principally at base-metal mineralisation, although potential for epithermal precious-metal mineralisation was identified in one area.

For the present study G-BASE data for the area between National Grid Eastings 360000 and 420000 and Northings 600000 and 650000 (3500 km²) were retrieved from the BGS Geochemical Database. Within this area, data for 1318 stream sediment samples are available for up to 35 major and trace elements (Figure 8.4). With the

exception of U, As and Sb, all elements were analysed by direct-reading DC arc emission spectrometry. Uranium was determined using delayed neutron activation and As and Sb by atomic absorption spectrometry (AAS).

Stream-sediment and panned-concentrate datasets were compiled from the various MRP surveys carried out over the Cheviot Volcanic Group and the Cheviot Granite. These provide nearly complete coverage of the area with a total of about 1100 samples at a density of approximately 0.8/km² (Figure 8.5). The plateau area of the Cheviot and eastwards for approximately 5 km were sampled at a lower density. In the Kingsseat Burn area additional follow-up surveys provide more detailed cover (Cameron et al., 1988). These data are described in more detail below (Section 8.5).

Geochemical analysis of panned-concentrate and stream-sediment samples were carried out by similar methods in each of the MRP surveys. All elements in panned concentrate samples were determined by X-Ray Fluorescence Spectrometry (XRF). In stream sediment samples, Cu, Pb and Zn were determined by AAS and other elements by Optical Emission Spectroscopy (OES).

8.3.2. Results

Summary univariate statistics for the G-BASE and MRP datasets are shown in Tables 8.2, 8.3 and 8.4.

Table 8.2 Summary statistics for G-BASE stream-sediment samples, Cheviot Hills
(all values in ppm)

| Element | no. samples | mean | minimum | maximum | 50% | 75% | 90% | 95% |
|---------|-------------|-------|---------|---------|-------|-------|-------|-------|
| Ag | 1318 | 0.1 | 0.1 | 1.5 | 0.1 | 0.2 | 0.3 | 0.4 |
| As | 508 | 13.1 | 1 | 117 | 10 | 15 | 23 | 32 |
| Ba | 1318 | 801.5 | 191 | 8117 | 720 | 899 | 1124 | 1282 |
| Be | 1318 | 2.8 | 0.4 | 18.1 | 2.4 | 3.4 | 4.7 | 5.5 |
| Bi | 1287 | 1.9 | 0.2 | 13 | 2 | 2 | 3 | 4 |
| Co | 1318 | 21.8 | 4 | 346 | 19 | 24 | 33 | 43 |
| Cu | 1318 | 17.7 | 3 | 85 | 16 | 20 | 27 | 33 |
| Fe | 1318 | 45541 | 9372 | 236677 | 42314 | 52455 | 68052 | 84837 |
| K | 1318 | 32613 | 5893.7 | 63005 | 32789 | 39596 | 45905 | 49308 |
| Li | 1318 | 59.9 | 17.4 | 188.6 | 57.7 | 75.8 | 93.3 | 104.2 |
| Mn | 1318 | 2295 | 60 | 94350 | 1400 | 2550 | 4550 | 6850 |
| Mo | 1318 | 0.3 | 0.1 | 36.4 | 0.1 | 0.1 | 0.7 | 1.5 |
| Ni | 1316 | 46.4 | 1 | 217 | 44 | 58 | 72 | 82 |
| Pb | 1318 | 58.4 | 16 | 708 | 48 | 68 | 100 | 126 |
| Rb | 1318 | 142.3 | 33 | 381 | 134 | 178 | 224 | 252 |
| Sb | 484 | 1 | 0.1 | 32 | 0.5 | 1 | 2.5 | 3 |
| Sr | 1318 | 144.4 | 42 | 492 | 122 | 183 | 237 | 275 |
| Ti | 1318 | 6642 | 3117 | 19124 | 6415 | 7254 | 8333 | 9232 |
| V | 1317 | 91.1 | 32 | 198 | 89 | 103 | 120 | 130 |
| Zn | 1318 | 213.7 | 2 | 2028 | 166 | 254 | 390 | 526 |

Table 8.3 Summary statistics for MRP stream-sediment samples, Cheviot Hills
(all values in ppm)

| Element | no. samples | mean | minimum | maximum | 50% | 75% | 90% | 95% |
|---------|-------------|-------|---------|---------|-------|-------|-------|-------|
| Ag | 145 | 0.5 | 0.1 | 1 | 0.1 | 1 | 1 | 1 |
| As | 700 | 14.8 | 0.5 | 162 | 12 | 17 | 24 | 32 |
| Ba | 1164 | 948.6 | 75 | 16000 | 750 | 1000 | 1300 | 1800 |
| Co | 1110 | 17.8 | 3 | 180 | 16 | 22 | 29 | 32 |
| Cr | 1029 | 104.7 | 17 | 1080 | 94 | 113 | 174 | 205 |
| Cu | 1148 | 16.4 | 5 | 120 | 15 | 20 | 25 | 30 |
| Fe | 1110 | 29570 | 5920 | 104000 | 28400 | 36500 | 45100 | 52455 |
| Mn | 1111 | 2095 | 59 | 130000 | 1270 | 2400 | 3890 | 5670 |
| Mo | 1110 | 0.6 | 0.1 | 10 | 0.1 | 1 | 2 | 2 |
| Ni | 1111 | 46.3 | 10 | 149 | 42 | 56 | 68 | 79 |
| Pb | 1149 | 49.4 | 10 | 740 | 40 | 60 | 80 | 90 |
| Sn | 1111 | 3.6 | 1 | 320 | 1 | 3 | 8 | 10 |
| Zn | 1150 | 149.3 | 30 | 920 | 130 | 180 | 260 | 330 |
| Zr | 1111 | 611.5 | 75 | 4920 | 420 | 761 | 1190 | 1600 |

Table 8.4 Summary statistics for MRP panned-concentrate samples, Cheviot Hills
(all values in ppm)

| Element | no. samples | mean | minimum | maximum | 50% | 75% | 90% | 95% |
|---------|-------------|-------|---------|---------|-------|-------|--------|--------|
| As | 792 | 23.2 | 0.5 | 612 | 10 | 23 | 53 | 80 |
| Ba | 1083 | 7592 | 2 | 418400 | 730 | 2021 | 11500 | 25500 |
| Bi | 792 | 1 | 0.2 | 220 | 0.2 | 1 | 2 | 3 |
| Ca | 825 | 4559 | 90 | 58800 | 2550 | 4090 | 11100 | 16100 |
| Ce | 1020 | 68 | 1 | 736 | 60 | 87 | 116 | 140 |
| Cu | 1025 | 23.7 | 1 | 1913 | 13 | 21 | 41 | 67 |
| Fe | 1082 | 71076 | 1680 | 7800000 | 48680 | 76550 | 127670 | 177640 |
| Mn | 1082 | 598.8 | 20 | 5440 | 410 | 720 | 1190 | 1690 |
| Mo | 843 | 3.7 | 0.1 | 51 | 2 | 4 | 8 | 12 |
| Ni | 1079 | 42.6 | 1 | 177 | 36 | 56 | 81 | 96 |
| Pb | 1069 | 83.2 | 1 | 10570 | 42 | 70 | 119 | 186 |
| Sb | 723 | 14.1 | 1 | 1771 | 6 | 11 | 18 | 30 |
| Sn | 1083 | 15.5 | 0.5 | 1155 | 5 | 14 | 34 | 54 |
| Zn | 1083 | 124.4 | 3 | 2886 | 92 | 149 | 234 | 302 |
| Zr | 1011 | 1089 | 1 | 23980 | 510 | 1125 | 2400 | 3720 |

Antimony (Sb): in the G-BASE stream-sediment data the median value is 0.5 ppm, with only 5% of samples exceeding 3 ppm. Two main anomalous zones are present: to the south-east of the Cheviot Granite east of Cushat Law, and, to the south-west of the granite extending south-westwards from the Kingsseat Burn area (Figure 8.6). A small linear group of anomalous sites is centred on the Halter Burn and Curr Burn catchments [384 627]. Other single-point anomalies occur sporadically, possibly related to contamination.

In the MRP panned concentrates the majority of samples with detectable Sb are derived from streams draining the Cheviot volcanics to the south-west of the granite, extending from the Kingsseat Burn catchment [385 618], south-south-eastwards towards Davidson's Burn [387 616] (Figure 8.7). No Sb minerals were detected in the heavy-mineral concentrates from this area, despite the presence of Sb levels up to 506 ppm, [386990 617620]. The elevated Sb is most commonly associated with enhanced As, with 50% of the highest Sb values accompanied by As greater than 100 ppm. Attendant enrichment in Ba, Cu, Mo and locally Sn also occur in samples with high Sb contents. For example, the highest Sb value (1771 ppm), which occurs in the Riddlees Burn catchment [382680 606620], also contains elevated levels of Cu (1913 ppm), Pb (10570 ppm) and Sn (1155 ppm). Some panned-concentrate anomalies may be due to Sb dispersed in Ti-Fe oxides, including those in Heatherhope Burn [380 617] and Cowielaw Sike [382 610] (Cameron et al., 1988).

Arsenic (As): the northern part of the Cheviot Volcanic Group is characterised by generally low As contents (< 6 ppm) in the G-BASE stream sediment data (Figure 8.8). In the central and southern parts As values are commonly greater, with the highest levels locally exceeding 100 ppm e.g. two sites to the east of Cushat Law [393 614], in an area underlain by volcanic rocks. Moderate As enrichment is also present around Kingsseat and Windy Gyle to the south-west of the granite.

The MRP data indicate a similar distribution pattern for As in both stream sediments and panned concentrates, despite the potential influence of secondary (hydrrous oxide) precipitation processes on stream sediments (Figure 8.9). The majority of elevated values in both stream sediments and panned concentrates occur in a west-south-west-trending belt, running from the western edge of the Cheviot Granite to the Jed Water catchment area, on the western margin of the lavas [369 614]. In panned concentrates, two anomalous zones may be identified: one is centred on Cocklawfoot [385 618] and the other to the south of Oxnam [370 618], close to the western margin of the Cheviot Volcanic Group outcrop. At Cocklawfoot the As enrichment is associated with Ti-Fe oxides which may be associated with mineralisation at Yearning Cleuch [387 618].

The source of the anomalies south of Oxnam, where As values in panned concentrates reach 369 ppm, is uncertain. The marked enrichment in the panned concentrates relative to the stream sediments in this area is consistent with the recorded presence of abundant Fe oxides in the form of specular hematite which is relatively enriched in the concentrates. In the Oxnam area As enrichment is associated with sporadic high values of several other elements, such as Ba, (up to 47600 ppm in the Camptown area [368 613]), Sb (up to 30 ppm), and low-tenor Sn and Pb enrichment. In none of these samples, however, are levels of these elements sufficiently enhanced to suggest significant base-metal mineralisation.

Elevated As values (>25 ppm) in MRP stream sediments occur in a zone about 6 x 4 km extending from the Calroust Burn catchment in the west [383 617] to Davidson's Burn in the east [389 617]. Arsenic levels in panned concentrates over the same area are also high, with a cluster of 21 values in excess of 100 ppm over a 9 km² area. Associations with other elements are variable, but marked enrichments in Sb (maximum 506 ppm), Mo (maximum 23 ppm) and Ba (several values > 20 000 ppm) are the most conspicuous.

Barium (Ba): there is marked enrichment in Ba over the southern half of the outcrop of the Cheviot Volcanic Group. The highest Ba values occur to the west of the Cheviot Granite, particularly in the Kingsseat Burn [387 618] and Bowmont Water [383 620] catchments. Localised Ba enrichment also occurs on the southern and western periphery of the Cheviot lavas.

MRP stream-sediment and panned-concentrate data have generally similar distribution patterns. Background concentrations in both sample types are high, with a median value of 750 ppm Ba in stream-sediment samples and 730 ppm in concentrates. High values, commonly exceeding 10 000 ppm, reported in panned concentrates are consistent with field observations of baryte during panning and are probably related to mineralisation. The highest levels occur within a zone to the west of the Cheviot Granite, stretching from Davidson's Burn in the south-east [388 617] to the Cutt Burn in the north-west [384 624] (Figure 8.10). A second zone of enrichment occurs along the southern margin of the volcanics, in the Southhope Burn [383 605] and Ridlees Burn catchments [385 606].

Beryllium (Be): in the G-BASE stream-sediment data a broad zone of Be enrichment extends over the volcanic rocks and the Cheviot Granite in a north-easterly direction along the line of the Gyle–Harthope Fault, including the Kingsseat area (Figure 8.11). Elsewhere Be values over the volcanic rocks are about 3–4 ppm in the north and slightly higher, 5–6 ppm, in the south.

MRP stream sediments show a similar Be distribution pattern, with elevated values along the same north-east trend. Two anomalous samples are derived from streams which traverse highly kaolinised porphyry in the Kingsseat Burn area. The most probable cause of this pattern is a concentration of Be in hydrothermal fluids and its retention in clay minerals following alteration.

Bismuth (Bi): the median Bi value in the G-BASE data is 2 ppm, with only 5% of values greater than 4 ppm. Most high values occur over the Cheviot Granite and in the central and southern sections of the volcanic outcrop (Figure 8.12). In MRP panned concentrates only 5% of values exceed 3 ppm Bi. These occur sporadically over the granite and in the south-eastern part of the volcanic outcrop (Figure 8.13). At one site in this sector [395 615], close to the granite margin, a value of 220 ppm Bi is accompanied by elevated Sb and As. A cluster of anomalous values (> 4 ppm) occurs in the Kingsseat Burn area in association with elevated As, Sb and Sn.

Boron (B): in the G-BASE data, B has a similar distribution pattern to Be, with a north-east-trending linear break between the north-western and south-eastern Cheviots. In the MRP panned concentrate data elevated levels in excess of 1000 ppm occur on the north-western margin of the Cheviot Granite, to the north and north-east of the Cheviot summit [390 620], where they are related to the presence of tourmaline within the granite. These occurrences support Haslam's (1975) suggestion that the northern granite is richer in tourmaline than the other variants.

Cobalt (Co): in G-BASE stream sediments Co enrichment occurs in the southern half of the Cheviot volcanics, particularly along, and to the south of, the Gyle–Harthope Fault (Figure 8.14). The highest values occur near the south-western margin of the Cheviot Granite, in the Kidland Forest area, and extend south-westwards along the line of the Gyle–Harthope Fault.

In both G-BASE and MRP stream-sediment datasets there is a common association of Co with Mn, Zn and Ni. This indicates the importance of co-precipitation on hydroxide phases as a control on the distribution of these elements at these localities.

Copper (Cu): sporadic high values in the G-BASE data occur around the periphery of the Cheviot Granite, along the line of the Gyle–Harthope Fault and in the Kingsseat Burn area (Figure 8.15). Chalcopyrite is recorded in concentrates derived from easterly-draining streams to the north-west of Thirl Moor [379 609] at the south-west end of the fault.

The distribution patterns for Cu in the MRP panned-concentrate and stream-sediment data are generally similar over the Cheviot Volcanic Group (Figure 8.16). Elevated values occur in the Kingsseat Burn area and in a south-west-trending belt, from the edge of the Cheviot Granite in the direction of Raven’s Knowe [376 606]. Low-tenor enrichment continues north-east across the granite along the Gyle–Harthope Fault. The four highest values in panned concentrates occur in the south of the area. Two of these sites show no enrichment in other elements and may therefore be due to contamination from the military ranges. The highest Cu value (1913 ppm), close to the southern margin of the volcanic rocks at [382680 606620], has attendant enrichment in Pb, Sb, Sn and Bi. A similar association occurs at a nearby site [382330 610760].

Gold (Au): was not determined in G-BASE or MRP samples.

Lead (Pb): values in the G-BASE dataset show a general enrichment over the volcanic rocks to the south-east of the Gyle–Harthope Fault (Figure 8.17). The MRP stream-sediment data for Pb have a similar distribution, with enhanced values occurring over the southern half of the Cheviot Volcanic Group (Figure 8.18). A zone of low-tenor enrichment occurs in the Kingsseat and adjacent catchments to the west of the Cheviot Granite. In general, the distribution of Pb in stream-sediment samples is similar to that of Cu.

Elevated Pb values in concentrates occur at several localities around the periphery of the volcanics. Anomalous sites are also present in the Kingsseat Burn area, along the Gyle–Harthope Fault and the southern margin of the Cheviot Granite. There is commonly a close association with Cu enrichment, although field observations indicate that some anomalies may be attributable to contamination from munitions. Galena was identified at a small number of localities, notably in the Allerhope Burn [3929 6103] and in the south-east fault-controlled Bleakhope tributary of the River Breamish [3922 6159]. Analytical Pb and Ba contents of these samples are also high. Pyromorphite and cerrussite or anglesite were recorded at several localities.

Manganese (Mn): in the G-BASE data Mn concentrations are high over the southern part of the Cheviot volcanics to the south-east of the Gyle–Harthope Fault (Figure 8.19). Elevated Mn values also occur in the Kingsseat Burn area immediately north of the fault.

Molybdenum (Mo): Mo concentrations in both the G-BASE and MRP stream-sediment data are low, with 95% of values less than 2 ppm and maxima of 36 ppm and 10 ppm respectively. In the G-BASE data high values occur at several sites in the vicinity of the Breamish Fault, while sporadic low-tenor enrichment (>3 ppm) occurs close to the western margin of the Cheviot Volcanic Group.

In MRP stream sediments, elevated Mo values occur at several localities in the southern part of the Cheviot Volcanic Group and over the Cheviot Granite (Figure 8.20). The highest values occur on the south-western margin of the volcanics in the Thirl Moor area east of Carter Bar [380 608], and in the Breamish Fault Zone in the Allerhope Burn and catchments to the east [393 614], where Pb mineralisation is also known. Minor enrichment is also present in the Kingsseat Burn area.

Anomalous Mo values occur in the MRP panned concentrates from the Kingsseat Burn area [386 616], with four values in excess of 40 ppm (Figure 8.21). Elsewhere Mo enrichment is noted in the southern part of the volcanic outcrop, especially along the Gyle–Harthope Fault

Silver (Ag): in the G-BASE stream-sediment data, less than 1% of all values are above the practical detection limit of 0.7 ppm, while in MRP stream sediments the maximum Ag value reported is 1 ppm. Clearly these data provide no evidence for Ag enrichment in the area.

Tin (Sn): G-BASE stream-sediment data indicate a slightly elevated background over the Cheviot Granite relative to the volcanics (Figure 8.22). Minor enrichment is also present in the Kingsseat Burn area to the west. A similar pattern is evident in the MRP stream-sediment data with sporadic single-site anomalies occurring widely within the volcanics.

The distribution pattern for Sn in panned concentrates is broadly similar to that in stream sediments, but no enrichment is present over the granite. Sporadic high Sn in MRP panned concentrates occurs to the west of the Cheviot Granite (Figure 8.23). The majority of elevated values are single-site anomalies and therefore may be due to contamination, either from the military ranges or domestic-agricultural sources. A few Sn anomalies can be related to natural causes. Those in the Kingsseat area are caused by appreciable amounts of Sn dispersed in Ti-Fe and Fe oxides. The relatively low levels of Sn in panned concentrates relative to stream sediments suggests that cassiterite is unlikely to be the source of anomalies.

Zinc (Zn): G-BASE (Figure 8.24) and MRP stream-sediment data distributions for Zn are generally similar and are broadly comparable with the patterns for Cu and Pb. Relatively high values occur over the south-eastern part of the volcanic outcrop, to the south-east of the Gyle–Harthope Fault, and low tenor enrichment is present in the Kingsseat Burn area.

Zinc in panned concentrates has a similar distribution pattern to stream sediments, with a general enrichment in the south-east part of the volcanic outcrop. In particular, several anomalies occur in the vicinity of the Breamish Fault and in the Ridleeshope area [385 606]. The low tenor of Zn values in panned concentrates suggests that most Zn is held in Fe-Ti oxides rather than as a sulphide.

8.3.3. Discussion

Cameron et al. (1988) provided a detailed discussion of the element associations and distribution patterns derived from the MRP reconnaissance drainage survey in the Cheviot Hills. The principal element groupings identified were:

- i. elements enriched in heavy metallic minerals, principally ilmenite and magnetite, including Ti, Fe, Mn, Ni and Zn, but also Cu, Sn, Sb and Pb which might occur in hydrothermal mineralisation
- ii. clays, precipitates and organic matter – V, Mn, Fe, Co, Cu, Zn and Pb which occur in fine and light fractions of stream sediments and which may be concentrated by scavenging on hydrous Fe and Mn oxides.
- iii. baryte – Ba and Sr have close association, independent of other variables. This supports the existence of a separate phase of baryte formation, unrelated to base-metal mineralisation and to events associated with ilmenite-magnetite formation.

The distributions of Zr, Cr and B were interpreted to be largely independent of other elements and to be unrelated to mineralisation processes. The role of contamination was regarded as of generally minor importance in this area.

Two targets with potential for epithermal gold mineralisation can be identified in the G-BASE and MRP datasets:

- i. the area around Kingsseat and Windy Gyle, where geochemical anomalies occur in an extensive suite of elements including As, Ba, Bi, Co, Cr, Cu, Fe, Mn, Mo, Ni, Pb, Sb, Sr, Ti.
- ii. Breamish Fault Zone, where enrichments occurs in As, Cu, Pb, Bi, Zn, Sb and Mo.

Another notable feature of the geochemical data is the transition which occurs in the distribution patterns of many elements across the line of the Gyle–Harthope Fault. Several elements, including Co, Cu, Pb, Zn and Mn, have higher background concentrations to the south-east of the fault than to the north-west. This may be due to relative movement along the fault, which has exposed a deeper level in the volcanic pile to the south-east. This interpretation is consistent with the greater abundance of dykes mapped in this sector of the Cheviot Volcanic Group. The presence of known and undiscovered occurrences of mineralisation in this zone may also contribute to the observed distributions of some of these elements, although the deeper erosion level in the south-east indicates lower favourability for the occurrence of epithermal mineralisation.

8.4. Geophysics

8.4.1. Bouguer gravity data

The Bouguer gravity anomaly map (Figure 8.25) shows a clear minimum over the Cheviot Granite, north-west of Hedgehope Hill, superimposed on a larger negative feature which extends from south of the granite north-eastwards into the Hetton Carboniferous trough. There is also a broad negative anomaly approximately over the south-east part of the Devonian volcanic outcrop. This may relate to the lavas; to a subsurface extension of the granite or to Devonian sedimentary strata beneath the lavas.

A qualitative explanation of the Bouguer gravity anomaly map can be obtained from measured rock densities in the region (Lee, 1982). The Cheviot Granite has a relatively low bulk saturated density [2.64 Mgm^{-3} (standard deviation 0.07)], with the central Standrop variety slightly less dense [$2.58 (0.07)$]. Carboniferous limestones [$2.68 (0.02)$], shales [$2.56 (0.04)$] and sandstones [$2.42 (0.03)$] have densities which overlap those of the granitic rocks, but the limestones adjacent to the intrusion are generally slightly denser. Devonian andesites have a variable density depending on petrology and weathering [$2.55\text{--}2.65 \text{ Mgm}^{-3}$]. Upper Devonian sandstones in the Midland Valley have saturated densities down to about 2.40 Mgm^{-3} while the Lower Devonian strata generally have densities close to 2.60 Mgm^{-3} . Lower Palaeozoic Silurian strata have densities close to 2.71 Mgm^{-3} . Consequently, while the exposed granitic rocks are directly associated with a closed gravity minimum, part of the regional low over the volcanic rocks might be due to a much larger area of buried granite, a wedge of andesitic rocks or a hidden basin of Lower Devonian sedimentary rocks.

Residual gravity anomalies (Figure 8.26) derived from a ‘continuation’ regional field (defined as the observed field after upward continuation by 5 km) show the Cheviot Granite anomaly superimposed on a broader negative anomaly which covers much of the south-east part of the outcrop of the Devonian lavas and extends to the north-east of the granite into the Hetton Trough. In this residual field there is a distinct closed negative anomaly at

Windy Gyle close to the Gyle–Harthope Fault. A second residual gravity low occurs about 5 km south-west of Cushat Law.

Regional Bouguer anomalies derived from the observed data sub-sampled at approximately one station in every eight with selective removal of data over, and close to, the mapped granite produces a field (Figure 8.27) reflecting the main features of the geological structure away from the granites. Residual anomalies derived from the data after subtraction of the sub-sampled regional field produce a residual field (Figure 8.28) which represents the main effect of the granite intrusion. This field has anomalies of about -10.5 mGal over the main phase of the granite, with minor residual lows in the Windy Gyle area and to the south-west of Cushat Law.

In both residual maps there is a clear negative anomaly over the main granite with a secondary low over the Windy Gyle area. The source of the Windy Gyle residual anomaly is of potential significance for epithermal mineralisation since it might reflect the presence of a high-level acid or intermediate intrusion into the lavas. Furthermore, detailed mapping by BGS suggests that the Gyle–Harthope fault system is more significant than on published maps. This north-east-trending structure might form an important feature in the basement and be a focus for the igneous intrusion and hydrothermal fluid flow. The broader negative anomaly over the andesites to the north-west of the fault, seen in the regional field derived from the sub-sampled data, is therefore likely to be due to a Lower Devonian basin beneath the lavas rather than extensive granite.

8.4.2. Aeromagnetic data

Total magnetic intensity data (TMI) (Figure 8.29) show a regional positive low-amplitude anomaly over the andesitic lavas with a more focused anomaly over the Cheviot Granite. Total field values over Cheviot are above 400 nT over the south and south-east parts of the intrusion. The data show a minor low-amplitude positive anomaly close to Windy Gyle. The polar TMI anomaly (Figure 8.30) at 800 m above ground level (after upward continuation by 500 m) suggests that the source of the main anomaly is the Cheviot Granite and its magnetic phases. Specifically, the maxima of the polar field lie inside the mapped granite outcrops. Lee (1982) quotes susceptibility values for the marginal granite types of about 0.030 SI; for the Standrop and granophyric varieties 0.006 SI and for some meta-andesites 0.034 SI. The andesites and rhyolites generally have a low mean susceptibility of about 0.003 SI. The polar magnetic anomaly can be interpreted to suggest that there is no evidence of a magnetic granite cupola at Windy Gyle south-west of the main granite. In this case any satellite mass in this area would be similar to the later more granitic Standrop phase of the Cheviot Granite. Detailed MRP mapping in this area, between the Kingsseat Burn and Windy Gyle, has identified biotite porphyry and biotite pyroxene porphyry as well as minor vent material (Cameron et al., 1988). However the alteration paragenesis documented in this area suggests that the porphyry intrusions are early and actually pre-date tourmalinisation associated with the Cheviot Granite.

8.4.3. 3-D gravity-magnetic model

Lee (1982) interpreted a -25 mGal residual gravity anomaly over the Cheviot Granite in terms of a large intrusion extending to a depth of about 9 km with a significant roof region. Shallow granite, at depths less than 2 km below sea-level, was interpreted across an area at least twice the present outcrop area of the granite, including the Windy Gyle area and a southerly extension along the Biddlestone anticline approximately 5 km from the outcrop margin. A separated residual field, due to near-surface Devonian lavas and sandstones, was interpreted in terms of a lava pile generally less than 500 m thick.

A simple 3-D model of the granite has been generated from the sub-sampled residual anomaly, assuming density contrasts of -0.04 (marginal phases) and -0.08 Mgm^{-3} (central phase). An initial surface was constructed from the residual anomaly assuming granite within the -1.0 mGal contour. This upper surface was then constrained so that granite extended to surface in zones compatible with the geological map. The initial base of the granite was approximately an inversion of the upper surface and extended to about 8 km below OD. With modulation of the base and minor adjustment of the densities this model approximately matches the residual field [RMS error 0.8 mGal]. The map showing the modelled depth to the top of the granite (Figure 8.31) indicates shallow non-magnetic granite beneath the Windy Gyle area and generally steep sides to the main outcrop at Cheviot. It provides a more compact granite solution than that described by Lee (1982).

A regional 2D ‘full-crust’ model of the gravity and magnetic data through the Cheviot Granite (Figure 8.32) interprets part of the regional gravity low over the Devonian lavas and granite as due to Lower Devonian strata beneath the andesite flows with minor intrusive material of laccolithic form adjacent to the granite. This is broadly consistent with the marginal magnetic aureole to the granite which suggests that the roof region of the granite is not much larger than the exposed surface.

8.4.4. Geophysical lineaments

A lineament analysis, similar to that described for the Ochil Hills and Lorn Plateau, has been carried out for gravity, magnetic and Landsat TM data over the Cheviot Hills (Figures 8.33, 8.34 and 8.35). A similar analysis has been undertaken for fault vectors from the 1:250 000 digital geological map. The azimuthal frequency diagrams for these lineament sets reflect the structural fabric of the region (Figure 8.36). Magnetic lineaments show a strong east-west orientation with a secondary population at about 120° . The gravity data show two orthogonal sets trending $60^\circ/150^\circ$ and $30^\circ/120^\circ$. The fault vectors have a strong north-east preferred orientation with population maxima at 50° and 60° . Landsat TM lineaments cluster at about 40° and 90° .

8.4.5. Discussion

All known gold occurrences in the district are located on, or close to, the Cheviot Granite, and are situated within the zone of positive ($>20 \text{ nT}$) polar magnetic anomaly at 800 m above ground level. There is also an association with residual gravity minima around Windy Gyle and Kings Seat. Magnetic susceptibility values on a suite of rock samples from this area indicate a low mean value for the exposed porphyry intrusive rocks (see Section 8.5.2). This may partly reflect hydrothermal alteration of these rocks, but the less altered samples also have low susceptibility, comparable to the granophyric or central granite types. Consequently, the gravity and magnetic data in the Windy Gyle area are consistent with the presence of a low-density, poorly magnetic magma. Other intrusions of this type might be present elsewhere in the volcanic pile but are poorly represented in the existing gravity data coverage and are not prominent in the regional magnetic data. Local gravity minima close to the granite have been included as key parameters in the prospectivity analysis.

South-east of the Gyle–Harthope Fault the gravity map suggests that the lavas are at a lower structural level and that this sector is intruded by more dykes than to the north-west of the fault. The relationship of mineralisation to lineaments is less clear, but north-east- and north-north-east-trending gravity lineaments are favoured and have been used in the prospectivity analysis.

8.5. Investigations in the Kingsseat Burn area

8.5.1. Previous work

The MRP reconnaissance drainage geochemical survey of the western Cheviot Hills identified prominent, multi-element geochemical anomalies in the Cocklawfoot–Kingsseat area (Figure 8.1). Follow-up surveys comprising geological mapping, a detailed drainage and rock geochemical survey and associated petrographic and mineralogical studies were carried out to identify the sources of these anomalies (Cameron et al., 1988).

Geology

The area is underlain by rocks of the Cheviot Volcanic Group and related intrusions. The eastern half is composed of dominantly andesitic lavas with subordinate pyroclastic and sedimentary strata and two main vent breccias. The rocks in the western half of the area were previously mapped as mica felsite or rhyolite (Carruthers et al., 1932; Robson, 1976). However, re-mapping during the MRP survey interpreted these rocks as intrusive in origin, comprising five distinct porphyritic lithologies which together make up the Cock Law Complex. The two main components are biotite porphyry and pyroxene-biotite porphyry, with subordinate pyroxene porphyry, biotite-quartz porphyry and granodiorite porphyry. The overall form of the complex is difficult to determine, but the available evidence suggests that it is laccolithic.

Several kaolinised minor intrusions of stock- or dyke-like form were also mapped in the Kingsseat Burn area, while at the head of Cheviot Burn, about 5.5 km north-east of Windy Gyle, exposures of pink biotite microgranite are possibly part of the Cheviot Granite complex.

All the volcanic and intrusive rocks in the area have undergone some form of alteration, which varies greatly in type and intensity. Seven main assemblages of alteration minerals were recognised: the most important are kaolinite-dominated assemblages which show a close spatial association with the porphyry intrusions, and sericite-dominant assemblages which are best developed in the volcanic sequence. The alteration assemblages exhibit complex spatial and temporal relations which make it difficult to establish any zoning sequence within the area related to a single event or a sequence of events. However, the following generalised scheme was proposed:

- i. deuteric alteration of lavas and intrusive rocks to sericite ± chlorite ± amphibole ± epidote
- ii. hydrothermal alteration of porphyry intrusions and country rocks to give kaolinite-dominant assemblages
- iii. carbonate alteration
- iv. tourmalinisation (bluish-green) associated with granite intrusion
- v. late polyphase events including hematite alteration, quartz and carbonate veining and gossan formation

No sulphide minerals were identified during the field surveys, but secondary copper minerals were recorded at a few localities. Malachite is fairly abundant in gossanous debris at the head of Yearning Cleuch [38760 61860] in reddened and fractured andesite which is locally brecciated and stockworked with carbonate and hematite. Quartz vein systems were found at two localities, both on the south side of Kings Seat, near the margin of the Cock Law Complex. At one locality [38778 61717] the country rock adjacent to a one-metre-thick quartz vein is silicified and penetrated by quartz veinlets, and at another [38731 61748], 500 m to the north-west, an anastomosing quartz vein complex about 2 m thick and including late baryte veins cuts brecciated volcanic rocks.

Drainage survey

A detailed drainage geochemical survey was carried out to supplement the reconnaissance data in this area. Stream-sediment and panned concentrate samples were collected from 93 sites. Analysis of concentrates was carried out by XRF, while stream sediments were analysed by AAS for Cu, Pb and Zn and by OES for other elements reported. These data have been added to the reconnaissance MRP drainage data and the distributions of various elements in the integrated dataset are shown in Figures 8.37–8.43.

This survey confirmed and located more precisely anomalies identified in the reconnaissance survey. The wide range of metal enrichments include As, Ba, Bi, Co, Cr, Cu, Fe, Mn, Mo, Ni, Pb, Sb, Sr, Ti, W and Zn. Comparison of stream-sediment and panned-concentrate results indicate that several of the enriched elements are contained mainly in heavy minerals. Detailed mineralogical studies of selected concentrates confirmed this observation for Mn, Ni, Cu, Zn, Mo and Sn, with enrichment observed in Fe and Fe-Ti oxides, principally ilmenite and magnetite. Barium anomalies reflect the distribution of baryte observed during panning, while scattered Pb anomalies are related, at least in part, to observed secondary Pb minerals. The distribution of Cu is more complex and may be explained by several processes including the presence of local secondary copper minerals in the Yearning Cleuch area, by high levels in andesites and in Fe-Ti oxides.

The sources of the As, Sb and W drainage anomalies are not readily explained. Their abundances are not closely correlated with Fe-Ti oxides and no discrete heavy minerals were identified in which these elements are major constituents. It is possible that the high As and Sb values in concentrates may be related to the breakdown of sulphosalt minerals (e.g. enargite, tetrahedrite) to hematite under oxidising conditions. No As or Sb data are available for stream-sediment samples from the follow-up investigations in the Kingsseat Burn area.

Lithochemochemistry

Geochemical analyses were carried out on 82 samples from the principal lithologies exposed in the Kingsseat area. A subset of 29 samples was analysed for Au by AAS. Summary statistics for these samples are presented in Table 8.5.

The distribution of rock samples with Au contents exceeding 10 ppb and of anomalous values (> 90th percentile) of As, Sb and Cu is shown in Figure 8.44. Two samples from the Yearning Cleuch area are enriched in a suite of elements indicating complex, multi-stage mineralising processes, possibly including an epithermal event. Sample NTR 54, comprising outcropping gossan, is enriched in Au (43 ppb), Ag, As, Ba, Cu, Fe, Mn, Mo, Pb, Sb and U. Sample NTR 56 which comprises blocks of breccia from a scree has a similar geochemical signature, although lacking Au, Mn and Ba enrichment. Elsewhere in the Cock Law Complex As enrichment is widespread, locally accompanied by high Sb values. For example, NTR 21, from the lower part of Bank Burn, comprises strongly hematitised porphyry containing high values of As, Sb and Mo, but lacking any enrichment in Au or Ag. Copper enrichment, without attendant As or Sb, is more widely developed in the volcanic rocks, while high-tenor Pb values alone are restricted to altered rocks from the Cock Law porphyry intrusions. The inter-element associations in the lithochemochemical data are displayed graphically in Figure 8.45.

Table 8.5 Summary statistics for lithochemical samples, Kingsseat Burn area
(all values in ppm, except Au ppb)

| Element | no. samples | mean | minimum | maximum | 50% | 75% | 90% | 95% |
|---------|-------------|---------|---------|---------|-------|-------|-------|-------|
| Au | 29 | 3.2 | 1 | 43 | 1 | 1 | 1 | 11 |
| Ag | 82 | 1.4 | 0.1 | 27 | 1 | 1 | 2 | 2 |
| As | 82 | 31.9 | 1 | 1181 | 7 | 16 | 37 | 84 |
| Ba | 82 | 572.5 | 51 | 1983 | 640 | 782 | 851 | 890 |
| Bi | 82 | 0.3 | 0.2 | 1 | 0.2 | 0.2 | 0.2 | 1 |
| Ca | 82 | 11022.1 | 70 | 257040 | 4110 | 14540 | 18350 | 21200 |
| Ce | 82 | 76.1 | 36 | 158 | 75 | 83 | 90 | 99 |
| Cu | 82 | 352.7 | 0.5 | 26079 | 11 | 20 | 40 | 55 |
| Fe | 82 | 46722 | 11880 | 470340 | 39520 | 45750 | 57090 | 65440 |
| Mn | 82 | 344 | 30 | 2830 | 350 | 460 | 540 | 660 |
| Mo | 82 | 3.3 | 0.5 | 117 | 1 | 2 | 3 | 4 |
| Nb | 82 | 14.8 | 1 | 23 | 15 | 17 | 19 | 20 |
| Ni | 82 | 31.4 | 1 | 84 | 33 | 44 | 54 | 58 |
| Pb | 82 | 31.8 | 5 | 305 | 24 | 30 | 41 | 58 |
| Rb | 82 | 165.1 | 1 | 302 | 181 | 216 | 241 | 276 |
| Sb | 82 | 10 | 0.2 | 271 | 3 | 7 | 19 | 24 |
| Sn | 82 | 1.5 | 0.5 | 5 | 1 | 2 | 4 | 4 |
| Sr | 82 | 208.5 | 13 | 569 | 170 | 316 | 409 | 460 |
| Th | 82 | 20.9 | 3 | 35 | 20 | 25 | 27 | 28 |
| Ti | 82 | 4557.9 | 690 | 8880 | 4320 | 5140 | 6030 | 6770 |
| U | 82 | 5.9 | 1 | 110 | 5 | 6 | 7 | 7 |
| W | 82 | 6.1 | 0.5 | 19 | 6 | 8 | 9 | 10 |
| Y | 82 | 18.8 | 3 | 61 | 18 | 20 | 22 | 27 |
| Zn | 82 | 61.4 | 2 | 200 | 59 | 80 | 100 | 126 |
| Zr | 82 | 296 | 18 | 434 | 287 | 348 | 368 | 380 |

8.5.2. PIMA analysis and magnetic susceptibility data

PIMA spectra were acquired in the current project in order to elucidate the alteration mineral assemblages previously identified (Cameron et al., 1988). Spectra were measured on reference hand specimens of samples collected during the MRP survey. A total of 85 spectra were recorded with a PIMA II instrument in the laboratory. Spectral analysis was carried out using The Spectral Geologist (TSG v.1.1) software package. A summary of the TSG analysis of the PIMA spectra is displayed in Figure 8.46. Corresponding magnetic susceptibility values (10^{-3} SI units) measured with a kappameter are shown in the same figure.

In general, the results of the PIMA analysis are in good agreement with the previously identified alteration minerals. Porphyritic rocks yield spectra dominated by kaolinite, locally accompanied by dickite, illite, montmorillonite, halloysite or, rarely, jarosite. The assemblage kaolinite-dickite-jarosite comprises an advanced argillic alteration suite, typically accompanied by quartz, which may relate to a high-sulphidation epithermal system. PIMA spectra for the andesites are more varied but indicate mainly muscovite (sericite), chlorite, illite, phengite and rare epidote. These minerals indicate sericitic (phyllic) and propylitic alteration assemblages which may be found in porphyry or distal epithermal settings.

Magnetic susceptibility values for the same suite of rock samples range up to a maximum of 5.51×10^{-3} SI. The distribution of magnetic susceptibility values around Kingsseat Burn and Windy Gyle is shown in Figure 8.47. In most porphyritic intrusive rocks values are less than 1, although several samples of variably altered, pyroxene-biotite porphyry have values exceeding 2×10^{-3} SI. The andesites are more varied, but rarely have susceptibilities greater than 2×10^{-3} SI.

The application of PIMA analysis has confirmed the presence of advanced argillic, sericitic and propylitic alteration in the Kingsseat area. However, the limited data availability and the complexity of the geology do not allow any clear relationships to be established between mineralisation, alteration and magnetic susceptibility.

8.5.3. Discussion

Available evidence from geochemical, geological and mineralogical studies indicates that complex multi-stage hydrothermal processes have operated in the area around Kingsseat and Windy Gyle. These have resulted in enrichment in an extensive suite of metals in rocks and drainage samples and have led to the development of complex alteration which varies markedly in type and distribution across the area.

Cameron et al. (1988) developed the following speculative timetable for igneous and mineralising events that affected the area:

- i. extrusion of andesite lavas with local Cu enrichment
- ii. intrusion of the Cock Law tonalitic porphyry complex, perhaps contemporaneously with the volcanism
- iii. argillic alteration of the porphyry and, locally, the volcanic pile, perhaps accompanied by weak W and other mineralisation
- iv. intrusion of the Cheviot Granite and contact metamorphism of the volcanics
- v. granite-related high temperature hydrothermal activity, tourmalinisation, silicification, and perhaps, locally, Sn mineralisation
- vi. epithermal mineralisation
- vii. baryte mineralisation
- viii. hematite and specularite formation, carbonate and quartz veining
- ix. gossan formation. Redistribution or introduction of some metals (Cu and U) associated with this or the previous event.

There are many uncertainties over the timing and sequence of these events, although the importance of the control of major fracture zones on the location of alteration and mineralisation is clear. Further work is required

to clarify the relationships between the various igneous episodes, the alteration assemblages and the phases of mineralisation. It is likely that some stages overlapped, while others were superimposed on the products of earlier events.

It is clear, however, that a phase of epithermal activity, of possible high-sulphidation style, affected the area. This may have been related to an early phase of high-level intrusions associated with the Cock Law Complex, rather than the later intrusion of the Cheviot Granite as suggested above. This is supported by the observation of Cameron et al. (1988) that the tourmalinisation event accompanying granite emplacement post-dates the lower temperature advanced argillic and sericitic alteration. Accordingly it is suggested that the main phase of epithermal mineralisation was associated with stage iii above, rather than stage vi.

The last two stages in the model proposed by Cameron et al. may have taken place at a later time, possibly related to Hercynian or Tertiary events in the region. Hematite alteration and gossan formation may have significantly affected the concentration of Au and other associated elements enriched in the epithermal environment. Oxidation of sulphosalt minerals, such as enargite and tetrahedrite which are common in high-sulphidation systems, can lead to the formation of hematite which, in the secondary environment, could give rise to the element associations observed in drainage samples in the Kingsseat area. The local enrichments in Mo and W are also consistent with geochemical abundances reported from high-sulphidation epithermal systems.

8.6. Data integration and prospectivity analysis

As for the other project areas, key exploration parameters for analysis of the prospectivity for epithermal gold mineralisation in the Cheviot Hills were defined on the basis of published deposit models, empirical observations of mineralisation in the district, and the availability of suitable multivariate digital data. Each parameter was assigned a zone of influence (number of cells), a style of influence (exponent) and a weighting (Table 8.6).

Seventeen parameters were considered in the analysis for this area. These included: enrichment in a suite of elements in drainage geochemical data; presence of negative residual gravity anomalies possibly related to high-level intrusions; various lineament intersections and faults, especially those associated with geochemical anomalies; and known mineral occurrences. The distributions of these parameters in the area are shown in the multi-dataset maps (Figure 8.48, 8.49, 8.50 and 8.51).

Several geochemical parameters are used in this analysis. This has the effect of highlighting areas where sample density is greatest and where multiple-site multi-element anomalies were identified. Even though individual parameters are given a low weight the cumulative effect is to generate high prospectivity where follow-up MRP sampling was carried out. This effect has been reduced by using the 95th, rather than the 90th, percentile values as the anomaly thresholds for the MRP datasets. Selective or arbitrary exclusion of data points is considered inappropriate due to the effect on the data distributions and the risk of excluding critical anomalous values. For the regional G-BASE data anomaly thresholds were set at the 90th percentile values.

The prospectivity analysis was carried out in X-MAP with a pixel size of 250 m square using the Boolean logic data model normalised to produce a binary weights-of-evidence map for the district (Figure 8.52). The main epithermal gold targets identified and their key features are summarised in Table 8.7. The area of the negative residual gravity anomaly to the south-west of Cushat Law is not identified as prospective as it lacks key geochemical and structural features which were used in the analysis.

Table 8.6 Index parameters used for prospectivity analysis, Cheviot Hills

| zone of influence | exponent | weight | parameter |
|-------------------|----------|--------|--|
| 0 | 2.0 | 0.1 | andesitic lavas from 1:250K map |
| 0 | 2.0 | 0.2 | pyroclastic rocks from 1:50K maps |
| 1 | 2.5 | 0.2 | major faults |
| 4 | 2.5 | 0.1 | intersections of north to north-east magnetic or gravity lineaments and faults |
| 4 | 2.5 | 0.1 | intersections of east to south-east magnetic or gravity lineaments and faults |
| 4 | 2.5 | 0.4 | gold occurrences |
| 4 | 2.5 | 0.1 | lead and copper mineral occurrences |
| 6 | 2.5 | 0.2 | negative residual gravity anomalies |
| 4 | 2.5 | 0.2 | G-BASE stream-sediment data, As > 23 ppm |
| 4 | 2.5 | 0.1 | G-BASE stream-sediment data, Cu > 27 ppm |
| 4 | 2.5 | 0.1 | G-BASE stream-sediment data, Sb > 2.5 ppm |
| 4 | 2.5 | 0.1 | MRP panned-concentrate data, Pb > 186 ppm |
| 4 | 2.5 | 0.1 | MRP panned-concentrate data, Bi > 3 ppm |
| 4 | 2.5 | 0.1 | MRP panned-concentrate data, As > 80 ppm |
| 4 | 2.5 | 0.1 | MRP panned-concentrate data, Mo > 12 ppm |
| 4 | 2.5 | 0.1 | MRP panned-concentrate data, Zn > 302 ppm |

Table 8.7 Main targets for epithermal gold, Cheviot Hills

| Area | Centre | Approx size (km ²) | Geology | Drainage geochemical anomalies | Negative gravity anomaly | Positive magnetic anomaly | Faults or intersections |
|------------------------|---------|--------------------------------|----------------------------|--|--------------------------|---------------------------|-------------------------|
| Kingsseat – Windy Gyle | 387 617 | 15 | andesite; porphyry complex | As, Ba, Bi, Co, Cr, Cu, Fe, Mn, Mo, Ni, Pb, Sb, Sr, Ti, W and Zn | ✓ | ✓ | ✓ |
| Breamish Fault | 394 615 | 4 | andesite | As, Cu, Pb, Bi, Zn, Sb and Mo | | ✓ | ✓ |

9. DISCUSSION AND CONCLUSIONS

The delineation of favourable resource areas and the identification of exploration targets have traditionally been carried out by manual inspection procedures. However, with the recent increased availability of high-quality digital geoscientific data of potential exploration significance, there is a growing need for systems which maximise the utility of these data through the application of quantitative, consistent and objective methods.

In this study, XMAP has been used to map the potential for epithermal gold mineralisation in the three main Lower Devonian volcanic terrains of northern Britain. Selection criteria were derived from published models and from assessments of known epithermal occurrences in these areas. The following key features were taken into account in the analysis: tectonic setting, regional structure, regional geochemistry, stratigraphy, lithology and buried intrusions and their contacts. Parameters which provide information on these features were extracted from regional and local-scale datasets held on relational databases at BGS. The datasets of greatest utility included:

- i. geology: lithology, age.
- ii. geochemistry: trace-element distributions in drainage geochemical samples, especially As, Sb, Bi and locally Mo, Ag, Cu, Pb and Zn; anomaly thresholds were set at 90th or 95th percentile values.
- iii. geophysics: lineations derived from regional aeromagnetic and gravity survey data; residual magnetic and Bouguer gravity anomalies from the same datasets.
- iv. remote-sensing: lineations taken from satellite images and topographic maps.
- v. mineral occurrences: metalliferous mineralisation in bedrock and in mine workings; incidence of alluvial gold grains in heavy mineral concentrates.

The key exploration criteria for epithermal gold mineralisation in each of the study areas are summarised in Table 9.1. Recognition of these criteria in the various datasets yields a positive prospectivity score in XMAP and thus allow predictions to be made of the locations of areas favourable for epithermal gold deposits in northern Britain.

9.1. Ochil Hills

Prospectivity analysis has confirmed the potential of an area of approximately 12 km² in the western part of the central Ochil Hills of the Midland Valley of Scotland. This area, to the north and west of Borland Glen, is identified by the widespread occurrence of alluvial gold, by drainage geochemical anomalies and by its favourable geological setting comprising high-level intrusions emplaced in andesitic volcanic rocks. Detailed investigations by the MRP had previously established the presence of extensive hydrothermal alteration in one area of Borland Glen. PIMA analysis of archived drillcore from that programme has confirmed the presence of sericitic alteration and silicification associated with low-tenor Au enrichment in bedrock in this area. Smaller prospective areas were also identified around Culteuchar Hill, 12 km north-east of Borland Glen, and on the north Fife coast of the Tay estuary. Coincidence of various geological, geophysical and geochemical parameters in the Tillicoultry area indicate potential for higher temperature, base-metal-dominated intrusion-related mineralisation. The erosion level in this sector is such that any overlying epithermal mineralisation is likely to have been removed.

Table 9.1 Key exploration criteria for Lower Devonian volcanic terrains in northern Britain

| Data class / area | Geology | Geochemistry | Geophysics | Mineral occurrences | Structures and lineaments |
|----------------------|--------------------------------------|--|---|---------------------|---|
| Ochil Hills | andesite; diorite; porphyry | As, Sb, Bi, Mo, Ag in stream sediments | residual gravity and magnetic anomalies | Cu, Pb: alluvial Au | intersections of north-west magnetic or gravity lineaments with any topographic or Landsat lineament |
| Lorn Plateau | andesite; acid lavas; tuffs; diorite | As, Bi, Cu, Pb, Zn in stream sediments; Sb, Cu, Pb, Zn in concentrates | residual gravity and magnetic anomalies | alluvial Au | major faults; selected inferred faults (north-west and north-north-east); north-west dykes; intersections of inferred faults and gravity lineaments |
| Cheviot Hills | andesite; tuffs | As, Cu, Sb in stream sediments; As, Bi, Mo, Pb, Zn in concentrates | residual gravity anomalies | Au, Cu, Pb | intersections of north-north-east gravity or magnetic lineaments and faults; intersections of east-south-east gravity or magnetic lineaments and faults |

9.2. Lorn Plateau

Little systematic exploration for gold has been undertaken in the Lower Devonian volcanic rocks of the Lorn Plateau in the south-west Highlands of Scotland. However, at Lagalochan, immediately south of the Lorn Plateau, epithermal-porphyry Cu-Mo-Au mineralisation is associated with a Lower Devonian intrusive complex in Dalradian metamorphic rocks. At Lagalochan drainage anomalies for As, Bi, Cu, Mo, Pb, Sb and Zn occur, together with a negative residual gravity and a positive magnetic anomaly. Emplacement of the complex appears to have been controlled by the intersection of north-east- and north-north-east-trending faults. At Bragleenbeg similar geophysical features and various geochemical anomalies are present along the inferred extension of the north-north-east trending fault and define an area of about 5 km² of the volcanic outcrop prospective for epithermal mineralisation. Potential is also indicated in two areas around Beinn Ghlas with a combined extent of about 8 km². High prospectivity over one of these is indicated by the coincidence of favourable geology, fault intersections and geochemical anomalies for several elements. However there are no indications from the mapped geology or from geophysical data of underlying high-level intrusions in the Beinn Ghlas area.

9.3. Cheviot Hills

In the Cheviot Hills prospectivity analysis indicates potential for epithermal mineralisation in two main areas of the Lower Devonian volcanic terrain. In the Kingsseat Burn area, to the south-west of the Cheviot Granite, multi-element geochemical anomalies are associated with a high-level porphyry complex intruded into the andesitic volcanic rocks. A complex alteration history has been documented by previous studies in this area. A reassessment of this data, in conjunction with PIMA analysis of archived rock specimens, suggests that the main phase of epithermal mineralisation may have been associated with intrusion of the porphyry complex prior to emplacement of the main granite. The prospective area extends over about 15 km² and, in addition to the multi-

element geochemical anomalies, is characterised by a negative residual gravity anomaly and intersections of a north-north-east-trending gravity lineament with north-east-trending faults, including the major Gyle–Harthope Fault. The hydrothermal alteration, including advanced argillic and sericitic assemblages, and the low-tenor gold enrichments previously reported in rock samples, confirm the potential of this area for epithermal mineralisation. A smaller prospective area is identified around the Breamish Fault, on the south side of the main granite, mainly on the basis of multi-element geochemical anomalies coincident with the major north-west-trending fault zone.

9.4. Exploration methods

Exploration methods for epithermal gold deposits have been discussed in Section 4 of this report. At the reconnaissance scale, permissive terrain can be identified by various techniques, including assessment of regional geological, geophysical and geochemical datasets. At the prospect scale, local conditions will determine the optimum methods to be used for target definition and resource evaluation. Detailed drainage surveys and basal overburden sampling have been effectively employed by BGS in numerous MRP project areas in northern Britain. Electrical and electromagnetic surveys are also particularly useful for studying alteration zones in epithermal systems, including targets which are buried beneath unaltered or exotic cover. Detailed geological mapping provides a basis for interpretation of the exploration data and can help to elucidate the palaeohydrology of the hydrothermal system and hence to identify fluid conduits and sites of mineral deposition. Detailed litho-geochemistry and associated petrographic and mineralogical studies provide information on the nature of the parent system and hence on the location, extent and morphology of the deposit.

The importance of applying new technologies and genetic concepts to exploration has been demonstrated in this study. PIMA analysis of archived drillcore and rock samples from two areas elucidated the hydrothermal alteration assemblages present and thus contributed to an improved understanding of the mineralising processes. Existing data from regional geochemical and geophysical surveys and from multi-disciplinary exploration projects have been reassessed in the light of recent genetic models for epithermal deposits thereby contributing significantly to the identification of new prospective targets.

9.5. Computer-based data analysis

Knowledge-based prospectivity mapping systems offer many advantages over traditional techniques of data integration and estimation of mineral potential. This technology provides systematic quantitative solutions for the integration of multi-disciplinary digital datasets which are increasingly becoming available, especially to geological surveys. However, the quality of the derived prospectivity maps is dependent on the reliability of mineral-deposit models and the availability of relevant, high quality data. As XMAP is a knowledge-based system it is reliant on the expertise of the user for the identification of the key exploration criteria, for the assignment of weights to those criteria and for definition of the extent and nature of their influence around the occurrence pixel.

The availability of complete and uniform data coverage over the entire study area is required for consistent and unbiased mapping of mineral potential. Commonly, however, this condition may not be fulfilled for all available datasets. For example, differences in sampling density and the elements determined in the two drainage geochemical surveys over the Ochil Hills results in the restricted availability of certain potentially useful exploration parameters. The regional survey provided uniform cover for a limited range of elements over the entire volcanic outcrop, but the later follow-up campaign for gold provided a higher sampling density in some smaller areas and generated data for additional elements of particular relevance to gold exploration. The extra

data are directly relevant to the present study of epithermal gold and have therefore been included in the prospectivity analysis. However, where such data are lacking, the derived potential will inevitably be under-rated.

The quality of the data used in prospectivity analysis is another important consideration. For certain chemical elements, such as Cu, Pb and Zn, reliable and sensitive analytical methods have been available for several decades and no problems should arise from their use in prospectivity mapping. The same cannot be said for some other elements, such as the chalcophile pathfinder elements (As, Sb and Bi) and the precious metals (Au and PGE). High-quality data for these elements are now widely available at reasonable costs, but effective and consistent anomaly recognition may be problematic in older datasets. Given geochemical data of adequate quality, it is also important to be sure that the samples were collected and prepared according to standards appropriate to the needs of a particular project.

Geological maps form the basis of any reserve assessment or prospectivity analysis. Where a regional study is being undertaken it is important to use geological data that have been acquired to uniform standards, with data recorded in a consistent fashion, preferably at a single scale. Fundamental geological data such as lithology and contacts provide important basic parameters, but variations in the amount of detail recorded by different geologists may mean that certain significant parameters cannot be included in the analysis.

The utility of certain datasets may be limited by the scale at which they were collected. Use of exploration parameters from a regional survey in a prospect-scale evaluation is likely to yield erroneous results. For example, the low resolution of the UK regional gravity and aeromagnetic survey data inevitably leads to locational errors in the position of lineaments derived from these data fields. Where event datasets are generated from intersections of regional lineament datasets these errors will be compounded. It is therefore important to be aware of the scale at which the data were acquired and to use them in an appropriate manner.

XMAP is a versatile and powerful tool for the identification and ranking of prospective targets and for the estimation of mineral potential. Further refinements in the data handling and processing and the incorporation of additional datasets will provide more robust modelling solutions and allow the system to be used more effectively. As our understanding of metallogenesis improves, so more reliable exploration criteria can be defined and the system applied with greater confidence to a range of mineralisation styles in addition to epithermal gold deposits. Future applications in quantitative mineral resource planning might include prediction of the number of mineral deposits expected in any given area and the tonnage of metals likely to be contained in them.

10. RECOMMENDATIONS

1. Follow-up surveys are recommended in the areas identified as prospective in each of the Devonian volcanic terrains studied. The investigations should include detailed geological mapping and alteration studies using mineralogical and geochemical techniques. Detailed drainage and overburden sampling should also be carried out together with ground geophysical surveys to investigate the extent and form of hydrothermal alteration.
2. The methodology used in this study can be applied elsewhere in Britain. Knowledge-based prospectivity mapping is a powerful generic tool which can increase exploration efficiency by focusing expensive field programmes. It can be used to map the potential for the occurrence not only of epithermal gold mineralisation, but also of a wide range of other mineral-deposit types.

3. Knowledge-based systems are dependent on the availability of appropriate expertise and well-founded deposit models for their effective application. Continued research on mineral-deposit genesis is required in order to define more reliable exploration criteria and hence to apply the methodology with greater confidence to a range of deposit types, both in the UK and overseas.
4. Prospectivity analysis requires high-quality, relevant digital datasets such as those held in various national geoscience databases by BGS. The continued maintenance and enhancement of these databases are therefore vital. Digitising of archived paper records should continue to ensure their long-term availability for strategic applications such as mineral-potential mapping.
5. The application of new technologies (e.g. PIMA, 3-D modelling) and genetic concepts to existing datasets or archived reference materials is recommended practice. This may provide significant additional information and new insights into the processes responsible for mineralisation and the location of deposits.

11. REFERENCES

ALEKSEEV, S G, DUKHANIN, A S, VESHEV, N A and VOROSHILOV, N A. 1996. Some aspects of practical use of geoelectrochemical methods of exploration for deep-seated mineralisation. *Journal of Geochemical Exploration*, 56, 79-86.

ALLEN P M, COOPER D C, PARKER M E, EASTERBROOK G D, and HASLAM H W. 1982. Mineral exploration in the area of the Fore Burn igneous complex, south-western Scotland. *IGS Mineral Reconnaissance Programme Report*, No. 55.

ALLIS, R G. 1990. Geophysical anomalies over epithermal systems. *Journal of Geochemical Exploration*, 36, 339-374.

ANDREW, C J. 1997. The geology and genesis of the Chelopech Au-Cu deposit, Bulgaria: Europe's largest gold resource. In: *Europe's Major Gold Deposits, IAEG-IMM Conference, Newcastle, County Down, Northern Ireland*, May 1997.

BAJC, A.F. 1998. A comparative analysis of enzyme leach and mobile metal ion selective extractions: Case-studies from glaciated terrain, northern Ontario. *Journal of Geochemical Exploration*, 61, 113-148.

BATCHELOR, R A. 1987. Geochemical and petrological characteristics of the Etive granitoid complex, Argyll. *Scottish Journal of Geology*, 23, 227-249.

BATESON, J H, JOHNSON, C C, and EVANS, A D. 1983. Mineral reconnaissance in the Northumberland Trough. *Mineral Reconnaissance Programme Report. Institute Geological Sciences*, 62.

BONHAM-CARTER, G F. 1994. Geographic information systems for geoscientists: modelling with GIS. (Pergamon: Canada.)

BONHAM-CARTER, G F. 1997. GIS methods for integrating exploration datasets. In: *Proceedings of Exploration '97: Fourth Decennial International Conference on Mineral Exploration*, edited by A. G. Gubins, GEO F/X, 59-64.

- BOYLE, R.W. 1979. Geochemistry of gold and its deposits. *Geological Society of Canada Bulletin*, No 20.
- BRERETON, N R, BROWNE, M A E, CRIPPS, A C, GEBSKI, J S, BIRD, M J, HALLEY, D N, and MCMILLAN, A A. 1988. Glenrothes borehole: geological well completion report. Investigation of the geothermal potential of the UK. British Geological Survey.
- BRITISH GEOLOGICAL SURVEY, 1990. Regional geochemical atlas, Argyll. (Keyworth, Nottingham: British Geological Survey).
- BRITISH GEOLOGICAL SURVEY. 1993. Regional geochemistry of southern Scotland and part of Northern England. (Keyworth, Nottingham: British Geological Survey)
- BRITISH GEOLOGICAL SURVEY. 1997. Colour shaded relief gravity anomaly map of Britain, Ireland and adjacent areas. Smith, I F and Edwards, J W F (compilers) 1:1,500,000 Scale (Keyworth, Nottingham: British Geological Survey).
- BRITISH GEOLOGICAL SURVEY. 1998. Colour shaded relief gravity anomaly map of Britain, Ireland and adjacent areas. Royles, C P and Smith, I F (compilers) 1:1,500,000 Scale (Keyworth, Nottingham: British Geological Survey).
- BROWN, J F. 1975. Rb-Sr studies and related geochemistry on the Caledonian calc-alkaline igneous rocks of N.W. Argyllshire. *D. Phil. Thesis, University of Oxford*.
- BUTT, C R M and ZEEGERS, H. (editors). 1992. Regolith exploration geochemistry in tropical and subtropical terrains. *Handbook of Exploration Geochemistry*, 4, 607pp, (Amsterdam: Elsevier).
- BUTT, C R M, LINTERN, M J and ANAND, R. R. 1997. Evolution of regoliths and landscapes in deeply weathered terrain – implications for geochemical exploration. In: *Proceedings of Exploration '97: Fourth Decennial International Conference on Mineral Exploration*, edited by A. G. Gubins, GEO F/X, 323-334.
- CAMERON, I B and STEPHENSON, D. 1985. The Midland Valley of Scotland. (Third edition). *British Regional Geology*, (London: HMSO).
- CARLILE, J C., DAVEY, G R, KADIR, R P, LANGMEAD, R P and RAFFERTY, W J. 1998. Discovery and exploration of the Gosowong epithermal gold deposit, Halmahera, Indonesia. *Journal of Geochemical Exploration*, 60, 207-227.
- CAMERON, D G, COOPER, D C, BIDE, P J, ALLEN, P M AND HASLAM, H H. 1988. A geochemical survey of part of the Cheviot Hills and investigations of drainage anomalies in the Kingsseat area. *Mineral Reconnaissance Programme Report, British Geological Survey*, No. 91.
- CARRUTHERS, R G, BURNETT, G A, ANDERSON, W, and THOMAS, H H. 1932. The geology of the Cheviot Hills (explanation of sheets 3 and 5). *Memoirs of the Geological Survey of Great Britain*, (London: HMSO).
- CHARLEY M J, HAZLETON R E, and TEAR S J. Precious metal mineralisation associated with the Fore Burn igneous complex, Ayrshire, south-west Scotland. *Transactions of the Institution of Mining and Metallurgy (Section B)*, 98, B48.

- CHINN, G T and ASCOUGH, G L. 1997. Mineral potential mapping using an expert system and GIS. In: *Proceedings of Exploration '97: Fourth Decennial International Conference on Mineral Exploration*, edited by A. G. Gubins, GEO F/X, 105-114.
- CIDU, R, FANFANI, L, SHAND, P, EDMUNDS, W M, VAN'T DACK, L and GIJBELS, R. 1996. Hydrochemical exploration for gold in the Osilo area, Sardinia, Italy. *Applied Geochemistry*, 95, 517-529.
- CLARK, J.R. 1997. Concepts and models for the interpretation of enzyme leach data for mineral and petroleum exploration. In: *Enzyme leach: Model, Sampling Protocol and Case Histories*. Activation Laboratories, Ontario.
- CLAYBURN, J A P, HARMON, R S, PANKHURST, R J and BROWN, J F. 1983. Sr, O and Pb isotope evidence for the origin and evolution of the Etive Igneous Complex, Scotland. *Nature*, 303, 492-497.
- CLOUGH, C T. 1888. The geology of the Cheviot Hills (English side, explanation of new Series sheet 5). *Memoirs of the Geological Survey Great Britain*, (London: HMSO).
- COATS, J S, SHAW, M H, GALLAGHER, M J, ARMSTRONG, M, GREENWOOD, P G, CHACKSFIELD, B C, WILLIAMSON, J P and FORTEY, N J. 1991. Gold in the Ochil Hills, Scotland. *British Geological Survey Technical Report WF/91/1* (BGS Mineral Reconnaissance Programme Report 116).
- COCHRAN-PATRICK, R W. 1878. Early records related to mining in Scotland. (Edinburgh: David Douglas.)
- COLLINS, R S (compiler). 1976. Gold. Mineral Dossier Mineral Resources Consultative Committee, No. 14.
- COLMAN, T B and COOPER, D C. 1998. The combined use of PIMA and VULCAN technology for mineral deposit evaluation based on their application to the Parys Mountain mine, Anglesey. British Geological Survey Technical Report WF/98/4/C.
- COX, D P and SINGER, D A (eds). 1986. Mineral deposit models. *USGS Bulletin 1693*, 379 pp.
- CRISS, R W, CHAMPION, D G and MCINTYRE, D H. 1985. $\delta^{18}\text{O}$, aeromagnetic and gravity anomalies associated with hydrothermally-altered zones in the Yankee Fork Mining District, Custer County, Idaho. *Economic Geology*, 80, 1277-1296.
- CRUMMY, J A. 1993. Geological processes of gold concentration and depletion in Caledonian terrains. *PhD thesis (unpublished)*, University of Glasgow.
- CRUMMY, J, HALL, A J, HASZELDINE, R S and ANDERSON, I K. 1997. Potential for gold mineralisation in east and central Sutherland, Scotland: indications from River Brora headwaters. *Transactions of the Institution of Mining and Metallurgy (Section B)*, 106, B9-14.
- DARNLEY, A G, BJÖRKLUND, A, BØLVIKEN, B, GUSTAVSSOM, N, KOVAL, P V, PLANT, J A, STEENFELT, A, TAUCHID, M. and XIE XUEJING. 1995. A global geochemical database for environmental and resource management. Recommendations for International Geochemical Mapping. *Final Report of IGCP Project 259*. UNESCO Publishing, Paris. 122pp.
- DAVISON, C. 1924. A history of British earthquakes. Cambridge.

DICKIE, D M and FORSTER, C W. (editors) 1974. Mines and Minerals of the Ochils. (Clackmannanshire Field Studies Society.)

DOLLAR, A T J. 1951. Catalogue of Scottish earthquakes, 1916–1949. Transactions Geological Society of Glasgow, 21, 283-361.

DIAKOW, L J, PANTELEYEV, A and SCHROETER, T G. 1991. Jurassic epithermal deposits in the Toodoggone River area, northern British Columbia: examples of well preserved volcanic-hosted precious metal mineralisation. *Economic Geology*, 86, 529-554.

DUBÉ, B, DUNNING, G and LAUZIÈRE, K. 1995. Geology of the Hope Brook mine, Newfoundland: a preserved Late Proterozoic high-sulphidation epithermal gold deposit and its implications for exploration. *Economic Geology*, 93, 405-436.

ELLIS, R A, COATS, J S, HASLAM, H W, ET AL. 1977. Investigations of disseminated copper mineralisation near Kilmelford, Argyllshire, Scotland. *Mineral Reconnaissance Report* No. 9. British Geological Survey.

EVANS, A L, MITCHELL, J G, EMBLETON, B J J, and CREER, K M. 1971. Radiometric age of the Devonian polar shift relative to Europe. *Nature, Physical Science*, 229, 50-51.

FETTES, D J, GRAHAM, C M, HARTE, B and PLANT, J A. 1986. Lineaments and basement domains: an alternative view of Dalradian evolution. *Journal of the Geological Society, London*, 143, 453-464.

FITCHES, W R and MALTMAN, A J. 1984. Tectonic development and stratigraphy at the western margin of the Caledonides: Islay and Colonsay, Scotland. *Transactions of the Royal Society of Edinburgh: Earth Sciences*, 75, 365-382.

FITTON, J G, THIRLWALL, M F, and HUGHES, D J. 1982. Volcanism in the Caledonian orogenic belt of Britain. In: *Andesites*: editor R S Thorpe. John Wiley and Sons.

FORTEY, N J. 1990. Mineralogy and petrography of rock samples and drillcore from the Borland Glen area, Ochil Hills, Scotland. *British Geological Survey Technical Report* WG/90/7R.

FRANCIS, E H, FORSYTH, I H, READ, W A and ARMSTRONG, M. 1970. The geology of the Stirling District (Explanation of One-inch Geological Sheet 39). *Memoir of the Geological Survey of Great Britain*.

FRENCH, W J, HASSAN, M D and WESTCOTT, J. 1979. The petrogenesis of Old Red Sandstone volcanic rocks of the western Ochils, Stirlingshire. In: Harris, A L, Holland, C H and Leake, B E. (editors), *The Caledonides of the British Isles – reviewed. Special Publication Geological Society of London*, No. 8.

FREYSSINET, P, LECOMTE, P and EDIMO, A. 1989. Dispersion of gold and base metals in the Mborguéne lateritic profile, East Cameroun. *Journal of Geochemical Exploration*, 32, 99-116.

FREYSSINET, P and ITARD, Y. 1997. Geochemical mass balance of gold under various tropical weathering conditions: application to exploration; 347-354, In: *Proceedings of Exploration '97: Fourth Decennial International Conference on Mineral Exploration*, edited by A. G. Gubins, GEO F/X, 1068pp.

- GEIKIE, A. 1897. The Old Red Sandstone of Lorn. *Nature*, 56, 157.
- GEIKIE, A. 1900. The Geology of Central and Western Fife and Kinross. *Memoirs of the Geological Survey of Scotland*. Sheet 40 and parts of Sheets 32 and 48.
- GEIKIE, A. 1902. The Geology of Eastern Fife. *Memoirs of the Geological Survey of Scotland*. Sheet 41 and parts of sheets 40, 48 and 49.
- GILL, J B. 1981. Orogenic andesites and plate tectonics. (Berlin: Springer-Verlag).
- GRAHAM, C M. 1986. Petrochemistry and tectonic significance of Dalradian metabasaltic rocks of the SW Scottish Highlands. *Journal of the Geological Society, London*, 132, 61-84.
- GOLDBERG, I S, ABRAMSON, G J, HASLAM, C O and LOS, V L. 1997. Mobile forms of elements: their use in geochemical mapping and exploration. In: *Proceedings of Exploration '97: Fourth Decennial International Conference on Mineral Exploration*, edited by A. G. Gubins, GEO F/X, 365-370.
- GRIMES, D J, MCHUGH, J B, FICKLIN, W H and MEIER, A L. 1993. Anomalous gold, antimony, arsenic and tungsten in groundwater and alluvium around disseminated Au deposits along Getchell Trend, Humboldt County, Nevada. In: *D.I. Fletcher (Editor), Integrated Methods in Exploration and Discovery Society of Economic Exploration*, USA.
- GROOME, D R, and HALL, A. 1974. The geochemistry of the Devonian lavas of the Northern Lorn Plateau, Scotland. *Mineralogical Magazine*, 39, 621-640.
- GUNN, A G, STYLES, M T, SHAW, M H and FLETCHER T A. 1991. Exploration for platinum-group elements in Caledonian igneous rocks of NE Scotland. *Paper presented at Exploration and the Environment, Ninth International Conference on Prospecting in Areas of Glaciated Terrain*, Edinburgh, September 1991.
- GUNN, A G, WIGGANS, G N, COLLINS, G L, ROLLIN, K E and COATS, J S. 1997. Artificial intelligence in mineral exploration: potential applications by SMEs in Britain. British Geological Survey Technical Report WF/97/3C, 58pp.
- HALL J, 1986. Geophysical lineaments and deep continental structure. *Philosophical Transactions of the Royal Society*, London A, 317, 33-44.
- HALL, I H S, GALLAGHER, M J and others. 1982. Investigation of polymetallic mineralisation in Lower Devonian volcanics near Alva, central Scotland. *Mineral Reconnaissance Programme Report Institute of Geological Sciences*, No. 53.
- HALLBERG, A. 1994. The Enåsen gold deposit, central Sweden: 1. A palaeoproterozoic high-sulphidation epithermal gold mineralisation. *Mineralium Deposita*, 29, 150-162.
- HARRIS, A L and BERRIDGE, N G. 1969. The geology of the Nant hydro-electric tunnels. *Bulletin of the Geological Survey of Great Britain*, 30. Institute of Geological Sciences (British Geological Survey).

- HARRIS, M, KAY, E A, WIDNALL, M A, JONES, E M, and STEELE, G B. 1988. Geology and mineralisation of the Lagalochan intrusive complex, western Argyll, Scotland. *Transactions of the Institution of Mining and Metallurgy (Section B)*, 97, 15-21.
- HASLAM, H W. 1975. Geochemical survey of stream waters and stream sediments from the Cheviot area. *Report Institute Geological Sciences 75/6*.
- HASLAM, H W. 1986. Mineral investigations in the Ben Nevis and Ballachulish areas of the Scottish Highlands. *Mineral Reconnaissance Programme Report British Geological Survey*, No. 80.
- HASLAM, H W. 1986. Pyroxenes and coexisting minerals in the Cheviot Granite. *Mineralogical Magazine*, 50, 671-674.
- HASLAM, H W and KIMBELL, G S. 1981. Disseminated copper-molybdenum mineralisation near Ballachulish, Highland Region. *Mineral Reconnaissance Programme Report British Geological Survey*, No. 43.
- HASLAM, H W and CAMERON, D G. 1985. Disseminated molybdenum mineralisation in the Etive plutonic complex in the western Highlands of Scotland. *Mineral Reconnaissance Programme Report British Geological Survey*, No. 76.
- HEALD, P., FOLEY, N.K. and HAYBA, D.O. 1987. Comparative anatomy of volcanic-hosted epithermal deposits. Acid-sulphate and adulaia-sericite types. *Economic Geology*, 82, 1-26.
- HEDENQUIST, J W and LOWENSTERN, J B. 1994. The role of magmas in the formation of hydrothermal ore deposits. *Nature*, 370, 519-527.
- HEDENQUIST, J W, IZAWA, E, ARRIBAS, A Jr and WHITE, N C. 1996. Epithermal gold deposits: styles, characteristics and exploration. *Resource Geology Special Publication Number 1*, (Society of Resource Geology; Tokyo).
- HEDENQUIST, J W, ARRIBAS, A Jr and REYNOLDS, T J. 1998. Evolution of an intrusion-centred hydrothermal system: Far Southeast-Lepanto porphyry and epithermal Cu-Au deposits. *Economic Geology*, 93, 373-404.
- HEDENQUIST, J W and ARRIBAS, A, Jr. 1999. The tops and bottoms of high-sulphidation epithermal ore deposits. In: *Mineral deposits: Processes to Processing*, Stanley et al. (eds), Balkema, Rotterdam, 515-518.
- HIPKIN, R G and HUSSAIN, A. 1983. Regional gravity anomalies: 1 Northern Britain. *Institute of Geological Sciences Report 82/10*, 45.
- INSON, P R and MITCHELL, J G. 1974. K-Ar isotope age determinations from Scottish mineral localities. *Transactions of the Institution of Mining and Metallurgy (Section B: Applied Earth Sciences)*, 83, B814-818.
- IRVINE, R J and SMITH, M J. 1990. Geophysical exploration for epithermal gold deposits. In: Hedenquist, J W, White, N C and Siddeley, G (editors), *Epithermal gold mineralisation of the circum-Pacific: geology, geochemistry, origin and exploration, II*. *Journal of Geochemical Exploration*, 36, 375-412.

- IZAWA, E, URASHIMA, Y, IBARAKI, K, SUZUKI, R, YOKOYAMA, T, KAWASAKI, K, KOGA, A and TAGUCHI, S. 1990. The Hishikari gold deposit: high grade epithermal veins in Quaternary volcanics of southern Kyushu, Japan. In: Epithermal gold mineralisation of the Circum-Pacific geology, geochemistry, origin and exploration, II, Eds. Hedenquist, J W, White, N C and Siddley, G. *Journal of Geochemical Exploration*, 36, 1-56.
- JASSIM, R Z, PATTRICK, R A D, and RUSSELL, M J. 1983. On the origin of the silver + copper + cobalt + baryte mineralization of Ochil Hills, Scotland: a sulphur isotope study. *Transactions of the Institution of Mining and Metallurgy (Section B: Applied Earth Sciences)*, 92, B213-216.
- JHINGRAN, A G. 1942. The Cheviot Granite. *Quarterly Journal of the Geological Society, London*, 98, 241-255.
- JOHNSON, I M and FUJITA, M. 1985. The Hishikari gold deposit: an airborne EM discovery. *CIM Bulletin*, 78, 61-66.
- KAY, E A. 1985. Hydrothermal mineralisation and alteration of the Lagalochan Au-Cu-Mo prospect, W Scotland. *Unpublished PhD Thesis, University of London*.
- KELLEY, K D, ROMBERGER, S B, BEATY, D W, PONTIUS, J A, SNEE, L W, STEIN, H J and THOMPSON, T B. 1998. Geochemical and geochronological constraints on the genesis of Au-Te deposits at Cripple Creek, Colorado. *Economic Geology*, 93, 981-1012.
- KIFF, I T and SPENCE, W H. 1988. Gold mineralisation and associated alteration patterns at the Haile mine, Lancaster County, South Carolina. In: *Southeast Geological Excursions*, ed. Secor, D T S., Carolina Geological Survey, 29-39.
- KNOX-ROBINSON, C M and GROVES, D I. 1997. Gold prospectivity mapping using a Geographic Information System (GIS) with examples from the Yilgarn Block, Western Australia. *Chronique de la Recherche Minière*, No 529, 127-138.
- KYNASTON, H, and HILL, J B. 1908. The geology of the country near Oban and Dalmally. *Memoir of the Geological Survey of Great Britain (Scotland)*.
- KRUPP, R E and SEWARD, T M. 1987. The Rotokawa geothermal system, New Zealand: an active epithermal gold-depositing environment. *Economic Geology*, 82, 1109-1130.
- LANG, B, EDELSTEIN, O, STEINITZ G, KOVACS, M and HALGA, S. 1994. Ar-Ar dating of adularia – a tool in understanding genetic relations between volcanism and mineralisation: Baia Mare area (Gutii Mountains), Northwestern Romania. *Economic Geology*, 89, 174-180.
- LATHAM, A G, and BRIDEN, J C. 1974. Paleomagnetic field directions in Siluro-Devonian lavas of the Lorn Plateau, Scotland, and their regional significance. *Geophysical Journal*, 43, 243-252.
- LAWRANCE, L M. 1995. Redox controls on the formation of supergene gold deposits. *Extended abstract of paper presented at 17th International Geochemical Exploration Symposium*, Townsville, Queensland.
- LEAKE, R C, and HASLAM, H W. 1978. A geochemical survey of the Cheviot area in Northumberland and Roxburghshire using panned mineral concentrates. *Report Institute Geological Sciences 78/4*.

- LEE, G W, and BAILEY, E B. 1925. The pre-Tertiary geology of Mull, Loch Aline, and Oban. *Memoirs of the Geological Survey of Great Britain (Scotland)*. Part of Sheets 35, 43, 44, 45 and 52 (Scotland).
- LEE, M K. 1982. The regional geophysics of the Cheviot area. *Report Institute Geological Sciences ENPU 82/2*.
- LEHMANN, B, HEINHORST, J, HEIN, U, NEUMANN, M, WEISSER, J D and FEDESEJEV, V. 1999. The Bereznjakovskoje gold trend, southern Urals, Russia. *Mineralium Deposita*, 34, 241-249.
- LOVE, D A, CLARK, A H, HODGSON, C J, MORTENSEN, J K, ARCHIBALD, D A and FARRAR, E. 1998. The timing of adularia-sericite-type mineralisation and alunite-kaolinite-type alteration, Mount Skukum epithermal gold deposit, Yukon Territory, Canada: ^{40}Ar - ^{39}Ar and U-Pb geochronology. *Economic Geology*, 93, 437-462.
- MANN, A W, BIRRELL, R D and MANN, A T. Relationships between mobile metal ion (MMI) and conventional (total digestion) geochemistry. In: *Abstracts volume for 19th International Geochemical Exploration Symposium*, Vancouver, Canada.
- MILLER, H. 1887. The geology of the country around Otterburn and Elsdon (explanation of new series sheet 8). *Memoirs of the Geological Survey of Great Britain*, HMSO, London.
- MITCHELL, J G. 1972. Potassium-argon ages from the Cheviot Hills, Northern England. *Geological Magazine*, 109, 121-426.
- MORRISON, G W and BEAMS, S D. 1995. Geological setting and mineralisation style of ore deposits of northeast Queensland. In: *Mineral deposits of Northeast Queensland: Geology and Geochemistry*, ed. S D Beams. EGRU Contribution 52, 17th International Geochemical Exploration Symposium, Townsville, Australia, May 1995.
- MORRISON, G, GUOYI, D and JAIRETH, S. 1990 Textural zoning in epithermal quartz veins. Gold Research Group, James Cook University of North Queensland, *AMIRA Project P247*.
- MÜLLER, D and GROVES, D I. 1993. Direct and indirect associations between potassic igneous rocks, shoshonites and gold-copper deposits. *Ore Geology Reviews*, 8, 383-406.
- NELSON, C E and GILES, D L. 1985. Hydrothermal eruption mechanisms and hot spring gold deposits. *Economic Geology*, 80, 1633-1639.
- NESBITT, B.E. 1988. Gold deposit continuum: A genetic model for lode Au mineralization in the continental crust. *Geology*, 16, 1044-1048.
- NICHOL, I, HALE, M and FLETCHER, W K. 1994. Drainage geochemistry in gold exploration. In: *Drainage Geochemistry*, edited by M Hale and J A Plant; *Handbook of Exploration Geochemistry*, Vol. 6.
- PARNELL, J and SWAINBANK, I G. 1984. Interpretation of Pb isotope compositions of galenas from the Midland Valley of Scotland and adjacent regions. *Transactions of the Royal Society of Edinburgh: Earth Sciences*, 75, 85-96.
- PATRICK, R A D and POLYA, D A (editors). 1993. *Mineralisation in the British Isles*. (London: Chapman and Hall).

- PLANT, J A and 29 others. 1998. Multidataset analysis for the development of exploration models in western Europe. *British Geological Survey Research Report SF/98/1*, 143pp, (edited by A G Gunn and J A Plant).
- RADFORD, N. 1996. BLEG sampling in gold exploration: an Australian view. *Explore*, No. 92, 8-10.
- RICE, C M and DAVIES, B. 1979. Copper mineralisation associated with an appinite pipe in Argyll, Scotland. *Transactions of the Institution of Mining and Metallurgy, (Section B: Applied Earth Science)*, 88, 154-160.
- RICE C M and TREWIN, N H. 1988. A Lower Devonian gold-bearing hot-spring system, Rhynie, Scotland. *Transactions of the Institution of Mining and Metallurgy, (Section B: Applied Earth Science)*, 97, 141-144.
- RICE, C M, ASHCROFT, W A, BATTEN, D J, BOYCE, A J, CAULFIELD, J B, D. FALLICK, A E, HOLE, M J, JONES, E. PEARSON, M J, ROGERS, G, SAXTON, J M. STUART, F. M. TREWIN, N H and TURNER, G A. 1995. Devonian auriferous hot spring system, Rhynie, Scotland. *Journal of the Geological Society of London*, 52, 229-250.
- ROBERT, F, POULSEN, K H and DUBÉ, B. 1997. Gold deposits and their geological classification. In: *Proceedings of Exploration 97: Fourth Decennial International Conference on Mineral Exploration*, ed. Gubbins, A G., 209-220.
- ROBSON, D A. 1976. A guide to the geology of the Cheviot Hills. *Transactions of the Natural History Society of Northumbria*, 43, 1.
- ROBSON, D A. 1977. The structural history of the Cheviots and adjacent regions. *Scottish Journal of Geology*, 13, 255-262.
- ROY, J and PUTIKOV, O F. 1997. Overview on the electrogeochemical techniques. In: *Proceedings of Exploration '97: Fourth Decennial International Conference on Mineral Exploration*, edited by A. G. Gubbins, GEO F/X, 375-380.
- RUSSELL, M J. Base-metal prospecting in Scotland – theory and method. *Proceedings of the Society of Analytical Chemistry*, 9, 154-156.
- RUSSELL N and KESSLER S E. 1991. Geology of the maar-diatreme complex hosting precious metal mineralisation at Pueblo Viejo, Dominican Republic. *Geological Society of America Special Paper* 262, 203-216.
- SALLOMY, J T, and PIPER, J D A. 1973. Paleomagnetic studies in the British Caledonides – IV Lower Devonian lavas of the Strathmore region, Scotland. *Geophysical Journal*, 34, 47-68.
- SANDER, M V and EINAUDI, M T. 1990. Epithermal deposition of gold during transition from propylitic to potassic alteration at Round Mountain, Nevada. *Economic Geology*, 85, 285-311.
- SCHALUMAK, I B, ZUBIA, M, GENINI, A and FERNANDEZ, R R. 1997. Jurassic epithermal Au-Ag deposits of Patagonia, Argentina. *Ore Geology Reviews*, 12, 173-186.
- SENEHEN, D M. 1997. The applicability of partial extractions to mineral exploration in areas of transported overburden. *Queen's University, PhD thesis (unpublished)*.

SHAW, M H, FORTEY, N J, GIBBERD, A J and ROLLIN, K E. 1995. Gold exploration in the Duns area, Southern Uplands, Scotland. *Mineral Reconnaissance Programme Report*, British Geological Survey, No. 138.

SHAND, P. 1989. Later Caledonian magmagenesis in Southern Scotland. *Unpublished Ph.D. thesis, University of Aston in Birmingham*.

SHERLOCK, R L, TOSDAL, R M, LEHRMAN N J, GRANNEY, J R, LOSH, S, JOWETT, E C and KESLER, S E. 1995. Origin of the McLaughlin mine sheeted vein complex: metal zoning, fluid inclusion and isotopic evidence. *Economic Geology*, 90, 2156-2181.

SHIKAZANO, N, NAITO, K and IZAWA, E. (eds), 1993. High grade epithermal gold mineralisation – the Hishikari deposit. *Resource Geology Special Issue*, No. 14.

SIDDELEY, G and ARANEDA, R. 1986. The El Indio-Tambo gold deposits, Chile. In: *Proceedings of Gold '86 Symposium*, ed. A J MacDonald, Toronto, 445-456.

SILBERMAN, M L and BERGER, B R. 1985. Relationships of trace-element patterns to alteration in epithermal precious-metal deposits. In: *Geology and geochemistry of epithermal systems*, Berger, B R and Bethke, P M (eds). *Reviews in Economic Geology*, 2, 203-232.

SILLITOE, R H. 1993a. Epithermal models: genetic types, geometrical controls and shallow features. In: Kirkham, R V, Sinclair, W D, Thorpe, R I and Duke, J M., eds., *Mineral Deposit Modelling: Geological Association of Canada, Special Paper 40*, 403-417.

SILLITOE, R H. 1993b. Gold-rich porphyry copper deposits: geological model and exploration implications. In: Kirkham, R V, Sinclair, W D, Thorpe, R I and Duke, J M., eds., *Mineral Deposit Modelling: Geological Association of Canada, Special Paper 40*, 465-478.

SILLITOE, R H. 1995. Exploration and discovery of base- and precious-metal deposits in the circum-Pacific region during the last 25 years. *Metal Mining Agency of Japan*.

SIMON, G, KESLER, S E, RUSSELL, N, HALL, C M, BELL, D and PIÑERO, E. 1999. Epithermal gold mineralisation in an old volcanic arc: the Jacinto deposit, Camaguey District, Cuba. *Economic Geology*, 94, 487-506.

SMEE, B W. 1997. The formation of surficial geochemical patterns over buried epithermal gold deposits in desert environments: results of a test of partial extraction techniques. In: *Proceedings of Exploration '97: Fourth Decennial International Conference on Mineral Exploration*, edited by A. G. Gubins, GEO F/X, 301-314.

SO, C S, ZHANG, D Q, YUN, S T and LI, D X. 1998. Alteration-mineralisation zoning and fluid inclusions of the high sulfidation epithermal Cu-Au mineralisation at Zijinshan, Fujian Province, China. *Economic Geology*, 93, 961-980.

SPEIGHT, J M, and MITCHELL, J S. 1979. The Permo-Carboniferous dyke swarm in northern Argyll and its bearing on the dextral placement of the Great Glen Fault. *Journal of the Geological Society of London*, 136, 3-11.

- STEPHENS, W E and HALLIDAY, A N. 1984. Geochemical contrasts between late Caledonian granitoid plutons of northern, central and southern Scotland. *Transactions of the Royal Society of Edinburgh: Earth Sciences*, 75, 259-273.
- TAYLOR, B J, BURGESS, I C, LAND, D H, MILLS, D A C, SMITH, D B, and WARRIN, P T. 1971. Northern England. *British Regional Geology*, Institute of Geological Sciences, HMSO, London.
- THIERSCH, P C, WILLIAMS-JONES, A E and CLARK, J R. 1997. Epithermal mineralisation and ore controls of the Shasta Au-Ag deposit, Toadogone District, British Columbia, Canada. *Mineralium Deposita*, 32, 44-57.
- THIRLWALL, M F. 1981. Implications for Caledonian plate tectonic models of chemical data from volcanic rocks of the British Old Red Sandstone. *Journal Geological Society London*, 138, 123-138.
- THIRLWALL, M F. 1982. Systematic variation in chemistry and Nd-Sr isotopes across a Caledonian calc-alkaline volcanic arc: implications for source materials. *Earth and Planetary Science Letters*, 58, 27-50.
- THIRLWALL, M F. 1988. Geochronology of late Caledonian magmatism in northern Britain. *Journal of the Geological Society of London*, 145, 951-967.
- THOMPSON, J F H, LESSMAN, J and THOMPSON, A J B. 1986. The Temora gold-silver deposit: a newly recognised style of high sulphur mineralisation in the lower Palaeozoic of Australia. *Economic Geology*, 81, 732-738.
- TINGLEY, J V and BERGER, B R. 1985. Lode gold deposits of Round Mountain, Nevada. *Nevada Bureau of Mines and Geology Bulletin 100*, 62pp.
- TURNER, D D. 1997. Predictive GIS model for sediment-hosted gold deposits, north-central Nevada, USA. In: *Proceedings of Exploration '97: Fourth Decennial International Conference on Mineral Exploration*, edited by A. G. Gubins, GEO F/X, 115-126.
- VOLKERT, D F, MCEWAN, C J A and GARAY, E M. 1998. Pierina Au-Ag deposit, Cordillera Negra, north-central Peru. *Pathways '98 Extended Abstracts Volume, Conference of British Columbia & Yukon Chamber of Mines and The Society of Economic Geologists*, Vancouver, Canada.
- WHITE, N C and HEDENQUIST, J W. 1990. Epithermal environments and styles of mineralization: variations and their causes, and guidelines for exploration. *Journal of Geochemical Exploration*, 36, 445-474.
- WHITE, N C, LEAKE, M J, MCCAUGHEY, S N and PARRIS, B W. 1995. Epithermal gold deposits of the southwest Pacific. *Journal of Geochemical Exploration*, 54, 87-136.
- WILLIAMS, T M. 1999. Evaluation of enzyme and hydroxylamine hydrochloride leach soil reconnaissance methods over high sulphidation epithermal mineralisation at El Mozo, Azuay. Report No: EDM/99/02. *World Bank PRODEMICA Subcomponent 3.5*, Quito.
- WILLIAMS, T M and GUNN, A G. 1999. Enzyme leach soil survey of the Llano Largo low sulphidation epithermal gold prospect, Azuay, Ecuador. Williams and Gunn. Report No: EDM/99/03, *World Bank PRODEMICA Subcomponent 3.5*, Quito.

WILSON, G.V. and FLETT, J.S. 1921. The lead, zinc, copper and nickel ores of Scotland. *Special Report on the Mineral Resources of Great Britain*, 17, 159pp.

ZHOU, J. 1987 (a). Geology of the copper-bearing intrusive suite near Kilmelford, Argyllshire, Scotland. *Transactions of the Institution of Mining and Metallurgy (Section B)*, 96, 179-186.

ZHOU, J. 1987 (b). Lithogeochemical exploration for copper and gold in Kilmelford district, Argyllshire, Scotland. *Transactions of the Institution of Mining and Metallurgy (Section B)*, 96, 187-194.

ZHOU, J. 1988. A gold and silver-bearing subvolcanic centre in the Scottish Caledonides near Lagalochan, Argyllshire. *Journal of the Geological Society London*, 145, 225-235.

ZWASCHKA, M and SCHEETZ, J W. 1995. Detailed geology of the Brewer gold mine, Jefferson, South Carolina. *Society of Economic Geologists Guidebook Series*, 24, 95-141.

12. APPENDIX 1

Explanation of lithological codes used in Figures 6.29 and 6.30

| Code | Lithology |
|------|------------------|
| 1abh | felsite-porphyry |
| 1bc0 | andesite |
| 1dao | trachyte |
| 1jdo | tuff |
| 3800 | breccia |

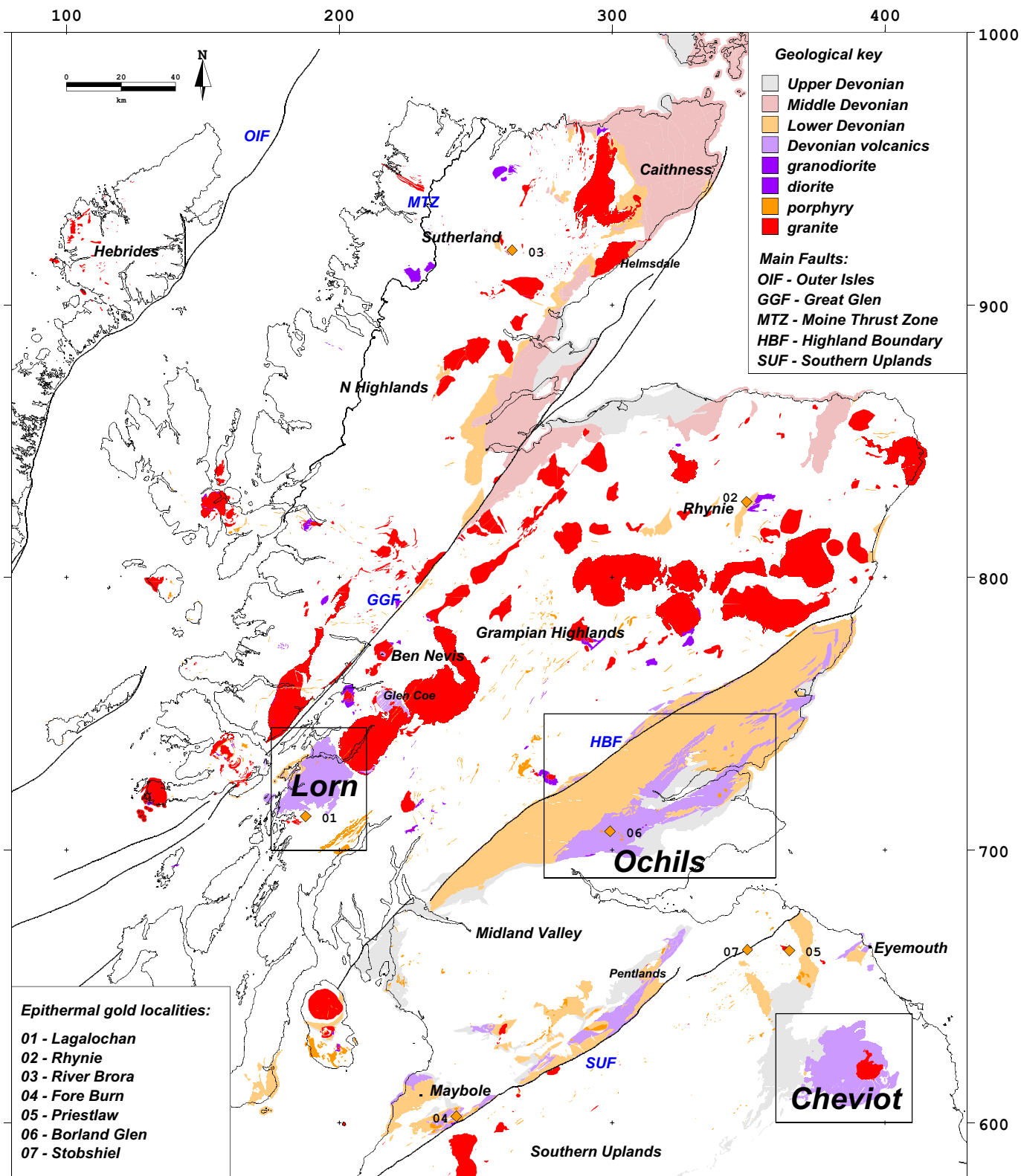


Fig 1.1 Devonian lavas and strata in northern Britain showing the locations of known epithermal gold mineralisation

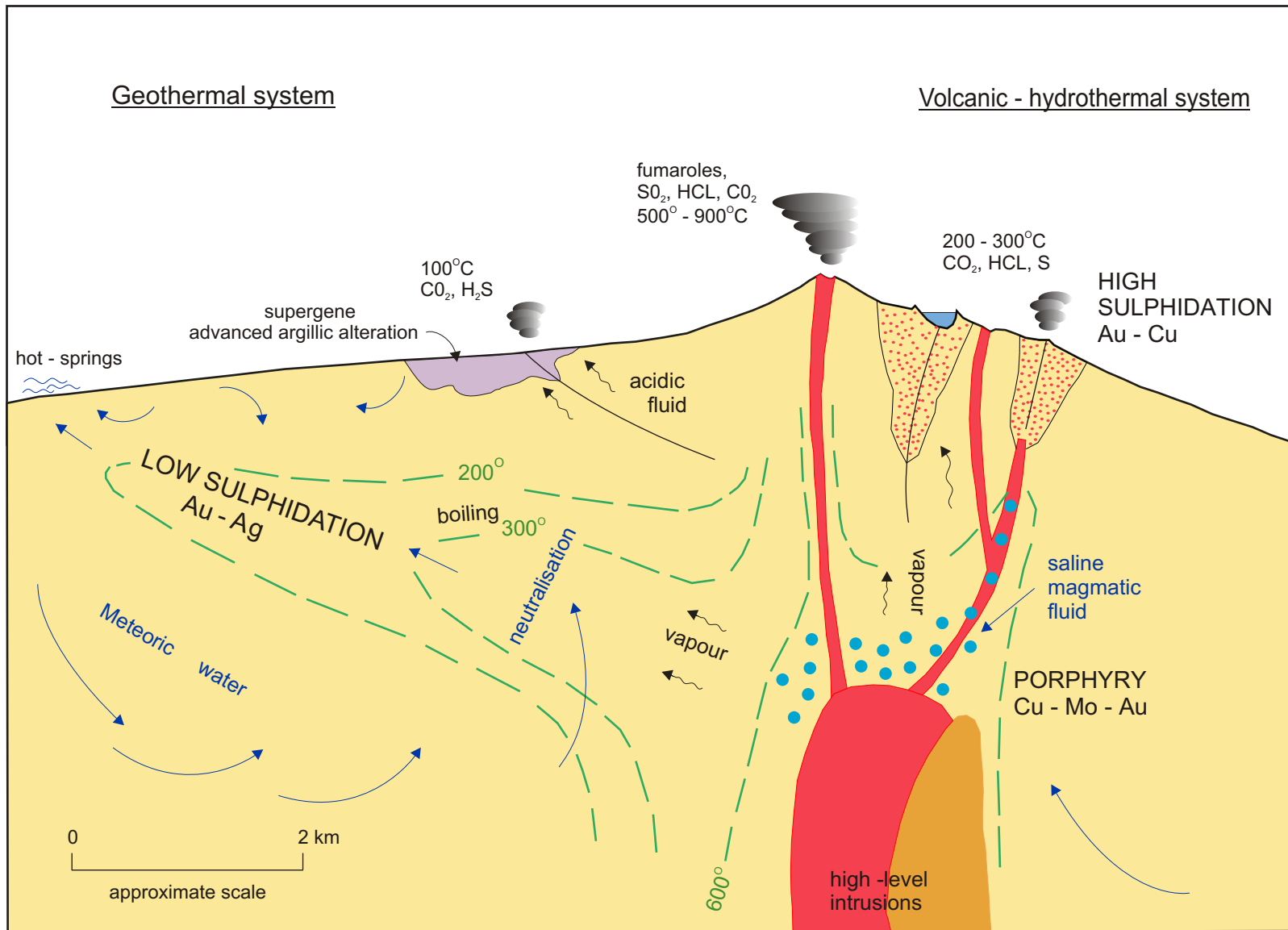


Figure 3.1 Schematic cross-section showing the environments of formation for porphyry Cu-Mo-Au and high- and low-sulphidation epithermal deposits (modified from Hedenquist and Lowenstern, 1994)

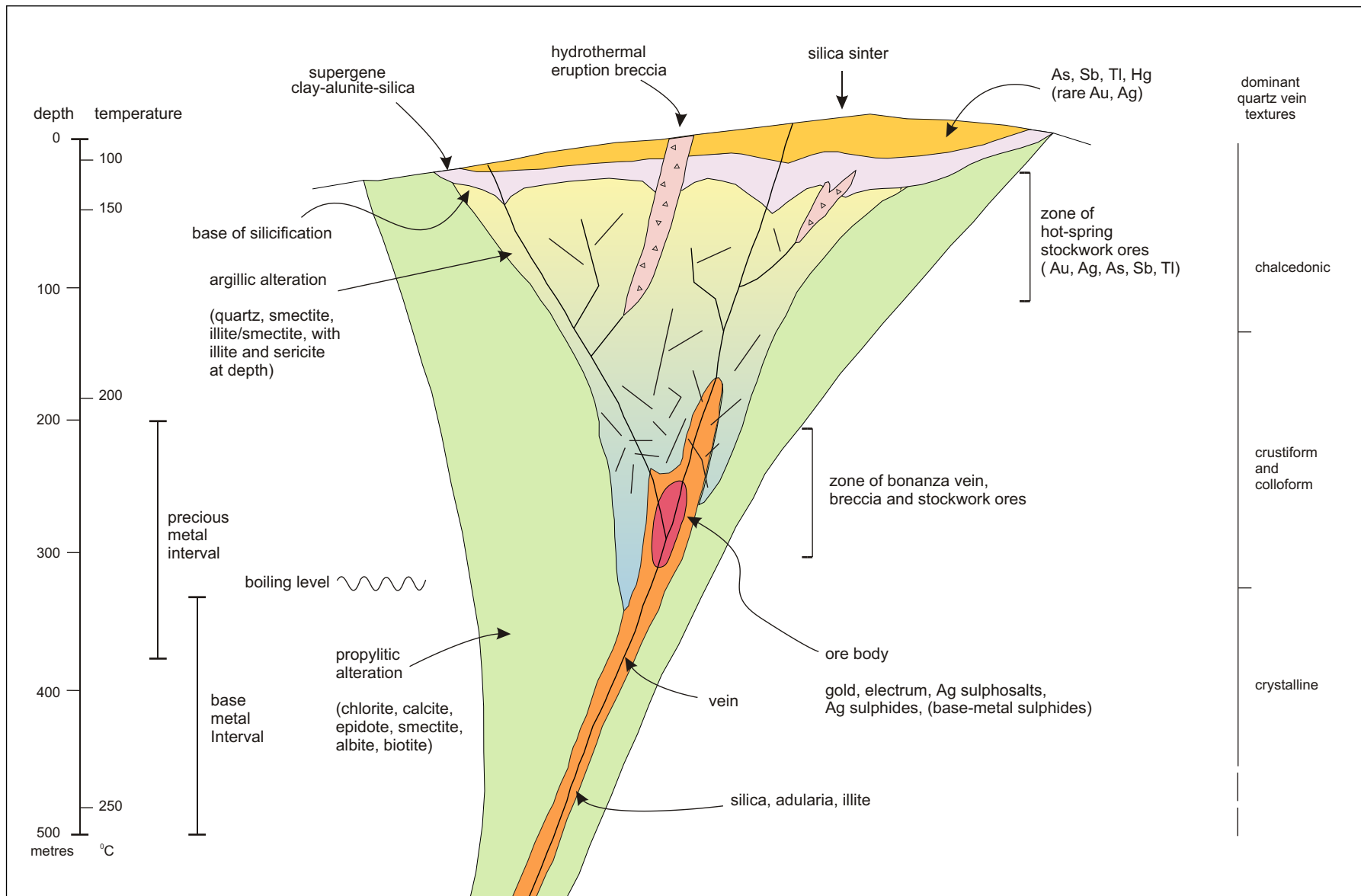


Figure 3.2 Schematic cross-section showing the architecture of a typical low sulphidation epithermal vein deposit

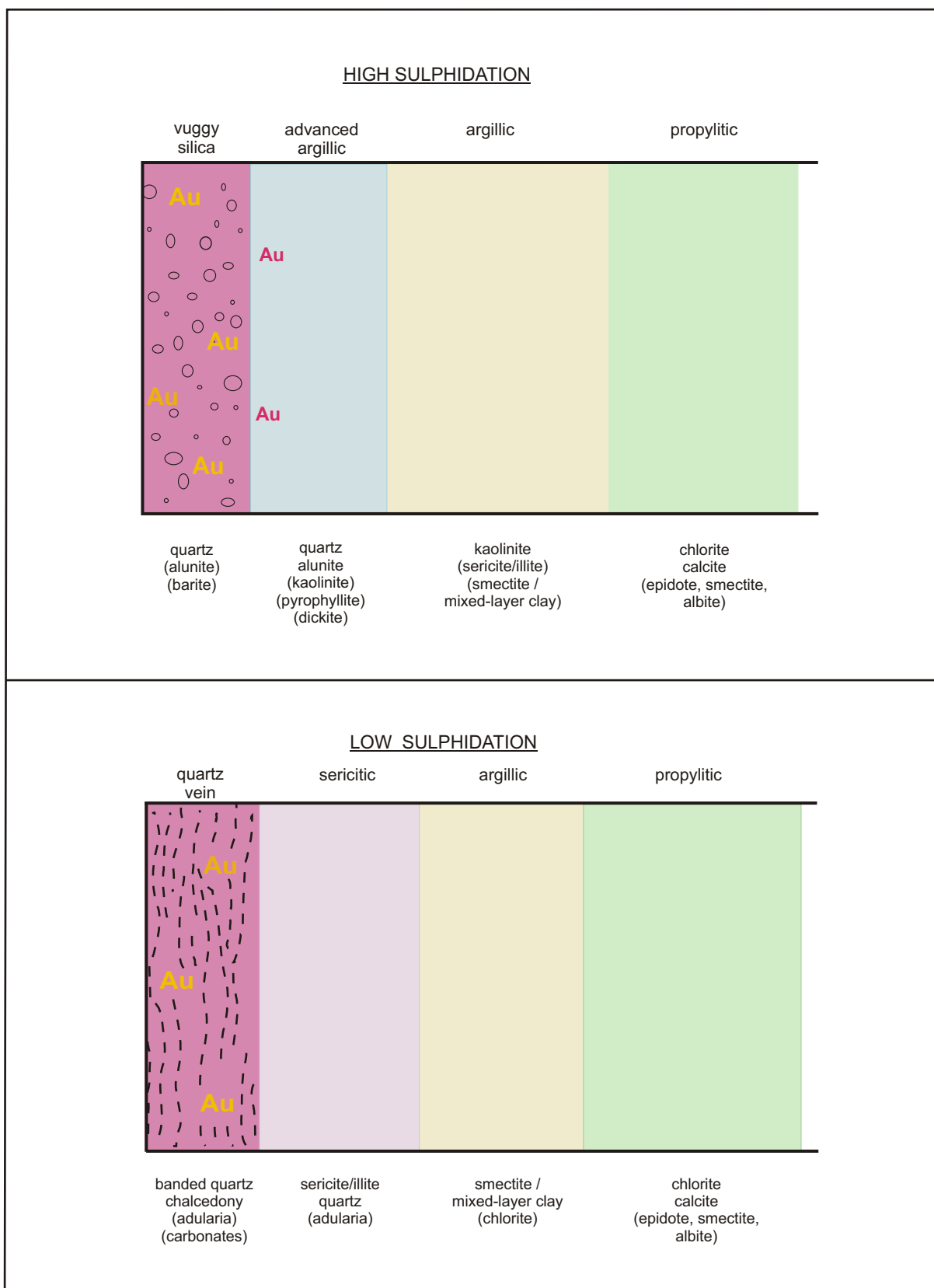


Figure 3.3 Simplified alteration zoning in high and low sulphidation epithermal deposits

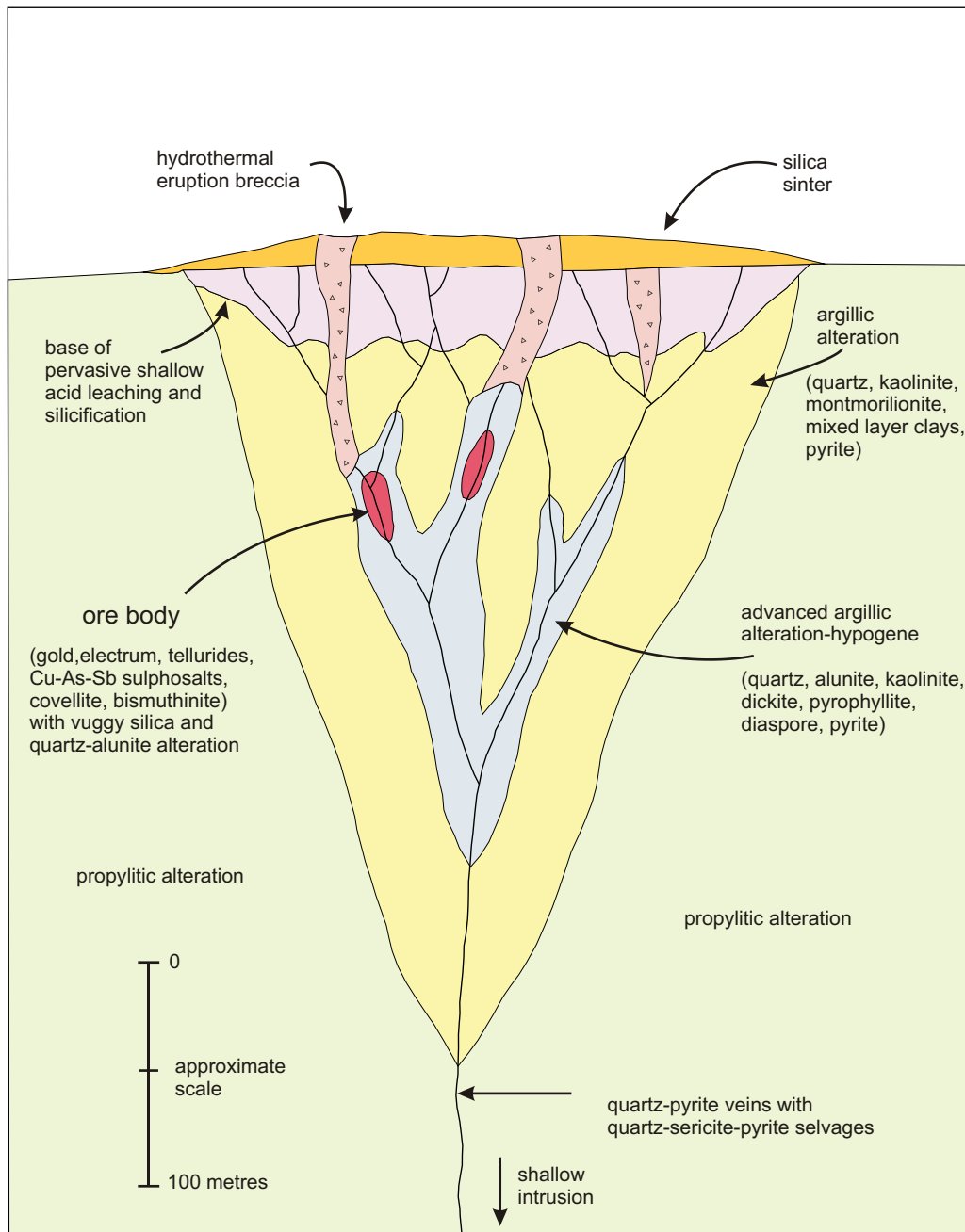


Figure 3.4 Schematic cross-section showing the architecture of a typical high sulphidation epithermal deposit (after Silberman and Berger, 1985)

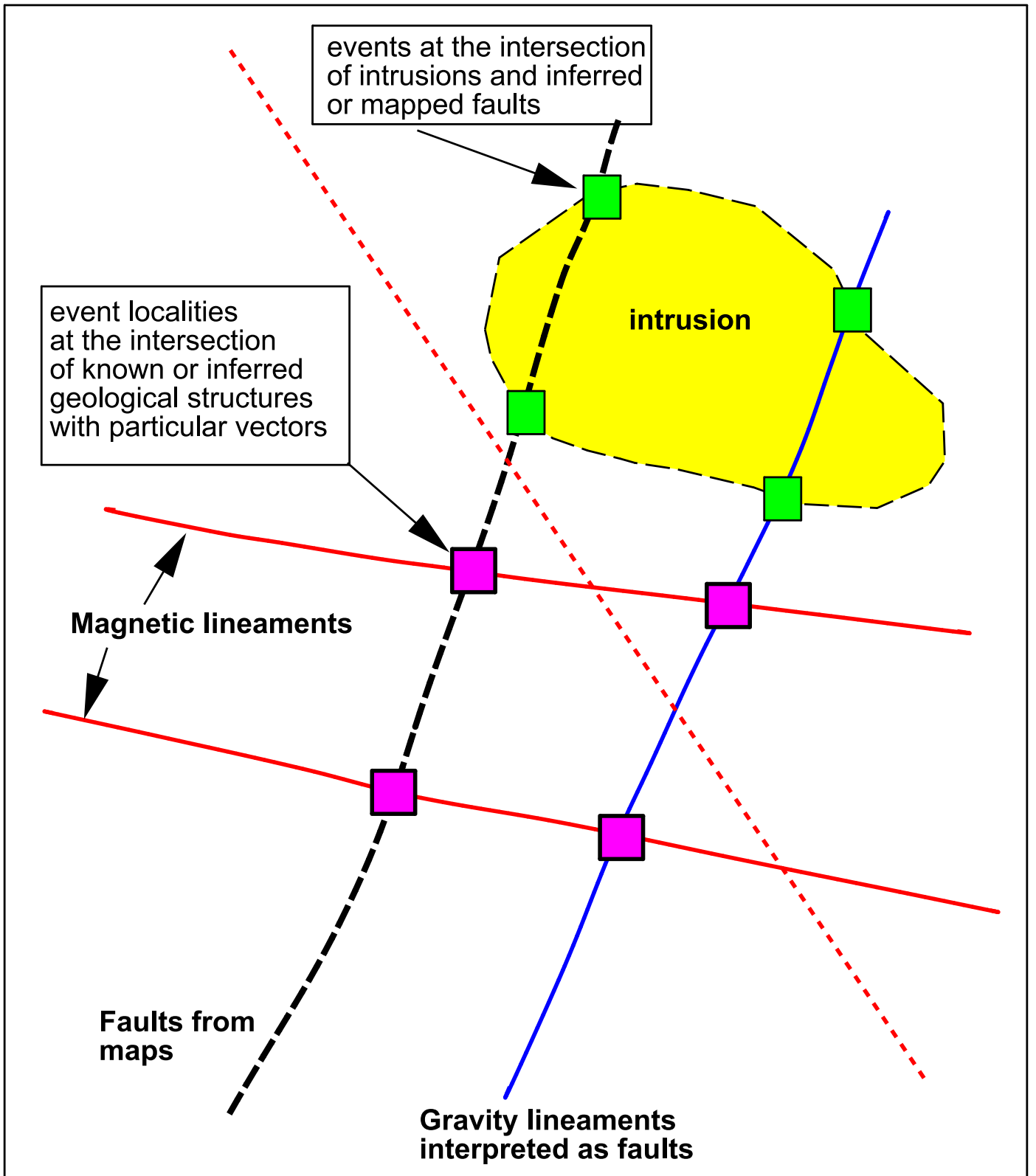


Fig 5.1 Event occurrences derived from digital geological and geophysical data

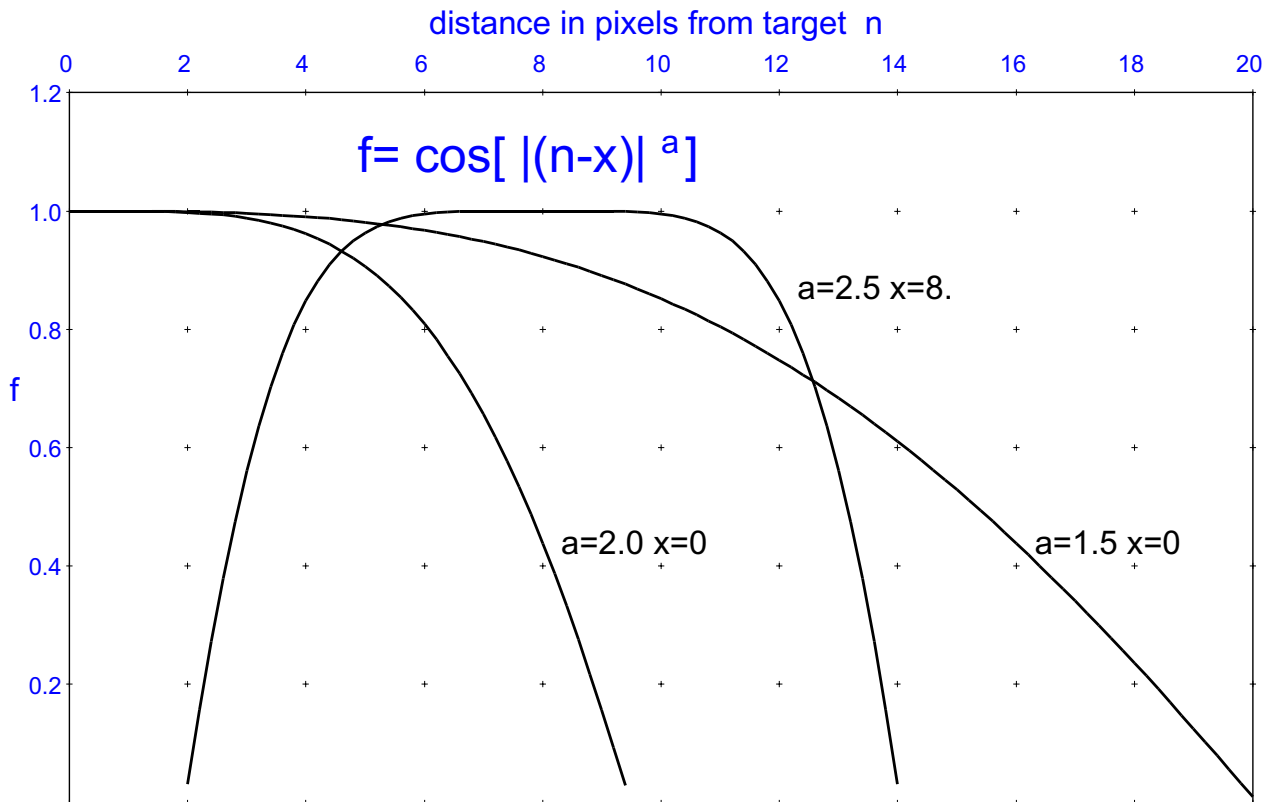


Fig 5.2 Prospectivity weight cosine function (f) for any pixel (n) is determined by the exponent (a) and the halo distance (x)

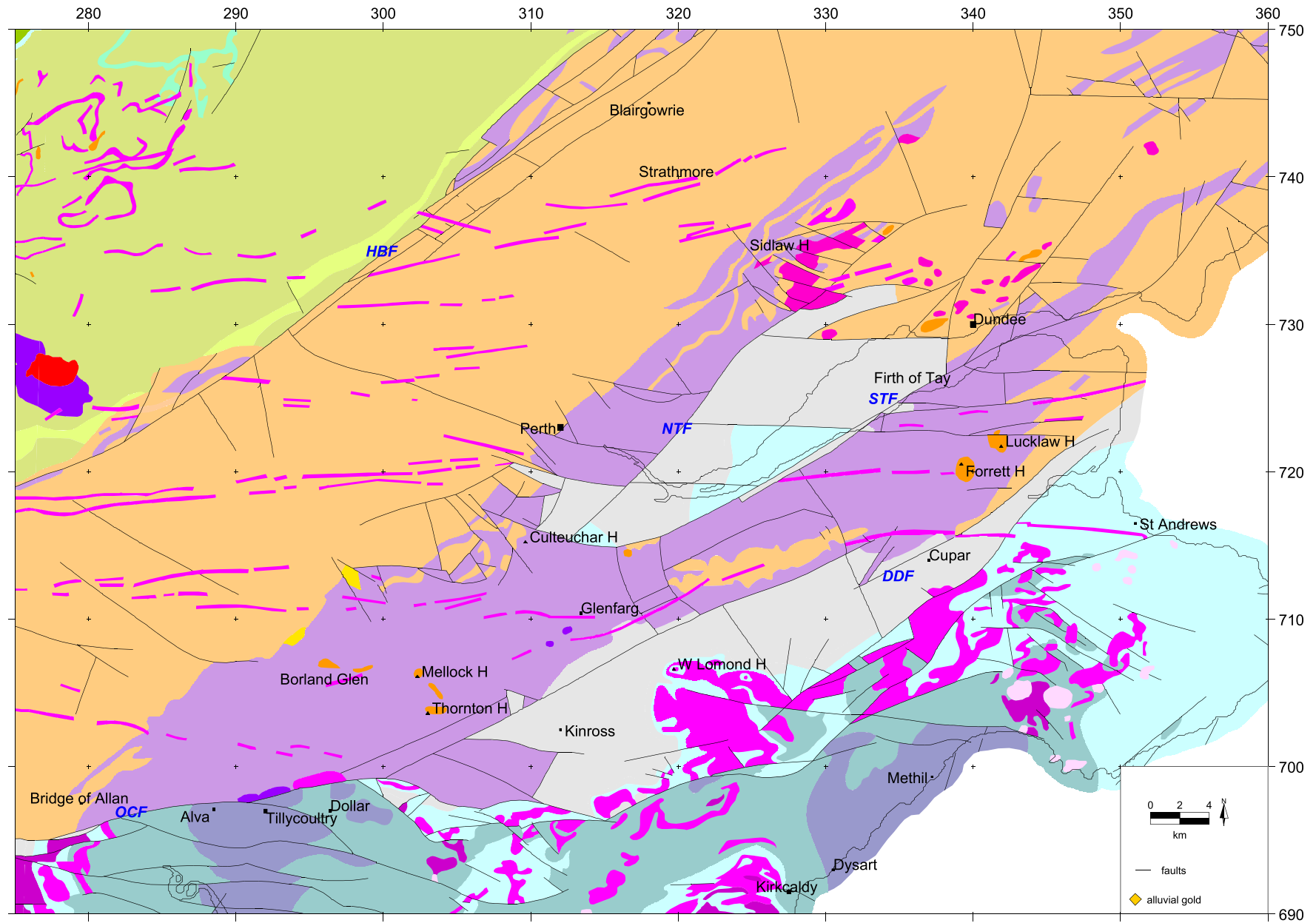


Fig 6.1 Solid geology of the Ochil Hills and surrounding area

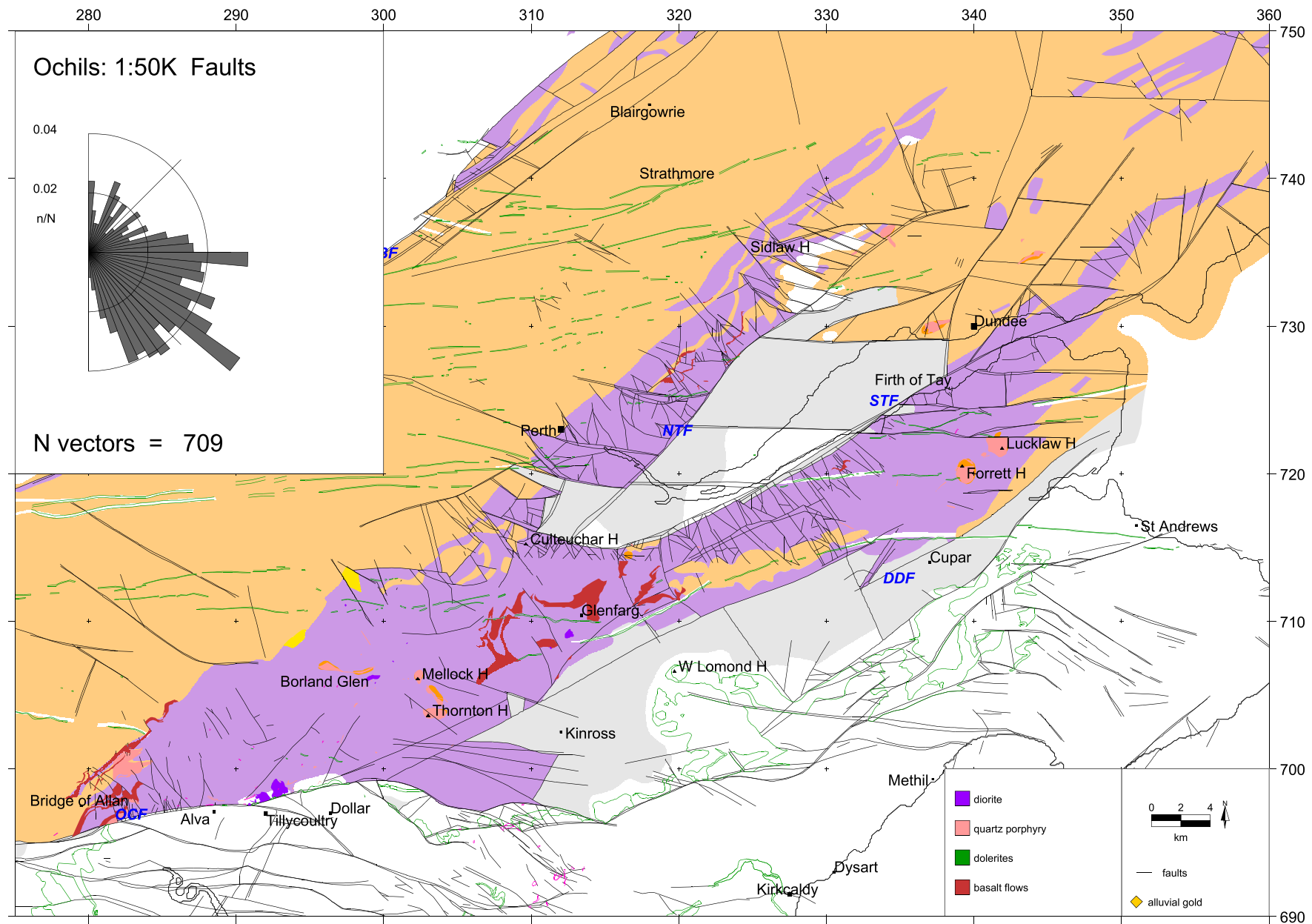


Fig 6.3 Ochils: selected elements of the geology based on the 1:50 000 map series

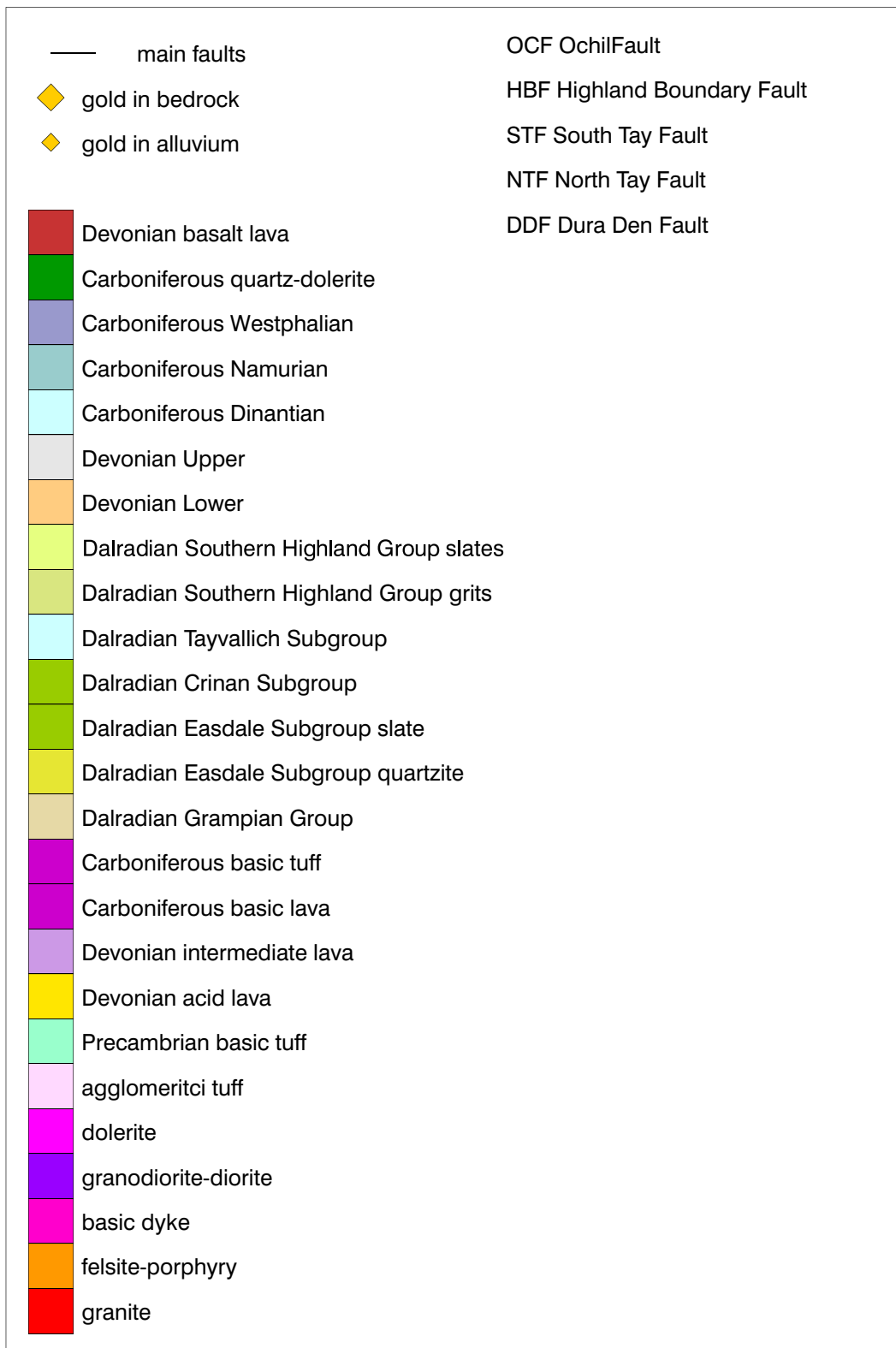


Fig 6.2 Legend for the solid geology map Figure 6.1

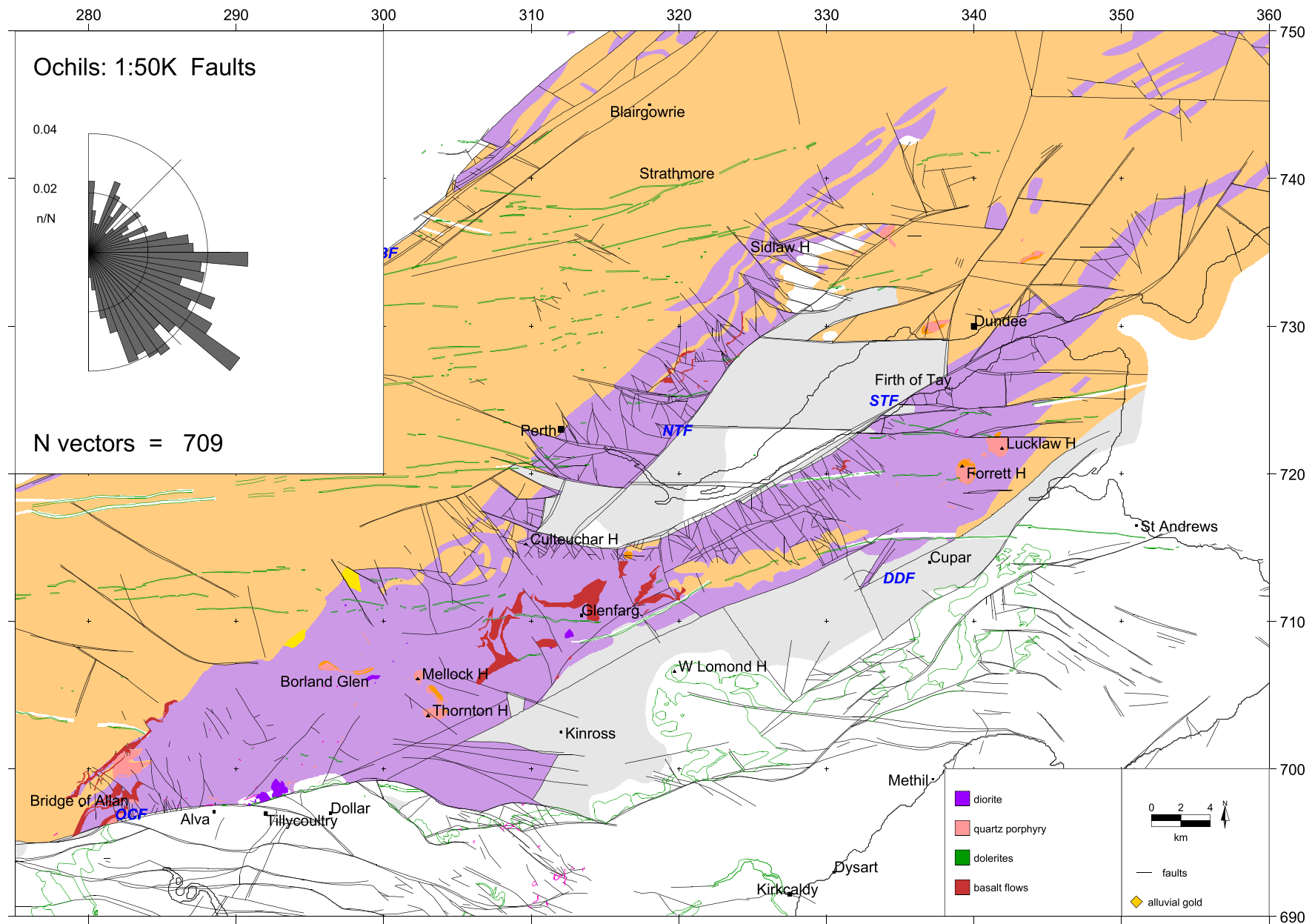


Fig 6.3 Ochils: selected elements of the geology based on the 1:50 000 map series

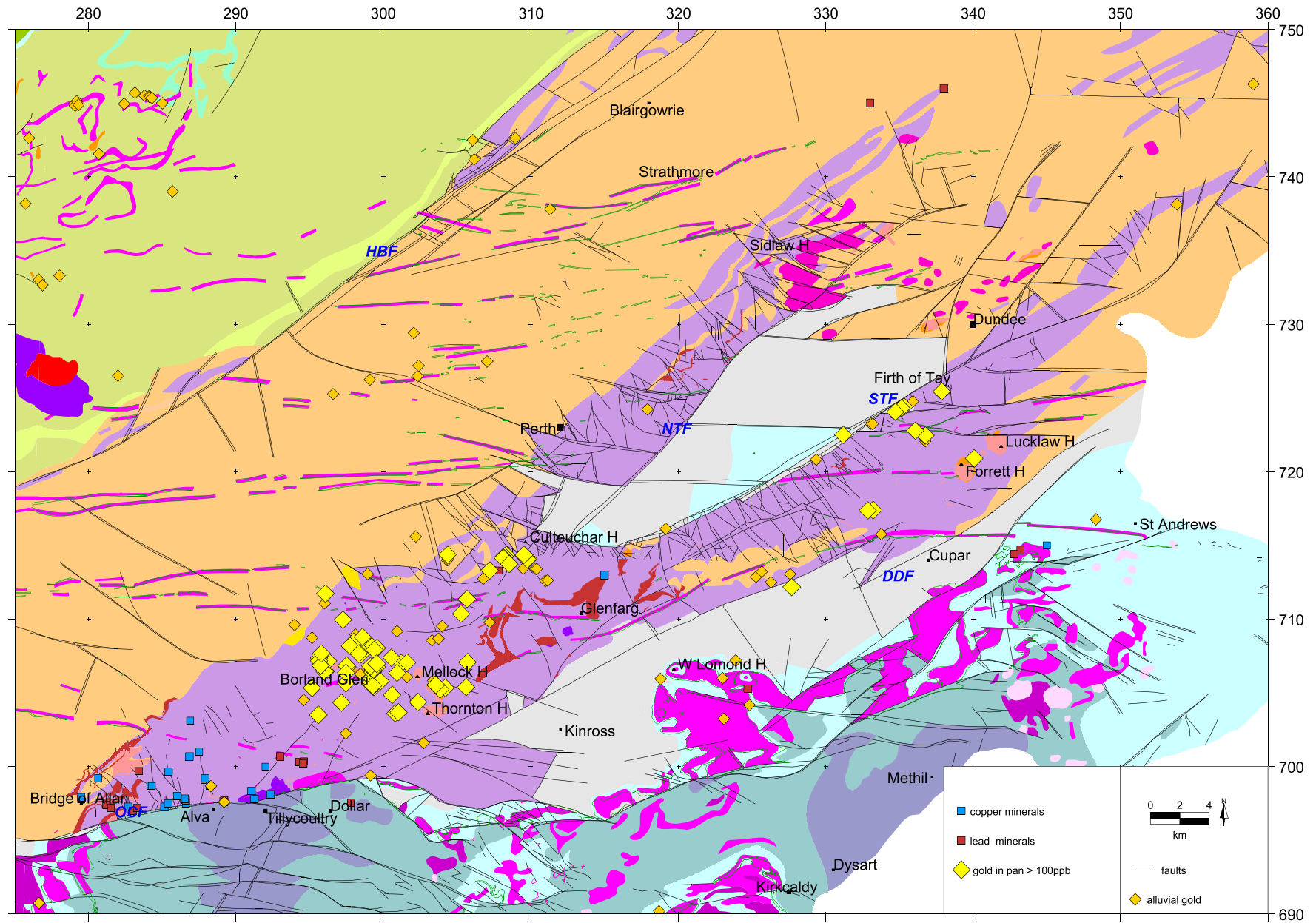


Fig 6.4 Ochils: occurrences of alluvial gold, copper and lead minerals

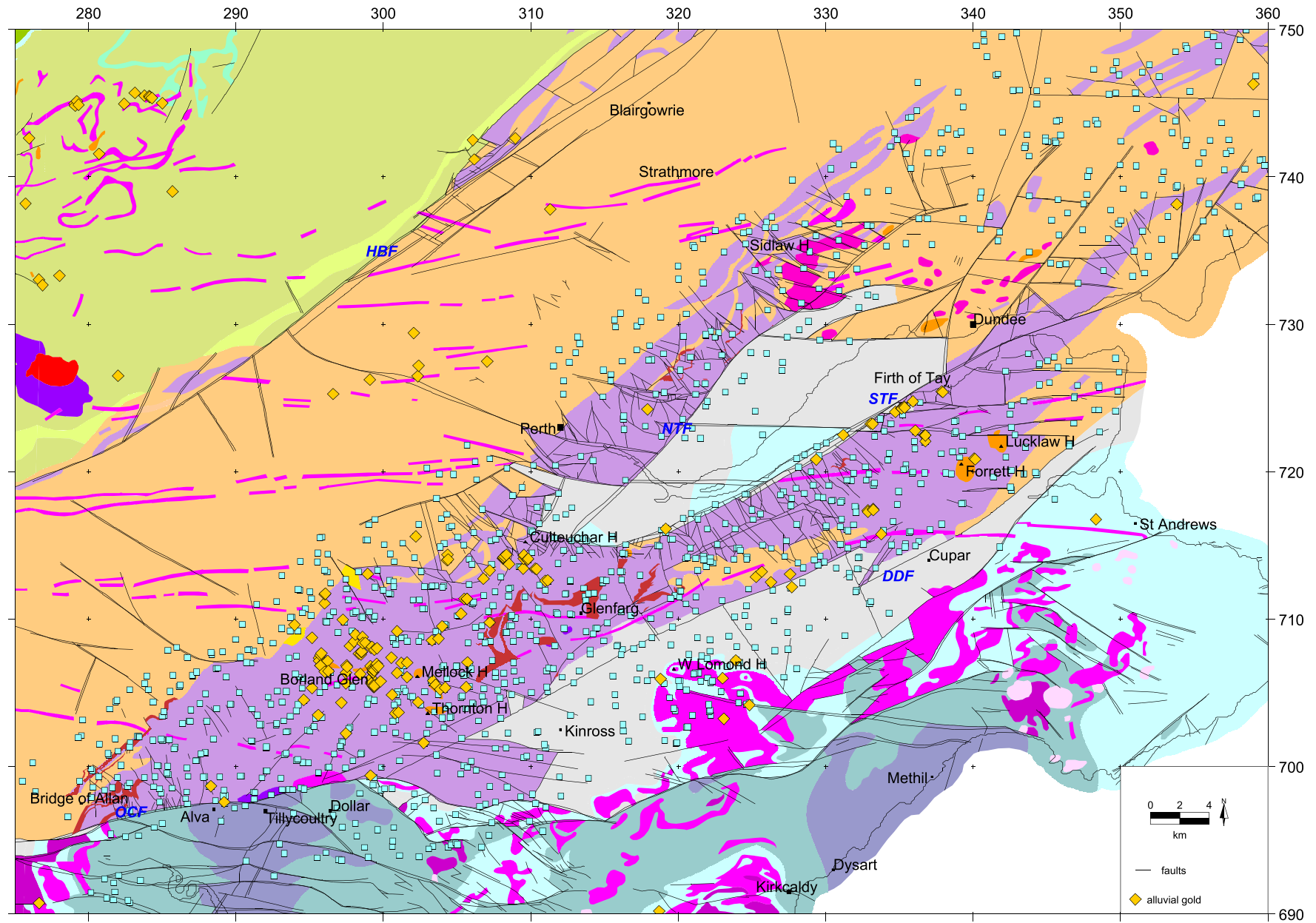


Fig 6.5 Ochils: location of G-BASE stream sediment samples

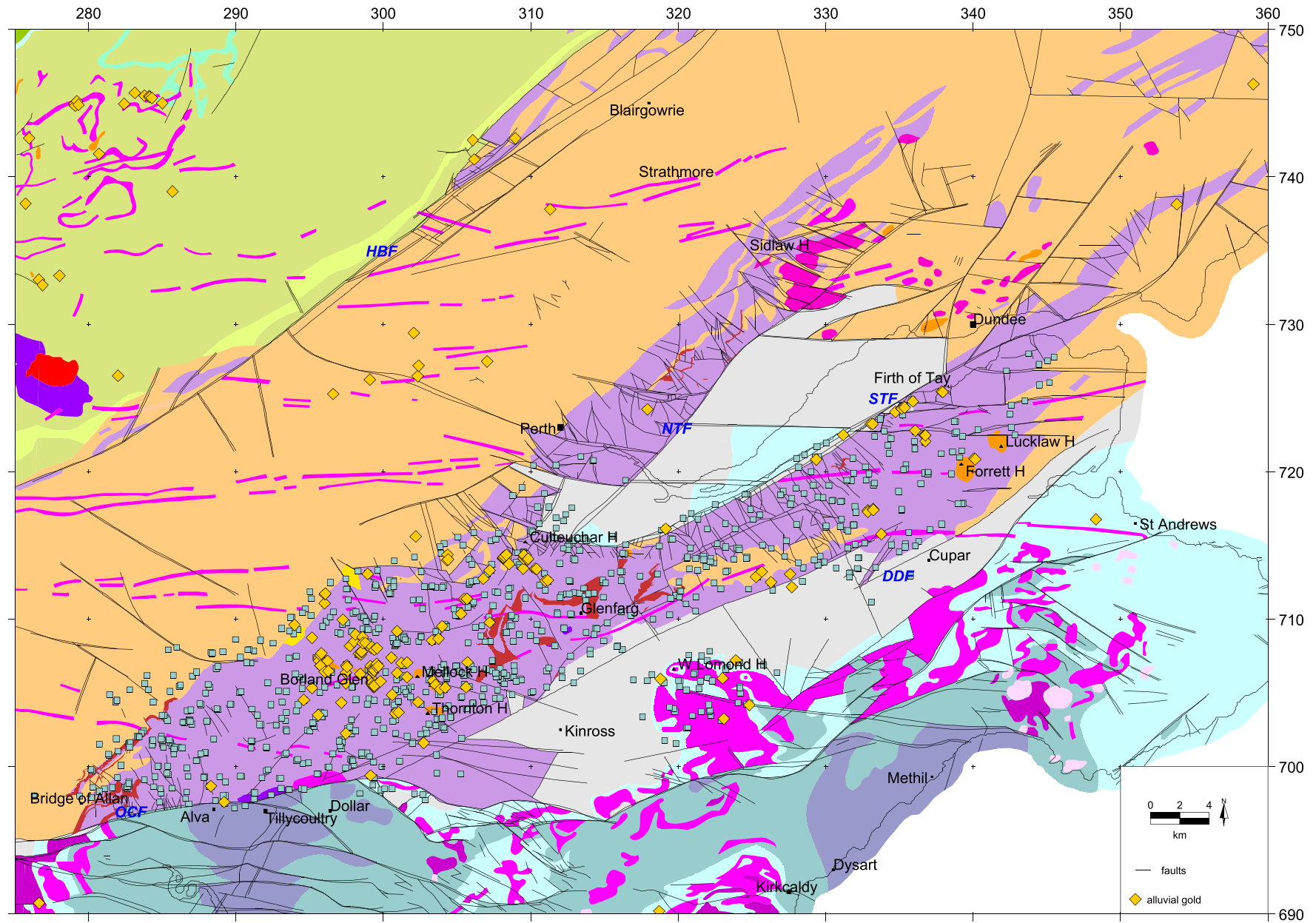


Fig 6.6 Ochils: location of MRP panned concentrate samples

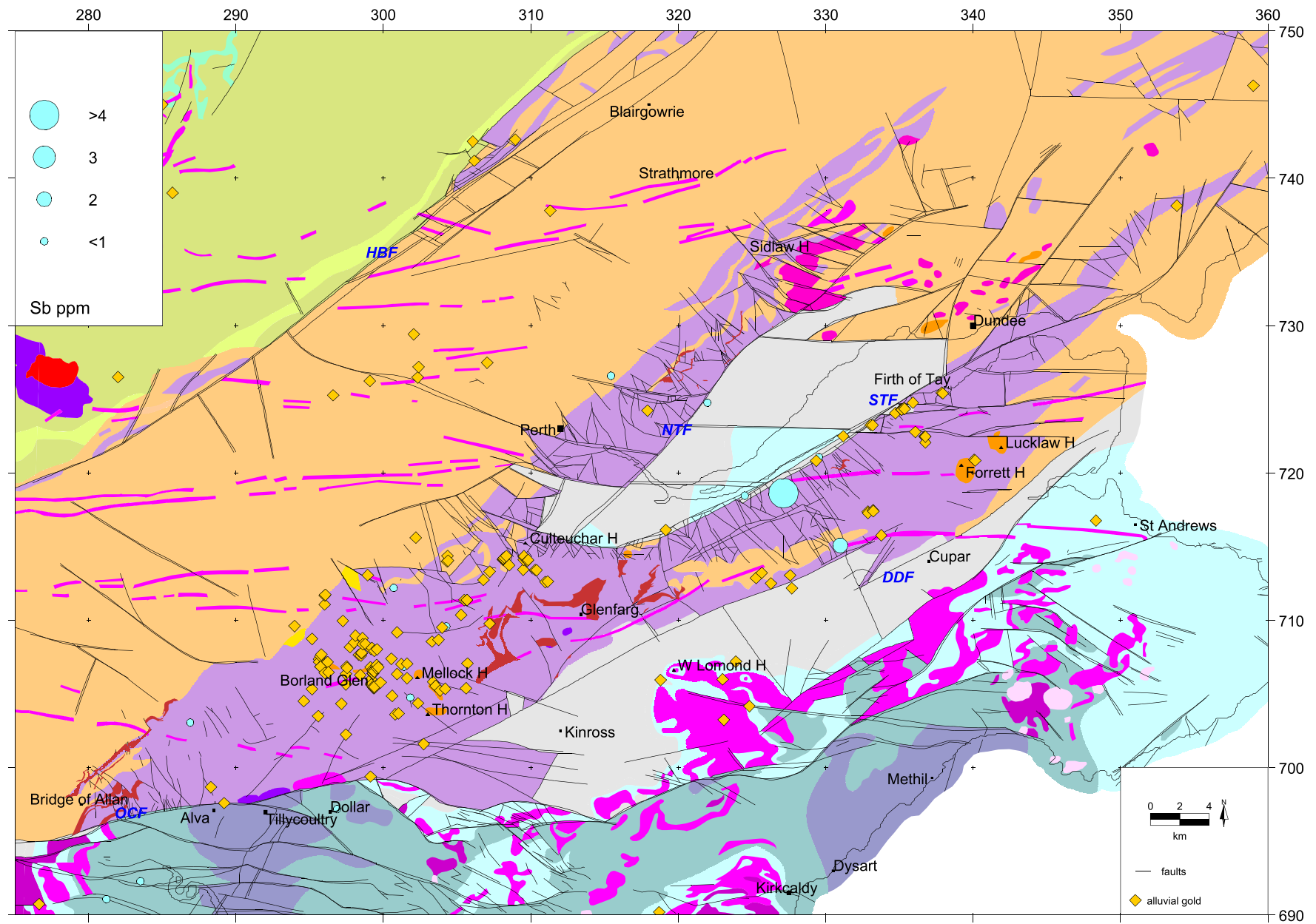


Fig 6.7 Ochils: antimony (Sb) in G-BASE stream sediment data

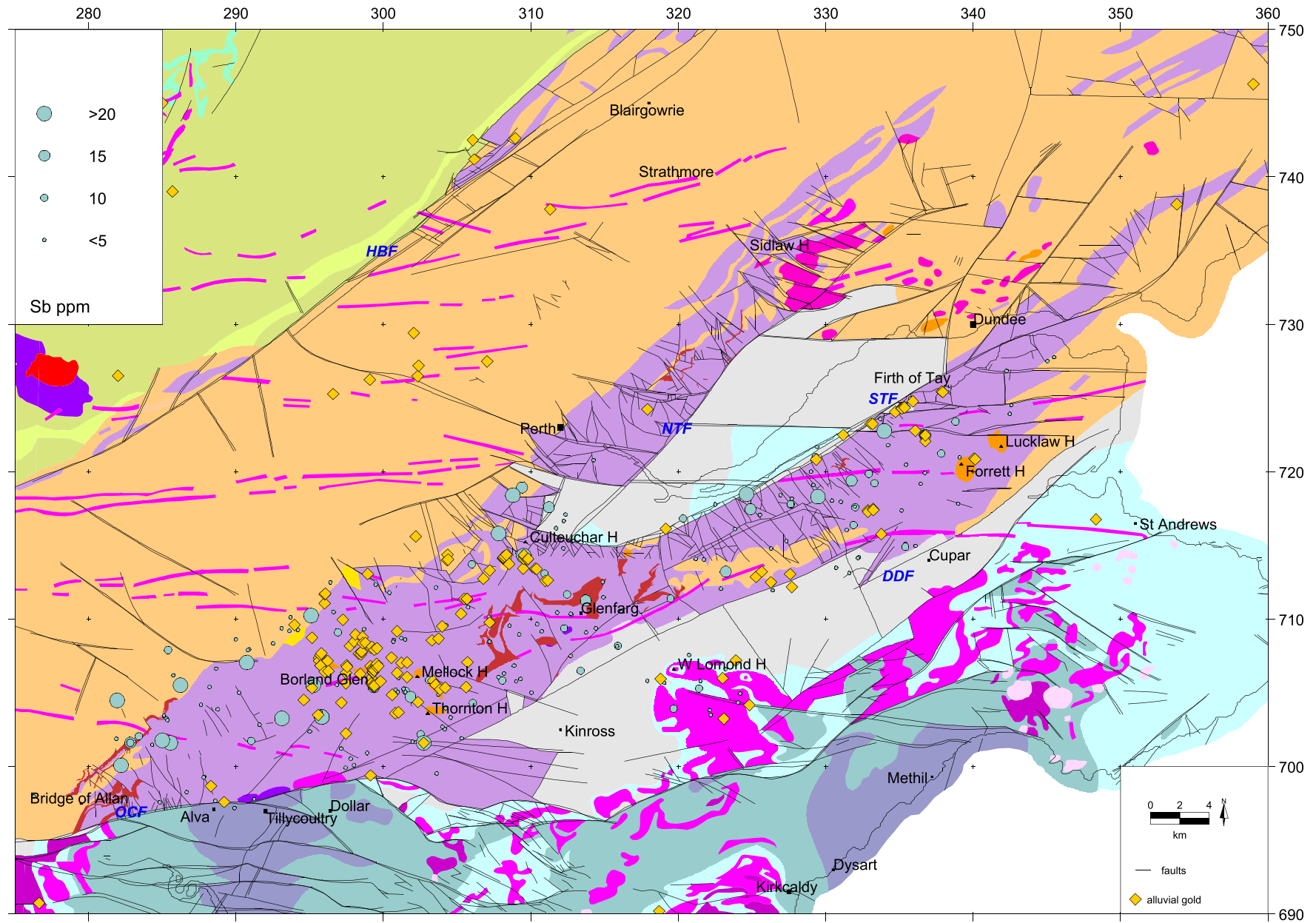


Fig 6.8 Ochils: antimony (Sb) in MRP panned concentrate data

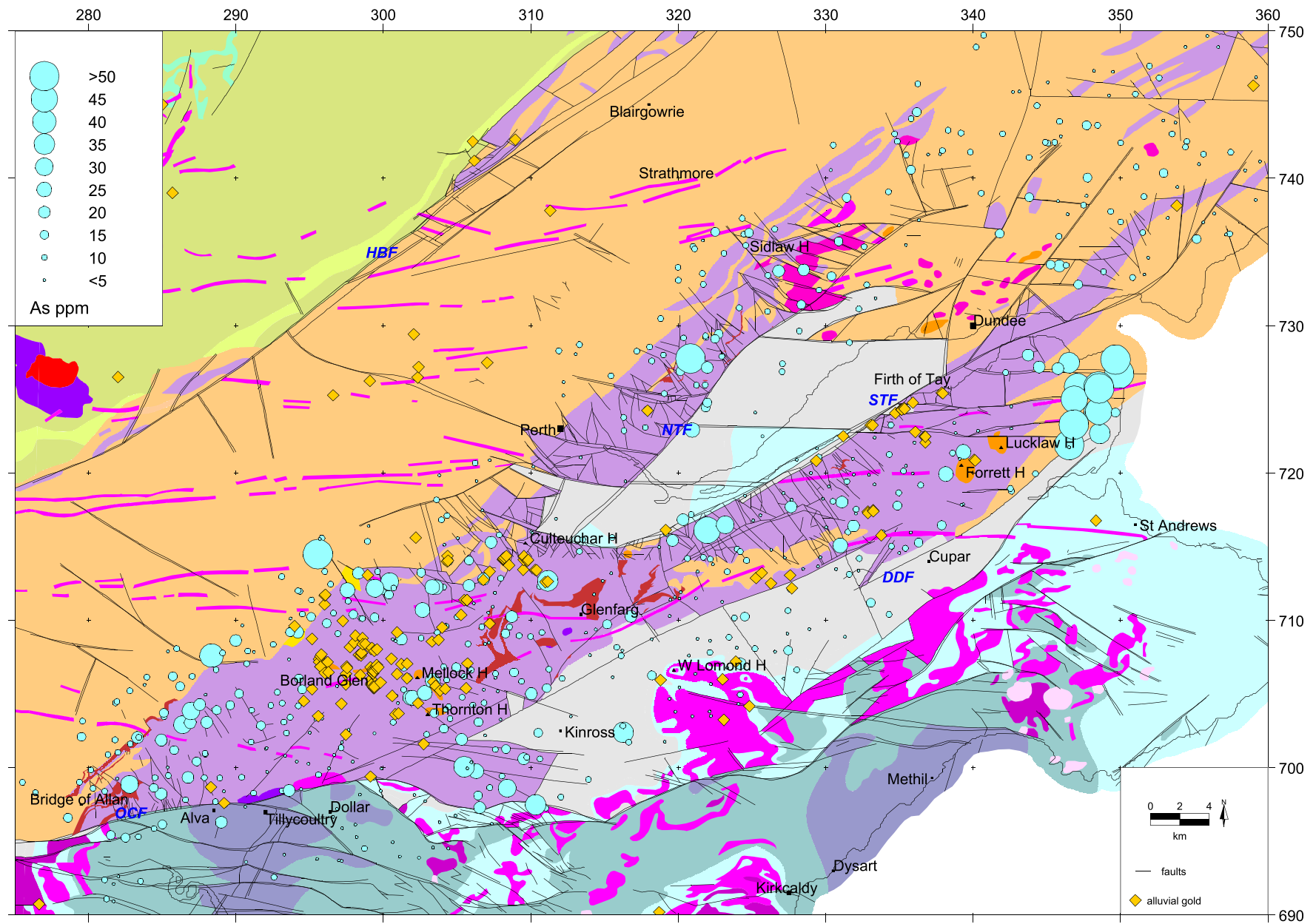


Fig 6.9 Ochils: arsenic (As) in G-BASE stream sediment data

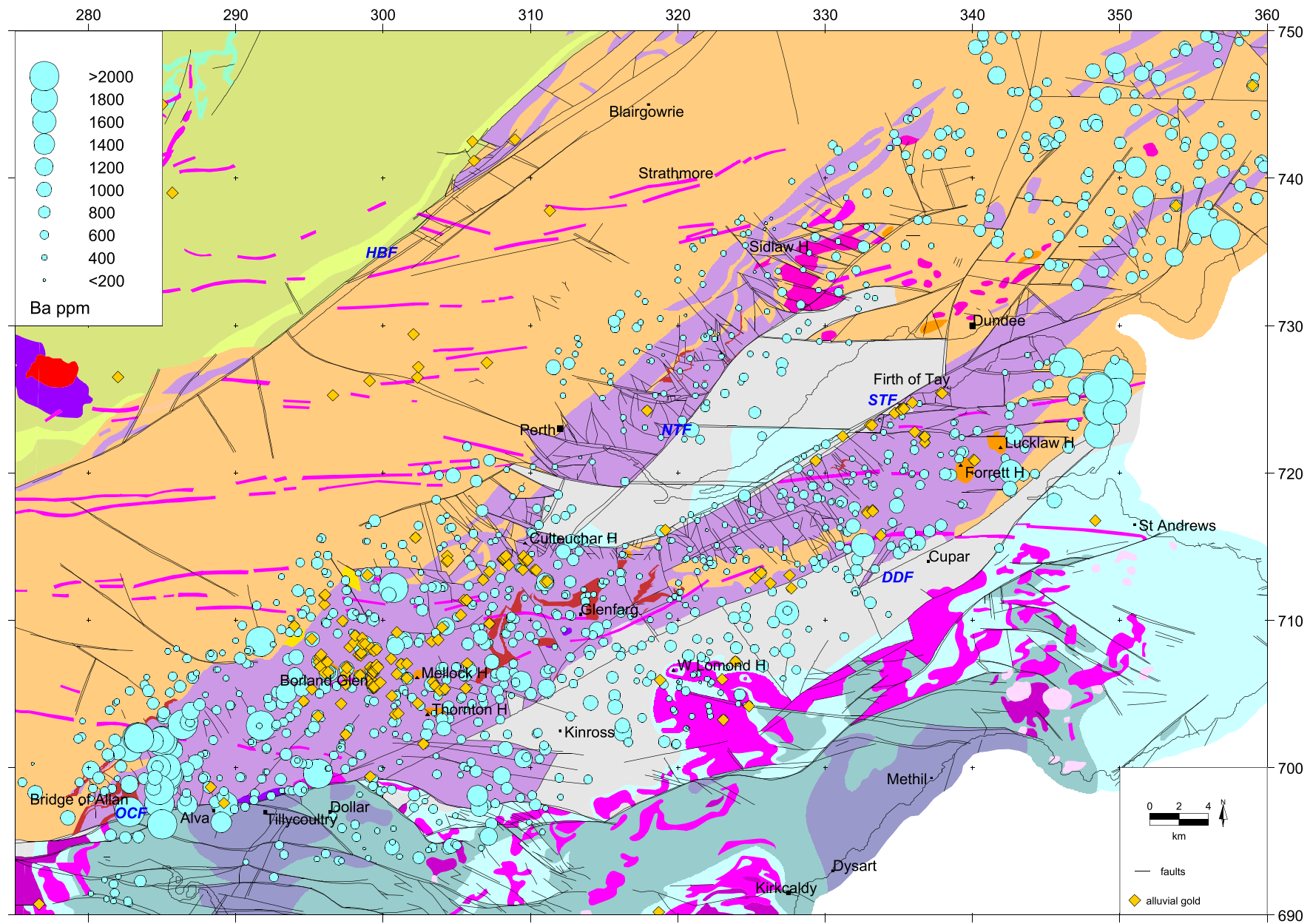


Fig 6.10 Ochils: barium (Ba) in G-BASE stream sediment data

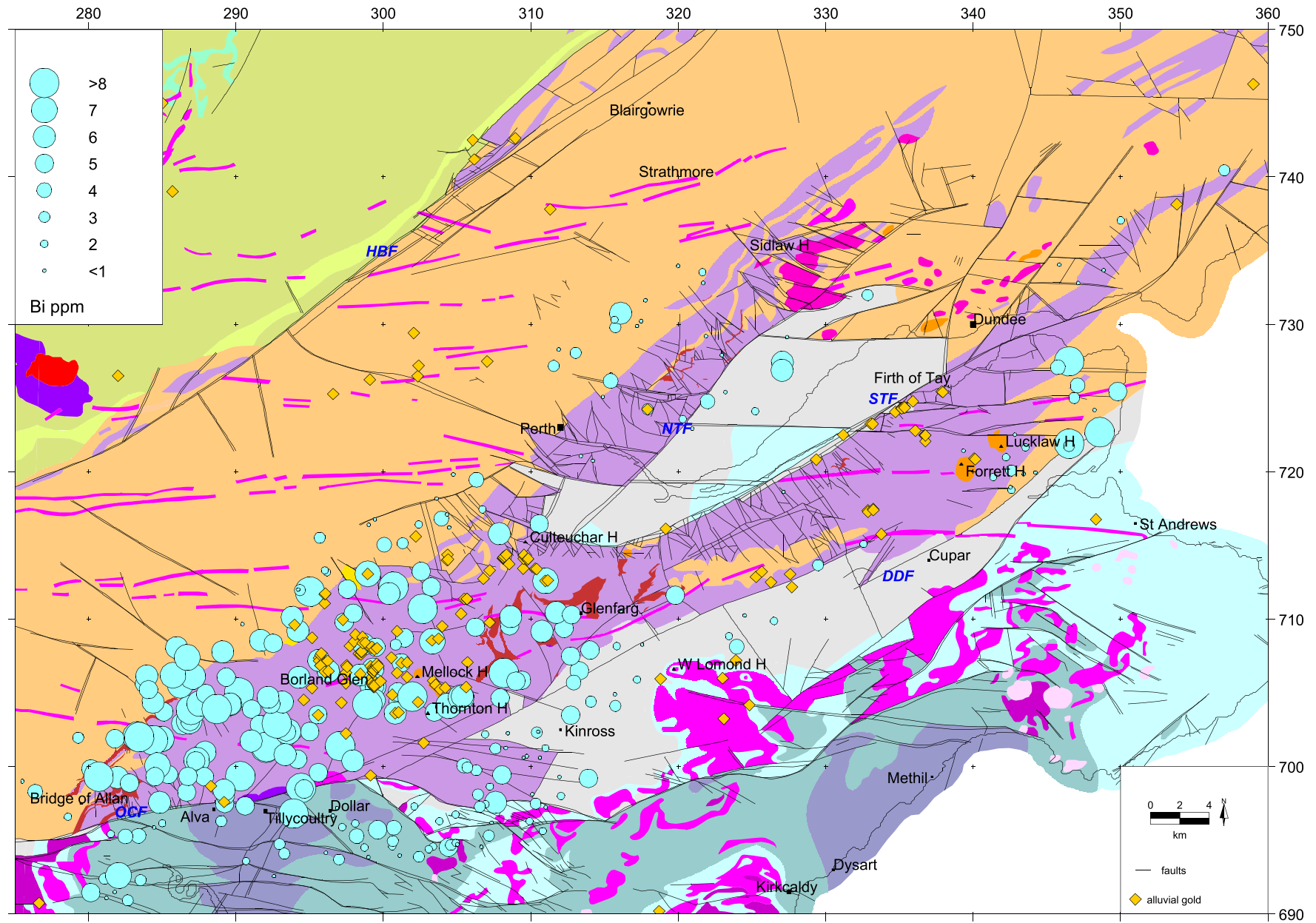


Fig 6.11 Ochils: bismuth (Bi) in G-BASE stream sediment data

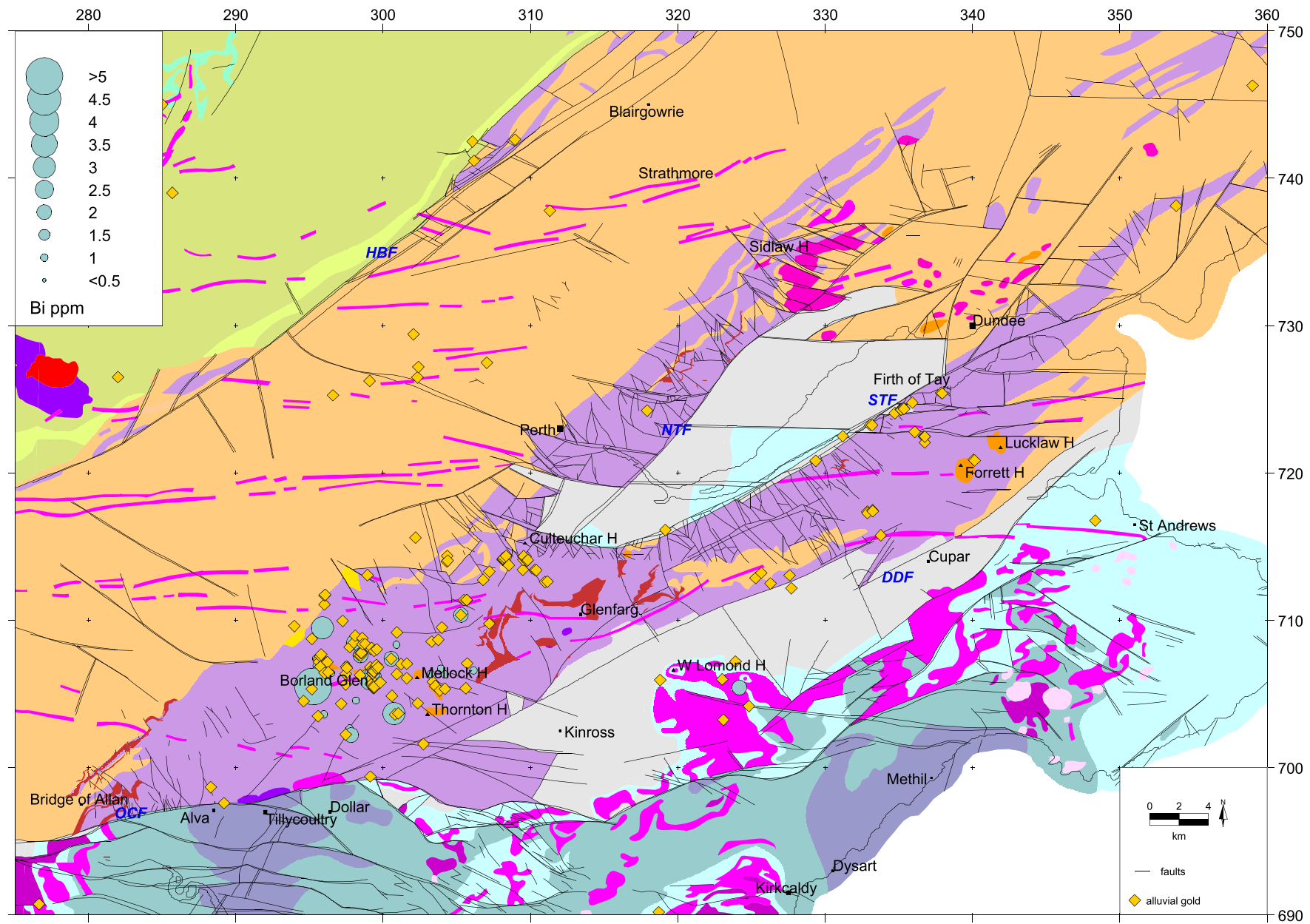


Fig 6.12 Ochils: bismuth (Bi) in MRP panned concentrate data

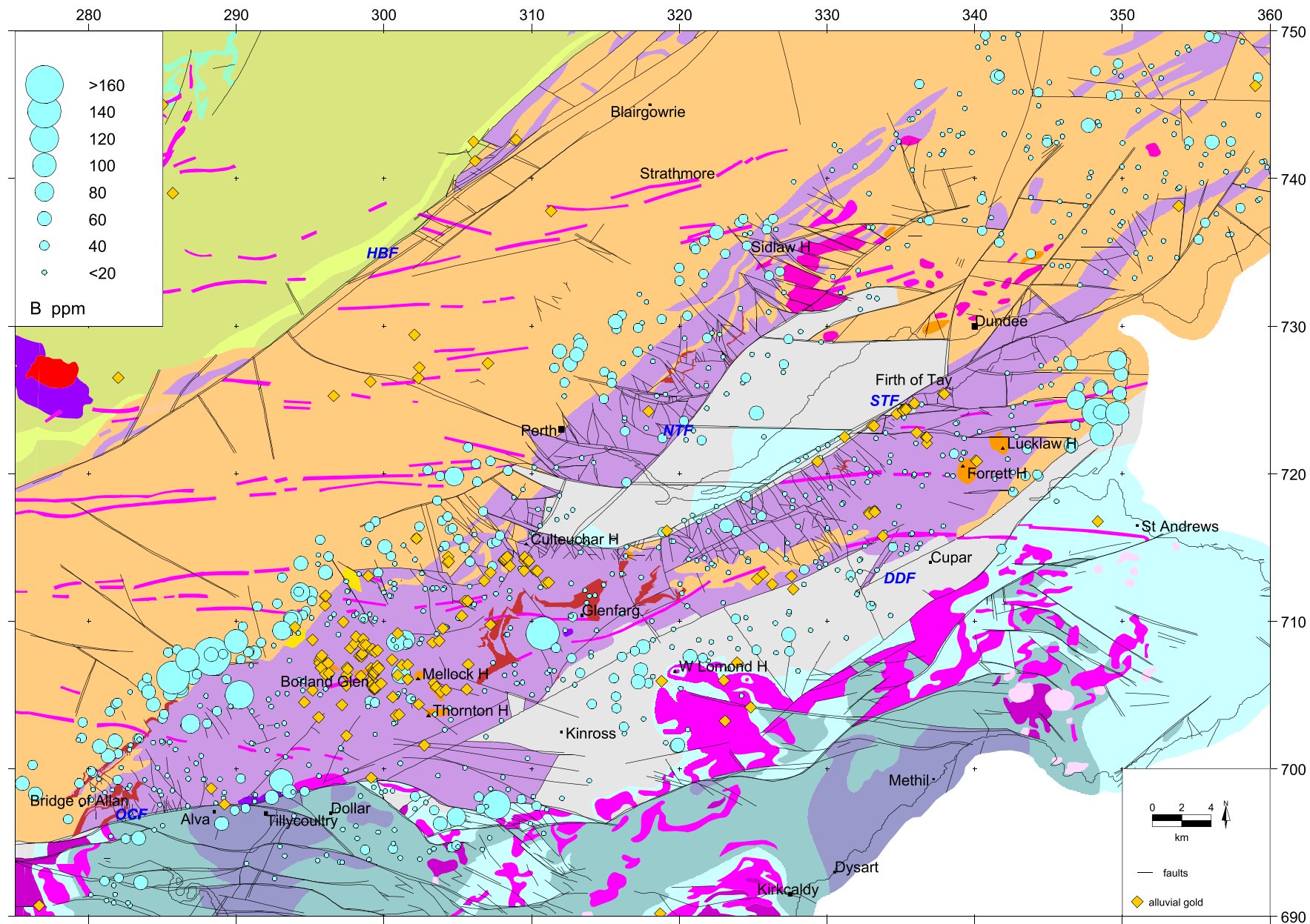


Fig 6.13 Ochils: boron (B) in G-BASE stream sediment data

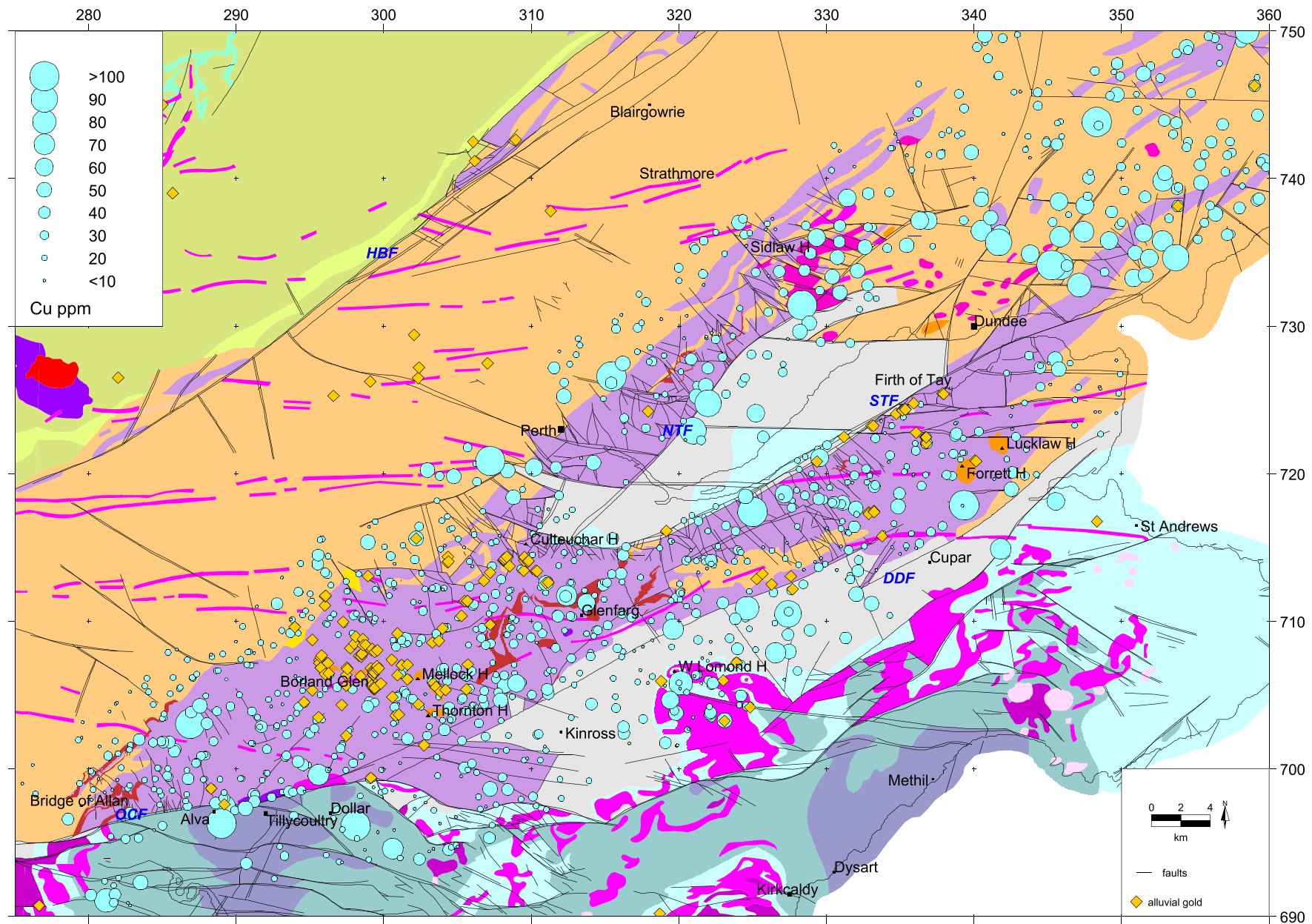


Fig 6.14 Ochils: copper (Cu) in G-BASE stream sediment data

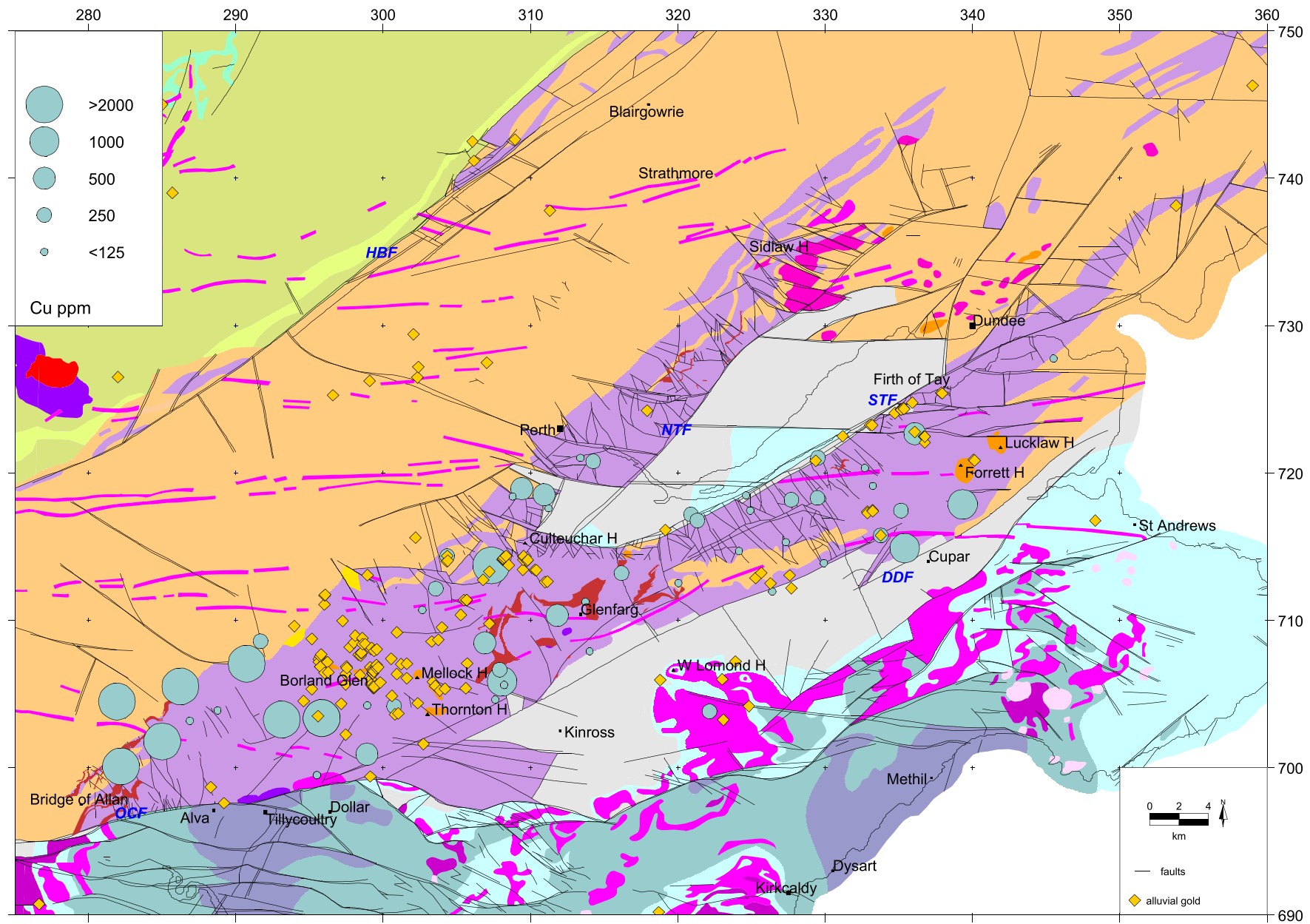


Fig 6.15 Ochils: copper (Cu) in MRP panned concentrate data

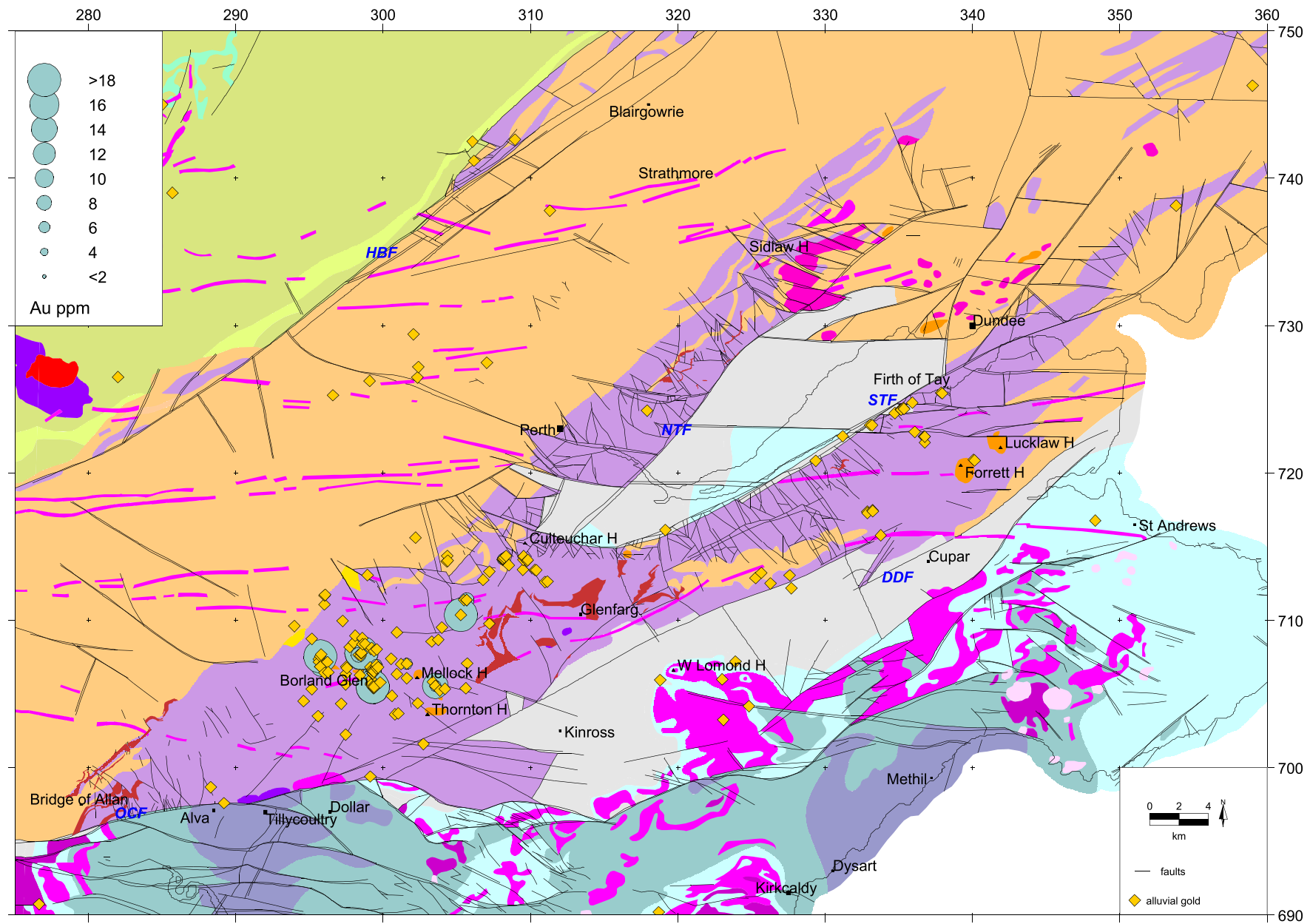


Fig 6.16 Ochils: gold (Au) in MRP panned concentrate data

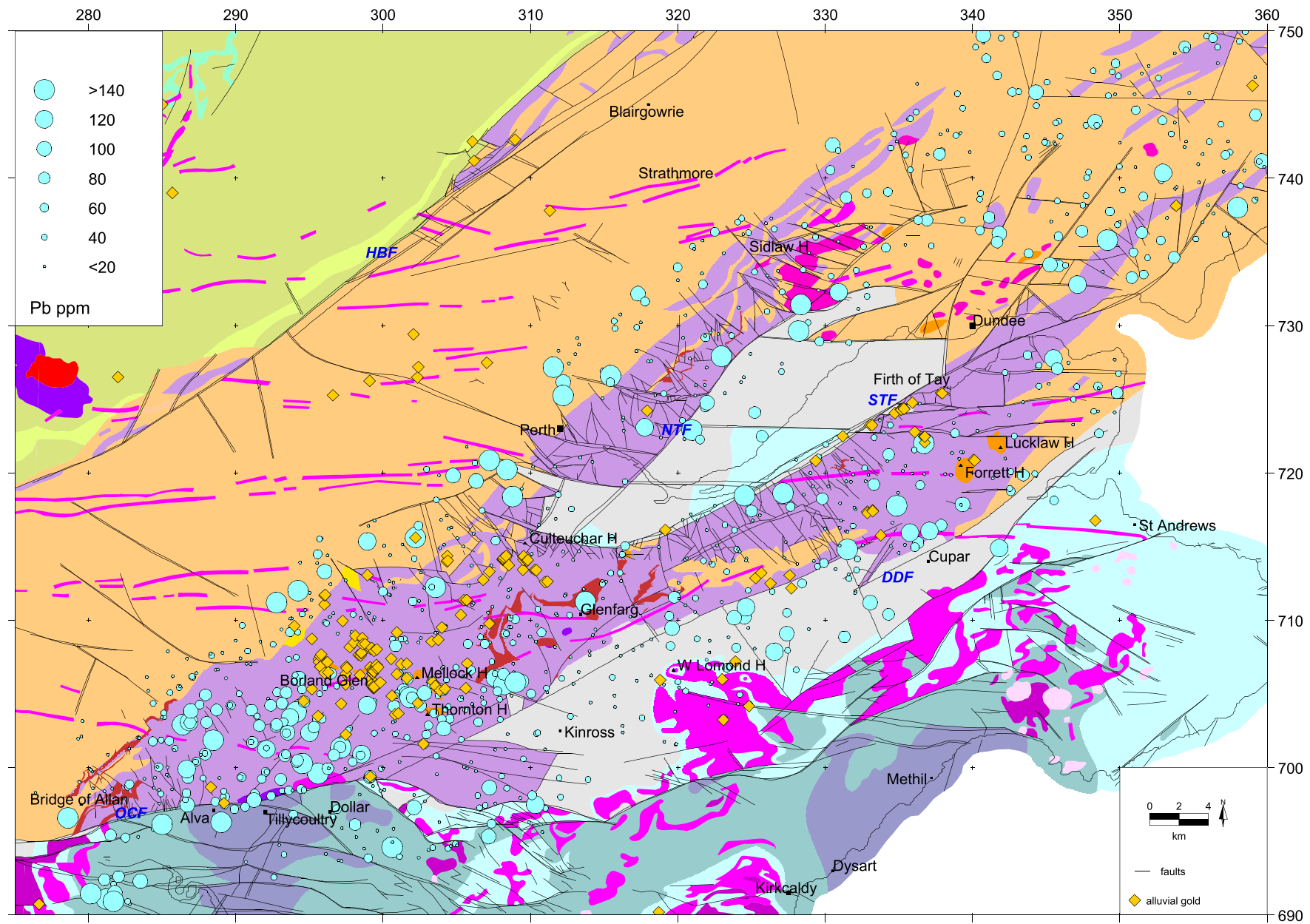


Fig 6.17 Ochils: lead (Pb) in G-BASE stream sediment data

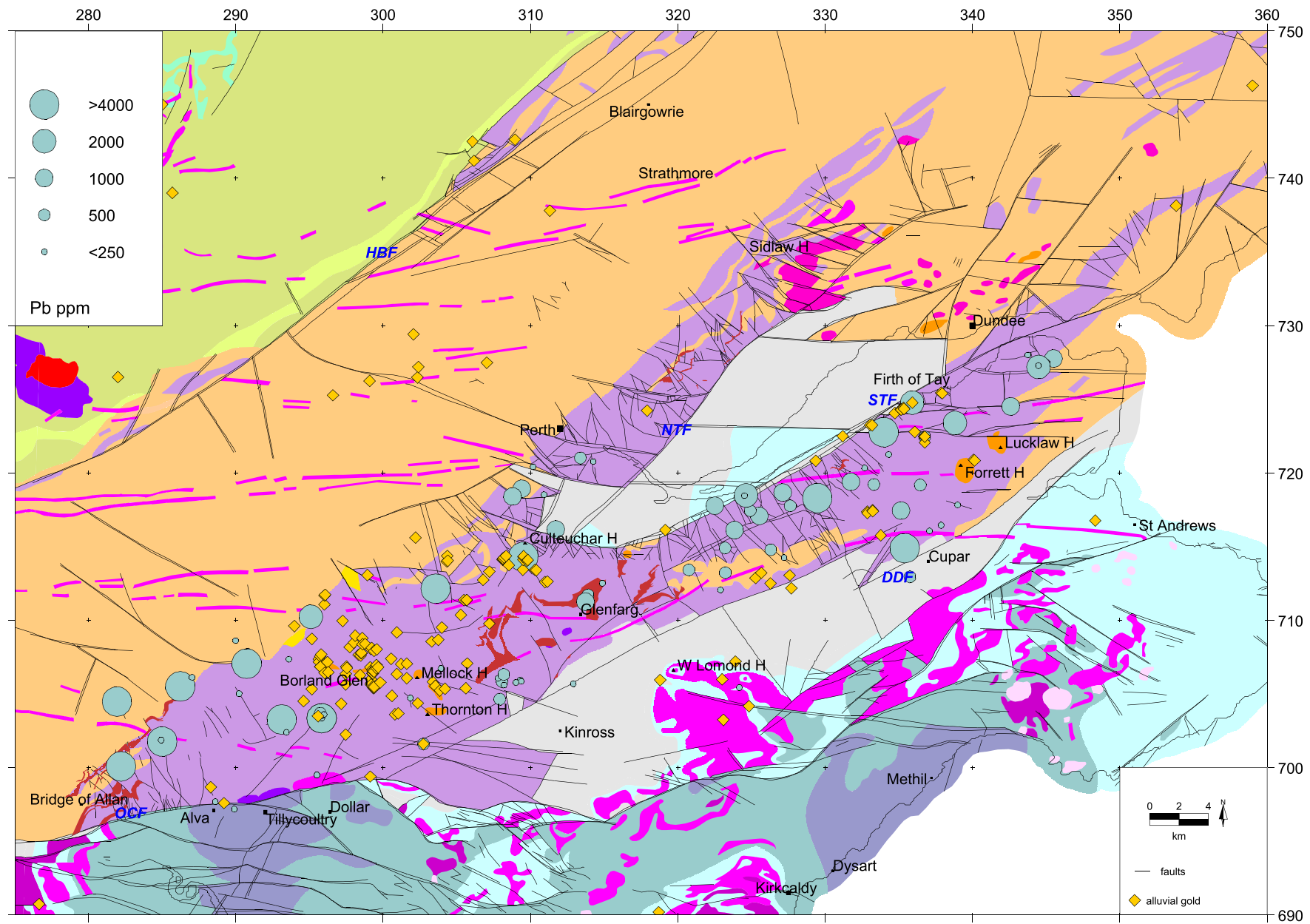


Fig 6.18 Ochils: lead (Pb) in MRP panned concentrate data

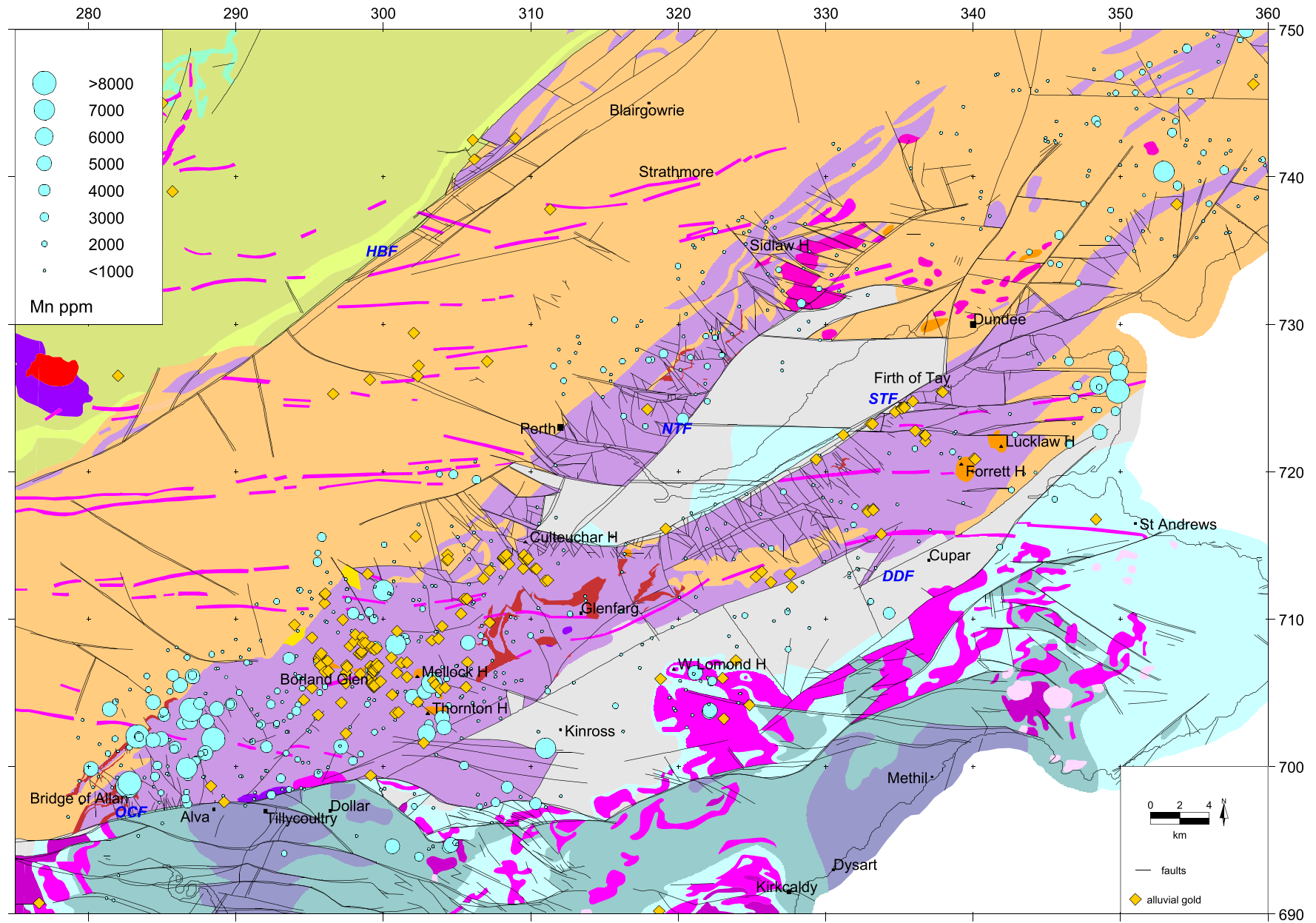


Fig 6.19 Ochils: manganese (Mn) in G-BASE stream sediment data

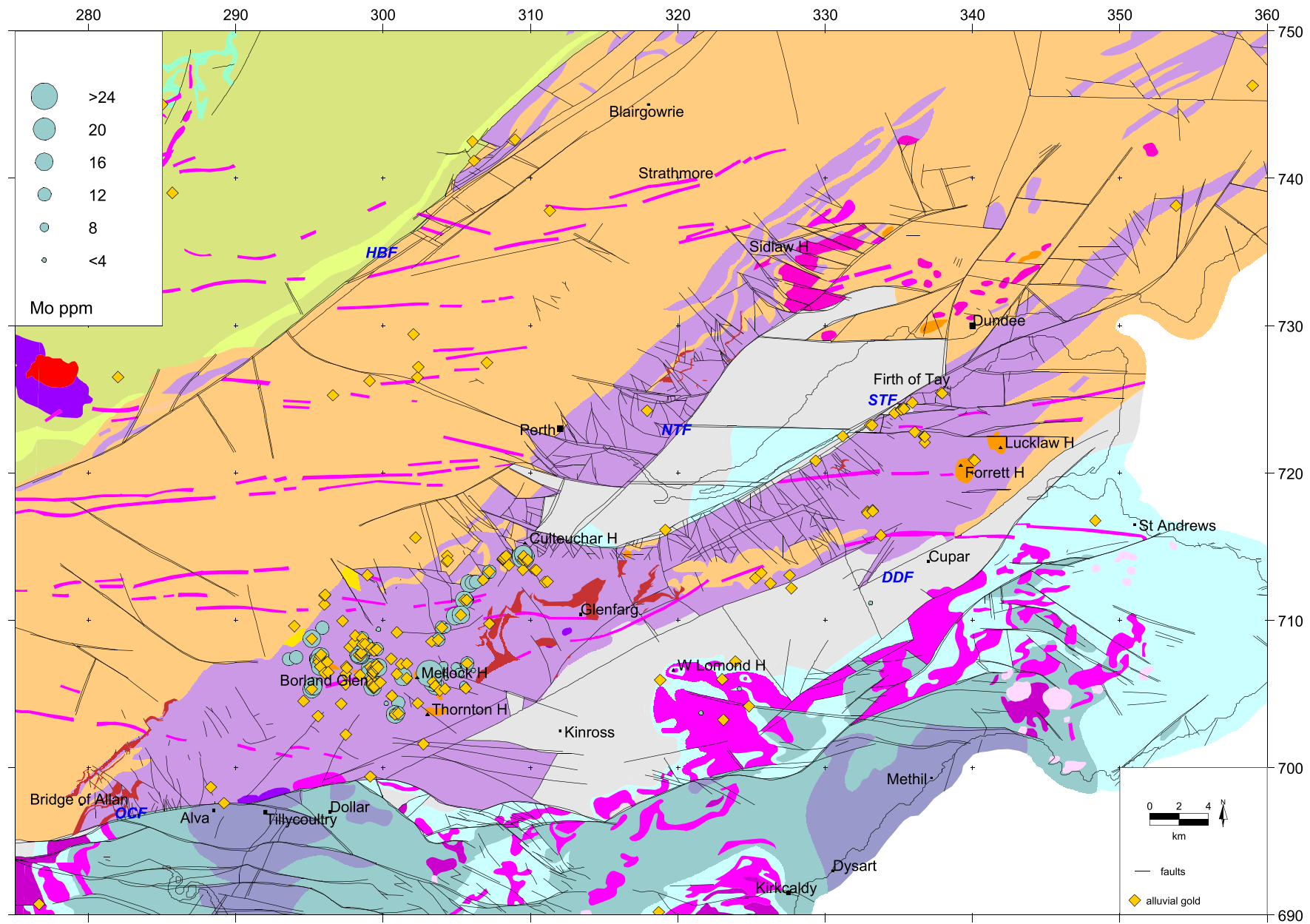


Fig 6.20 Ochils: molybdenum (Mo) in MRP panned concentrate data

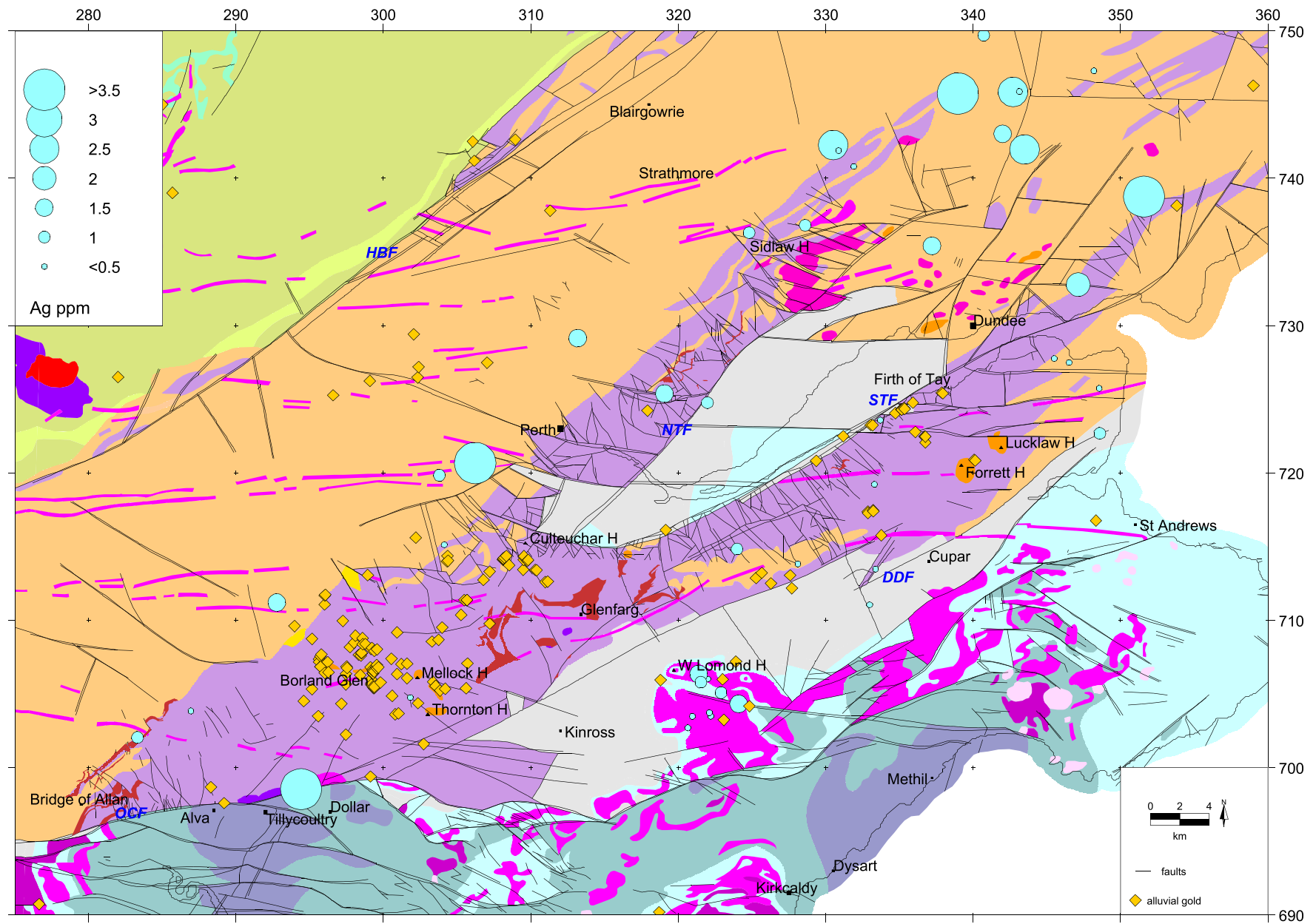


Fig 6.21 Ochils: silver (Ag) in G-BASE stream sediment data

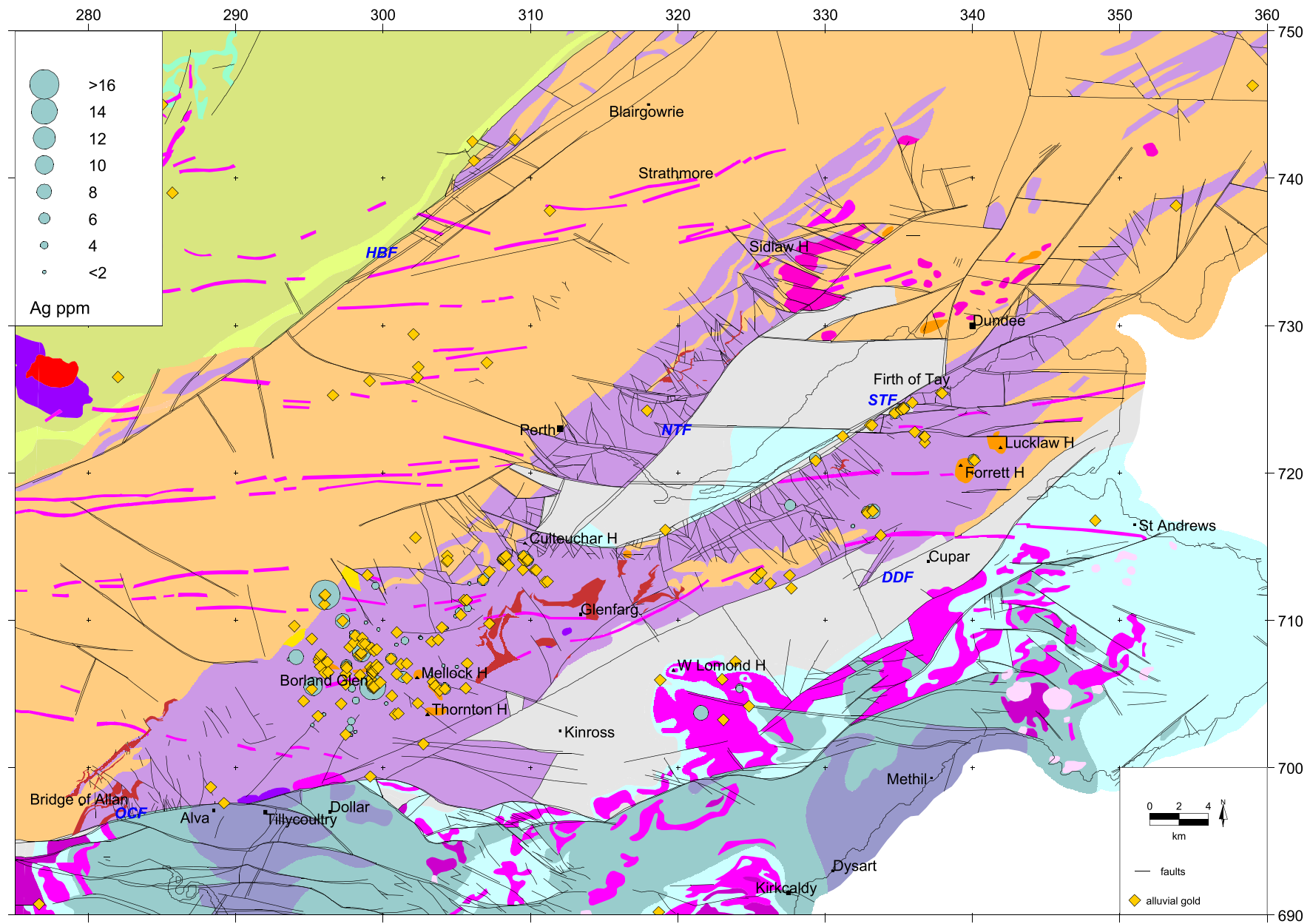


Fig 6.22 Ochils: silver (Ag) in MRP panned concentrate data

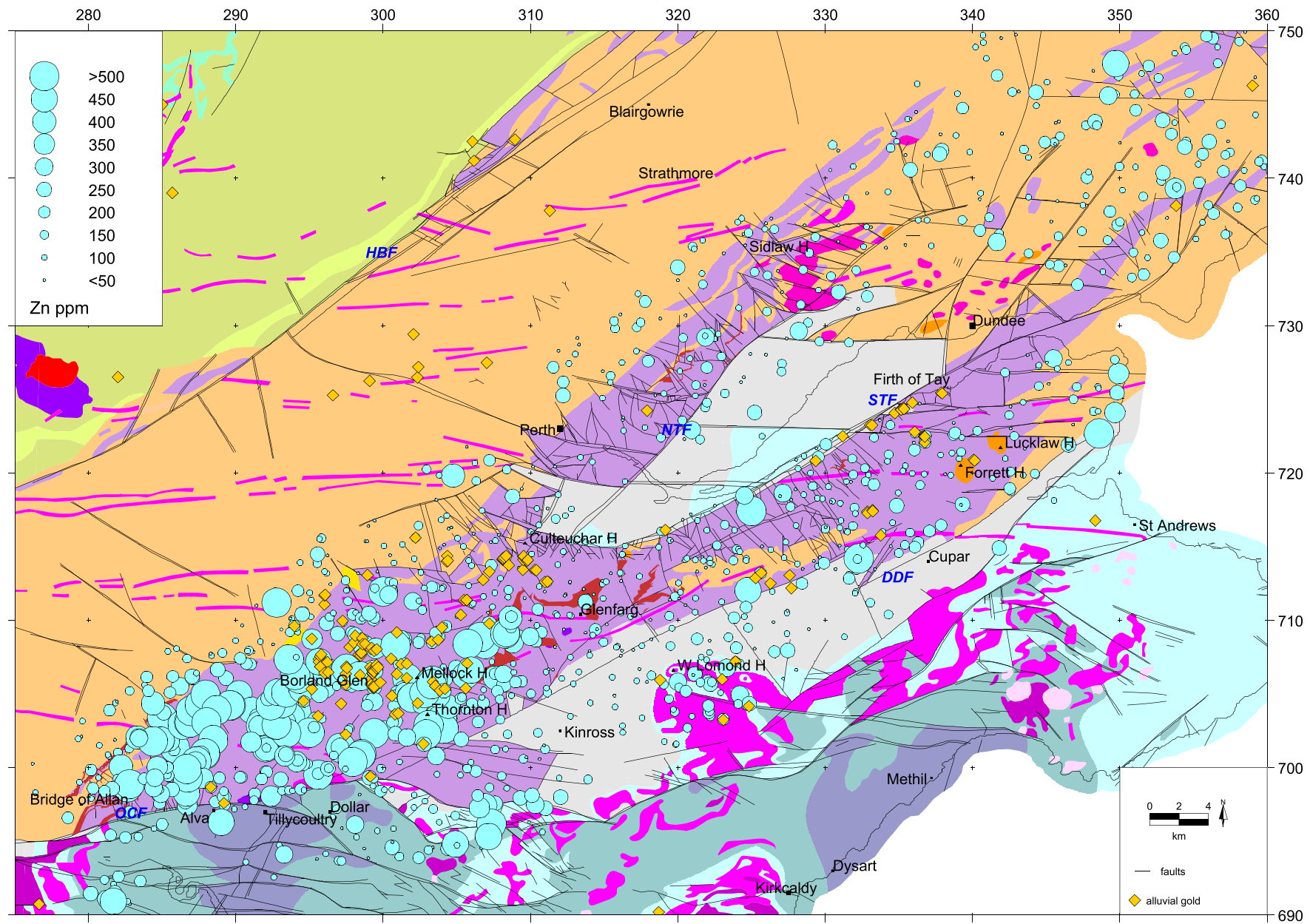


Fig 6.23 Ochils: zinc (Zn) in G-BASE stream sediment data

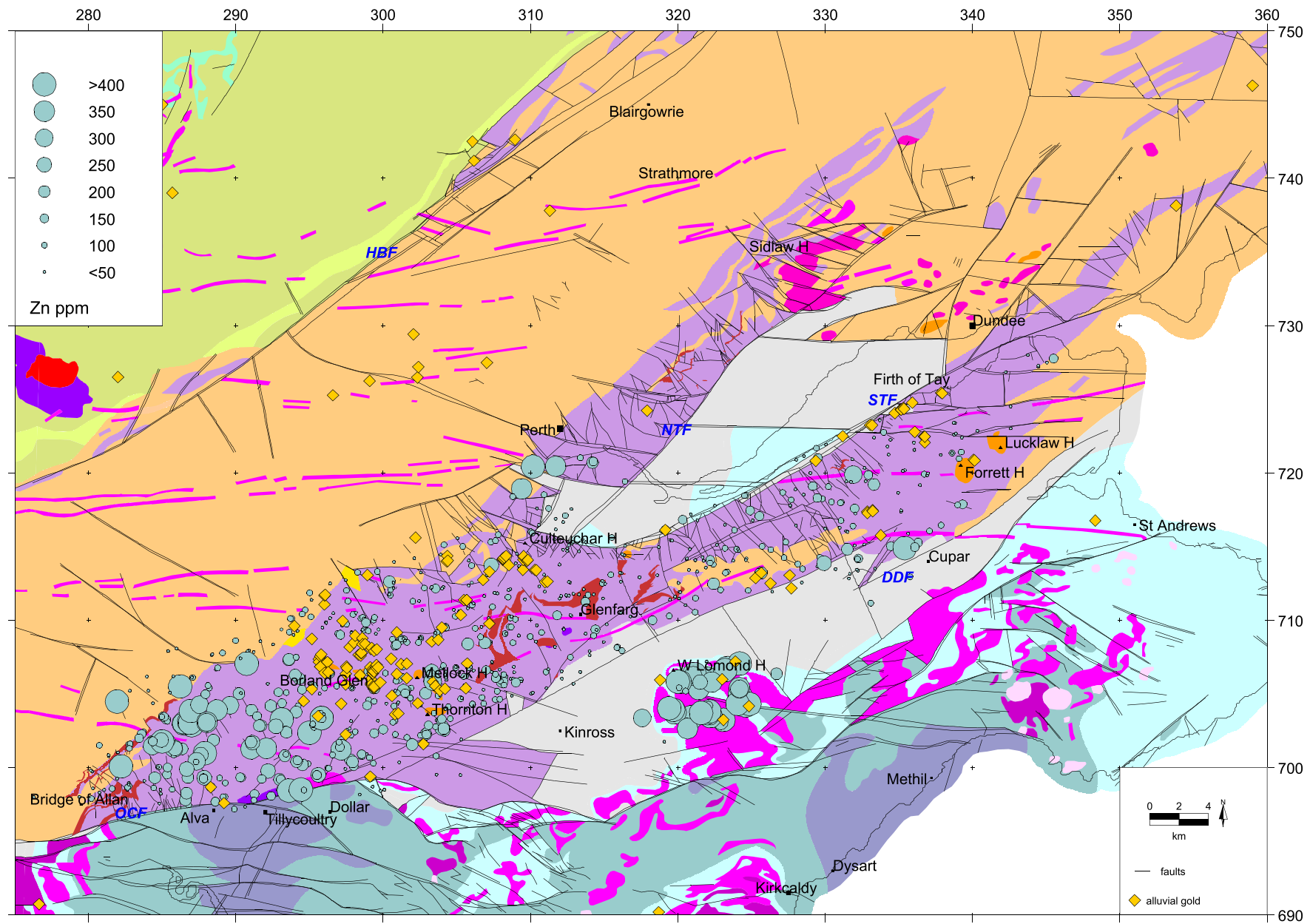


Fig 6.24 Ochils: zinc (Zn) in MRP panned concentrate data

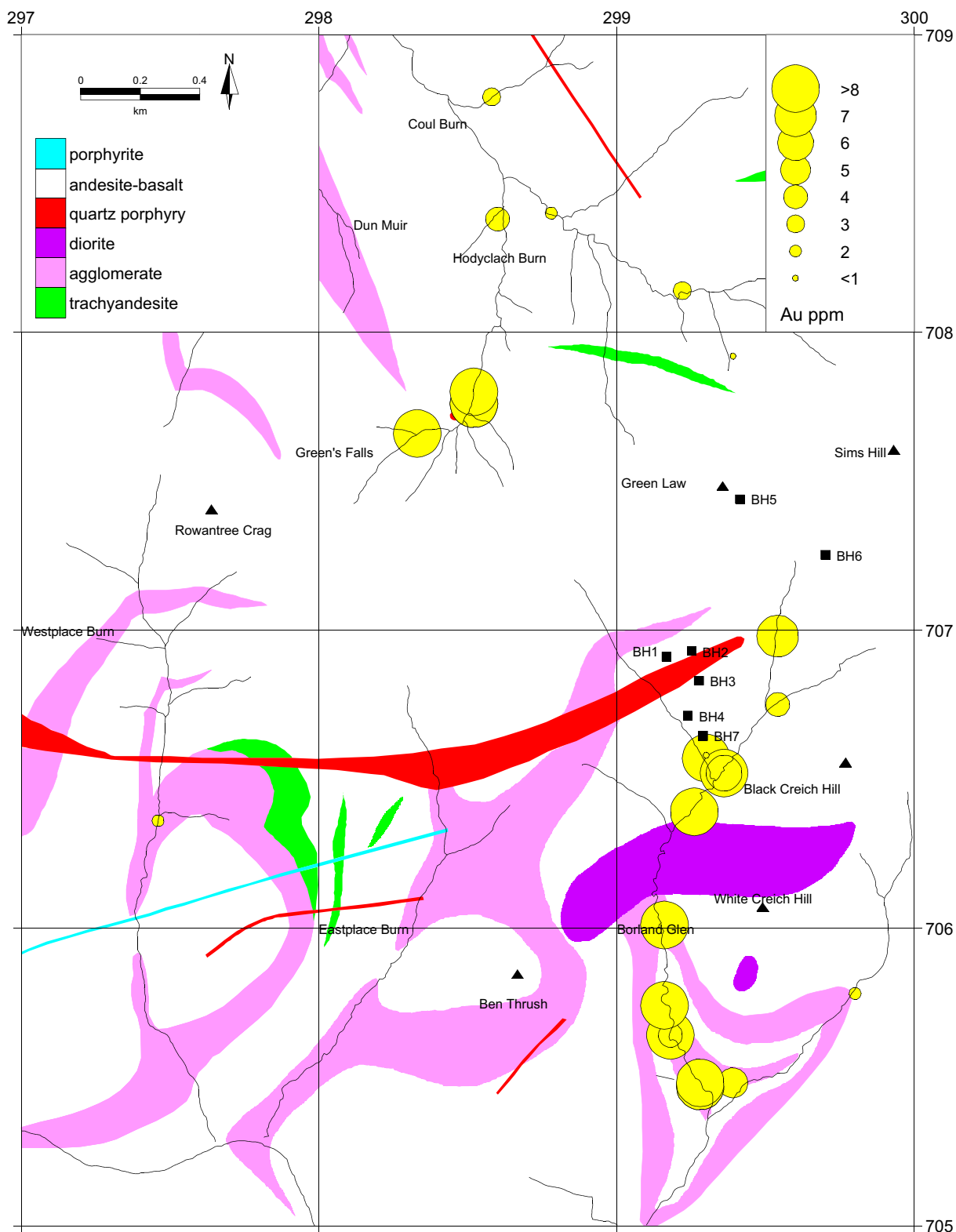


Fig 6.25 Ochils: detailed geology of Borland Glen showing gold (Au) in panned concentrate data

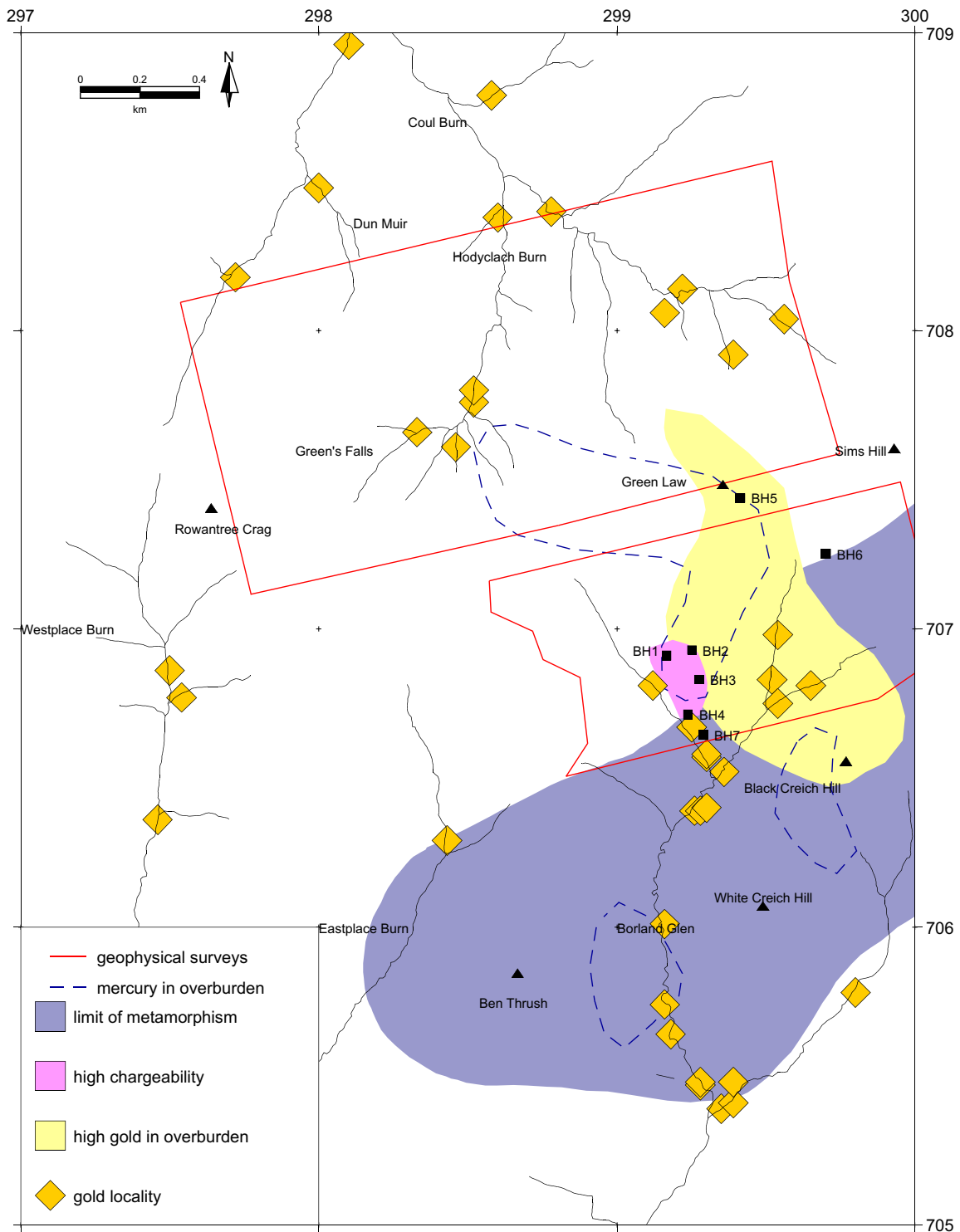


Fig 6.26 Ochils: distribution of alluvial gold in Borland Glen, geophysical anomalies and elevated mercury (Hg) values in overburden

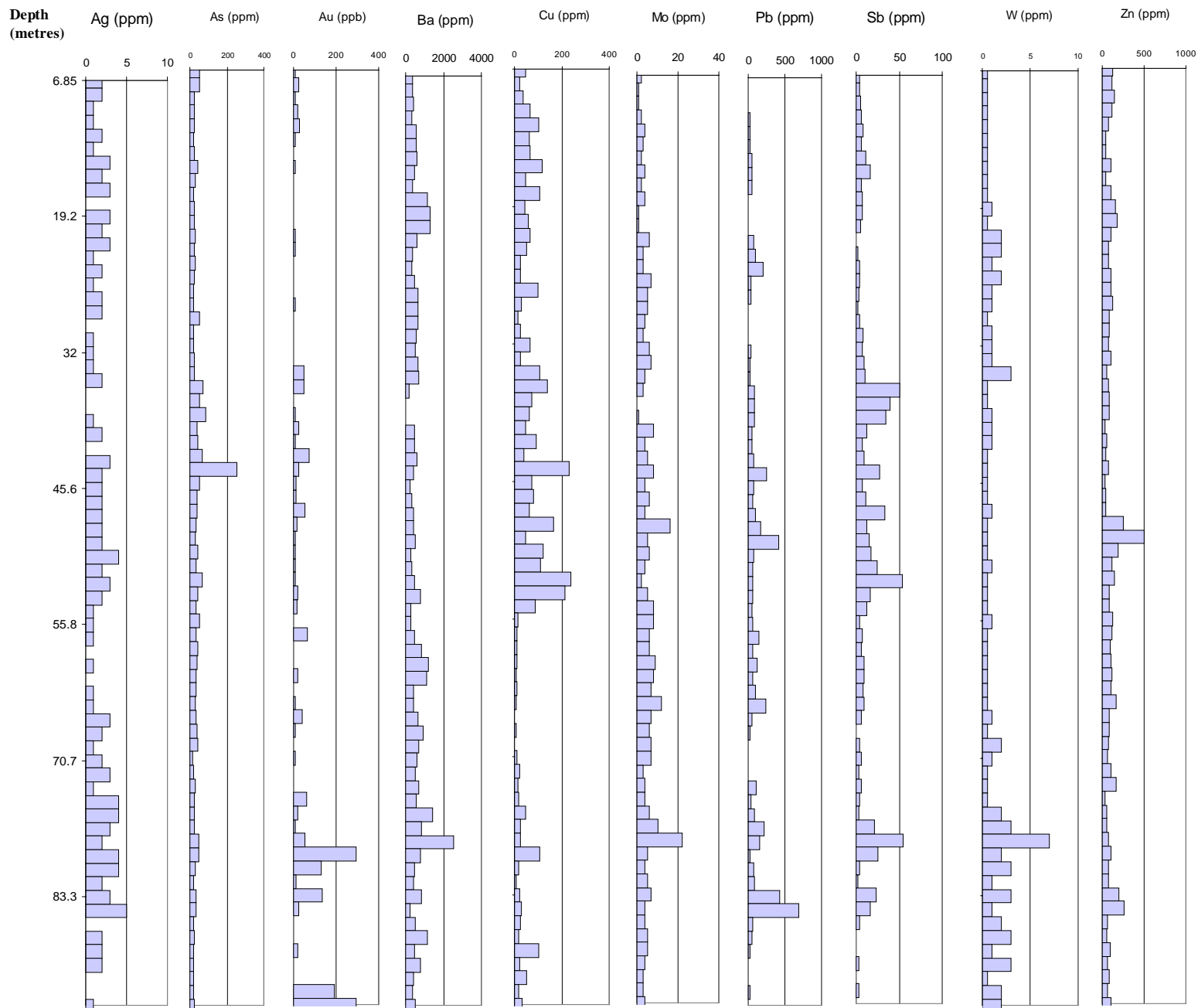


Figure 6.27 Ochils: geochemical log for borehole 2, Borland Glen

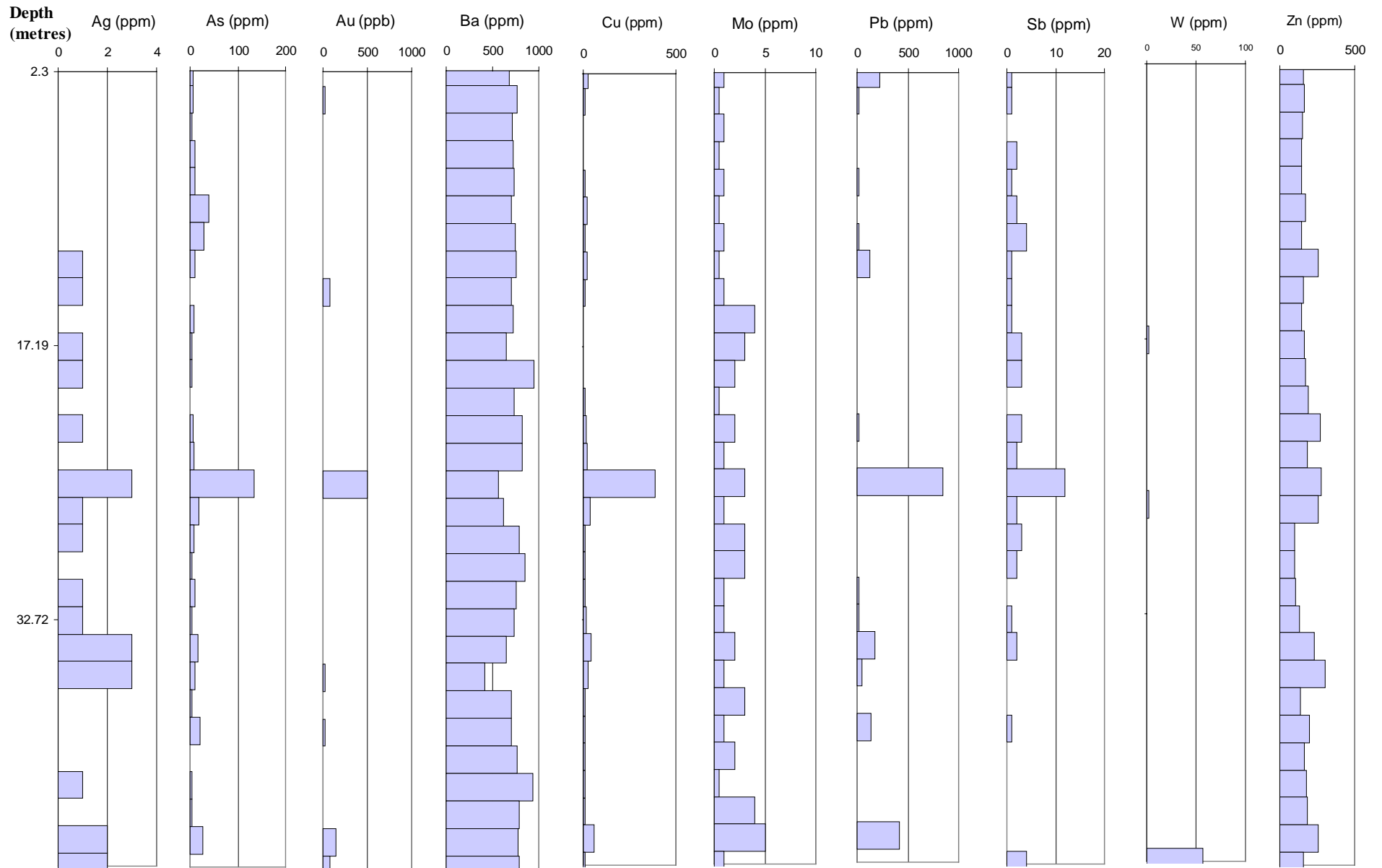


Figure 6.28 Ochils: geochemical log for borehole 5, Borland Glen

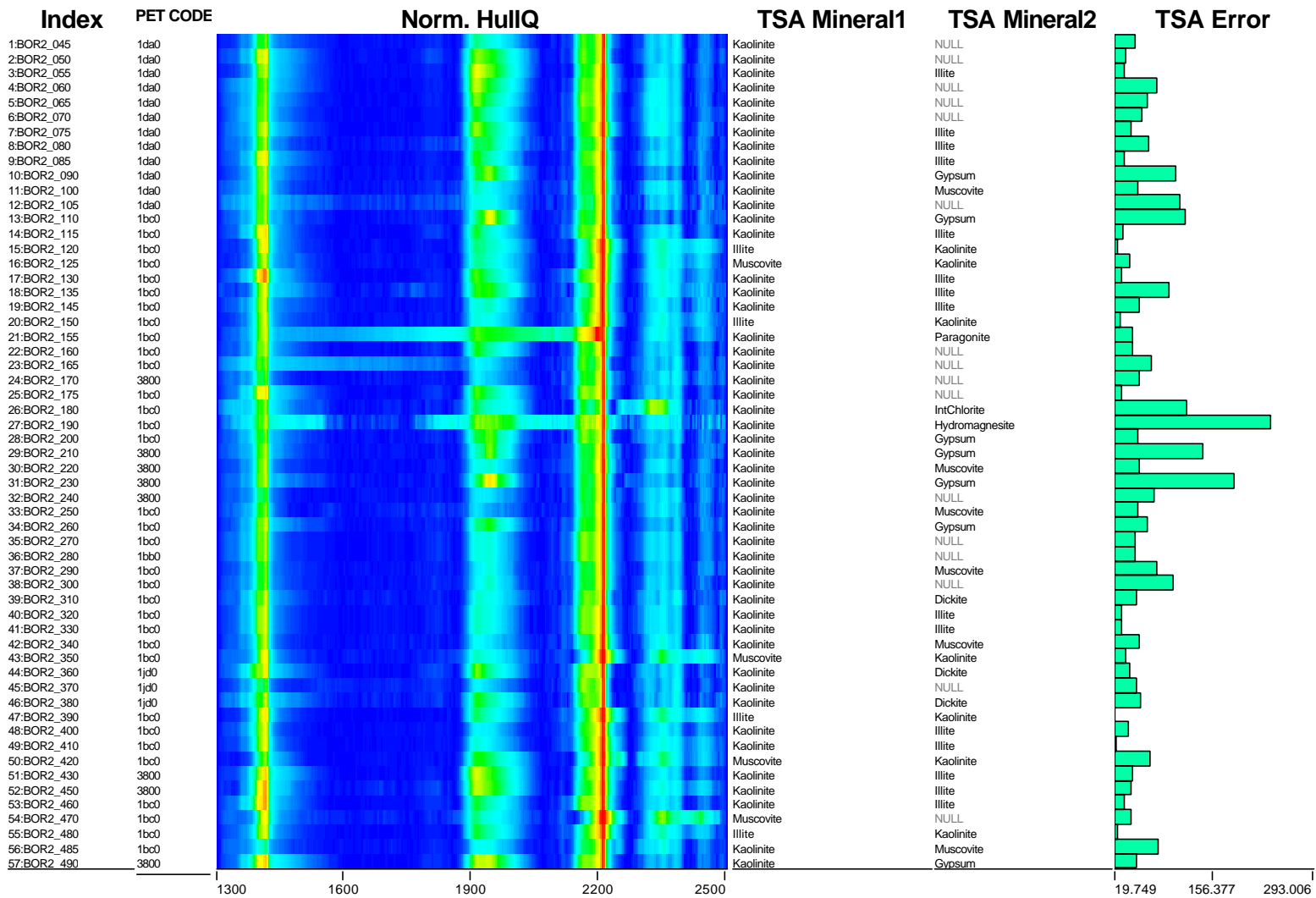


Figure 6.29 Ochils: summary of PIMA analysis for borehole 2, Borland Glen

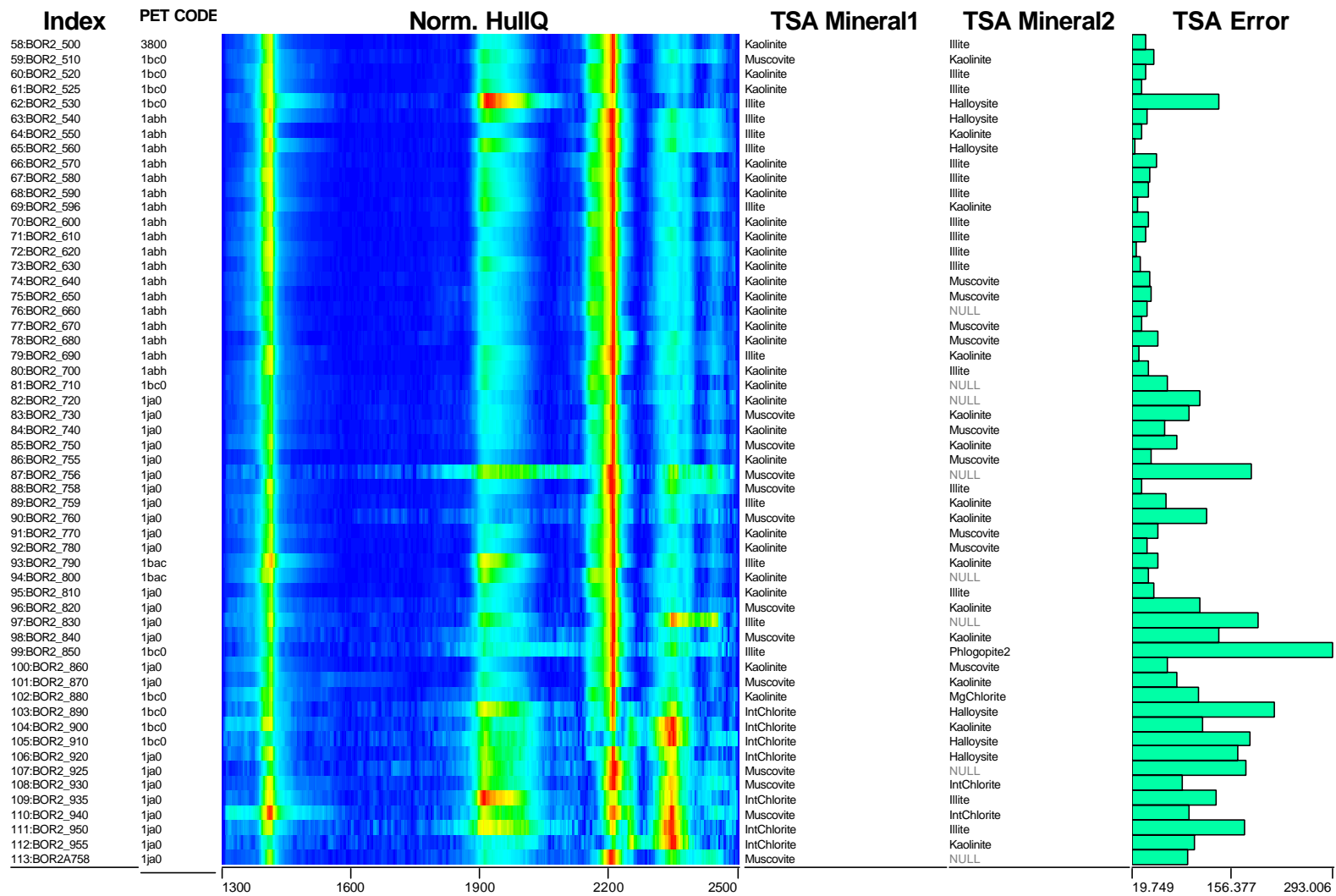


Figure 6.29 Ochils: summary of PIMA analysis for borehole 2, Borland Glen

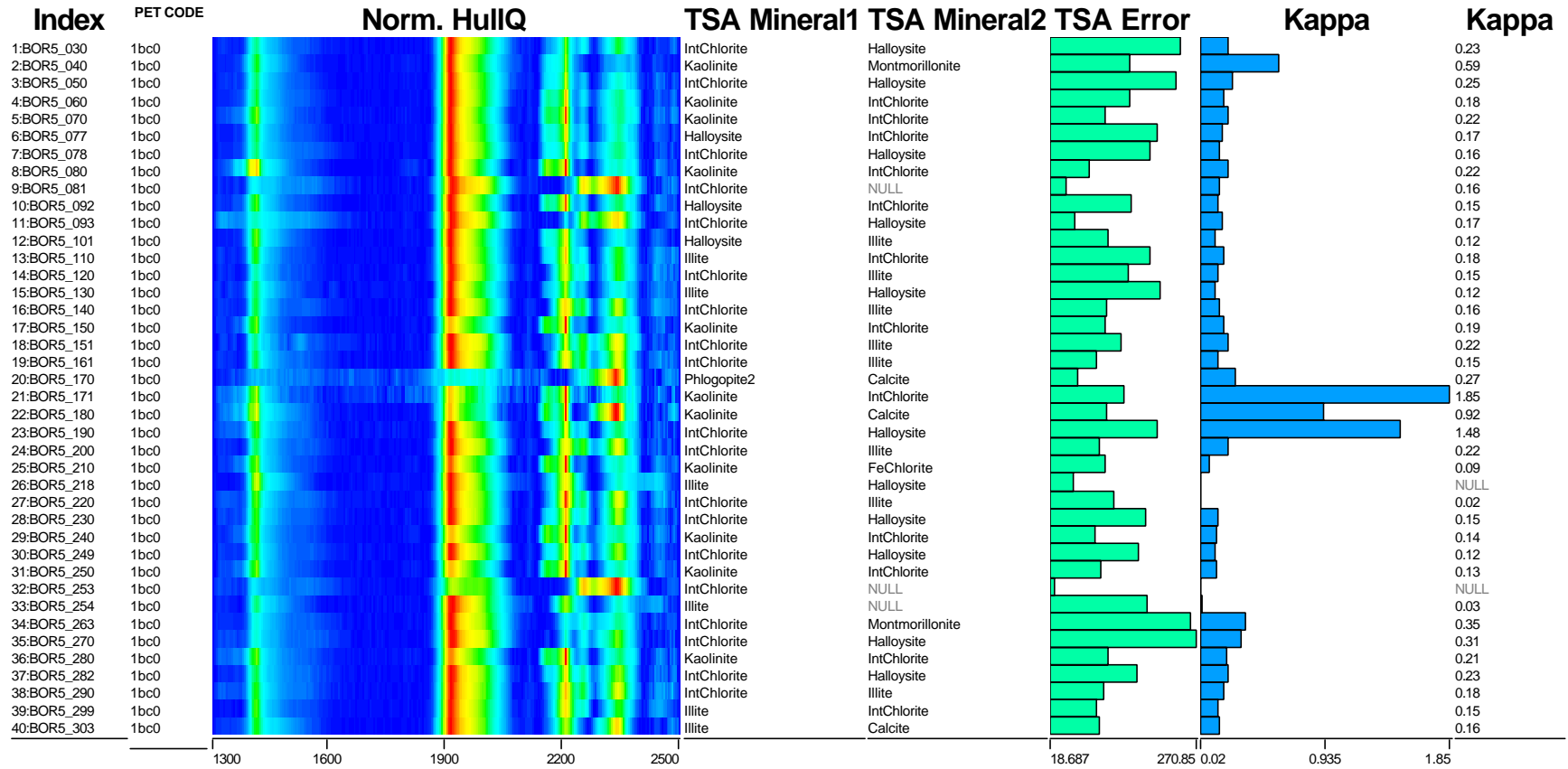


Figure 6.30 Ochils: summary of PIMA analysis for borehole 5, Borland Glen. Magnetic susceptibility values (10^{-3} SI) are also shown.

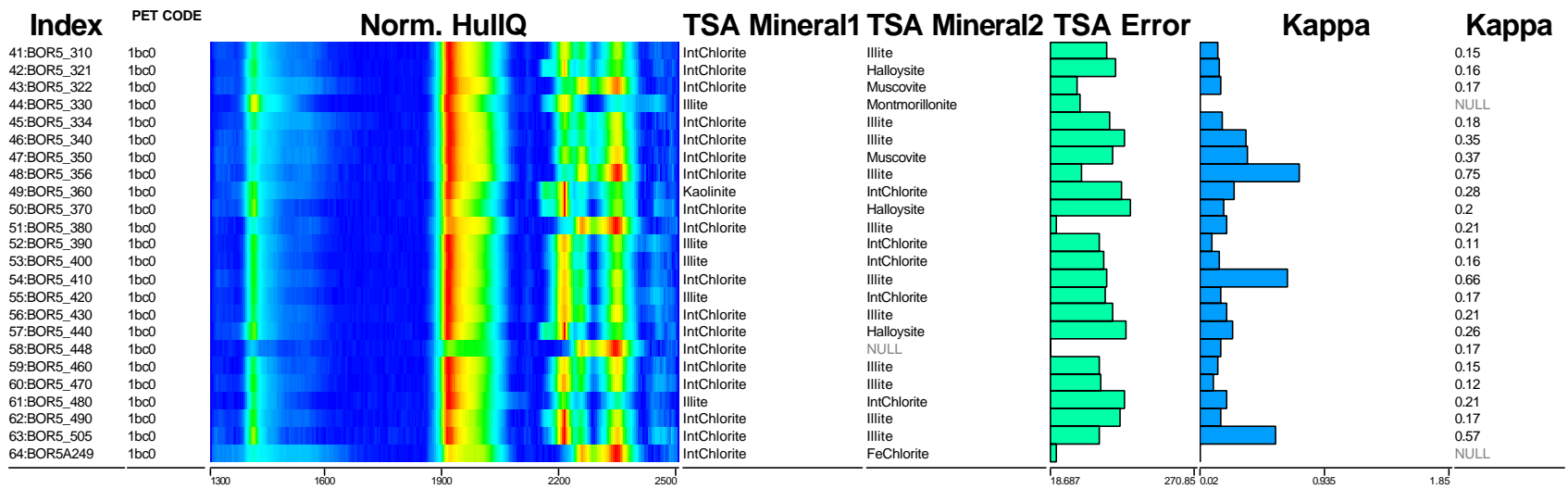


Figure 6.30 Ochils: summary of PIMA analysis for borehole 5, Borland Glen. Magnetic susceptibility values (10^{-3} SI) are also shown.

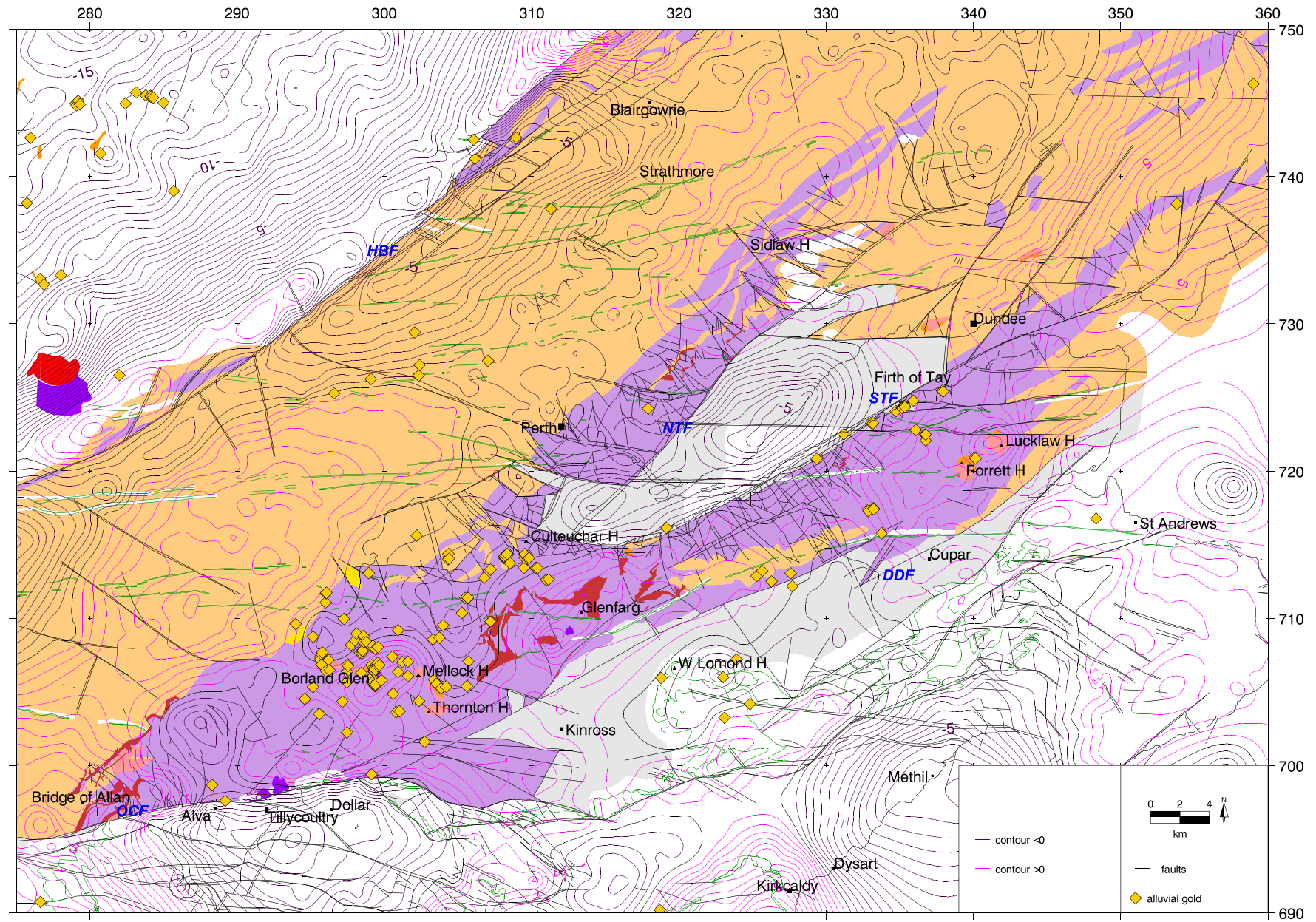


Fig 6.31 Ochils: Bouguer gravity anomaly, contour interval 0.5 mGal

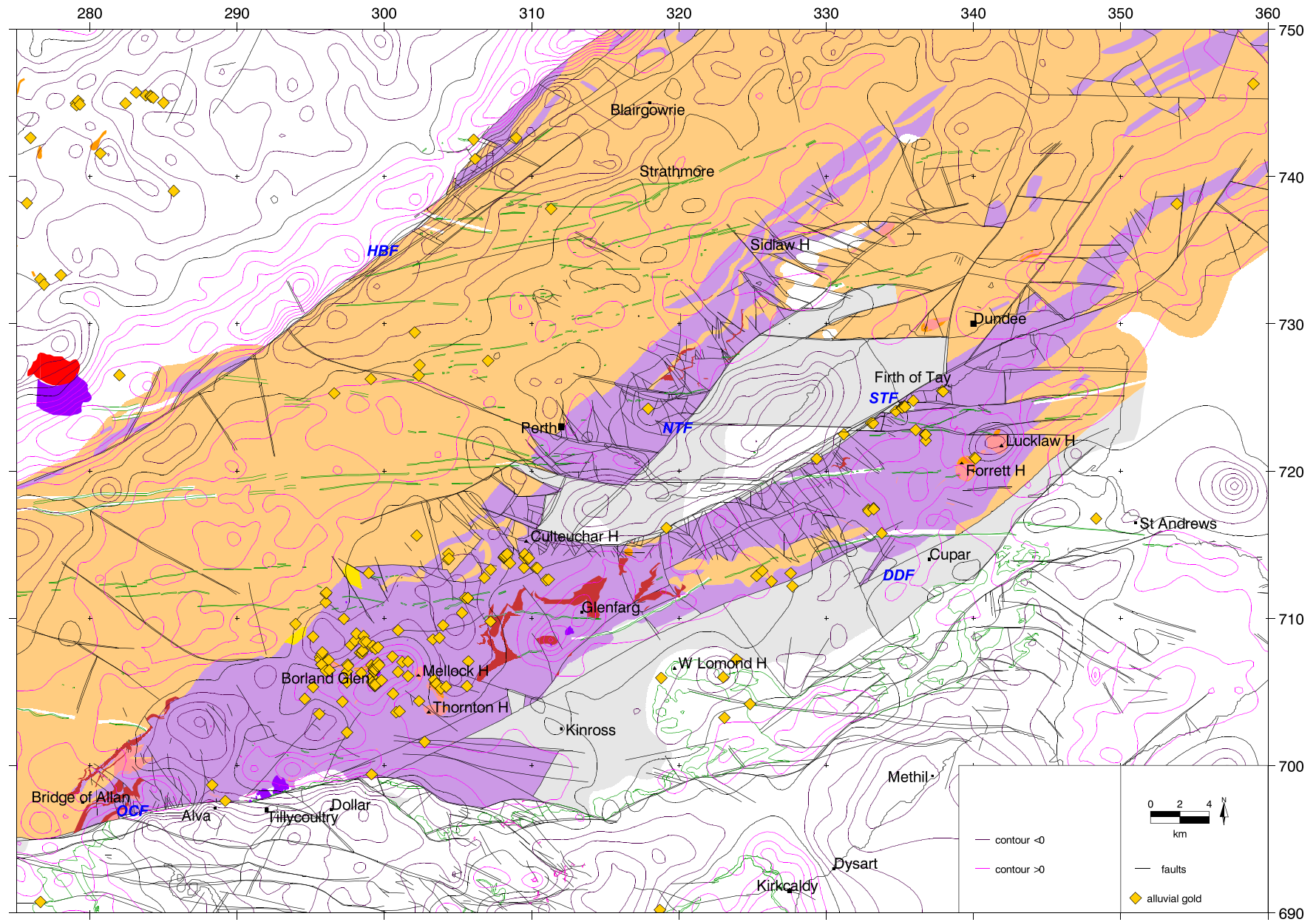


Fig 6.32 Ochils: Residual gravity anomaly, contour interval 0.5 mGal

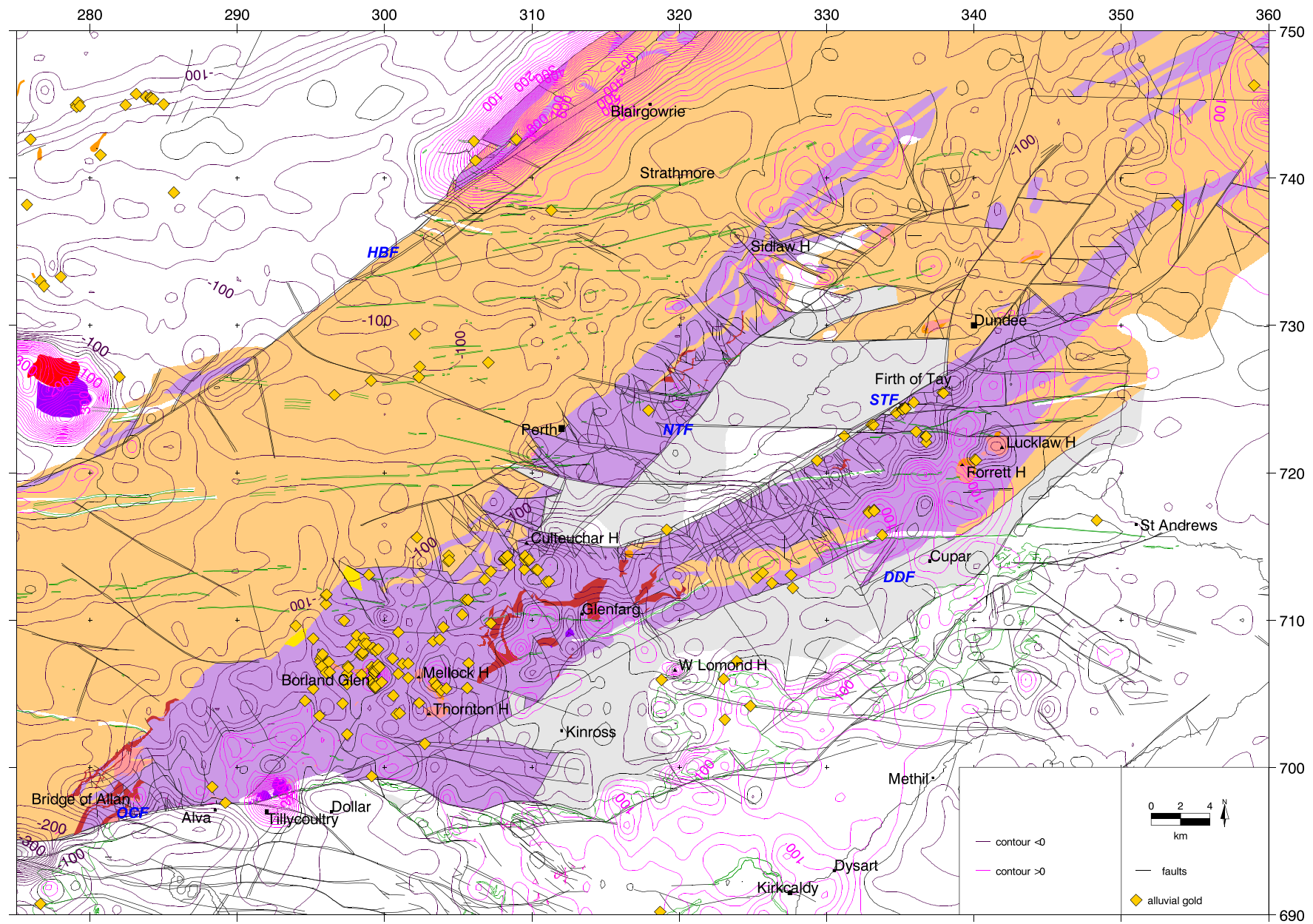


Fig 6.33 Ochils: Total Magnetic field anomaly contour interval 25 nT

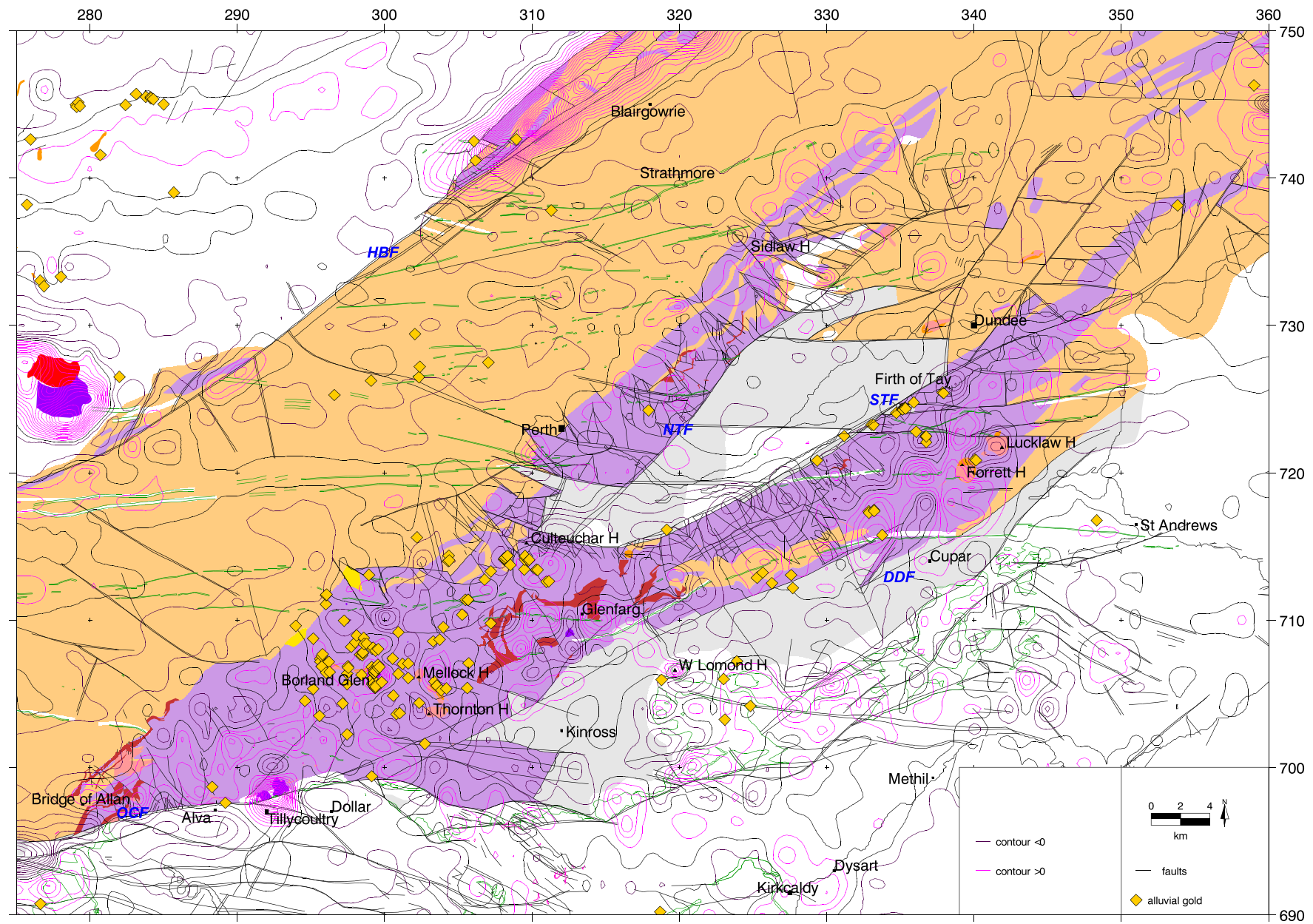


Fig 6.34 Ochils: Residual magnetic anomaly, contour interval 25 nT

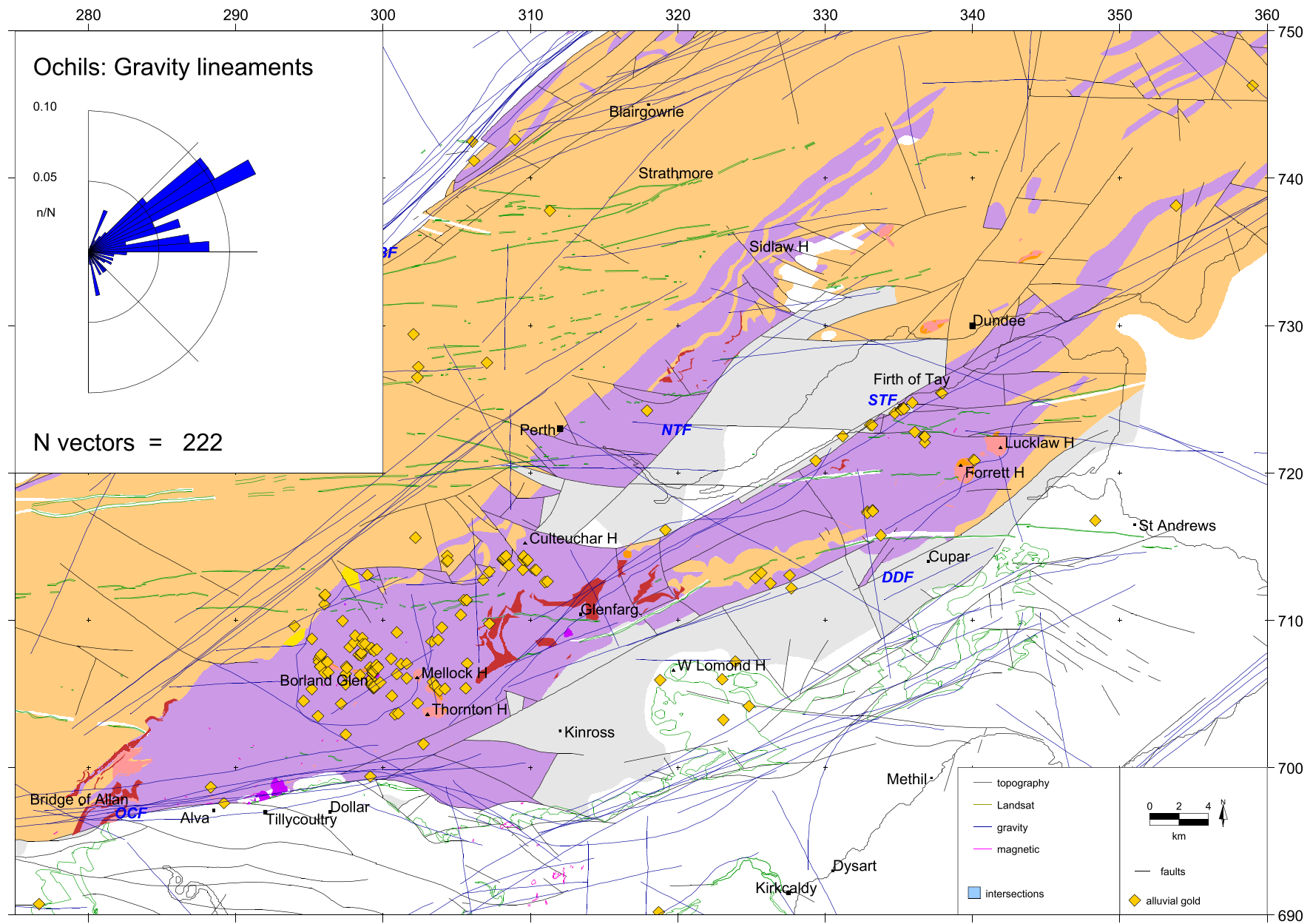


Fig 6.35 Ochils: gravity lineaments

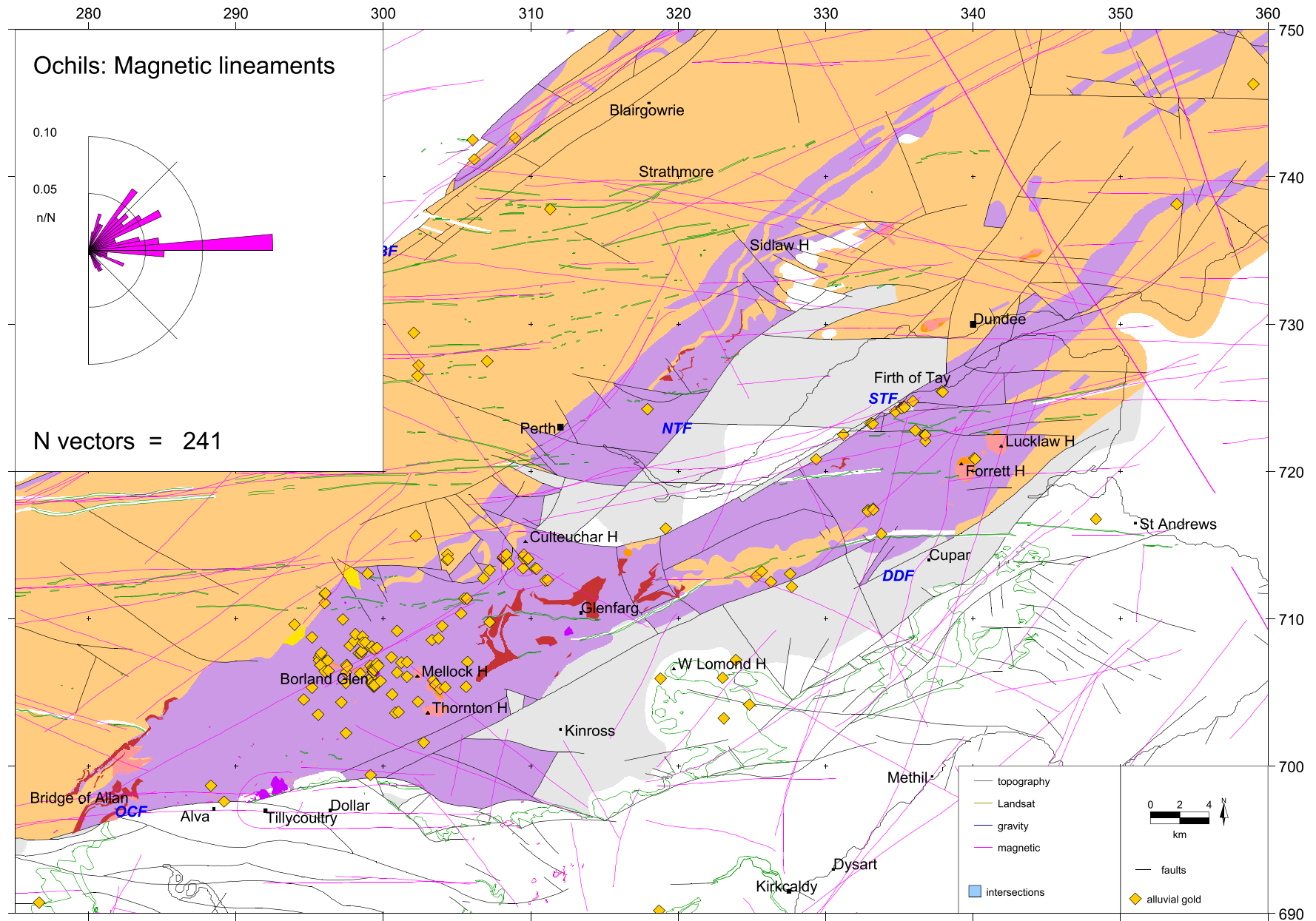


Fig 6.36 Ochils: magnetic lineaments

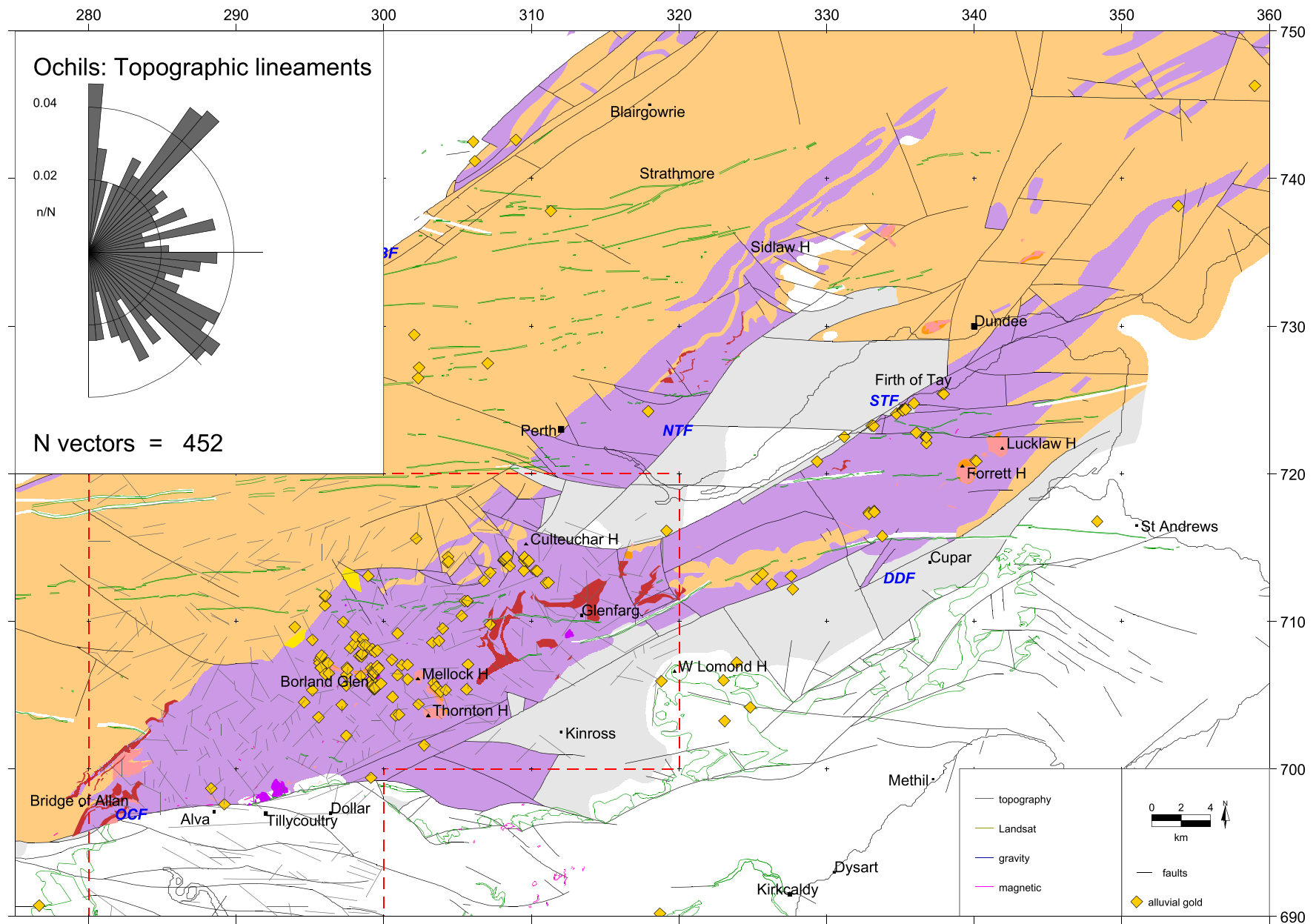


Fig 6.37 Ochils: lineaments from digital topography. Red dashed line defines area of data availability

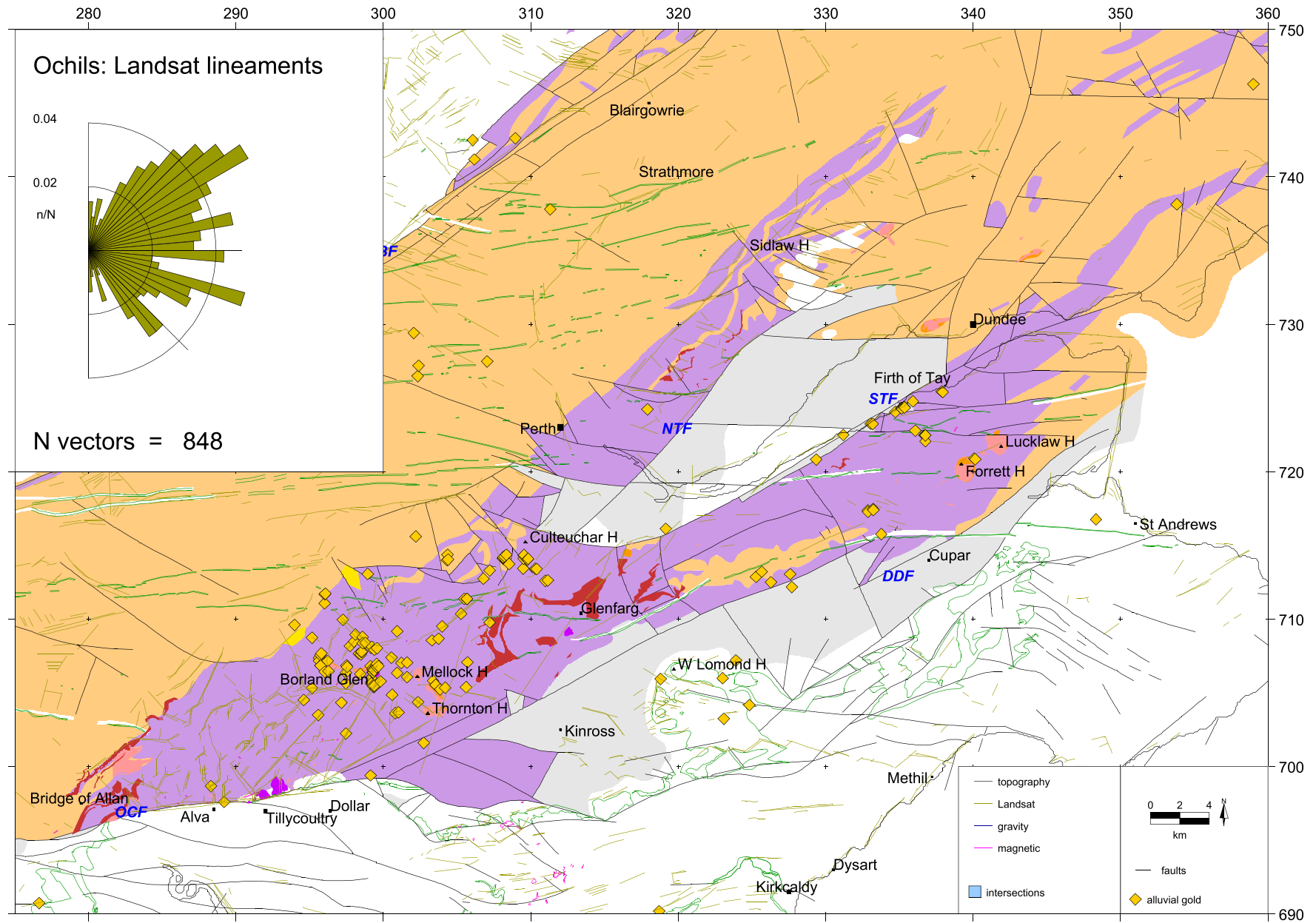


Fig 6.38 Ochils: Landsat TM lineaments

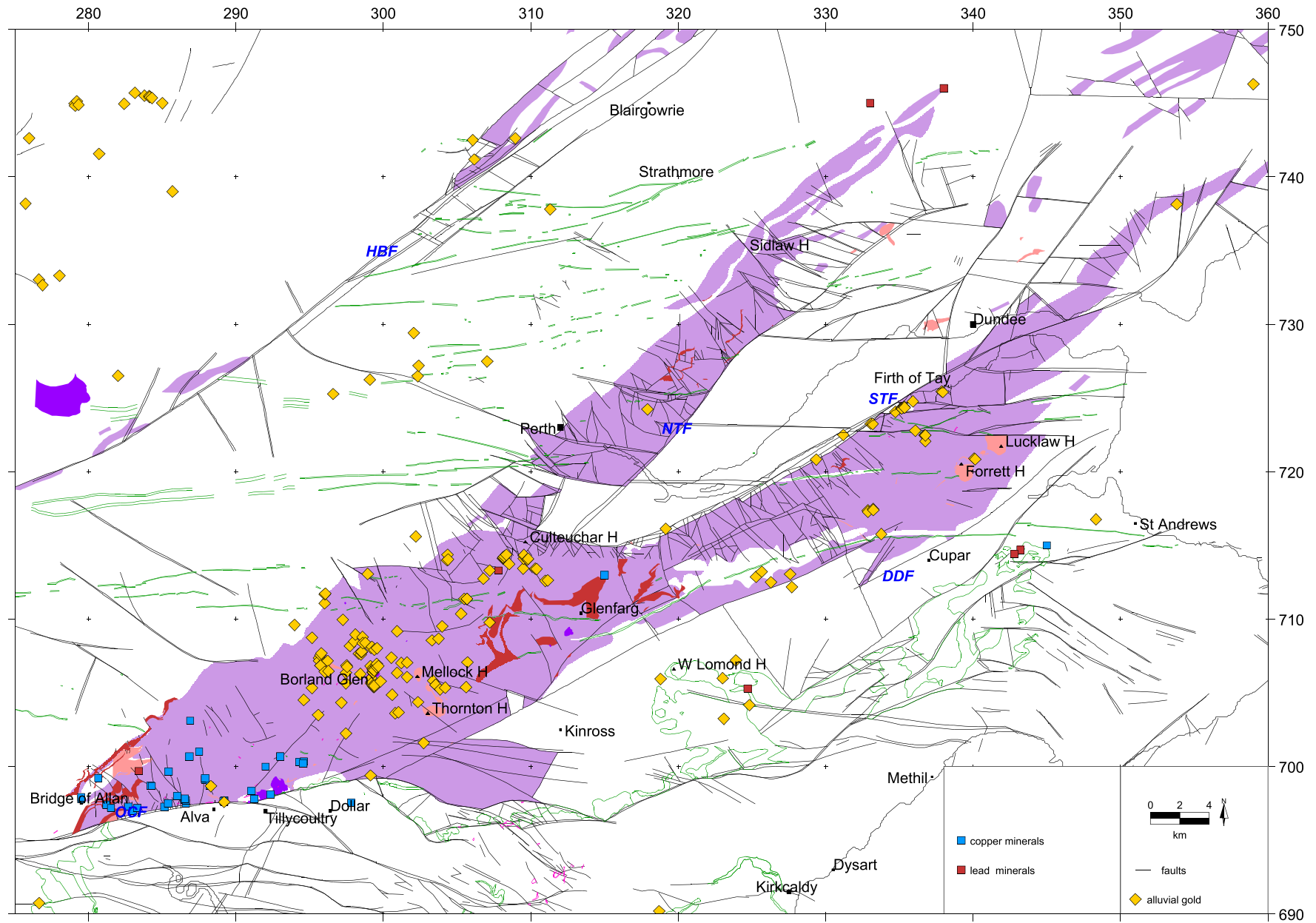


Fig 6.39 Ochils: selected geology layers for prospectivity analysis

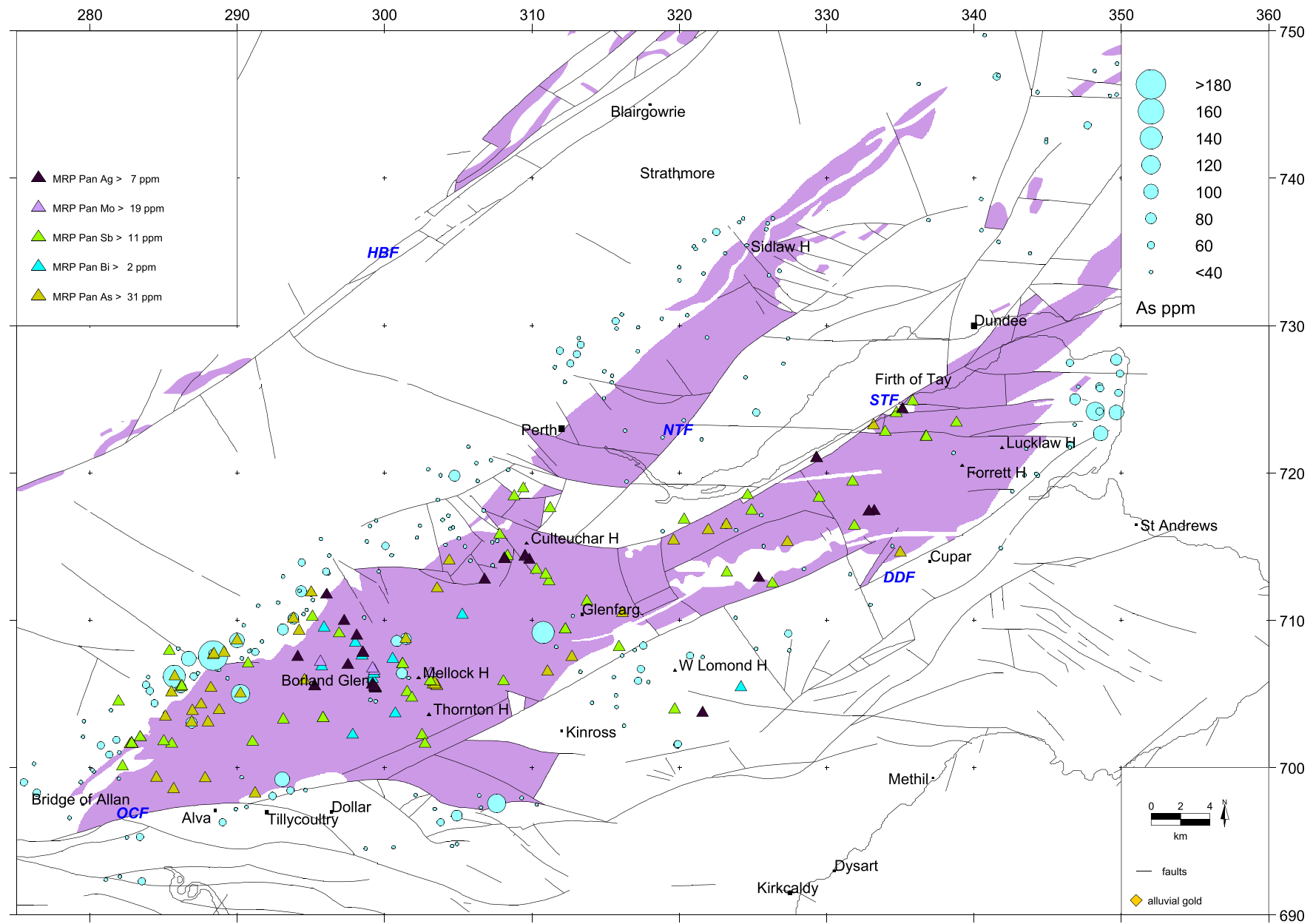


Fig 6.40 Ochils: selected geochemistry layers for prospectivity analysis

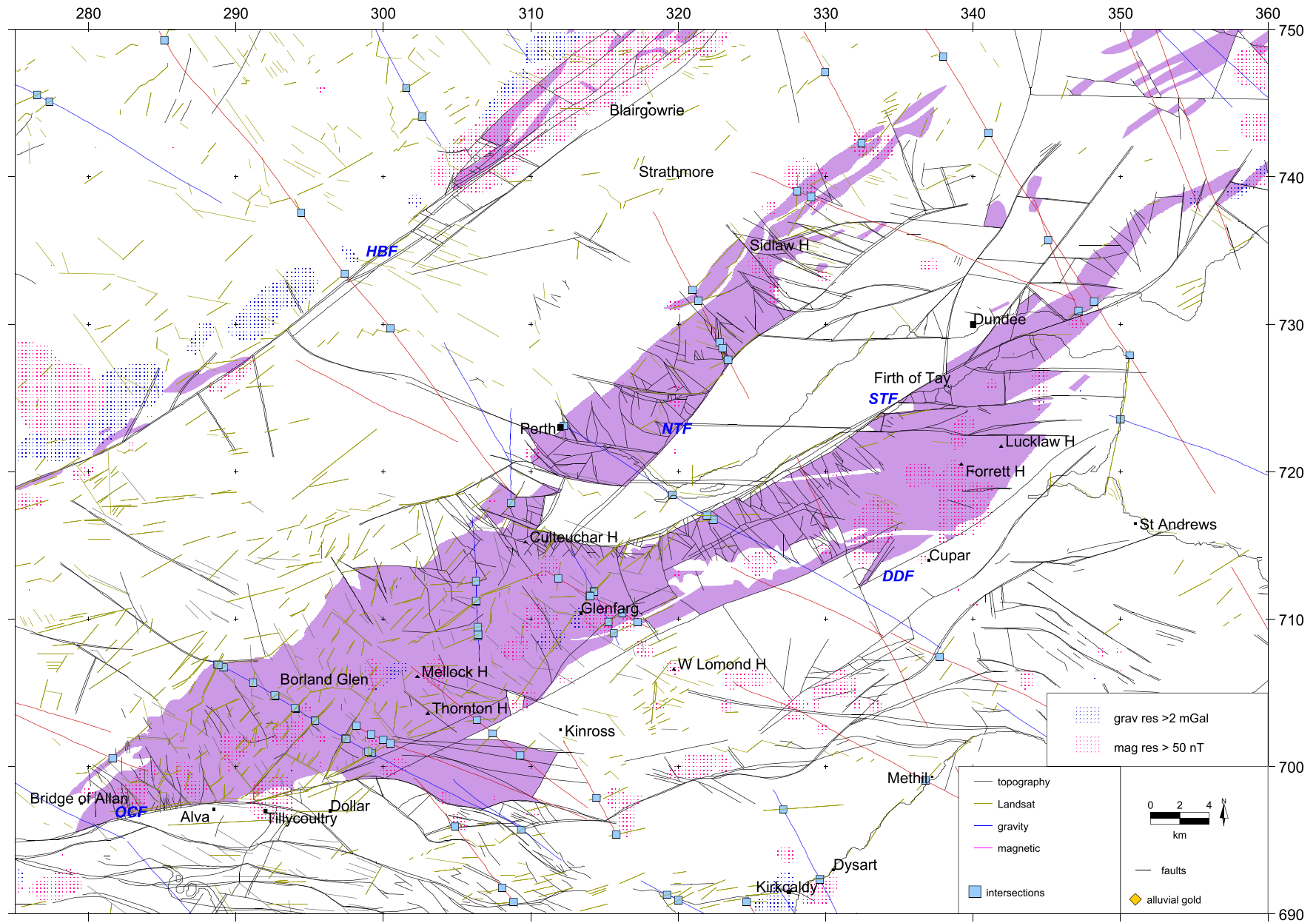


Fig 6.41 Ochils: selected geophysical layers for prospectivity analysis

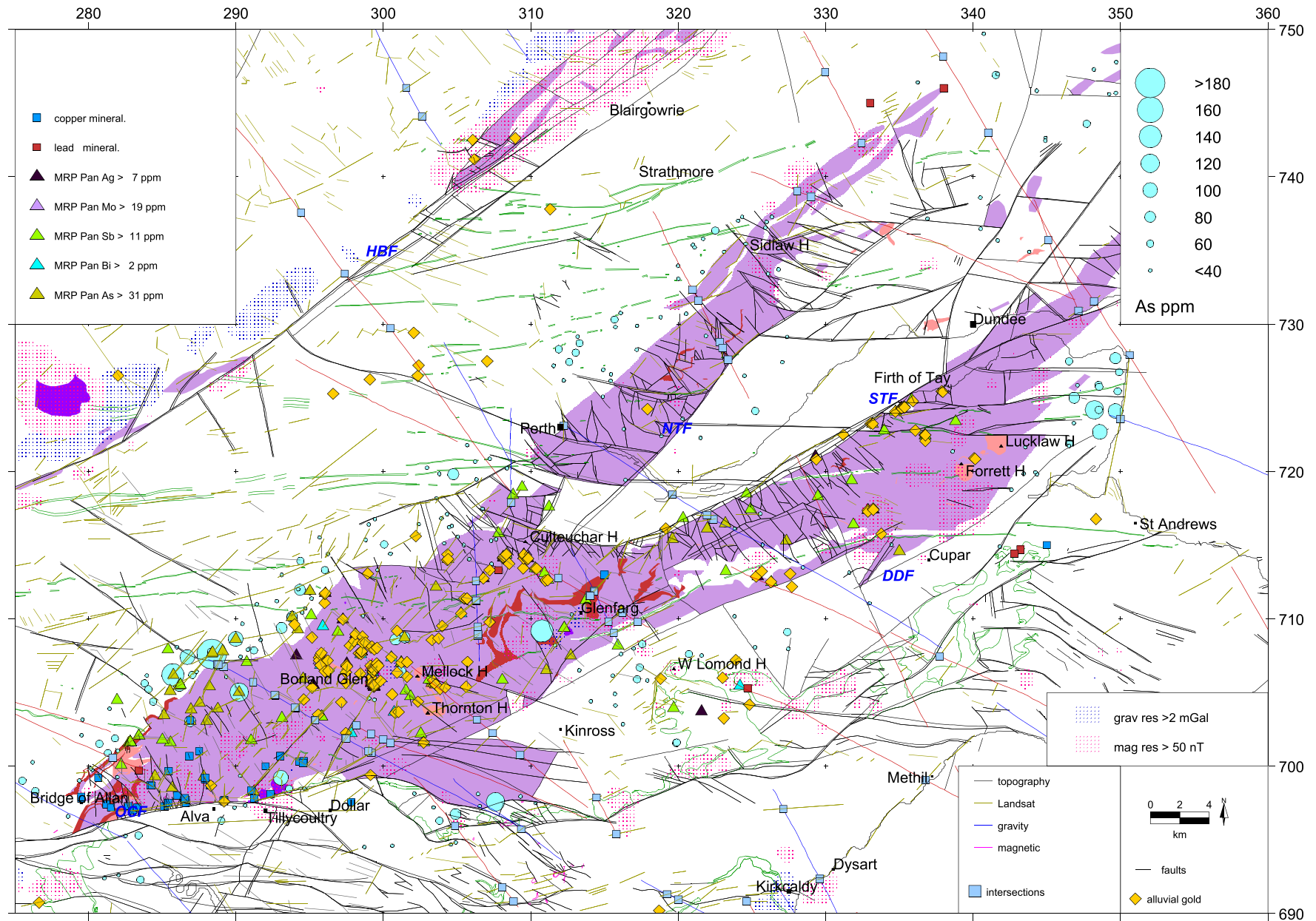


Fig 6.42 Ochils: all selected data layers for prospectivity analysis

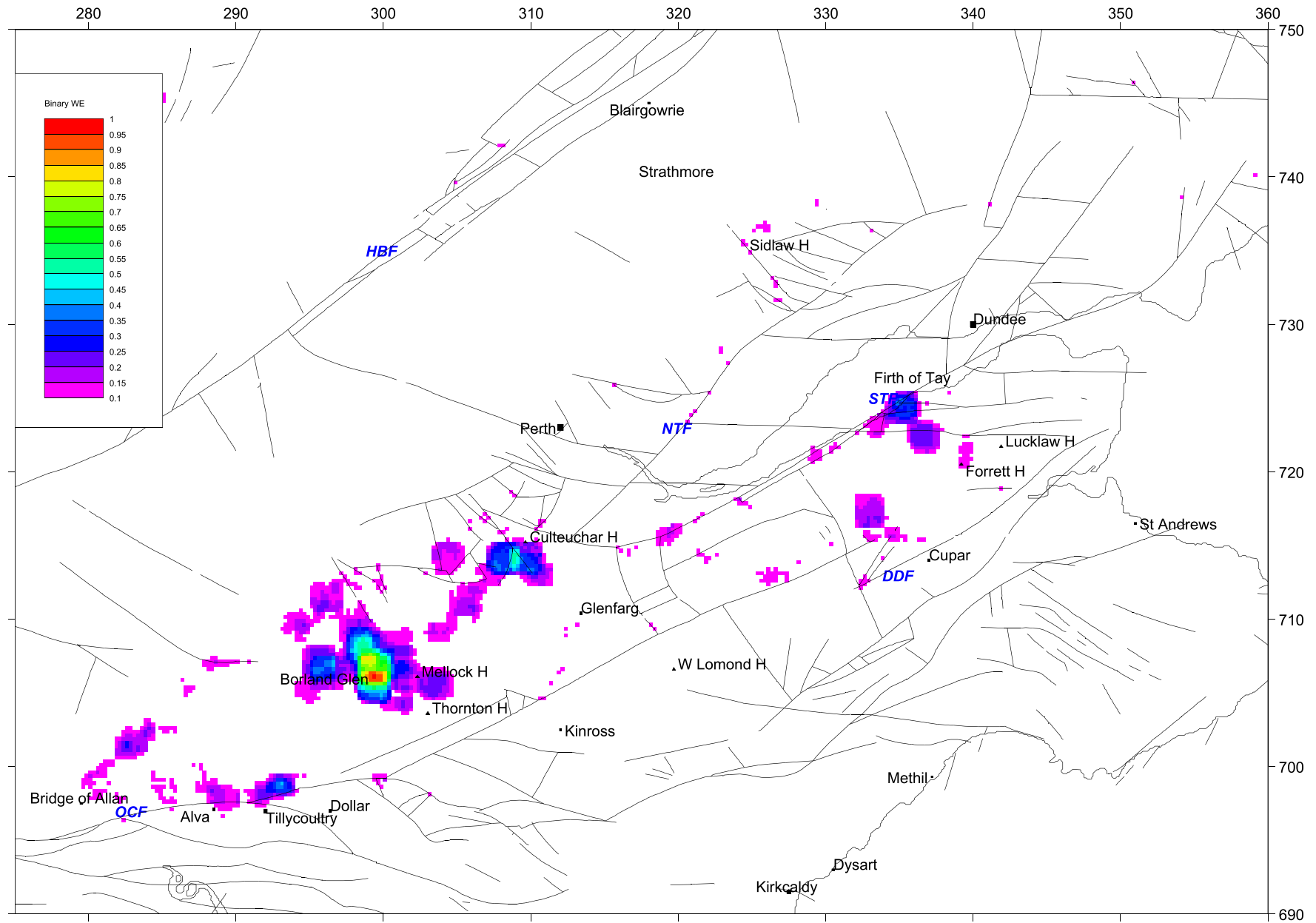


Fig 6.43 Ochils: binary weights of evidence (BWE) prospectivity map for epithermal gold mineralisation

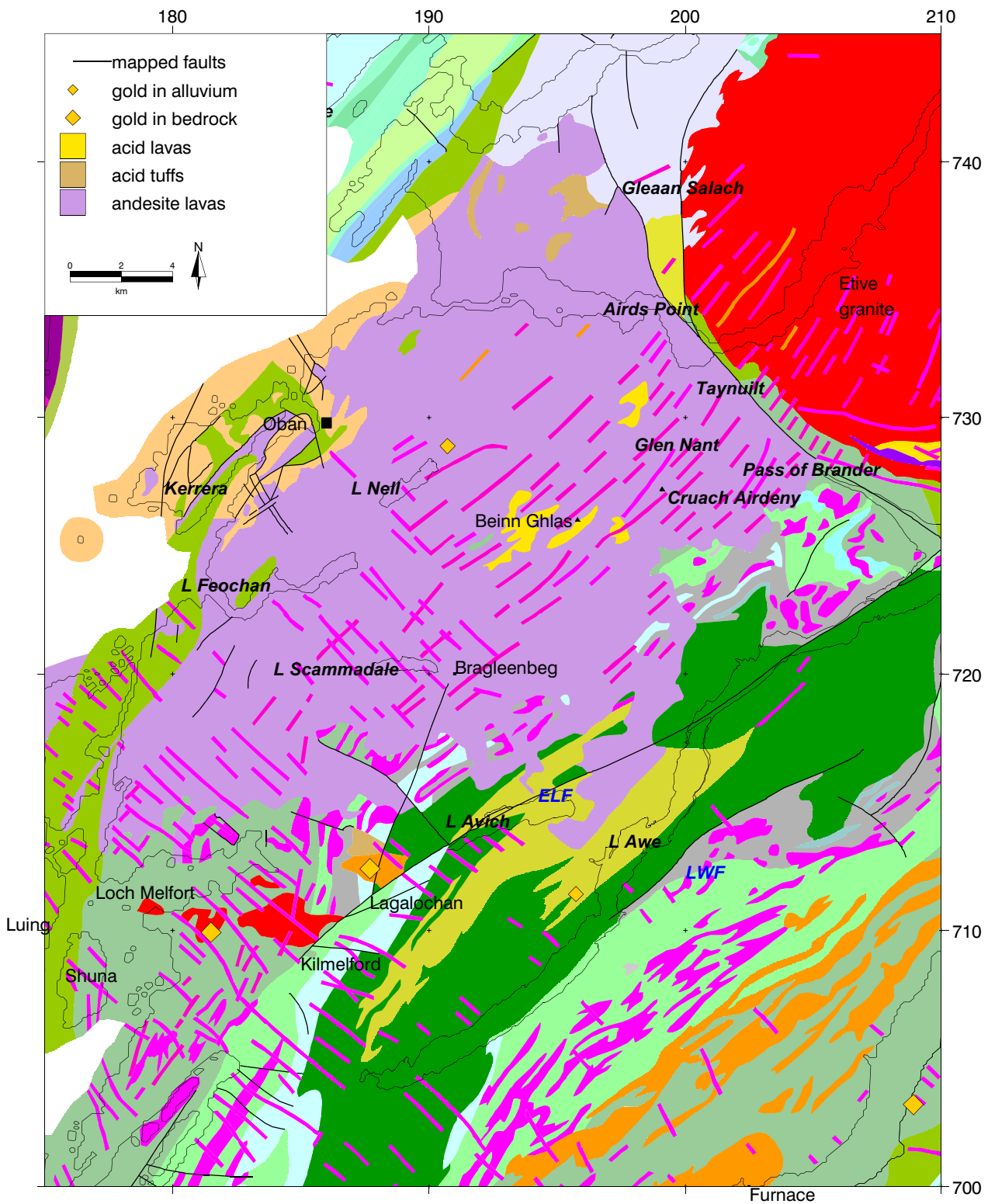


Fig 7.1 Solid geology of the Lorn Plateau region

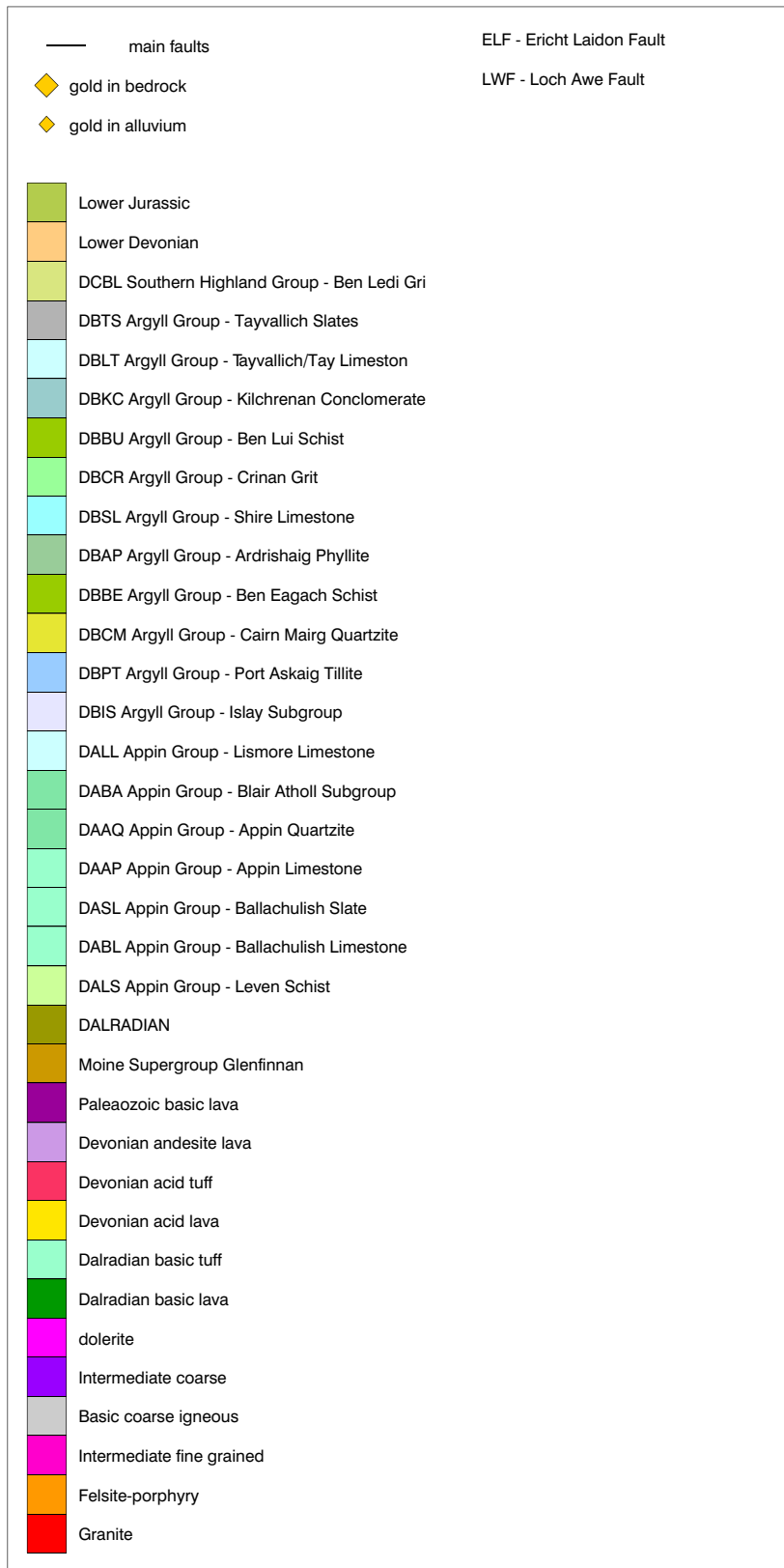


Fig 7.2 Lorn: Legend for the solid geology map Figure 7.1

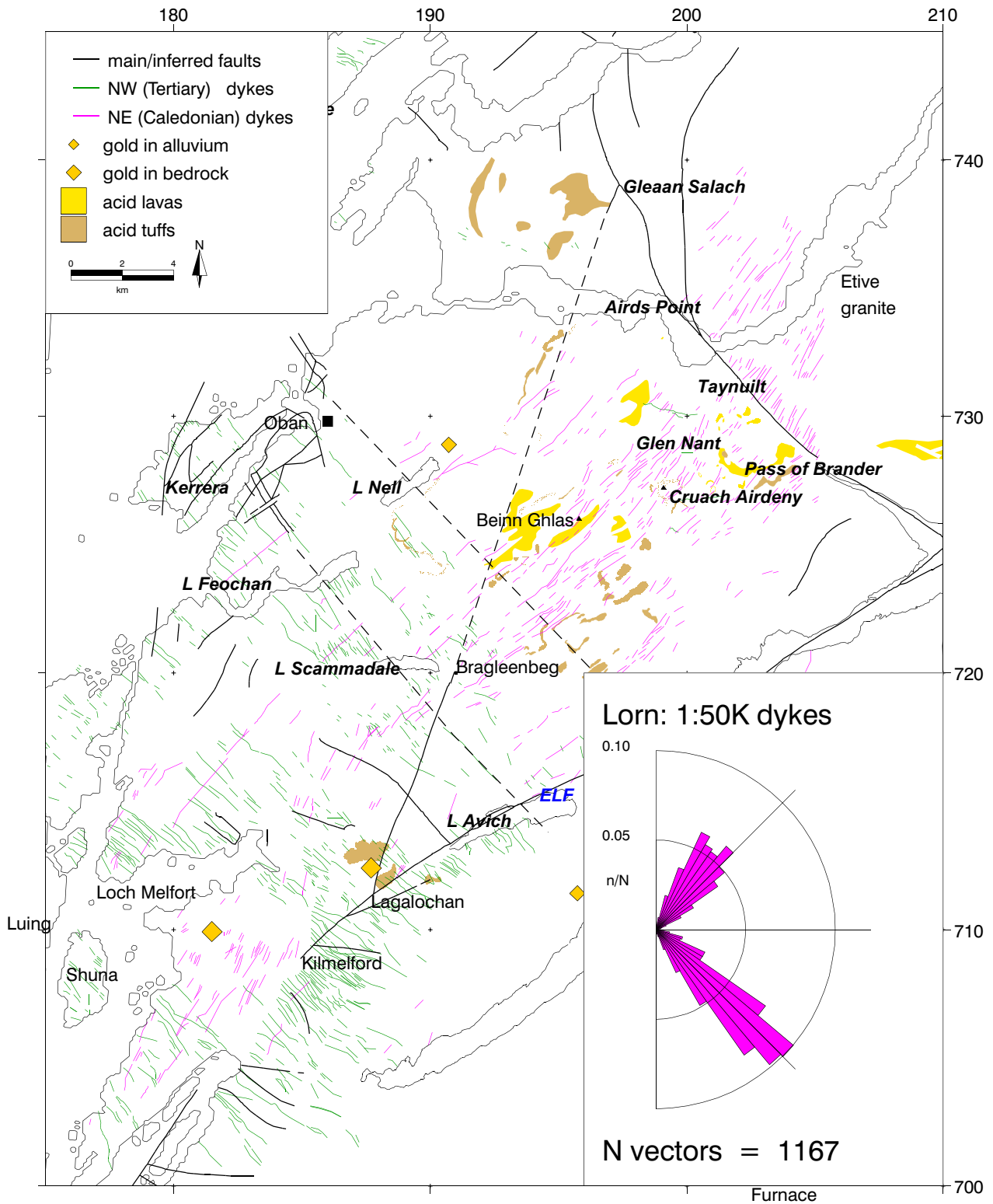


Fig 7.3 Geology of the Lorn Plateau region based on the 1:50000 map series
 Inset shows the orientations of mapped dykes in the region

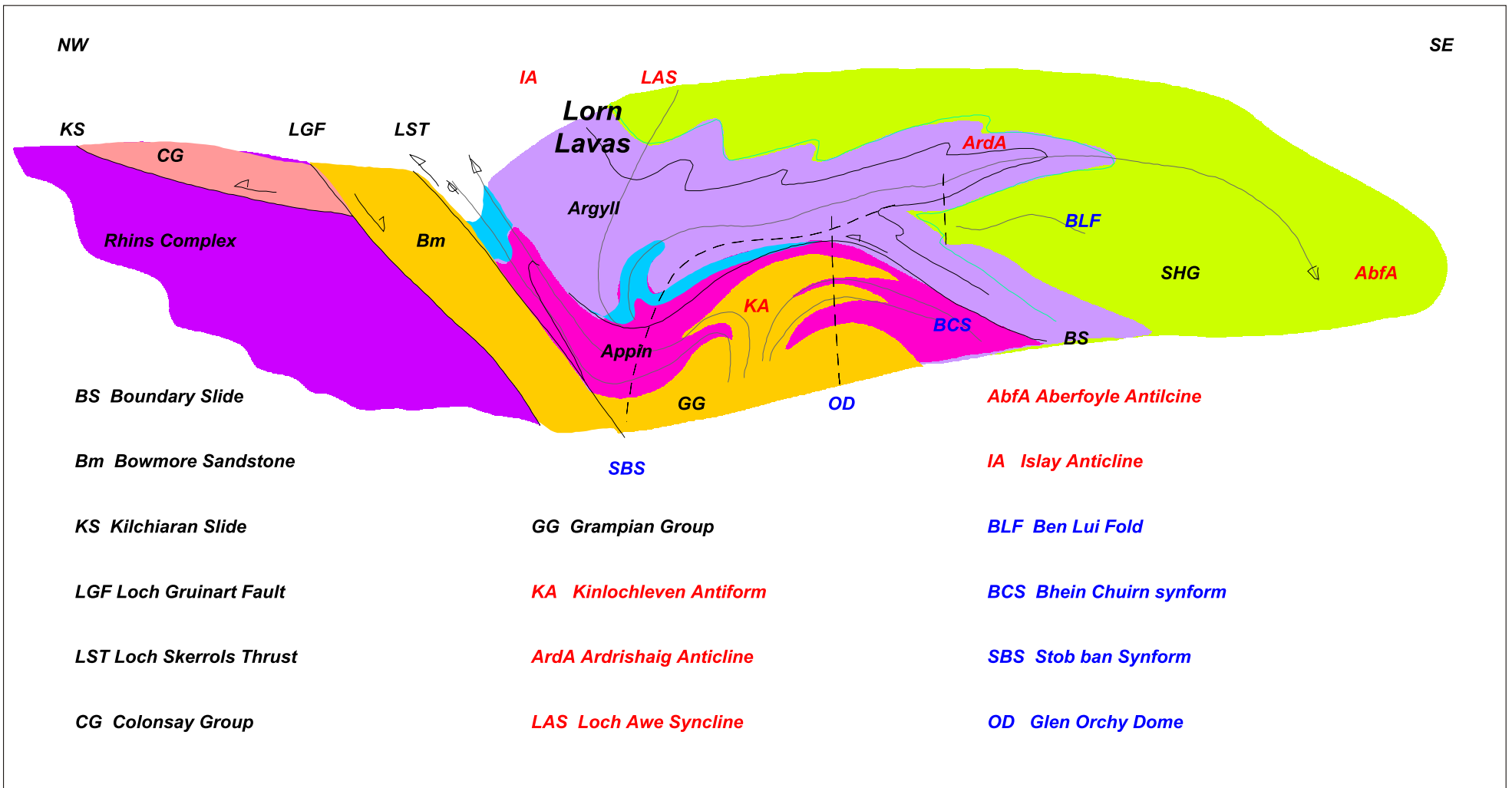


Fig 7.4 Cartoon structural cross-section through the SW Grampian Highlands showing the location of the Lorn Plateau lavas

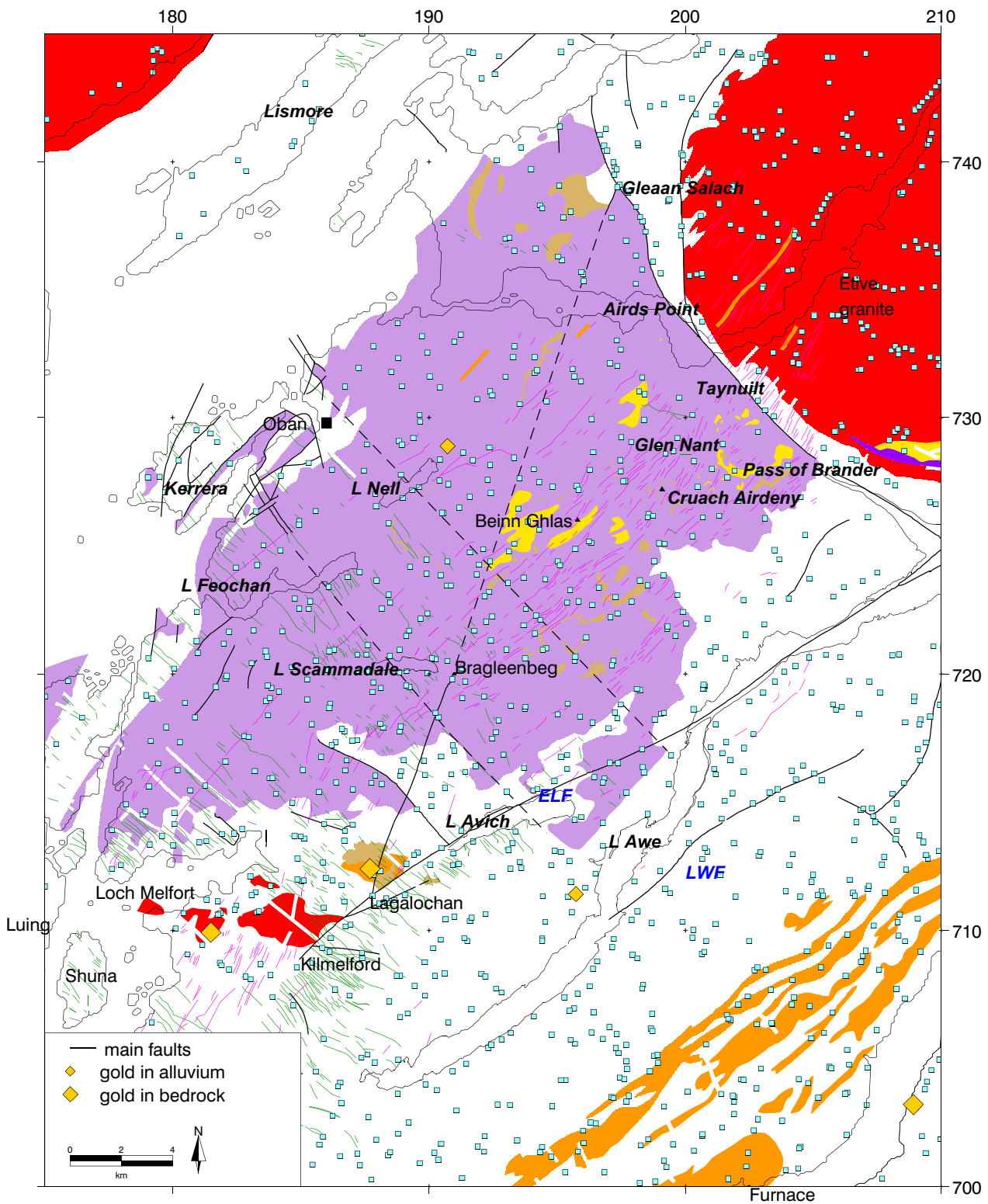


Fig 7.5 Lorn: location of G-BASE stream sediment samples

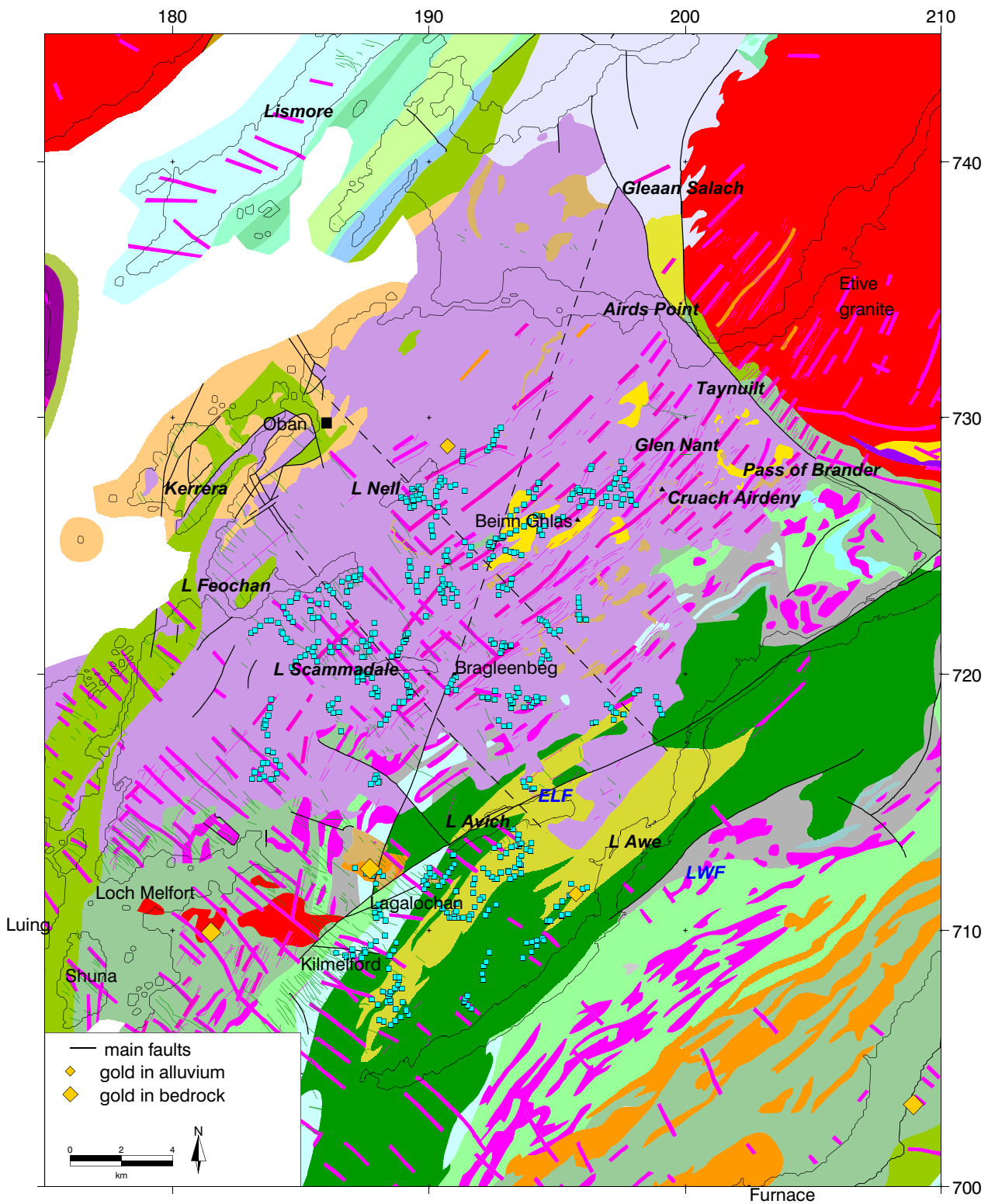


Fig 7.6 Lorn: location of MRP drainage geochemical samples

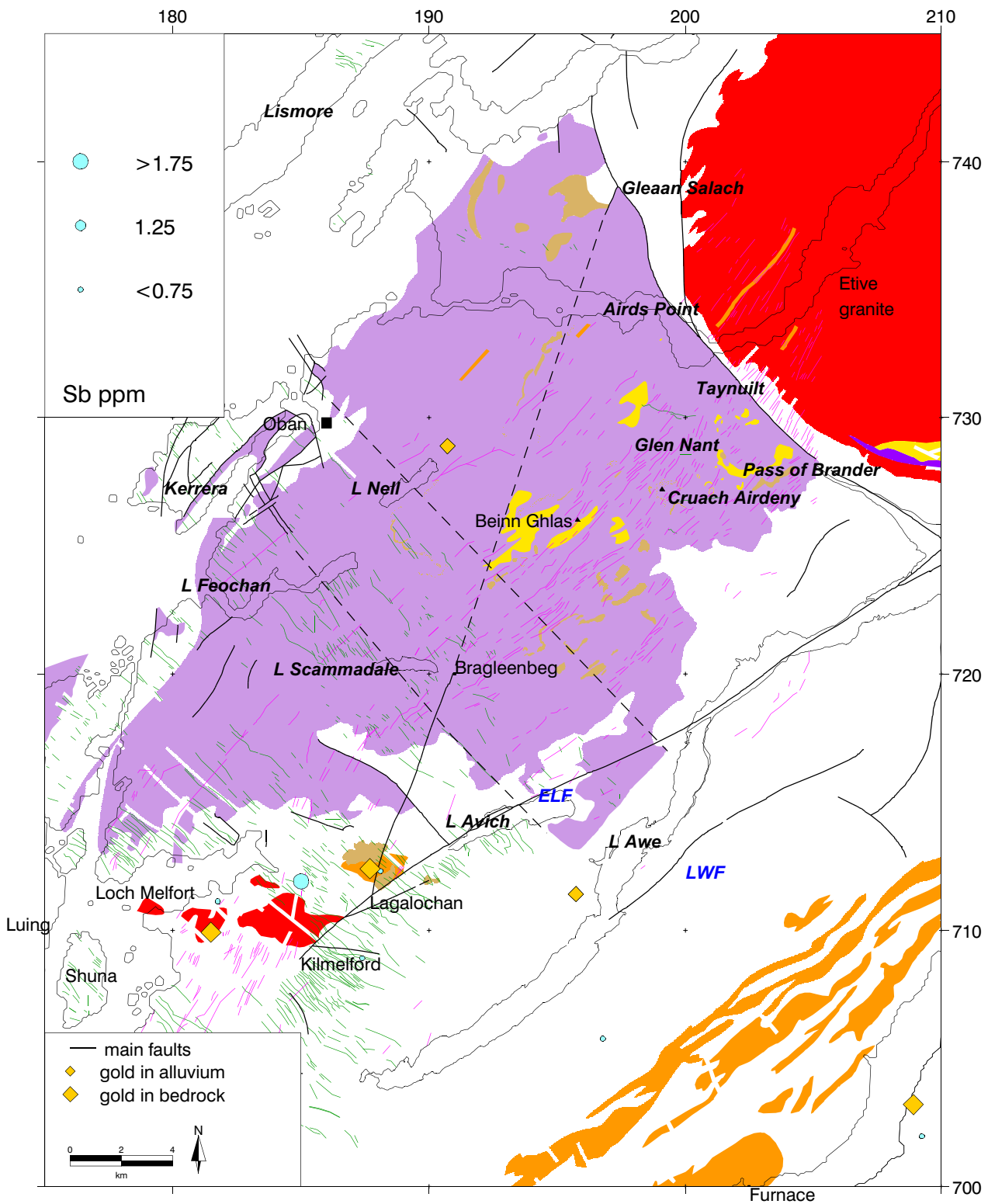


Fig 7.7 Lorn: antimony (Sb) in G-BASE stream sediment data

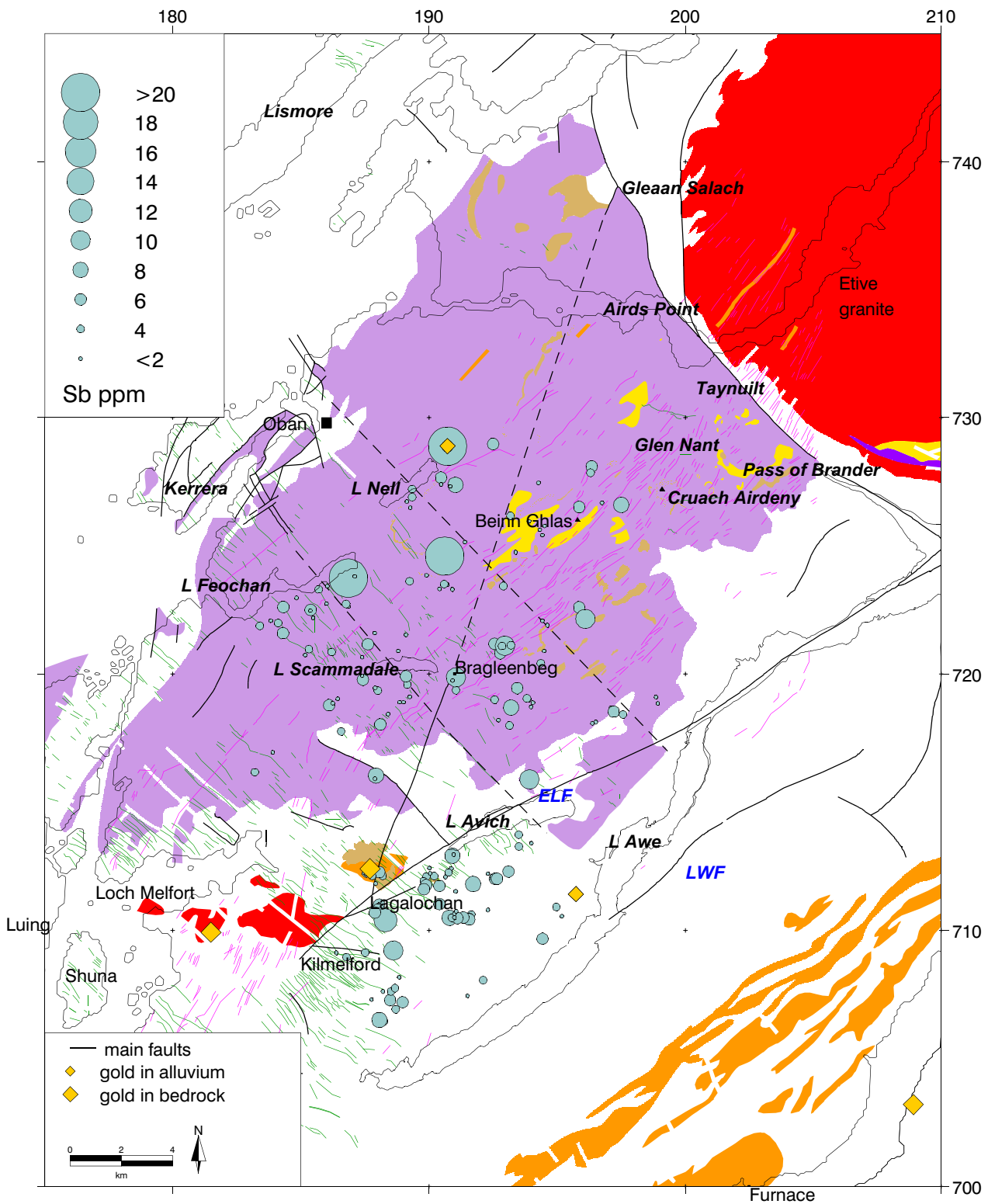


Fig 7.8 Lorn: antimony (Sb) in MRP panned concentrate data

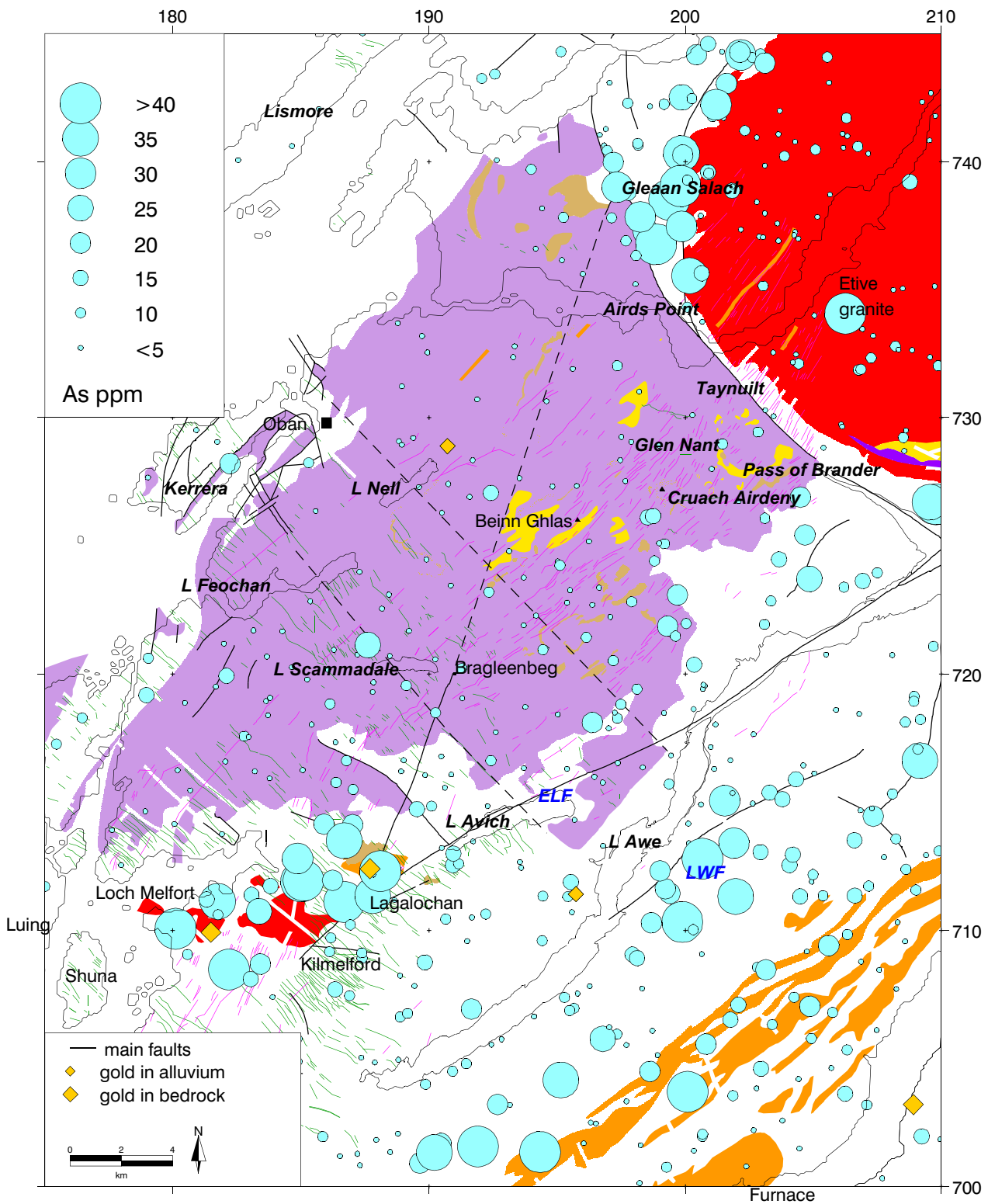


Fig 7.9 Lorn: arsenic (As) in G-BASE stream sediment data

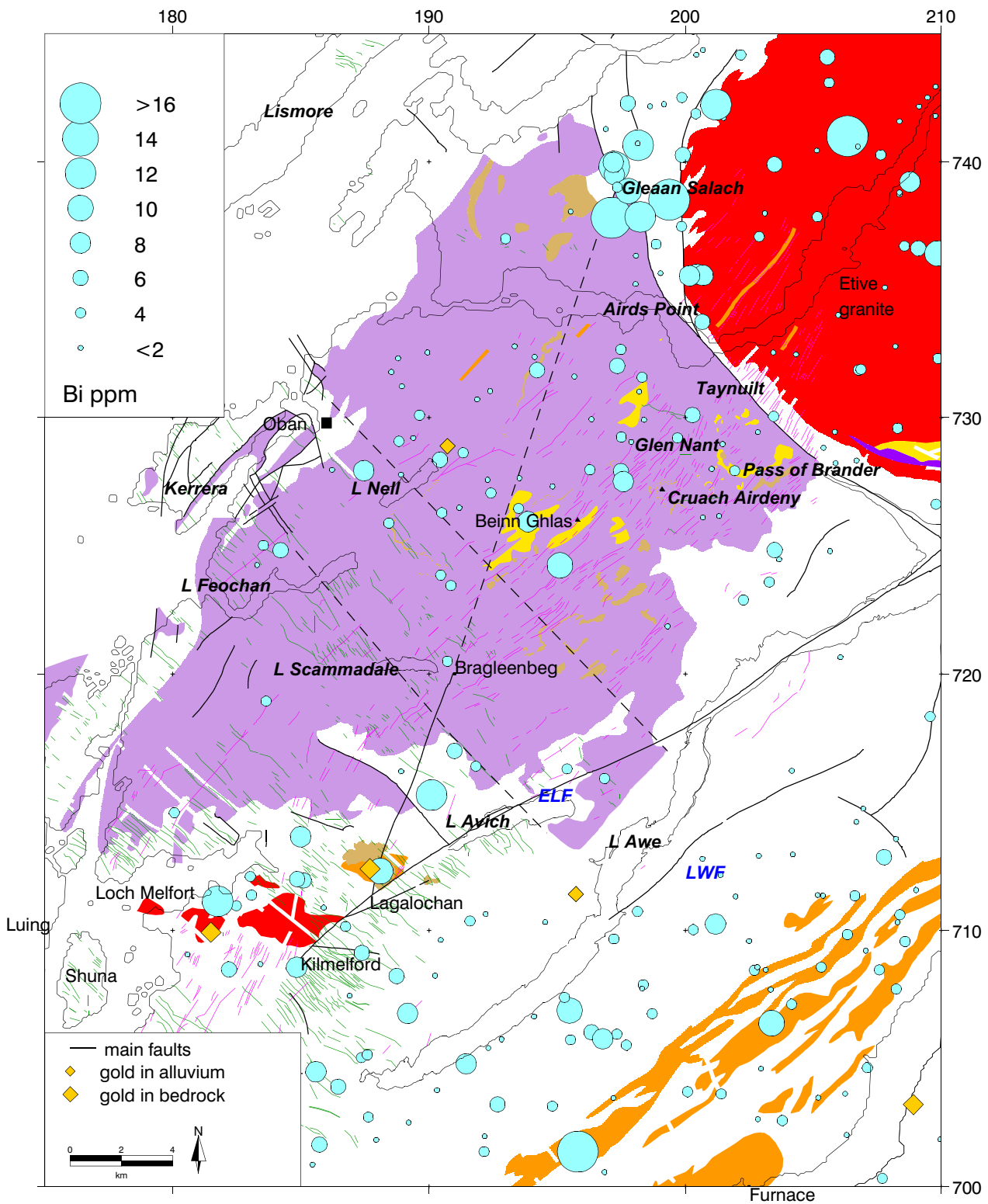


Fig 7.10 Lorn: bismuth (Bi) in G-BASE stream sediment data

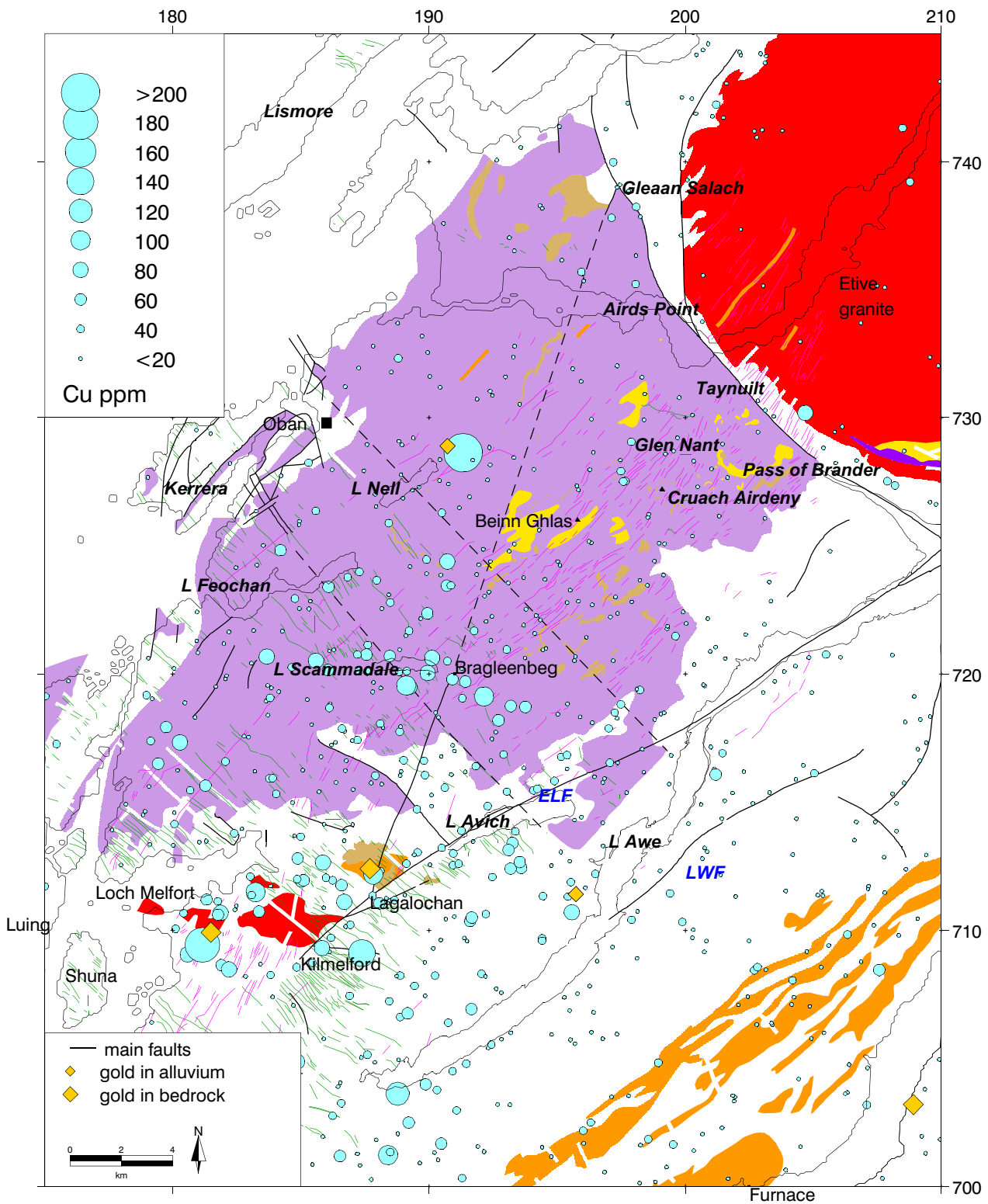


Fig 7.11 Lorn: copper (Cu) in G-BASE stream sediment data

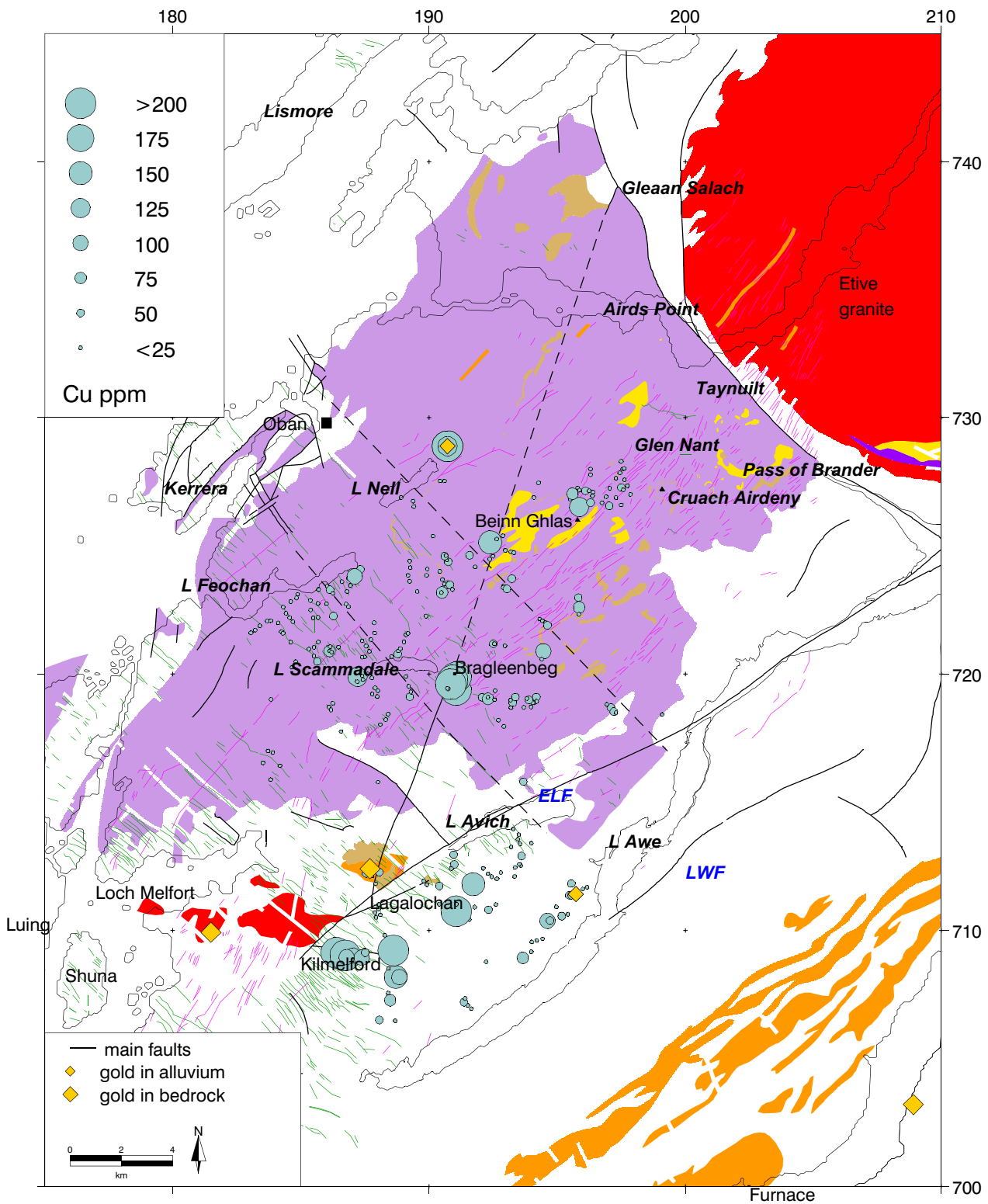


Fig 7.12 Lorn: copper (Cu) in MRP panned concentrate data

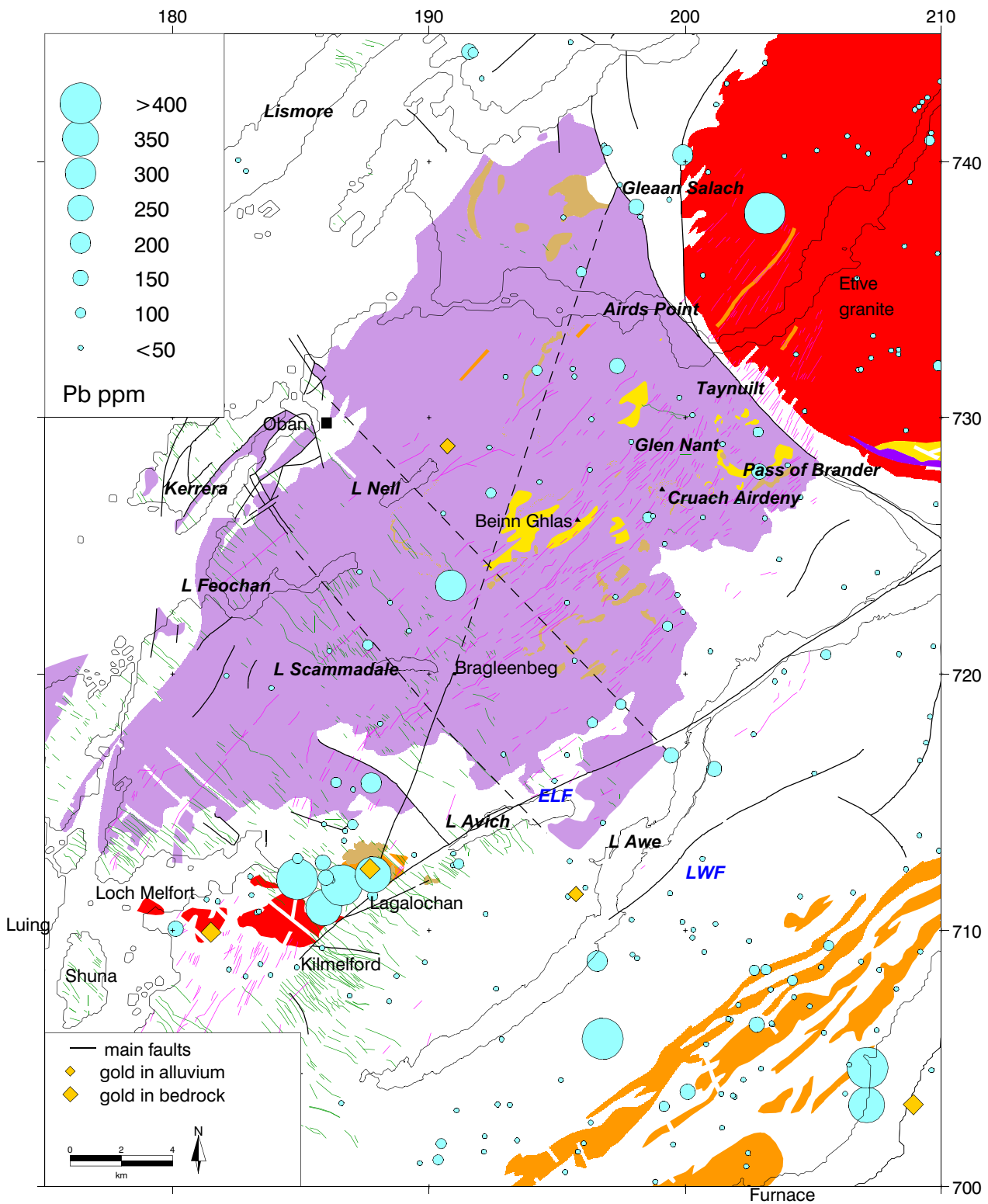


Fig 7.13 Lorn: lead (Pb) in G-BASE stream sediment data

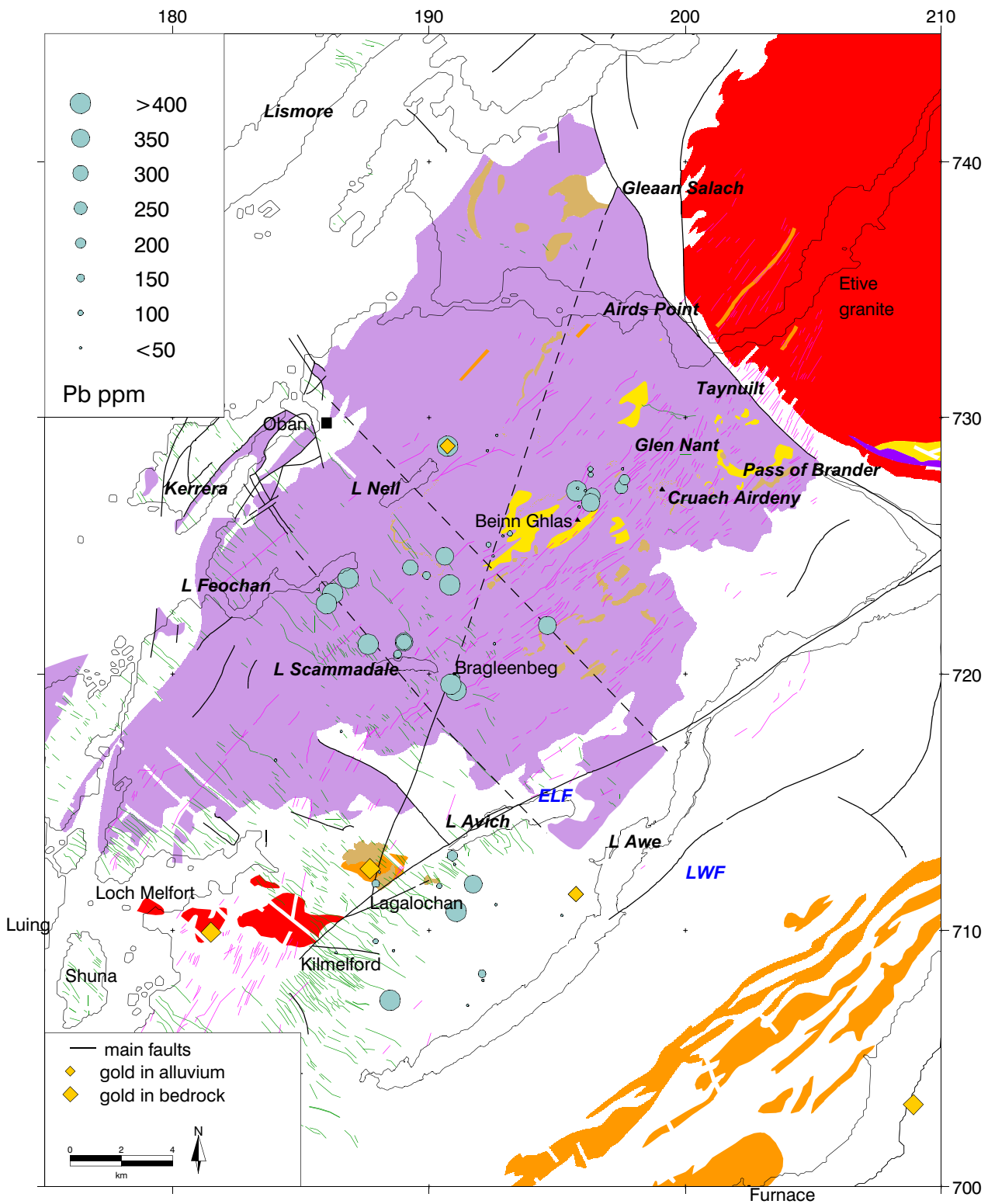


Fig 7.14 Lorn: lead (Pb) in MRP panned concentrate data

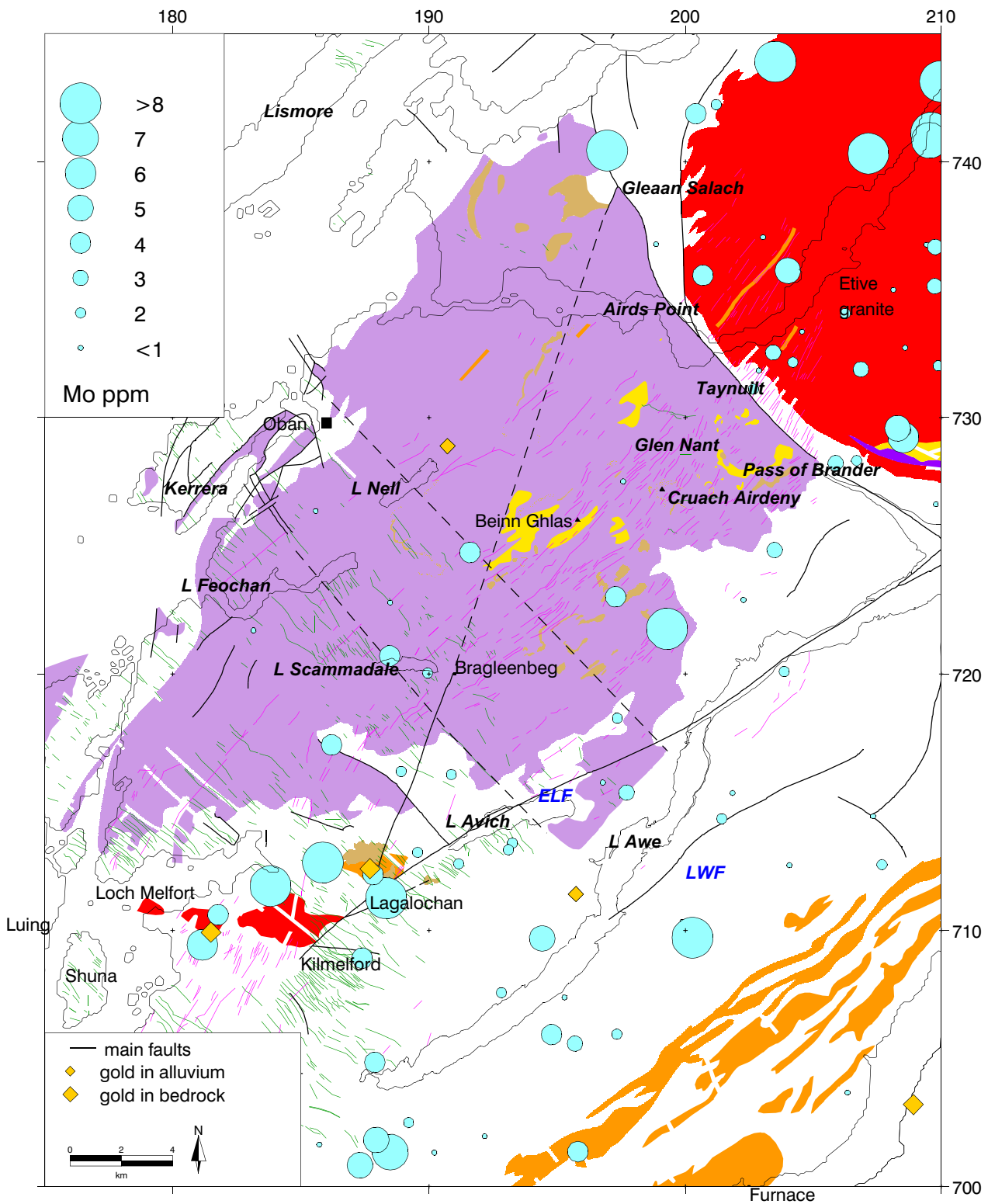


Fig 7.15 Lorn: molybdenum (Mo) in G-BASE stream sediment data

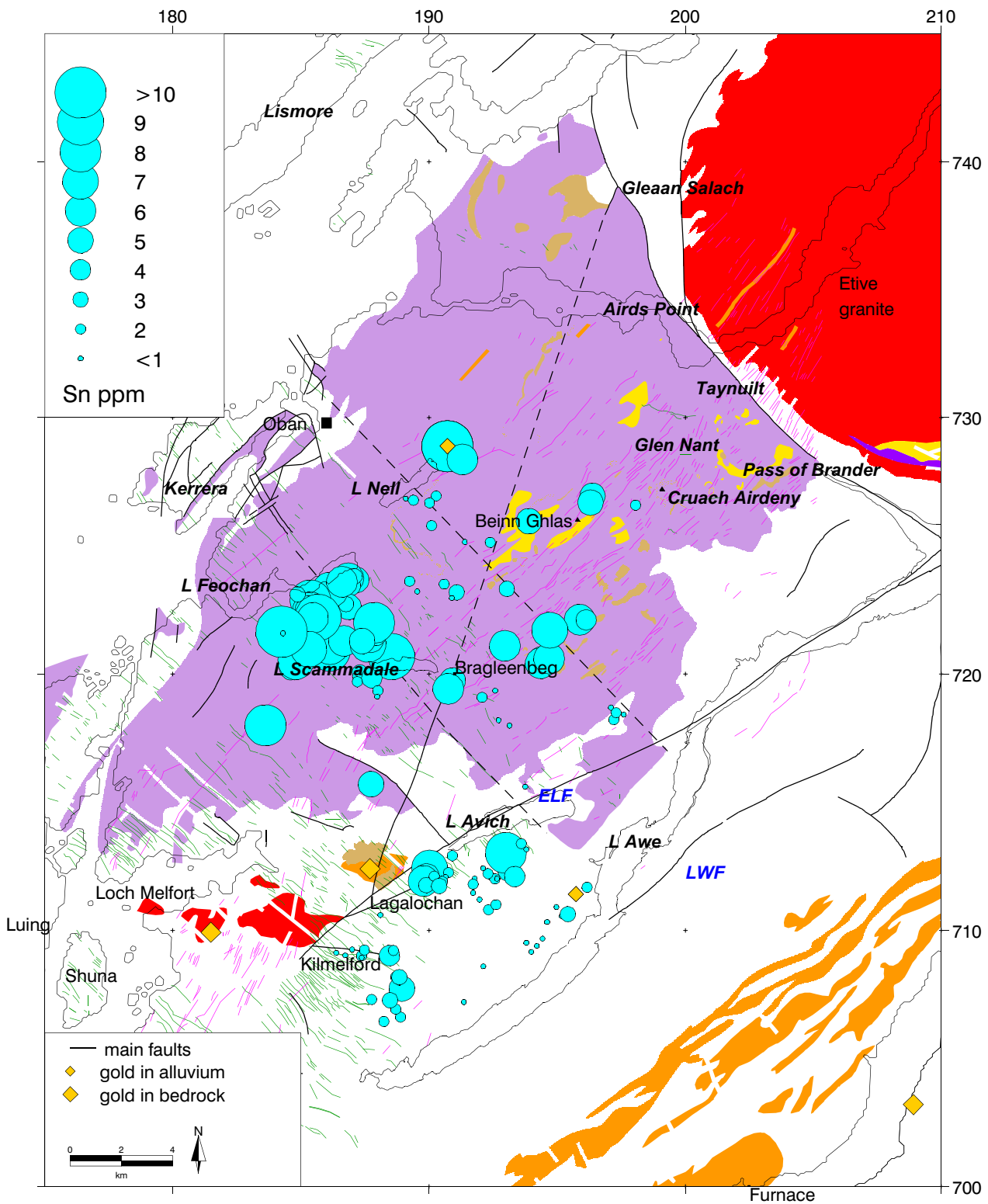


Fig 7.16 Lorn: tin (Sn) in MRP stream sediment data

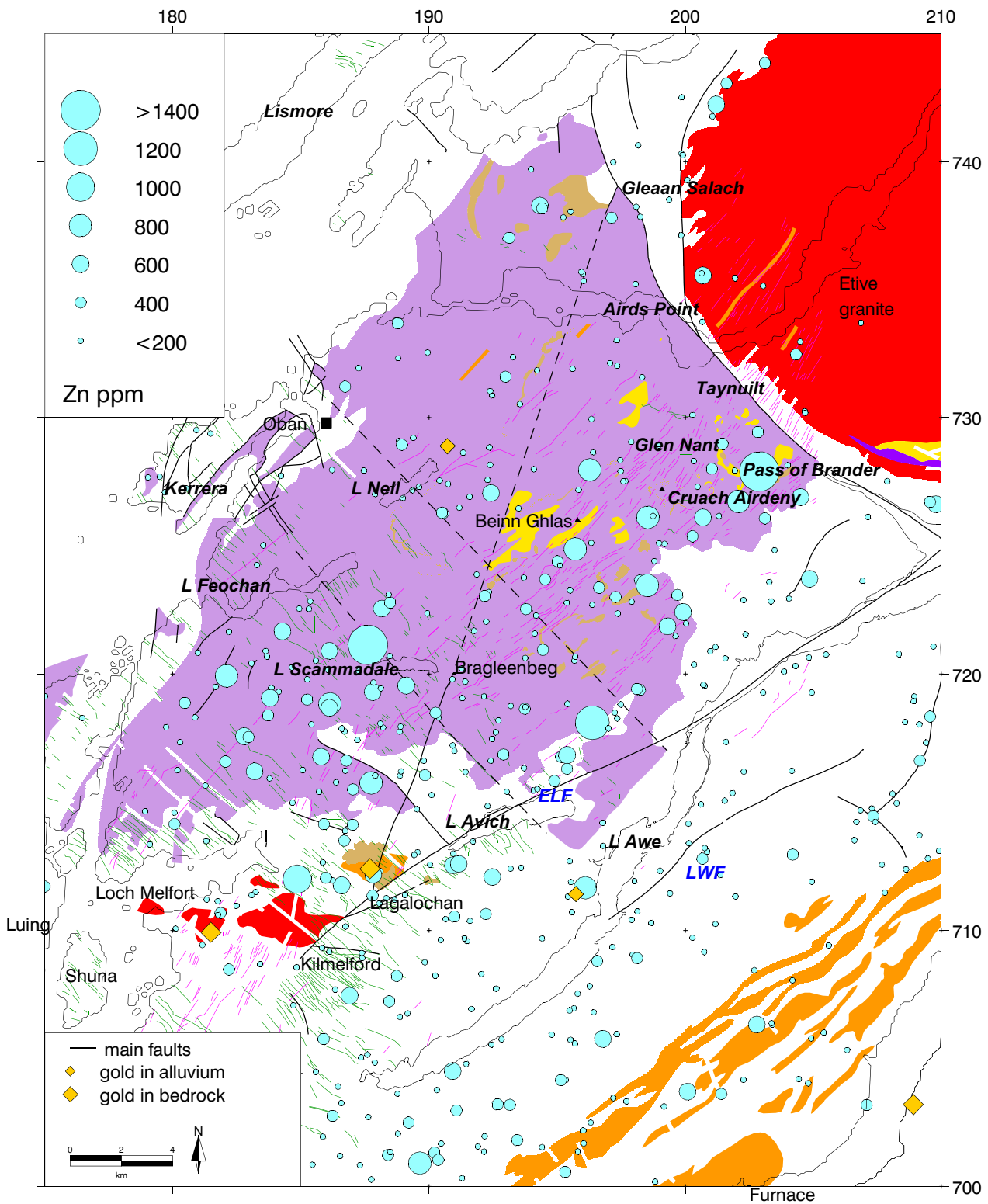


Fig 7.17 Lorn: zinc (Zn) in G-BASE stream sediment data

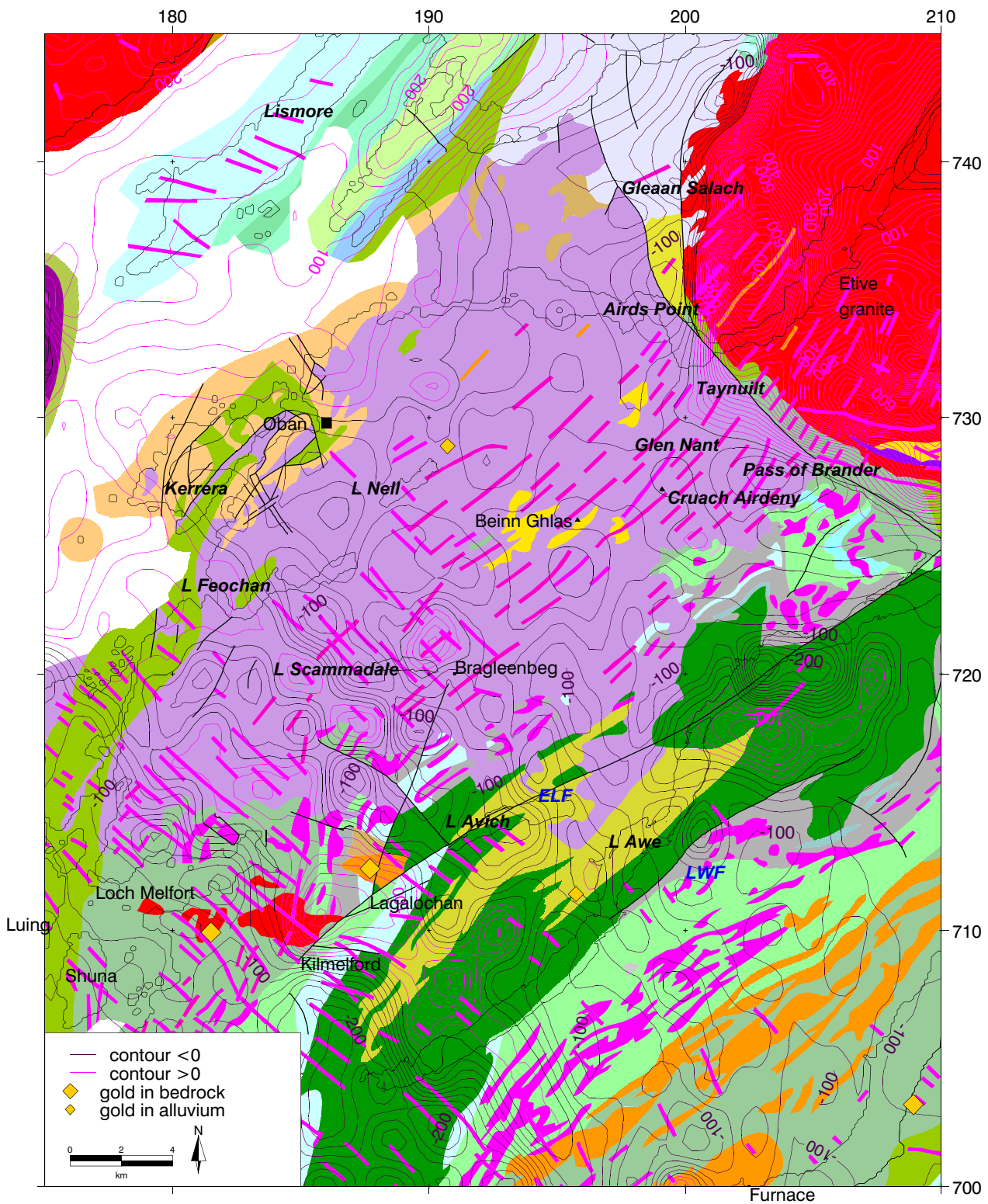


Fig 7.18 Lorn: total magnetic field anomaly (contour interval 25 nT)

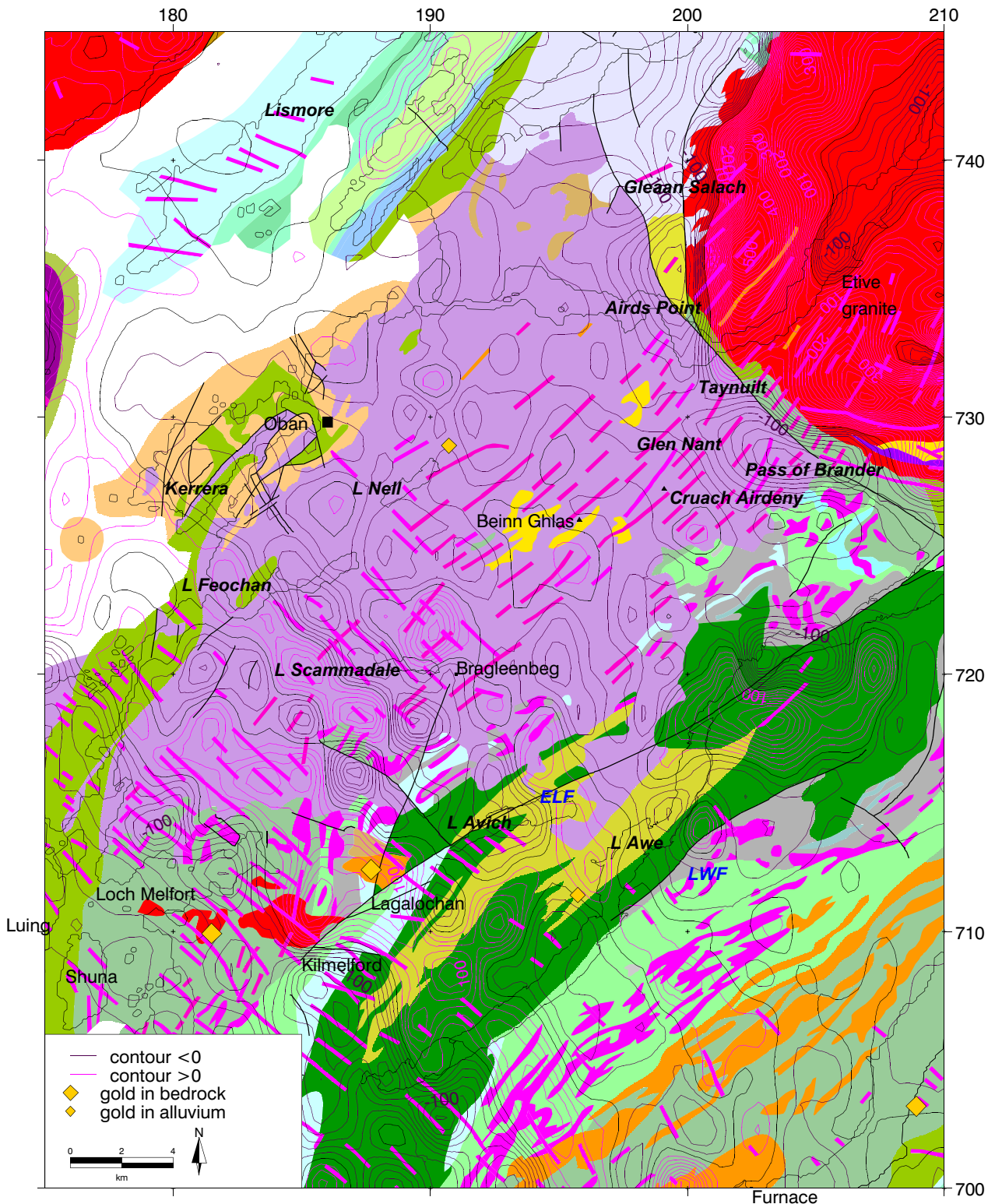


Fig 7.19 Lorn: residual magnetic field anomaly (contour interval 25 nT) Regional from observed field continued to 2km and reduced to the pole

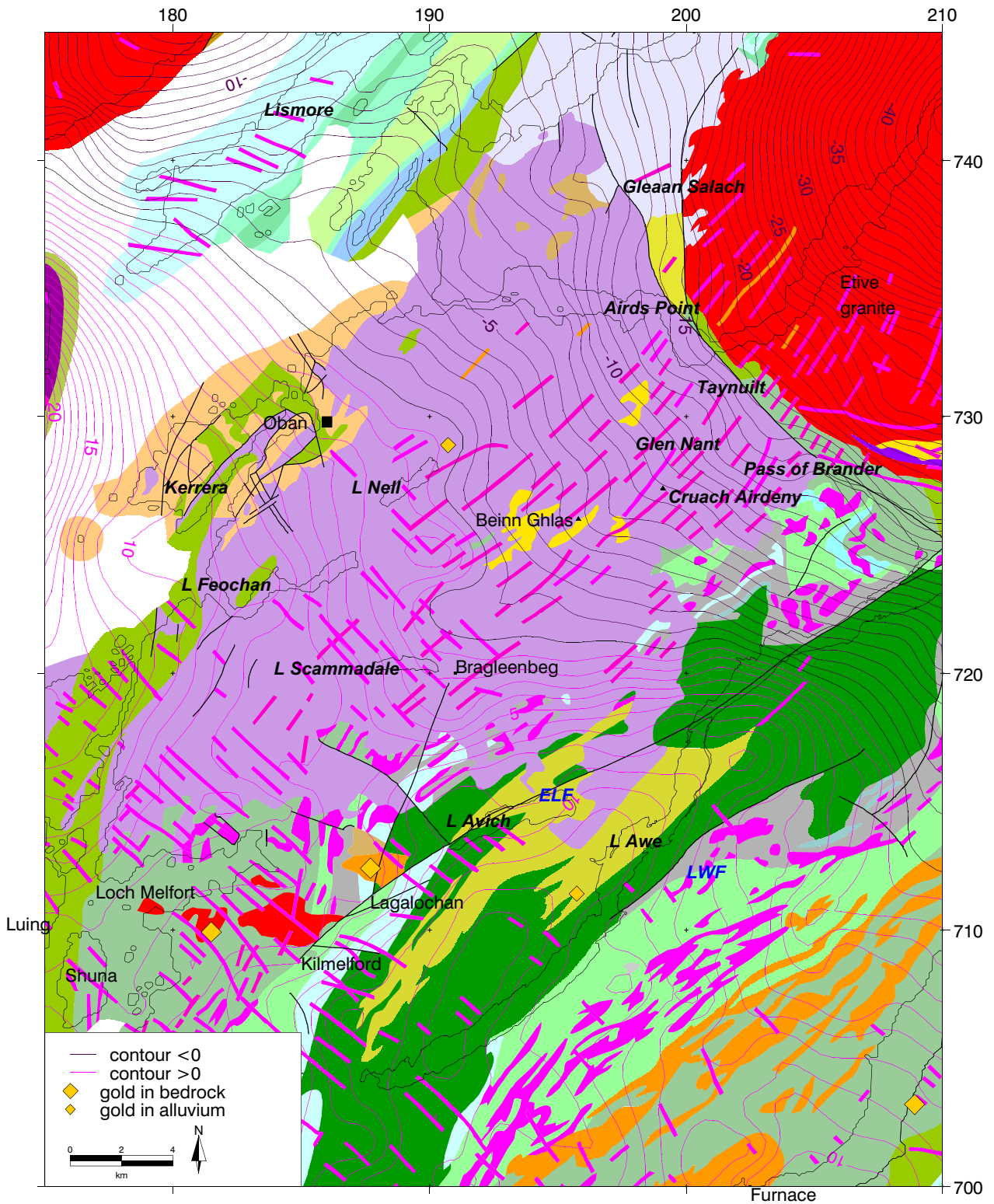


Fig 7.20 Lorn: Bouguer gravity anomaly (contour interval 1 mGal)

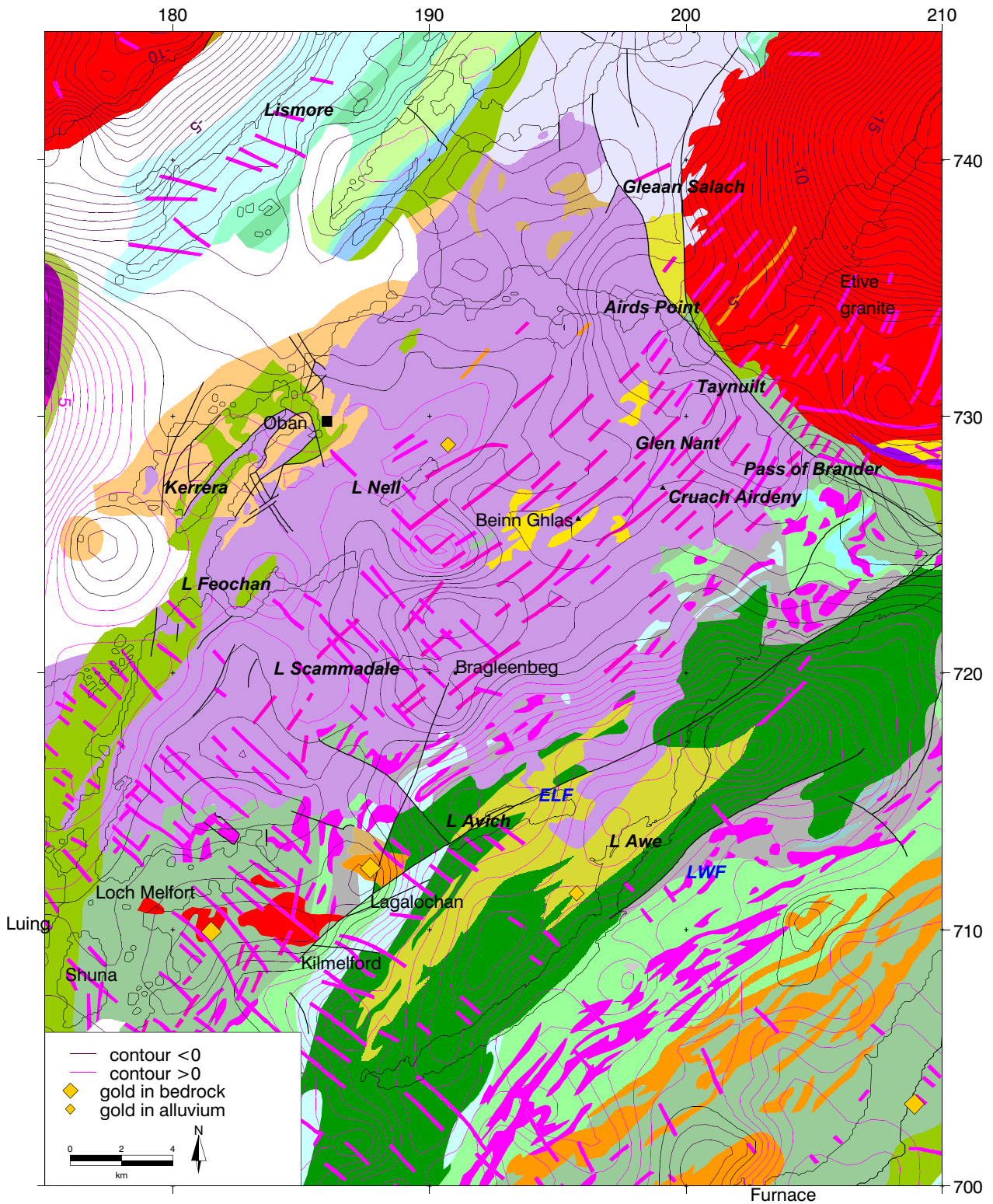


Fig 7.21 Lorn: residual gravity anomaly (contour interval 0.5 mGal)
Regional from observed field continued to 5km

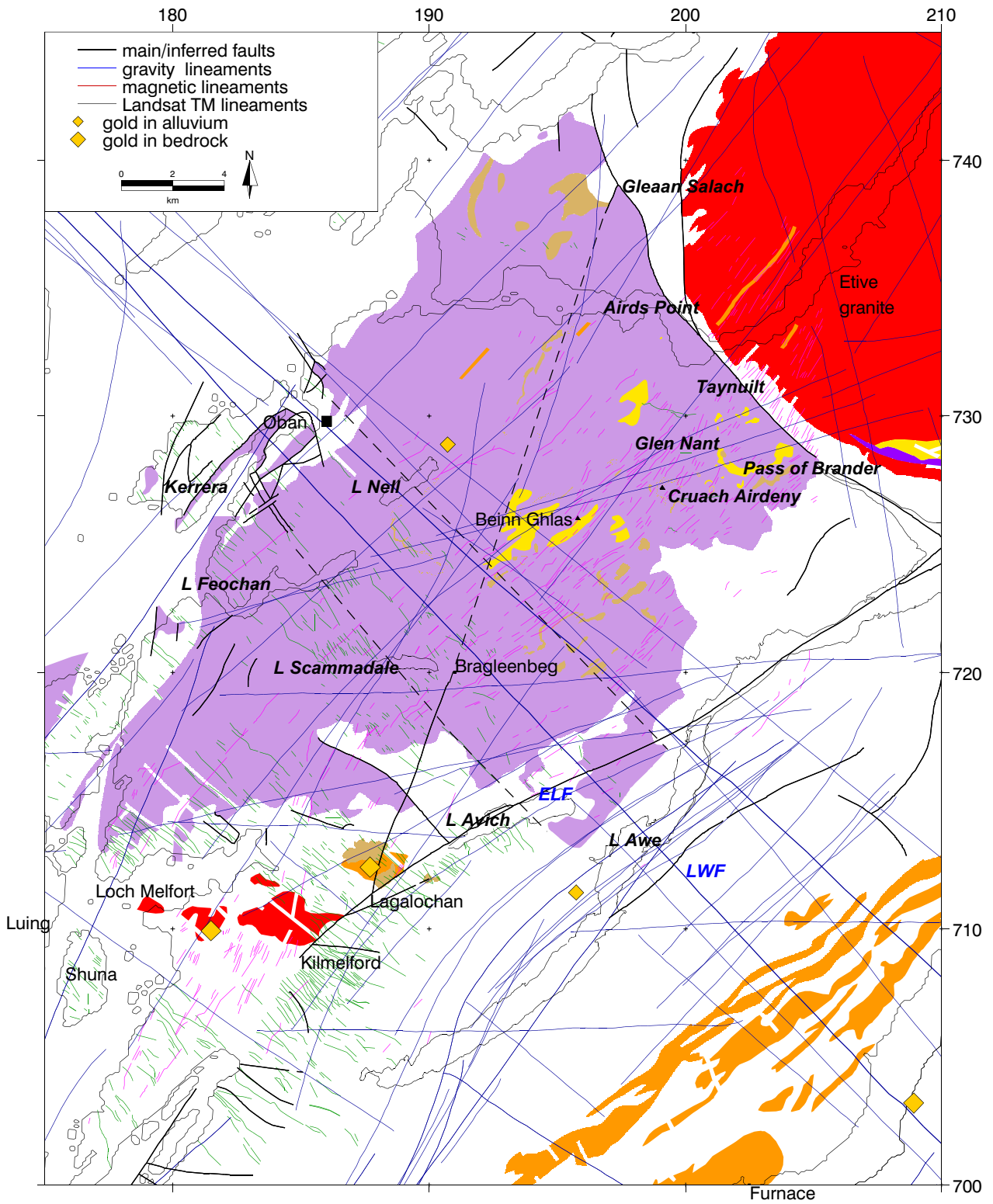


Fig 7.22 Lorn: gravity lineaments

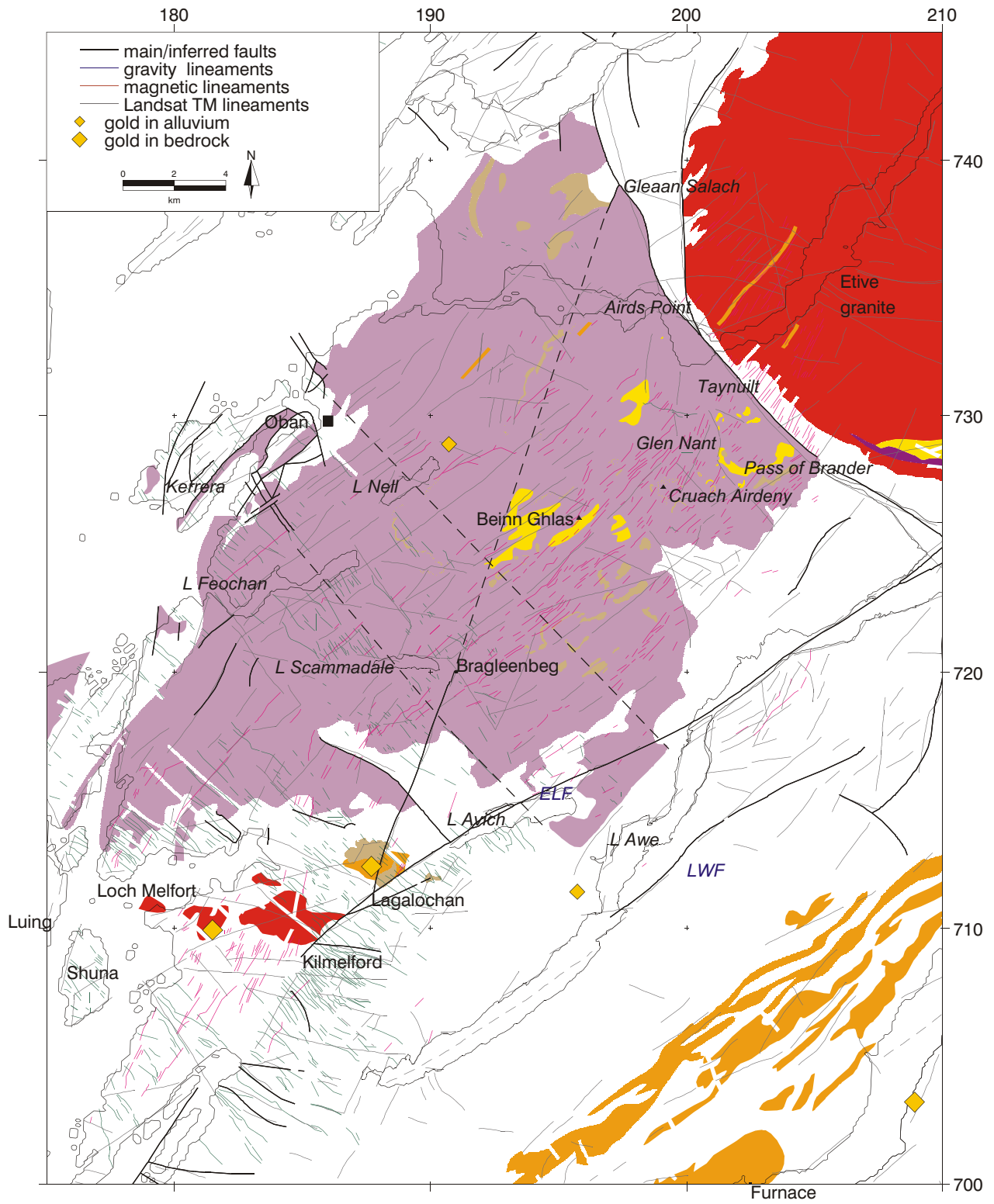


Fig 7.24 Lorn: Landsat TM lineaments

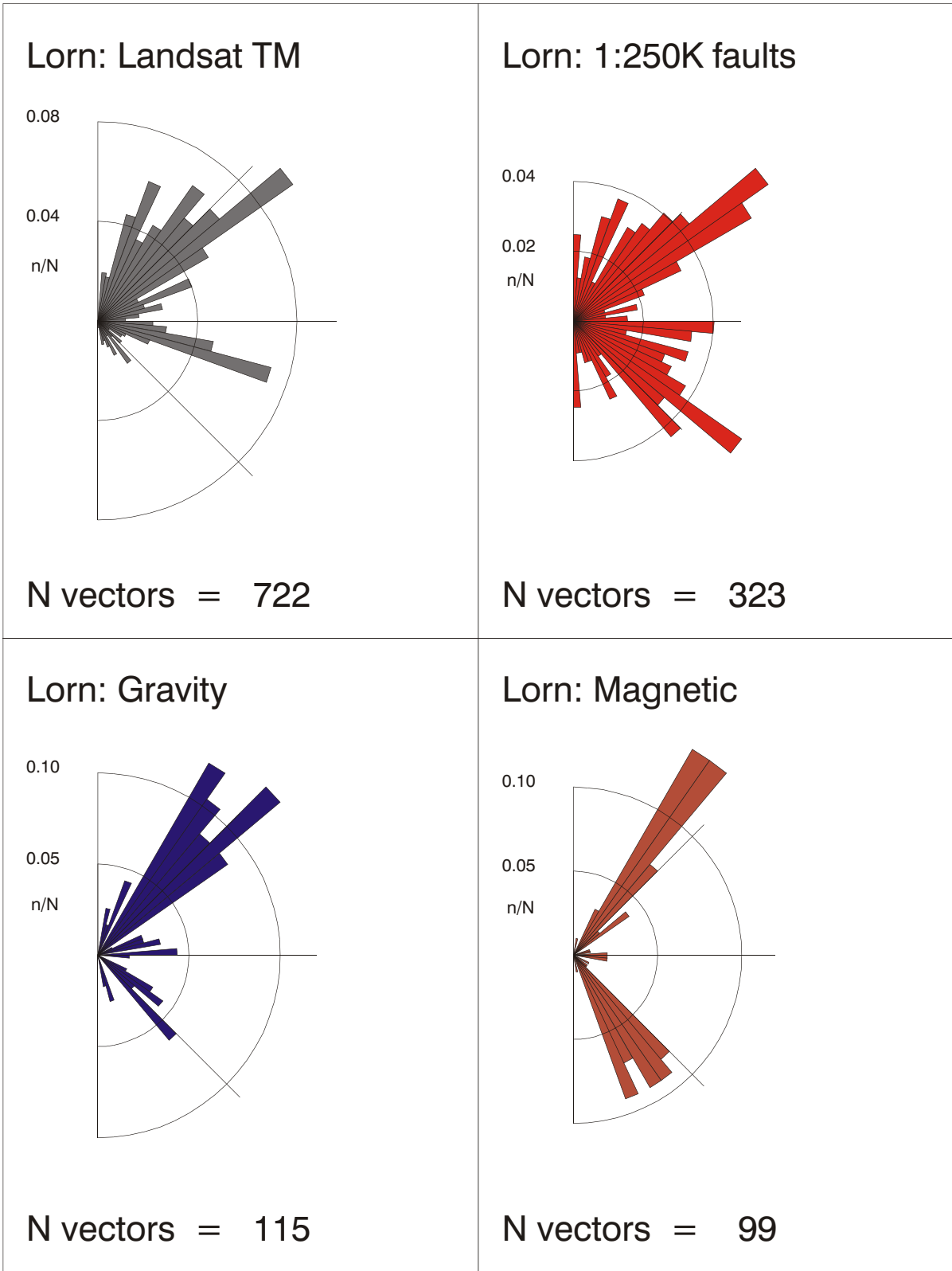


Fig 7.25 Lineament azimuths over the Lorn Plateau region

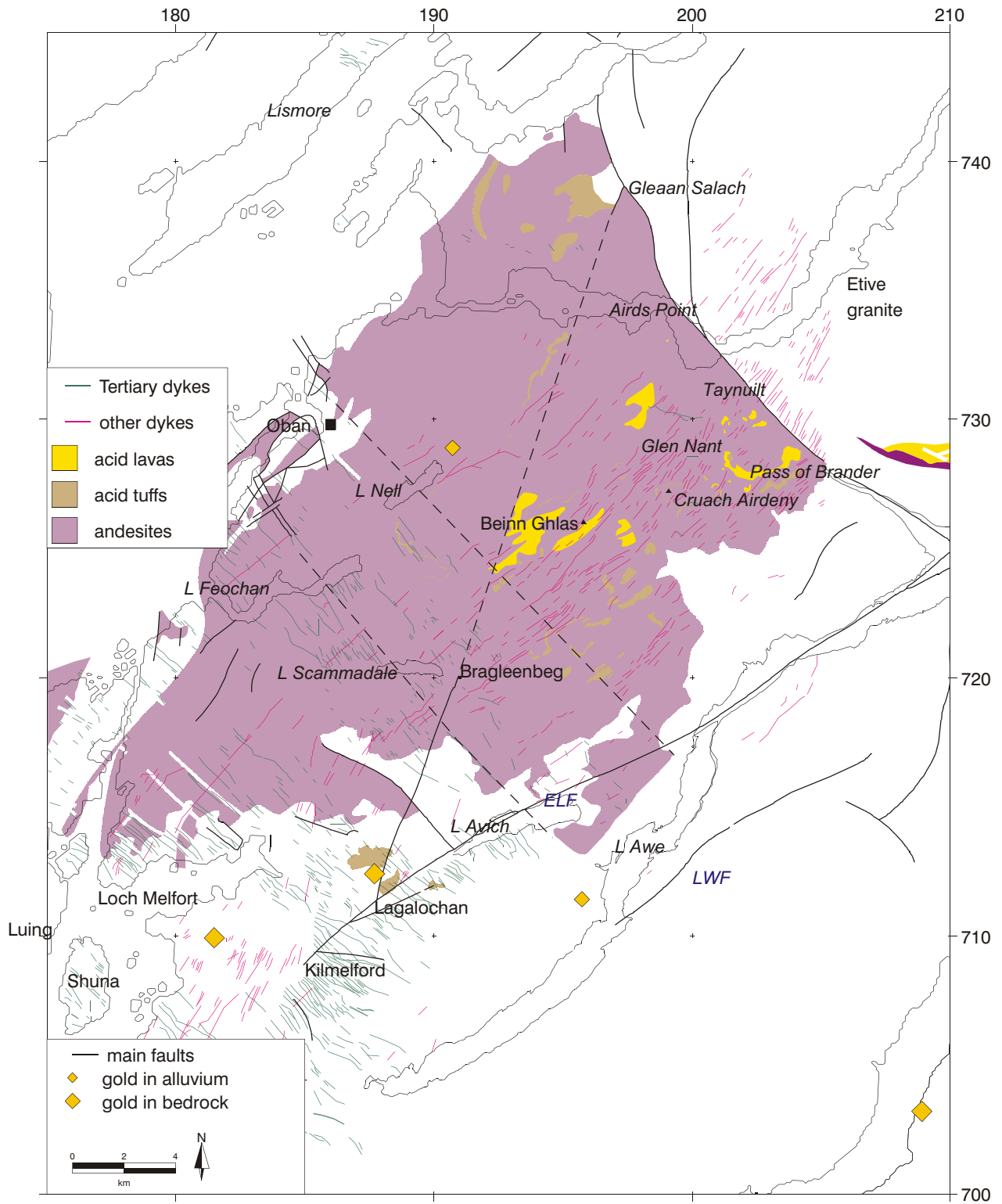


Fig 7.26 Lorn: Selected geological data layers

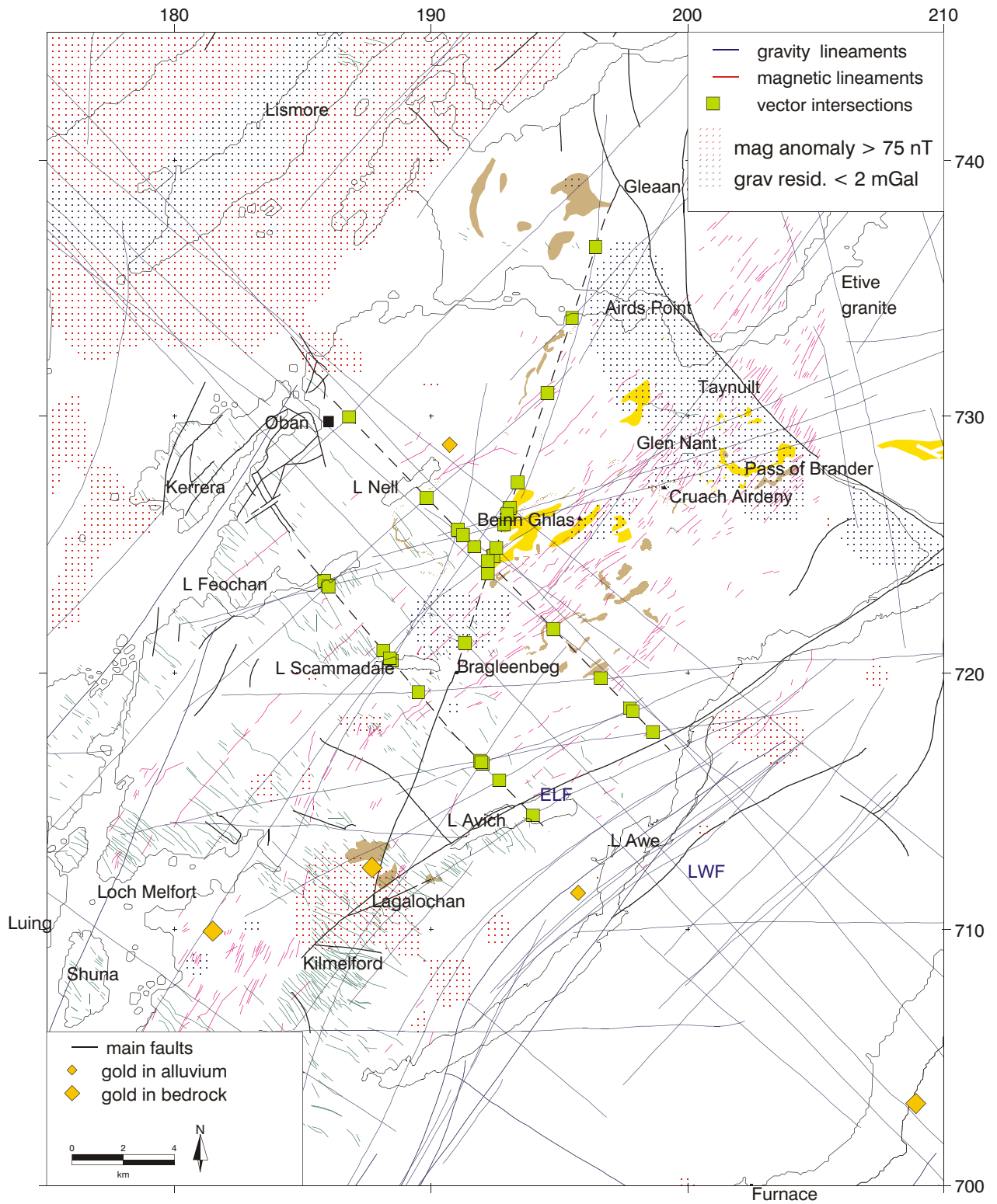


Fig 7.28 Lorn: selected geophysical data layers

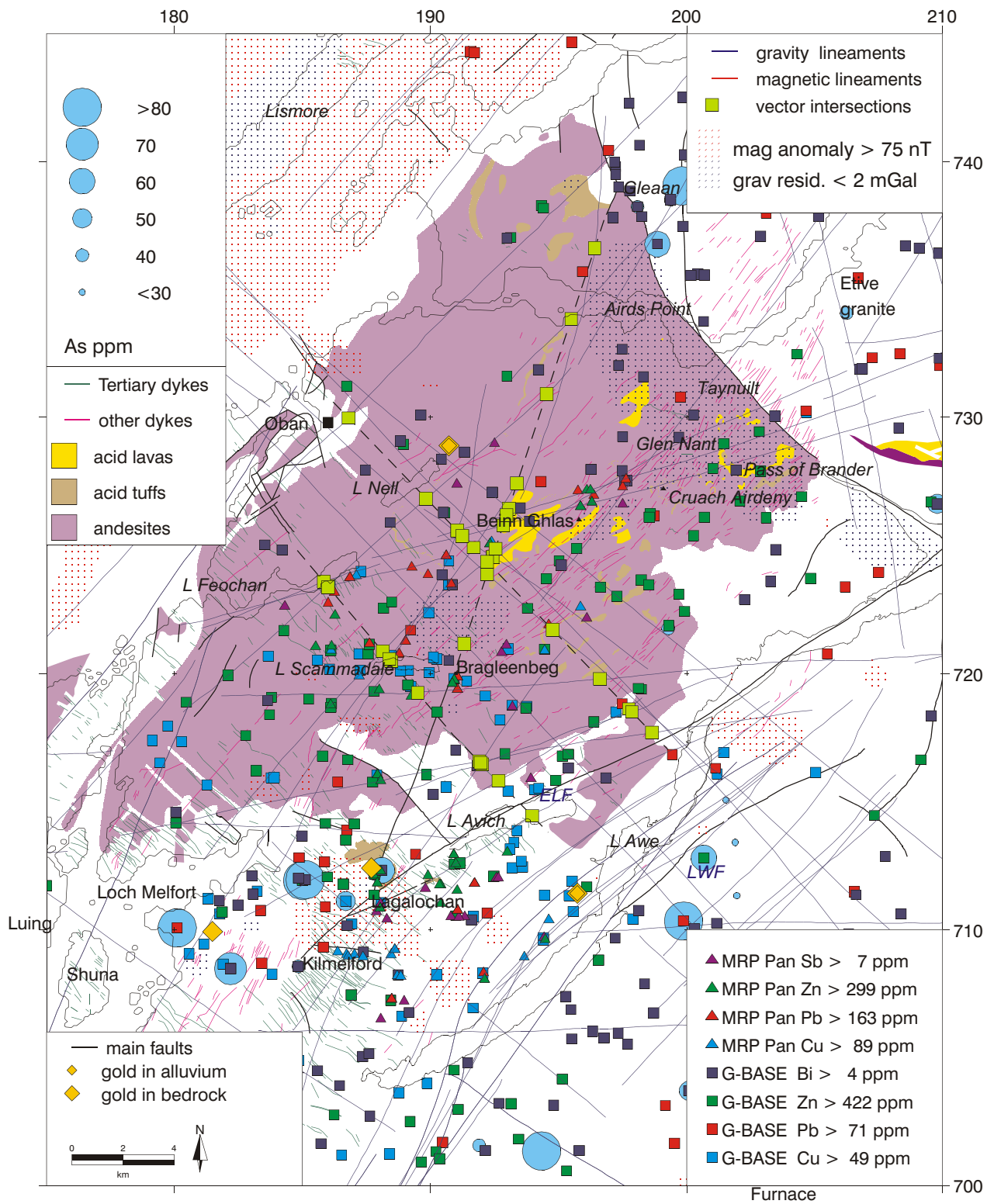


Fig 7.29 Lorn: all selected data layers for prospectivity analysis

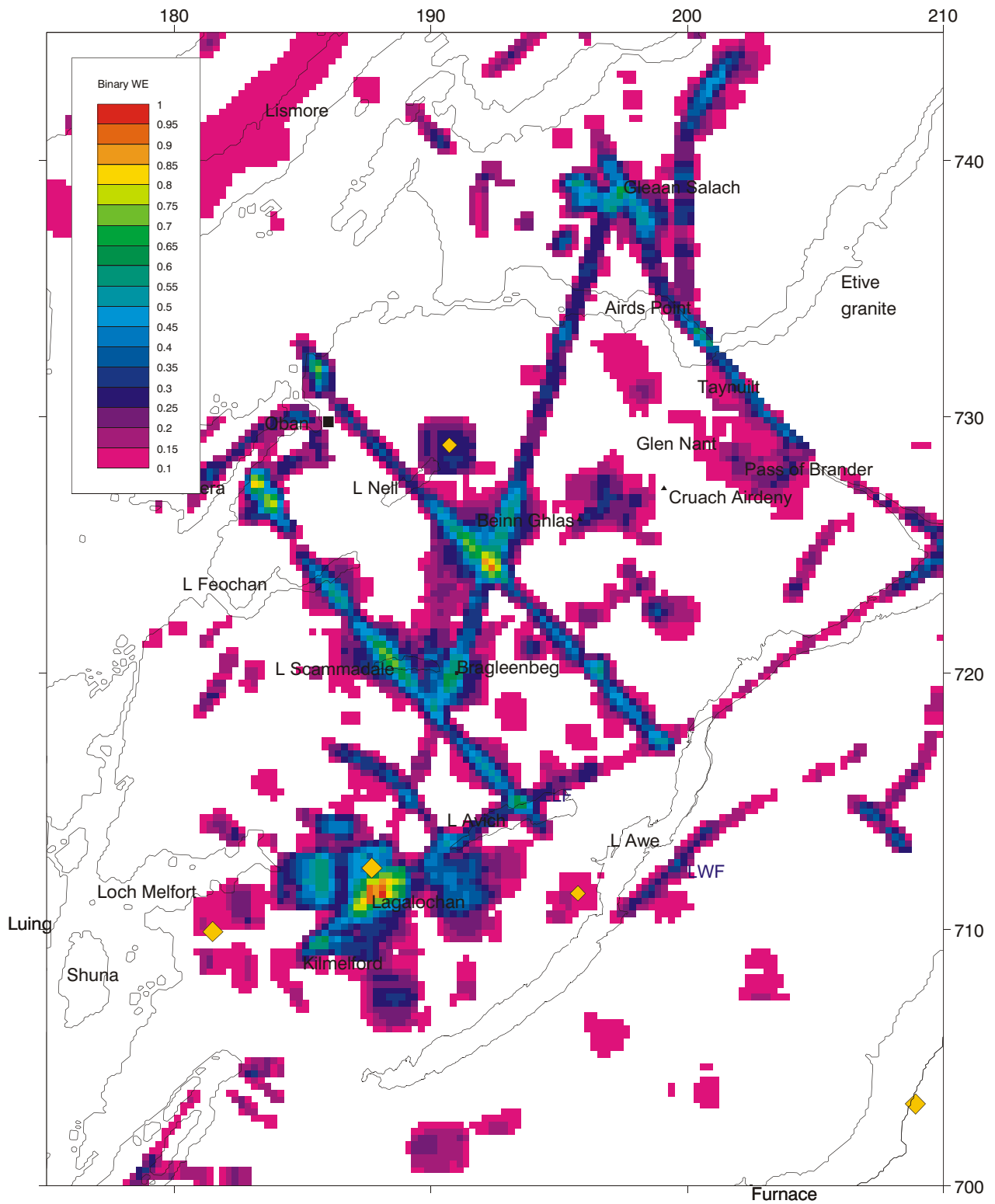


Fig 7.30 Lorn: binary weights of evidence (BWE) prospectivity map for epithermal gold mineralisation

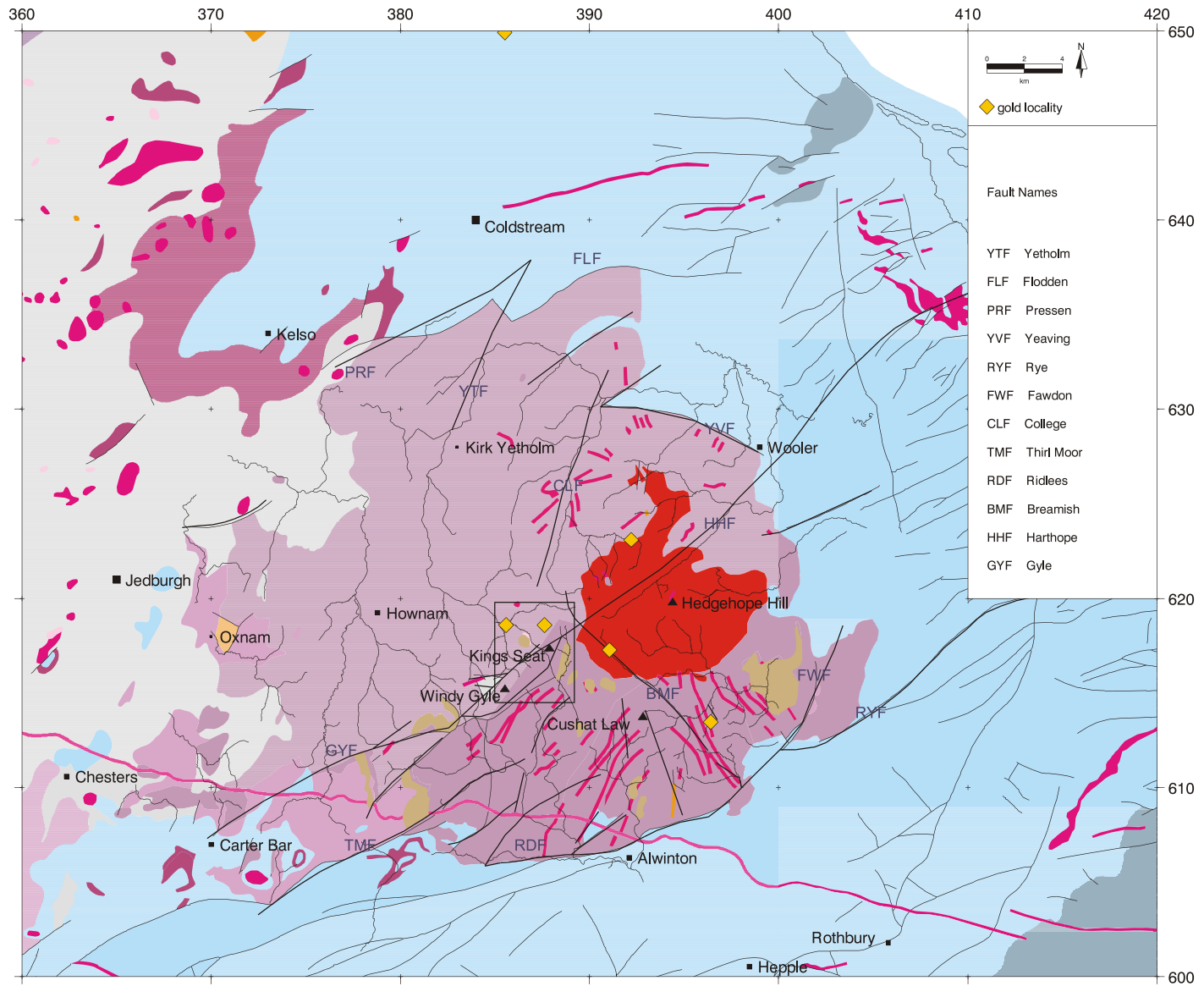


Fig 8.1 Solid geology of the Cheviot Hills area.
Boxed region is the Kingsseat Burn area.

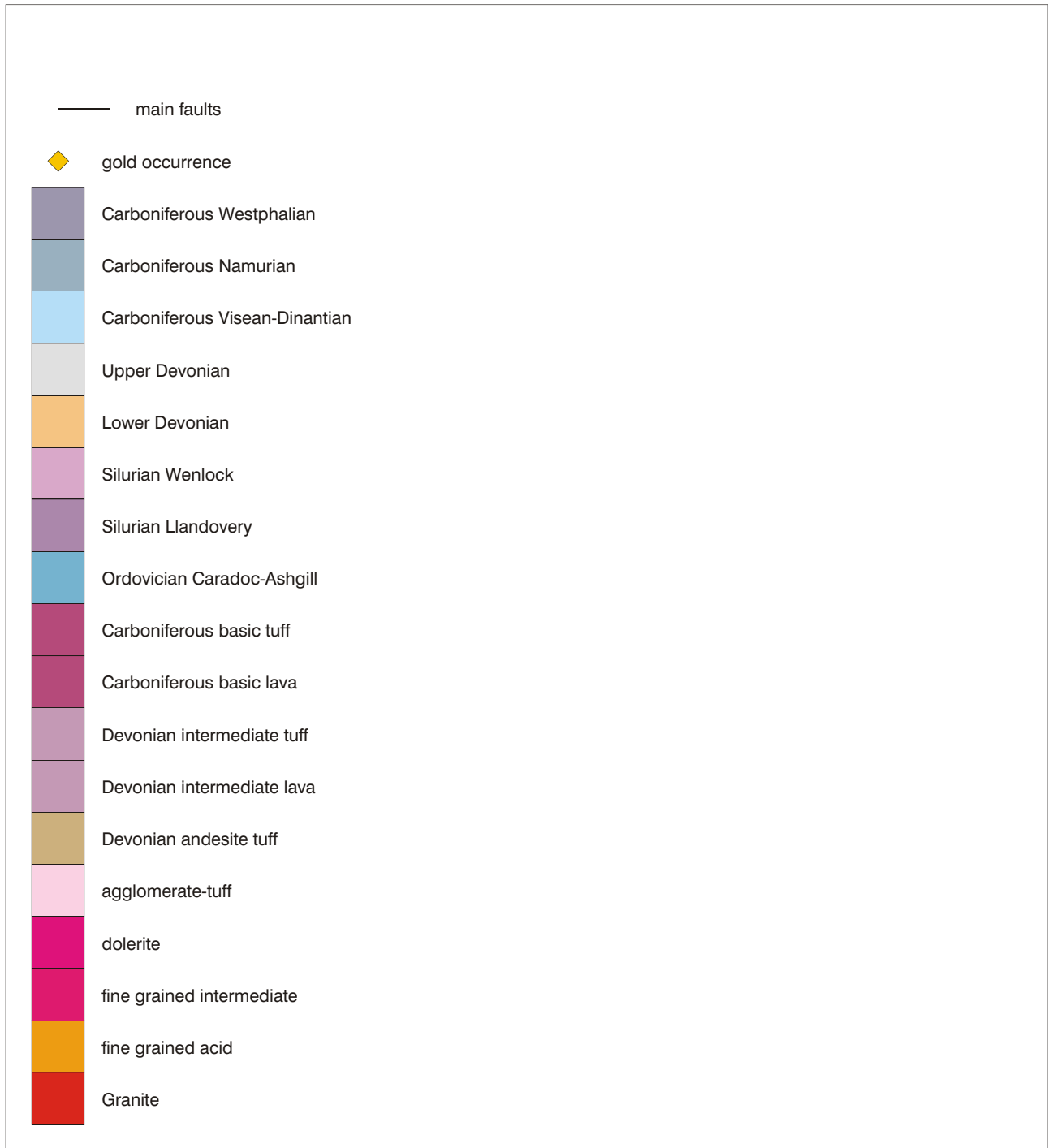


Fig 8.2 Cheviot: legend for the solid geology map Figure 8.1

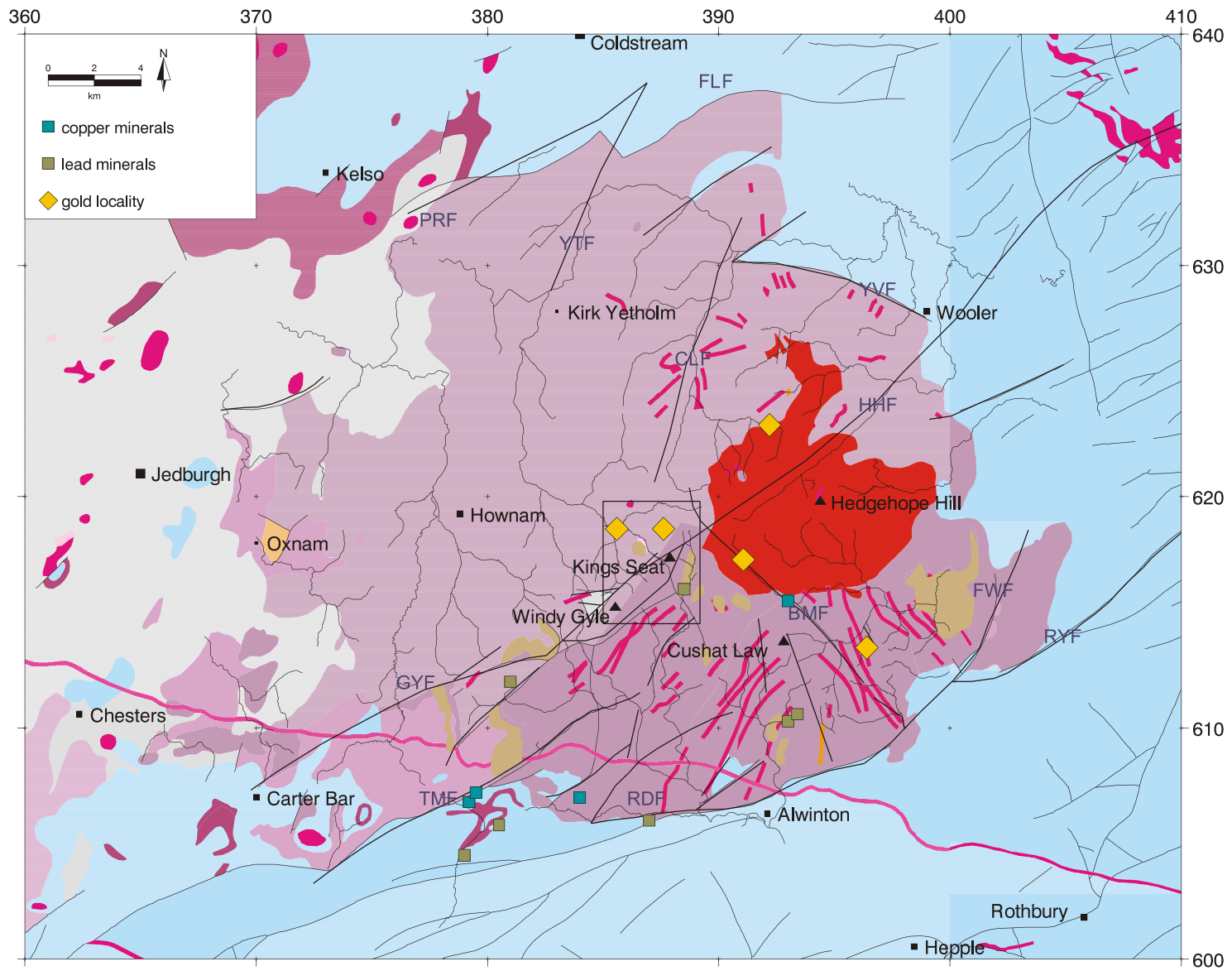


Fig 8.3 Cheviot: location of gold, copper and lead occurrences

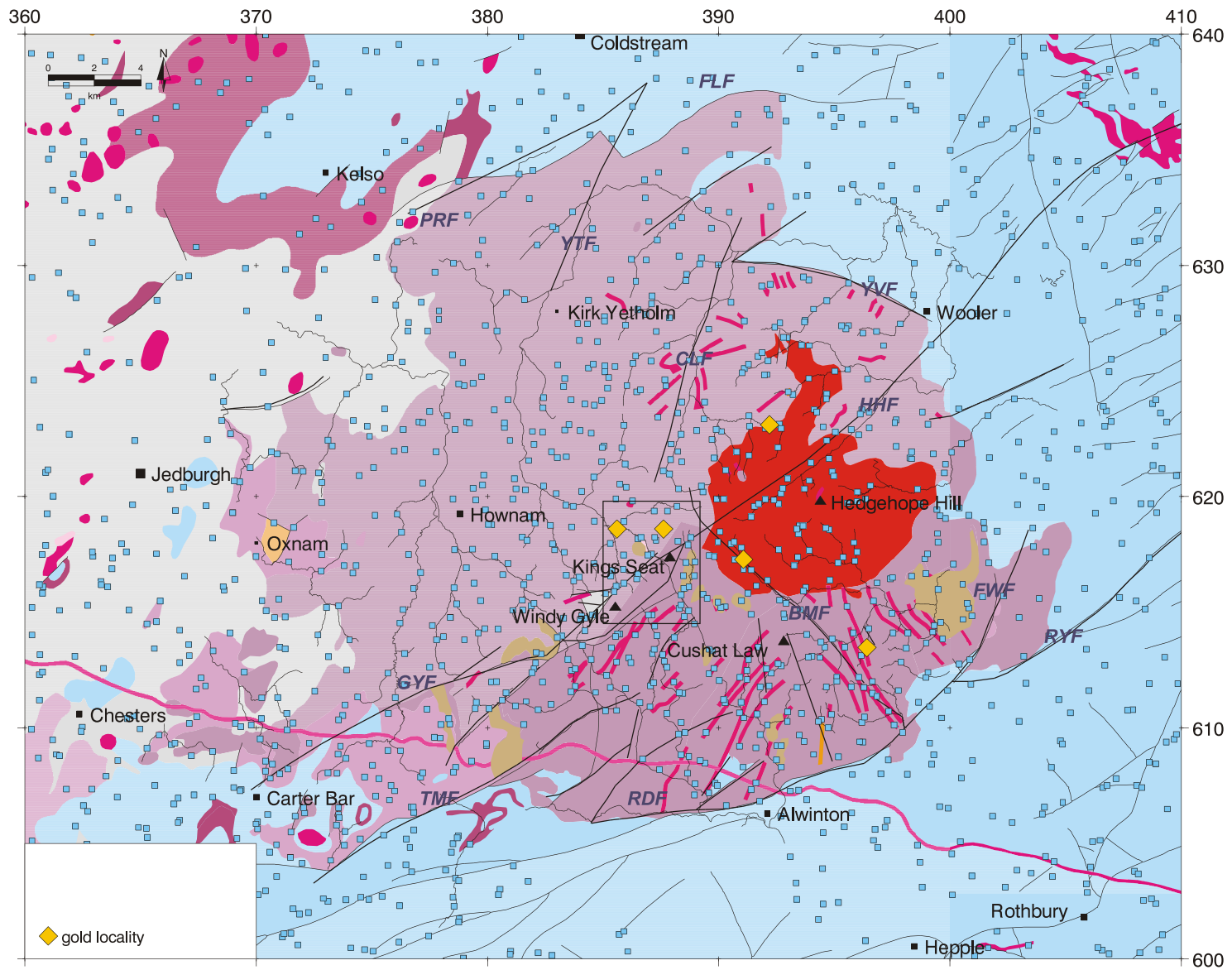


Fig 8.4 Cheviot: Location of G-BASE stream sediment samples

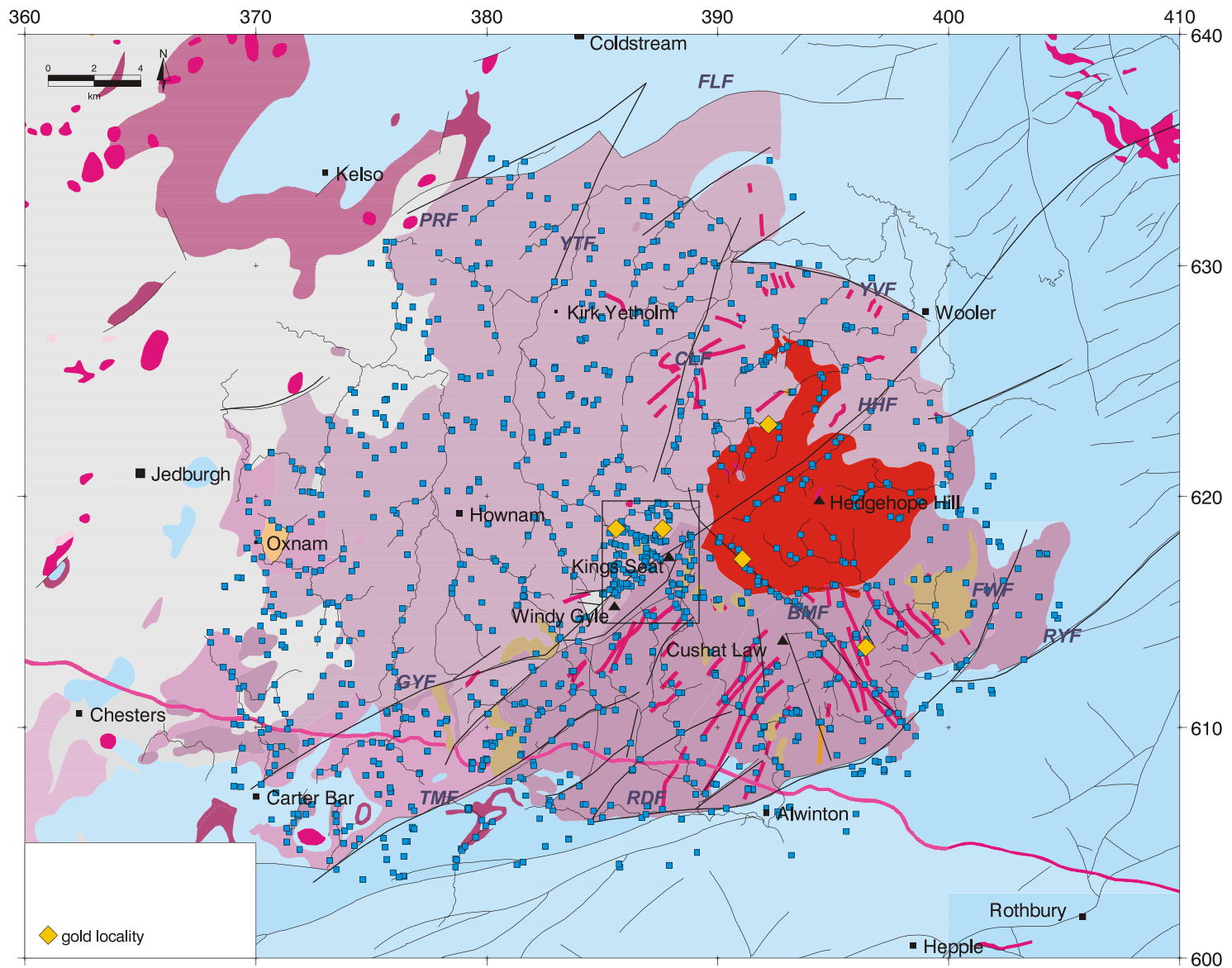


Fig 8.5 Cheviot: location of MRP stream sediment samples and panned concentrate samples

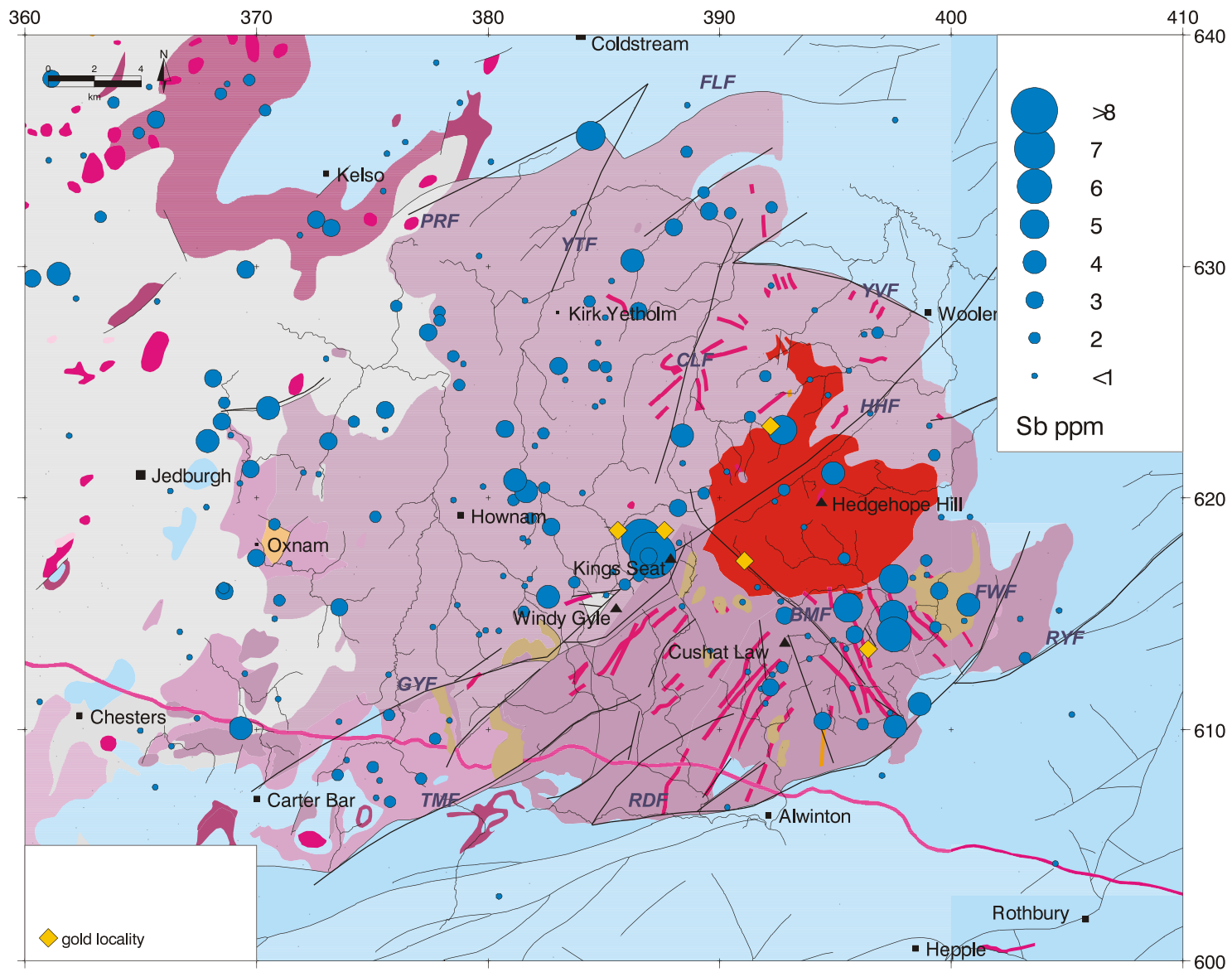


Fig 8.6 Cheviot: antimony (Sb) in G-BASE stream sediment data

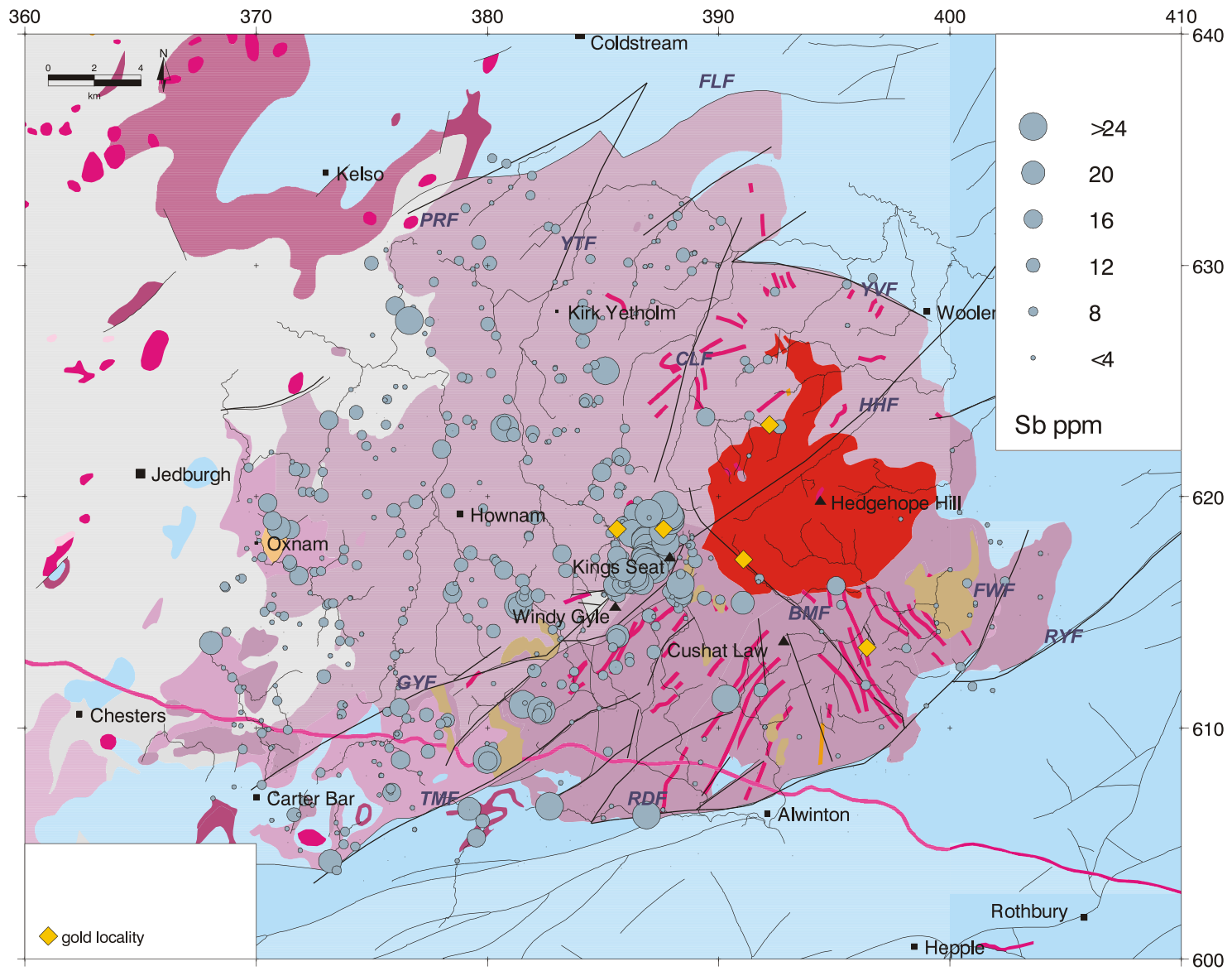


Fig 8.7 Cheviot: antimony (Sb) in MRP panned concentrate data

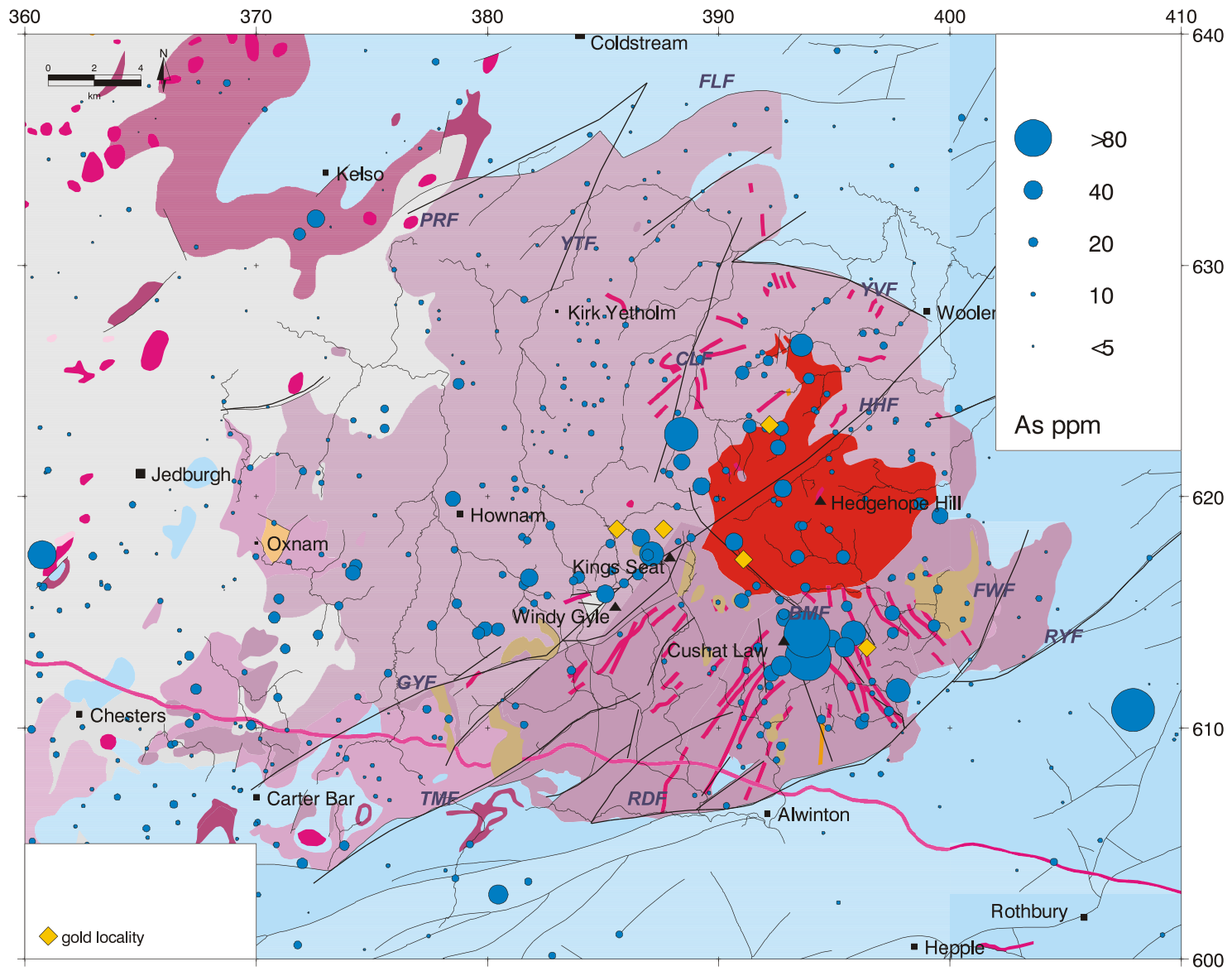


Fig 8.8 Cheviot: arsenic (As) in G-BASE stream sediment data

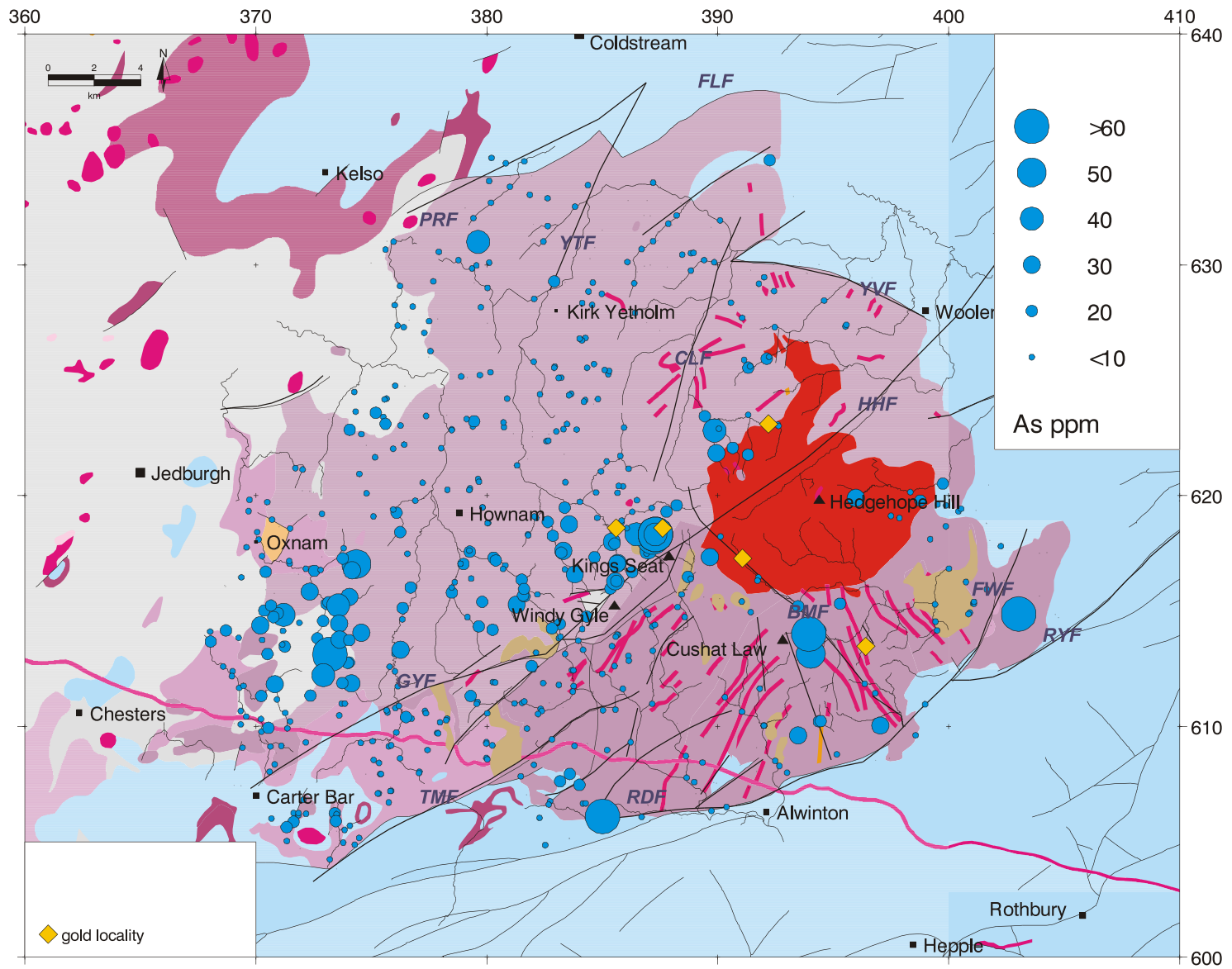


Fig 8.9 Cheviot: arsenic (As) in MRP stream sediment data

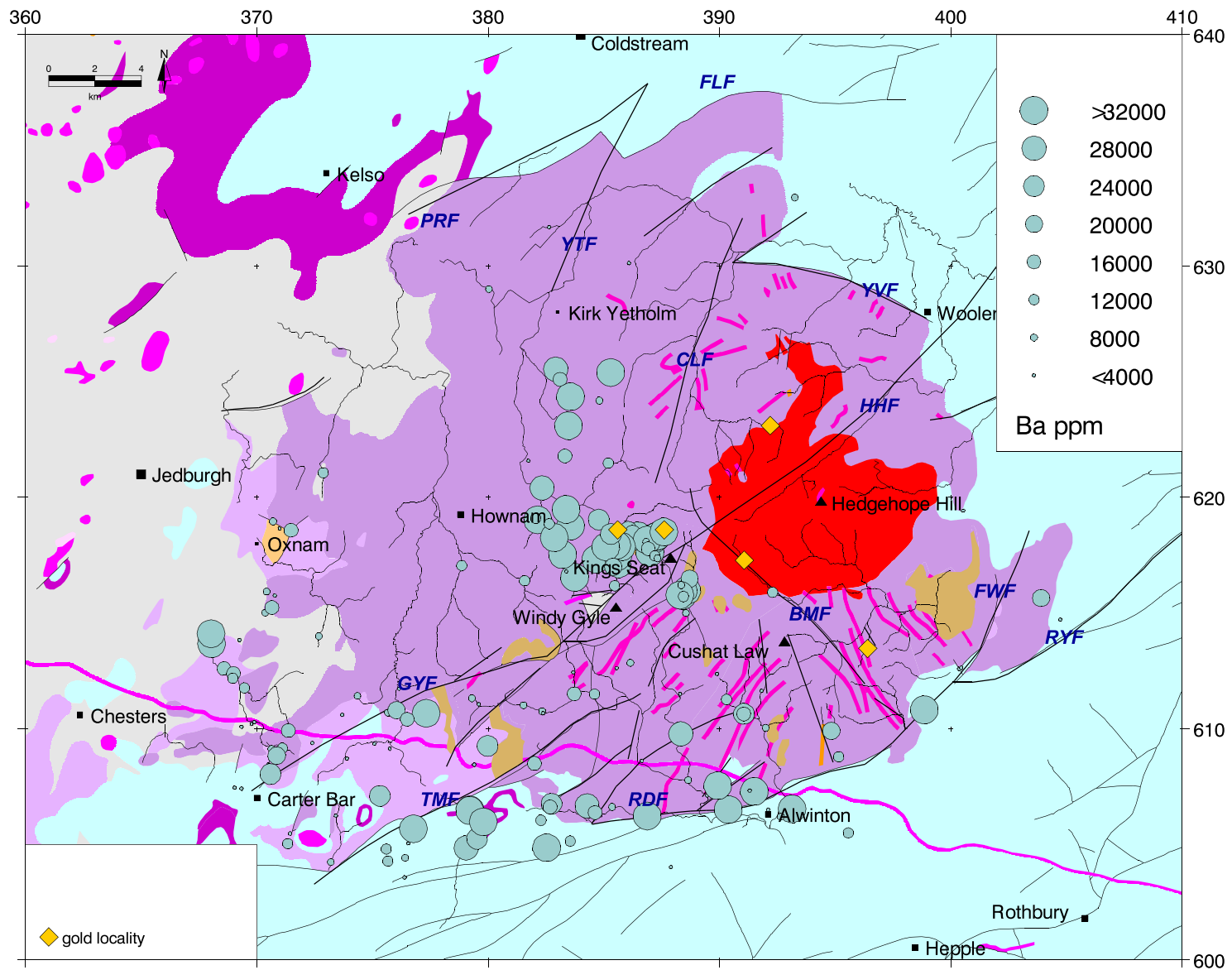


Fig 8.10 Cheviot: barium (Ba) in MRP panned concentrate data

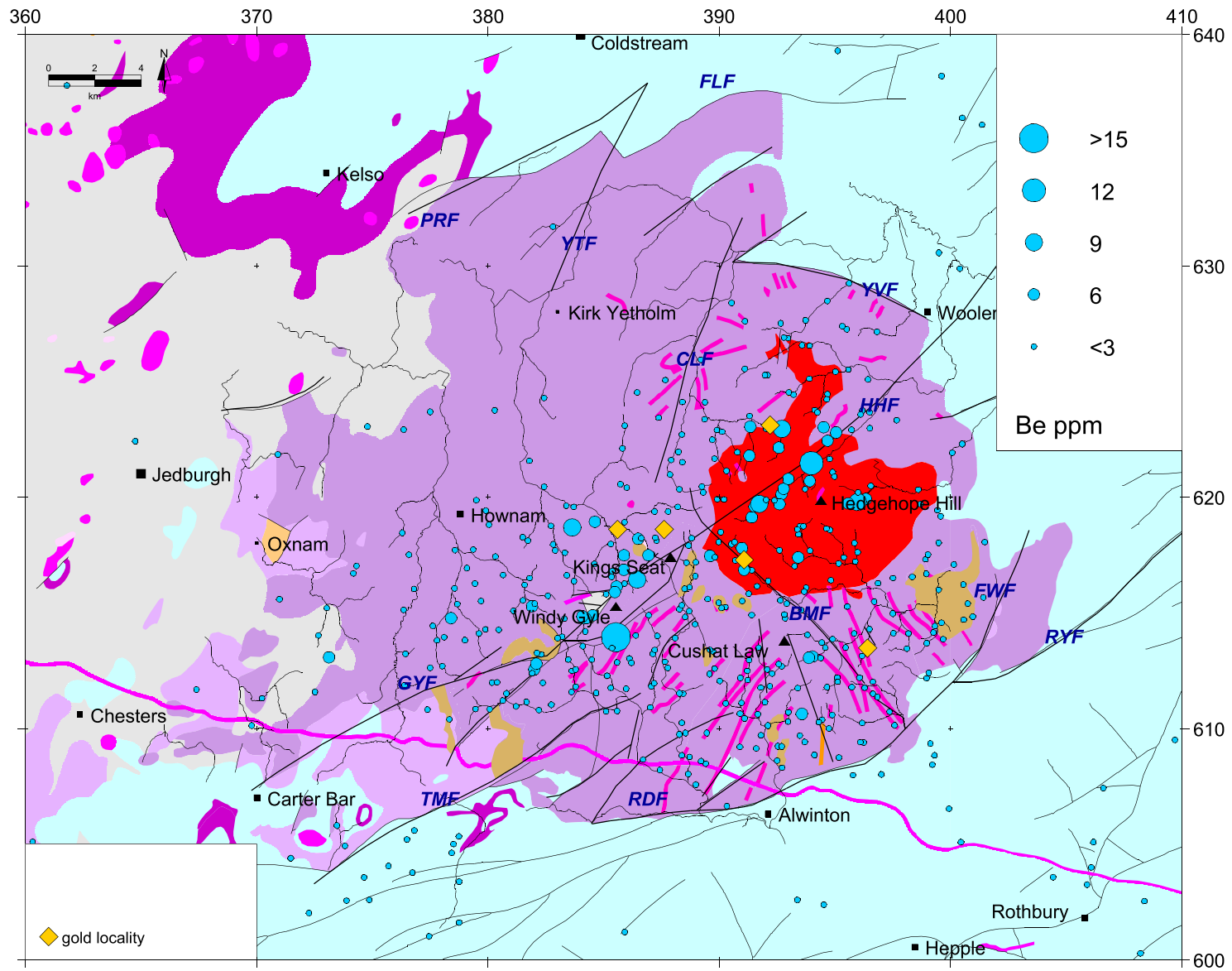


Fig 8.11 Cheviot: beryllium (Be) in G-BASE stream sediment data

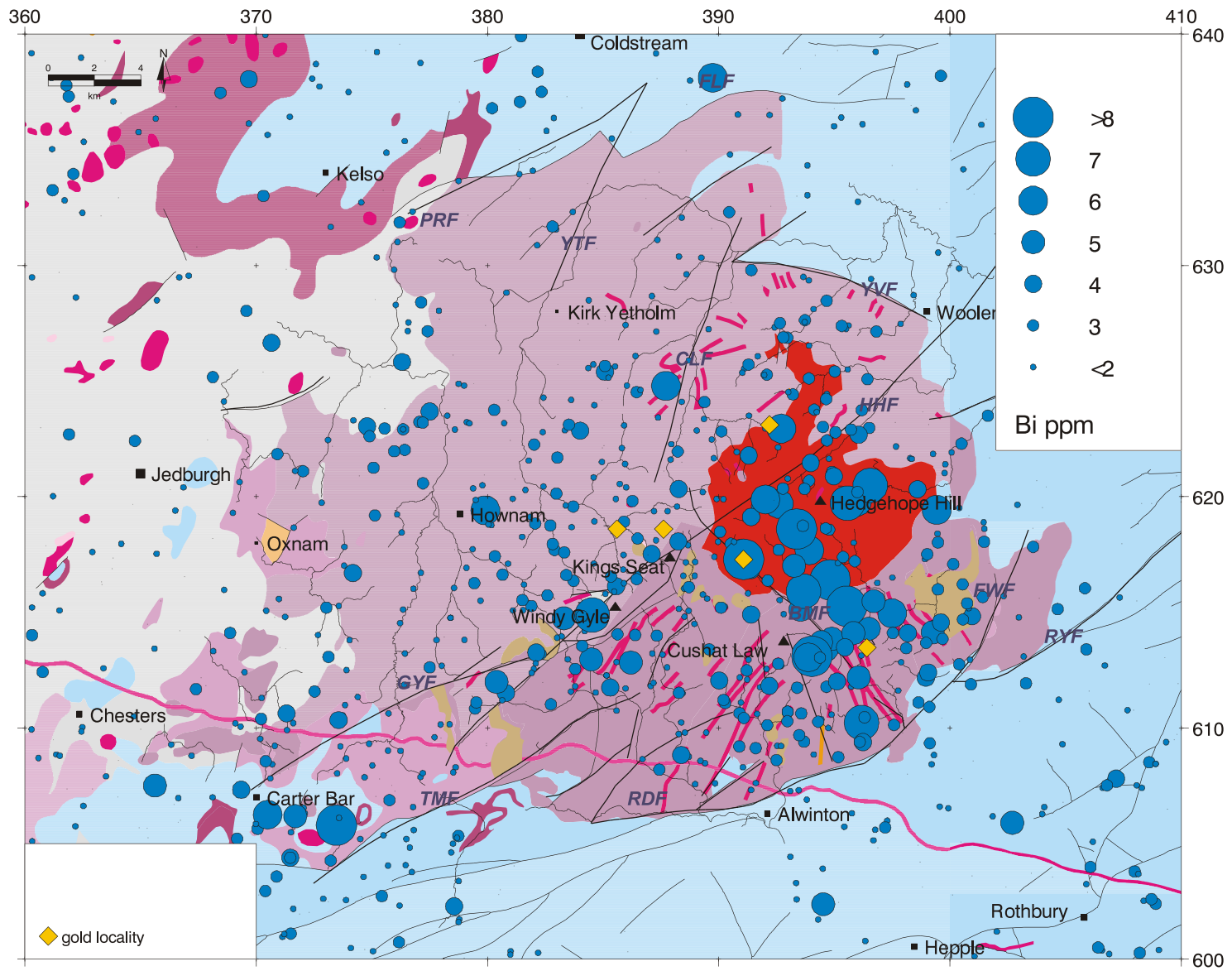


Fig 8.12 Cheviot: bismuth (Bi) in G-BASE stream sediment data

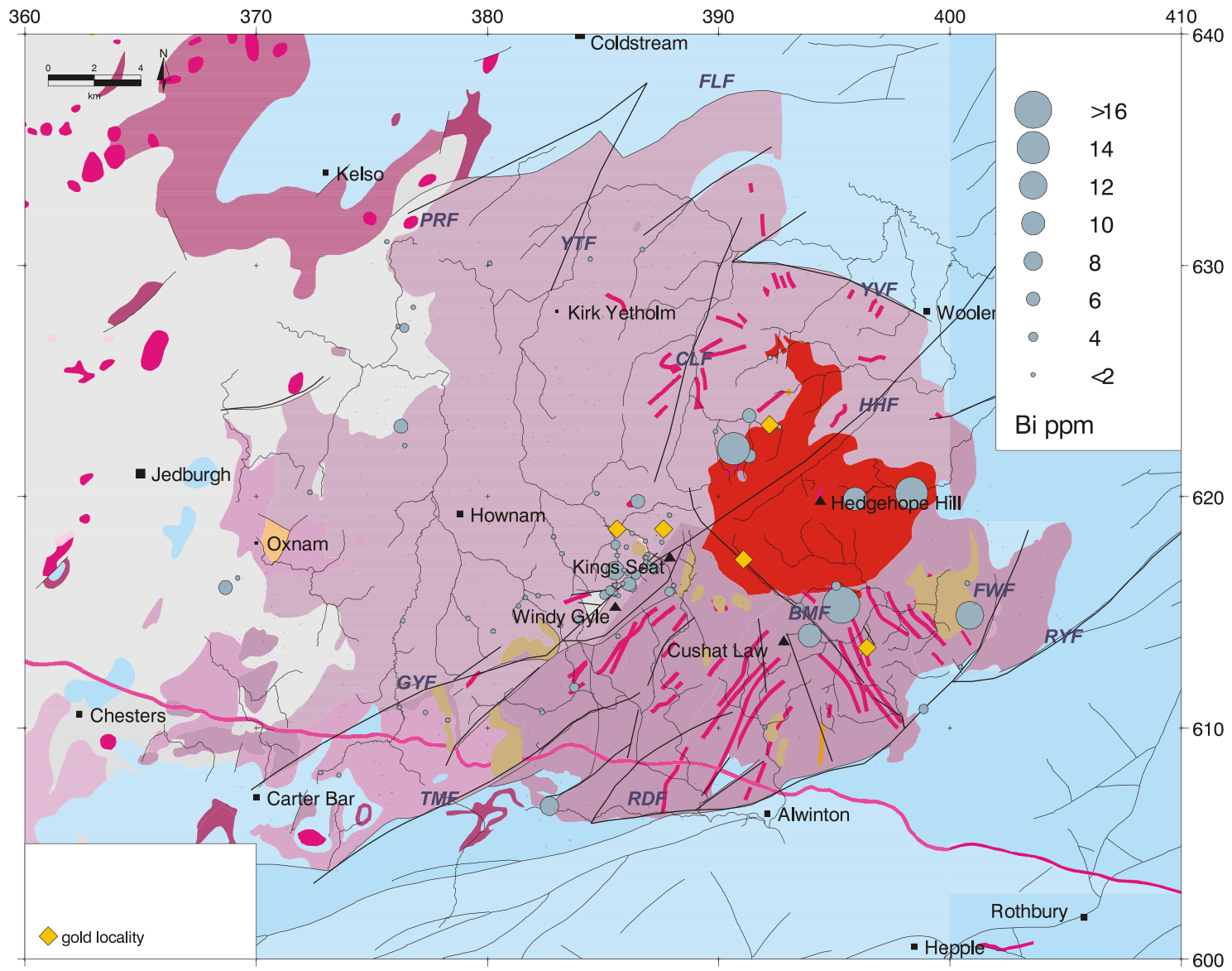


Fig 8.13 Cheviot: bismuth (Bi) in MRP panned concentrate data

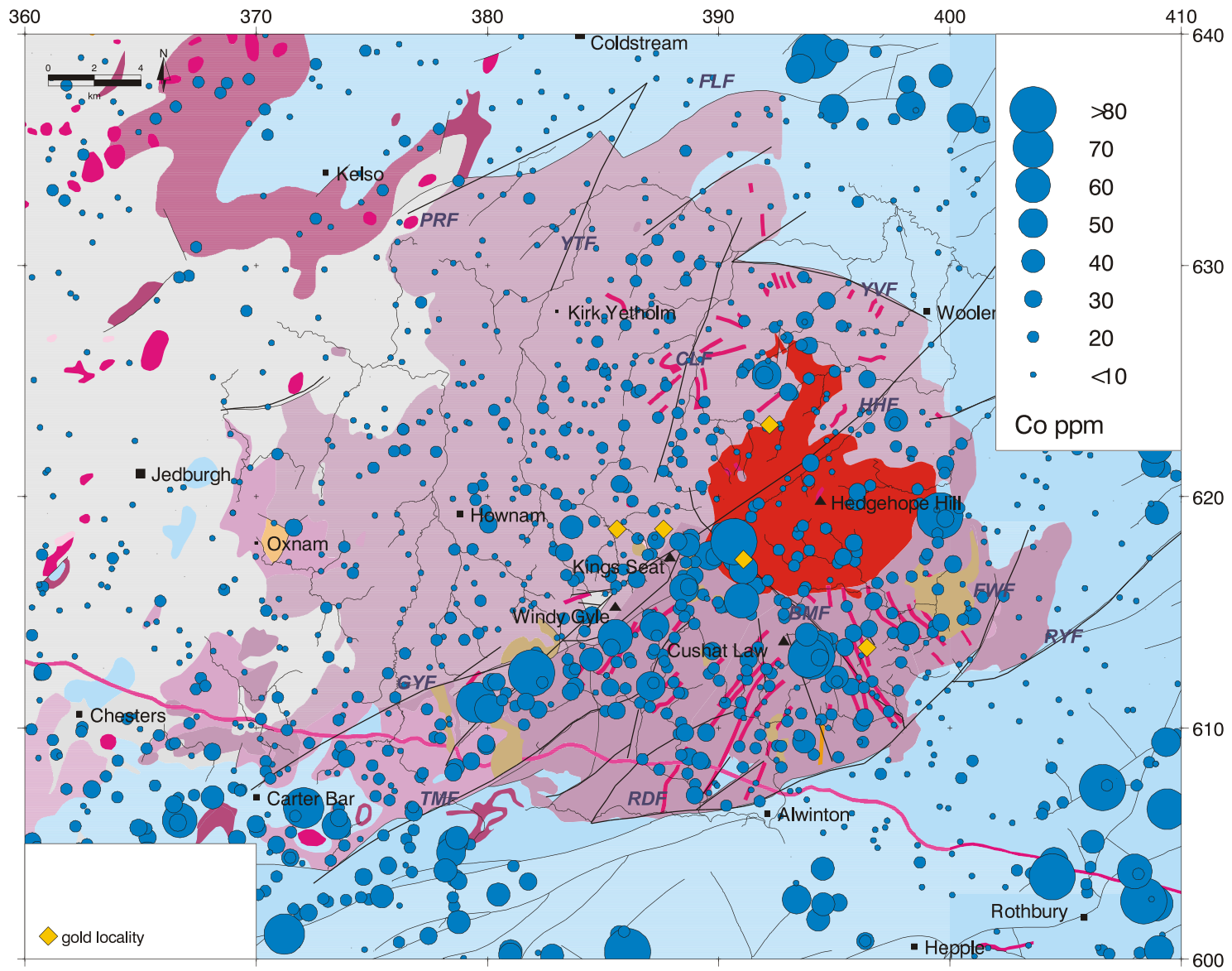


Fig 8.14 Cheviot: cobalt (Co) in G-BASE stream sediment data

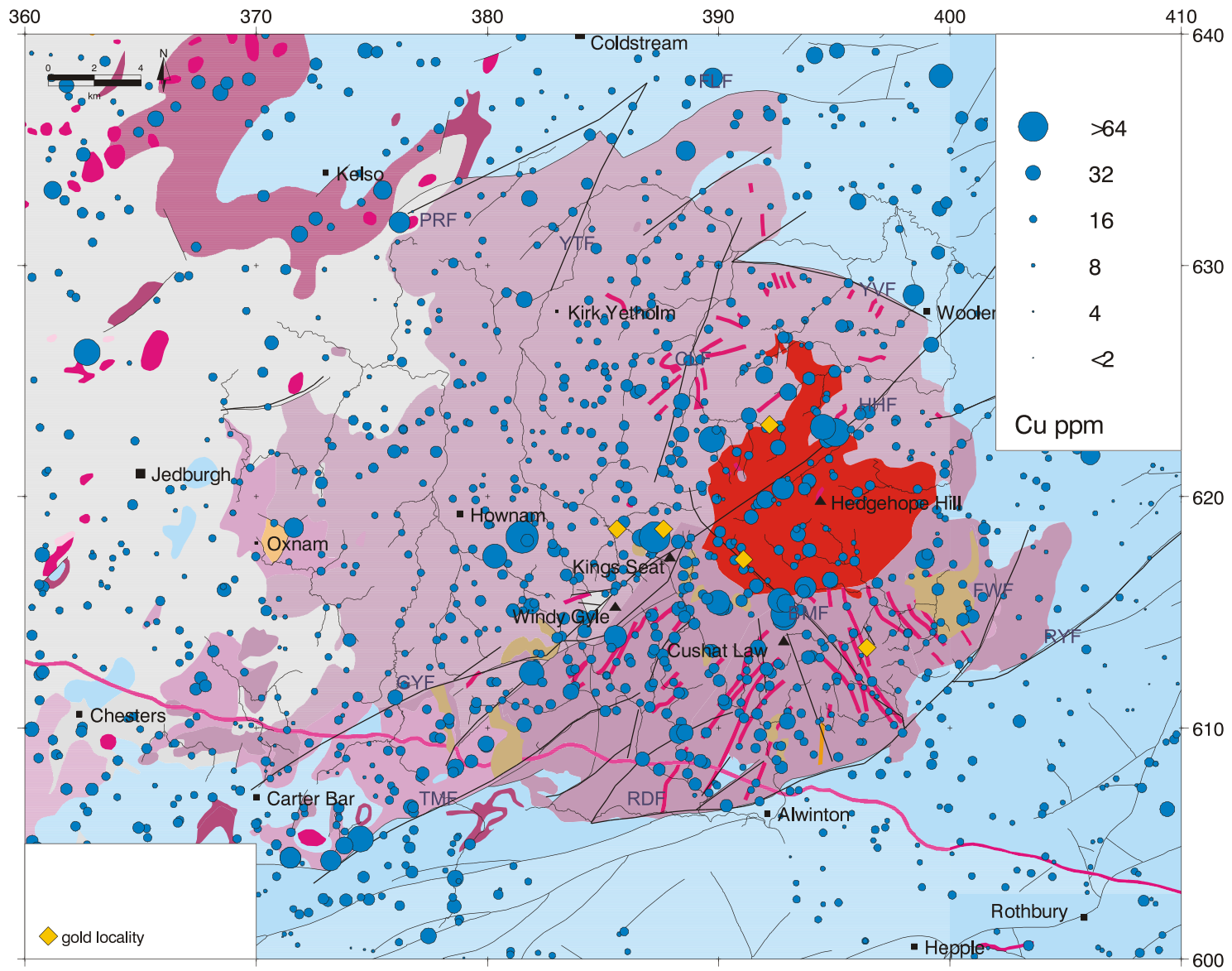


Fig 8.15 Cheviot: copper (Cu) in G-BASE stream sediment data

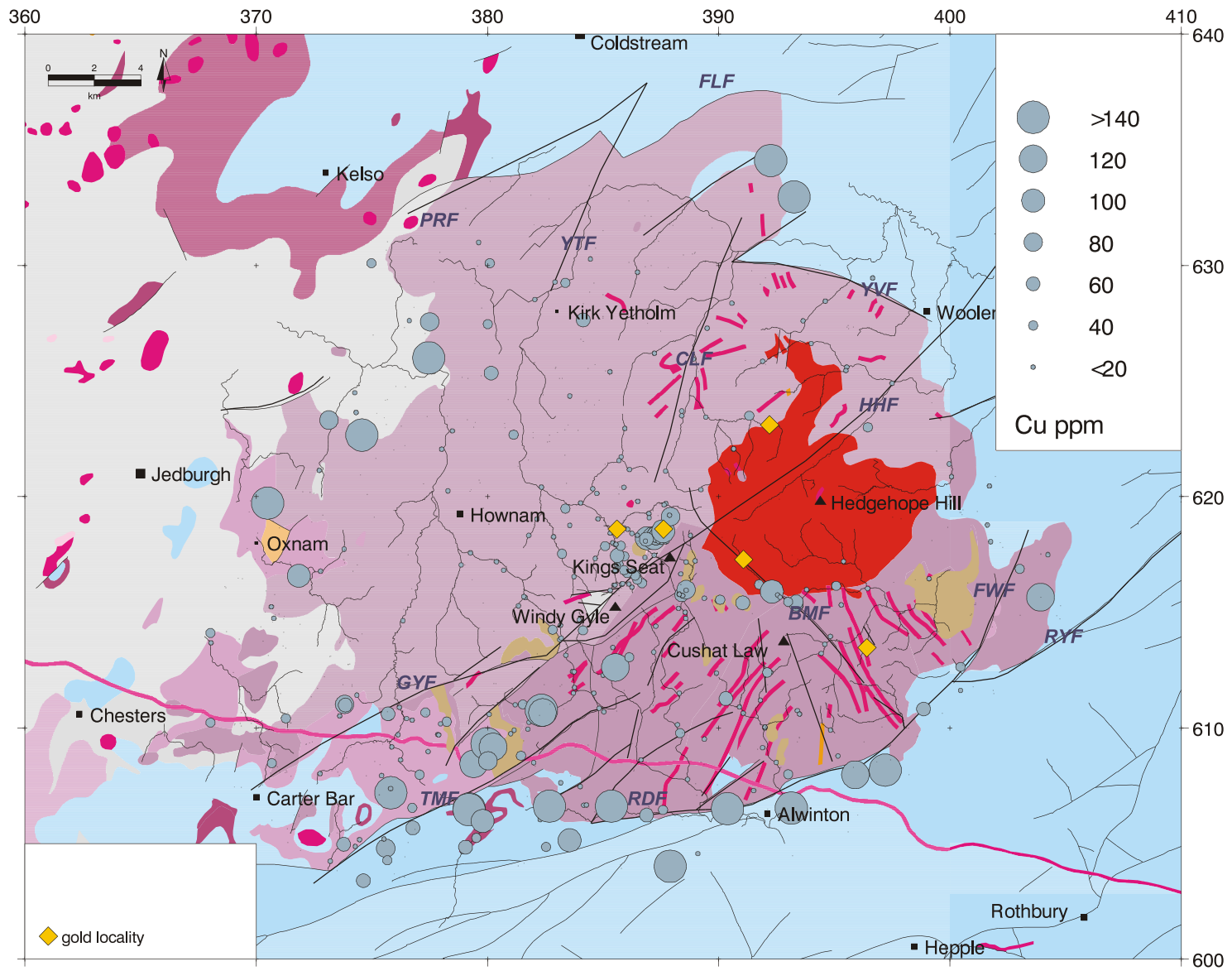


Fig 8.16 Cheviot: copper (Cu) in MRP panned concentrate data

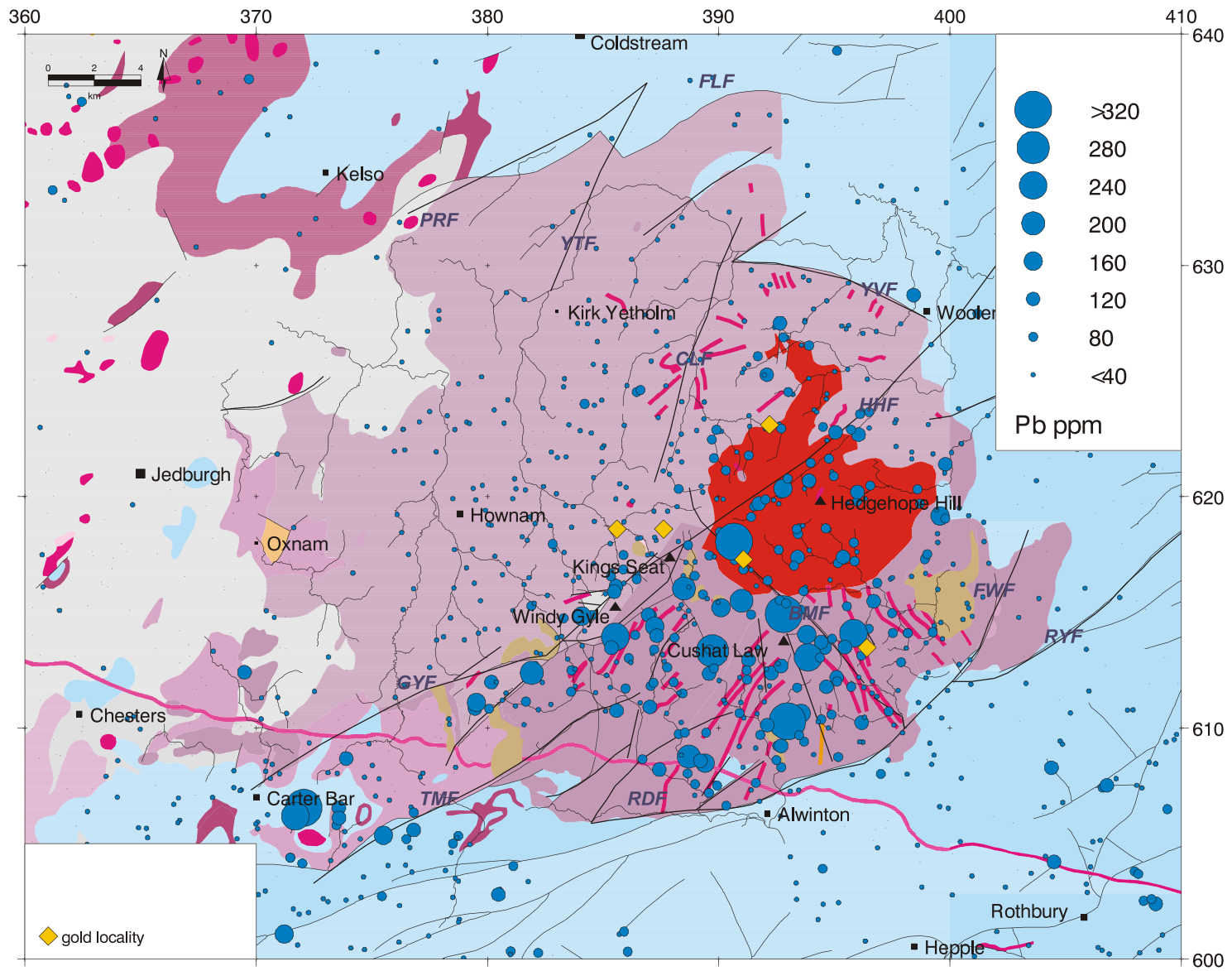


Fig 8.17 Cheviot: lead (Pb) in G-BASE stream sediment data

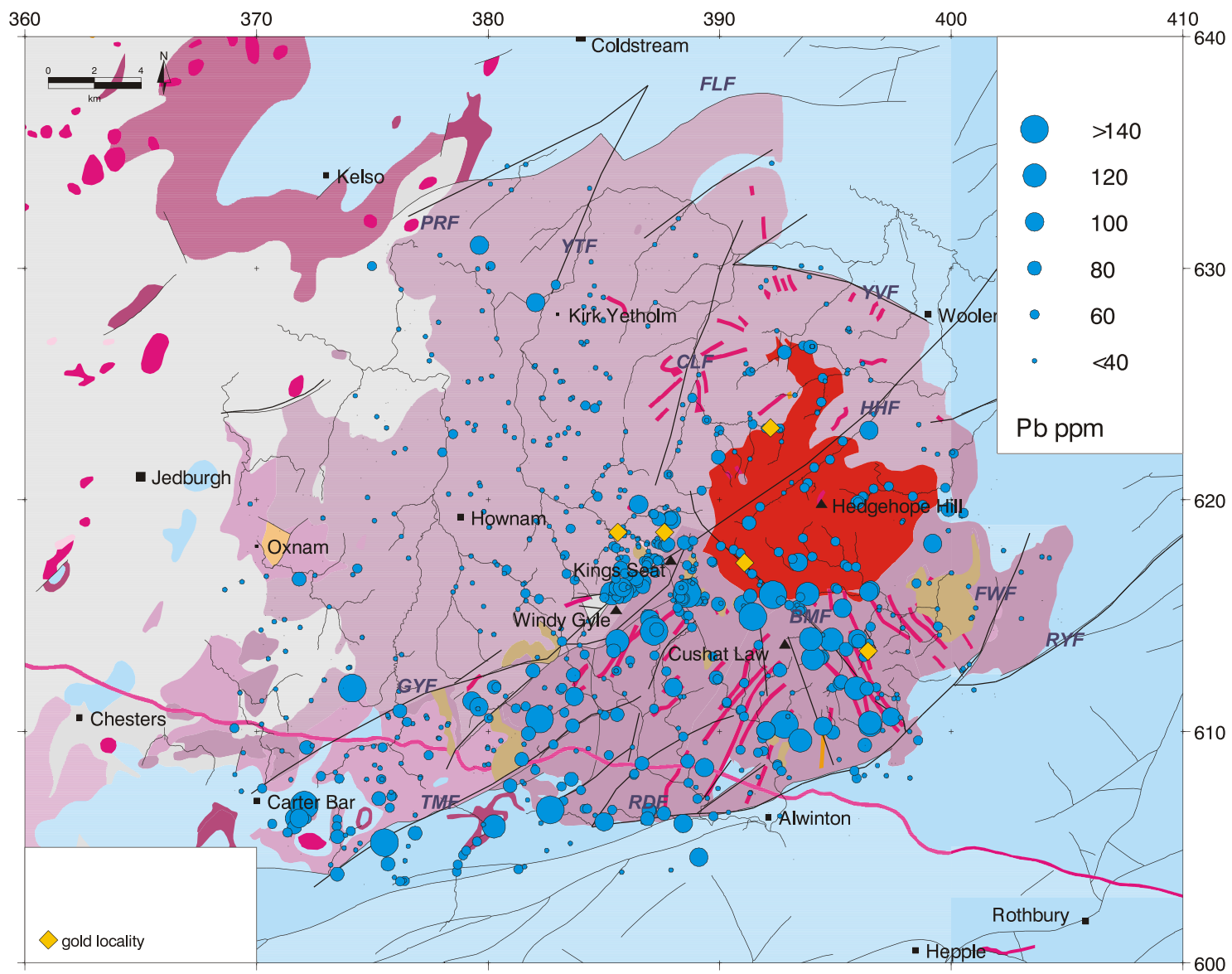


Fig 8.18 Cheviot: lead (Pb) in MRP stream sediment data

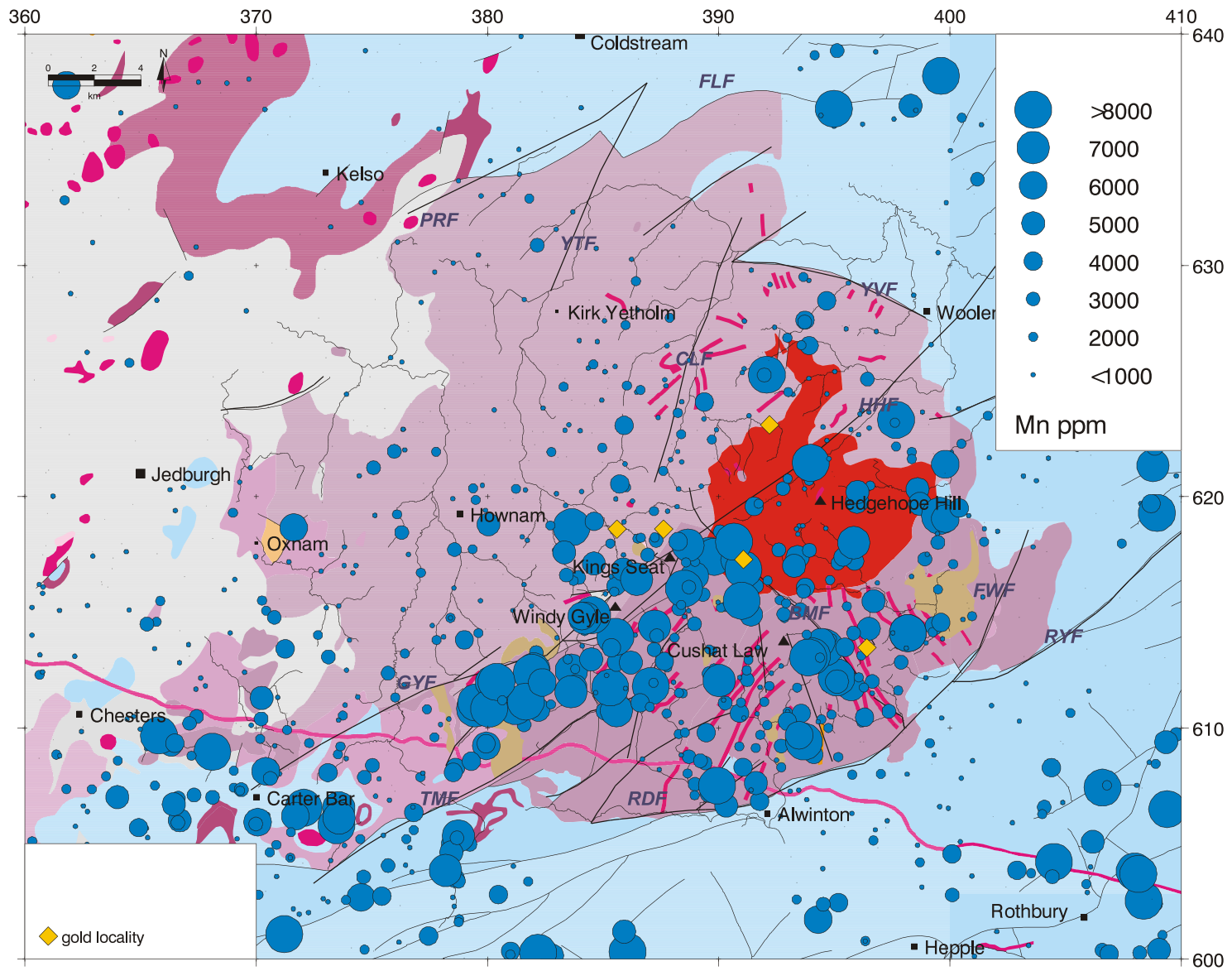


Fig 8.19 Cheviot: manganese (Mn) in G-BASE stream sediment data

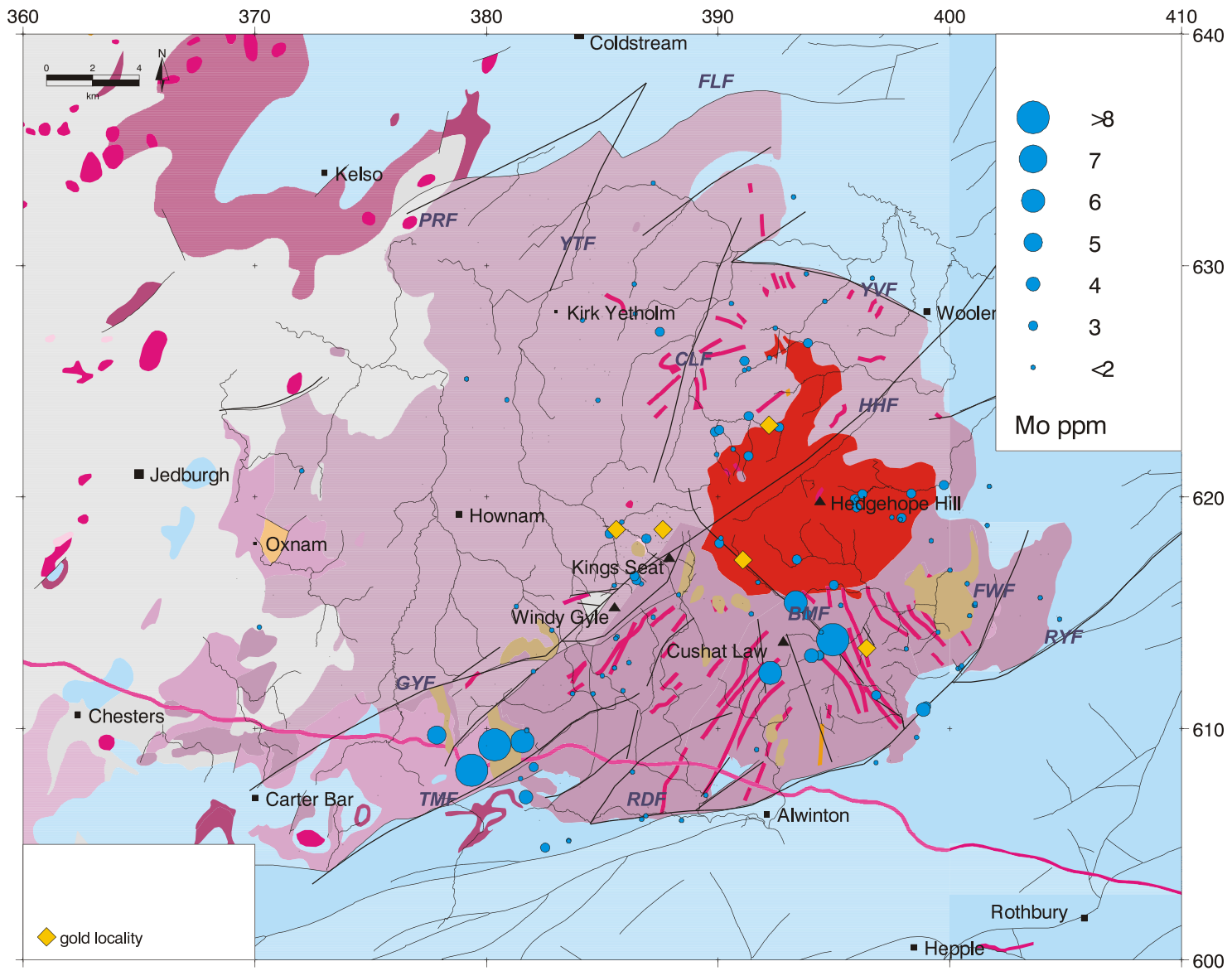


Fig 8.20 Cheviot: molybdenum (Mo) in MRP stream sediment data

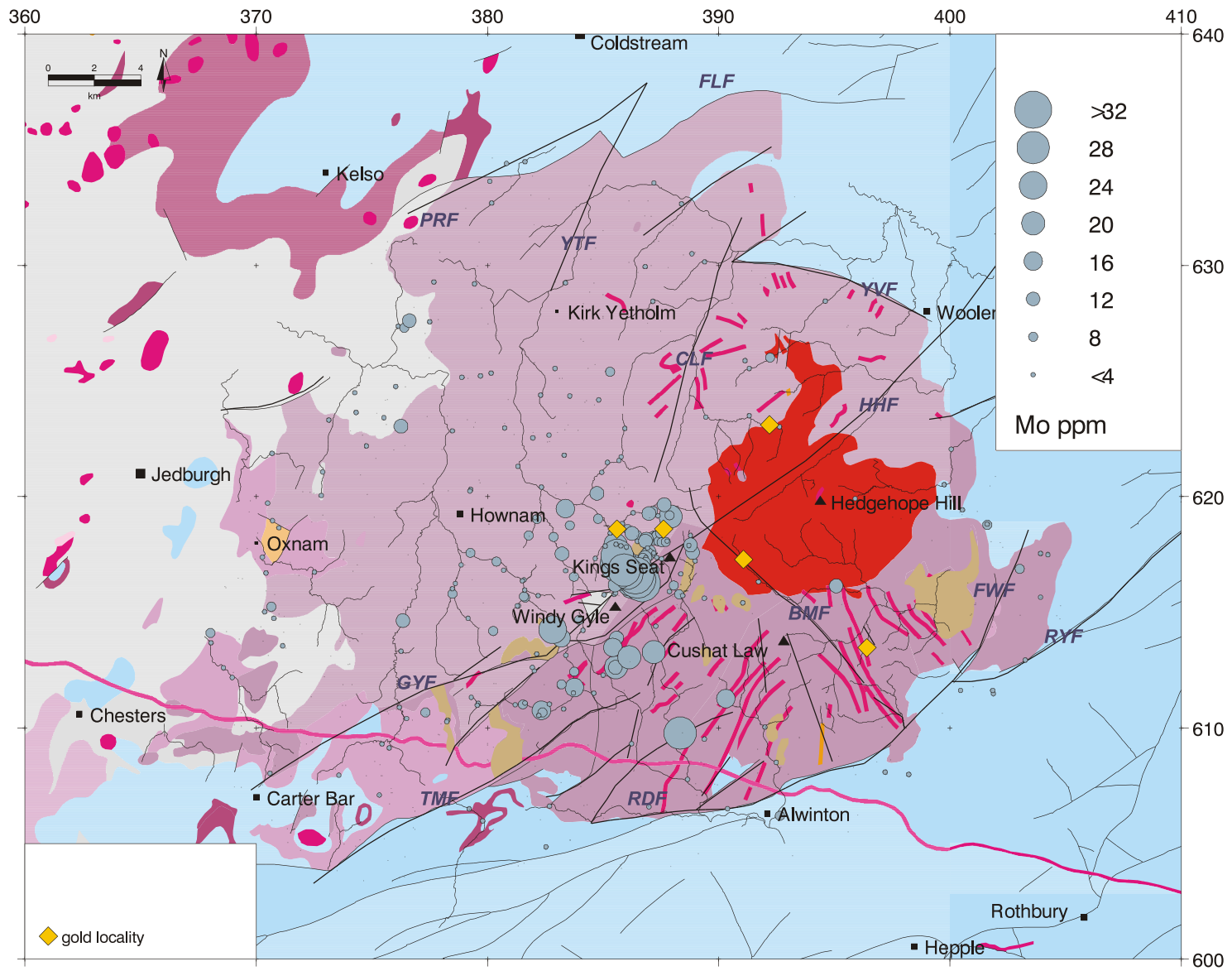


Fig 8.21 Cheviot: molybdenum (Mo) in MRP panned concentrate data

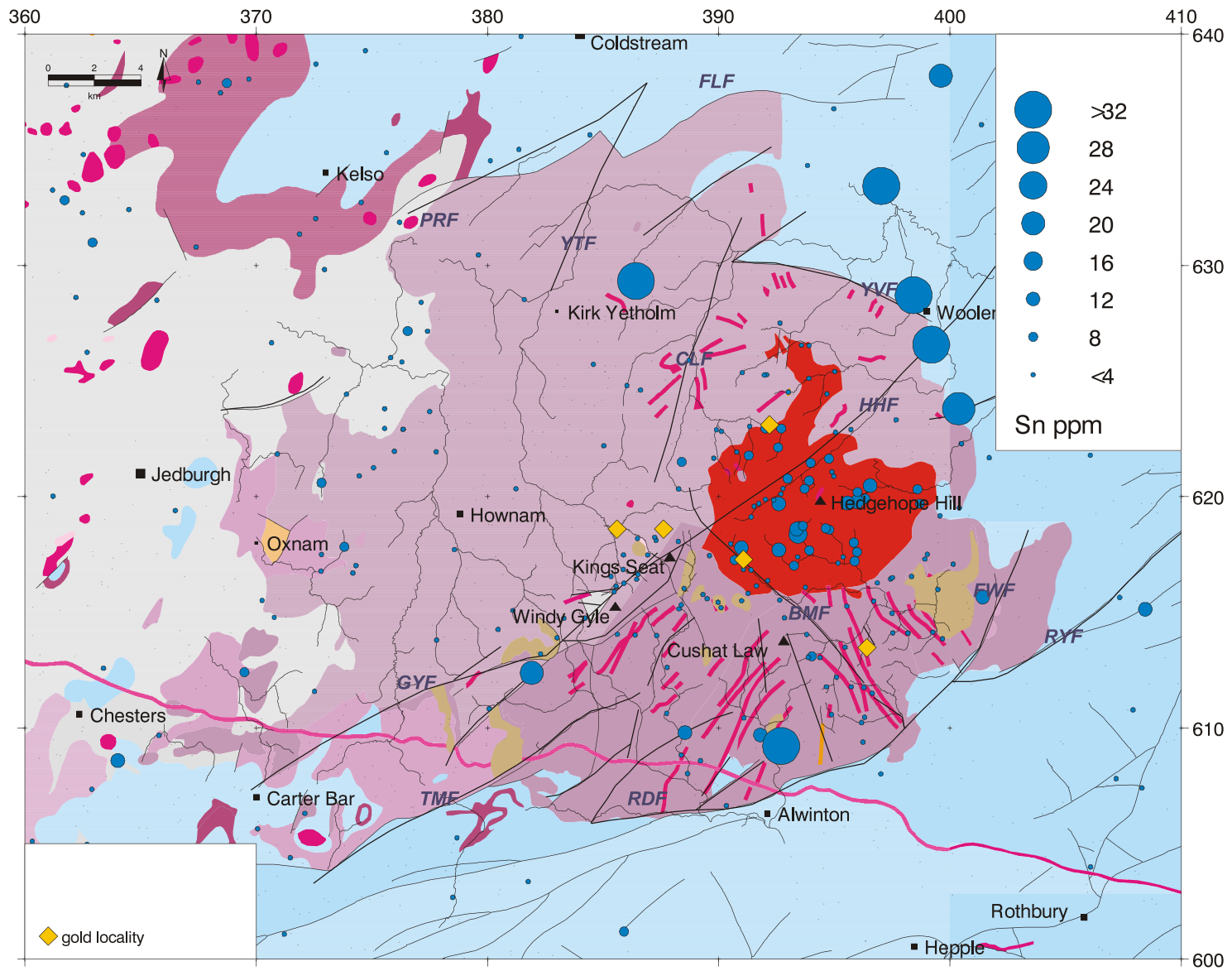


Fig 8.22 Cheviot: tin (Sn) in G-BASE stream sediment data

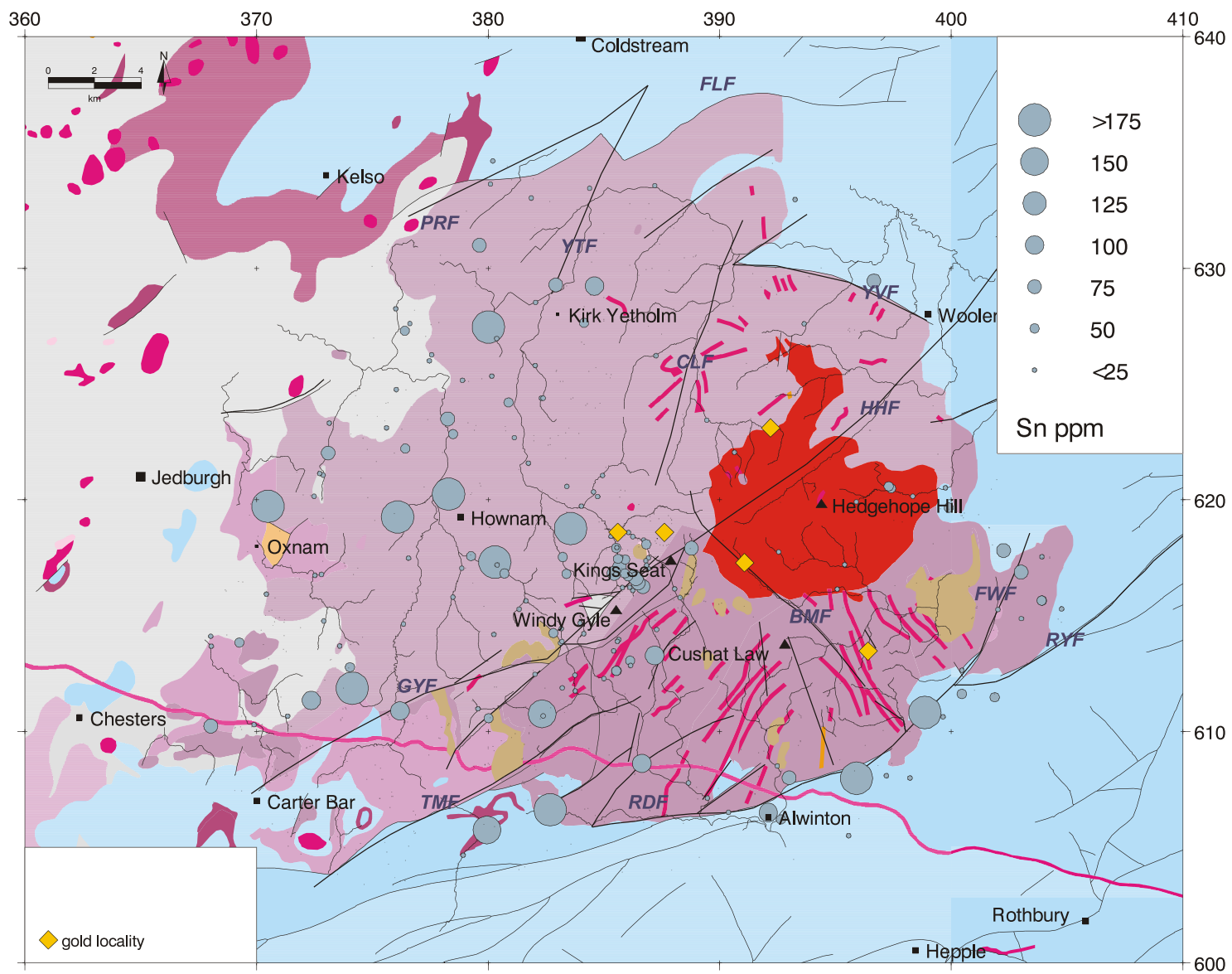


Fig 8.23 Cheviot: tin (Sn) in MRP panned concentrate data

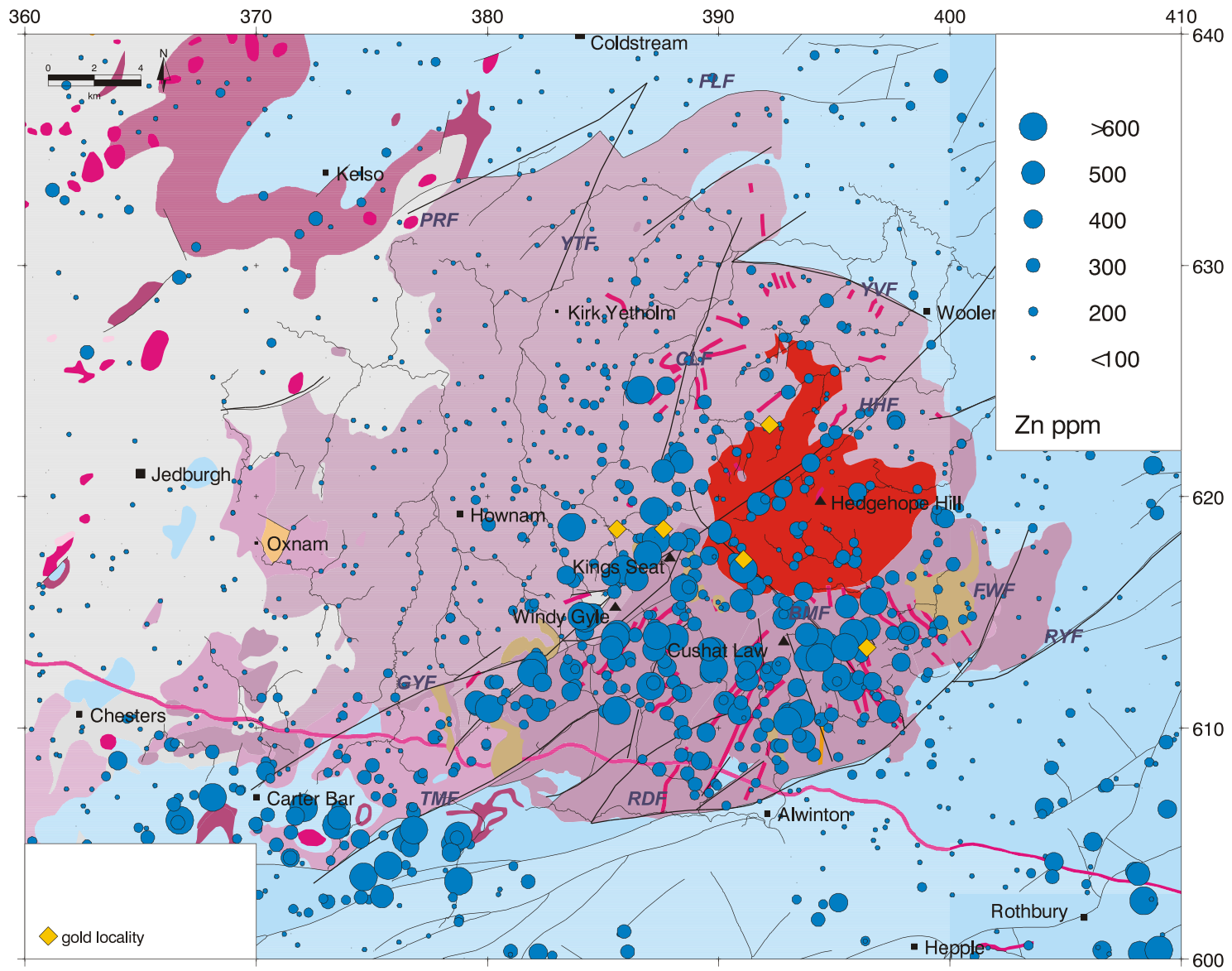


Fig 8.24 Cheviot: zinc (Zn) in G-BASE stream sediment data

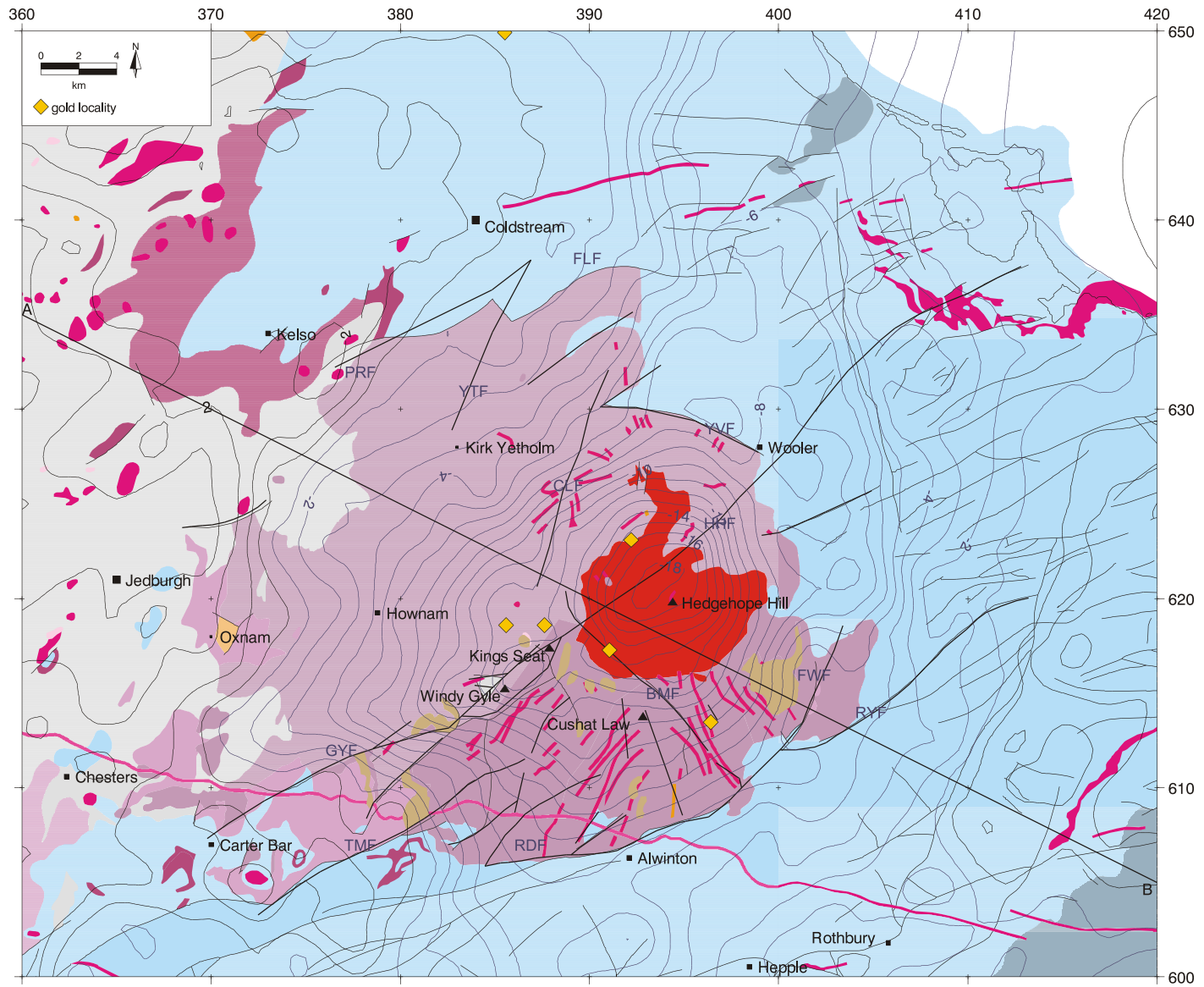


Fig 8.25 Cheviot: Bouguer gravity anomaly map.
 Line AB is the location of the 2D model profile in Figure 8.32

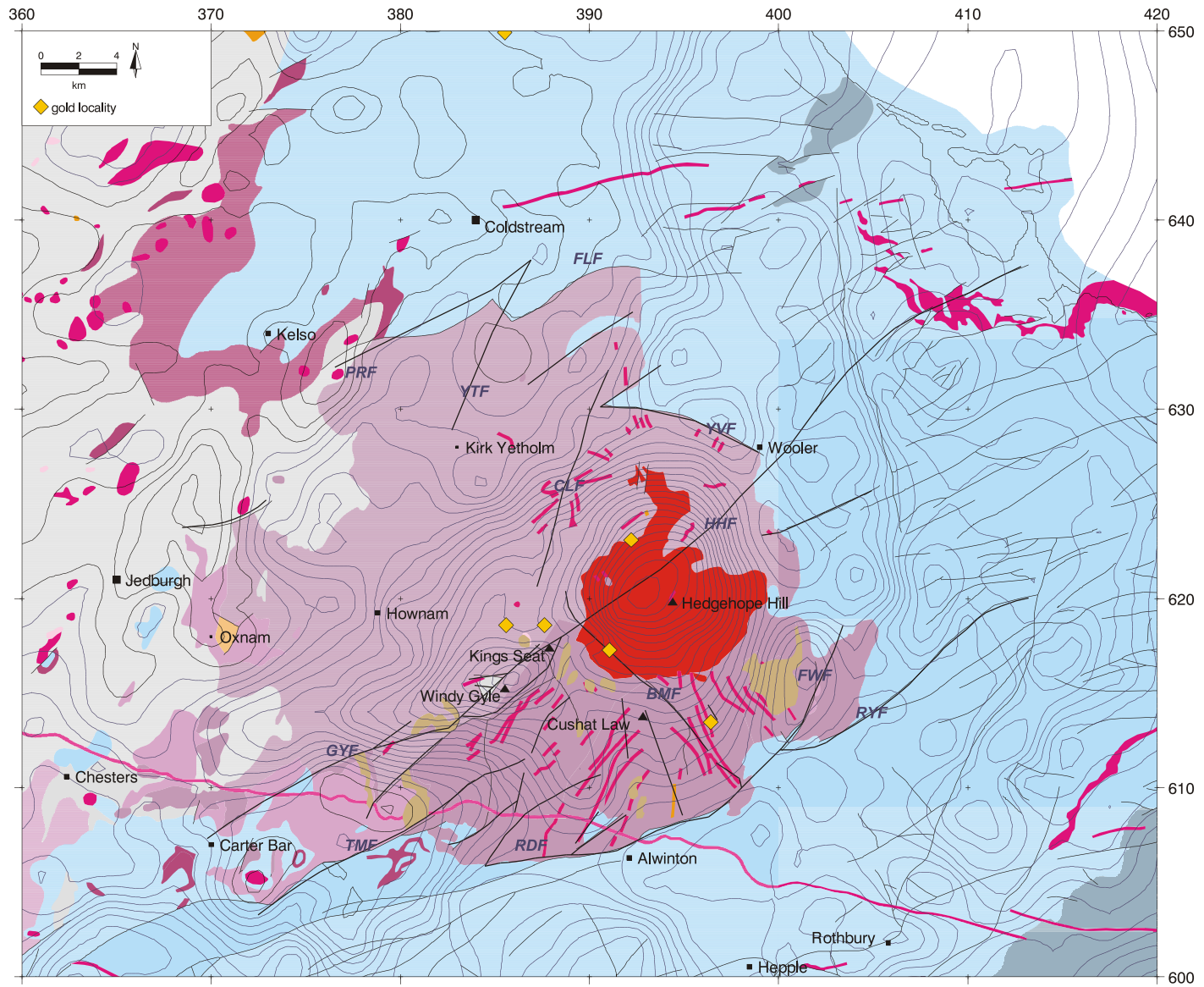


Fig 8.26 Cheviot: Residual gravity anomaly based on a continued (+5km) regional field. Contour interval 0.5 mGal

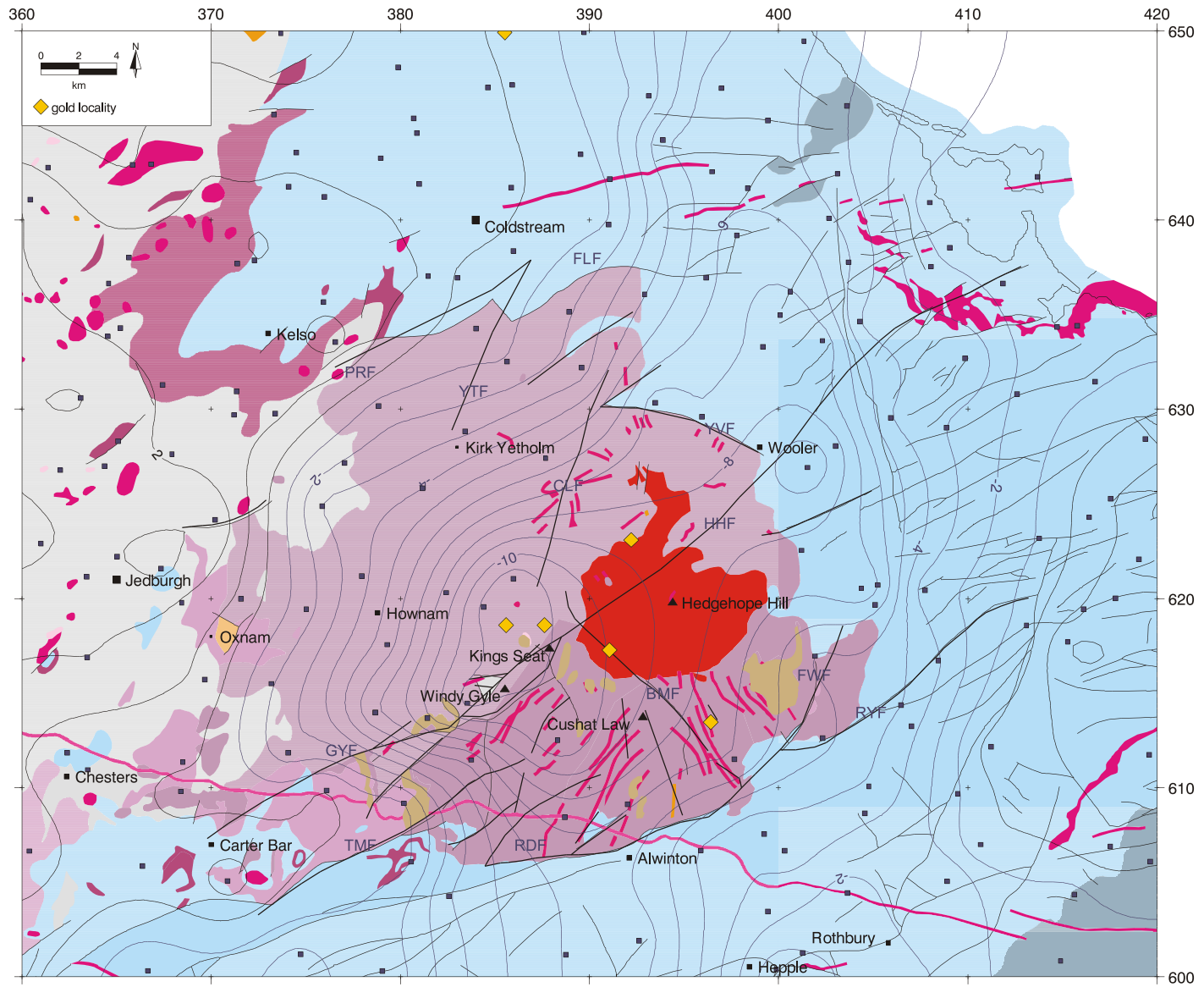


Fig 8.27 Cheviot: Regional gravity anomaly based on subsampled data away from granites. Contour interval 1.0 mGal

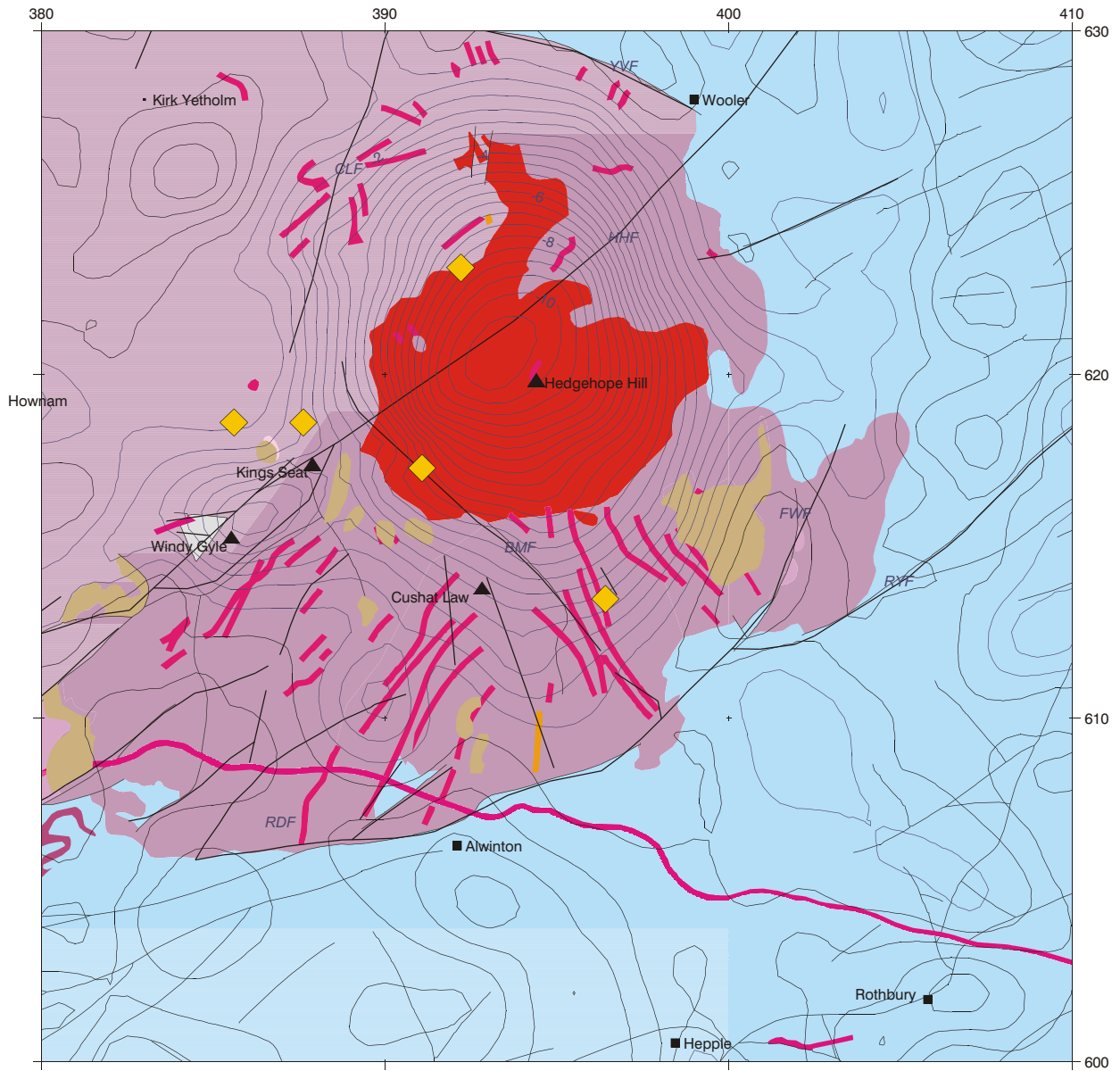


Fig 8.28 Cheviot: Residual gravity anomaly over the granite based on subsampled regional field. Contour interval 0.5 mGal

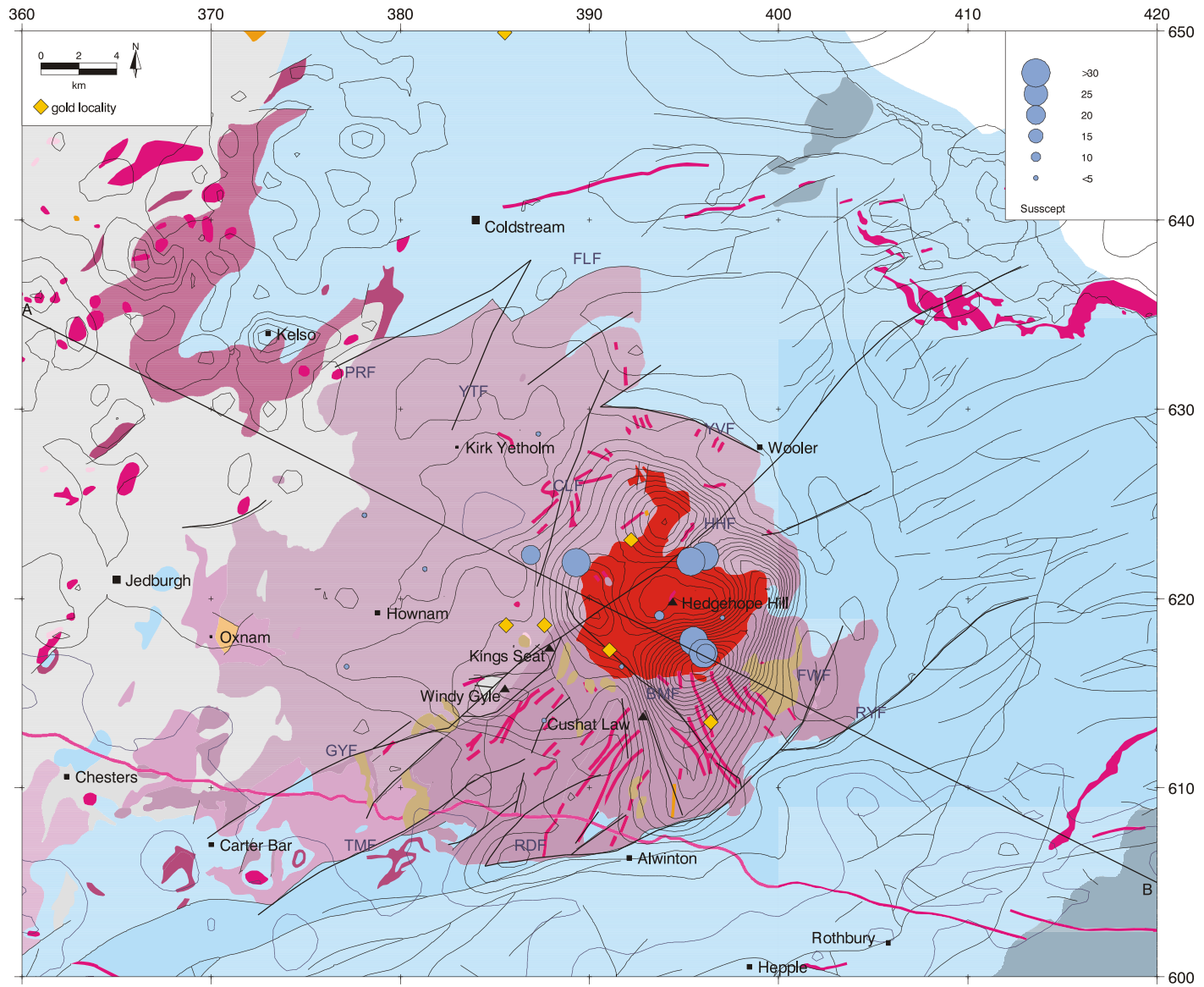


Fig 8.29 Cheviot: Total field magnetic anomaly at 305m above ground level. Contour interval 20 nT

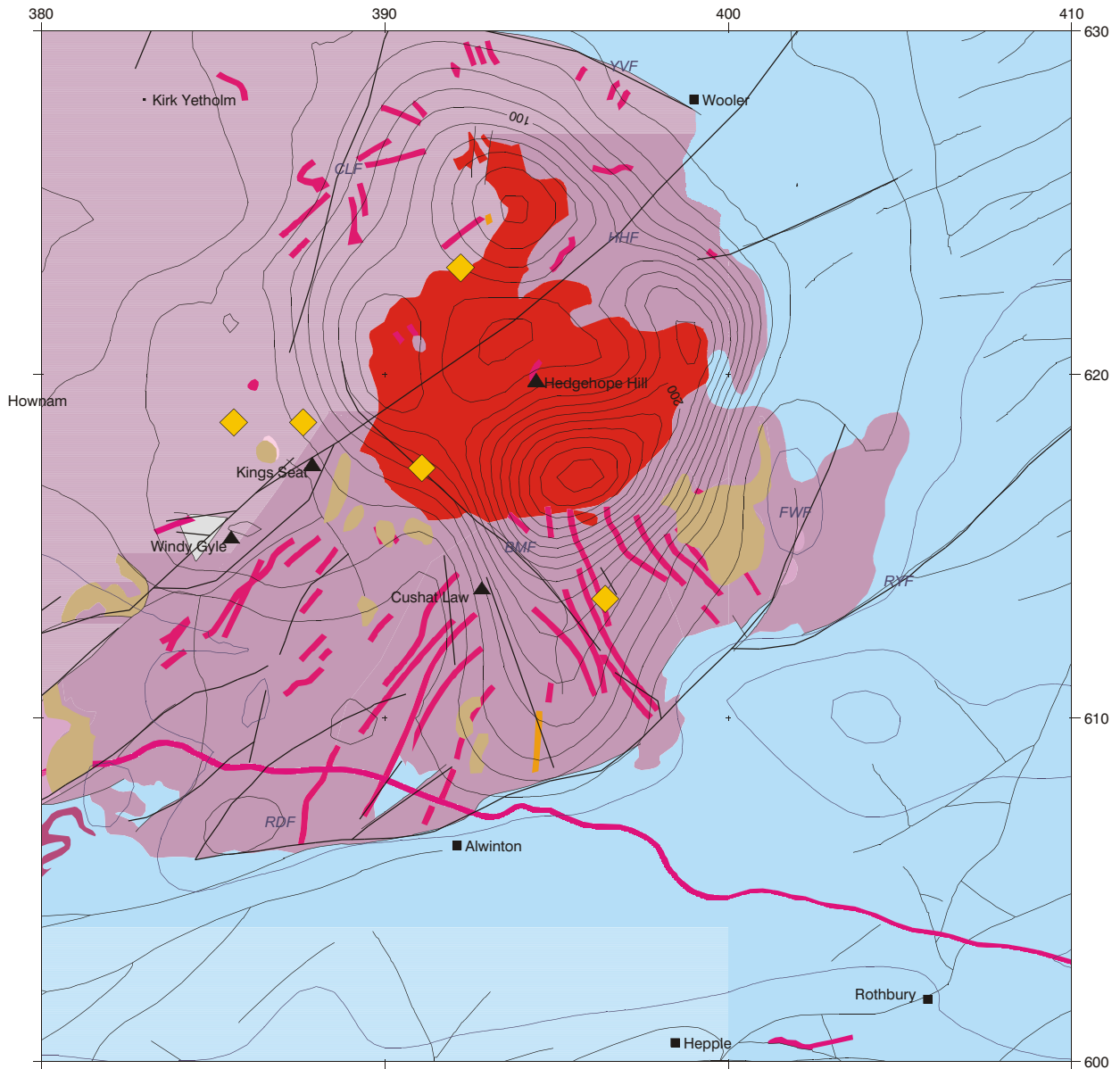


Fig 8.30 Cheviot: Polar Total field magnetic anomaly at 800m above ground level. Contour interval 20 nT

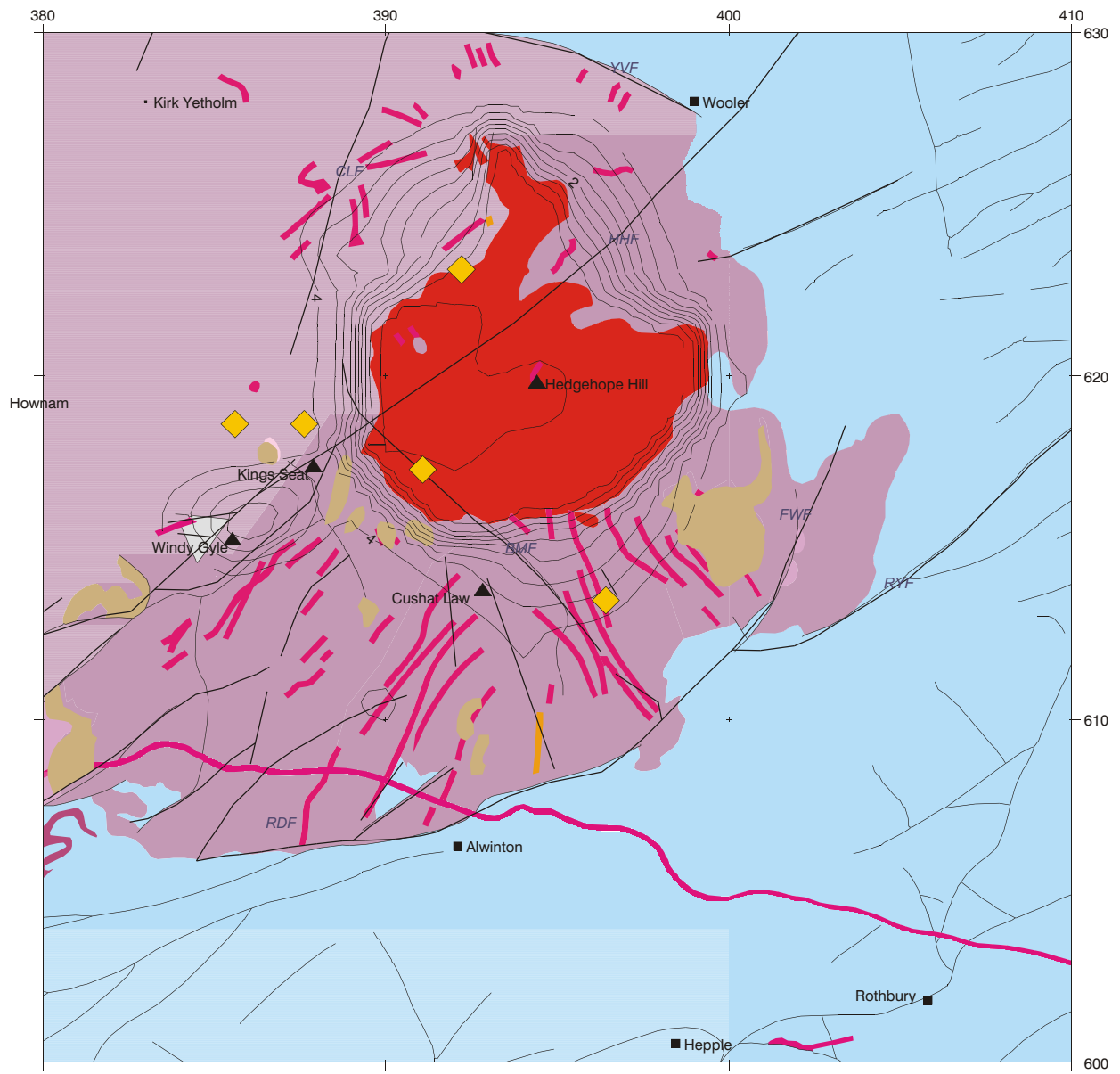


Fig 8.31 Cheviot: modelled depth (km) to the top of the granite
Contour interval 0.5 km

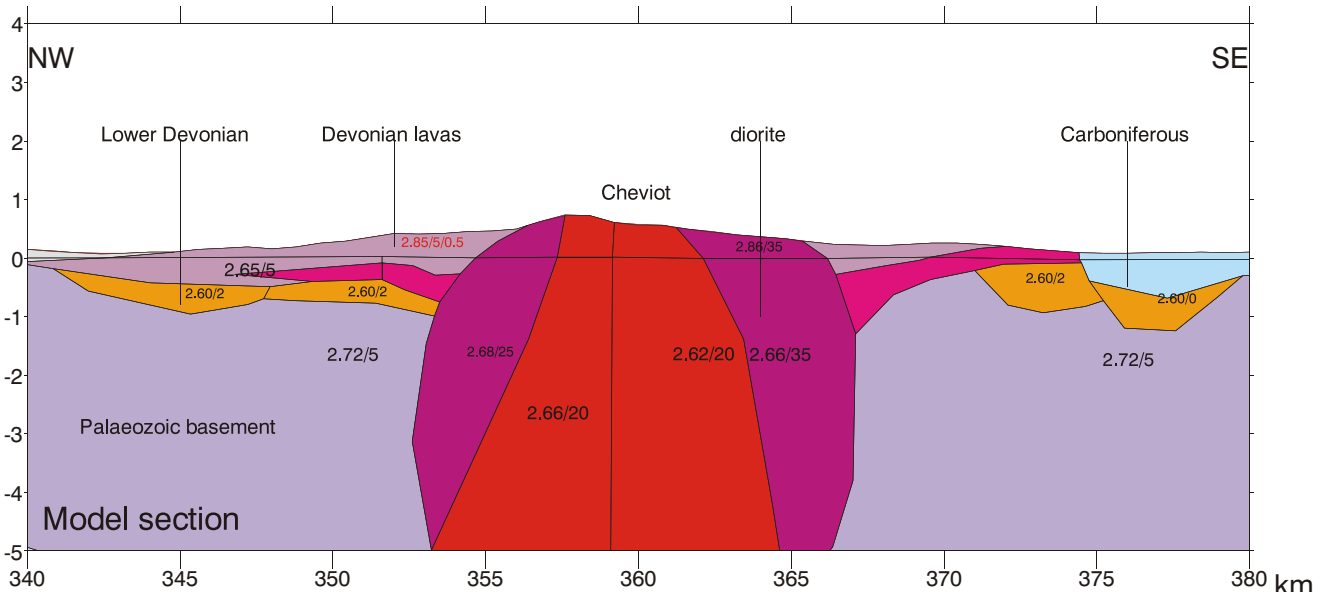
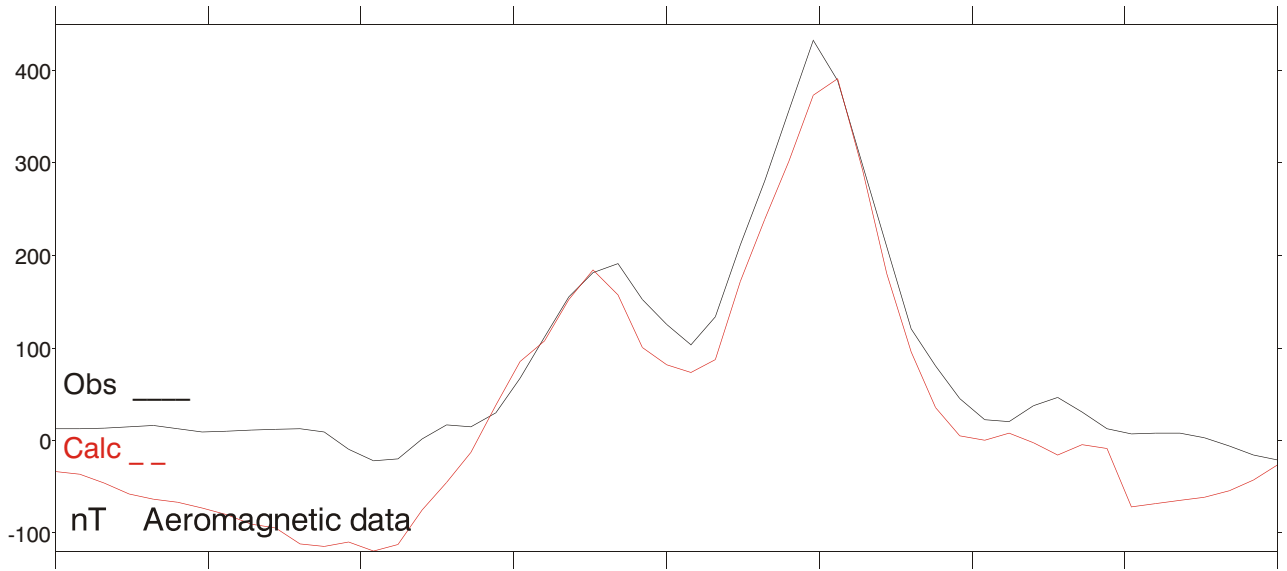
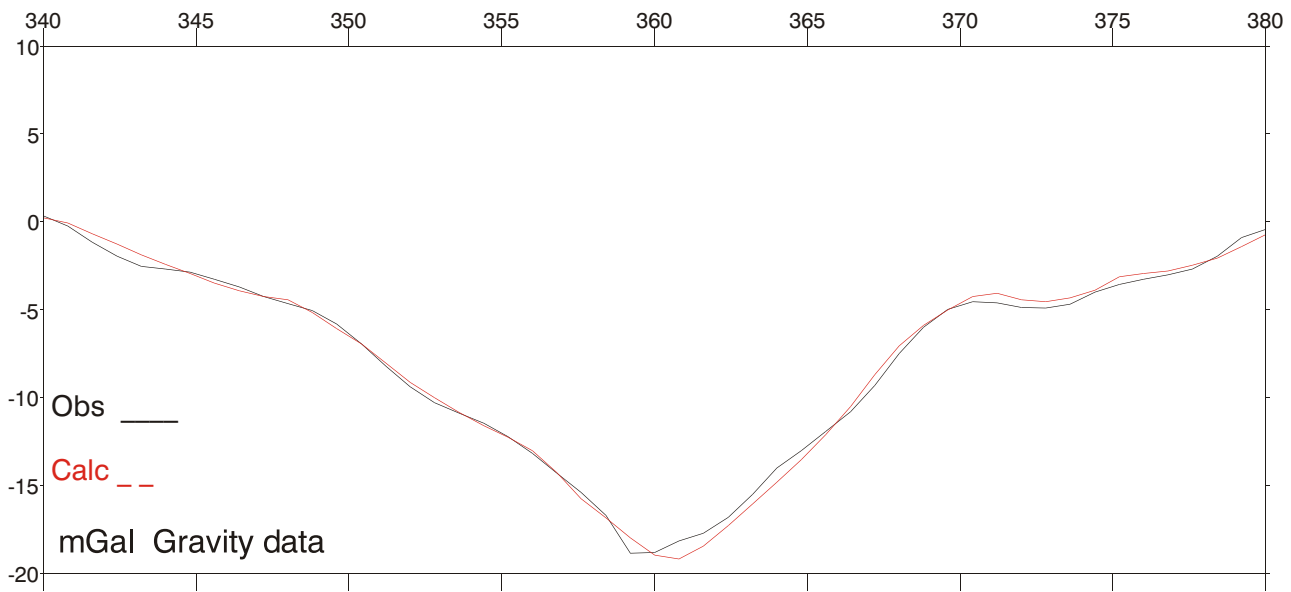


Fig 8.32 Cheviot: part of a 2D NW-SE section through the granite and lava field.
Line of section is shown in Figure 8.25

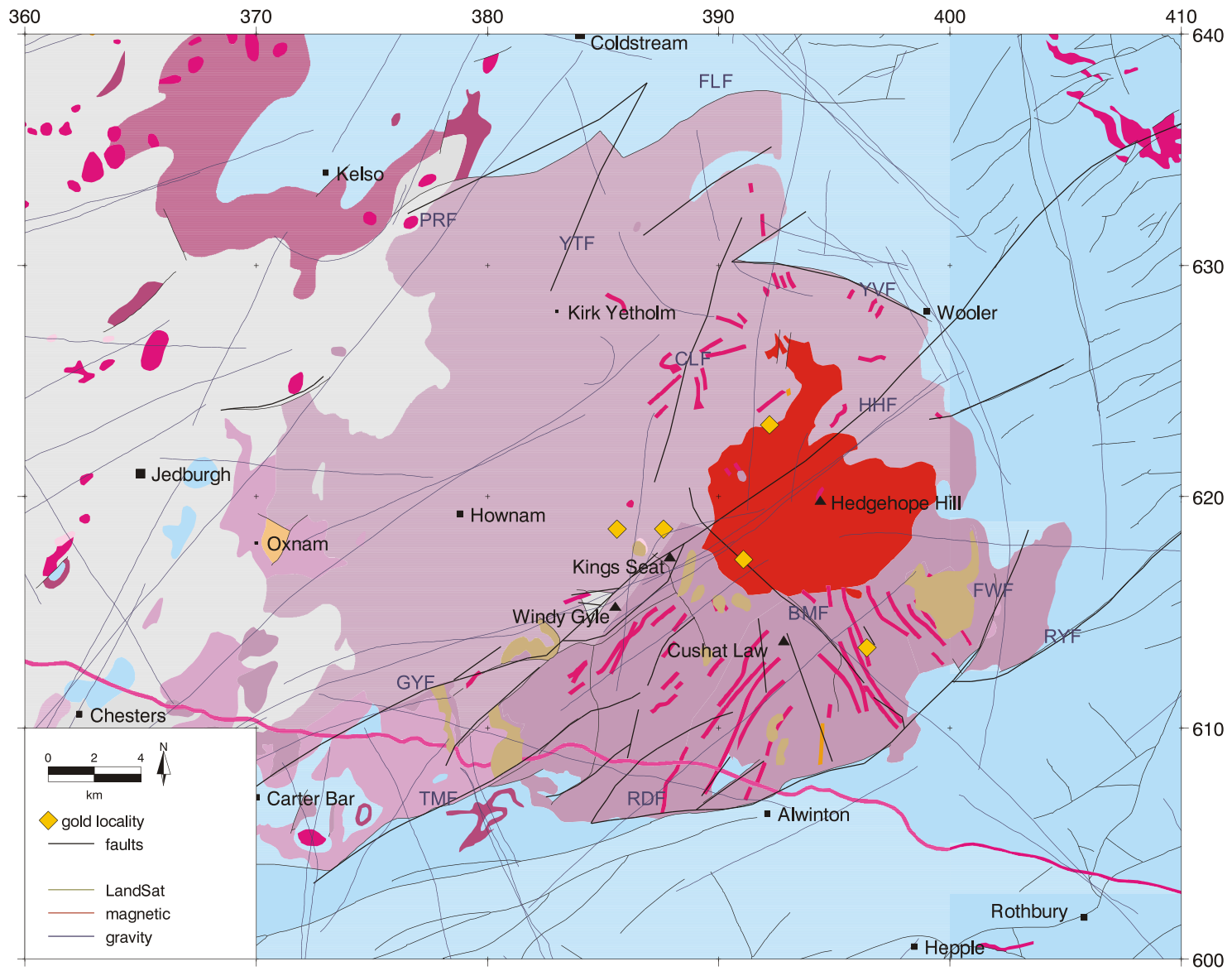


Fig 8.33 Cheviot: Gravity lineaments

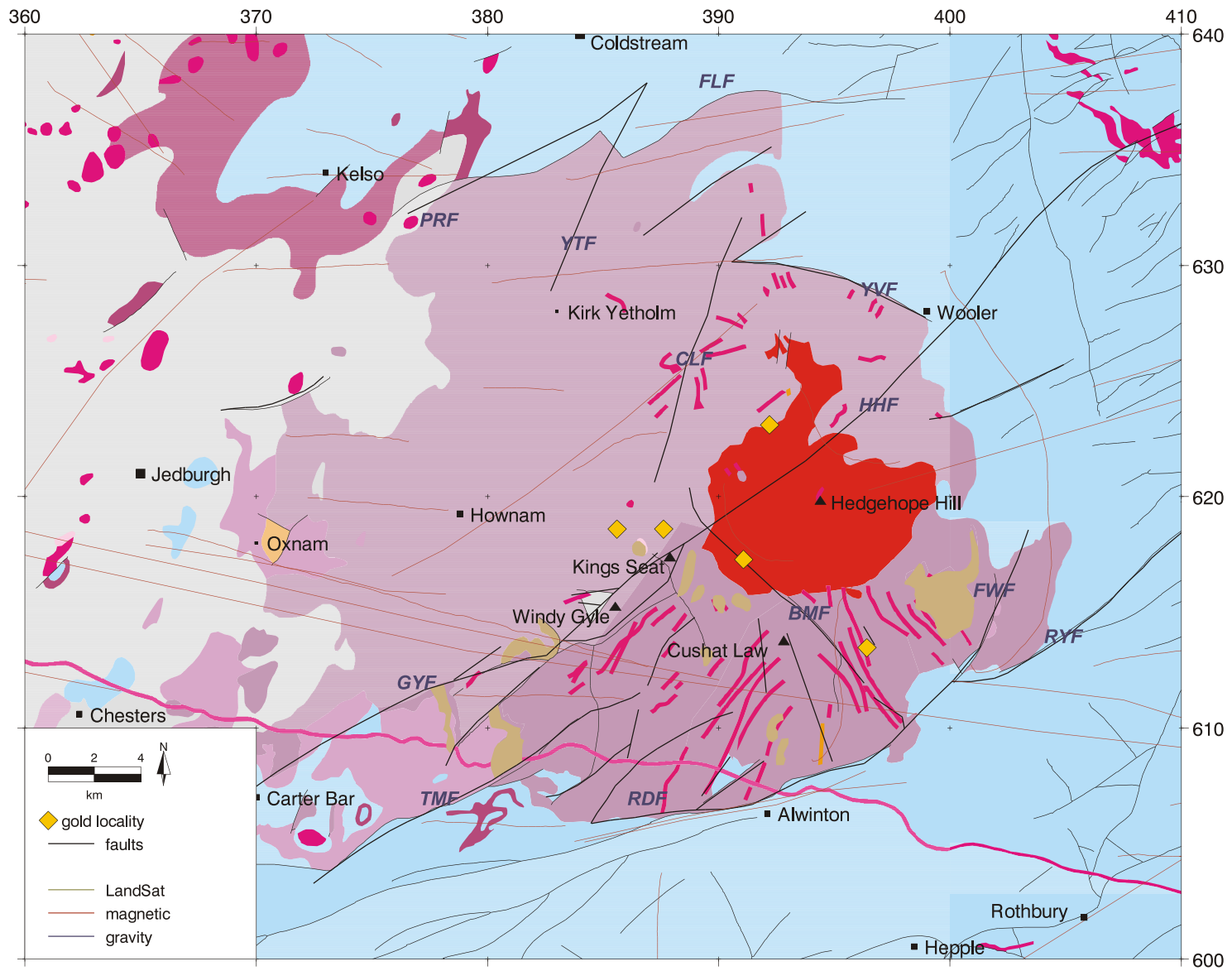


Fig 8.34 Cheviot: Magnetic lineaments

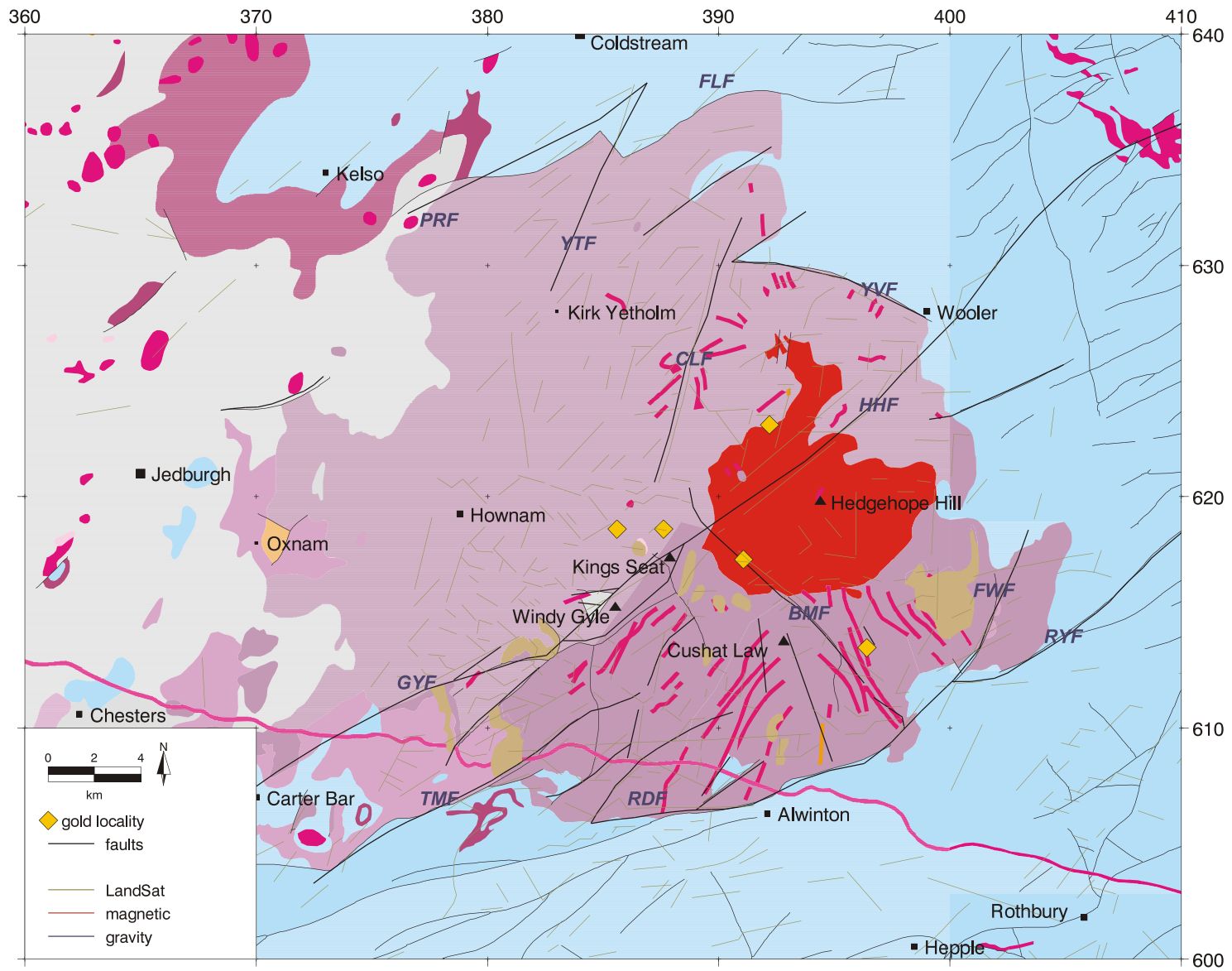


Fig 8.35 Cheviot: Landsat TM lineaments

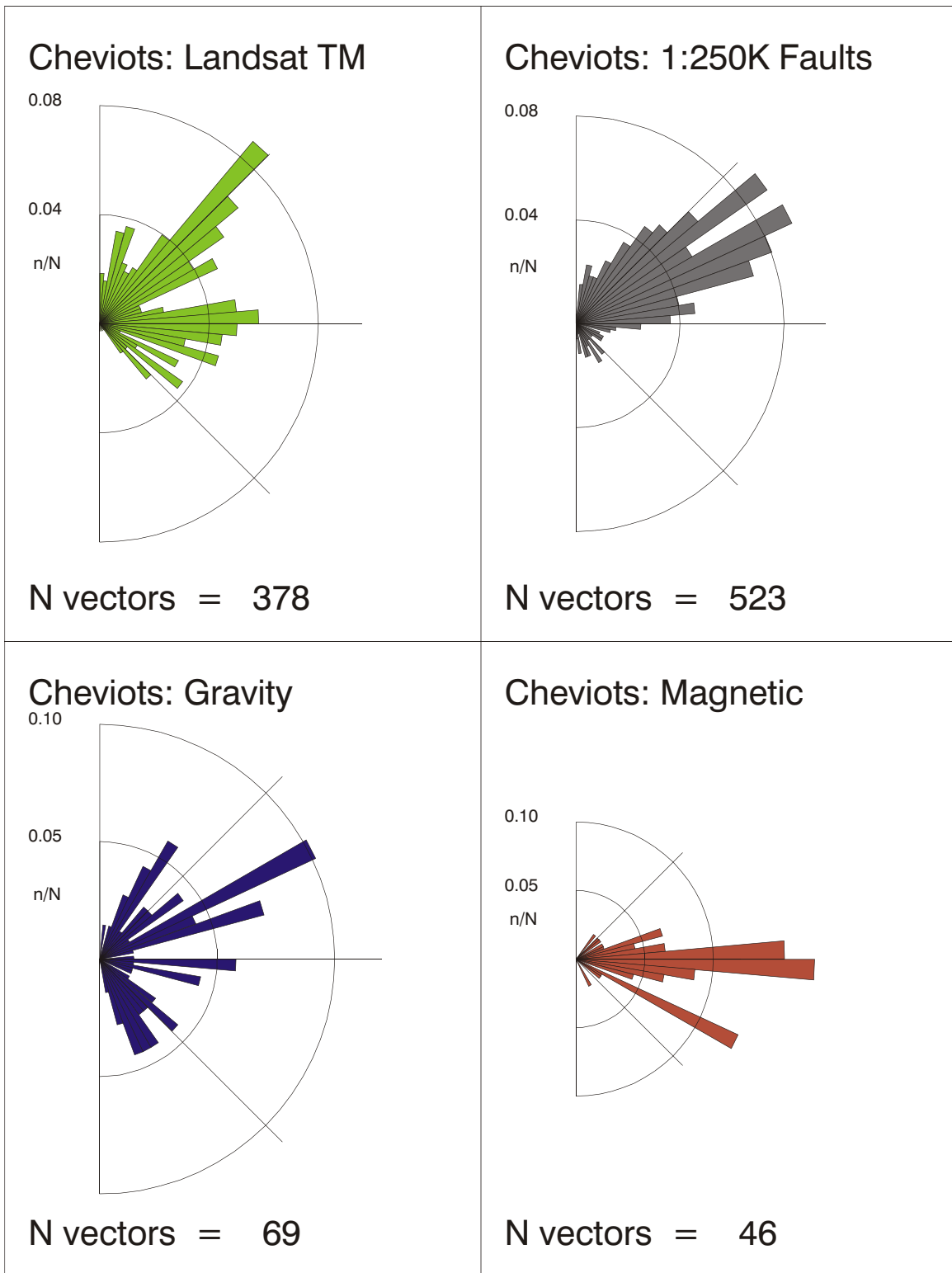


Fig 8.36 Azimuthal frequency plots for lineaments in the Cheviot region

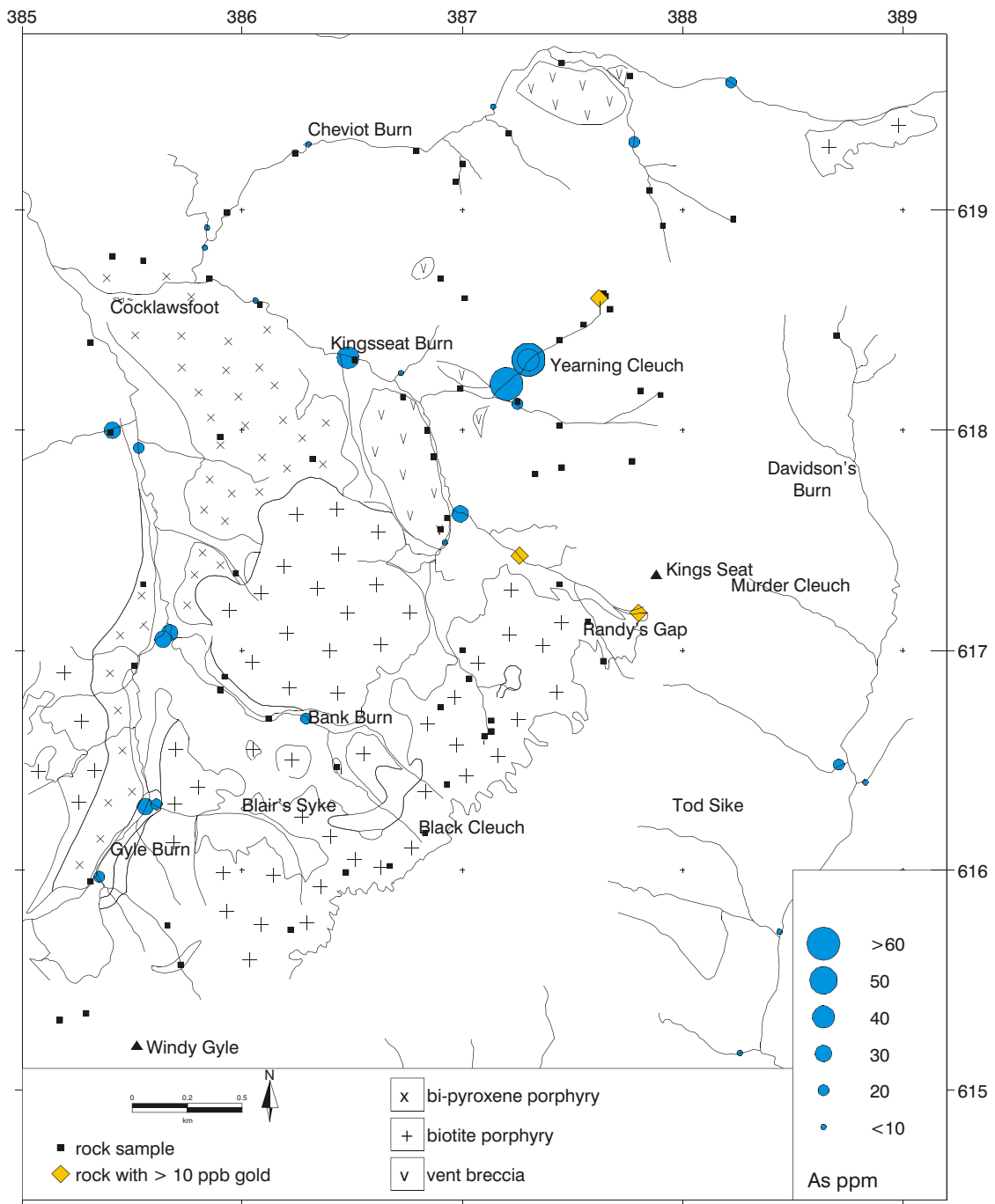


Fig 8.37 Kingsseat Burn: arsenic (As) in MRP stream sediment data

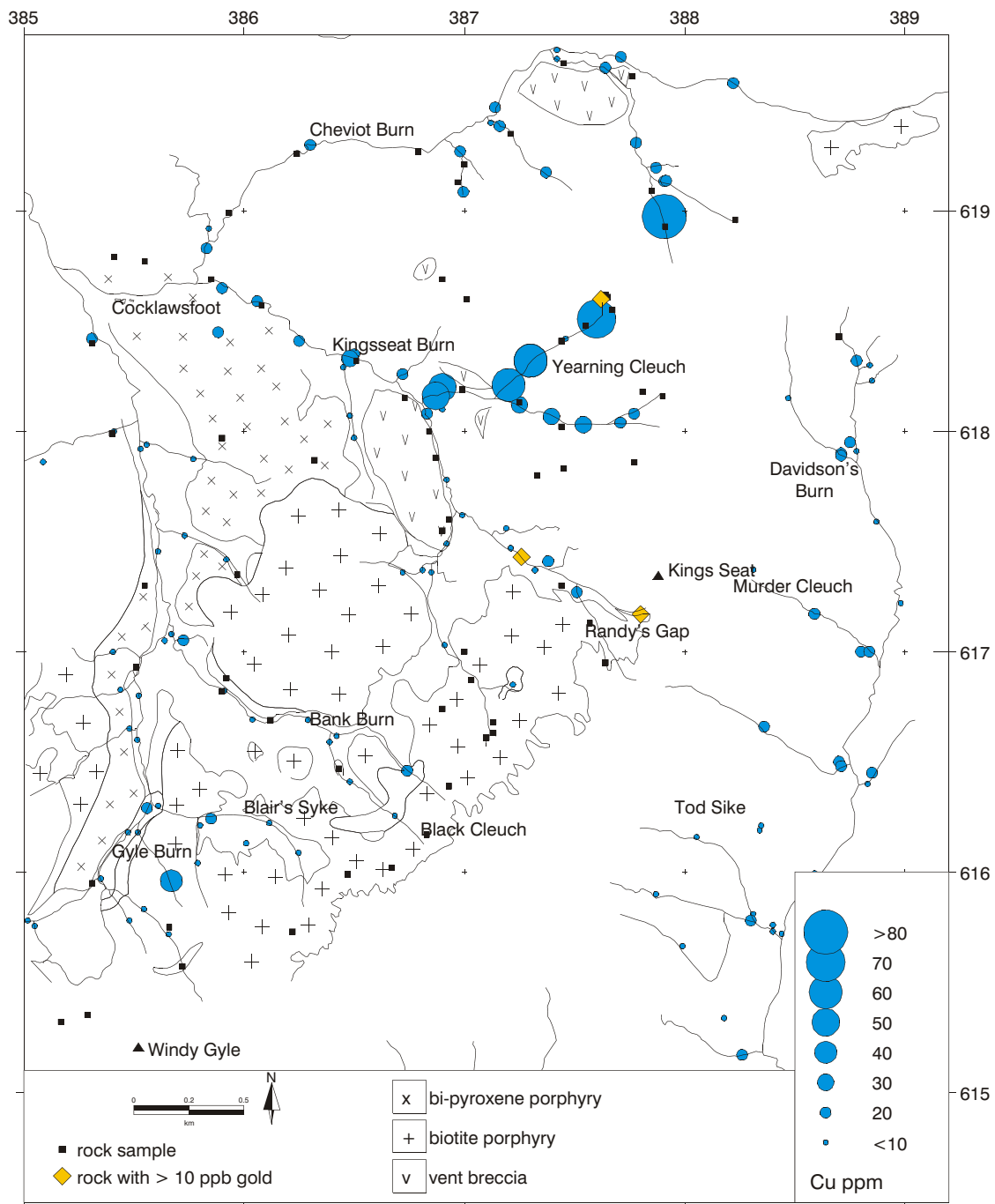


Fig 8.38 Kingsseat Burn: copper (Cu) in MRP stream sediment data

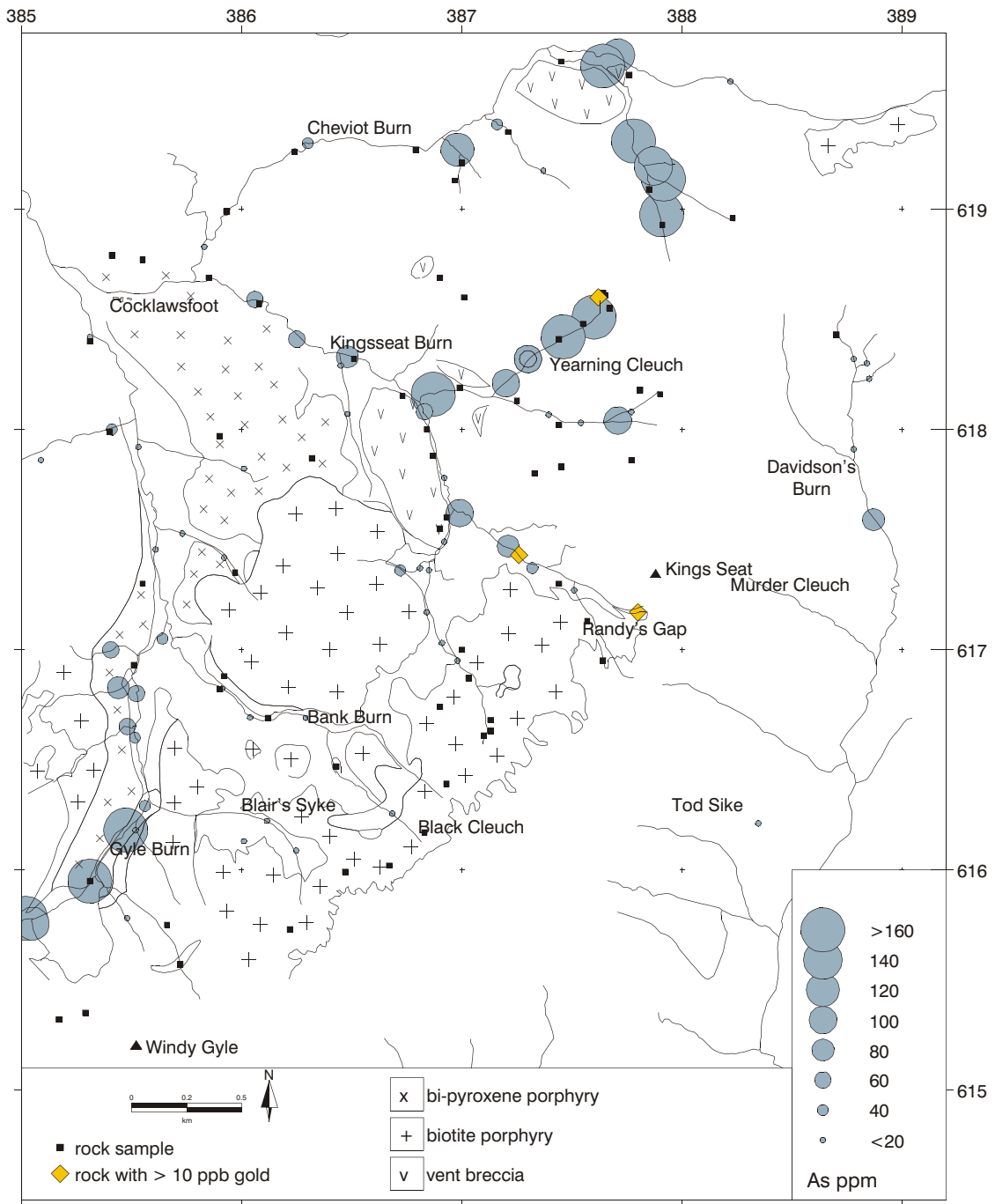


Fig 8.39 Kingsseat Burn: arsenic (As) in MRP panned concentrate data

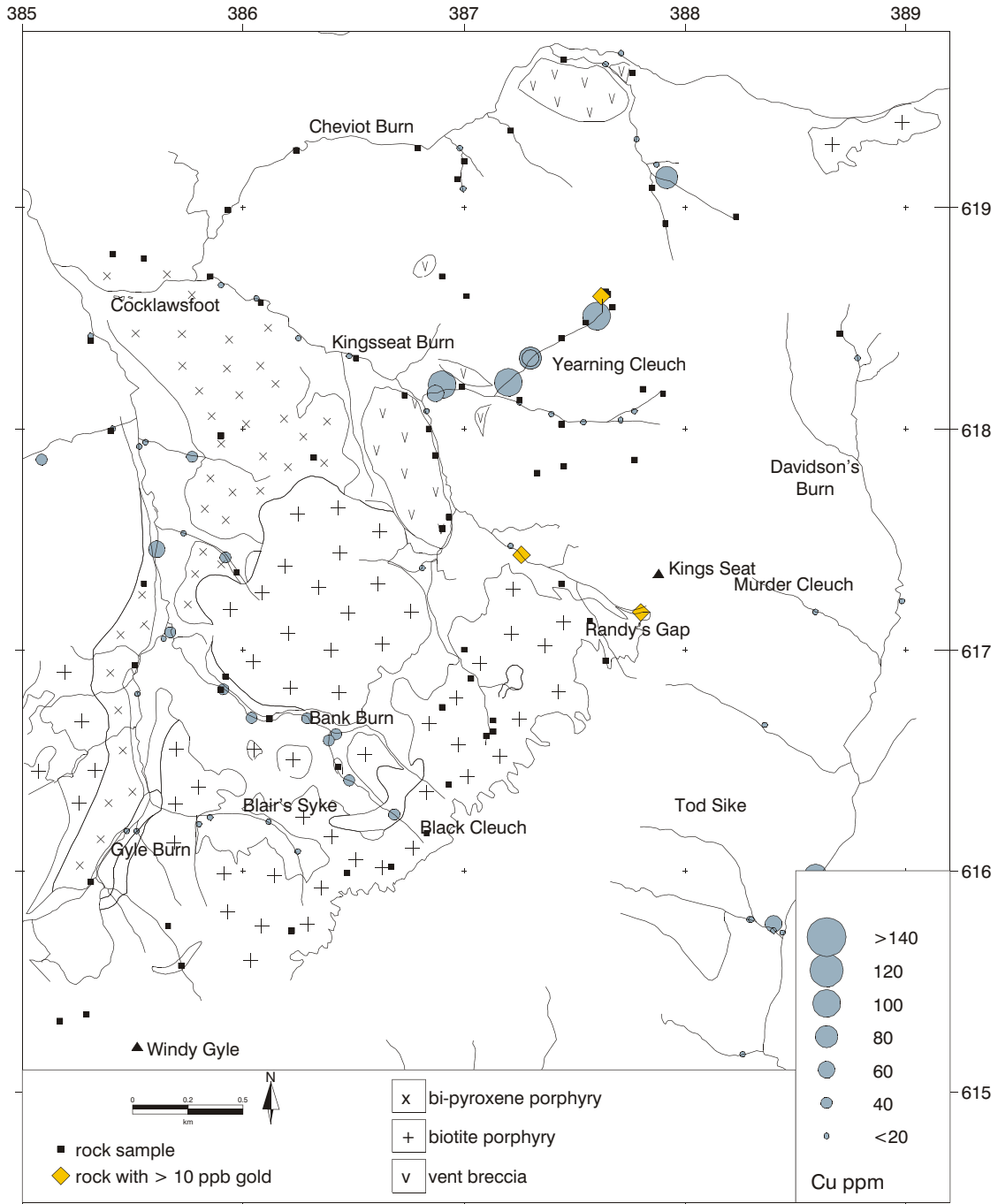


Fig 8.40 Kingsseat Burn: copper (Cu) in MRP panned concentrate data

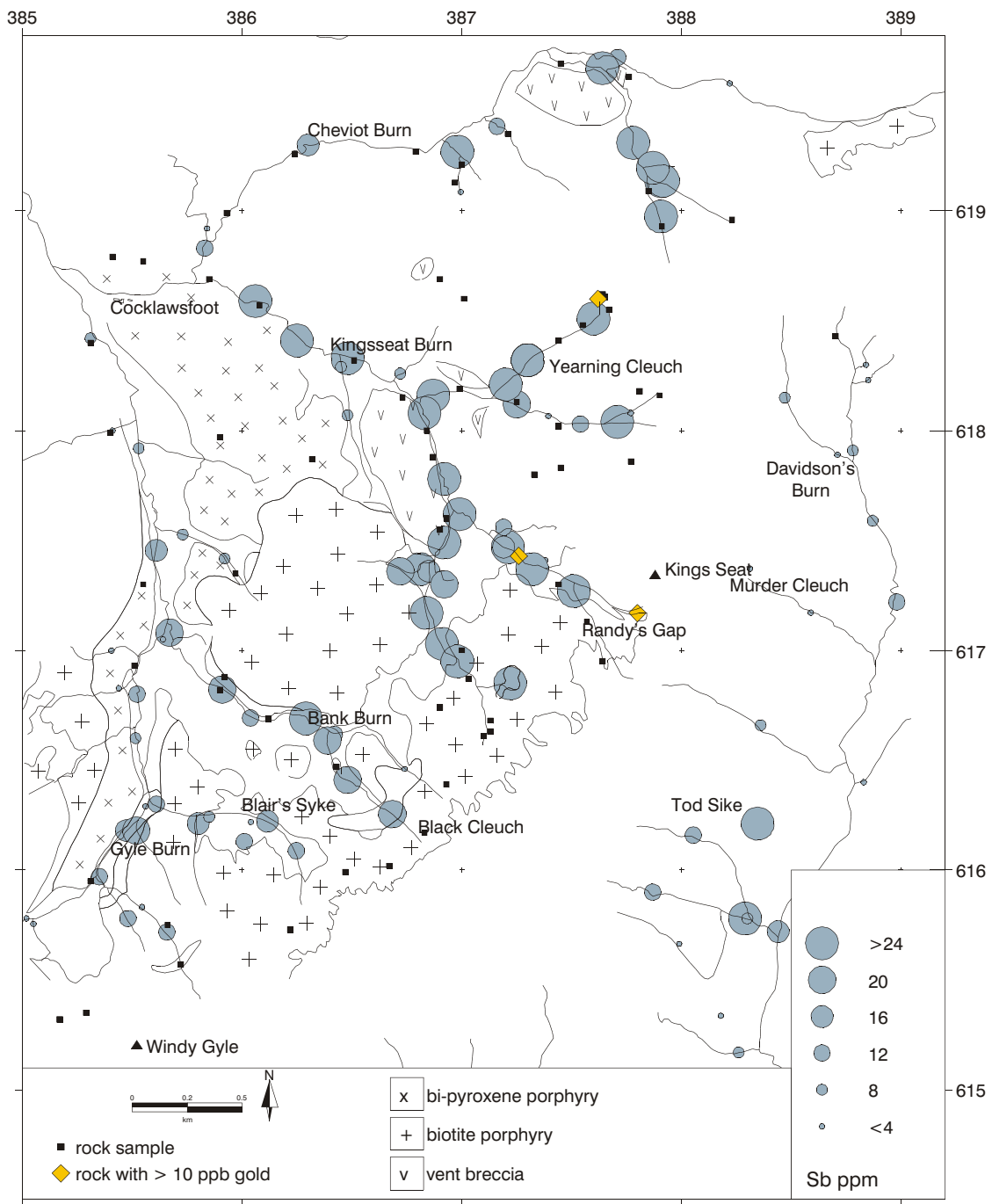


Fig 8.41 Kingsseat Burn: antimony (Sb) in MRP panned concentrate data

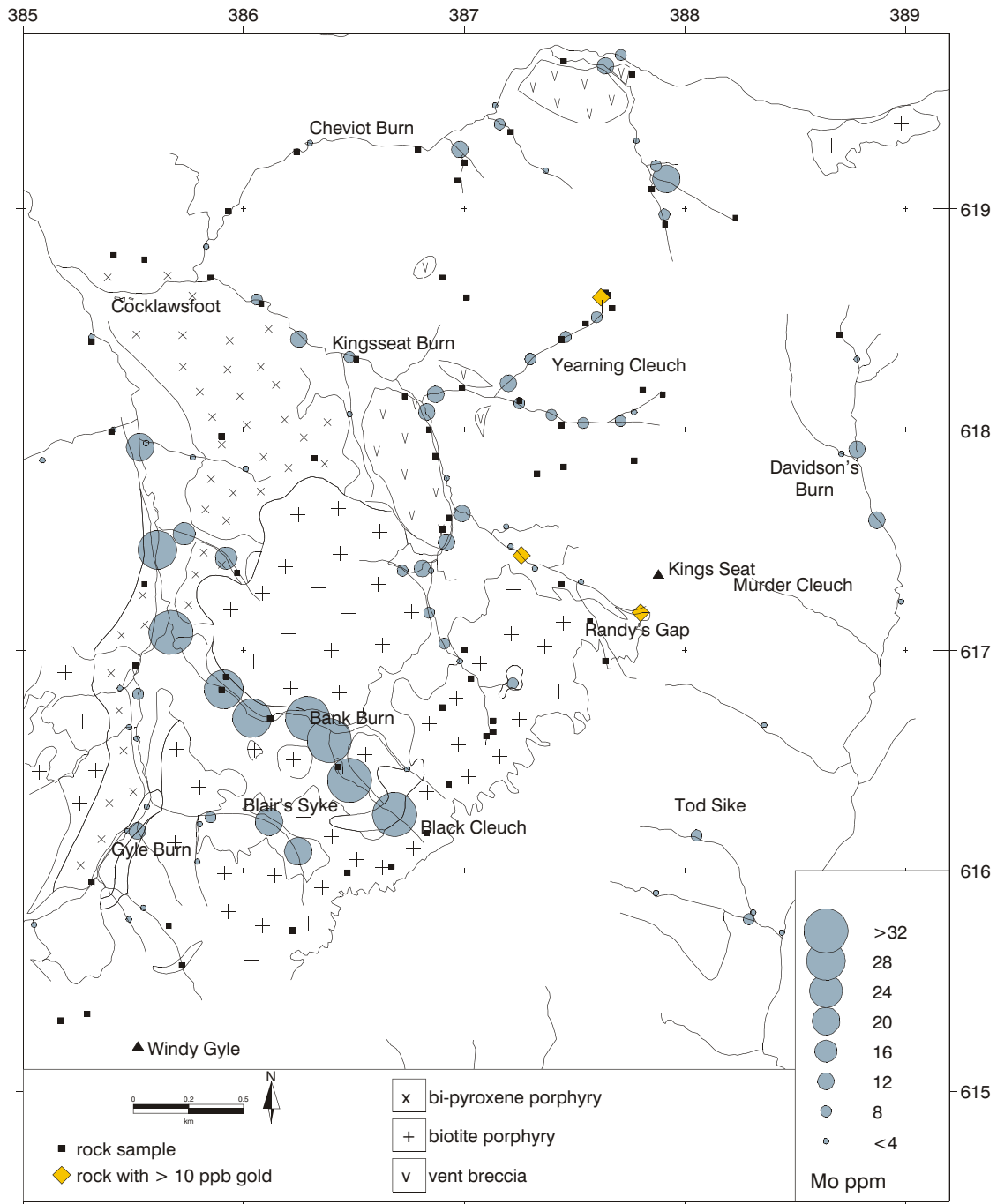


Fig 8.42 Kingsseat Burn: molybdenum (Mo) in MRP panned concentrate data

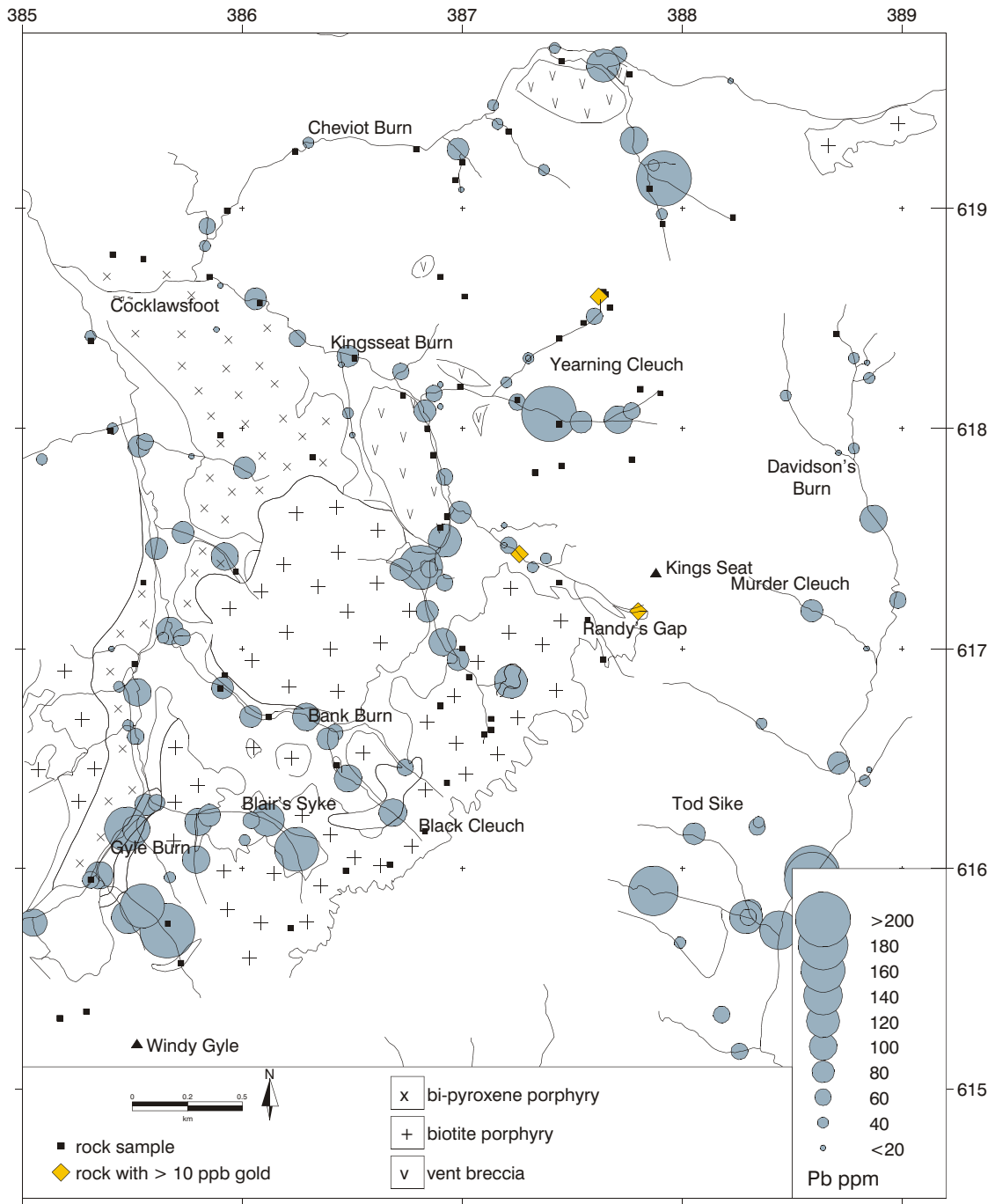


Fig 8.43 Kingsseat Burn: lead (Pb) in MRP panned concentrate data

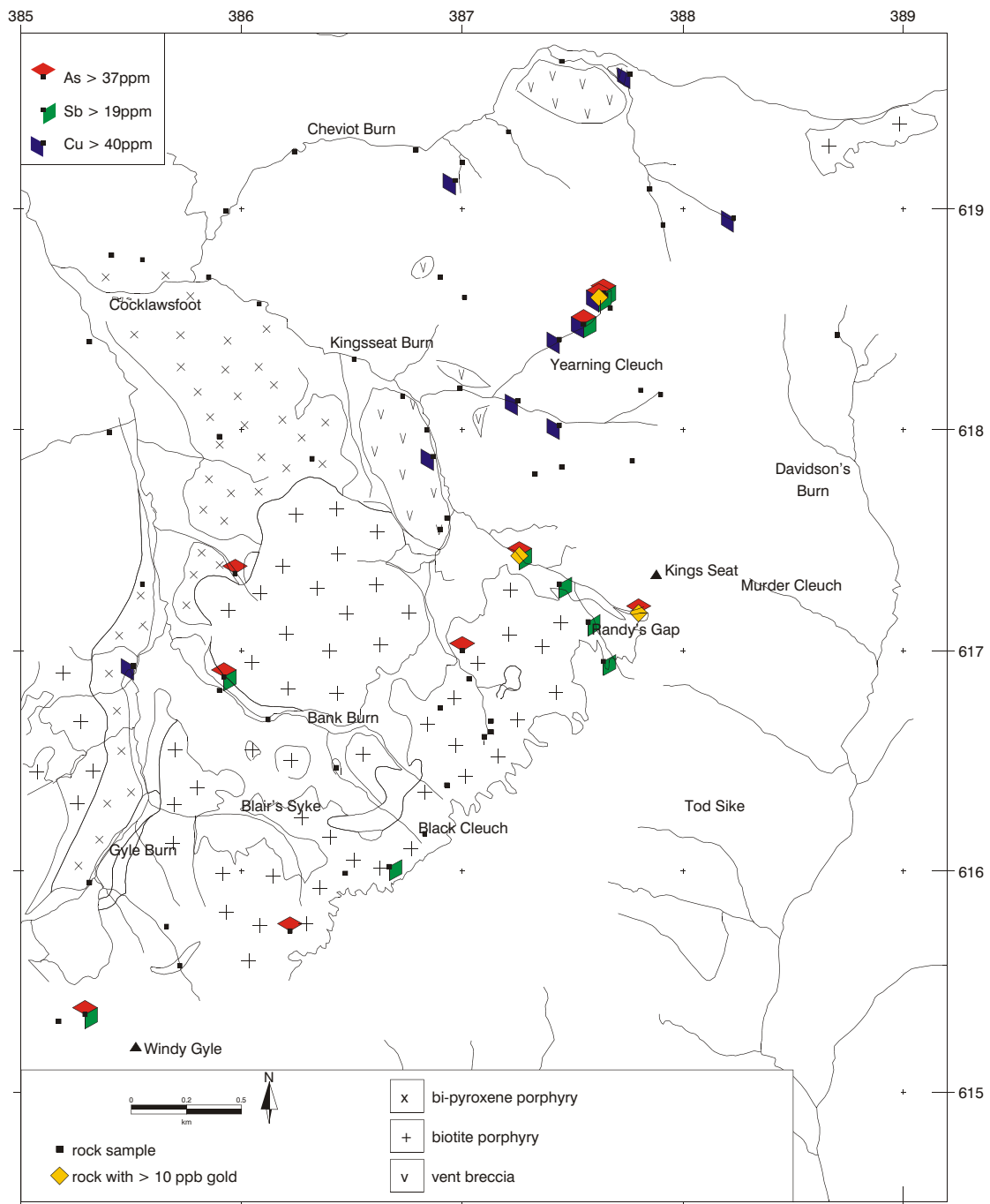


Fig 8.44 Kingsseat Burn: distribution of anomalous values of Au, As, Sb and Cu in rock samples

Figure 8.46 Kingsseat Burn: summary of alteration minerals in rock samples identified by the Spectral Geologist. Magnetic susceptibility values (10^{-3} SI) are also shown.

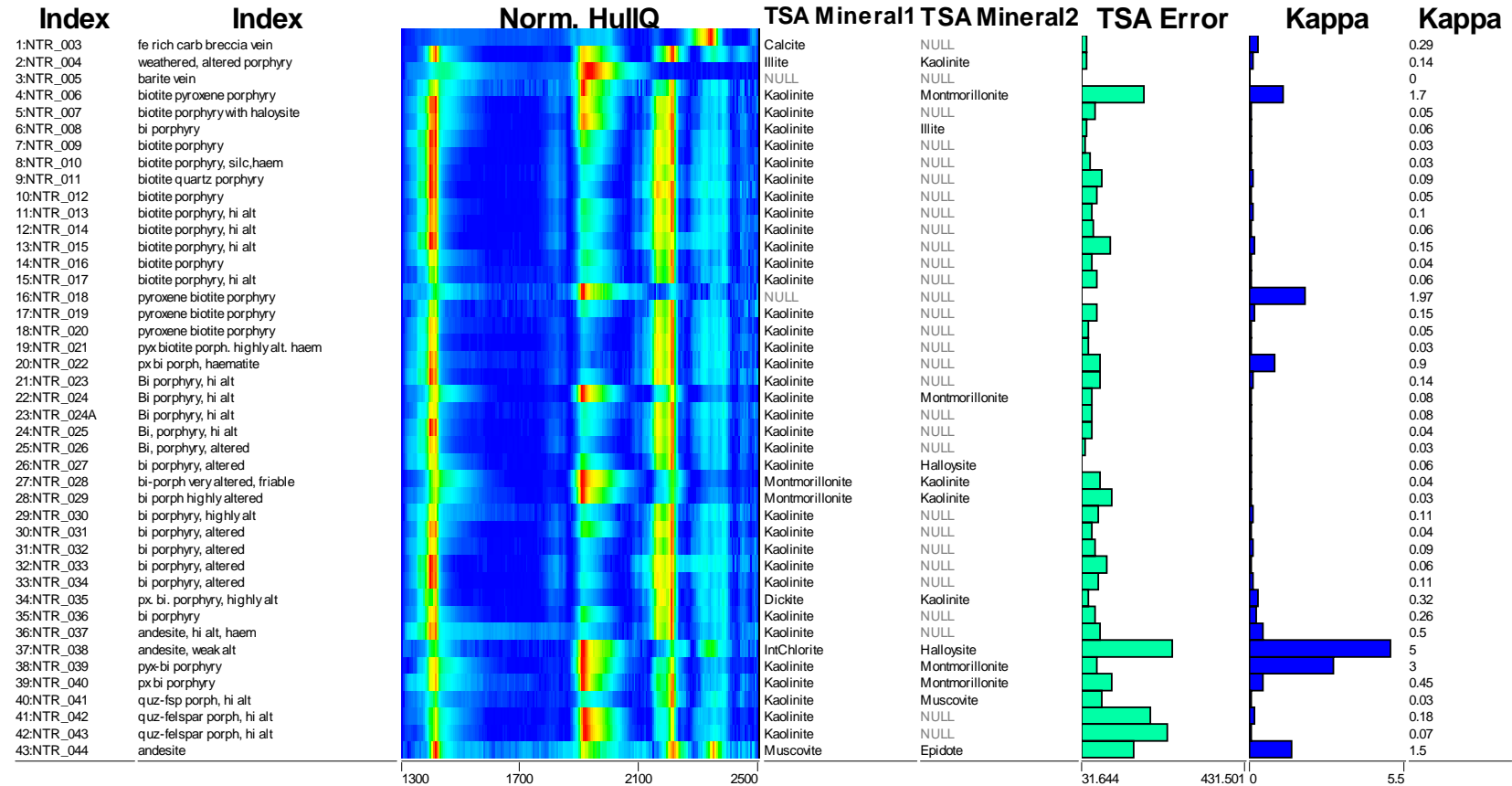
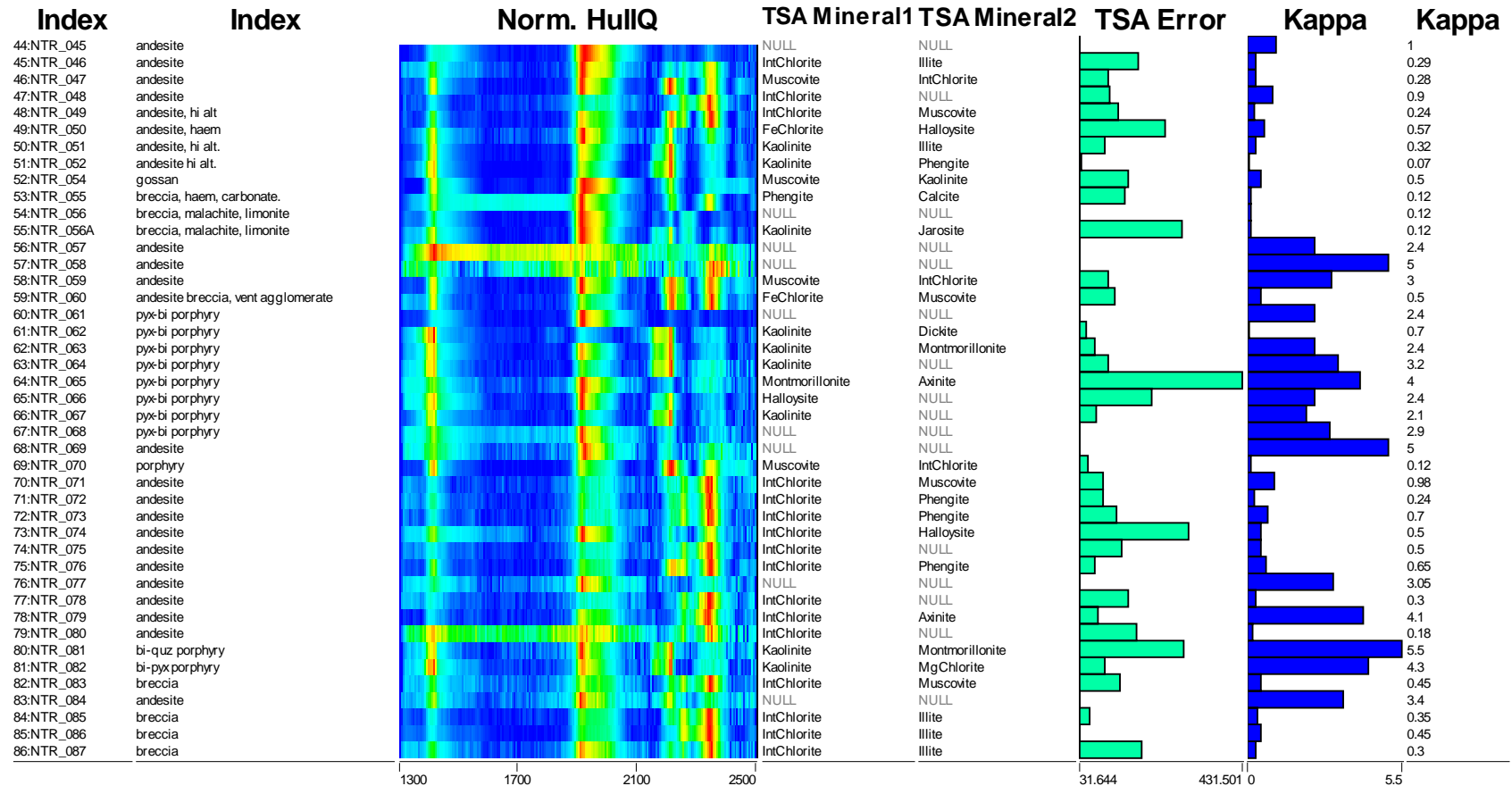


Figure 8.46 Kingsseat Burn: summary of alteration minerals in rock samples identified by the Spectral Geologist. Magnetic susceptibility values (10^{-3} SI) are also shown.



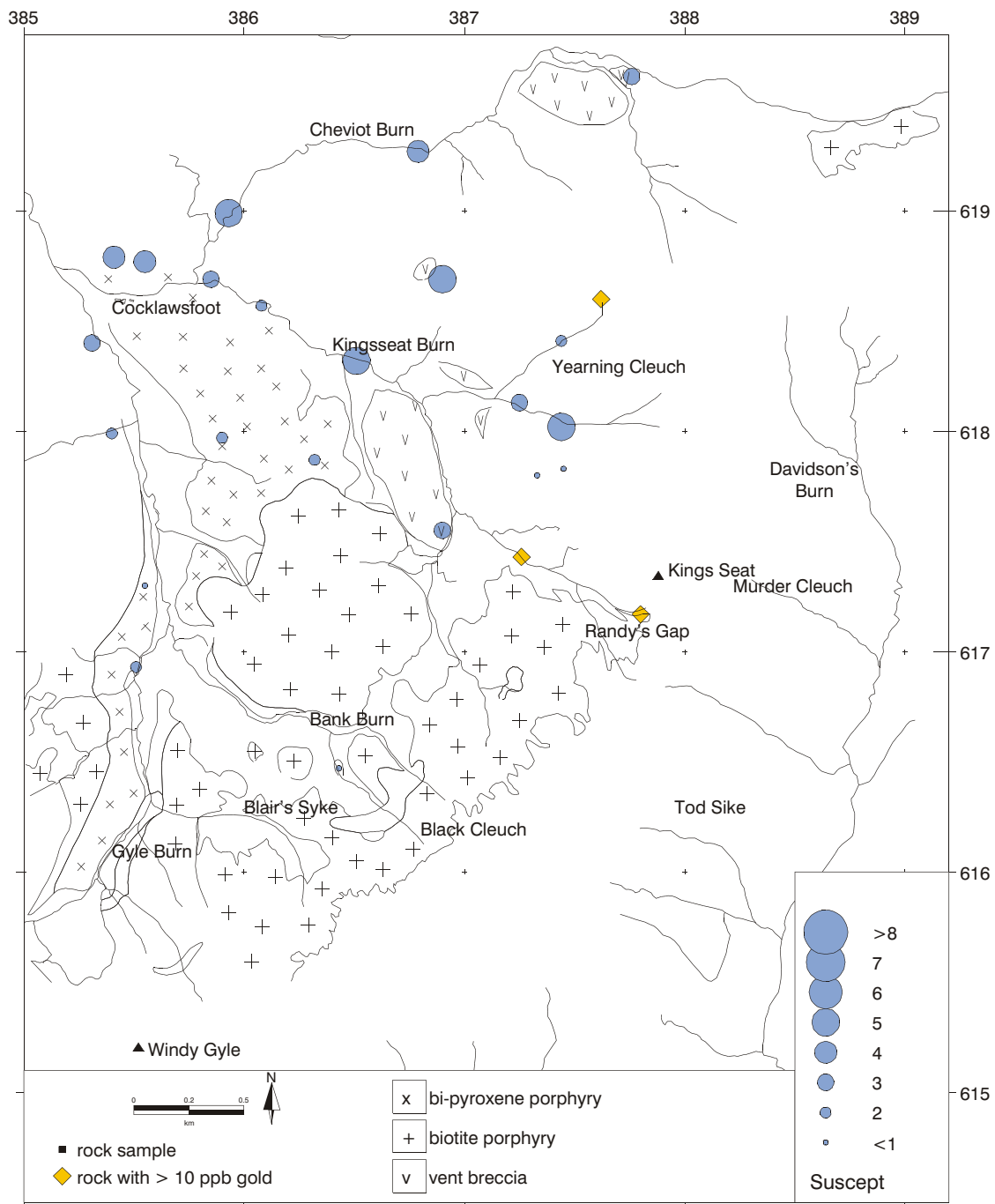


Fig 8.47 Kingsseat Burn: distribution of magnetic susceptibility in rock samples

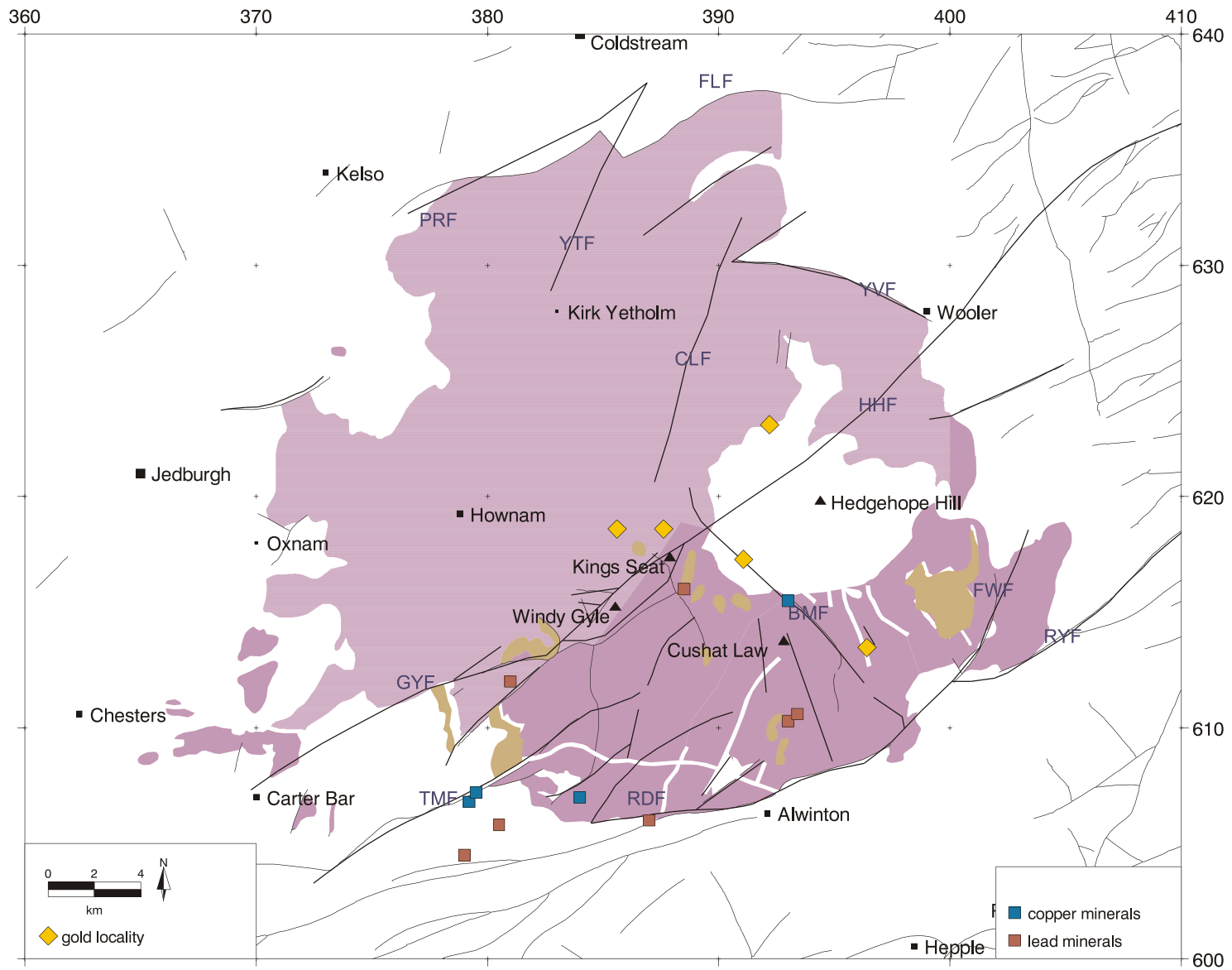


Fig 8.48 Cheviot: selected geological data for prospectivity analysis

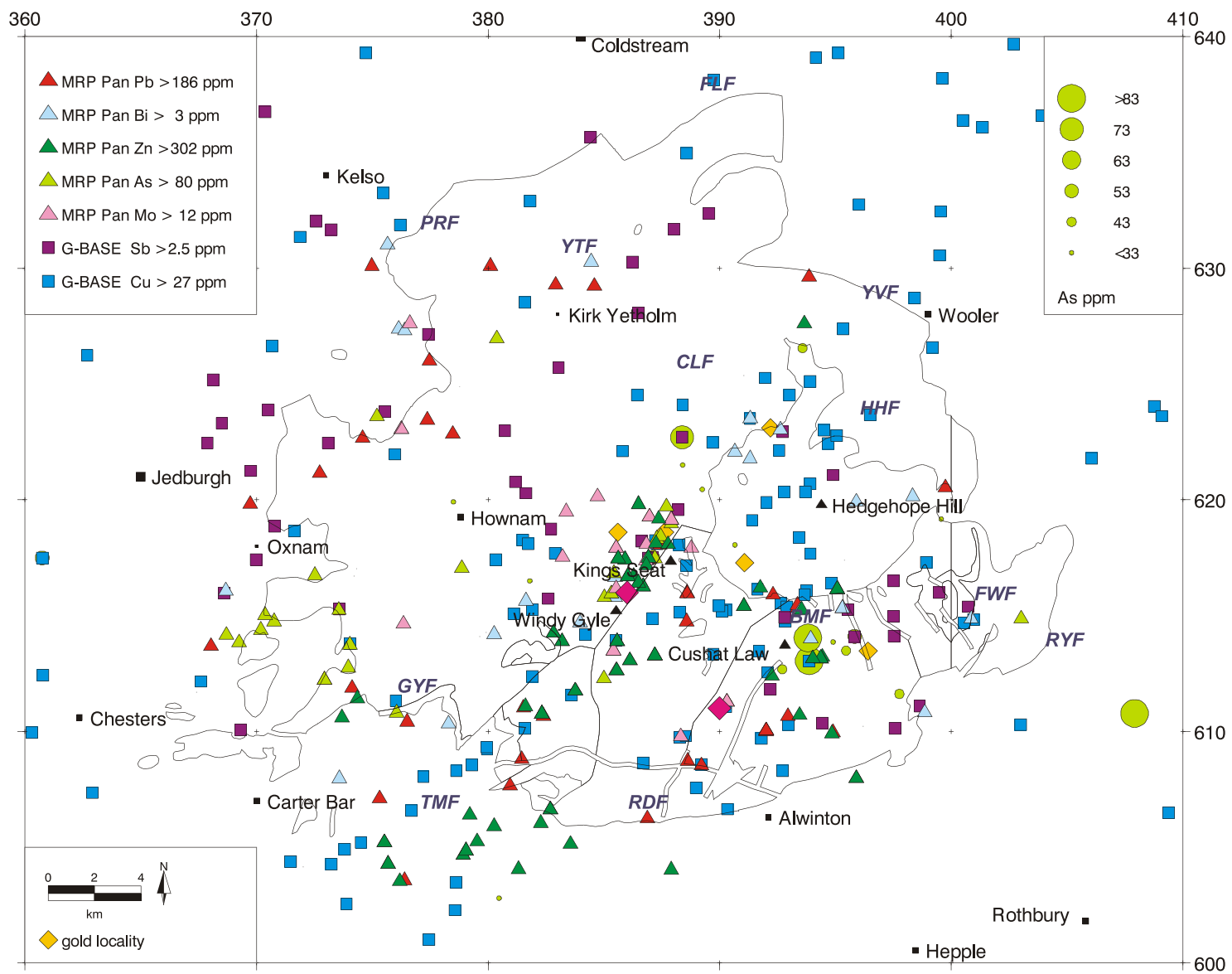


Fig 8.49 Cheviot: selected geochemical data for prospectivity analysis

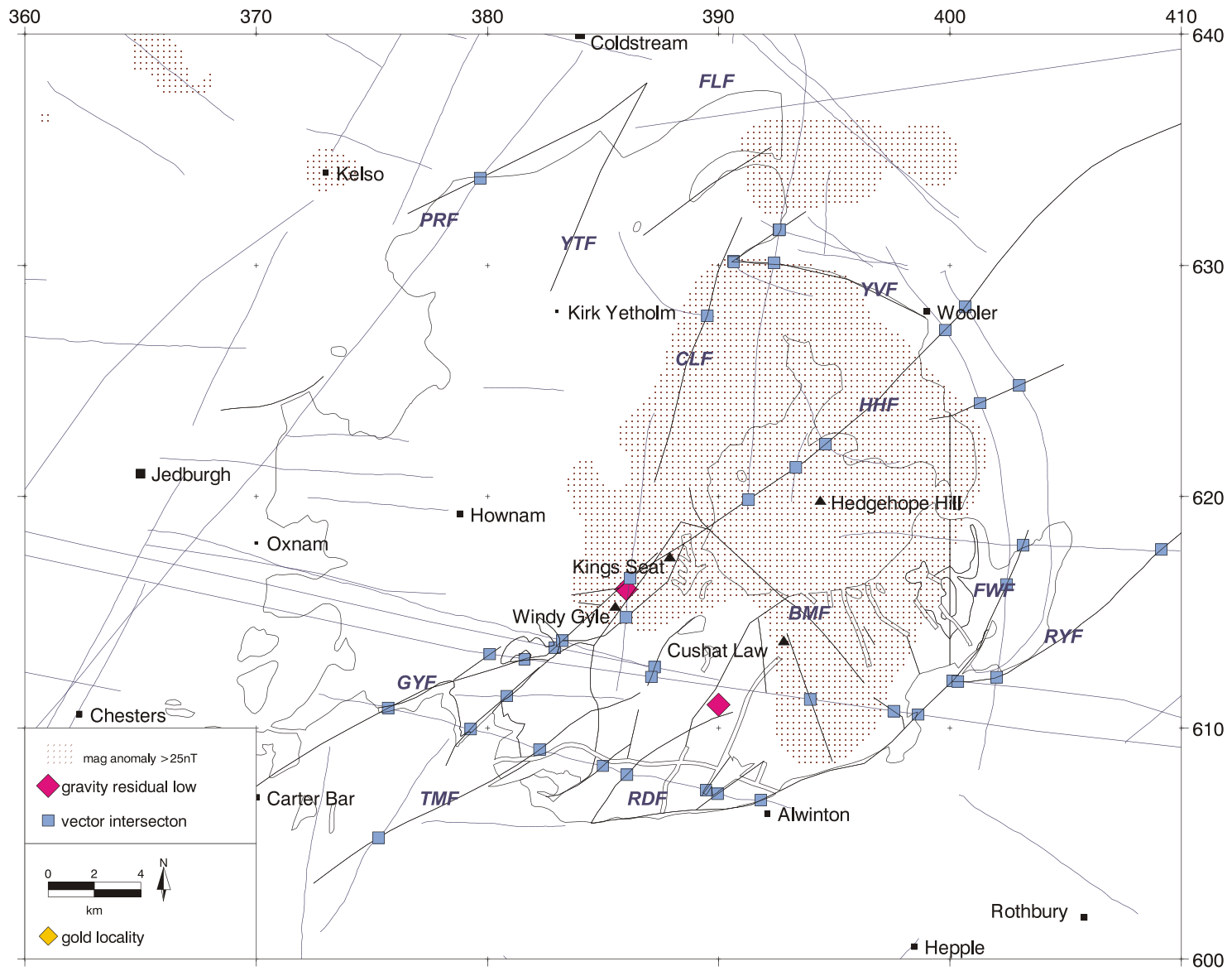


Fig 8.50 Cheviot: selected geophysical data for prospectivity analysis

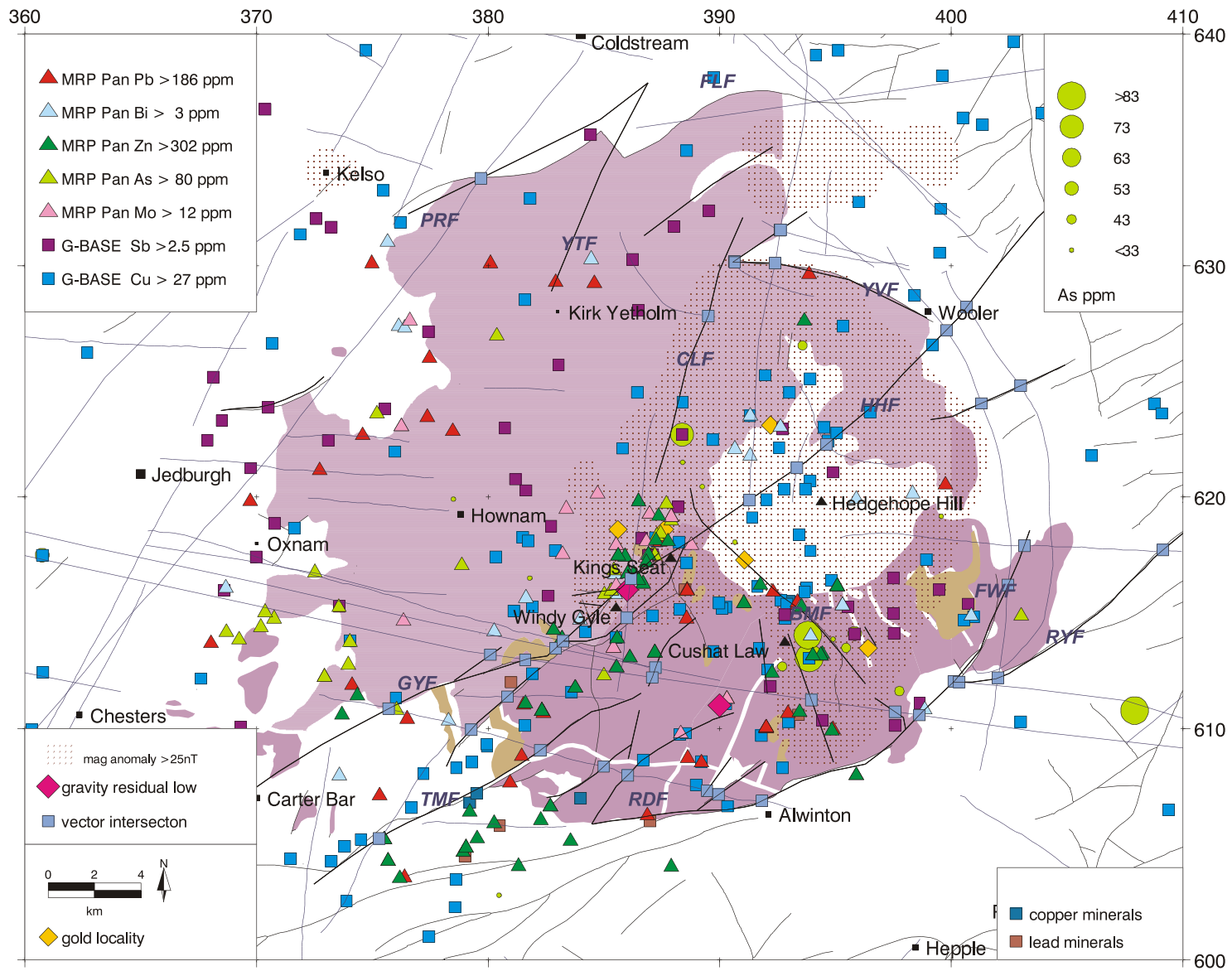


Fig 8.51 Cheviot: all selected data for prospectivity analysis

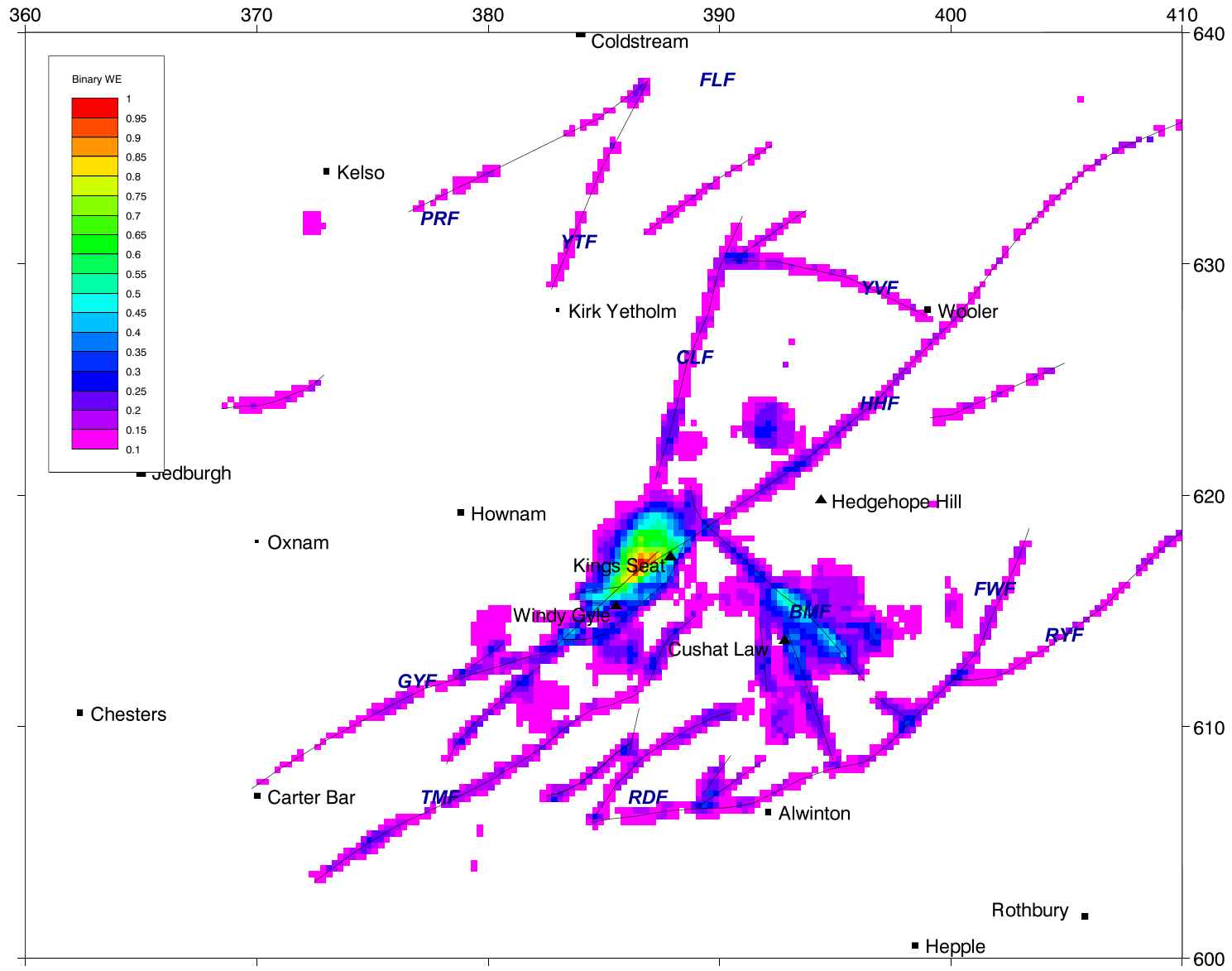


Fig 8.52 Cheviot: binary weights of evidence (BWE) prospectivity map for epithermal gold mineralisation